THE EFFECTS OF STREPTOMYCIN AND DIVALENT CATIONS ON THE DEVELOPMENT AND FINE-STRUCTURE OF SAPROLEGNIA SPP.

VOLUME I

by

Gordon William Beakes, B.Sc., A.R.C.S.

A thesis submitted for the degree of Doctor of Philosophy of the University of London and for the Diploma of Imperial College

June 1976

Department of Botany and Plant Technology,
Imperial College of Science and Technology,
London SW 7.

ABSTRACT

An ultrastructural account of growth and reproduction in Saprolegnia spp. is given to illustrate the normal patterns of differentiation in these fungi. Particular attention is given to oogonium and oospore development. Gametangial nuclear divisions are described and the evidence indicating their meiotic development discussed. Primary oospore formation is effected by the discharge of wall vesicles whereas subsequent accretion of the inner endospore wall is not vesicle mediated. The mature endospore wall is bounded on both sides by unit membranes, the origins of which are discussed. Ultrastructural changes in fertilisation tube and nuclear morphology confirm that in S.furcata both fertilisation and karyogamy take place during oospore maturation.

The effects of streptomycin on growth and reproduction in Saprolegnia spp. are also described. Although development at all stages in the life cycle is inhibited, reproductive differentiation is more sensitive than vegetative development. Streptomycin delays normal reproductive development and increases the proportion of gemmae which develop. As with other eukaryotes the toxic effects of streptomycin are greatly reduced by calcium ions.

Streptomycin causes widespread cytoplasmic lysis in induced hyphae but little effect is observed on the cytoplasm of growing hyphae. In colonies induced to sporulate it stimulates wall development and alters the structure of vacuolar and densebody vesicles and nuclear cytology. The effects of other protein synthesis inhibitors are described and compared with those of streptomycin. Streptomycin also reduces oxygen uptake and, above certain critical concentrations, causes the leakage of ions and UV-absorbing material from the cells. These effects are discussed in relation to metabolic lesions induced by antibiotics on other organisms.

The inhibitory effects of tap water, EDTA and divalent cations (Mn, Ca, Mg) on reproduction are also described. Tap water inhibition appears to be related, at least in part, to the high divalent cation content of the water. The EDTA and cation effects are compared with the antibiotic observations.

It is proposed that in Saprolegnia streptomycin acts by competing for particular cellular divalent cation ligands. In doing so it disrupts cellular metabolism governed by calcium and other cations. The availability of suitable binding sites is considered to be an important factor governing the susceptibility of these fungi to streptomycin.

CONTENTS

Volume I

	ABSTRACT	
	CONTENTS	1
	ACKNOWLEDGEMENTS	4
0.1	INTRODUCTION	5
0.2	MATERIALS AND METHODS	7
0.2.1	Fungi	7
0.2.2	Culture media	7
0.2.3	Culture techniques	9
0.2.4	Sporulation induction techniques	10
0.2.5	Light microscopy	10
0.2.6	Ultrastructural techniques	11
1.	ULTRASTRUCTURAL ASPECTS OF THE LIFE CYCLE OF SAPROLEGNIA AND PHYTOPHTHORA	17
1.1	LITERATURE REVIEW	18
1.1.1	The vegetative thallus	18
1.1.2	Zoosporangium morphogenesis	21
1.1.3	Gametangium morphogenesis	28
1.2	OBSERVATIONS	34
1.2.1	Vegetative development	34
1.2.2	Asexual reproduction	36
1.2.3	Sexual reproduction: Gametangium development	43
1.2.4	Sexual reproduction: Oospore maturation	51
1.2.5	Septum formation and structure in Saprolegnia	61
1.2.6	Sporangium development in Phytophthora cactorum	63
1.3	DISCUSSION	66
1.3.1	The parallel arrays of endoplasmic reticulum	66
1.3.2	Densebody vesicle function	66
1.3.3	Gametangial nuclear divisions	68
1.3.4	Fertilisation	71
1.3.5	Wall development	71
2.	THE EFFECT OF STREPTOMYCIN ON GROWTH AND REPRODUCTION IN SAPROLEGNIA	76a
2.1	LITERATURE REVIEW	76
2.1.1	Structure of streptomycin	76
2.1.2	The effect of streptomycin on prokaryotes	76
2.1.3	The effect of streptomycin in eukaryotes	78
2.1.4	Streptomycin uptake	81
2.1.5	Cation antagonism	82
2.1.6	Streptomycin resistance and dependence	82

2.2 MATERIALS AND METHODS 84

2.2.1 Antibiotic stock solutions 84
2.2.2 Antibiotic media 84
2.2.3 Divalent ion solutions 84
2.2.4 Experimental procedures to determin antibiotic effects 84
2.2.5 Methods used in physiological studies of antibiotic action

2.3 RESULTS 88

2.3.1 Effects of streptomycin on Saprolegnian growth 88
2.3.2 The effects of streptomycin on asexual reproduction in Saprolegnia 92
2.3.3 The effect of streptomycin on sexual reproduction in Saprolegnia 97
2.3.4 The effects of streptomycin on reproduction in Phytophthora cactorum 101
2.3.5 The addition or removal of streptomycin at varying stages in the induction cycle 103
2.3.6 The effect of other divalent cations on streptomycin toxicity 106
2.3.7 The effects of other protein synthesis inhibitors on sexual reproduction in Saprolegnia 109
2.3.8 The effect of antibiotics on gross morphology and cytology 111
2.3.9 The effect of antibiotics on organelle ultrastructure 123
2.3.10 Physiological effects of streptomycin 131

2.4 DISCUSSION 137

2.4.1 The toxic effects of streptomycin on Oomycetes 137
2.4.2 The inhibition of cytoplasmic cleavage 137
2.4.3 The extension of the post-induction lag phase 140
2.4.4 The antagonism of streptomycin toxicity by divalent cations 140
2.4.5 Cell wall enhancement 141
2.4.6 The mechanism of streptomycin action in Saprolegnia 141
2.4.7 Variations in streptomycin toxicity 146

3. THE EFFECTS OF TAP WATER AND DIVALENT CATIONS ON THE REPRODUCTIVE DIFFERENTIATION OF SAPROLEGNIA SPP. 149

3.1 LITERATURE REVIEW 150

3.1.1 The induction of sporulation in Saprolegnia 150
3.1.2 Changes in cellular biochemistry which accompany induction 151

3.2 MATERIALS AND METHODS 153

3.2.1 Water types used in induction experiments 153
3.2.2 Divalent cation and EDTA stocks 153

3.3 OBSERVATIONS 154

3.3.1 The effect of mains tap water and its pre-treatment in Saprolegnian reproduction 154
3.3.2 The effect of divalent metal cations and EDTA on sexual reproduction in S.furcata 158

3.4 DISCUSSION 164

3.4.1 The effects of tap water 164
3.4.2 The effects of EDTA 164

	3.4.3	Divalent cation toxicity	166
	3.4.4	Morphological and ultrastructural effects of excess Ca^{2+} ions	166
	3.4.5	Comparison of divalent cation, EDTA, and antibiotic effects	167
4.	SUMMARY		170
5.	REFERENCES		176

Volume 2

6.	PHOTOGRAPHIC PLATES		1
6.1	ABBREVIATIONS		1
	6.1.1	Fixatives	1
	6.1.2	Optical systems	1
	6.1.3	Inducing solutions	1
	6.1.4	Plates and legends	2
6.2	PLATES		
	1.	Ultrastructural aspects of the life cycle of Saprolegnia and Phytophthora	3
	2.	The effect of streptomycin on growth and reproduction in Saprolegnia	76
	3.	The effects of tap water and divalent cations on the reproductive differentiation of Saprolegnia	141

ACKNOWLEDGEMENTS

I would like to express my thanks and gratitude to my supervisor, Dr. J.L. Gay for his help and encouragement throughout the course of this project. I am also indebted to the technical staff, particularly Miss Marion Martin, of the Electron Microscope Unit (Department of Botany, Imperial College) for their endless assistance and patience. I am grateful to the Geology Department, Imperial College, for the use of their S.E.M. elemental analysis facilities and to Dr. S. Bullivant for the demonstration of his freeze-fracture apparatus. Thanks also go to my colleagues, Dr. Rosemary Reeves and Francisco Gil for their helpful discussions and useful technical advice. I must also thank Miss G. Williams for performing a minor miracle and converting my handwriting into typescript. Finally a word of appreciation to all my long suffering friends for all they have had to endure from me during the course of this work.

This work was carried out under the tenure of a Science Research Council Studentship.

0.1 INTRODUCTION

Vegetative colonies of the aquatic Saprolegniales can be induced to sporulate by the simple manipulation of the growth medium, and nearly synchronous development follows. Such a system is ideal for the study of both organelle and biochemical changes associated with reproductive differentiation. Not surprisingly during the past decade there have been a number of such studies on reproduction in this group. Ultrastructural changes associated with sporangium development were first described by Gay and Greenwood (1966) for Saprolegnia ferax, and later in Saprolegnia monoica by Hagedorn and Weinert (1974). Most of the complementary biochemical studies on asexual differentiation have been carried out on Achlya spp. (Griffin & Breuker, 1969; Cameron & LéJohn, 1971; Timberlake et al., 1972; O'Day & Horgen, 1974; Horgen & O'Day, 1975). Oogonium development and oospore formation in Saprolegnia follows a similar course of structural changes to those described in sporangia, although the nuclear cytology is more complex (Howard & Moore, 1970; Gay, Greenwood & Heath, 1971). This present study was initiated as a direct continuation of the structural studies on Saprolegnia. It was hoped to further the understanding of the spore cleavage process and structural aspects of sexual differentiation not previously investigated.

Studies on members of the Peronosporales have shown that sublethal concentrations of streptomycin induce abnormal cleavage patterns in the sporangia (Griffin & Coley-Smith, 1971). Since the employment of selective inhibitors has been widely used to further the understanding of normal patterns of differentiation in other organisms, it was hoped that the study of the effects of streptomycin on Saprolegnian development would yield similarly useful information. Although streptomycin inhibits the development of Oomycete fungi it has little affect on fungi with chitinous walls (Vörös, 1963). The biochemical basis of streptomycin toxicity to this group of fungi is not known (Griffin & Coley-Smith, 1971; McMeekin, 1973). Although streptomycin is also toxic to algae and higher plants it was thought to act mainly through inhibiting plastid development (Brock, 1966). It was hoped that this study on Saprolegnia might give some indication of the mode of streptomycin action against this fungal group, and perhaps other eukaryotes as well. Knowledge of the mode of streptomycin action in this group is especially desirable now that streptomycin resistance has been used as a genetic marker in Phytophthora (Shaw & Elliott, 1968; Shattock & Shaw, 1975).

During the course of these investigations the inhibitory effect of tap water to sexual reproduction in Saprolegnia furcata was observed. In

addition to providing useful information on the otherwise intractible problem of mature oospore structure, a number of similarities between the tap water and streptomycin effects were also noted. This led to a comparative study of the inhibitory effects of excess divalent cations and a chelating agent on Saprolegnian differentiation.

This account is divided into three main parts, each with a literature review and discussion. The first part describes normal growth and reproduction in Saprolegnia; the second examines the effects of streptomycin, and the third includes the tap water and cation studies. These sections are preceeded by a description of the materials and methods used throughout the course of this work.

0.2 MATERIALS AND METHODS

The materials and general experimental methods used throughout the course of this study are described in this section. Other experimental details will be included where appropriate in the relevant subsections.

0.2.1 Fungi

A list of the Oomycete species and strains used in this study is given in Table 0.1. The first Saprolegnia ferax isolate (1) was isolated and described by Manton, Clarke and Greenwood (1951), and has subsequently been used in the ultrastructural studies of A.D. Greenwood and his associates (see literature review, Section 1.1). All three S.ferax(1,2 & 3)isolates have lost their ability to reproduce sexually. In contrast the two S.fucata isolates (4 & 5) mainly reproduce sexually, and isolate 4 was used in the ultrastructural study of Gay, Greenwood and Heath (1971). The Phytophthora cactorum isolate was chosen both for its ability to produce large numbers of sporangia, and its previous use in a streptomycin study by Shaw and Elliott (1968).

0.2.2 Culture Media

All the media were prepared using Analar grade chemicals (unless otherwise indicated), made up using single glass distilled water (Fistream still, Fisons Ltd.), and sterilised by autoclaving at 120°C for 15 minutes.

0.2.2.1 Glucose, Yeast extract, Peptone, Salts Medium (GYPS)

Glucose	10.0 g
Yeast extract (Oxoid no. L21)	0.1 g
Peptone	1.0 g
KH_2PO_4	1.0 g
$MgSO_4.7H_2O$	0.3 g
Distilled water	1.0 l
Agar (Oxoid no.3 or Ionagar no. 2)	15.0 g

This was the standard liquid (om itting agar) and solid medium used throughout this work. The most satisfactory colony growth for experimental purposes was obtained using half-strength GYPS. In some of the antibiotic experiments the $MgSO_4$ was omitted from the medium.

0.2.2.2 Oatmeal Agar (OA)

Oatmeal (Quaker oats)	30.0 g
Agar (BDH, Fine Powder Agar)	20.0 g
Distilled water	1.0 l

The oatmeal was suspended in distilled water and steamed for 1 h before straining through fine muslin. The filtrate was made up to a litre with distilled water and the agar added. This was the standard growth medium used for Phytophthora cactorum.

Table 0.1. The Oomycete fungi used in the experimental work

Species	Origin	Reference Number
Saprolegniales		
1. Saprolegnia ferax (Gruith.) Thuret	A.D. Greenwood Imperial College, London	-
2. Saprolegnia ferax (Gruith.) Thuret	H. Fuller University College, Dublin	-
3. Saprolegnia ferax (Gruith.) Thuret	H. Fuller University College, Dublin	-
4. Saprolegnia furcata Maurizio	J. Gay* Imperial College, London	APC 205a
5. Saprolegnia furcata Maurizio	A.P.C.C., Reading	APC 205b
6. Saprolegnia hypogyna Pringsheim	A.P.C.C., Reading	APC 206a
7. Saprolegnia litoralis Coker	A.P.C.C., Reading	APC 207a
8. Saprolegnia megasperma Coker	A.P.C.C., Reading	APC 208a
9. Saprolegnia parasitica Coker	A.P.C.C., Reading	APC 211d
10. Saprolegnia turfosa Gaumann	A.P.C.C., Reading	APC 213a
Peronosporales		
11. Phytophthora cactorum (Lebert and Cohn) Schroeter	C.M.I., Kew	IMI 21168

A.P.C.C. Aquatic Phycomycete Culture Collection, Reading.

C.M.I. Commonwealth Mycological Institute, Kew.

* This isolate has been subcultured in the laboratory at Imperial College since 1967 from a culture supplied by Dr. M. Dick, Reading.

0.2.2.3 Pea Extract Agar (PEA)

Frozen Peas (Waitrose)	400.0 g
Sucrose	20.0 g
Agar (BDH Fine Powder Agar)	10.0 g
Distilled water	1.0 l

The peas were boiled in about 0.5 l of distilled water for 5 min., and partially drained before homogenisation (Polytron homogeniser). The homogenate was made up to 1 l with distilled water and boiled for 30 min. before straining through a double layer of fine muslin. The volume of this extract was adjusted to 1 l with hot distilled water and the sucrose and agar added. This medium was always autoclaved in two 500 ml aliquots. This medium was used for sporangium production in P.cactorum.

0.2.2.4 Water Agar

Agar (BDH Fine Powder Agar, or Oxoid no. 3)	8.0 g
Distilled water	1.0 l

0.2.3 Culture techniques

0.2.3.1 Maintainance of Stock Cultures

Saprolegnia cultures were maintained on GYPS agar slopes in metal capped Pyrex test tubes or universal bottles, and Phytophthora cultures on similar OA slopes. All stock cultures were stored at 4°C and subcultured at 6-monthly intervals. Any colonies showing signs of bacterial contamination on subculture were decontaminated by growing through glass 'Raper' rings as described by Raper (1937).

0.2.3.2 Routine Culture

Routine sub-culturing was carried out by cutting 4 mm discs from the margin of 48 h colonies grown on GYPS agar, using a flame-sterilised stainless steel borer. These discs were transferred aseptically with a flame-sterilised needle to fresh agar plates. Colonies were incubated in the dark, at 25°C for Saprolegnia and at 20°C for Phytophthora.

0.2.3.3 Liquid Culture

Saprolegnia species grow well in liquid-GYPS medium to produce a more or less flat circular colony ideal for use in sporulation-induction experiments. Initially 4 mm colony-plugs were used as inoculum, but were later replaced by infested nylon discs prepared in the following way. Suitable discs were punched from a nylon sheet (45 µm mesh, Henry Simon Ltd.) using a redhot 4 mm cork borer. These were sterilised by autoclaving and then placed around the margin of an actively growing vegetative colony. The plates were then left for 24 h to become infested with the fungus before transferring the discs to liquid medium. Usually 4 such discs were inoculated into a single 8 cm plastic Petri dish (Sterilin) containing approximately 20 ml of medium. These discs were incubated for between 16-20 h at 20°C to produce suitable

colonies for induction experiments.

0.2.4 Sporulation Induction Techniques

0.2.4.1 Induction of Sporangia and Oogonia in Saprolegnia

As described by Klebs (1899) vegetative colonies of Saprolegnia can be induced to sporulate by transfer to a nutrient-free medium. Preliminary experiments showed that the incubation of suitable inocula in 1/2 GYPS - liquid medium at 20°C for about 18 h produced colonies of suitable diameter (15-20 mm) and hyphal density for use in induction experiments. Suitable colonies were transferred to a large volume (200 ml) of sterile distilled water and gently agitated to remove all traces of nutrient solution. Washed-colonies were transferred aseptically to plastic 8 cm Petri dishes containing 15 ml of inducing solution. In normal experiments this was sterile glass-distilled water (Fistream or Scorah stills). In most experiments two colonies were placed in each dish and incubated in the dark at 20°C or 25°C, depending on the species.

0.2.4.2 Induction of Sporulation in Phytophthora

Phytophthora cactorum was induced to produce sporangia using the procedure described by Shaw and Elliott (1968). Vegetative colonies were grown on PEA medium at 25°C for between 4-5 days to allow the fungus to overgrow the dish. The colony was then cut into strips, c. 5.0 x 1.0 cm in size, using a flame-sterilised scalpel. These strips were transferred to plates of water agar (0.8%) and incubated at 20°C in the dark. Sporangia develop very quickly on these strips, and were harvested after 48-72 h using the following procedure. The water agar plates were flooded with 10 ml of sterile distilled water and the surface gently scraped with a sterilised glass spatula. The resulting suspension was first passed through a double-layer of muslin to remove the larger debris, and then filtered through a nylon mesh filter (45 µm mesh, Henry Simon Ltd.). The isolated sporangia were spun down by centrifugation at 500 r.p.m. for 3 minutes (Autopoise Centrifuge, Griffin and George Ltd.) The pellet was resuspended in 2% dextrose to prevent zoospore lysis (Shaw and Elliott, 1968). Zoospore formation (indirect germination) was induced by chilling the sporangial suspension at 4°C for 3 min. before incubating at 16°C.

0.2.5 Light Microscopy

Routine low-power examination of colonies was carried out by the direct observation of the petri dish cultures under a Vickers binocular microscope (x 10 eyepiece, x 10 objective). However, for more critical high-power (x 40, x 100 objectives) examination of hyphae, sporangia and oogonia small portions of colony were removed using a flame-sterilised scalpel and transferred to a microscope slide. Most high-power observations were made on a Reichert 'Zetopan' microscope, equipped with positive, negative (Anoptral) and differential interference (Nomarski) phase optical systems and Koehler

illumination. This microscope was also fitted with a Reichert prismatic beamsplitter and an EXA camera back.

Most of the photographs of living material, either under ordinary or anoptral phase contrast, were taken using a Zeiss 'Ukatron' flash unit (at either 30 or 60 W) usually fitted with a green interference filter, and recorded on Ilford pan F film (A.S.A. 50). Photographs of material examined under Nomarski phase optics were obtained with the microscope illuminated by the fitted 30 W tungsten lamp, and recorded on Ilford HP3 film (A.S.A. 400).

For the high-power (x 100 objective) time-lapse photographic sequence of oospore maturation a simple observation cell was constructed. A coverslip (3.0 x 2.0 cm) was mounted on a microscope slide over a narrow (4 mm) strip of filter paper (Whatman no. 50) and sealed with liquid paraffin. Prior to mounting the specimen was placed in the centre of the coverslip in a drop of water contained by a ring of vaseline (10 mm diameter).

0.2.6 Ultrastructural Techniques

0.2.6.1. Processing Procedures

Colonies of Saprolegnia were simply processed by transferring them with a needle to the appropriate fixative solution (3.5 ml), contained either in covered embryo cups or in capped 10 ml-glass vials. Suspensions of cells (Phytophthora sporangia and Saprolegnia cysts) were pelleted by centrifugation (2-3 min.at 50 r.p.m. for sporangia and 2000 r.p.m. for cysts) before resuspending in the appropriate fixative solution. Once the fixative schedule was completed the cell suspensions were resuspended and spun-down in molten agar (Oxoid Ionagar No. 2, 2% w/v) prior to dehydration and embedding. These agar-embedded pellets were cut into convenient-sized blocks and processed in the same way as whole colonies.

0.2.6.2 Fixation Procedures

The fixation procedures used in this study are basically those described by Heath (1969). Cacodylate buffer was used in preference to phosphate buffer however since it is believed to result in less vacuolar-membrane disruption (Gay, personal communication). Most of the fixatives and embedding materials were supplied by TAAB Laboratories, and were stored in the deep freeze when not in use. The main fixation schedules will now be described:

1. Osmium Tetroxide (Os)

Material was fixed for 1 h at room temperature (20-24°C) in 1% osmium tetroxide (OsO_4) in 0.1 M sodium cacodylate buffer at pH 7.0. This is an extremely dangerous and volatile chemical and fixations were always carried out in a fume cupboard. The fixative solution was prepared by mixing drops of 4% OsO_4 stock solution (TAAB) with drops of 0.2 M cacodylate buffer and double glass distilled water, in the ratio of 1:2:1.

This was the most widely used fixative procedure used in this study since it gave particularly good preservation of the vacuolar systems. It

did not however preserve nuclear or cytoplasmic microtubules.

2. Glutaraldehyde-Osmic (GaOs)

Material was first fixed in 2% glutaraldehyde in 0.1 M cacodylate buffer at pH 7.0, for 3 h at room temperature. The fixative was prepared by diluting a 25% glutaraldehyde stock solution(TAAB) with appropriate volumes of 0.2 M buffer and distilled water. The material was then washed in 4 changes of buffer (14 min. each change), before post-fixing for 1 h in 1% OsO_4 using the procedure described above.

This fixative procedure gave the best overall preservation of cytoplasmic structure and was mainly employed in the study of nuclear cytology and hyphal structure.

3. Potassium Permanganate ($KMnO_4$)

Material was fixed at room temperature in unbuffered 2% potassium permanganate ($KMnO_4$) for varying periods of time ranging from 2-25 min. This fixative mainly preserves internal cell membranes, and often reveals cell wall sustructure. It also proved the most satisfactory fixative for the study of mature oospore structure.

4. Potassium Permanganate-Osmic Acid ($KMnO_4$-Os)

This fixative combination was used for some of the oospore preparations and gave a better preservation of peripheral lipid droplets than $KMnO_4$ alone Between the $KMnO_4$ and Os fixations the material was washed in 4 changes of buffer (4 x 10 min.).

0.2.6.3 Dehydration and Embedding

Fixed material was dehydrated in a graded series of ethanol solutions, in 10% steps from 20% to 100%. Approximately 10 min. was allowed for each change up to absolute ethanol. This was followed before 4 x 30 min. changes in absolute ethanol to complete the dehydration. The material was then transferred to epoxyresin via a series of epoxypropane mixtures as outlined in Table 0.2.

Table 0.2. Summary of the infiltration and embedding procedure

		Solution composition v/v				
Stage		Ethanol	Epoxy-propane	Epon 812	Time h	Temp. °C
	1	1	1	0	0.5	20-24
	2	0	1	0	0.5	"
Infiltration	3	0	2	1	2	"
	4	0	1	1	12-18	4
Embedding	5	0	0	1	24	20-24
Polymerisation	6	0	0	1	48	60

The resin used was Epon 812 (TAAB laboratories) which was prepared according to the formulations of Luft (1962), the components of which are as follows:

A mix	Epon 812	46.0 g
	Dodecenyl succinic anhydride (DDSA)	61.8 g
	Benzyl demethylamine (BDMA)	2.0 ml
B mix	Epon 812	69.0 g
	Methyl nadic anhydride (MNA)	57.0 g
	BDMA	2.0 ml

The hardness of the resin is determined by the ratio of hardener (DDSA + MNA) and accelerator (BDMA), and for the early work the very hard B resin was usually used, but later this was replaced by the moderately hard 1A:1B mix.

Following impregnation in resin at room temperature the material was transferred to polythene embedding dishes (c. 2.5 cm x 0.5 cm) for polymerisation at 60°C. The infiltrated fungal colonies were carefully teased apart and distributed around the margin of each dish before polymerisation. Usually a layer of resin was partially polymerised in each dish before adding the specimen to prevent sinkage during polymerisation. The agar-embedded pellets were either polymerised in the apex of BEEM capsules (Polaron) or in small polypropanol moulds.

0.2.6.4. Trimming and Sectioning

Suitable portions of colony were selected from the flat-embedded discs under the light microscope, and sawn-out with a small fret-saw. These pieces were then mounted on the end of a short piece of perspex dowel (2.5 cm in length x 1.0 cm in diameter) with Durofix adhesive (Rawplug Ltd.). The mounted specimen-blocks were held in a chuck for trimming under a stereomicroscope (x 90, Bausch and Lomb). The mounted blocks and capsule-embedded material were trimmed using pieces of degreased stainless-steel razor blade (Wilkinson Sword Ltd.) held in a small pin-vice. Blocks were trimmed to a trapezium-topped pyrimid containing a single hypha, sporangium or oogonium of a known stage and orientation. The trimmed-blocks were usually faced with a glass-knife on an ultramicrotome before sectioning was commenced.

Sections were cut either on an 'LKB Ultratome 1'(LKB-Produkter AB Ltd.) or on a 'Reichert OmU_2' ultramicrotome (C. Reichert AG), using glass (prepared using an LKB 'Knife Maker' 7800) or diamond-knives (I.V.I.C. or Ge-Fe-Ri). The cut sections were floated onto double-distilled water, and section thickness was assessed according to their interference colours at the water surface (Peachey, 1958: grey, <60n,; silver, 60-90 nm; gold, 90-150 nm). Silver-gold sections were cut for low-power studies (<10,000) and silver-grey sections for higher-resolution studies.

Ribbons of cut sections were collected on formvar-coated copper grids (100 or 200 mesh; Polaron, Smethurst, Mason & Morton). The sections were picked up by carefully lowering the grids onto the sections with fine curved forceps. The coated grids were prepared by casting a formvar (TAAB) film onto a clean water surface, from a coated glass slide (prepared with a 0.6% formvar solution in chloroform) and loading with grids. The grids were then collected on clean nylon or copper mesh and stored in a desiccator. The collected sections were stored on hardened filter paper (Whatman no. 40) in glass Petri dishes prior to staining.

0.2.6.5. Staining Procedures

1. Uranyl Acetate - Lead Citrate (UaPb)

Most fixed material lacks sufficient contrast to be examined directly under the light-microscope without staining. Most grids were double-stained with uranyl acetate and lead citrate. The droplets of stain were placed on cleaned polythene sheets in plastic petri dishes. The grids were incubated in droplets of 2% aqueous uranyl acetate at 60°C for 30 minutes. The grids were then rinsed well in a stream of clean distilled water before staining in droplets of Reynolds lead citrate (Reynolds, 1963). To prevent lead carbonate precipitation in the lead citrate droplets, atmospheric carbon dioxide was removed by the addition of KOH pellets to the Petri dish chamber. The grids were stained in lead citrate for 10 minutes at room temperature before rinsing in a stream of distilled water. The grids were dried on hardened-filter paper and stored in gelatin capsules (Parke-Davis) mounted between strips of card.

2. Periodic Acid - Silver Methenamine (PASM)

The histochemical localisation of cellular polysaccharides was determined using the periodic acid-silver methenamine staining procedure described by Dhir and Boatman (1972). However, in this study the sections were not picked up on gold grids, but were transferred through the various solutions using a small platinum loop. The sections (GaOs & Os-fixed) were first peroxidised in 0.005 M periodic acid for 20 minutes at room temperature (22°C). After washing by transferring through several changes of distilled water the sections were incubated in the silver methenamine (hexamine) solution (Dhir & Boatman, 1972) at 60°C for 1 h. Following washing the sections were treated for 2 minutes with 0.5% sodium thiosulphate to remove the covalently-bound silver. The sections were then given a final series of washes and picked up on copper grids.

0.2.6.6. Freeze-fracture Replicas

Oogonia containing mature oospores were isolated by homogenisation of induced-colonies in a Sorvall Omnimix microhomogeniser (10 ml). The homogenate was passed through muslin to remove the larger debris and then

filtered through a 45 µm nylon-mesh filter (Henry Simon Ltd.). The resulting oogonial suspension was concentrated by centrifugation and loaded in a specimen holder of the freeze-fracture device developed by Bullivant and Ames (1966). A freeze-fracture replica was prepared by Dr. S. Bullivant using the procedure outlined by Bullivant (1973). The replica was cleaned in 10% sodium hypochlorite for 30 minutes before picking up on a formvar-coated 200 mesh copper grid.

0.2.6.7 Electron Microscopy

The specimens were examined either on an A.E.I. EM 6 or EM6B electron microscope, at accelerating voltages of 60 and 75 kV respectively. The magnification of each microscope was calibrated using an AEI diffraction grating (2,160 lines/mm). Electron micrographs were recorded either on Ilford N 50 or Agfa C plates or on Agfa 'F071P' cut film. The exposed plates or film were developed in Kodak D 19 Developer and fixed in Ilford 'Ilfofix'.

0.2.6.8. Printing and Stereology

Routine electron micrograph prints were made on Agfa-Gevaert Rapido-print paper (25.4 x 20.3 cm), using an Agfa-Gevaert L21 Processor. Estimates of the volume fractions of various cytoplasmic components were made from these routine prints (print magnification 10,500) using a simple point-lattice (1cm) as described by Freere and Weibel (1967).

0.2.6.9. Electron Microscopic Elemental Analysis

The elements in biological material can be determined under the scanning electronmicroscope (SEM) by the energy dispersive analysis of the emitted X-rays(EDAX). The basic principles of this elemental analysis has been recently reviewed by a leading manufacturer of EDAX equipment (Anon., 1972). The SEM image of the surface of a biological specimen is mainly formed from the low energy secondary electrons derived from atoms in the sample excited by the high energy incident electrons. These secondary electrons are collected by a single crystal semiconductor linked to a multichannel analyser. This is a special-purpose digital computer which counts the number of pulses in each energy-band, and produces a complete energy-spectrum of the emitted X-rays from the specimen.

In this study portions of induced S.furcata colonies (120 h) with mature oogonia were dried down either onto aluminium or carbon rivet supports. These were then vacuum-coated with aluminium or carbon respectively in an A.E.I. coating unit. These specimens were examined under a Cambridge scanning electron microscope operated at an accelerating voltage of 20 kV. The elemental analysis of the selected specimens (magnification, 10,000) was compiled using a single point source of incident electrons, with count times of 500 or 1000 seconds to suit the specimen. The resulting spectra

were plotted-out from the multichannel-analyser using a potentiometric recorder.

PART I

ULTRASTRUCTURAL ASPECTS OF THE LIFE CYCLE OF SAPROLEGNIA AND PHYTOPHTHORA

This first section describes the observations made on various stages in the life cycle of Saprolegnia ferax and Saprolegnia furcata, and on the sporangia of Phytophthora cactorum. Most of these observations were made on material set up and fixed as controls in the antibiotic and ion experiments to be described in following parts of this thesis. Certain aspects of the Saprolegnian life history which have been subject to controversy, such as the gametangial nuclear divisions and the occurrence of fertilisation, or are poorly documented, like oospore maturation, will be described and discussed in some detail.

1.1 LITERATURE REVIEW

1.1.1 The Vegetative Thallus

1.1.1.1 The Hyphal Apex

In common with most fungi the Oomycete thallus consists of a branching system of filamentous hyphae, which in this group are coenocytic. Hyphal extension is confined to the tapered apical region (Burgeff, 1915; Smith, 1923b). Not surprisingly this region possesses many interesting morphological and physiological properties (see reviews by Robertson, 1965; Bartnicki-Garcia, 1973a), which gave impetus to the ultrastructural study of the hyphal apex.

However none of the early ultrastructural accounts of Oomycete hyphae included apical profiles, although they revealed the presence of many organelles previously described in higher plants and algal cells (Hawker, 1963; Hawker & Abbott, 1963; Hendy, 1966; Gay & Greenwood, 1966; Shatla, Yang & Mitchell, 1966; Marchant, Peat & Banbury, 1967). The first unequivocable description of a hyphal apex was given by McClure, Park and Robinson (1968) for Neurospora crassa. This was quickly followed by similar accounts for a wide range of species including the following Oomycete fungi; Saprolegnia ferax (Heath, 1969; Heath, Gay & Greenwood, 1970), Phytophthora parasitica (Hemmes & Hohl, 1969. This species was later re-identified as P.palmivora, Hemmes & Hohl, 1972). Saprolegnia monoica (Hagedorn & Weinert, 1971), Pythium ultimum (Grove, Bracker & Morré, 1970; Grove & Bracker, 1970), Aphanomyces euteiches (Hoch & Mitchell, 1972a), and Lagendium collinectes (Gotelli, 1974a).

It was found in all these studies that the apex (<10 μm) contained a large number of small membrane-bound vesicles. In Oomycetes these vesicles were of two distinct sizes; the smaller and more abundant approximately 60 nm in diameter, and the larger about 150 nm in diameter (Grove & Bracker, 1970). However these different-sized vesicles are not segregated into specialized regions as they are in the apices of both the Zygomycetes and septate fungi (Grove & Bracker, 1970).

These apical vesicles are believed to be produced by the sub-apical Golgi dictyosomes, and then migrate to the apex where they are discharged (Grove, Bracker & Morré, 1970; Heath, Gay & Greenwood, 1971). In addition to contributing membrane to the expanding plasmalemma (Grove & Bracker, 1970) they also release cell wall precursors and probably lytic enzymes (Girbardt, 1969; Grove & Bracker, 1970; Heath, Gay & Greenwood, 1971). Although these vesicles have not been extracted and analysed biochemically, they have been shown to be rich in polysaccharides by the periodic acid-silver hexamine staining technique (Heath, Gay & Greenwood, 1970). They

do not however contain preformed microfibrils (Bracker, 1971), which have been shown to be assembled extracellularly (Wang & Bartnicki-Garcia, 1969). Bartnicki-Garcia (1973a) proposed the polarised discharge of vesicles at the apex would establish the gradients of wall deposition (Bartnicki-Garcia & Lippman, 1969; Gooday, 1971) and wall plasticity (Robertson, 1965) necessary for apical extension. However the means by which the polarity of vesicle deposition is determined is still unknown.

1.1.1.2 Organelle Zonation

In addition to the apical vesicles there is further organelle zonation in the hyphal tip region. Immediately behind the vesicular zone there is a mitochondrial zone before the first nuclei and large vacuolar vesicles appear (Grove, Bracker & Morré, 1970; Heath, Gay & Greenwood, 1970). Further from the apex the hyphal cytoplasm becomes increasingly vacuolate and there is an increase in storage products such as lipid (Hawker, 1963; Gay & Greenwood, 1966; Shatla, Yang & Mitchell, 1966; Grove, Bracker & Morré, 1970).

Histochemical (Zalokar, 1959) and growth studies (Trinci, 1971) on fungal hyphae have shown that the main synthetic capacity of the fungal cytoplasm resides in the subapical zone, up to 500 µm behind the tip. This is in effect the hinterland which supports each growing apex. In Oomycetes this subapical zone contains abundant Golgi dictyosomes, which produce the vesicles which are transported to the apex (Grove, Bracker & Morré, 1970). Each dictyosome is associated with either a cisterna of endoplasmic reticulum (ER) or nuclear envelope; both of which contribute small vesicles to the proximal dictyosome cisterna (Grove, Bracker & Morré, 1970; Heath, Gay & Greenwood, 1970). Nuclei and mitochondria are also abundant in this subapical zone, and profiles of the latter of up to 10 µm in length are not uncommon (Gay & Greenwood, 1966).

1.1.1.3 Wall Composition and Morphology

The cell walls of Oomycete fungi are unusual in that they contain cellulose and not chitin as the microfibrillar component (Zervenhuisen & Bartnicki-Garcia, 1969). Oomycete walls have now been analysed for a wide range of species, and all show a remarkably similar composition (Parker, Preston & Fogg, 1963; Bartnicki-Garcia, 1966; Novaes-Liden & Jimenez-Martinez, 1968; Sietsma, Eveleigh & Haskin, 1969; Poa & Aronson, 1970). Proteins account for between 5-10% of the wall and β-glucans (1,3-,1,4- and 1,6- linked) the remaining 90-95%. Of the latter crystalline cellulose only constitutes between 15-25%. Hunsley and Burnett (1970) have shown that the cellulose microfibrils are embedded in an inner proteinaceous matrix, with the amorphous β-glucans forming the outer wall layer.

Shadowed whole-mount preparations of Oomycete walls from hyphae (apical and subapical) cysts and sporangia all show randomly orientated cellulose microfibrils (Heath, 1969; Tokunga & Bartnicki-Garcia, 1971; Hunsley & Burnett, 1970; Hegenauer & Hohl, 1974).

Oomycetes also have a variety of membranous bodies associated with their cell walls. These bodies have been the cause of much speculation concerning their function and confusion over their terminology. Such bodies were first described in chitinous fungi by Moore and McAlear (1961) who called them lomasomes, and were subsequently reported in Oomycetes (Hendy, 1966) and higher plants (reviewed by Marchant and Robards, 1968). Marchant and Robards (1968) proposed the collective name paramural body for these structures, and differentiated them into lomasomes and plasmalemmasomes depending on whether they were formed from internal membranes, or from plasmalemmar elaborations. As Heath and Greenwood (1970a) pointed out, such a distinction was difficult if not impossible to apply and proposed plasmalemmasome should be applied to membraneous material trapped between the cell wall and the plasmalemma, and lomasome to membraneous material actually sequestered within the wall. Hemmes and Hohl (1969) also differentiated lomasomes into types 1 and 2 on a similar basis. The terminology of Heath and Greenwood (1970a) was accepted by Marchant and Moore (1973), although many contemporary accounts still continue to use the term lomasome indiscriminately (e.g. Bimpong & Hickman, 1975).

Lomasomes have been implicated in a number of cellular functions including chitin synthesis and enzyme secretion (reviewed by Marchant & Robards, 1968). Bracker (1967) pointed out that most of the suggestions for lomasome function were mostly based on speculation, and suggested they may even be fixation artefacts. However it is now accepted that plasmalemmasomes develop as a way of removing excess plasmalemma which forms when vesicle deposition exceeds surface expansion (Hemmes & Hohl, 1969; Heath & Greenwood, 1970a; Marchant & Moore, 1973). As the plasmalemmasomes become sequestered by wall material they become classifiable as lomasomes (Heath & Greenwood, 1970a; Marchant & Moore, 1973).

1.1.1.4 Nuclear Cytology

Most accounts of nuclear division in Oomycete hyphae have indicated a form of direct (amitotic) division in which a sponge-like mass of chromatin separates as the nucleus elongates into a dumbell-shaped body and divides (Trow, 1895; Smith,1923a; Bakerspigel, 1960; Slifkin, 1967). The amitotic nature of these divisions is further supported by their apparent resistance to mitotic poisons such as colchicine (Slifkin, 1967) and griseofulvin (Stuart & O'Gorman, 1971).

However Hartog (1891) claimed that nuclear division was achieved by the

duplication and separation of distinct chromosomes in a normal mitotic fashion. This has been supported by more recent studies in which both chromosomes and spindle bodies have been reported in dividing Saprolegnian nuclei (Marks, 1965; Flanagan, 1970; Robinow cited by Heath & Greenwood, 1970b).

Ultrastructural studies have confirmed that hyphal nuclei undergo an intranuclear mitotic division in both the Saprolegniales (Heath & Greenwood, 1968 and 1970b; Howard & Moore, 1970; Hoch & Mitchell, 1972b; Heath, 1974a) and Peronosporales (Hemmes & Hohl, 1973). Nuclear division is achieved by the formation of an intranuclear spindle between two pairs of polar centrioles. The chromosomes divide and segregate along this spindle as the nucleus elongates into the dumbell-shaped profiles. Chromatin is not distinguishable in the Oomycete nucleoplasm, although chromosome number can be estimated by the presence of the rather indistinct kinetochore bodies (Heath & Greenwood, 1970b; Heath, 1974a). The spindle microtubules are widely spaced and Heath (1974a) suggests the motive force for nuclear elongation is supplied by the interaction of the nuclear envelope and cytoplasmic microtubules, rather than by spindle microtubule interactions.

Each interphase nucleus is associated with a pair of centrioles which lie in a shallow pocket in the nuclear envelope (Heath & Greenwood, 1968, 1970b; Heath, 1974b). These centrioles are similar in structure to those described in animal cells (Brinkley & Stubblefield, 1970), although are somewhat shorter. In the Saprolegniales they are always aligned end to end rather than at right-angles, which is a feature shared by relatively few other groups (see Heath, 1974b).

1.1.2 Zoosporangium Morphogenesis

1.1.2.1 Organelle changes and associations

In both Saprolegnia (Gay & Greenwood, 1966; Hagedorn & Weinert, 1972, 1974) and Phytophthora (Christen & Hohl, 1972) sporangium development is achieved by the migration of cytoplasm into expanding hyphal apices until they are delimited by the insertion of a basal septum. An apical papilla develops and the cytoplasm then differentiates into zoospores.

In Saprolegnia the early stages of sporangium development are accompanied by a massive increase in rough ER; the cisternae of which become aligned in elaborate parallel arrays around both the nuclei and mitochondria (Hagedorn & Weinert, 1972; Heath & Greenwood, 1971). Comparable increases in ER have not been described in Phytophthora sporangia (Christen & Hohl, 1972) although ER cisternae are reported around the nuclei (King, Colhoun & Butler, 1968; Williams & Webster, 1970).

In delimited sporangia the mitochondria are markedly shorter than in the vegetative hyphae, although are otherwise similar in their structure

(Gay & Greenwood, 1966; Hagedorn & Weinert, 1974). Many of the sporangial Golgi dictyosomes in Saprolegnia are associated with mitochondria, together with an intervening ER cistena (Heath & Greenwood, 1971b; Hagedorn & Weinert, 1974). This has also been reported in the Vaucherian algae (Greenwood, 1959; Ott & Brown, 1974a,b) and led Heath and Greenwood (1971) to suggest the association evolved to facilitate efficient energy transfer in these coenocytes.

Golgi dictyosomes increase in abundance during the early stages of sporogenesis in Saprolegnia and dividing Golgi have been shown associated with the nuclei of S.monoica (Hagedorn & Weinert, 1972, 1974). During this period the dictyosomes are still producing the vesicles involved in wall, septum and papilla development (Heath, Gay & Greenwood, 1970; Christen & Hohl, 1972). However once cleavage commences the dictyosomes become clustered around the pyriform nuclei and change their function. In Saprolegnia they become temporarily quiescent, before assuming a role in contractile vacuole development in the differentiated zoospores (Heath & Greenwood, 1971b), while Phytophthora dictyosome vesicles are involved in cleavage vacuole development (King & Butler, 1968; Elsner et al., 1970).

During sporangial differentiation a number of specialised organelles appear in the cytoplasm which often take part in later stages in development. One of the earliest of these specialised bodies to appear in Saprolegnia is the capsule-shaped bar (Gay & Greenwood, 1966). These have a polysaccharide rich matrix which surrounds a number of rather short electron-dense rods. In the differentiated zoospores these bars migrate to the cell periphery (Gay & Greenwood, 1966). On encystment they are immediately discharged, depositing the electron dense outer layer of the cyst wall in which the tufts of rods (spines) remain embedded (Heath & Greenwood, 1971).

The bar equivalents in Aphanomyces and Phytophthora both lack spines and therefore appear as amorphous spherical bodies. These have usually been overlooked in differentiating sporangia. However they are readily recognised in the zoospores by their peripheral distribution, and have been called peripheral or fibrous bodies (Hoch & Mitchell, 1972a, b; Hemmes & Hohl, 1971; Sing & Bartnicki-Garcia, 1975; Bimpong & Hickman, 1975). Recently it has been shown in Phytophthora that these bodies are composed of glucoprotein and have an adhesive function on discharge (Sing & Bartnicki-Garcia, 1975; Bimpong & Hickman, 1975).

Following septum insertion bundles of 15-20 nm diameter tubules contained in inflated ER cistemae appear in the sporangial cytoplasm (Heath, Greenwood & Griffiths, 1970; Williams & Webster, 1970). These tubules are the flimmer (mastigoneme) hairs which are liberated into the flagellar groove and assemble themselves around the tinsel flagellum (Heath, Greenwood & Griffiths, 1970).

In Pythium middletonii these flimmer tubules form in ER-cistemae lying adjacent to mitochondria, and are then passed through the dictyosome complex prior to discharge (Heintz, 1971). Recently bundles of flimmer tubules have been shown to occur in the vegetative hyphae of Lagenidium callinectes (Gotelli, 1975a).

Spherical microbody-like bodies have been described in both Phytophthora sporangia and cysts (Hemmes & Hohl, 1969, 1971; Williams & Webster, 1970; Elsner et al., 1970; Bimpong & Hickman, 1975). Recently catalase activity has been demonstrated histochemically with these bodies in Phytophthora palmivora, and they have been extracted from the cell by density gradient centrifugation (Phillipi, Pansh, & Hohl, 1975).

In Achlya sporangium formation is associated with a massive increase in lysosomal enzyme activity (O'Day & Horgen, 1974; Horgen & O'Day, 1975). This may correlate with the appearance of the membrane-bound multivesicular bodies noted in pre-cleavage sporangia of Saprolegnia monoica (Hagedorn & Weinert, 1972), since these bodies resemble the lysosmal autophagic vesicles described in other biological material (Ericsson, 1969).

1.1.2.2 Reserve Products

During sporangium(Hagedorn & Weinert, 1974; Christen & Hohl, 1972) and oogonium (Gay, Greenwood & Heath, 197); Howard & Moore, 1970; Vujičić, 1971; Hemmes & Bartnicki-Garcia, 1975) development in the Oomycetes there is a striking increase in both lipid and osmiophilic reserve granules. The droplets of neutral lipid are not membrane-bound, and in senescing sporangia of Phytophthora frequently coalesce into larger aggregates (King, Colhoun & Butler, 1968). The neutral lipid droplets are largely extracted in permanganate fixations, and the resulting product has been variously identified as vacuolar vesicles (Chapman & Vujičić, 1965) and glycogen 'polygonalen vesikles' (Hagedorn & Weinert, 1974). Glycogen has however been reported as a reserve product in Phytophthora sporangia (Hohl & Hamamoto, 1967; King, Colhoun & Butler, 1968) but has not been confirmed histochemically.

The second major reserve body in differentiating sporangia and oogonia are the electron dense (300-450 nm diameter) granules which are contained in membrane-bound vesicles. Because of their extreme osmiophilia Gay and Greenwood (1966) named these granules densebodies, although in other accounts they have been referred to as osmiophilic granules (King, Colhoun & Bulter, 1968), opaque granules (Hoch & Mitchell, 1972a, b), storage granules (Howard & Moore, 1970), and lipid granules or liposomes (Chapman & Vujičić, 1965; Elsner et al., 1970; Williams & Webster, 1970). During cytoplasmic cleavage and in the differentiated zoospores and oospores, the densebody granules become associated with a series of lamellar, myelin-like arrays. These have a periodicity of between 8-15 nm, depending on the material and fixative.

These arrays are best preserved in Ga-Os fixations and have been variously described as myelin-like (Gay, Greenwood & Heath, 1971; Hoch & Mitchell, 1972a, b), crystalline (Ho, Zacchariah & Hickman, 1968; King, Colhoun & Butler, 1968; Reichle, 1969; Howard & Moore, 1970), striate (Elsner et al., 1970; Williams & Webster, 1970), and finger-print like (Hemmes & Hohl, 1971, 1972; Colt & Endo, 1972; Sing & Bartnicki-Garcia, 1975; Bimpong & Hickman, 1975 ; Hemmes & Bartnicki-Garcia, 1975). In Saprolegnia the myelin-like arrays are normally confined to the granule margins (Howard & Moore, 1970; Gay, Greenwood & Heath, 1971), whereas in Phytophthora they usually develop throughout the expanded granule (Reichle, 1969; Elsner et al., 1970; Williams & Webster, 1970).

The osmiophilic nature of the densebodies and the appearance of mycelin-like bands, such as form in hydrated polar lipids, suggest these bodies are composed of phospholipid material (Gay & Greenwood, 1966; Williams & Webster, 1970; Gay, Greenwood & Heath, 1971; Hoch & Mitchell, 1972a). These granules are partially extracted by lipid solvents (Williams & Webster, 1970; Hoch & Mitchell, 1972a; Bimpong & Hickman, 1975) which probably accounts for their relatively poor preservation in permanganate (Heath, 1969; Hagedorn & Weinert, 1974). Further support for the phospholipid nature of these granules comes from Gay, Greenwood and Heath (1971) who demonstrated that the formation of densebody granules of S.ferax correlates with the appearance of acetyl choline in cell-free extracts.

It has been proposed that the myelin arrays result from the partial hydrolysis of the phospholipid granules to provide endogenous energy both for spore cleavage (Elsner et al., 1970; Williams & Webster, 1970) and zoospore motility (Gay, Greenwood & Heath, 1971; Bimpong & Hickman, 1975). The role of densebodies in cleavage and oospore maturation will be described later.

1.1.2.3 Septum and Papilla Development

In the Saprolegniales septum formation is extremely rapid and takes only a few minutes to complete (Gay & Greenwood, 1966; Griffin, 1966). Although Dick (1969) reports that septa are inserted centripetally, recently the lateral insertion of sporangial septa has been demonstrated in Achlya (O'Day & Horgen, 1974). So far septum formation in Saprolegnia has not been followed ultrastructurally, although their mature structure is well documented (Heath, Gay & Greenwood, 1971; Hagedorn & Weinert, 1974). Saprolegnia septa have a curious tripartite structure consisting of two layers of wall material enclosing a layer of vesicular material, and the occasional lipid droplet Heath, 1969). This is quite unlike the septal structure of any other fungal group, although is similar to that recently described in Vaucheria (Ott & Brown, 1974b). This is yet another example of the close structural similarity

between the Saprolegniaceae and Vaucheriaceae (discussed by Manton, 1965; Heath & Greenwood, 1971), and suggests a close phylogenetic affinity between the two groups.

The formation of the septal plug in Phytophthora sporangia has been described by Christen and Hohl (1972). In this group the sporangial stalk simply becomes centripetally occluded by peg-like ingrowths of the wall. This plug contains abundant pockets of entrapped vesicular material (lomasomes) and has been described as having a vesiculated or spongy appearance (Chapman & Vujičić, 1965; Hohl & Hamamoto, 1967; King, Colhoun & Butler, 1968; Elsner et al., 1970; Williams & Webster, 1970). The mature septal plug is between 2-3 μm thick and becomes overlaid by the thick inner sporangial wall. Similar vesiculated septal plugs have also been described in the oogonium stalks of Phytophthora, although these are not overlaid by a wall layer (Vujičić, 1971; Hemmes & Bartnicki-Garcia, 1975). However Hemmes and Bartnicki-Garcia (1975) have shown that the antheridial septum in Phytophthora palmivora is much thinner (< 0.5 μm) and appears to have a tripartite structure reminiscent of the Saprolegnian septa.

In Saprolegnia the apical papilla develops as a simple pimple-like outgrowth of the sporangium tip, which is preceded by an accumulation of wall vesicles at the apex (Heath, Gay & Greenwood, 1971). In contrast the papilla of Phytophthora sporangia is a plug of refractile wall-like material which is accreted centripetally between the tapered inner wall layers at the sporangium apex (Christen & Hohl, 1972). It remains capped by the thin outer sporangial wall layer and has a lamellate or fibrous substructure (Hohl & Hamamoto, 1967; King, Colhoun & Butler, 1968; Elsner et al., 1970; Williams & Webster, 1970). King, Colhoun and Butler (1968) have shown that the papillae of Phytophthora infestans are partially digested by both pectinase and protease enzymes.

1.1.2.4 Cytokinesis in the Oomycetes

The ultrastructural studies of spore differentiation in Oomycete fungi reveal that cytokinesis is effected in a number of different ways. These can be divided into three groups on the basis of cleavage apparatus generation.

Group A

Species in which cleavage is effected by the development or redistribution of large internal vacuolar vesicles. The vacuoles delimit the spore initials and cleavage is achieved by the fusion of the tonoplast and the plasmalemma. This mode of cleavage is characteristic of both zoospore (Gay & Greenwood, 1966; Hoch & Mitchell, 1972a; Hagedorn & Weinert, 1974) and oospore (Howard & Moore, 1970; Gay, Greenwood & Heath, 1971) differentiation in the Saprolegniales, and has been termed centripetal sporogenesis by Dick (1969). Flagellum development, if it occurs, does not take place until after

cleavage (Gay & Greenwood, 1966; Heath & Greenwood, 1971).

In Saprolegnia it was suggested that cleavage vacuoles are derived from the expansion and coalescence of the densebody vesicles (Gay & Greenwood, 1966; Gay, Greenwood & Heath, 1971). Densebody granules were not observed in the developing vacuoles and it was suggested that their conversion into a soluble osmotically-active derivative might motivate the vacuolar expansion (Gay, Greenwood & Heath, 1971). However densebody granules are discharged into the developing vacuoles of germinating cysts (Heath, Gay & Greenwood,1971; Hemmes & Hohl, 1971; Colt & Endo, 1972; Hoch & Mitchell, 1972b)although this is probably related to their breakdown (Bimpong & Hickman, 1975).

Heath and Greenwood (1971) proposed that the extensive microtubular roots which surround the peripheral nuclei during cleavage may stabilise the surrounding cytoplasm in such a way that the cleavage furrows form along lines of 'weakness' between them. Cytoplasmic microtubules have not however been seen aligned along the presumptive lines of cleavage.

In Aphanomyces euteiches the zoospores differentiate within unspecialised hyphae by the simple redistribution of existing vacuolar and cytoplasmic components. Cleavage is effected by only the partial coalescence of the plasmalemma and tonoplast, which results in the formation of a chain of uninucleate spores each connected by a fine cytoplasmic strand (Hoch & Mitchell, 1972a).

Group B

Species in which narrow cleavage vesicles align themselves along fairly well-defined presumptive lines of cleavage and coalesce. This type of a cleavage pattern occurs in Phytophthora sporangia (Hohl & Hamamoto, 1967; King, Colhoun & Butler, 1968; Elsner et al., 1970; Williams & Webster, 1970), and in the vesicle of La genidium callinectes (Gotelli, 1974b). In both these cases flagellum formation precedes cleavage. Cleavage therefore involves both the coalescence of cleavage and axonemal vesicles, although the extent of plasmalemmar incorporation appears variable. Indeed Hohl and Hamamoto (1967) suggest that the ephemeral vesicle in which the zoospores of Phytophthora parasitica are liberated is a double-membraned sac, derived from the plasmalemma and the fusion products of axonemal and cleavage vesicles. In Lagenidium most of the unincorporated membrane which remains after zoospore differentiation is also believed to be of plasmalemmar origin (Gotelli, 1974b).

The cleavage vesicles in this system appear to be derived both from the Golgi dictyosomes (King & Butler, 1968; Elsner et al., 1970) and from the redistribution of existing vacuolar vesicles (Williams & Webster, 1970; Gotelli, 1974b). However it is not known what determines the alignment of

these vesicles into well-defined cleavage furrows.

Group C

In this final group cytokinesis is achieved by the invagination of the plasmalemma. The spores are eventually delimited by the coalescence of the invaginated cleavage furrows either with each other, or with internal vacuoles. This type of cleavage pattern has been described in the sporangia of the marine Oomycete, Thraustochytrium (Kazama, 1975) and in the vesicle of Pythium middletonii (Heintz, 1971).

In the former the developing cleavage furrow is guided by cytoplasmic microtubules which align themselves along the plane of cleavage. The interaction of the cytoplasmic microtubules with the plasmalemma is believed to generate the motive force required for plasmalemmar invagination (Kazama, 1975). In Pythium however the extra plasmalemma required for cleavage furrow development is generated by the discharge of dictyosome cisternae and Golgi vesicles in the region of the flagellar pit (Heintz, 1971; Bracker personal communication).

In addition to these different modes of zoospore delimitation some Oomycete species, such as Pythium and Lagenidium, discharge their sporangial contents into a thin-walled vesicle prior to zoospore formation (Heintz, 1971; Gotelli, 1974b). However in Pythium zoospore differentiation takes place entirely within the vesicle, whereas in Lagenidium it is initiated before discharge and completed in the vesicle. In contrast Phytophthora species liberate their zoospores into a vesicle after cleavage is completed (Blackwell, 1943; Chapman & Vujičić, 1965; Williams & Webster, 1970).

To conclude this review on Oomycete cleavage systems some reference must be made to the differentiation of oospores in the unisporiate Peronosporalean oogonia. In these bodies the cytoplasm appears to differentiate into a central zone (the coenocentrum) containing the functional nuclei, and a peripheral layer (the periplasm) in which the supernumerary nuclei degenerate (Dick, 1969). Following fertilisation the coenocentrum develops into the functional oospore while the periplasm condenses to form an outer wall layer, the exospore (de Bary, 1887). Dick (1969) has termed this mode of differentiation centrifugal sporogenesis.

However it is still far from clear how this differentiation of the cytoplasm is achieved. The ultrastructural accounts on Peronosporalean oogonia to date have either not followed oospore differentiation (Marchant, 1968; Vujičić, 1971) or present conflicting accounts of development (Hemmes & Bartnicki-Garcia, 1975; McKeen, 1975). The light-microscopic accounts of oospore differentiation suggests a central vacuole forms during cleavage (Trow, 1901; Blackwell, 1943) in much the same way as described in

unisporiate Saprolegnia species (Dick, 1969). Hemmes and Bartnicki-Garcia (1975) suggested the periplasm may even be the contents of the antheridium which are injected into the oogonial compartment during fertilisation. However in his study on Pythium, McKeen (1975) still considers the periplasm to be a differentiated layer of the oogonial cytoplasm; although he does not describe how this is achieved.

1.1.2.5 Zoospores and Cysts

Saprolegnia is diplanetic, which means it produces two distinct zoospore types. The morphology and behaviour of these spores have been described by Crump and Branton (1966). The primary zoospores which are liberated from the sporangia are pyriform in shape and have apically-inserted flagella. After a period of encystment secondary zoospores are liberated, which are reniform in shape and have laterally inserted flagella. Many families of the Saprolegniaceae do not produce primary zoospores (e.g. Dictyuchus and Aphanomyces; Cotner, 1930) and liberate only secondary zoospores, as do the Peronosporales (Ho, Hickman & Telford, 1966).

The ultrastructural morphology of a number of zoospores has been described, including the primary zoospores of S.ferax (Heath, 1969; Heath & Greenwood, 1971), and the secondary zoospores of Aphanomyces euteiches (Hoch & Mitchell, 1972b) and a range of Phytophthora spp. (Ho, Zacchariah & Hickman, 1968; Reichle, 1969; Hemmes & Hohl, 1972b; Bimpong & Hickman, 1975). All show the same basic morphology, with a larger pyriform nucleus, linked by elongate kinetosome bodies to the flagellar bases. Dictyosomes are clustered around the nuclear apex, and produce the 'hairy' alveolar vesicles, which are involved in contractile vacuole formation (Heath & Greenwood, 1971).

On encystment the primary zoospores retract their flagella whereas the secondary zoospores shed their flagella (Crump & Branton, 1966), leaving transient knob-like scars (Hoch & Mitchell, 1972b). The primary cysts contain both remnants of the axonemal tubules and abundant flimmer vesicles (Heath, 1969). Otherwise the primary and secondary Oomycete cysts are similar in their overall structure (Heath, 1969; Grove, 1970; Hemmes & Hohl, 1971a; Hoch & Mitchell, 1972b; Bimpong & Hickman, 1975). Following the almost immediate discharge of bar bodies or their equivalents on encystment an inner wall layer is deposited by the Golgi-derived wall vesicles. Prior to cyst germination, a localized accumulation of peripheral wall vesicles develops and the nuclei divide (Grove, 1970; Heath, Gay & Greenwood, 1970; Hemmes & Hohl, 1971a; Hoch & Mitchell, 1972b).

1.1.3 Gametangium Morphogenesis

1.1.3.1 Hormonal Control of Sexual Reproduction

Before describing some of the ultrastructural aspects of sexual reproduction it should be noted that sexual differentiation in the

Saprolegniales is initiated and co-ordinated by a series of diffusible hormones. This was elucidated by the classic studies of Raper on heterothallic Achlya spp. which have been extensively reviewed (e.g. Raper, 1952; Machlis, 1966, 1972; Barksdale, 1969). The hormonal control pattern for homothallic species is believed to be similar to that described for the heterothallic species (Raper, 1952). Briefly the hormonal control of sexual differentiation in the Saprolegniaceae is as follows. (The hormonal notation of Raper will be used);

(1) Sexual reproduction is initiated by the female thallus which secretes hormone A, which induces the formation of antheridial hyphae on the male thallus. There are at least four hormonal components involved in this initiation step, which act in concert to regulate the intensity of the sexual response (Raper, 1950).

(2) The male thallus then secretes hormone B which initiates oogonium development on the female thallus.

(3) The developing oogonial initials secrete hormone C which directs the growth of the antheridial hyphae towards them and governs antheridium delimitation once contact has been made. Barksdale (1963) recently demonstrated that the effects of hormone C can be mimicked by hormone A adsorbed onto polystrene beads, and proposed they were the same hormone. Machlis (1972) has however questioned the purity of her hormonal extracts.

(4) The delimited antheridia finally secrete hormone D which governs oogonium delimitation and oospore differentiation.

During the past decade Barksdale and her associates have succeeded in isolating hormone A and chemically characterising it (reviewed by Barksdale, 1969), and it has been named antheridiol. Similar attempts with the other hormones involved in this system have so far proved unsuccessful (Machlis, 1972).

1.1.3.2 Gametangial Organelle Changes

Cytoplasmic differentiation in the oogonia and antheridia of Saprolegnia (Howard & Moore, 1970; Gay, Greenwood & Heath, 1971) and Peronosporalean Oomycetes (Vujičić, 1971; Hemmes & Bartnicki-Garcia, 1975; McKeen, 1975) follows a similar pattern to that described in their sporangia. The mitochondria in the oogonia of Saprolegnia terrestris were frequently cup-shaped and closely associated with droplets of lipid or densebody vesicles (Howard & Moore, 1970). Such mitochondrion-lipid associations are frequently linked with starvation conditions (see Howard & Moore, 1970).

In Saprolegnia the antheridia are less densely packed with cytoplasmic organelles than the oogonia (Howard & Moore, 1970; Ellzey, 1974). This is less apparent in the Peronosporalean antheridia (Hemmes & Bartnicki-Garcia,

1975; McKeen, 1975). In both groups wall vesicles accumulate in the peripheral cytoplasm where the oogonium and antheridium make contact (Heath, Gay & Greenwood, 1970; Hemmes & Bartnicki-Garcia, 1975).

1.1.3.3 Gametangial Nuclear Division

Gametangium development in the Oomycetes is accompanied by the synchronous division of the nuclei (Dick, 1972; Dick & Win-Tin, 1973). The controversy over the nature of these divisions is a long and fascinating one and has recently been given a detailed historical review by Dick and Win-Tin (1973). The main debate has centered around the position of meiosis in the life cycle; did it occur during oospore germination, as expected in fungi with haploid thalli, or did it occur during gametogenesis, indicating the vegetative thallus of Oomycetes is diploid.

In spite of some early accounts suggesting gametangial meiosis (e.g. Trow, 1904) it became generally accepted that Oomycetes, in common with other fungi, underwent zygotic meiosis. Most of the evidence in favour of zygotic meiosis was based on the failure to observe two consecutive gametangial nuclear divisions (Dick & Win-Tin, 1973), although there were a few accounts of meiotic nuclei in germinating oospores (Claussen, 1908; Zeigler, 1953).

The debate was reopened by Sansome (1961, 1963) who, using squash preparations, described meiotic configurations in the gametangia of a number of Oomycetes. Her observations have since been confirmed in similar cytological studies by a number of other workers (e.g. Barksdale, 1968; Bryant & Howard, 1969; Flanagan, 1970; Howard & Bryant, 1970; Win-Tin & Dick, 1975; Brasier & Sansome, 1975). These cytological accounts of gametangial meiosis have been substantiated by recent genetic studies (Mullins & Raper, 1965; Barksdale, 1966; Shaw & Khaki, 1971; Elliott & McIntyre, 1973; Lasure & Griffin, 1974), and the microspectrophotometric analysis of nuclear DNA content (Bryant & Howard, 1969; Howard & Bryant, 1971). Nevertheless there is one important school, based at Riverside, California, ~~who~~ which still favours zygotic meiosis, at least in the genus Phytophthora, on the basis of both their genetic (Timmer et al., 1970) and cytological studies (Stephenson, Erwin & Leary, 1974).

The only complete ultrastructural account of gametangial meiosis is that of Howard and Moore (1970) for Saprolegnia terrestris, although prophase I stages have also been described for Achlya ambisexualis (Ellzey, 1974) and Thraustotheca clavata (Heath, 1974a). In S.terrestris there appear to be two successive nuclear divisions, which occur within the same nuclear envelope. However the retention of the nuclear envelope after prophase I has been questioned both by Flanagan (1970) and Win-Tin and Dick (1975), in their light-microscopic studies. Howard and Moore (1970) suggest the following features are indicative of gametangial meiosis.

1. The occurrence of two successive intranuuclear divisions resulting in the characteristic four-lobed cruciate nuclear profiles at the late second divisional stage.
2. The relative sizes of the interphase, prophase I, and gametic nuclei (2:4:1) are consistent with a meiotic division.
3. The appearance of condensed uniaxial elements in the large prophase I nuclei and their apparent homology to the lateral elements of meiotic synaptinemal complexes.
4. The different centriolar behaviour to that associated with mitotic divisions.

All these features except 1, were also shown in A.ambisexualis (Ellzey, 1974) and in T.clavata (Heath, 1974a) suggesting this is the standard pattern of division throughout the Saprolegniales. However there is ample evidence from light-microscopic studies that there is a good deal of variation in gametangial nuclear behaviour, and several abnormal divisional patterns have been described (Dick, 1972; Dick & Win-Tin, 1973; Win-Tin & Dick, 1975). Recently polyploidy has been demonstrated in both Achlya and Pythium, and multiple chromosome associations have been described in the prophase I nuclei of a number of species, including S.furcata (Win-Tin & Dick, 1975).

1.1.3.4 Fertilisation and Oospore Maturation

The occurrence of true fertilisation in the Saprolegniaceae was also much debated amongst the late-nineteenth century mycologists, following the initial disagreement of de Bary and Pringsheim (reviewed by Dick, 1972; Dick & Win-Tin, 1973). In spite of Trow's (1905) unequivocal demonstration of oospore fertilisation by antheridial nuclei in Achlya polyandra, the functional importance of the fertilisation tube in all antheridiate species is still questioned (Dick, 1969, 1972; Flanagan, 1970). Although the fertilisation of oospores in Saprolegnia has not been directly observed in ultrastructural studies both Howard and Moore (1970) and Gay (published in Beckett, Heath & McLaughlin, 1974) have shown a curious thickening of the oospore wall in the region of fertilisation tube contact.

Ultrastructural studies of the Peronosporales show the penetration of the antheridial fertilisation tube into the oogonium compartment occurs before oospore differentiation (Hemmes & Bartnicki-Garcia, 1975; McKeen, 1975). After the discharge of the antheridia cytoplasm into the oogonial compartment, the fertilisation tube collapses against the oogonial wall (Hemmes & Bartnicki-Garcia, 1975).

Karyogamy does not normally accompany plasmogamy. In most species however it is achieved before the final maturation of the oospore, although in some it may be delayed until germination (Dick & Win-Tin, 1973). Following fertilisation (where it occurs) the oospores acquire a thick wall and

undergo considerable reorganisation of their internal cytoplasm (Dick, 1969).

The thick inner oospore wall is called the endospore (de Bary, 1887) and is apparently a storage layer containing both cellulosic and proteinaceous components (de Bary, 1887; Trow, 1895; Blackwell, 1943; Dick, 1969). Recently the combined oogonial and oospore walls of Phytophthora var. sojae have been extracted and analysed (Lipmann, Erwin & Bartnicki-Garcia, 1974). The major carbohydrate component of the oospore wall is a β-1,3 glucan, which accounts for about 70% of the wall, with cellulose contributing a further 7%. The oospore wall also contains appreciable amounts of protein (12.5%) and lipid (10%), and an exceptionally high level of phosphorous (0.55%).

Ultrastructurally the endospore wall appears very electron transparent and has little apparent substructure (Howard & Moore, 1970; Hemmes & Bartnicki-Garcia, 1975; McKeen, 1975). Endospore accretion occurs independently of the usual wall secreting vesicles (Hemmes & Bartnicki-Garcia, 1975). McKeen (1975) suggests the periplasm contributes material to the developing endospore in Pythium.

Following oospore differentiation in Saprolegnia the spores immediately secrete a thin wall around themselves (Howard & Moore, 1970; Gay, Greenwood & Heath, 1971). De Bary (1887) calls this wall layer the epispore, and it appears similar in structure to other Saprolegnian cell walls (Heath, Gay & Greenwood, 1970). On the other hand the Peronosporales do not appear to secrete such a wall but instead they acquire a thin osmiophilic outer layer derived from the condensation of the surrounding periplasm (Hemmes & Bartnicki-Garcia, 1975; McKeen, 1975). Once the endospore layer forms the oospores become virtually impermeable to fixatives which has proved a great hindrance to both critical light-microscopic (Trow, 1895) and ultrastructural studies (Marchant, 1968; Vujičić, 1971).

The internal cytology of mature oospores is well documented, if poorly understood, since it is of considerable taxonomic importance (Coker, 1923; Dick, 1969; Howard, 1971). Most mature oospores acquire a large, more or less centrally located compartment, which in the Peronosporales appears uniformly refractile and in most Saprolegniales contains small granules in Brownian motion (Dick, 1969). Howard and Moore (1970) demonstrated in Saprolegnia terrestris that this body was derived from the expansion and coalescence of the oospore densebody vesicles. This has also been confirmed in the Peronosporalean oospores (Hemmes & Bartnicki-Garcia, 1975; McKeen, 1975). This membrane-bound vacuole has been called the ooplast (Howard & Moore, 1970), and oospores are classified according to its spatial relationship with the lipid droplets in the surrounding cytoplasm (Howard, 1971).

Where the lipid reserves occur as small droplets, spores with a centrally located ooplast are called centric, and spores with an eccentrically placed ooplast are called sub-centric. Where the lipid droplets coalesce into larger aggregates, the spores are called eccentric or sub-eccentric depending upon whether the lipid occurs as a single or as several large droplets.

The peripheral oospore cytoplasm usually contains one or two large optically transparent bodies, which de Bary named pellucid spots and correctly interpreted as the oospore nuclei (Dick, 1969). Ultrastructural studies have also revealed mitochondria scattered throughout the peripheral oospore cytoplasm, but have not shown ribosomes and ER (Howard & Moore, 1970; Hemmes & Bartnicki-Garcia, 1975; McKeen, 1975).

Following their maturation oospores require a period of dormancy before germination can occur. Dormancy may last for only a few days as in Achlya americana (Trow, 1899), although more usually extends for several months (Zeigler, 1953; Mullins & Raper, 1965). Germination is initiated by the swelling of the oospores, during which the endospore layer is eroded away and the ooplast dispersed (Blackwell, 1943; Zeigler, 1953; Flanagan, 1970). Most oospores then produce a short germtube, which is usually terminated by a zoosporangium (Zeigler, 1953, Flanagan, 1970). However in some species the oospore cytoplasm may differentiate directly into zoospores as in Achlya americana (Trow, 1899). There have been no ultrastructural accounts of oospore germination in Oomycetes.

1.2 OBSERVATIONS

1.2.1 Vegetative Development

1.2.1.1. Hyphal Morphology and Ultrastructure

The overall morphology and ultrastructural cytology of the vegetative hyphae of Saprolegnia furcata (Figs. 1.4-1.21) proved similar to that previously described for S.ferax (Heath, 1969). Vegetative hyphae from colonies grown in a weak nutrient medium such as 1/2 GYPS are fairly narrow (10-15 µm) and contain sparse lipid reserves compared with hyphae grown from infested hemp seed or insect inocula (e.g. S.monoica,Hagedorn and Weinert, 1970) The first lateral branches are produced between 200 and 300 µm behind the characteristically tapered transparent apices (Fig. 1.4). Nomarski phase optics however reveal the presence of filamentous mitochondria, spherical lipid droplets and nuclei (Fig. 1.5) streaming into and out of the hyphal tip. Ultrastructural profiles of this region show the typical fungal apical organisation (Fig. 1.5). There is a terminal zone of apical vesicles which intergrades into a short mitochondrial zone, before the first nuclei and large vacuolar vesicles appear 20-30 µm behind the tip (Fig. 1.6). Further from the apex vacuolar vesicles become increasingly abundant as shown in Figs. 1.7, 1.10. Similar zonation is shown in the young lateral branch in Fig. 1.8, although the zones are much compressed, with the first nucleus occurring only 5 µm behind the tip.

The apical vesicle zone is composed of at least two types of vesicles (Fig. 1.6). The smaller and more abundant vesicles have a spherical or tubular profile (60-80 nm) and contain electron dense fibillar contents (Figs. 1.6, 1.9), whereas the larger (150-200 nm) vesicles are always spherical and almost contentless (Fig. 1.6).

In the older regions of the hypha the vacuolar vesicles become aligned along the hyphal axis (Fig. 1.7) and coalesce and expand until the hyphal cavity is almost completely vacuolate (Figs. 1.14, 1.15). In these regions the mitochondria, nuclei, and lipid droplets are confined to the peripheral band of cytoplasm (Figs. 1.14, 1.15), which in some regions is reduced to only 200-500 nm in diameter (Fig. 1.16). The vacuoles themselves contain small osmiophilic granules, and are partitioned by fine strands of cytoplasm (Fig. 1.14, 1.15).

There is a high density of ribosomes throughout the hyphal cytoplasm (Figs. 1.9, 1.11, 1.12, 1.16 and 1.18). Ribosomes are frequently seen attached to cisternae of 'rough' ER which are aligned around nuclei, mitochondria and vacuolar vesicles (Fig. 1.10). Golgi dictysomes are abundant in the subapical hyphal zone (Fig. 1.10) where they are usually associated with either mitochondria (Fig. 1.13) or nuclei (Figs. 1.21, 1.22). In vegetative hyphae the dictyosome membranes are very osmiophilic and occur

in compact stacks of 4 to 5 cisternae (Fig. 1.12, 1.13, 1.22). The hyphal dictyosomes produce small electron dense vesicles from their cisternal margins (Fig. 1.12).

Mitochondria are particularly abundant in the apical region of the hyphae (Fig. 1.6). In vegetative hyphae the mitochondria are often very elongate, and profiles of up to 6 µm are not uncommon (Fig. 2.228). The mitochondrial matrix is of similar density to that of the surrounding cytoplasm, and contains ribosome particles that are clearly smaller than their cytoplasmic counterparts (Figs. 1.13, 1.18). The inner mitochondrial membrane is folded into abundant peripheral cristae, which are roughly spherical and between 80-100 nm in diameter (Figs. 1.13, 1.17, 1.18).

The vegetative hyphae of S.furcata lack the osmiophilic densebody granules which are so common in the reproductive stages. They do however contain large numbers of small (250-400 nm) electron-dense myelin-like membraneous whorls (Fig. 1.11) which are distributed throughout the cytoplasm. The origin and function of these bodies is not known, although similar structures have been widely reported in fungal cytoplasm (Marchant, Peat and Banbury, 1969; Marchant and Robards, 1967; Bimpong and Hickman, 1975).

The hyphal wall is very thin (85-95 nm) and almost completely electron-transparent (Figs. 1.9, 1.11). Apart from at the hyphal apex, wall vesicles are very sparsely distributed in the peripheral cytoplasm (Figs. 1.10, 1.16). Lomasomes and plasmalemmasomes are scarce in vegetative hyphae grown under normal conditions.

1.2.1.2. Nuclear Cytology

The interphase nuclei in the apical hyphal zone, up to 100 µm behind the tip, are usually ovoid and approximately 3.0 µm x 2.0 µm in size (Figs. 1.6, 1.8, 1.10, 1.17). However, in the distal vacuolate regions the nuclei become drawn out into elongate spindle-shaped bodies, which can be up to 6.0 µm in length (Fig. 1.21). The nucleoplasm appears uniformly particulate in GaOs-fixed material, and contains a more electron dense nucleolar region (Figs. 1.8, 1.10, 1.17, 1.19, 1.21). The nuclear envelope is perforated by pores (60-80 nm diameter) which when viewed in tangential section have electron-dense particulate rims (Fig. 1.18).

Each interphase nucleus is associated with a pair of microtubular centrioles which are orientated in the end to end (180°) Oomycete fashion (Fig. 1.22). Each centriole is approximately 200 nm in length, and of similar diameter. The microtubules are of slightly different lengths which give the centrioles their typical wedge-shaped proximal profile in L.S. (Fig. 1.22). In T.S. each centriole is composed of a tubular array of 9 blades, made up of three fused microtubules (Figs. 1.18, 1.96). Each triplet blade is

connected to a central hub by an electron-dense spoke, forming the characteristic cartwheel arrangement clearly shown in Fig. 1.96. Each pair of centrioles lies in a shallow pocket in the nuclear envelope (Figs. 1.18, 1.21).

Profiles of dividing nuclei were scarce in these hyphae. This may indicate the hyphae were fixed outside the period of synchronous nuclear division which occurs in Saprolegnia (Smith, 1923a). A number of nuclei did, however, contain intranuclear spindle-microtubules characteristic of mitotically-dividing nuclei(Fig. 1.20). However, the non-median profiles made it impossible to determine the precise divisional stage (Fig. 1.20) However, the elongate dumbell-shaped nucleus in Fig. 1.19 is almost certainly a late telophase stage since the nucleolus has clearly divided and the remnants of the spindle are still associated with the centriolar pocket (Fig. 1.22).

1.2.2. Asexual Reproduction

1.2.2.1 Zoosporangium formation on induced-colonies of Saprolegnia

Vegetative colonies (16-20 h) of Saprolegnia ferax were induced to sporulate using the procedure described in Section 0.2.4.1. The rate of sporangium formation depended both on colony size and the efficiency with which the nutrient medium was removed. Sporangial production on typical 18 h-colonies is summarised in Fig. 1.1, which also shows the high degree of synchrony in zoospore differentiation.

The morphological development of sporangia in S.ferax is summarised in Figs. 1.23-1.35 and described in the accompanying plate legends. Relatively few undifferentiated gemma bodies (Figs.2.70, 2.73) are produced on these colonies compared with hempseed grown colonies, although gemmae still account for most of the 'uncleaved sporangia' scored 20 h after induction in Fig. 1.1. The sporulation process is extremely efficient in this species and by the end of the 20-30 h sporulation period nearly all the original hyphal cytoplasm is converted either into zoospores or gemmae.

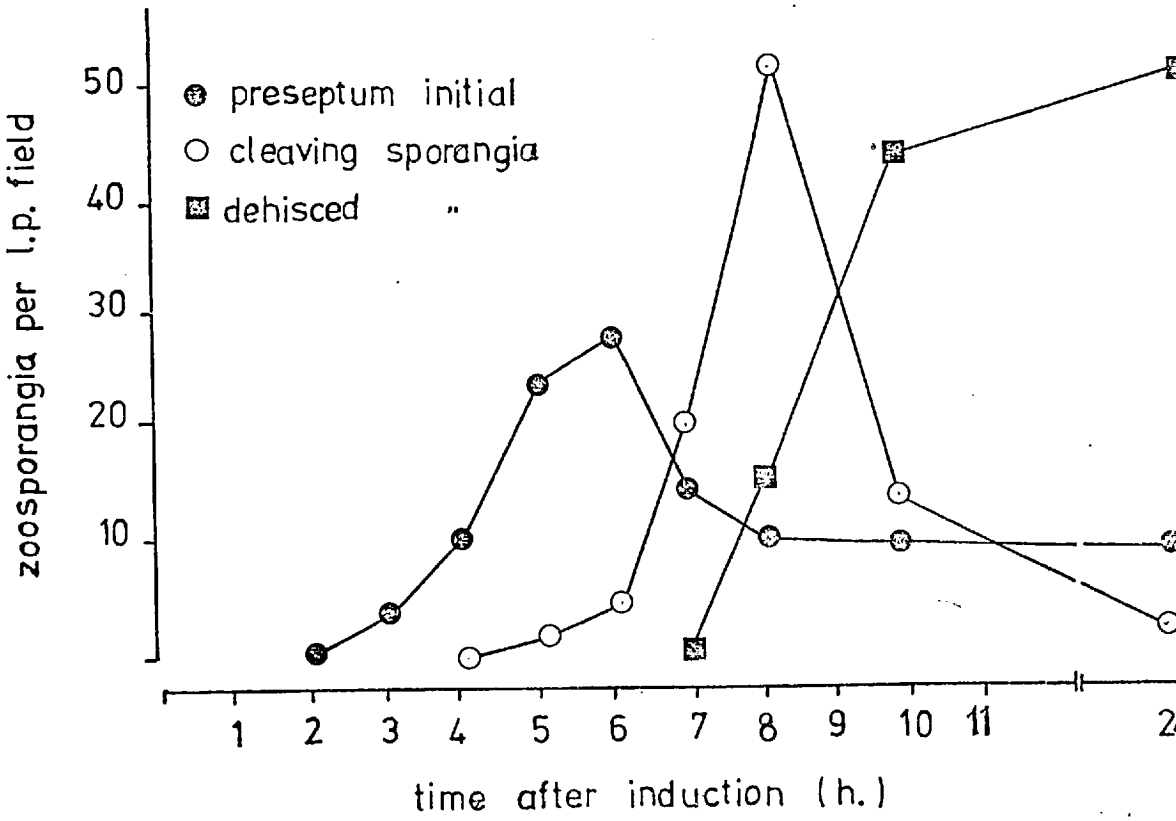
Whereas in S.ferax zoosporangia develop at hyphal apices throughout the colony, in S.furcata their production is confined to the marginal hyphae. Sporangium development in S.furcata follows a similar pattern to that described for S.ferax in Figs. 1.27-1.37, although proliferation does not occur in this species.

1.2.2.2. Ultrastructural aspects of Sporangium development

Cleavage vacuole formation

The L.S. profile of a newly delimited S.ferax sporangium in Fig. 1.36 shows the almost complete absence of aggregated vacuolar vesicles at this stage. However, following apical papilla development, an axial vacuole quickly forms in the sporangia (Figs. 1.26, 1.27). This is apparently achieved by the expansion and coalescence of vacuolar vesicles along the sporangium

Fig. 1.1. Sporangium development on 18 h - induced colonies of Saprolegnia ferax.



axis as shown in Fig. 1.44. Gay and Greenwood (1966) suggest the patches of fibrillar material clearly seen in some of these vacuoles (Fig. 1.44) may represent the remnants of expanded densebody granules (Fig. 1.39).

The fully-expanded vacuole occupies between 40-45% of the sporangium volume (Fig. 1.47) although remains divided into compartments by fine strands of cytoplasm. Cleavage furrows develop in the peripheral cytoplasm between the nuclei at this stage (Fig. 1.47). These will eventually coalesce with the main vacuole to delimit the uninucleate zoospore initials (Gay and Greenwood, 1966; Hagedorn and Weinert, 1974) which are so clearly visible in the light microscope (Fig. 1.28). Zoospore differentiation is achieved by the fusion of the tonoplast and plasmalemma around the initials.

1.2.2.3. Organelle Changes and Associations

Prior to septum insertion organelles such as mitochondria and ER cisternae are orientated parallel to the long axis of the sporangium as cytoplasm streams into the expanding initials (Fig. 1.37). After septum formation this orientation is lost (Figs. 1.36, 1.42) and the previously elongate mitochondria (Fig.s 1.37, 1.38) break up into shorter profiles (Fig. 1.42, 1.49).

ER occurs abundantly in precleavage sporangia such as shown in Fig. 1.36, in which parallel arrays of 2-6 cisternae align themselves around the nuclei and mitochondria (Fig. 1.49). Connections between the nuclear envelope and ER cisternae are also frequently seen at this stage (Fig. 1.49). During cleavage vacuole formation however, there seems to be a reduction in cytoplasmic ER and the nuclear connections are lost (Fig. 1.44, 1.47, 1.48).

Golgi-dictyosomes are also most abundant during the pre-cleavage stages, during which dictyosome-derived vesicles are involved in the formation of the expanding sporangial wall and in septum and papilla development (Fig. 1.206, 1.42). Most dictyosomes at this stage show the characteristic ER-mitochondrian associated (Fig. 1.52). This is clearly illustrated in the profile of the sporangium apex shown in Fig. 1.42 in which there are no less than 14 dictyosomes; 11 of which are associated with mitochondria and only 3 with nuclei. It is noticeable that sporangial dictyosomes have much more conspicuously inflated cisternal peripheries than their hyphal counterparts (cf. Fig. 1.52 and Fig. 1.12). Face views of Os-fixed Golgi also reveal the abundant electron-dense vesicles associated with the dictyosomes in precleavage sporangia (Figs. 1.39, 1.40).

During cleavage-vacuole development cytoplasmic dictyosomes are reduced in number (Hagedorn and Weinert, 1974), leaving the remaining dictyosomes clustered around the apex of pyriform nuclei. Perhaps the close association of the dictyosome in Fig. 1.48 with both the nucleus and a mitochondrion represents an intermediate stage in the transfer of

dictyosome allegiance from mitochondria to nuclei as reported in Vaucheria (Ott & Brown, 1974b).

Small numbers of wall vesicles are present in the peripheral sporangial cytoplasm throughout development (Figs. 1.44, 1.47, 1.52). The frequent pocket-like invaginations of the plasmalemma are suggestive of vesicle fusion (Fig. 1.43). However, accumulations of the dense Golgi-vesicles or larger wall vesicles occur both in the basal stalk prior to septum insertion (Fig. 1.206) and in the sporangial apex prior to papilla formation (Fig. 1.42). Both of these regions appear refractile under the light-microscope (Figs. 1.200, 1.41).

The sporangial wall remains electron-transparent throughout development and is usually barely discernable (Figs. 1.43, 1.44, 1.47). Nevertheless wall thickness increases from c.80 nm in early preseptal sporangia (Fig. 1.43) to between 150-200 nm at the time of cleavage. As in the hyphae plasmalemmasomes and lomosomes are rare in normal sporangia.

Sporangial cytoplasm contains both droplets of neutral lipid and osmiophilic densebody granules, which each account for 4-5% of the total cytoplasmic volume fraction in mature sporangia (Fig. 1.47). The irregular profiles of the lipid droplets are typical of Os-fixed material (Figs. 1.37, 1.39). However, $KMnO_4$ extracts most of the neutral lipid, and the resulting product is usually difficult to distinguish from the vacuolar vesicles (Fig. 1.52). Densebody granules are present in the sporangial cytoplasm throughout development even though they do not occur in the vegetative hyphae. In pre-septal sporangia they are quite small (c. 200-250 nm) and contained in a membrane-bound vesicle together with small osmophilic particles (Fig. 1.39). During sporangium development the granules increase in diameter (< 350 nm) and become more osmiophilic (Fig. 1.44). However, the myelin-like arrays which frequently become associated with the densebody granules (Gay and Greenwood, 1966) were not observed in this material.

Bars are present even in pre-septal sporangia (Fig. 1.38). In Os-fixed material bars are regular capsule-shaped bodies (150 nm x 350 nm) composed of a peripheral matrix of amorphous material surrounding a series of electron dense rods (Fig. 1.55). In pre-septal sporangia the amorphous bar matrix is both less extensive and less electron dense than in post-septal bodies suggesting it is accreted during sporangium maturation (cf. Figs. 1.38, 1.55 with 1.40, 2.173). $KMnO_4$-fixed bars were often less regular in profile and contained coiled rods (Figs. 1.53, 1.54).

Flimmer vesicles (Heath, Greenwood and Griffiths, 1970), which appear in delimited sporangia, were not particularly well preserved in Os-fixed sporangia and were not observed at all in $KMnO_4$-fixed sporangia. A typical Os-fixed flimmer vesicle with poorly-preserved tubules is shown in Fig. 1.40.

This flimmer vesicle appears to be associated in the peripheral vesicles of a dictyosome, a feature also noted in Pythium (Heintz, 1971).

1.2.2.4. Nuclear Cytology

Pre-cleavage sporangia contain typical ovate interphase nuclei similar to those described in the vegetative hyphae (Fig. 1.45). $KMnO_4$-fixed nuclei have poorly-preserved nucleoplasm and a rather irregular undulating nuclear envelope (Fig. 1.49). The delimited sporangium shown in Fig. 1.36 contained many nuclei which were clearly in various stages of autolysis (Figs. 1.42, 1.46). The two irregular nuclear profiles shown in Fig. 1.46, are being isolated from the surrounding cytoplasm by the electron-dense cisternae and small vesicles which surround them. A poorly preserved centriolar profile is contained in a deep pocket formed by the invagination of the nuclear envelope (Fig. 1.46). Following nuclear isolation the nuclear envelope begins to disintegrate as shown in two of the nuclei in Fig. 1.42. The nucleus probably then breaks up to form a series of autophagic multivesicular bodies such as shown in Figs. 1.50 and 1.51, since similar bodies have been shown to be the end product of organelle autolysis in vegetative hyphae (Heath, 1975a).

During cleavage-vacuole development the remaining nuclei become peripherally distributed, and acquire a pyriform shape (Figs. 1.47, 1.48). The lateral centrioles (Fig. 1.45) migrate to the nuclear apex and become converted into kinetosomes prior to flagellum development (Fig. 1.48).

1.2.2.5 Zoospores and Encysted Spores: Behaviour and Morphology

The rapid discharge from the sporangium is shown in Fig. 1.31. The possible mechanisms for this have been discussed by Gay and Greenwood (1966). The primary zoospores are ovoid to pyriform, with their flagella arising from the pointed apex (Fig. 1.31). They swim weakly in a rather erratic fashion for between 10-20 minutes before settling, withdrawing their flagella and encysting. Under normal conditions the primary cysts germinate within 10 h to produce the faster-swimming secondary zoospores. However, in isolated suspensions primary cysts frequently germinate directly by producing a germtube.

The secondary zoospores are reniform and their flagella arise from a lateral groove (Fig. 1.33). The spores are the main swarming phase and swim actively for periods of up to 10 h before encysting. Unlike the primary zoospores, the secondary zoospores shed their flagella on encystment and always germinate directly by producing a germtube (Fig. 1.34). Frequently the secondary zoospores encyst in large clumps, often around a dehisced sporangium (Fig. 1.34). It is possible that spent sporangia may attract the spores by chemotaxis.

1.2.2.6. Cyst Ultrastructure

Zoospore ultrastructure was not examined in this study. However, profiles of primary cysts shortly after encystment and after 8 h incubation are shown in Figs. 1.56-1.57 and in Figs. 1.60-1.64 respectively. Each cyst is approximately 10 μm in diameter and contains only a single nucleus (Figs. 1.56, 1.60). Prior to germination the cyst nucleus reverts to the normal ovoid interphase morphology (Fig. 1.59). Cyst germination is accompanied by nuclear division.

The cyst mitochondria are peripherally distributed (Figs. 1.56, 1.57, 1.60) and are shorter and have much more elongate tubular cristae than mitochondria in either the hyphae (Fig. 1.17) or sporangia (Figs. 1.37, 1.38). However, during germination the mitochondria once more become elongate and the cristae shorten (Figs. 1.62, 1.63) as they revert to their vegetative morphology.

Young cysts also contain very active Golgi dictyosomes which always lie close to the nucleus (Figs. 1.56, 1.57). However, in older cysts (Fig. 1.60, 1.61) the dictyosomes are more widely dispersed and appear less active. Wall vesicles occur in the peripheral cyst cytoplasm (Fig. 1.58) and are involved in the deposition of the electron-transparent inner cyst wall and in germtube development. The bar bodies are discharged on encystment and deposit the thin outer electron dense wall layer, in which the short rods (or spines) remain embedded (Fig. 1.57). Lomasomes are not uncommon in the primary cyst walls (Figs. 1.62, 1.63) and plasmalemmosomes usually occur at the germtube apex (Fig. 1.64).

Flimmer vesicles are abundant in ungerminated cysts and tubule pockets of up to 1.0 μm in length are not infrequent (Fig. 1.59, 1.61). However, once indirect (Fig. 1.62) or direct (Fig. 1.64) germination is underway flimmer vesicles are no longer visible. Newly-encysted spores also contain small vacuolar vesicles, droplets of neutral lipid and densebody vesicles (Fig. 1.56).

All the cysts shown in Figs. 1.56 - 1.64 were incubated in the absence of exogenous nutrients, and were therefore dependent on their endogenous energy reserves for both indirect and direct germination. Some of the cysts germinated indirectly by liberating their protoplast as a secondary zoospore; an early stage of which is shown in Fig. 1.62. Other cysts germinated directly by producing short, rather twisted germtube (Fig. 1.64). Direct germination is always accompanied by the partial or complete vacuolation of the cytoplasm (Figs. 1.61, 1.63). In cysts with germtubes, the organelle-containing cytoplasm is confined to a narrow peripheral band (Fig. 1.64). The germtubes develop by the deposition and extension of the inner wall layer. The developing germtubes rupture the outer osmophilic layer as they grow out (Fig. 1.64).

Fig. 1.2. Sporangium and oogonium development on 18 h-induced colonies of Saprolegnia furcata.

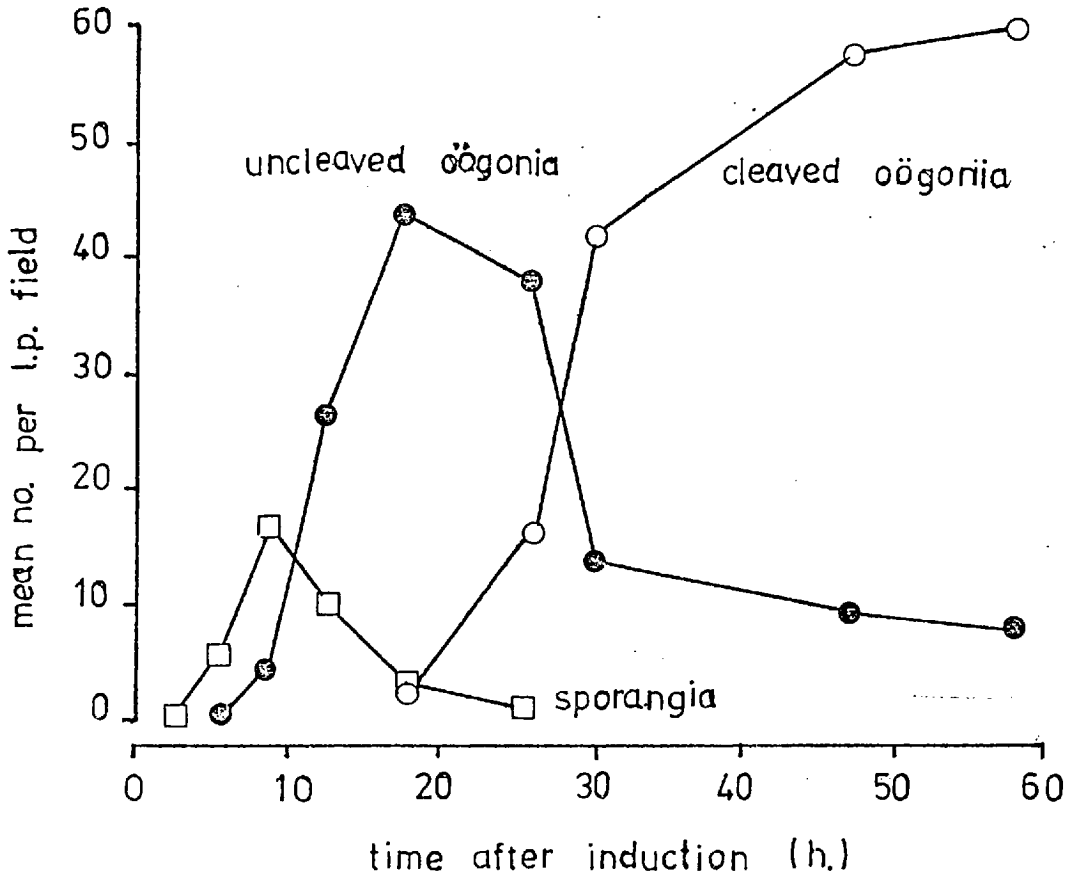
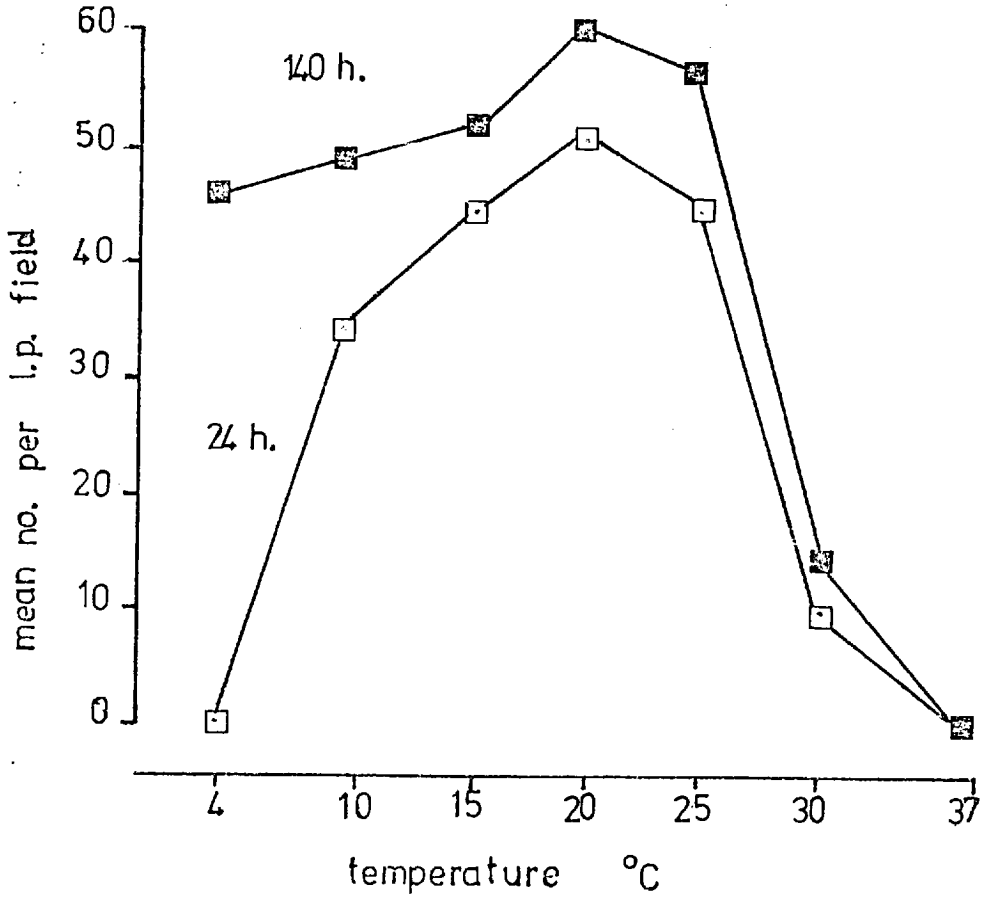


Fig. 1.3. The effect of temperature on oogonium development in Saprolegnia furcata assessed 24 h and 140 h after induction.



As the vacuoles develop the osmiophilic densebody granules expand and acquire electron-transparent cores (Fig. 1.65, 1.66, 1.67). This continues until the densebodies are reduced to narrow osmiophilic rings, up to 1.5 μm in diameter (Fig. 1.67). This presumably is related to the mobilisation of these phospholipid reserves to provide energy for germination. This behaviour contrasts with spores germinated in a nutrient solution, in which the densebody granules are simply deposited in the expanding vacuole (Gay, Heath & Greenwood, 1971). It should also be noted that in the absence of an exogenous energy supply, the vacuolar vesicles are only partially coalesced, so that the mature cyst vacuoles remain divided by a fine network of cytoplasmic strands (Figs. 1.63, 1.64).

1.2.3 Sexual Reprodution: Gametangium development

1.2.3.1 Gametangium formation on induced colonies of Saprolegnia furcata

Vegetative colonies (16-20 h) of S.furcata were induced to sporulate using the procedure described in Section 0.2.4.1. Gametangium production on typical 18 h colonies is summarised in Fig. 1.2, which clearly shows the prevalence of sexual differentiation in this species (cf. Figs. 1.1 and 1.2). The first oogonial initials appear on induced-colonies between 6-12 h after induction, compared with $1\frac{1}{2}$-2 h taken for the first sporangia to develop (Fig. 1.2).

In preliminary experiments carried out at 25°C it was noted that many of the oogonia failed to differentiate normally. A temperature sensitivity experiment was carried out and the results are summarised in Fig. 1.3. Maximal oogonial production occurs at temperatures between 15-25°C, but at the higher temperature the proportion of undifferentiated oogonia is increased. At temperatures above 25°C there is a rapid decline in oogonium production, and therefore it is clear that 25°C is near the upper limit of temperature tolerance. Therefore oogonium induction experiments were all carried out at 20°C, which gave optimum oogonium production, and the highest proportion of differentiated oogonia. Even at this temperature between 5-10% of the uncleaved oogonial bodies scored after 72 h (Fig. 1.2) could be classified as vegetative gemmae, such as shown in Figs. 1.190-1.197.

The development of gametangia takes between 10-15 h at 20°C, and for convenience will be divided into a number of stages, each designated with a Roman numeral:

Stage I: Oogonial-initial formation. Cytoplasm accumulates in the characteristic hooked tips (Fig. 1.68) which develop on the main hyphae and short lateral branches, to form the spherical oogonial initials (Fig. 1.69).

Stage II: Antheridial branch development. Antheridial branches develop androgynously from the oogonial-initial stalk and spiral up until they make contact with the oogonium body (Fig. 1.71). The tips of the antheridial

branches then swell and are delimited by the insertion of a basal septum (Fig. 1.77).

Stage III: Oogonium delimitation. The oogonial initials expand to their full diameter (40-60 µm) before they are delimited by the formation of a septum in the oogonial stalk (Fig. 1.77).

Stage IV: Vacuolation. A large central vacuole forms in the oogonium, and conspicuous transparent prophase I nuclei become visible in the cytoplasm (Fig. 1.77). Following meiosis the cytoplasm once more appears uniformly dense (Fig. 1.79).

Stage V: Oosphere initial formation. The final stage in oogonium differentiation before clearage involves the redistribution of the peripheral cytoplasm into distinct hemispherical mounds (Figs. 1.80, 1.124). Cleavage is effected as in the sporangium by the fusion of the tonoplast with the plasmalemma (Fig. 1.124).

Throughout Stages III-V little change can be observed in the antheridial cytoplasm under the light-microscope (Figs. 1.77, 1.79, 1.80).

1.2.3.2. Ultrastructural aspects of gametangium development: Vacuole formation

The cytoplasm in Stage I oogonial initials is similar in overall appearance and organelle composition to comparable sporangial organelles (Fig. 1.70). However, there is no evidence of bars or other specialised sporangial organelles, indicating the clear differentiation of sexual organs from their initiation. During Stages II and III while the oogonial bodies are still expanding, many small vacuolar vesicles appear in the cytoplasm which can account for nearly 20% of the cytoplasmic volume fraction (Fig. 1.74). Following oogonium delimitation (Stage IV) these vesicles enlarge by expansion and coalescence to form the large oogonium vacuole (Figs. 1.75, 1.76). During this stage the densebody vesicles are often greatly expanded and are indistinguishable, except for their osmiophilic granules, from vacuolar vesicles (Fig. 1.86). However osmiophilic granules are never seen in the expanded vacuoles, even though the occasional densebody vesicles in the peripheral cytoplasm may expand into the vacuolar compartment (Fig. 1.91).

The vacuole can occupy upto 50% of the total cytoplasmic volume in Stage IV oogonia. In Os-fixed oogonia this vacuole remains partitioned by fine strands of cytoplasm (Fig. 1.76), which are occasionally visible in living material (Fig. 1.124). However, these strands are not preserved in GaOs-fixed material (Fig. 1.75). The redistribution of the vacuolar and cytoplasmic fractions which occurs during Stage V could not be followed ultrastructurally.

The vacuoles in the newly delimited Stage III antheridia are quite small and usually peripherally distributed (Fig. 1.73) and account for approximately 20% of the cytoplasmic volume fraction. Following meiosis (late

Stage IV-Stage V) the antheridia become increasingly vacuolate (< 50% volume fraction) and the cytoplasm peripherally concentrated (Fig. 1.82).

1.2.3.3 Organelle Changes and Associations

Developing oogonia and antheridia (< Stage IV) lack the conspicuous arrays of ER noted in comparable sporangia (Figs. 1.70, 1.73, 1.74, 1.78b) The mitochondria are similar in appearance to those in developing sporangia, and contain abundant electron-transparent cristae (Figs. 1.83, 1.101).

Golgi dictyosomes occur abundantly in both antheridial and oogonial cytoplasm, and as in the sporangia the ER-mitochondrial association is the most common (Figs. 1.83, 1.85, 1.91). Golgi activity judged by the abundance of peripheral vesicles is probably greater in developing oogonia than in either hyphae or sporangia (cf. Figs. 1.83-1.85, with Figs. 1.12, 1.52) The portion of peripheral oogonial cytoplasm shown in Fig. 1.85 clearly illustrates the proposed (Heath, Gay and Greenwood, 1971) derivation of the peripheral wall vesicles from the Golgi dictyosomes. Unlike in the zoosporangia, cytoplasmic Golgi-dictyosomes remain active throughout the period of spore delimitation (Stages IV-V).

As in developing sporangia wall vesicles are present in abundance in the peripheral cytoplasm of oogonia, and to a lesser extent in antheridia. Localised accumulations of wall vesicles also arise where the oogonium and antheridium make contact (Stage II-III), (Fig. 1.78a) However these wall vesicle accumulations do not persist after Stage IV (Figs. 1.81, 1.82). The larger more electron dense vesicles noted by Heath, Gay and Greenwood, (1971) in the region of gametangium contact (Fig. 1.78a) were not observed in this study.

The cell walls of oogonia are slightly more electron-dense than comparable sporangial walls (Fig. 1.85), and reach a thickness of between 200-300 nm by the time cleavage takes place (Stage V). Plasmalemmasomes and lomosomes are rarely present in the walls of normal gametangia, except perhaps in the region of antheridium contact.

Neutral lipid and densebody reserves are much more abundant in oogonia than in comparable sporangia (cf. Figs. 1.75 and 1.47). The cytoplasmic volume fraction of neutral lipid increases from 5% in Stage I oogonia to between 15-18% by Stage IV (Figs. 1.70, 1.75), and that of densebody granules from 5% to between 12-15%. This accumulation of storage reserves does not occur in antheridia, where the combined lipid and densebody fractions only account for 2-3% of the total volume fraction (Figs. 1.73, 1.78b, 1.71, 1.82).

The appearance of densebody granules in Stage I oogonia is similar to those described in preseptal sporangia (cf. Figs. 1.83 and 1.39). The similarity between the fibillar material and small osmiophilic particles in the densebody vesicles and the contents of inflated ER cisternae shown in

Fig. 1.83, suggests the former may arise from the latter. After the marked expansion of densebody vesicles during vacuole development (Fig. 1.86), the Stage IV-vesicles are usually little bigger than the densebody granules. The densebodies at this stage are between 400-500 nm in diameter and are frequently of variable electron-density (cf. Figs. 1.89 and 1.90). In some Stage-IV oogonia the densebody vesicles membranes are poorly preserved (Figs. 1.87, 1.89). During vacuole development (Stage IV) the densebody granules become associated with concentric arrays of a myelin-like material, with a regular periodicity of between 8-9 nm (Figs. 1.87, 1.90). In a few of the GaOs fixed densebody vesicles the associated matrix material appears as a network of osmiophilic granules, rather than the usual myelin arrays (Fig. 1.88). These myelin-like arrays persist in the differentiated oospores, where they reach their maximum extent (cf. Figs. 1.90 and 1.162).

1.2.3.4. Nuclear Cytology

The nuclear divisions which accompany gametangium development are not initiated until the oogonium is fully vacuolate (Stage IV). As noted in S.terrestis by Howard and Moore (1970) the gametangial nuclear divisions in S.furcata occur synchronously (Figs. 1.75, 1.77) at least as far as anaphase I. Nuclear divisions are also initiated simultaneously in both the oogonium and antheridium (Fig. 1.75) and remain in phase until synchrony is lost. The main nuclear stages recognised in differentiating gametangia are as follows. Centriolar behaviour will be described separately.

Interphase Nuclei

Up to Stage IV oogonia and antheridia both contain typical interphase nuclei (Figs. 1.70, 1.73, 1.74, 1.92, 1.94). Prior to nuclear division the nuclei become regularly distributed throughout the peripheral oogonial cytoplasm (Fig. 1.75). No observations were made of autolysing nuclei in developing oogonia prior to nuclear division, although this has been reported in light microscopic accounts (Win-Tin & Dick, 1975).

Prophase I

At the onset of prophase I there is a rapid expansion of nuclear size, from approximately 3.0 to 4.5 μm (Figs. 1.92, 1.94, 1.95, 1.100, 1.104). These large prophase I nuclei are clearly seen in oogonia under the light microscope (Fig. 1.77) and are visible for a period of 2 h or more.

In GaOs-fixed material as the nuclei enlarge the particulate nucleoplasm becomes more electron-transparent (Figs. 1.92, 1.93, 1.100) and the nucleolus condenses into an electron-dense spherical body, some 600-800 nm in diameter. This condensed nucleolus always lies close to the nuclear envelope (Figs. 1.93, 1.95) and is retained at least until metaphase I (Fig. 1.106).

However the ultrastructural morphology of the oogonial nuclei depends

on the fixative employed (Figs. 1.95, 1.104). Most of the GaOs-fixed nuclei have reasonably smooth ovate profiles (Figs. 1.93, 1.104) which are comparable to the bodies visible in the light microscope (Fig. 1.77). However, the Os-fixed nuclei have deeply lobed profiles and retain their dense particulate nucleoplasm throughout prophase (Fig. 1.95). Frequently these nuclei are even more divided than the nucleus shown in Fig. 1.95. In contrast there is little difference between GOs and Os fixed nuclei in the antheridia (Figs. 1.99, 1.100).

During the period of enlargement a series of electron-dense linear or crescent shaped elements condense in the nucleoplasm, and may reach lengths of up to 1.5 μm (Figs. 1.78b, 1.93, 1.95, 1.99, 1.104). Because of their close resemblance to the lateral elements of the meiotic synaptinemal complex (SC) Howard and Moore (1970) suggest these bodies represent the condensing bivalent chromosomes, and named them uniaxial elements. In common with the lateral elements of the SC the uniaxial elements terminate against a straight segment of nuclear envelope, which is frequently associated with cytoplasmic microtubules (Fig. 1.100). The GaOs-fixed elements are between 80-90 nm in diameter and are made up of a core of electron-dense particles from which fibrillar material radiates (Fig. 1.102). The Os-fixed elements are narrower (50-60 nm) but still composed of a particulate core and lateral fibrils, although these are somewhat obscured by the dense groundplasm (Fig. 1.103).

At a stage Howard and Moore (1970) interpreted to be late zygotene, the uniaxial elements become aligned in pairs approximately 150-160 nm apart. (Figs. 1.101, 1.104). Possible pairs of elements are indicated in Fig. 1.104, although without a serial-section reconstruction of the nucleus it is not possible to determine pairing with absolute certainty. However, there was never any sign of the central core and lateral fibrils which link the paired lateral elements in the normal SC (Moses, 1968).

As prophase I progresses the uniaxial elements become less distinct as they revert to the more diffuse chromation masses, and an intranuclear spindle appears (Fig. 1.104). As in mitotic nuclei the spindle microtubules terminate adjacent to the nuclear envelope, in the region of the by now polar centriole pockets (Figs. 1.105, 1.106, 1.107).

Metaphase I

Metaphase I nuclei are difficult to distinguish with certainty from the late prophase I stages. However, the nuclei shown in Figs 1.105 and 1.106 both contain well developed spindles and the electron dense chromation material is more or less concentrated in the region of the nuclear equator. This suggests the alignment of the chromosomes on the meta phase plate

Anaphase I

During Anaphase I the chromation segregates towards the nuclear poles, as a result of nuclear elongation and probably spindle microtubule contraction.

The near median L.S. profile of an anaphase I nucleus in Fig. 1.107 clearly shows the spindle apparatus spanning the nucleus between the two pairs of apical centrioles and the separating chromatin material. In some sections spindle microtubules were seen terminating in the electron dense chromatin material, although no specialised kinetochore (attachment) structure was observed.

Telophase I and Second Divisional Stages

As the nuclei elongate during telophase a contriction develops resulting in the formation of bilobed dumbell-shaped profiles, such as shown in Fig. 1.108. In S.terrestris the centrioles are reported to separate at this stage and migrate to initiate new spindle poles at right-angles to the axis of the first division (Howard & Moore, 1970). Serial sections of the nucleus shown in Fig. 1.108 reveal centrioles in positions consistent with the onset of prophase II. Win-Tin and Dick (1975) report that this species frequently (c. 40% of nuclei) shows an unequal segregation of chromatin at anaphase I, which may account for the marked size-difference of the two lobes in Fig. 1.108.

The two antheridial nuclei lying side by side in Fig. 1.109 are both undergoing synchronous division with their spindles orientated parallel to each other. Serial sections indicate these two nuclei may be connected by a narrow isthmus of nucleoplasm, although insufficient serial profiles were salvaged to unequivocably confirm this. However, the presence of only a single centriole at each nuclear pole (Fig. 1.109) is indicative of a second divisional stage (Howard & Moore, 1970).

Howard and Moore (1970) report the final stage of gametangial meiosis to be the formation of a 4 lobed cruciate body prior to separation. The closely associated nuclear profiles in both the antheridial (Fig. 1.81) and oogonial cytoplasm (Fig. 1.110), may represent oblique sections through such cruciate bodies outside of the narrow plane of interconnection. Certainly the 3 nuclei in Fig. 1.110 all appear to be converging to the same point and all contain spindle microtubules.

Therefore although the evidence is rather sketchy it seems likely the second divisional stages in S.furcata follow a similar pattern to those described in S.terrestris by Howard and Moore (1970). Recent light-microscopic accounts of gametangial meiosis in Saprolegnia have suggested the nuclear envelope may breakdown after telophase I (Flanagan, 1970; Win-Tin & Dick, 1975), but there is no ultrastructural evidence to confirm this.

Gametic Nuclei (Post-divisional).

Post-divisional gametic nuclei from antheridia are shown in Figs. 1.82, 1.111. These nuclei are characterised by their small, rounded profiles (c. 2.0 x 1.5 μm). Otherwise their nucleoplasm is similar to that previously

described in interphase nuclei, with particulate contents and diffuse electron-dense nucleolar region (Fig. 1.111).

The female gametic nuclei appear slightly larger (c. 2.5 x 2.0 μm) and have a pyriform profile (Fig. 1.128). Following the gametangial nuclear divisions (Stage V) the oogonial cytoplasm contains many autolysing nuclei, similar to those shown in Fig. 2.226. This supports the findings of Trow (1895) that supernumery oogonial nuclei abort after nuclear division.

1.2.3.5. Centriolar Behaviour

Prior to the initiation of nuclear divisions the pair of centrioles associated with each nucleus have a normal interphase morphology, such as described in section 2.212 (Figs. 1.96, 1.97). During early Prophase I the centrioles separate and replicate (Fig. 1.98) as they migrate to the nuclear poles to act as foci for the spindle apparatus. However, it was not possible to determine whether this separation was associated with spindle formation as it is in mitotic divisions (Heath & Greenwood, 1970b; Heath, 1974a), although studies on other Saprolegnian species indicate that it is probably not (Howard & Moore, 1970; Ellzey, 1974).

Between prophase I and anaphase I a number of changes occur both in centriole structure and their organisation in relation to the nucleus, which are not reported during mitosis. The first of these structural changes involves the enveloping of the centriole by a layer of electron dense material, 40-50 nm in diameter, which Howard and Moore (1970) called the 'sheath' (Figs. 1.114-1.116, 1.118-1.123). This material is never associated with interphase (Fig. 1.97, 1.96, 1.117) or mitotic centrioles. This sheath is retained throughout gametangial nuclear divisions (Fig. 1.109). Howard and Moore (1970) claim it does not disappear until after fertilisation, although this could not be ascertained in this study. Centriole TS profiles in the region of the sheath show that both fibrillar material and aster microtubules radiate from the amorphous sheath (Figs. 1.118, 1.119, 1.120).

During prophase I centriolar triplet microtubules elongate so that by anaphase I the centrioles are more than double their original length (450-500 nm cf. 200 nm: Figs. 1.97, 1.113, 1.116, 1.122). This elongation has not been reported in the other Saprolegnian species examined (Howard & Moore, 1970; Ellzey, 1974). The presence of the amorphous sheath enveloping the proximal 200-300 nm of the centriole (Figs. 1.115, 1.116, 1.122) makes it difficult to tell if all three triplet microtubules elongate equally. It seems likely, from Figs. 1.113-1.116, that only the inner two microtubules of each triplet elongate. These elongate centriolar profiles were only observed upto Anaphase I, after which the centrioles revert to their usual interphase length (Fig. 1.109).

Some changes also occur in the central cartwheel structure during prophase I. The most obvious of these is that the previously continuous lamina of the

centriolar spokes (Heath & Greenwood, 1970b) becomes divided into a series of 5-6 rib-like sections. This gives the LS profiles a rather striate appearance (Figs. 1.113, 1.116). Divided centriolar lamina are also reported in algae (Cavalier-Smith, 1972) and animals (Brinkley & Stubblefield, 1970).

In addition these structural changes the centriole pairs also move apart during prophase I, with the intracentriolar space increasing from 20 nm (Figs. 1.113, 1.114) to between 80-100 nm (Figs 1.115, 1.116, 1.122). In LS each separated centriole can be seen to lie in its own shallow pocket in the nuclear envelope. The spindle microtubules nearly always terminate against the nuclear envelope in the region between the two separated centrioles (Fig. 1.116).

Finally, between late prophase I and anaphase I the centrioles become surrounded by a cisternal 'cap', which is similar in its staining properties to nuclear envelope and ER (Figs. 1.115, 1.116, 1.118-1.123). At this stage the two pairs of centrioles lie at the poles of the elongating nucleus, and both pairs are orientated in approximately the same plane (Fig. 1.107). The endomembrane cisternae in S.furcata form an open-ended tunnel-like cap enclosing the two centrioles (Figs. 1.116, 1.122, 1.118, 1.119, 1.123). This contrasts with the other Saprolegnian species in which this cap has been described, where endomembrane encloses both the centriolar ends and intervenes into the intracentriolar space (Howard & Moore, 1970; Ellzey, 1974). This endomembrane cap does not seem to be continuous with the nuclear envelope, although it is perforated by pores through which aster microtubules pass (Figs. 1.118, 1.119). Other aster microtubules appear to terminate against the endomembrane cap itself (Fig. 1.118). This cap does not persist beyond anaphase I (Fig. 1.109) and its mode of development is unclear.

1.2.3.6. Gemma Morphology and Ultrastructure

As mentioned in Section 1.2.3.1 a number of delimited bodies which develop on induced colonies of S.furcata do not form antheridia or differentiate into oospores. These gemma bodies are relatively uncommon in colonies of S.furcata induced under the conditions employed in this study (Fig. 1.2). Gemmae are usually smaller than oogonia, rarely axceeding 30 μm in diameter (Figs. 1.191-1.195), and have a much less dense cytoplasm (cf. Figs. 1.191-1.195 with Figs. 1.79, 1.80). Some gemmae remain as simple spherical bodies (Fig. 1.194). Many, however, form part of an acropetal succession of delimited bodies, usually of decreasing diameter (Figs. 1.191-1.193, 1.195).

Most of the gemmae are vacuolate (Figs. 1.191, 1.194) although the peripheral cytoplasm in these bodies is more unevenly distributed than in comparable oogonia (cf. Fig. 1.190 with Figs. 1.75, 1.76). The gemma cytoplasm contains the same organelles as oogonia, although both densebody vesicles and neutral lipid reserves are less abundant (Figs. 1.190, 1.196, 1.197). It

should, however, be noted that the lipid droplets have not been preserved in the $KMnO_4$ fixed gemma illustrated. In this 6-day old gemma the golgi dictyosomes appear quiescent (Fig. 1.197) and peripheral wall vesicles are scarce (Figs. 1.190, 1.196, 1.197) indicating active wall synthesis has probably ceased. The gemma wall is fairly thin (200-250 nm in diameter), and lomasomes were not observed.

All the gemmae nuclei observed in ultrastructural studies were in interphase, as shown in Figs. 1.196, 1.197. There is never any sign of the distinctive large prophase I nuclei in the cytoplasm of living gemmae (Figs. 1.191-1.195), confirming meiosis does not occur in these bodies.

When mature induced-colonies (5-10 days) were transferred to fresh inducing solution (distilled water), many gemmae produced vegetative germtubes as shown in Fig. 1.194. The germtubes which form are always narrow (7-10 μm) and grow linearly.

Induced-colonies of S.ferax also produce gemmae, (Section 1.2.2.1), which share many of the features described above, except that they are more elongate club-shaped bodies (Fig. 2.73). Sporangial gemmae also contain bars, although flimmer vesicles are not observed. Their nuclei do not undergo the changes in morphology that are associated with zoospore differentiation.

1.2.4. Sexual Reproduction: Oospore maturation

1.2.4.1. Oospore development

Following cleavage the differentiated oospores take between 24-48 h to reach maturity, after which no further cytological changes occur before germination. As with gametangium development, oospore maturation has been divided into a number of stages, designated by Roman numerals following on from those used for the gametangial stages.

Stage VI: Naked Oospores. The immediate post-cleavage stage during which there are marked changes in spore size and shape (Fig. 1.124:6-13) and the primary spore wall is deposited.

Stage VII: Immature oospores. This stage lasts from 5-10 h during which the oospores have uniformly dense cytoplasm (Fig. 1.124: 14-28). During this period the antheridium produces a fertilisation tube which makes contact with the oospores, and presumably plasmogamy follows (Fig. 1.124: 14-21).

Stage VIII: Endospore wall development. A refractile inner wall layer is laid down centripetally over a period of 10-20 h, and reaches a thickness of 1-1.5 μm. During its formation the cytoplasm becomes less uniform in appearance (Fig. 1.124: 28-32).

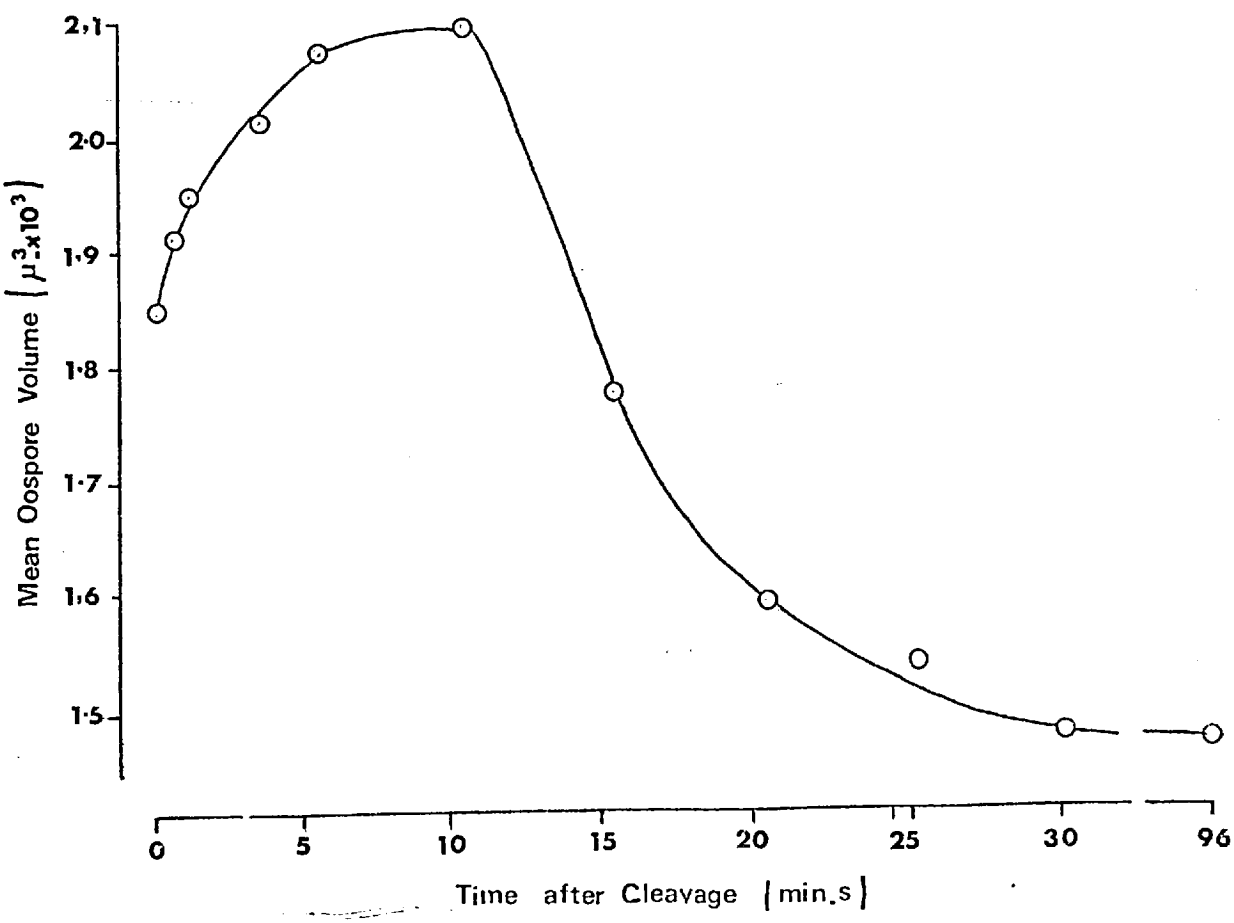
Stage IX: Ooplast development. After endospore deposition small vacuoles appear in the cytoplasm and coalesce to form a single large vacuole, the ooplast (Figs. 1.124: 33-36, 1.136-1.140). The mature ooplast in this species is slightly displaced to one side of the spore, characteristic of sub-centric spores (Figs. 1.124:36, 1.144).

Table 1.1. Changes in oospore volume following cleavage

Time after cleavage mins	Spore Diameter* µm max	min	Mean spore volume μm^3	% volume change from the time of cleavage (0 min)
0	18.0	14.0	1850	0
0.8	18.1	15.3	1950	+4
3.0	17.4	15.2	2020	+9
5.0	17.3	15.3	2040	+13
10.0	17.1	15.4	2100	−13
15.0	15.7	14.7	1780	−4
20.0	15.7	14.1	1600	−12
25.0	15.0	14.1	1560	−16
30.0	14.3	14.1	1480	−20
96.0	14.3	14.1	1480	−20

* mean of the 3 spores shown in Fig. 1.124.

Fig. 1.112 Changes in spore volume in S. furcata following cleavage, assessed from the spores shown in the photographic sequence.



Stage X: Final maturation: The endospore wall layer differentiates into two distinct layers (Fig. 1.148) and refactable particles in Brownian motion appear in the ooplast (Figs. 1.144-1.147).

As indicated most of the developmental stages (VI-IX) are shown in the photographic sequence of a single oogonium in Fig. 1.124. It should be noted that oospore maturation, particularly after Stage VII, is much delayed in the small photographic cell, perhaps due to oxygen limitation. In this study the term oosphere will be restricted to the naked Stage VI spores, although it is normally applied to pre-fertilisation spores (Dick, 1969). However, the precise time of fertilisation is impossible to ascertain under the light microscope, whereas the pre-wall stage is easily distinguishable.

Oospore maturation within a single oogonium is clearly synchronous (Fig. 1.124) although there is some variation in the rate of ooplast vacuole coalescence during Stage IX. Under normal conditions ($20^{o}C$) only a small proportion of the delimited oospores (< 1%) do not mature, although this proportion is greatly increased at higher temperatures ($>25^{o}C$) and in badly contaminated cultures. The cytoplasmic changes in oospore maturation will now be described in detail.

1.2.4.2. Oosphere wall formation

Following the fusion of the tonoplast and plasmalemma surrounding the hemispherical initials, the oospheres separate from the oogonium wall and round off (Fig. 1.124:3-8). The newly differentiated spores have an irregular continually changing outline (Fig. 1.124:5-13). The spore volume changes during these early stages were assessed from the measurement of the three spores shown in Fig. 1.124. The volume was calculated using the formula for a prolate spheroid($4/3\pi ab^2$, where a is the maximum radius and b is the minimum radius) used by Christen and Hohl (1972) to measure sporangial volume in Phytophthora and the results are summarised in Table 1.1 and Fig. 1.112. Immediately following cleavage there was an increase in volume (<.13%, Table 1.1) as the spores swell in the absence of a restraining wall. In some oogonia this spore swelling is so pronounced that individual oospores become indiscernible, as in the homogeneous sporangial phase (Fig. 1.29).

The oospheres remain in this expanded state for between 5 and 10 minutes before volume reduction commences (Table 1.1, Figs. 1.112, 1.124). During their expanded phase the oospheres exhibit much surface activity and have been claimed by Trow (1895) to exhibit amoeboid movement. The oospores then start to shrink and the spore volume is reduced by nearly 30% in a period of 10-15 minutes (Table 1.1, Fig. 1.112). However, unlike in zoospore volume reduction contractile vacuoles are not observed in these spores, and the mechanism of volume reduction is not known (Fig. 1.124:10-14).

Nevertheless oospheres do produce irregular cytoplasmic protuberances during the period of shrinkage (Fig. 1.124:9-12) and some of these are completely extruded from the spores (Fig. 1.124:11). Some of these extruded portions of cytoplasm migrate across the intersporal space and appear to be reabsorbed by neighbouring spores as shown in frames 10-12 in Fig. 1.124. Others simply lyse and disperse.

Ultrastructural profiles of three Stage VI oospheres are shown in Fig. 1.125 and confirm the absence of the cell wall at this stage. The uneven profile of the plasmalemma in these spores is due to the displacement of the membrane by both the abundant peripheral wall vesicles, and the complex whorls of expanded peripheral membrane (Figs. 1.126, 1.127). The wall vesicles in the naked oospheres are slightly larger (100-200 nm) than the comparable vesicles in hyphae, sporangia and gametangia (Figs. 1.126, 1.127). They are also much more closely adpressed to the plasmalemma. Some of these vesicles appear to have fused with the plasmalemma (Fig. 1.126), indicating they are being actively discharged at this stage.

The membraneous whorls, responsible for the larger bulges of the spore surface, may include small fragments of entrapped cytoplasm (Fig. 1.127). These bodies are possibly the origin of the large protuberances observed in the light microscope (Fig. 1.124). The intrasporal space in this oogonium contains abundant fragments of membraneous material (Fig. 1.125), which possibly originates from the breakup of extruded lumps of cytoplasm.

The formation of the primary oospore wall in Saprolegnia is indicated by the attainment of a stable, smooth spore outline (Fig. 1.124:13-14), and the cessation of shrinkage (Table 1.1, Fig.1.112). This usually occurs between 20-30 minutes after cleavage. If the spores are placed in 0.8 M sucrose at this stage they plasmolyse and the newly formed wall can be seen. The primary wall of the oospore is similar in appearance to the electron transparent walls of the hyphae and gametangia (Fig. 1.130, 1.131), and there is no sign of an electron dense outer layer such as present in cysts (Fig. 1.57). Wall vesicle-mediated wall deposition continues for some time after the initial appearance of the cell wall (Fig. 1.30) and the primary oospore wall usually reaches a thickness of between 100-150 nm under normal conditions (Figs. 1.130, 1.131). However the absence of wall vesicles from the peripheral cytoplasm in late Stage VII oospores (Fig. 1.129, 1.131) indicates primary cell wall development is completed before endospore deposition begins. It also suggests these vesicles are not involved in the formation of the latter. Lomasomes are present in small numbers in the primary oospore wall, particularly in the region of fertilisation tube contact (Figs. 1.171, 1.172).

1.2.4.3. Endospore Wall Formation

The inner endospore wall layer is accreted centripetally until it reaches a thickness of between 1.0-1.5 μm (Figs. 1.148-1.150, 1.153-1.158). This means it accounts for between 25-35% of the total oospore volume. It is hardly surprising its development is accompanied by a reduction in cytoplasmic density (Figs 1.136-1.1.139). In the light-microscope the endospore wall appears uniformly refractile (Fig. 1.144), and the two layers reported by Dick (1969) could not be discerned. The developing endospore wall appears uniformly electron-transparent in GaOs and Os-fixed spores (Fig. 1.132-1.135, 1.141-1.143) although it has a fine granular texture in $KMnO_4$-fixed material (Fig. 1.133). However, immediately following the initiation of endospore formation, the spores become relatively impermeable to fixatives and the quality of organelle preservation in GaOs and Os-fixations is very poor (Figs. 1.32, 1.141-1.143). This effect is strikingly illustrated in Fig. 1.134 in which even though the endospore layer is no more than 100 nm thick no internal membranes are preserved. Fortunately $KMnO_4$ gives slightly better fixation and preservation of internal membranes, at least in Stage VIII spores (Fig. 1.133).

There is no evidence of wall vesicle involvement in endospore accretion (Figs. 1.33-1.35) as has recently been noted in Peronosporalean oospores (Hemmes and Bartnicki-Garcia, 1975; McKeen, 1975). In addition no membrane can be traced between the endospore and the cytoplasm, even though cisternae of ER are aligned fairly close to the inner margin of the wall (Fig. 1.33). However, there is always a clearly-defined electron-dense layer (c. 10 nm - 15 nm thick) separating the primary wall and the endospore (Figs. 1.133, 1.135). In many parts this layer has a tripartite membrane-like structure (Figs. 1.133-1.135), and this is particularly clearly shown in mature oospores (Figs. 1.153, 1.159, 1.161). The presence of this membrane-like layer between the endospore and the primary wall and the absence of a membrane between the endospore and cytoplasm (at least in these early stages) suggests endospore accretion occurs inside the plasmalemma. This supports Dick's (1969) suggestion that the endospore wall may be a peripheral phase separation of reserve products.

During the final stages of oospore maturation (Stage X) an inner, usually more electron-dense layer, differentiates within the endospore. This is not however revealed in all fixation procedures (Figs. 1.152, 1.153, 1.156, 1.157). The mature endospore structure is poorly preserved in GaOs-fixed spores in which it is uniformly electron-transparent and more uneven and narrower than in other preparations (Fig. 1.152). Most Os and $KMnO_4$-fixations reveal a granular substructure to the endospore matrix and differentiate an electron-dense inner layer, which varies from 200 to 500 nm in thickness

(Figs. 1.153, 1.156). This inner layer is probably formed by the uneven impregnation of additional cytoplasmic components into the differentiated endospore layer, as described in some Ascospore walls (Stiers, 1974). This would also account for the irregular, crennate, margin of this inner layer (Figs. 1.153, 1.156). In some of the shorter $KMnO_4$-fixations (5 minutes) this electron dense inner layer is not revealed, (Fig. 1.157), whereas in others it appears completely electron transparent (Fig. 1.150).

The localisation of polysaccharides within the mature oospore wall was determined using the PASM staining technique described by Dhir and Boatman (1972) on Os-fixed sections comparable to those shown in Fig. 1.153. Silver granules are deposited more or less uniformly throughout the endospore wall, although show a slightly reduced density in the region of the inner layer. This indicates the latter is not of polysaccharide origin. The highest density of deposited silver granules coincides with the electron-dense membrane-like layer separating the primary and endospore layers.

A number of oospores were founded to have a rather different endospore wall structure from that outlined above. This was normally associated with tap water induced oospores, which were also abnormally swollen (Figs. 3.10, 3.11). The endospore wall in such spores is frequently of reduced thickness (0.5-0.8 μm cf. 1.5-2.0 μm) and contains small osmiophilic globules which are between 40-100 nm in size (Figs. 1.155, 1.158, 1.161). These globules are either distributed uniformly throughout the wall (Figs. 1.158, 1.161) or occur in localised bands (Fig. 1.151, 1.155). Sometimes a lamellate substructure to the endospore matrix was also revealed in these spores (Fig. 1.155). These abnormal endospore walls are always associated with spores which have extraordinarily well-preserved cytoplasm (Figs. 1.151, 3.11). This suggests the endospore structure is critical in governing spore permeability.

The other interesting feature of these abnormal oospores is that they demonstrate the presence of a membrane between the endospore layer and the cytoplasm (Figs. 1.158, 1.160, 1.161) which cannot be unequivocally shown in normal spores. This implies that the mature endospore wall layer is probably bounded on both sides by a membrane, as in Fig. 1.161.

1.2.4.4. Organelle changes and associations during oospore maturation

During the early stages of oospore maturation (Stages VI-VII) the main cytoplasmic organelles such as ribosomes, ER, mitochondria and Golgi remain similar in abundance and appearance to those described in the peripheral cytoplasm of the Stage IV oogonia (Figs 1.125, 1.126, 1.128-1.131). Following endospore imitation (Stage VIII) the poor cytoplasmic preservation makes it difficult to follow the changes in organelle composition and structure during the final stages of maturation (Stages VIII-X). It was a matter of good fortune that the well-fixed tapwater-induced oospores (Fig. 3.10, 3.11) had

a similar internal cytoplasmic organisation to that of the normal oospores. Whether the organelles in these abnormal oospores are comparable to those in normal spores is not known, but it will be assumed they are similar. The reasonably well preserved $KMnO_4$-fixed oospores also enable changes in the membraneous cytoplasmic organelles to be followed (Figs. 1.113, 1.151).

In the $KMnO_4$-fixed Stage VIII oospores the mitochondria become reduced in number and have rather small less regularly distributed cristae. In the mature Stage IX-X oospores relatively few mitochondria remain in the peripheral cytoplasm (Figs. 1.151, 1.188). These mitochondria have rather electron dense membranes, which contrast with the much more electron transparent matrix at this stage (Figs. 1.188, 3.12). Golgi dictyosomes were not observed in the oospore cytoplasm after Stage VII (Figs. 1.130) which confirms they are not involved in endospore accretion.

The status of ER cisternae and ribosomes in Stage IX-X oospores is more difficult to ascertain with certainty. Neither ribosomes nor clearly defined ER cisternae were discernible in the peripheral cytoplasm of the Os-fixed tapwater-induced spores (Figs. 1.188, 1.189, 3.12). However a number of very osmiophilic swollen cisternum-like profiles were seen in some of these spores (Fig. 1.161), and may represent vestigial ER cisternae. However the peripheral cytoplasm in these spores contain abundant membran ous fragments (Fig. 1.88), which in some spores are organised in elaborate whorl-like arrays as shown in Fig. 1.158. These observations suggest the widespread dissociation of cytoplasmic organelles during oospore maturation (Stages VIII-X). This is supported by the extremely transparent appearance of the peripheral cytoplasmic matrix in the light microscope (Figs. 1.137-1.139, 1.144, 1.145).

Unlike the membran ous and proteinaceous organelles the lipid and densebody reserves are relatively well preserved throughout oospore maturation, and the changes in their relative distributions have been carefully followed.

In the early Stage VI-VII spores the neutral lipid droplets and densebody granules account for between 55-65% of the total spore volume, with the lipid contributing 35-40% (Figs. 1.125, 1.128, 1.129). Following cleavage the lipid droplets and densebody vesicles are randomly distributed throughout the cell with respect to each other (Fig. 1.125). However, as the spores enter Stage VII the densebody vesicles tend to segregate to the spore periphery and the lipid to the spore centre (Figs. 1.128, 2.140). This is the organisation at the time of fertilisation (Fig. 1.171), but prior to endospore initiation (Stage VIII) these two components once more intermix as shown in Fig. 1.129. Throughout these changes the oospore cytoplasm appears uniformly dense under the light-microscope (Fig. 1.124:13-27).

During stages VI-VII the densebody granules are still associated with myelin like material (8-9 nm periodicity) which appeared during oogonium

vacuolation (Figs. 1.162, 1.163). In GaOs-fixed spores this material forms elaborate concentric arrays around the densebody granules (Figs. 1.162, 1.163) whereas in Os-fixed spores it is less extensive (Fig. 1.164). A freeze-fractured profile of an unfixed oospore also revealed multilayered bodies (Fig. 1.166) similar to those ascribed to phospholipid in yeast cells (Mar & Mühlethaler, 1963). This suggests these lamellar arrays are not fixation artefacts, even though their morphology depends on the fixative used. Prior to endospore wall formation the densebody vesicles start to expand (Fig. 1.129) and they acquire more elaborate, less regular arrays of matrix material, as shown in Fig. 2.157.

Following endospore wall formation (Stage VIII) small vacuoles become visible in the oospore cytoplasm under the light-microscope (Figs. 1.136, 1.137), which progressively enlarge by expansion and coalescence until the ooplast is formed (Figs. 1.137-1.140). In spite of the poor quality of cytoplasmic preservation the comparable ultrastructural profiles (Figs. 1.132, 1.141-1.143) clearly show that these vacuoles develop from the densebody vesicles. During this period of expansion the densebody vesicles remain embedded in a dense osmiophilic matrix, which was best preserved in GaOs-fixed oospores induced in cycloheximide (Fig. 1.142-1.143).

In normal GaOs-fixed spores (Fig. 1.132) ooplast matrix material contains numerous electron-transparent holes, giving it a sponge-like appearance (Figs. 1.152, 1.165). However, the embedded densebody granules are often still associated with myelin arrays, although these have a reduced periodicity of c. 5 nm (Figs. 1.167, 1.168). In the cycloheximide-induced spores the matrix material appears more uniform, and is extremely osmiophilic (Figs. 1.142, 1.143). Frequently the densebody granules are not preserved, and their presence is demonstrated by holes in the matrix (Fig. 1.142). In Os-fixed spores the contents of the ooplast are never preserved, although a few densebodies still remain attached to the vacuole margin (Figs. 1.141, 1.143).

The mature ooplast vacuole is approximately 10 µm in diameter and accounts for approximately 40% of the oospore volume (Figs. 1.140, 1.143, 1.44-1.150). There is no apparent reduction in the cytoplasmic volume fraction of densebody granules during oospore maturation (15-20%, Stage VI and Stage X), which suggests the ooplast matrix is not derived directly from expanded granules. The boundaries between the peripheral cytoplasm and the ooplast is clearly defined in living oospores (Figs. 1.140, 1.144, 1.145, 1.147) and is almost certainly delineated by a membrane (Fig. 1.152). However, the boundary between cytoplasmic and ooplast phases can rarely be distinguished in $KMnO_4$-fixed spores (Figs. 1.149-1.151).

In the final stages of oospore maturation (Stage X) minute granules in Brownian motion appear in the ooplast, giving it a particulate appearance (cf.

Figs. 1.140 and 1.144-1.147). The fact that the densebodies are in Brownian motion shows the liquid nature of the mature ooplast contents (Howard and Moore, 1970). This liquifaction of the ooplast matrix is apparently inhibited in cydoheximide-induced spores where the ooplasts remain uniformly transparent (Fig. 2.251). The ultrastructural appearance of the mature ooplast vacuole is quite varied as there are variations both in the matrix density and densebody granule osmiophilia (e.g. Figs. 1.149-1.152). The mature ooplast of the tapwater-induced oospores (Fig. 3.11) contains remnants of the matrix material, in which a small number of densebody granules are still embedded (Fig. 1.169). This matrix contains the characteristic myelin-like arrays, which at this stage have a periodicity of 5-6 nm (Fig. 1.170).

During ooplast expansion the neutral lipid droplets remain confined to the intervening cytoplasm (Figs. 1.132, 1.141-1.143). In the mature oospores the lipid droplets lie in ordered arrays in the peripheral cytoplasm (Figs. 1.143, 1.149-1.152). These closely packed lipid droplets are clearly shown in Nomarski-phase optics (Figs. 1.146-1.147) and account for most of the cytoplasmic volume fraction. In $KMnO_4$-fixed material the lipid droplets have irregular divided profiles and show varying degrees of extraction (Figs. 1.149-1.151). In mature oospores the neutral lipid fraction accounts for between 20-25% of the spore volume (based on GaOs-fixed spores, Figs. 1.143, 1.152), which indicates a reduction of 10-15% during maturation. This suggests some of the lipid reserves are re-distributed during oospore maturation, possibly into the endospore layer.

1.2.4.5. Ultrastructural Aspects of Fertilisation

The photographic sequence in Fig. 1.124 shows that fertilisation tube development is initiated after oospore wall formation, approximately 30 minutes after cleavage. The fertilisation tube penetrates the oogonium wall, and then grows through the oogonium space (at c.200 μm/h) until it contacts the spores. As it extends the hind region of the fertilisation tube clearly becomes vacuolate (Fig. 1.124:18-19, Fig. 1.171). The apex of the extending fertilisation tube contains the usual accumulation of wall vesicles (Fig.1. 171) and is densely packed with organelles, including gametic nuclei and mitochondria (Figs. 1.171-1.173).

Where the fertilisation tube makes contact with the oospore there is a concentration of wall vesicles in the peripheral spore cytoplasm and the primary wall becomes locally thickened (Fig. 1.171). This results in lomasome formation in the oospore walls in the region of fertilisation tube contact, and this is particularly well shown in streptomycin-treated spores (Fig. 1.172). However, fertilisation tubes were never observed penetrating living oospores (Fig. 1.124), and the only ultrastructural profile of a

fertilisation tube penetrating into the oospore cytoplasm was obtained in a streptomycin-treated oogonium (Fig. 1.174, 2.148). It seems likely that this streptomycin-treated penetration peg is larger than in normal spores and is described in detail in Section 2.3.8.7. (Fig. 2.148). It is clear that the fertilisation tube penetrates the primary oospore wall in much the same way as it does the oogonium wall (Fig. 1.174), but it does not rupture the oospore plasmalemma (Fig. 2.148).

The fertilisation tube presumably ruptures and discharges its contents, including the male gamete nucleus, into the oospore. This empty fertilisation tube then becomes compressed against the primary oospore wall as the endospore wall is accreted (Fig. 1.175). In mature Stage X oospores the fertilisation tube is reduced to a lomasome-like scar lying between the primary wall and the endospore (Figs. 1.177, 1.178). In streptomycin-treatments the collapsed fertilisation tube is much larger than in control spores and results in a clear distortion of the endospore wall (Fig. 1.176). Therefore there seems to be good structural evidence that the fertilisation tube is functional in Saprolegnia furcata, and this is supported by the nuclear studies.

1.2.4.6. Nuclear Cytology

Serial sections through immature Stage VI and many Stage VII oospores reveal only a single more or less centrally located female nucleus (Figs. 1.125, 1.128). This nucleus is pyriform in shape and approximately 2.0 x 1.5 µm in size (Figs. 1.128, 1.181, 1.18). In Stage VII oospores the nucleus lies in a lipid-free zone, 3-5 µm in diameter, which contains ER, mitchondria and Golgi in addition to the nucleus (Figs. 1.128, 1.181, 1.182). These nuclei are associated with an electron-dense apical body (Figs. 1.181, 1.183). Normal centriolar profiles were not observed, even though cytoplasmic microtubules are closely associated with these pyriform nuclei (Fig. 1.184).

Some of the Stage VII oospores contained two nuclear profiles, suggesting these were post-fertilisation spores (Fig. 1.185). The two nuclei shown in Fig. 1.185 were located in the peripheral oospore cytoplasm which has been reported by Trow (1905) to be typical of the immediate post-fertilisation stage.

During Stage VIII the nuclei return to their central position, and although poorly preserved two nuclear profiles can be clearly seen in Fig. 1.132. A nuclear profile can also be seen in the centre of Stage VIII spores in the light-microscope (Fig. 1.124:28) although it is not possible to discern whether there are one or two nuclei present.

However, the mature Stage X oospores contain only a single, peripherally-located pellucid spot whose large size (4.0 x 2.0 µm) suggests nuclear fusion has occurred (Figs. 1.144, 1.145, 1.147). This nucleus was not preserved in

mature $KMnO_4$-fixed spores, although its position can be determined by the absence of neutral lipid, and by the less uniform nature of the granular matrix (Figs. 1.149, 1.150). The mature tapwater-induced oospores contain a single large nucleus, approximately 4.0 x 2.0 µm in size (Figs. 1.188, 1.189). These fusion nuclei have an exceptionally electron transparent fibrillar nucleoplasm, more typical of expanding prophase I nuclei (Fig. 1.99) than of vegetative interphase nuclei (Fig. 1.94). The centrally-located nucleus from a tapwater-induced Stage IX oospore (Fig. 1.189) has an irregular lobed profile suggesting it might be an immediate post karyotic stage. Therefore it seems likely that karogamy takes place during ooplast development in this species.

The gametic nuclei which remain in the fertilisation tube after oospore fertilisation has been completed undergo autolysis by the inflation and then dissolution of their nuclear envelopes (Fig. 1.187)

1.2.5. Septum Formation and Structure in Saprolegnia

1.2.5.1 Septum Development

The development of the septa which delimit the sporangia, gametangia and gemmae follows the same pattern throughout. However, in this study, septum formation was most carefully observed in the sporangia of S.ferax and S.furcata. In these bodies the septum forms at the base of the swollen sporangium body (Figs. 1.198-1.205) approximately 2½-3 h after the initials appear.

Septum initiation is heralded by the appearance of a refractile zone in the sporangium stalk (cf. Figs. 1.198-1.200). This zone accumulates over a period of about 20 minutes, reaches a thickness of 10-15 µm, and occupies the full width of the sporangium stalk (Fig. 1.200). An optically dense band then differentiates within this refractile zone (Fig. 1.201), and the septum forms along the upper boundary of this band. Although the insertion of a dozen or more septa was observed, the precise way in which it formed could not be determined. Septa appear to develop uniformly across the full width of the hypha and there was no sign of either the centripetal or lateral patterns of insertion reported in other members of the Saprolegniales (Dick, 1969; O'Day & Horgen, 1974). The septum took several minutes to become distinct (Figs. 1.202-1.203) during which time the refracticle and dense zones disappeared. During the next 10-15 minutes the septum visibly thickens (cf. Figs. 1.202-1.205) and acquires its bowed (convexo-concave) profile, presumably as a result of the higher turgor pressure within the subtending hypha.

An ultrastructural profile of a preseptal sporangial stalk (Fig. 1.206) reveals it contains a large number of small electron dense vesicles which are derived from the Golgi dictyosomes. The high concentration of small vesicles

would account for the refractile appearance of this zone (Fig. 1.200).

The LS profile of the sporangial stalk in Fig. 1.207 reveals a more complex organisation than the region shown in Fig. 1.206, and probably represents a more advanced stage in septum development. There is a distinct zone in the sporangium stalk, in the region of presumed septal insertion, which can be distinguished from both the upper sporangial and lower hyphal cytoplasm (Fig. 1.207). This region is composed of three blocks of densely staining groundplasm, and contains mainly membrane cisternae, small electron dense vesicles and the occasional mitochondrion (Fig. 1.208). It seems likely that the dense blocks are part of a single zone, corresponding to the dense band observed in the light microscope (Fig. 1.201), which has become slightly broken during fixation. The striking feature about these dense blocks of cytoplasm is that they are delimited by a more or less continuous boundary membrane (Figs. 1.207, 1.208). It is suggested that in developing septa this membrane between the dense and normal phases may eventually extend the entire width of the stalk, and form a suitable 'surface' at which wall material can be discharged.

Unfortunately no further intermediate stages between this, and the fully inserted tripartite septum (Fig. 1.209) have been found. Therefore the way in which the curious tripartite structure of the septum arises must still be a subject of conjecture.

In spite of the oblique, peripheral, profile of the septum shown in Fig. 1.209, it almost certainly represents a newly inserted septum because of the thinness of the two wall layers, which are only 60 nm in diameter. This septum also has an extraordinarily broad vesicular layer, which closely resembles both in its density and membraneous composition the dense material described in the preseptal sporangial stalk (Fig. 1.208).

As the septum matures the two wall layers thicken (from 50-60 nm to 100-150 nm) and the intervening vesicular layer becomes much compressed and apparently reduced (Fig. 1.210). This suggests the entrapped vesicular layer might also contribute some material to the septal wall layers, in addition to the wall accretion from the surrounding cytoplasm. The vacuolation of the subtending hyphal stalk and the distended convexo-concave profile of the mature sporangial septum are both clearly shown in Fig. 1.210.

1.2.5.2 Gametangial Septa

Mature oogonial and antheridial septa are shown in Figs. 1.211 and 1.212 respectively. Both of these septa have the characteristic tripartite structure described above for the sporangia, and appear to be formed in the same way. The oogonial septum (Fig. 1.211) has a concavo-convex profile, indicating a higher turgor pressure in the differentiating oogonium than in the subtending hypha. However, after cleavage this distension of the septum

is lost (Fig. 3.11). The upper layer of the oogonial septum is always much thicker (200-300 nm) than the lower wall layer (100 nm), and reflects the greater synthetic capacity of the oogonial cytoplasm. The entrapped vesicular layer is between 100-350 nm thick, and is composed mostly of small electron-dense vesicles (Fig. 1.213). This vesicular layer frequently has strands of wall-like material threading through it, but under normal conditions never contained large vacuolar compartments or lipid material (Figs. 1.211, 1.213).

The antheridial septum (Fig. 1.212) is curious in that the two septal wall layers diverge markedly as they approach the side of the stalk adjacent to the oogonium body. This gives it a trumpet-like appearance in profile (Fig. 1.212). The upper and lower wall layers are almost of equal thickness in the antheridial septum.

1.2.6. Sporangium Development in Phytophthora cactorum

This brief and rather limited account of the ultrastructural cytology of the sporangia of P.cactorum, shows that this species is similar in its structure to other Phytophthora species (see literature review, Section 1.1). Sporangium formation was not followed in this study and only the morphology and cytology of the deciduous sporangia will be described.

1.2.6.1 Sporangium cytology

The sporangia of P.cactorum are borne on aerial sporangiophores from which they are easily detached. Each ovoid sporangium is approximately 40 x 30 µm in size and has a rounded refractile papilla at its apex Each sporangium is delimited by a plug of wall material in the basal stalk. Both the papilla and basal plug are composed of amorphous electron-transparent material (Fig. 1.216) although the latter contains vesicular pockets. The sporangium wall in Phytophthora is much thicker (<1.5 µm) than in Saprolegnia sporangia and is composed of two distinct layers (Fig. 1.215). The outer wall layer is thin (80-90 nm) and is continuous with the sporangium stalk and caps the papilla. It is in effect the morphological equivalent of the wall in Saprolegnia. The inner amorphous wall layer is about 1.5 µm thick (Fig. 1.216) and may increase in electron density towards its periphery (Fig. 1.218). The sporangial cytoplasm is quite dense and has a lumpy texture (Fig. 1.215).

The sporangial groundplasm contains a high denstiy of ribosomes and abundent cisternae of single ER (Figs. 1.222-1.224). The latter are frequently organised in parallel arrays of 2-3 cisternae in the sporangial cytoplasm. The mitochondria usually have short rounded profiles and contain small electron-transparent cristae (Figs. 1.223). Although sporangial dictyosomes are quite common they do not show the close mitochondrial association which was so common in Saprolegnia (Fig. 1.224). At this stage the Golgi produce small electron transparent vesicles (Fig. 1.224), which apparently contribute to the

vacuolar and axonemal vesicle systems (King & Bulter 1968, Elsner et al. 1970).

However, these sporangia still contain the usual peripherally distributed wall vesicles, which have fine granular contents in this GaOs-fixed material (Figs. 1.222, 1.223). In addition to the wall vesicles, the sporangia also contain a number of slightly larger (c.100 nm) vesicles, with more electron dense particulate contents (Fig. 1.223). These are the so called fibrous bodies which migrate to the periphery of the zoospores and behave as bar equivalents (Hemmes & Hohl, 1972a).

The electron transparent vacuolar vesicles in these sporangia are usually rather small, and rarely exceed 400 nm in diameter (Fig. 1.223). They are normally randomly distributed throughout the cytoplasm (Fig. 1.216) although in some of the older sporangia they aggregate and coalesce to form a small vacuole similar to that which develops in germinating bodies (Fig. 1.217).

The sporangial cytoplasm contains a high density of neutral lipid and densebody granules, which together account for over 50% of the cytoplasmic volume (Fig. 1.216). The densebody granules are very varied in their appearance, particularly in GaOs-fixed material (Figs. 1.220-1.221, 1.223). The densebody granules are between 200-400 nm in size, and are frequently elipsoidal in profile (Fig.1.223). These bodies usually contain electron transparent cores and are embedded in a matrix of amorphous material (Fig. 1.223). Occasionally the densebody vesicles become lamellate throughout, with a regular periodicity of 10 nm (Fig. 1.220), showing their structural homology to the densebody vesicles in the Saprolegniaceae. In contrast the Os-fixed densebody vesicles are composed of a uniform amorphous material with an electron-transparent core (Fig. 1.219).

The nuclei in these sporangia are randomly distributed and have ovate or spherical profiles (Fig. 1.223). They have a densely particulate nucleoplasm and a more electron dense nucleolus. Centrioles were not observed with these nuclear profiles.

1.2.6.2. Zoospore differentiation

The sporangia are induced to differentiate into zoospores by chilling at 4°C for 2 minutes before incubating at 16°C. A central vacuole soon develops in the sporangial cytoplasm and the nuclei become peripherally orientated (Fig. 1.217). As in Saprolegnia the nuclei acquire a pyriform morphology, but flagellar differentiation commences immediately. As the flagella microtubules are generated by the basal apparatus they are ensheathed in an axonemal vacuole (Fig. 1.222) and lie parallel to the cell wall (Fig. 1.217). The peripheral vacuolar vesicles also start to enlarge and become aligned between the nuclei (Fig. 1.217).

As cleavage progresses the protoplast starts to rock gently as the flagella become active. Zoospore cleavage then takes place and the individual spores can be seen moving in the sporangium. At dehiscence the papilla dissolves and the zoospores escape, enclosed in a transparent vesicle. The vesicle ruptures a few seconds after release and the zoospores swim away. The zoospores of Phytophthora cactorum are reniform and resemble the secondary spores of Saprolegnia (Fig. 1.33). Providing the suspension is induced in 2% dextrose the zoospores remain active for several hours before encysting. If the zoospores are liberated in distilled water, however, they lyse within a few minutes of their release. Quadriflagellate zoospores, which have not fully separated, are not uncommon in this species. The final stages of cleavage were not followed ultrastructurally.

1.3 DISCUSSION

The ultrastructural development of Saprolegnia and Phytophthora described in this study follows the same pattern of development to that previously described for these or closely related Oomycete species (see literature review, Section 1.1). Nevertheless some of the organelle associations and developmental stages require some re-evaluation in the light of the present studies and other recent findings.

1.3.1 The Parallel Arrays of Endoplasmic Reticulum

In their study on S.ferax, Heath and Greenwood (1971) suggested that the parallel arrays of rough ER which occur in developing sporangia might be an effect of cytoplasmic dehydration during cleavage, since similar arrays had been reported in dehydrated seeds. However this does not explain, a) why the maximal arrays of ER occur before vacuolation (Hagedorn & Weinert, 1974), and b) why similar arrays do not occur in developing oogonia during cleavage. Podbielkowska et al. (1975) have recently reviewed the occurrence of similar ER arrays in higher plant cells. They concluded that these arrays developed in response to either a high turn-over or rapid depletion of protein synthesis products.

In Saprolegnia sporangia the immediate precleavage period is associated with the synthesis of flimmer tubules and bars, both of which have proteinaceous components (Heath, Greenwood & Griffiths, 1970; Bimpong & Hickman, 1975). In addition, biochemical studies on Achlya bisexualis have also shown that lysosomal enzyme activity reaches its maximal extent during this period (O'Day & Horgen, 1974; Horgen & O'Day, 1975). These lysosomal (lytic) enzymes are associated with a membrane-bound fraction of cell organelles approximately 400-500 nm in diameter. In Saprolegnia ferax the only cell organelle of this size to reach its peak during the precleavage period are the multivesicular bodies (Hagerdorn & Weinert, 1972). This supports the claim that these bodies are associated with the lysosomal autolysis of cell organelles (Heath, 1975a).

Thus the conditions of high protein synthetic activity and rapid product utilisation necessary for the formation of parallel ER arrays are both fulfilled in precleavage sporangia. The absence of similar arrays in developing oogonia probably indicates a lower turnover of proteinaceous components, due to the lack of bar and flimmer tubule production.

1.3.2 Densebody Vesicle Function

This study has confirmed that in Saprolegnia colonies grown on dilute nutrient media such as GYPS, densebody vesicles are confined exclusively to the reproductive structures (Gay, Greenwood & Heath, 1971). The evidence for the phospholipid nature of these bodies outlined in the literature review (Section 1.1.2.2) is further supported by the demonstration of

phosphatid-like bodies (Moor & Mühlethaler, 1963) in the freeze-fracture profiles of oospores. In spite of their widespread occurrence very little is known of the genesis of densebody granules. There is some circumstantial evidence in this study that densebody granules may be accreted in expanded cisternae of smooth ER. This is also the proposed origin of vacuolar vesicles in fungi (McClure, Park & Robinson, 1968), and suggests both densebody and vacuolar vesicles may have a common origin. However the suggestion of Gay, Greenwood and Heath (1971) that the densebody vesicles are the sole origin of cleavage vacuoles should be questioned on the following counts:

1. The relatively small number of densebody vesicles present among the elaborate vesicle complexes which proceed vacuolation (Figs. 1.44, 1.74).
2. The almost complete absence of densebody granules in developing vacuolar vesicles.
3. The failure to observe a decline in the volume fraction of densebody granules during vacuolation.

Although it was proposed that densebody granule dissolution may be the motive force behind vacuolation (Gay, Greenwood & Heath, 1971), the presence of intact densebodies in expanding cyst and oospore vacuoles indicate this is not necessarily so. Therefore, although the utilisation of a small number of densebody vesicles during cleavage-vacuole formation in Saprolegnia cannot be excluded, it is probably best not to look upon these bodies primarily as part of the cleavage apparatus. Certainly, these bodies play no part in cleavage-vacuole formation in Phytophthora.

The failure to observe densebody granules in germinating cyst vacuoles (described by Gay, Greenwood & Heath, 1971; Colt & Endo, 1972; Hoch & Mitchell, 1972b; Bimpong & Hickman, 1975) deserves comment. Bimpong and Hickman (1975) have demonstrated in Phytophthora zoospores that lipid metabolism is far less important in germinating cysts than in zoospores. The excess densebody granules are deposited in the cyst vacuole prior to their reabsorption. In the absence of exogenous energy reserves the zoospores of S.ferax need to hydrolyse their densebody granules to provide the energy necessary for germination, and therefore the disposal of densebody reserves into the vacuole does not take place.

The role of densebody vesicles in ooplast formation proposed by Howard and Moore (1970) in their study on S.terrestris has been confirmed in S.furcata. However this study has revealed that changes take place in the structure of the ooplast matrix material during maturation which are not detectable in $KMnO_4$-fixed spores. It is suggested that during ooplast vacuole formation the densebody granules remain embedded in a colloidal gel. Both the osmiophilic nature of this matrix and the presence of myelin-like configurations within it suggest this material is a polar lipid. The formation of

colloidal gels in suitable polar lipid:water dispersions is well documented and is favoured by a high lipid:water ratio and the presence of divalent cations (Kavanau, 1965). The necessary dehydration of the oospore cytoplasm is probably brought about by the formation of the endospore wall layer. Certainly the development of the rather similar cortex in bacterial spores has been shown to dehydrate the protoplast (Gould & Dring, 1975). If the matrix material is of similar optical density to the densebody granules the latter will not be distinguishable in the ooplast. The final stage of ooplast development in Saprolegnia must therefore involve the liquifaction of the matrix, enabling the granules to undergo Brownian motion. This final stage is inhibited by cycloheximide, which probably indicates it is an enzymic autolysis.

Oospores with uniformly transparent ooplasts have been termed 'expersate' by Howard (1971), and this is considered to be an important taxonomic feature. Dick (1971) has reported that there is considerable variation in the presence of motile ooplast granules in the genus Aphanomyces. In some species he was even able to detect what were apparently stationary granules. He therefore concluded that granules were always present in the ooplast vacuoles in the Saprolegniaceae, even though they were not always visible under the light microscope.

However Dick (1969, 1971) suggested that the Saprolegnian ooplast was probably not homologous with the central oospore globules which occur in the Peronosporales. However recently ultrastructural accounts of Peronosporalean oospores have demonstrated that the large reserve globule in these, is also derived from the expansion and coalescence of densebody vesicles (Hemmes & Bartnicki-Garcia, 1975; McKeen, 1975). Indeed the ooplast in these spores appeared almost identical to the ooplast described in cycloheximide induced oospores of Saprolegnia. It is therefore proposed that the structural homology of the ooplast vacuole in oospores extends throughout the Oomycetes, and not just to the Saprolegniales as suggested by Dick (1971).

1.3.3 Gametangial Nuclear Division

This account of the ultrastructure of gametangial divisions in S.furcata indicate they follow the same pattern, at least during prophase I, to those described in S.terrestris (Howard and Moore, 1970), A.ambisexualis (Ellzey, 1974) and T.clavata (Heath, 1974a). Most of the features which have been used to identify these divisions as meiotic (Outlined in literature review, Section 1.1.3.3) were observed in S.furcata. The condensed uniaxial elements which appear in the expanded prophase I nuclei are morphologically homologous to the lateral elements of the synaptinemal complex (Howard & Moore, 1970). These elements are believed to form between the sister chromatids of each chromosome during leptotene (Moses, 1968; Westergaard & von Wettstein, 1972).

The absence of the synaptinemal complex between these paired uniaxial elements is a common feature of all the members of the Saprolegniaceae so far described. It also distinguishes this group from the meiotic prophase I nuclei of most other fungi (e.g. Myxomycetes: Aldrich & Mims, 1970; Yeast: Zickler, 1970; Moens & Rapport, 1971; higher Ascomycetes: Westergaard & von Wettstein, 1970; and Basidiomycetes: Lu, 1970; Gull & Newsam, 1975).

This observation has significant genetic implications. It is now generally accepted that the synaptinamal complex is not necessary for homologeus chromosome pairing, but is essential for chiasma formation and crossing-over (Westergaard & von Wettstein, 1972). However recent light-microscopic studies on prophase I nuclei have demonstrated chiasma in both the Saprolegniales and Peronosporales (Win-Tin and Dick, 1975; Brasier and Sansome, 1975). There are several explanations which could account for these apparently conflicting observations:

1) The small number of species so far examined ultrastructurally are all genuinely achiasmate.

2) The Saprolegniales may be a rare, possibly unique, example of chiasma formation independent of SC development.

3) The SC is not preserved in the prophase I nuclei of these species.

4) The presence of the SC is so transitory that it has not yet been detected in the ultrastructural studies.

Certainly the preservation of the SC in fungi can be variable, and its absence has been noted in a few strains of yeast and some other fungal species (P.Moens, personal communication). However unlike these fungi the overall preservation of Oomycete nuclei is very good, and therefore it is rather surprising that the SC is not observed in this group. Furthermore the distance between the uniaxial elements (150 nm) is typical of the pre-synaptinemic separation noted in other fungi during early zygotene (Westergaard & von Wettstein, 1972). The formation of the SC draws the two lateral elements together and reduces the distance to c. 100 nm. This suggests the Saprolegniaceae may be truely asynaptinemic. Obviously a much wider range of species, including those in which chiasma have been observed in the light microscope, need to be examined to verify this. Future genetic studies may also be able to confirm whether crossing-over occurs in this group or not.

Win-Tin and Dick (1975) have recently shown multiple chromosome associations in prophase I nuclei in a number of Oomycete species including S.furcata. In ultrastructural studies on higher plant polyploids, the homologous lateral elements usually become aligned side by side, and the SC switches between the different pairing partners (Moens, 1970). However there was never any sign of more than two aligned unaxial elements in S.furcata nuclei.

Many of the light-microscopic studies on gametangial nuclear divisions in Saprolegnia revealed prominant aster bodies associated with the prophase I nuclei. These were retained until after oospore fertilisation (e.g. Trow, 1904; Weston, 1918; Zeigler, 1953). Aster bodies were not however observed in the light microscope in mitotic divisions. However ultrastructural studies have not shown the aster microtubules associated with meiotic centrioles to be conspicuously more abundant than those associated with mitotic centrioles (Heath and Greenwood, 1970b; Heath, 1974a). It is interesting that the development of the electron-dense sheath which surrounds the prophase I centrioles correlates with the appearance of the prominant aster bodies in the light-microscope, and also persists until about the time of fertilisation (Howard and Moore, 1970).

This electron-dense sheath resembles the pericentriolar halo which forms around the centrioles during nuclear division in both mammals (Robbins, Jentzsch and Micali, 1968; Rattner, 1972) and in the lower fungus, Sorosphaera (Braselton and Miller, 1973). In both these examples the amorphous sheath material is believed to be involved in microtubule generation. Aster microtubules similarly terminate in the sheath material in Saprolegnia, which suggests it is homologous to the above structures. This sheath may develop to facilitate the enhanced aster development suggested by the light-microscope accounts, but not revealed in ultrastructural preparations.

The enclosing of the centrioles by an endomembrane between late prophase I and anaphase I is associated with the period when the centrioles are located at the poles of the elongating nuclei. This cap is superficially similar to the cisternal cap which forms adjacent to the microtubule organising center in meiotic ascomycete nuclei (e.g. Zickler, 1970; Moens and Rapport, 1971). However, in the latter this cisternal cap then extends to delimit the ascospores, whereas in Saprolegnia it disappears before the onset of prophase II.

The elongation of the centriole microtubules during prophase I has not been reported before. The only other stage in the life cycle at which the elongation and separation of the centrioles take place is during kinetosome formation, which accompanies zoospore cleavage (Heath & Greenwood, 1971). This may therefore be a vestigial developmental pattern remaining from an ancestral form which possessed motile sexual gametes. In relation to this, it is interesting to note that the structurally-similar Vaucherian algae (Manton, 1965; Heath & Greenwood, 1971) produce motile male gametes (Ott & Brown, 1974b).

The amorphous body which replaces the centriole in the oosphere nuclei of S.furcata resembles a procentriole. Similar bodies have been described in both Phytophthora sporangia (Williams & Webster, 1970) and in mammal cells

(Robbins, Jentzsch, & Micali, 1968). However Heath (1974b) questioned the presence of such a body in the former, and suggested it may simply represent a poorly-fixed centriole. However the loss of centrioles during meiosis has also been reported in mammal oocysts (Szallosi, Calarco & Donahue, 1972). Therefore it is likely that the female and possibly the male centriole reverts to a procentriolar state following meiosis. Centriolar behaviour in Saprolegnia also differs from that described in mammal sperm, in that the centrioles do not replicate prior to prophase II (Rattner, 1972) but simply separate.

1.3.4. Fertilisation

The occurrence of fertilisation in the Saprolegniaceae has been the centre of much controversey, which has been reviewed by Dick (1972) and Dick and Win-Tin (1973). This ultrastructural study on S.furcata indicates that oospore fertilisation does proceed via the fertilisation tube as demonstrated in Achlya polyandra by Trow (1904). Recently Flanagan (1970) claimed that the antheridial nuclei are released into the oogonium prior to cleavage, and that karyogamy has already taken place at the time of oospore differentiation. He considered the fertilisation tube to be non-functional. From this study there is no evidence to support the formation of a hypothetical pore between the antheridium and oogonium during Stage IV suggested by Flanagan (1970). In addition the nuclear number and size changes during oospore maturation are not consistent with such a hypothesis.

Since fertilisation tube formation occurs after the oospheres have acquired their outer wall, fertilisation does not take place at the naked protoplast stage as suggested in many early accounts (e.g. Trow 1895, 1904). Indeed oospore penetration appears to be strictly comparable to oogonium penetration. Although the rupture of the fertilisation tube and the release of its contents was not observed there is good indirect evidence that it takes place. The collapsed profiles of the fertilisation tubes in Stage VIII-X spores are similar to the post-fertilisation tubes observed in Phytophthora (Hemmes & Bartnick-Garcia, 1975). These fertilisation tubes have been regularly observed discharging their contents in the light-microscope (e.g. Blackwell, 1943).

In S.furcata nuclear fusion (karyogamy) probably takes place during or shortly after ooplast formation. This seems to be the commonest situation in the Saprolegniaceae (Dick & Win-Tin, 1973). The large size of the fusion nucleus and its unusual ultrastructural cytology may explain why the first division of this nucleus has often been misinterpreted as meiotic (Claussen, 1904; Zeigler, 1953).

1.3.5 Wall Development

1.3.5.1 Golgi-mediated Wall Deposition

The occurrence of small membrane-bound vesicles at all sites of wall formation (Heath, Gay and Greenwood, 1970) has been confirmed in this study.

The claim that these wall vesicles are derived from Golgi dictyosomes (Grove, Bracker and Morré, 1970; Heath, Gay and Greenwood, 1971) is also supported, although it is clear the Golgi-vesicles expand and acquire further contents as they migrate to the cell periphery. Additional evidence for the role of the Golgi dictyosomes in wall synthesis comes from the correlation of the Golgi-ER-mitochondrion association, with periods of active wall synthesis. In studies on the transport of secretory proteins in the pancreatic exocrine cell it has been shown that the secretion of vesicles from the periphery of the Golgi-complex is energy dependent (Jamieson and Palade, 1968). Therefore, the intimate mitochondrion-Golgi association observed in Saprolegnia would always provide a coupled energy supply to ensure the efficient dispatch of wall precursors from the dictyosome. This may be an important adaptation in a coenocyte such as Saprolegnia.

By regulating its organelle associations, the cell may also be able to govern the function of an organelle such as the dictyosome. Thus in the sporangia when the dictyosomes transfer their allegiance from the mitochondria to the nuclei they also change their function from wall synthesis to alveolar vesicle production (Heath and Greenwood, 1971). This may account for the absence of the mitochondrion-Golgi association in mature Phytophthora sporangia, in which all the developmental stages requiring wall synthesis have been completed. In addition such a system in which dictyosome function is related to its organelle association would afford the possibility of the cell being able to employ the dictyosomes in several different functions at the same time.

1.3.5.2 Septum Development

The development of the basal septum in Saprolegnia sporangia and gametangia is still enigmatic. Heath (1969) suggested the rapid rate of crosswall insertion may account for the entrapped vesicular layer, but did not speculate on why such a uniform tripartite structure always results. The accumulation of small electron dense vesicles in the sporangium stalk described by Heath (1969) has also been shown in this account. They appear to be unchanged Golgi vesicles rather than wall vesicles. It is proposed that as septum development proceeds these small vesicles become compacted into a well-defined zone which can be distinguished as a dense band in the light-microscope. This zone eventually becomes delimited by the membrane-cisternae which can be seen aligning themselves along its margins. This vesicular zone may prove structurally rigid enough to isolate the sporangial and hyphal protoplasts. This would allow the wall layers to be accreted in the usual way along both the upper and lower edge of this proposed 'vesicular plate.' The exact way in which wall accretion proceeds, and whether both upper and lower layers

develop concurrently is unclear.

Once the two wall layers are inserted they are rapidly thickened by both material from the surrounding cytoplasm and probably from some of the entrapped vesicles. The latter suggestion is supported both by the frequent observation of strands of wall-like material threading through the vesicular layer. The central parts of the septum become compacted by the turgor pressure exerted by the surrounding cytoplasm. Such a developmental sequence would account for the tripartite nature of the Saprolegnian septum, and explain why the rim of the septum is always wider than the central parts. The tumpet-like profiles of the antheridial septa can be explained by the development of a wedge-shaped rather than disc-like vesicular layer. This develops because of the polarised attraction of Golgi vesicles to the side of the antheridial stalk closest to the oogonium body.

1.3.4.3 Oospore Wall Formation

The occurrence of a tru ly naked phase after oospore delimitation was questioned by Gay, Greenwood and Heath (1971), but has been clearly demonstrated in this account. As in other stages of the life-cycle the formation of the primary wall around the oospores appears to be initiated solely by the discharge of the typical peripheral wall vesicles. In this respect oospore wall formation closely resembles that described in isolated fungal protoplasts (Gibson & Peberdy, 1972; Carbonell, Gil & Yegres, 1973). In oospores however wall formation is completed within 30 minutes, whereas it takes between 24-48 h in protoplasts. As in the encysting zoospores (Bartnicki-Garcia, 1973b) there is no evidence of preformed wall microfibrils being deposited by the wall vesicles, and it is likely that these assemble themselves at the plasmalemma surface.

The mechanism by which the oospores decrease their volume during the period of wall formation is rather obscure. The observed volume reduction (c. 30%) could be achieved by the discharge of approximately 5 extruded globules of c. 5 μm diameter per spore. However in generally only one large globule of this size was observed being extruded by most spores, although a number of smaller globules were also liberated. This cytoplasmic extrusion probably accounts for only some of the observed shrinkage. The discharge of the material necessary for wall development from the spore cytoplasm may also contribute to the volume reduction. It is still difficult to explain the apparent reabsorption of some of the discharged cytoplasmic globules by neighbouring spores, as this would increase spore volume.

The centripetal accretion of the thick endospore wall layer in Saprolegnia oospores is of considerable interest in that it occurs independently of the usual wall vesicles, as has been noted in Phytophthora (Hemmes and Bartnicki-Garcia, 1975). It differs in this respect from the

superficially similar sporangial wall in Phytophthora (Christen and Hohl, 1972) and thick spore walls of other fungi (e.g. Arcyia cinerea: Mims, 1972; Poronia punctata: Stiers, 1974). The following observations suggest the endospore wall is accreted inside the original oospore plasmalemma:

a) The absence of a detectable membrane between the endospore layer and the oospore cytoplasm, at least during the period of wall accretion.

b) The presence of a well-defined tripartite membrane-like layer between the primary wall and the endospore wall.

c) The lack of membrane-bound vesicles in its deposition.

These observations support Dick's (1969) suggestion that the endospore wall may be looked upon as the peripheral phase separation of oospore reserve products. However the trapping of the plasmalemma between two wall layers is extremely unusual, although it has been reported during the formation of the casparian strip in barley roots (Robards et al., 1972).

There is little doubt however that the mature oospores have an inner membrane between the endospore layer and the spore cytoplasm. Therefore it seems probable that the endospore wall is bounded on both its inner and outer surface by a membrane. A similar arrangement exists in Ascomycete fungi, in which the wall is accreted between the double-membraned cisternae which delimits the spores (e.g. Stiers, 1974). This clearly cannot occur in Saprolegnia oospores.

Two questions must be asked; what is the origin of the two membranes and which is the functional plasmalemma? The gram negative bacteria are another group of organisms with two membrane-like layers associated with their walls. In this group the outer membrane is an additional polar lipid layer, whose formation is governed by the inner membrane, which is the functional plasmalemma (Rogers, 1970; Fox, 1972). An outer tripartite membrane-like layer also forms outside the walls of Chlorella, and it was suggested this layer was composed of sporopollenin (Atkinson, John and Gunning, 1974). If a similar material to this is present in Saprolegnia oospores this may account for the impermeability of oospores and explain the apparently high polysaccharide deposit in this region. However recently polysaccharides have been demonstrated with the membrane sheath of powdery mildew haustoria (F.Gil & J. Gay, personal communication). Therefore the high polysaccharide content of this outer layer does not exclude its plasmalemmar origin.

If it is assumed, as suggested, that the inner membrane is not the original plasmalemma, its origin has to be explained. The literature contains no accounts of denovo plasmalemmar assembly on a 'naked' inner wall surface. Most studies on membrane genesis have shown that membranes develop by the intersusception of new components into existing membrane structures (Novikoff & Holtzman, 1970; Finean, Coleman & Michell, 1974). It is therefore

possible that the abundant membran ous fragments in the peripheral oospore cytoplasm may become aligned along the inner surface of the endospore and coalesce to form the new plasmalemma. There are a few profiles of tapwater-induced oospores in which the inner endospore membrane is only partially complete. Clearly these studies need to be extended to resolve the true nature of the two endospore membranes, preferably using a technique such as freeze-fracture to overcome the fixation difficulties.

The formation of the inner electron dense layer within the accreted endospore wall, is similar to the differentiation of the thickened wall of many ascospores (e.g. Poronia punctata ascospores; Stiers, 1971). Since this inner layer cannot be differentiated in GaOs-fixed spores it may explain the absence of such a layer in Peronosporalean oospores (Hemmes & Bartnicki-Garcia, 1975; McKeen, 1975). Since the formation of this inner endospore layer coincides with the observed reduction in spore organelles, it is probably composed of organelle breakdown products, (e.g. lipids and proteins). There is some evidence this occurs in Phytophthora oospores. Although ribosomes cannot be isolated from mature oospores, ribosomal subunit components are extracted with the cell wall fraction (Leary, Roheim and Zentmeyer, 1974).

The composition of the endospore wall is likely to be quite complex since it accounts for over 30% of the mature oospore volume, and is derived in its entirety from the spore protoplast. In Pythium there is some evidence that the surrounding periplasm may contribute material to the differentiating endospore (McKeen, 1975) but this cannot occur in Saprolegnia. A recent biochemical analysis of the oospore walls of Phytophthora megasperma var. sojae, indicate that a β1-3 linked glucan is the major component, with proteins and lipid accounting for a further 25% (Lippman, Erwin & Bartnicki-Garcia, 1974).

In Saprolegnia, PASM staining indicates polysaccharides (probably glycoproteins, Thiery & Rombourg, 1974) are distributed more or less uniformly throughout the endospore layer, and are probably the major constituent of the wall matrix.

The sequence of events discussed above in relation to the formation of the oospore wall is summarised diagramatically in Fig. 1.225.

PART 2

THE EFFECT OF STREPTOMYCIN ON GROWTH AND REPRODUCTION IN SAPROLEGNIA

This section describes in detail the morphological, cytological and physiological effects of streptomycin on the growth and reproduction of Saprolegnia spp. In addition, both the effects of this antibiotic on spore formation in a Phytophthora sp. and of two other protein synthesis inhibitors, chloramphenicol and cycloheximide, are included for comparison. The latter are both known inhibitors of Oomycete mitochondrial (Marchant & Smith, 1968) and cytoplasmic protein synthesis (Timberlake et al.) respectively. The antibiotic names are abbreviated in the results section using the notation given in Section 6.1.3.

2.1 LITERATURE REVIEW

The effect of streptomycin on micro-organism and plants

'Streptomycin = an inhibitor of bacterial metabolic activity with a pronounced stimulation of human investigatory activity'.

Gale et al. (1972).

2.1.1 Structure of Streptomycin

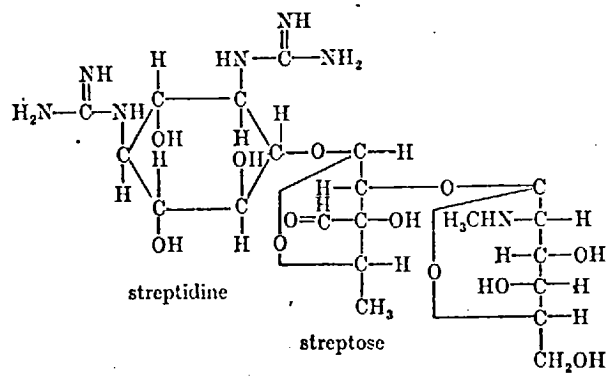
Streptomycin was isolated from two strains of Streptomyces griseus after the intensive screening of many thousands of micro-organisms (Schatz, Bogie and Waksman, 1944). Accounts of the biological, chemical and physical properties of streptomycin and its derivatives have been given in reviews by Regna (1959), Brock (1966) and Kazybski et al. (1967). Streptomycin is a triacidic base, with an empirical formula of $C_{21}H_{39}N_7O_{12}$, and is composed of the following subunits; streptidine, streptose and N-methyl-L-glucosamine. These three subunits are linked by glycosidic bonds as shown in Fig. 2.1. Nuclear magnetic resonance studies show that the aldehyde group undergoes an intramolecular reaction with the secondary amine to produce a carbolamine tautomer, from which a quatenary iminium hydroxide is established (Fig. 2.1, Aronson, Meyer & Brock, 1964). The two guanido groups ionize in aqueous solution, so that streptomycin normally behaves as a divalent cation (Fried & Wintersteiner, 1947). Streptomycin readily forms a variety of salts and the most common commercial formulations are the sulphate, trihydrochloride and calcium double salts

2.1.2 The Effect of Streptomycin on Prokaryotes

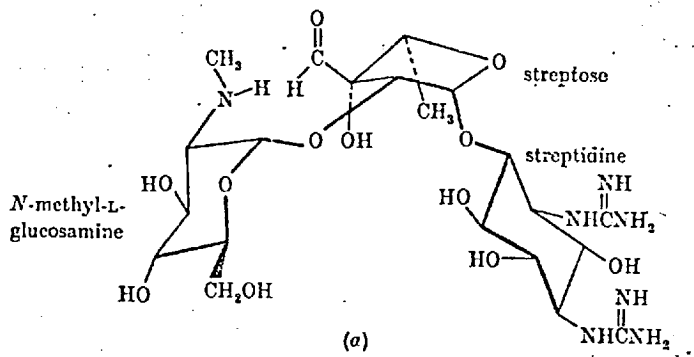
Most of the work on the effects of streptomycin on prokaryote organisms is beyond the scope of this review. A brief account of the main effects of streptomycin on this group will be given for cross reference with the eukaryote studies. The extent to which the understanding of the mode of streptomycin action on bacterial cells has advanced over the past two decades is illustrated by the frequent reviews of antibiotic action (Eagle & Saz, 1955; Goldberg and Luckey, 1959; Brock, 1966; Jacoby and Gorini, 1967; Pestka, 1971; Gale et al.,1972; Vasquez, 1974).

Streptomycin results in a wide variety of metabolic lesions when added to actively growing bacterial cells. These effects are probably best summarised in the study of Dubin, Hancock and Davis (1963) who described the sequential series of events which followed antibiotic addition to an exponentially growing culture of Escherichia coli cells. The first observable antibiotic effect was an immediate efflux of potassium ions (K^+) which was followed by a transient stimulation in RNA synthesis. Protein synthesis then ceased and there was a secondary uptake of antibiotic into the cells. This coincided with the leakage of macromolecules from the intracellular pools

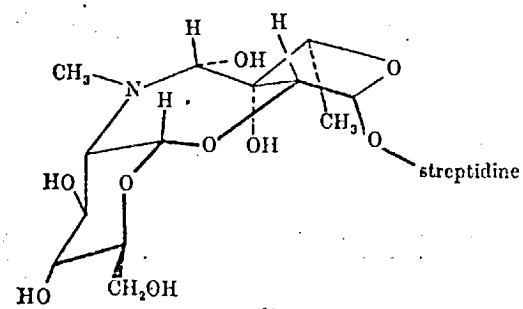
Fig. 2.1 The chemical structure and molecular conformation of streptomycin (From Brock, 1966)



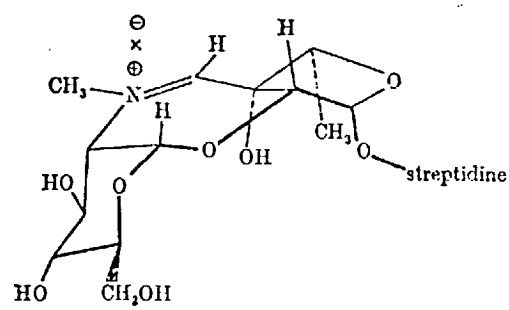
Streptomycin.



(a)



(b)



(c)

(a) Streptomycin; (b) carbinolamine form of streptomycin; (c) streptomycin cyclic iminium salt.

and the concommittant loss of cell viability. Finally respiration ceased, some 40 minutes after the addition of the antibiotic.

Since ion leakage was the first detectable streptomycin effect, it was suggested the cell membrane might be the primary target for antibiotic activity (Anand, Davis & Armitage, 1960; Dubin, Hancock & Davis, 1963). However the acquisition of streptomycin resistance or dependence has been shown to be the result of changes in a single 30S ribosomal subunit protein (Ozaki, Mizushima & Nomura, 1969) which suggests ribosomes are the primary antibiotic target. However in some bacterial species the acquisition of streptomycin resistance also affects the composition of the cell wall, indicating several cellular sites may be involved in the acquisition of resistance (Lawrence, 1969 cited by Pestka, 1971). Polglase (1965) suggested that streptomycin exerts its effects by binding non-specifically to all intra-cellular cationic sites, including ribosomes.

Experiments on cell-free protein synthesising systems showed that streptomycin interfered with the fidelity of the translation of certain synthetic messengers (Flahs, Cox, & White, 1962). The occurrence of streptomycin-induced misreading of mRMA in living cells has also been demonstrated (e.g. Gorini and Kataja, 1965) although its importance in relation to the loss of cell viability is disputed (Gorini & Kataja, 1964; Branscomb & Galas,1975).

Studies into the effects of streptomycin on cellular protein synthesis in Escherichia coli have been carried out by Modelell and Davis (1969) and Luzzato, Apirion and Schlessinger (1969). Although these two groups propose slightly different models to explain the streptomcyin effects, both show the antibiotic results in the breakdown of polyribosomes with the concomitant formation of aberrant initiation complexes. These are unable to function in further protein synthesis, and their accumulation is responsible for the loss of cell viability (Luzzato, Apirion and Schlessinger, 1969; Miskin and Zamir, 1974). All the varied effects of streptomycin on protein synthesis can be explained by the binding of the antibiotic to the acceptor (A) site on the 30S ribosomal subunit. The antibiotic-distorted A site is then unable to carry out its normal functions and protein synthesis is inhibited (Gale et al., 1972; Vasquez, 1974).

2.1.3 The Effect of Streptomycin on Eukaryotes

2.1.3.1 Mammalian Cells

Eukaryote organisms are considered to be relatively unaffected by streptomycin, probably as a result of their apparent impermeability to the antibiotic (Goldenbaum & Fukui cited by Brock, 1966). Some mammalian tissue-culture cells are killed by very high streptomycin concentrations (c.10,000 mg/l), but only in the presence of cysteine (Moskevitz & Kelker, 1965). The toxicological effects of streptomycin on mammals include damage to the

vestibular and cochlear branches of the 8th nerve, which results in vertigo and deafness (Mückter, reviewed by Brock, 1966). However eukaryote 80S ribosomes (from rabbit reticulocytes) are apparently resistant to streptomycin (Brock, 1966).

2.1.3.2 Algae and Higher Plants

The toxic effects of steptomycin on higher plants were largely discovered during the screening of antibiotics for their effectiveness against plant pathogens. These studies have been reviewed by Brian (1957) and Goodman (1959). Streptomycin (< 200 mg/l) usually results in a general stunting of plant growth. Its morphological effects include chlorosis (Anderson and Nienow, 1947;Von Euler, 1948; Rosen, 1954a), stem shortening and incomplete leaf expansion (Rosen, 1954a) and the inhibition of root growth (Rosen, 1954a; Gray, 1955;Alcorn and Ark, 1956; McMeekin, 1973). Although higher plants show considerably variation to streptomycin toxicity (Marlatt, 1956; Alcorn and Bachelder,1956) the meristematic and embryonic tissues are always the most sensitive (Goodman, 1959). Perhaps related to this, it was noted that streptomycin induced chromosomal abnormalities in the root-tip cells of Tradescantia, similar to those produced by other mutagens (Tanaka and Sato, 1952 cited by Goodman, 1959).

Induced chlorosis is probably the most widespread antibiotic symptom in higher plants and suggests streptomycin may be acting primarily on the chloroplasts. Biochemical studies show that streptomycin inhibits both chlorophyll and carotenoid formation (reviewed by Goodman, 1959). The inhibition of chloroplast development has also been demonstrated in unicellular algae. In Euglena gracilis chloroplast development is inhibited by streptomycin concentrations below those which inhibit vegetative growth, which results in the bleaching of the cells (Pringsheim and Pringsheim, 1953). In this species streptomycin inhibits both the synthesis of chlorophyll a and b, in addition to certain carotenoids (Kirk, 1962). The addition of the antibiotic to an actively growing culture of Euglena gracilis results in the progressive reduction in plastid lamellae over 5 or 6 generations, until they regress to the proplastid state (Ben Shaul & Ilana, 1970). Similar changes to these have also been described in Protosiphon botryoides (Berkaloff & Jupin, 1974) and Clamydomonas reinhardi (Behn & Arnold, 1975a).

Plastids contain ribosomes with similar sedimentation properties (70S) to those described in prokaryote cells (Eistenstadt & Brawerman, 1964). It seems probable that streptomycin exerts its effect on chloroplast function by inhibiting the 70S-ribosome directed chloroplast protein synthesis necessary for normal plastid development (Hoober, Siekevitz and Palade, 1969; Margulis and Brubaker, 1970; Bovarnick et al., 1974).

However streptomycin has also been shown to inhibit both RNA and protein synthesis in excised higher plant tissues (Parthier, 1965; Venis,

1967). Furthermore Venis (1968) demonstrated that streptomycin inhibited cytoplasmic protein synthesis at concentrations far below those which inhibited chlorophyll development (50 mg/l cf. 400 mg/l). The effect of streptomycin on chlorophyll synthesis in higher plants may therefore be of secondary importance. However the basis of the streptomycin inhibition of cytoplasmic protein synthesis is unclear since higher plant ribosomes (80S) are apparently insensitive to the antibiotic (App & Rees, cited by McMeekin, 1973). Streptomycin has also been reported to affect mitochondrial morphology in Clamydomonas reinhardi, again as a result of its effect on 70S ribosomes (Behn and Arnold, 1975a).

2.1.3.3 Fungi

Apart from Oomycetes, most fungi appear to be relatively insensitive to streptomycin (Goodman, 1959; Vörös, 1965). Both the cytoplasmic and mitochondrial ribosomes of Saccharomyces cerevisae and Neurospora crassa are reported to be insensitive to streptomycin (reviewed by Lloyd, 1974). Nevertheless Berliner (1954) reported that very high streptomycin concentrations (10,000 mg/l) resulted in the fragmentation of basidium chromatin in Gymnosporangium clavipes, and in Phycomyces blaksleeanus carotogenesis is inhibited (Goodman, Griffiths and Modi, 1956). Recently studies on another aquatic Phycomycete, Allomyces arbuscula shows that streptomycin, whilst not inhibiting gametangial formation, altered the usual synchrony of male and female differentiation (Fähnrich, 1974).

In contrast Oomycete fungi have been widely reported to be sensitive to streptomycin (Goodman, 1959). A list of Oomycete plant pathogens against which streptomycin has proved to be an effective fungicide is given in Table 2.1

Table 2.1 Streptomycin control of plant diseases caused by Oomycetes

Pathogen	Host	Authority
Peronospora tabacina	Tobacco	Grosso, 1954; Anderson, 1956.
Peronospora cubensis	Curcurbits	Coe, 1955; Ark & Thompson, 1957.
Peronospora parasitica	Cabbage	Natti,1957; Altman & Davis, 1958; McMeekin, 1973.
Phytophthora infestans	Tomato	Zaumeyer & Doolittle, 1956; Crosse et al., 1960.
Phytophthora infestans	Potato	Muller, MacKay & Friend, 1954; Vörös, Kiraly & Farkas, 1957.
Pseudoperonospora humuli	Hop	Horner & Maier, 1957; Maier, 1959; Ogawa, McCain & Hall, 1960; Hine, 1963; Coley-Smith, 1966; Griffin and Coley-Smith, 1971.
Plasmopara halstedii	Sunflower	Cohen & Sackston, 1973.

The effectiveness of this antibiotic, both as an eradicant and a protectant fungicide, depended upon the time of application, the formulation used, and the method of application (Goodman, 1959).

It was initially proposed that streptomycin exerted its fungicidal effects by stimulating the production of antifungal substances in the host plant (Muller, MacKay and Friend, 1954). This hypothesis was supported by the demonstration that streptomycin increased phenolase activity in potato tissue (Voros, Kiraly & Farkas, 1957). However Maier (1959) reported that streptomycin caused a reduction in sporangium production in Pseudoperonospora humuli in infested hop tissue. In addition the antibiotic resulted in the formation of distorted sporangia which produced fewer zoospores. This suggests streptomycin acts directly on the fungus, in addition to any effects it might have on the host.

The susceptibility of Oomycete fungi to streptomycin was confirmed by growth studies in agar culture. Antibiotic concentrations of between 20-200 mg/l completely inhibited vegetative growth in a wide range of Phytophthora and Pythium species (Eckert & Tsoa, 1962; Hine, 1962; Voros, 1963, 1965; Shaw & Elliott, 1968; McMeekin, 1973; Shattock & Shaw, 1973). There was often considerable variation in the toxicity of streptomycin to Oomycetes even between closely related species. Aphanomyces euteiches, the only species of Saprolegniales so far examined, proved relatively insensitive to streptomycin and was little affected by concentrations of 200 mg/l and above.

The effect of streptomycin on Oomycete sporulation has only been examined in any detail in Ps.humuli (Griffin & Coley-Smith, 1971). In addition to inhibiting sporangium formation and germination, streptomycin also induced abnormal zoospore cleavage patterns resulting in the release of abnormally large multiflagellate zoospores. Streptomycin also caused widespread cyst lysis, although apparently had little effect on zoospore motility and germtube growth.

2.1.4 Streptomycin Uptake

Streptomycin shows a typical two-phase uptake into bacterial cells (Hancock, 1962; Anand, Davis & Armitage, 1960). The antibiotic is first adsorbed onto the cell wall before transportation into the cell by an energy-dependent, membrane located carrier. In higher plants streptomycin is absorbed into the plants through the roots (Anderson & Nienow, 1947; Pramer, 1953), cut stems (Alcorn & Ark, 1954; Goodman, 1959), and leaves (Dowler and Goodman, 1958). Since streptomycin is both accumulated against the concentration gradient (Pramer, 1953) and has a high Q_{10} for uptake (Goodman & Goldberg, 1960), it is probably absorbed into plant cells by an active uptake process.

However the most detailed account of streptomycin-uptake into plant cells has been carried out using the giant cells of the alga Nitella clavata (Pramer, 1955, 1956; Litwack and Pramer, 1957). It was conclusively demonstrated, using ^{14}C-labelled antibiotic, that streptomycin-uptake is energy dependent and followed Michaelis-Menton type kinetics, indicating it is mediated by a specific ion-carrier.

Vörös (1965) was able to show that streptomycin-uptake into Oomycete hyphae was slightly depressed by the addition of metabolic poisons, suggesting that it also is at least partially energy dependent. However the recent study of ^{14}C-labelled streptomycin uptake into Ps.humuli sporangia only demonstrated a temperature-independent adsorption of the antibiotic onto the cell wall (Griffin & Coley-Smith, 1975).

2.1.5 Cation Antagonism

It has been widely reported that many of the toxic effects of streptomycin on eukaryote cells are supressed by other divalent cations. This has been reported in higher plants (Rosen, 1954; Gray, 1955; Zahn, 1962; Venis, 1968; McMeekin, 1973), algae (Kirk, 1961), and Oomycetes (McMeekin, 1973; Griffin & Coley-Smith, 1975). The antagonism of streptomycin activity was a fairly specific effect, with Mn^{2+}. Ca^{2+} and Mg^{2+} in descending order of effectiveness. In most studies optimum antibiotic-interference was obtained by molar-concentrations of antagonist between 5-10 times in excess of the antibiotic (Gray, 1955; McMeekin, 1973; Griffin & Coley-Smith, 1975). Griffin and Coley-Smith (1975) have recently demonstrated that Mn^{2+} and Ca^{2+} displace over 90% of the irreversibly adsorbed antibiotic from the sporangial walls of Ps.humuli. In addition in Nitella clavata both Ca^{2+} and Mg^{2+} competatively inhibit streptomycin-uptake (Pramer, 1956; Litwack and Pramer, 1957). Therefore with these ions reducing both phases of antibiotic-uptake, they are likely to result in a considerable reduction in the amount of antibiotic reaching the non-exchangeable intranuclear pools.

Although the non-specific cationic antagonism of streptomycin toxicity in bacteria has been widely reported (e.g. Plotz, Dubin & Davis, 1961) much higher concentrations of ions are required than for eukaryotes (McMeekin, 1973). McMeekin (1973) suggests this indicates a fundamentally different mode of streptomycin action in the two groups.

2.1.6 Streptomycin Resistance and Dependence

The development of high level streptomycin resistant and dependent strains in bacteria is related to changes in a single protein component (S12) in the 30S ribosome subunit (Ozaki et al., 1969; reviewed by Davis & Nomura, 1972). Ribosomes from streptomycin-sensitive cells bind the antibiotic to their A site on the 30S subunit, and changes to resistance alter the binding properties at this site (Gale et al., 1972). Whereas resistant

ribosomes are unable to bind the antibiotic, dependent ribosomes require bound-antibiotic for normal function of the A-site.

In eukaryotes streptomycin-resistant and dependent mutants have been isolated from Clamydomonas reinhardi (Sager, 1954; Sager & Tsubo, 1962; Behn & Arnold, 1972a & b) and Phytophthora spp. (Shaw & Elliott, 1968; Shattock & Shaw, 1975). Recently streptomycin-resistant tobacco plants have been raised from haploid tissue culture (Maliga, Sz-Breznovits & Marton, 1973).

In Clamydomonas reinhardi the streptomycin resistance phenotype appeared to be governed by both nuclear and cytoplasmic genes (Sager & Tsubo, 1962) although the resistance determinant is not known. Behn & Arnold (1974a) reported that a streptomycin-dependent mutant of C.reinhardi possessed streptomycin-resistant chloroplast ribosomes, but had streptomycin dependent mitochondrial ribosomes. This suggests that as in prokaryotes the streptomycin phenotype in eukaryotes may still be governed by the structure of the 30S ribosomal subunit. The latter however is known to be determined by both cytoplasmic and nuclear genes (Behn and Arnold, 1974a & b). Studies on Phytophthora cactorum suggest that streptomycin resistance and dependence phenotypes are cytoplasmically determined in this species (Shaw and Elliott, 1968).

2.2 MATERIALS AND METHODS

2.2.1 Antibiotic Stock Solutions

Streptomycin: This antibiotic was supplied as streptomycin sulphate ($(C_{21}H_{39}N_7O_{12})_2\ 3H_2SO_4$, Glaxo Pharmaceuticals), in sealed glass vials which each contained 1.0 g of antibiotic base. Streptomycin stock solutions (10,000 mg/l) were prepared by dissolving the contents of each vial in sterile distilled water (1.5-3.0 ml). The dissolved antibiotic was then transferred to a sterile volumetric flask (100 ml) using a sterile plastic syringe (5 ml, Gilette) and made up to volume with sterile distilled water.

Chloramphenicol: Stock solutions (1000 mg/l) of chloramphenicol ($C_{11}H_{12}N_2O_5$, Boehinger-Mannheim) were prepared by dissolving 0.1 g antibiotic in 1.0 ml of ethanol in a volumetric flask (100 ml) and making up to volume with distilled water. This solution was sterilised by membrane-filtration (0.45 µm, Millipore filter). Control colonies were always induced in sterile distilled water to which equivalent amounts of ethanol were added.

Cycloheximide: Stock solutions (100 mg/l) of cycloheximide ($C_{14}H_{20}NO_4$, Sigma Chemicals) were prepared by dissolving 0.1 g of antibiotic in a 100 ml of distilled water, and sterilising by membrane-filtration.

All of these stock solutions were stored in the dark at 4°C for periods of up to 6 weeks. All subsequent antibiotic dilutions were made up in bunged 150 ml-conical flasks, with sterile distilled water.

2.2.2 Antibiotic Media

Streptomycin-agar media was prepared by adding appropriate volumes of stock or diluted antibiotic solutions to molten 10 ml-aliquots of 1/2 GYPS agar, from which the $MgSO_4$ had been omitted. The tubes were mixed by rotation and poured into 8 cm plastic petri-dishes (Sterilin). Streptomycin-liquid media were similarly prepared by mixing antibiotic solutions (< 10 ml) with 1/2 GYPS liquid (-$MgSO_4$) medium (< 100 ml) in sterile cotton-wool bunged conical flasks (150 ml). This was then dispersed in 15 ml aliquots into 8 cm plastic Petri dishes.

2.2.3 Divalent Ion Solutions

Stock solutions of Mn^{2+}, Ca^{2+} and Mg^{2+} cations were prepared as described in Section 3.2.2.

2.2.4 Experimental Procedures to determine Antibiotic effects

2.2.4.1 Effect on Saprolegnian Growth

Radial growth rate (colony-extension rate) has been shown to be a good measure of the antibiotic inhibition of fungal growth (Trinci & Gull, 1970). Colonies were inoculated onto a range of streptomycin agar media as described in Section 0.2.3.2, and the plates inverted and incubated at 25°C in the dark. The colony diameter was measured at regular intervals by taking the mean value of two opposing diameters. In most experiments 10 replicate

colonies were set up for each treatment, and the averaged colony-diameter at each time interval calculated. These measurements were then plotted to calculate the averaged colony-extension rate at each antibiotic concentration.

The effect of streptomycin on colony dry-weight increase in liquid culture was assessed by harvesting nylon-disc inoculated colonies from a range of antibiotic-liquid media, after 68 h incubation at 25°C. The colonies were blotted on filter paper and placed on weighed-aluminium trays and dried to constant weight in a 60°C oven. As in the previous experiment 10 replicate colonies were inoculated for each antibiotic treatment and the mean dry-weight calculated.

2.2.4.2 Effect on Saprolegnian Reproduction

Saprolegnia colonies (18-20 h) were induced in a range of antibiotic solutions using the procedure described in Section 0.2.4.1. In most experiments 4 replicate colonies were induced for each antibiotic treatment (2 colonies per Petri dish). These colonies were scored at regular intervals for reproductive structures by examination under the low power objective (x 10) of a Vickers binocular microscope (L.P. field area 1.72 mm^2). It was found during the preliminary experiments that reasonably consistent assessments of sporangium and oogonium production could be obtained by scoring 5 random L.P. fields for each of the 4 replicate colonies. To ensure all the reproductive bodies in each field were scored the microscope was always focussed through the whole colony. The quantitative assessments of reproductive bodies were expressed as the mean number of bodies scored in a single L.P. field of 1.72 mm^2 area.

2.2.4.3 The effect on reproduction in Phytophthora

The effect of streptomycin production in P.cactorum was assessed by transferring 6 mm discs of colony, growing on PE agar, into a range of antibiotic solutions. Subjective assessments of sporangium number were made over a 3-4 day period.

The effect of streptomycin on zoospore formation in induced sporangia of P.cactorum was determined using the procedure described by Griffin and Coley-Smith (1971) in their studies on Pseudoperonospora humuli. An isolated sporangial suspension was prepared as described in Section 0.2.4.2, and adjusted to a concentration of 10^5 sporangia per ml. This was done by determining the density of the sporangial suspension in a heamocytometer (Hawksley Improved Neubauer type), and adjusting the volume accordingly. The sporangial suspension was then mixed with an equal volume of antibiotic solution in a small Pyrex test tube (6 ml). Samples withdrawn using a Pasteur pipette, and single drops (c. 0.05 ml) placed on a cleaned microscope slide; 3 droplets per slide. Each droplet was retained by a ring of silicone grease,

10 mm in diameter. In all 3 replicate droplets were set up for each antibiotic-treatment, and it was arranged that each was on a separate slide. The loaded slides were incubated in a plastic box moistened with filter paper. After briefly chilling the slides at 4°C, they were incubated for the remainder of the experiment at 16°C. The slides were examined after 6 h, 8 h and 24 h incubation and scored for germinated sporangia. This was assessed by the absence of the apical papilla and the discharge of most of the sporangial contents.

A similar germination experiment was also carried out for a suspension of Saprolegnia cysts. These were isolated by filtering the inducing-solution of several 12 h-induced colonies of S.ferax through a 10 µm nylon mesh filter (Henry Simon Ltd.) and concentrated by centrifugation (2000 rpm, 10 minutes). The cysts were incubated at 20°C, and scored for germtube formation.

2.2.4.4 Analysis of Antibiotic-inhibition Effects

Toxicological studies on organisms have shown that typical dose-mortality curves are sigmoidal (Bliss, 1935). A number of statistical transformations have been devised to convert these curves into linear regressions, and the most commonly used of these is the so-called probit analysis (Bliss, 1935; Finney, 1971). This is based on the assumption that differences in the susceptibility of individual organisms to a poison follows the usual normal distribution pattern. The proportion of organisms which are killed at a given concentration of poison will include all individuals with a sensitivity at or below that level on the normal distribution curve. Percentage-kill data can therefore be expressed in terms of units of normal distribution, the most usual of which is standard deviation (σ). The dose which results in 50% mortality is the median point on the distribution curve, where σ is equal to 0. To avoid the necessity of employing negative values of σ, Bliss (1935) introduced a statistical unit, the probit, which was given a value of 5 at the median point, and values of σ added or subtracted from it. Since biological variation follows a geometric rather than arithmetic progression the probits were plotted on the ordinate against the logarithm of the dose (Bliss, 1935). This double transformation usually results in a linear plot, the gradient of which is characteristic of the response of an organism to a given poison (Cochrane, 1958; Finney, 1971). Subsequently probit analysis has been applied to sigmoidal dose-response curves, other than those which result in the death of the organism (Finney, 1971).

The inhibitory effects of streptomycin were expressed as a percentage of the control value and converted into probits using the tables given by either Bliss (1935) or Finney (1971). These were plotted against the log of the dose and the regression fitted by eye as described in Finney (1971). The median effective dose (ED50) was read for these plots and used to compare

the toxicity of streptomycin at different stages in the Saprolegnian life cycle.

2 .2.5 Methods used in the Physiological Studies of Antibiotic Action

2.2.5.1 Colony Respiration

Oxygen uptake by respiring Saprolegnia colonies was determined in a Rank oxygen electrode (Rank Bros. Ltd.), with a 5.0 ml cell and operated at an applied voltage of 6.5 mV. The changes in electrode current were recorded using a Servoscribe potentiometric recorder (RE.511.20, Phillips). The electrode cell was kept at a constant temperature of 20°C by a water jacket maintained by a Julabo 'Paratherm II' heater (Scienco Western Ltd.). The electrode was calibrated with air-saturated distilled water, which contains 0.29 μ mole O_2/ml at 20°C, and zeroed using a few granules of sodium dithionate. A colony (18-48 h) was placed in the cell with 3 ml of distilled water or 1/2 GYPS medium. Oxygen uptake was measured over a period of 5-30 minutes, depending on the respiratory activity, during which time the contents of the cell were continuously agitated with a rotating magnetic flea. This was found to damage the colonies, which as noted in the earlier Warburg studies considerably reduces respiratory activity (Darby & Goddard, 1950). This difficulty was satisfactorily overcome by separating the colony from the flea by a disc of coarse (2 mm) nylon mesh.

2.2.5.2 Flame Photometric Assay of K^+ and Ca^{2+} ions

The leakage of K^+ and Ca^{2+} ions from antibiotic-induced colonies of Saprolegnia was determined by assaying samples of inducing solution for these ions, using an Eel Flame photometer (Evans Electroselenium Ltd.). The photometer was calibrated, using the appropriate K and Ca filters, using stock solutions containing 10 mg/l K^+ and 40 mg/l Ca^{2+} and zeroed using glass distilled water.

2.2.5.3 Measurement of UV-Absorbing Material

The loss of cellular membrane-integrity is usually indicated by the leakage of low molecular weight metabolites, which can be detected by their strong UV-absorbance (Olsen, 1971a). Samples (5 ml) of inducing solution were withdrawn and passed through a membrane filter (0.45 μm) before placing in a quartz cuvette. The absorption spectra of these samples was measured in the UV-range of a Pye Unicam SP800 spectrophotometer.

2.3. RESULTS

2.3.1 Effects of Streptomycin (Str) on Saprolegnian Growth

2.3.1.1 Colony-extension Rate

A representative series of growth-curves for S.furcata colonies grown on a range of Str-agar concentrations (10-100 mg/l) at 25°C is shown in Fig. 2.2. There is a lag phase of between 5 to 10 h before a constant rate of radial growth is attained. The colony extension rates were calculated from the linear parts of these growth curves. The results of three separate antibiotic series are summarised in Table 2.2, and Fig. 2.3. The 'A' series results for S.ferax and S.furcata were obtained at the same time using the same media and inocula and therefore are directly comparable. The 'B' series data for S.furcata comes from a separate experiment and is included to show the typical variation which occurs between replicate experiments.

Colony-extension rates show a linear regression when plotted against the log of Str concentration (Fig. 2.3). A similar relationship has also been described in other antibiotic studies on fungal growth, although the basis for it is unclear (Trinci & Gull, 1970). This linear relationship is less convincingly shown by the S.ferax data (Fig. 2.3) perhaps because this species is less sensitive to Str.

Comparison of the two sets of data for S.furcata (Table 2.2, Fig. 2.3) shows that although there is considerable variation in the observed toxicity of Str (ED 50 for A is 750 mg/l, ED 50 for B is 50 mg/l) the dose response curves have approximately the same gradient. Parallel dose response curves are taken to indicate a similar response to the toxin, and often result from differences in antibiotic potency (Finney, 1971).

Str also increases the variability in colony diameter measurements which is reflected by the relatively higher standard deviation values in Str (Table 2.2). This is both the result of the inherent variation in the response of the fungus to the antibiotic and due to appearance of faster growing sectors on some plates (>100 mg/l Str) after 24 h incubation or more. The nature of these sectors is unclear since when they were subcultured and retested they failed to show a significantly higher Str resistance.

The effect of Str on a wider range of Saprolegnia isolates was assessed in a single comparative experiment, using agar containing 500 mg/l Str. The results are summarised in Table 2.3. Two S.ferax isolates (1 and 2, Table 0.1) are the least sensitive to Str, showing less than 2% inhibition of growth. In contrast isolates of S.furcata (4), S.turfosa (10) and S.parasitica (9) are all inhibited by over 40% or more at this concentration. Differences in Str-sensitivity also occurred amongst isolates of S.ferax (1 to 37%) and S.furcata (37 to 48%). Therefore there is both inter and intra specific variation in sensitivity to Str in the Saprolegniaceae.

Table 2.2 The effect of streptomycin on colony diameter (45 h) and colony-extension rate for S.ferax (A') and S.furcata (A & B) at 25°V

Streptomycin Conc.n mg/l	Mean+ Colony Diameter mm			Colony-Extension Rate µm/h		
	A'	A	B	A'	A	B
0	59.0±1.4	55.2±0.4	57.1±0.7	750	728	657
10	-	-	41.3±2.1	-	-	443
32	57.3±1.2	48.6±2.9	-	745	650	-
50	-	-	33.7±1.2	-	-	338
100	56.8±1.8	41.2±1.7	28.6±1.2	740	570	263
200	-	-	24.7±1.4	-	-	231
320	54.0±2.2	33.5±3.6	-	705	445	-
500	52.8±2.9	31.0±3.9	19.4±1.4	685	390	152
1000	49.9±3.5	20.4±5.3	14.8±0.8	600	333	100

+Mean of 10 replicate colonies
(The A series results come from a single experiment)

Table 2.3 The effect of streptomycin (500 mg/l) on colony diameter (36 h) and colony-extension rate for a range of saprolegnia spp., at 25°C

Species	Controls		Streptomycin Treatments 500 mg/l		
	Mean+ colony Diameter(mm)	Colony Extension Rate(µm/h)	Mean colony Diameter(mm)	Colony Extension Rate(µm/h)	% Inhibition by 500 mg/l Sr
S.ferax 1	50.7±1.0	882	50.6±0.5	875	1
S.ferax 2	48.7±3.3	815	43.3±1.0	805	2
S.ferax 3	31.7±1.8	555	22.1±0.9	350	37
S.furcata 4	37.7±0.9	610	24.7±1.5	318	48
S.furcata 5	43.6±1.4	740	31.3±1.0	470	37
S.hypogyna 6	46.3±0.6	760	33.3±3.5	535	30
S.litoralis 7	39.3±1.5	695	35.7±0.5	595	15
S.megasperma 8	28.8±0.7	500	25.4±0.5	375	23
S.parasitica 9	51.0±0.9	855	34.0±4.5	487	43
S.turfosa 10	27.0±0.9	455	16.7±2.2	250	45

+Mean of 8 replicate colonies

Fig. 2.2 The increase in the colony-diameter of S. furcata at 25°C on a range of streptomycin-agar plates.

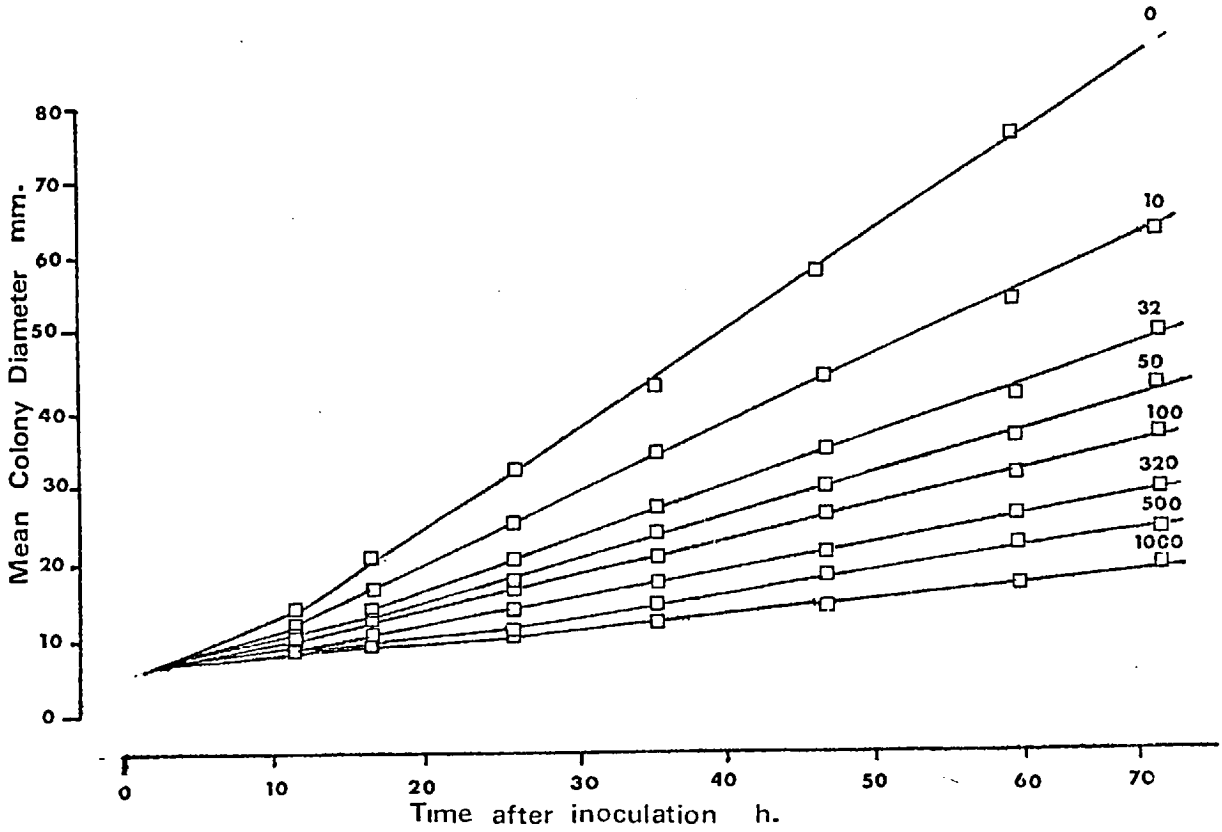


Fig. 2.3 The effect of streptomycin on the extension-rate of S. ferax and S. furcata colonies at 25°C.

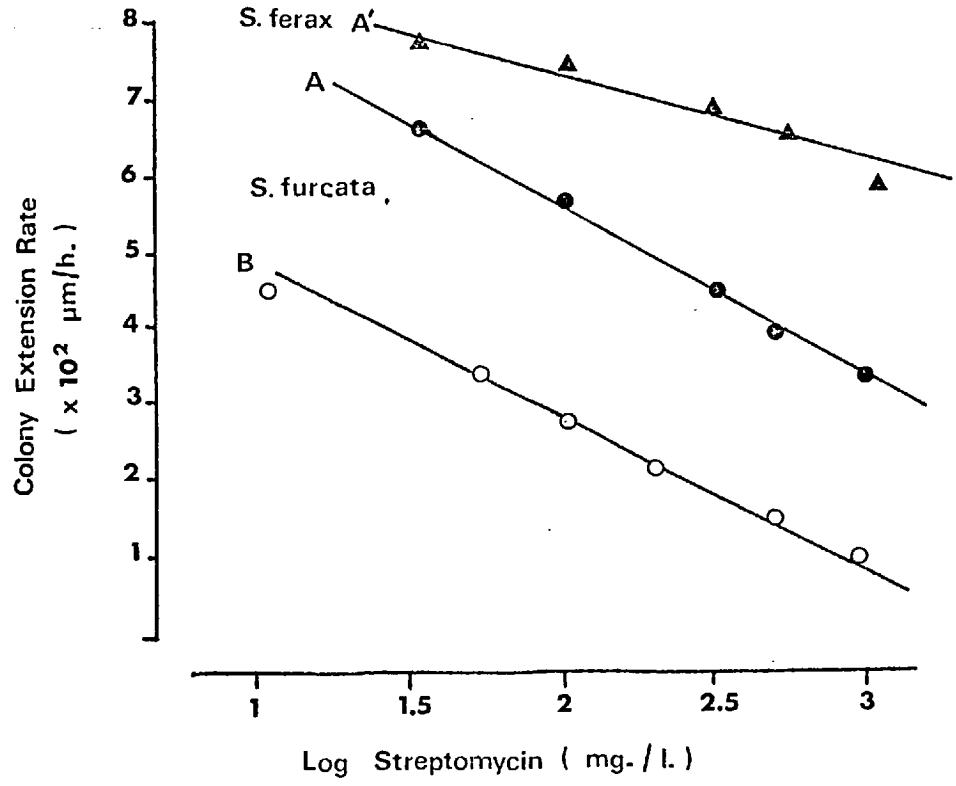


Fig. 2.4 The effect of streptomycin on the dry-weight of 68h-colonies of S. ferax and S. furcata grown in 1/2 GYPS liquid medium at 25°C.

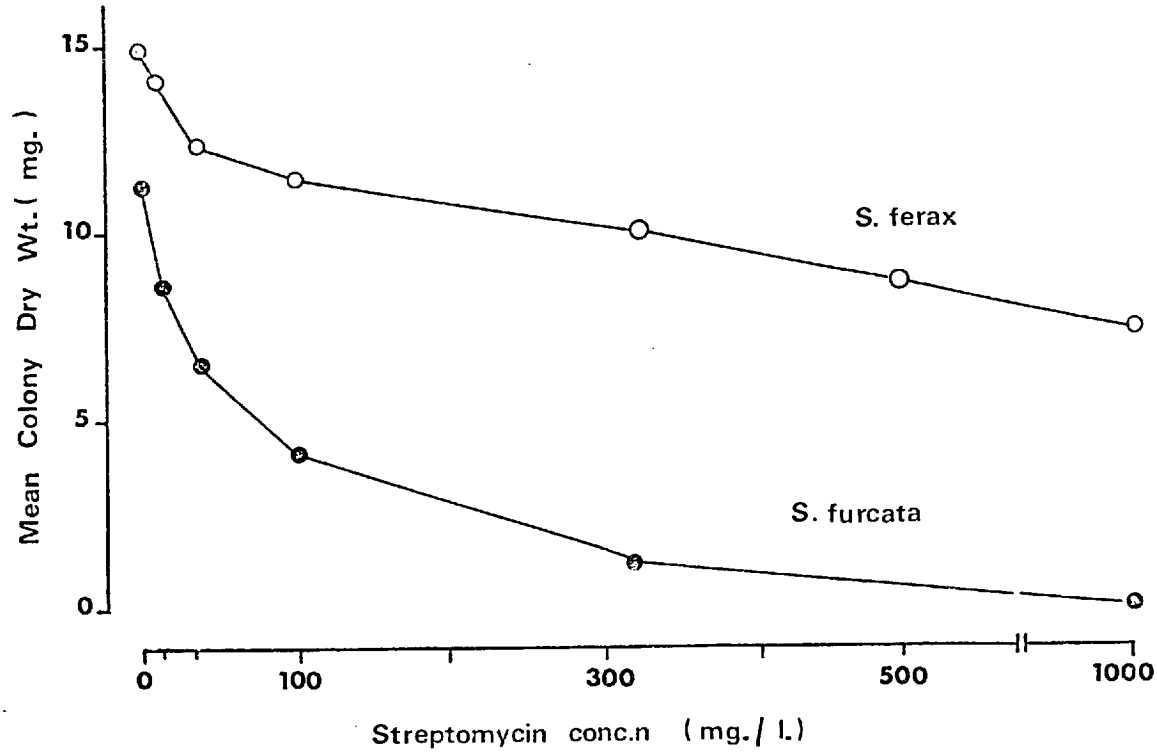
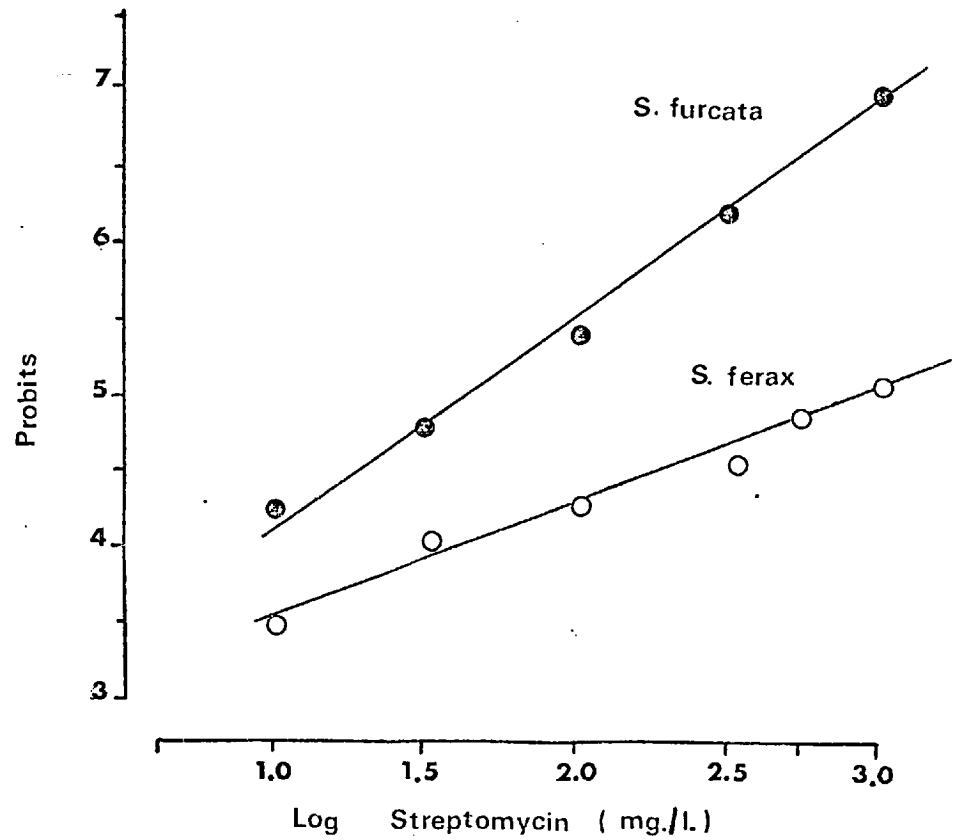


Fig. 2.5 Probit (% 68h-Colony dry-weight inhibition) against log streptomycin concentration.



2.3.1.2 Colony dry weight

The effects of Str on the increase in colony dry weight for S.ferax and S.furcata are summarised in Table 2.4 and in Fig. 2.4. Again Str markedly inhibits colony dry weight increase, although S.furcata is clearly more sensitive to the antibiotic. The percentage inhibition of colony growth was calculated for each antibiotic treatment and then plotted on a probability scale against the log of the dose (Fig. 2.5). The resulting plots give linear regressions and the respective ED50 values for S.ferax and S.furcata read from these curves are 1000 mg/l and 45 mg/l. The kinetics of Str-inhibition of vegetative growth in Saprolegnia is similar on both solid media and liquid culture, although the fungus is more sensitive to the antibiotic in the latter.

Table 2.4. The effect of streptomycin on colony dry weight increase assessed after 68 h incubation in liquid culture at 25°C

Streptomycin Conc. n (mg/l)	S.ferax		S.furcata	
	Mean+ Colony Dry Weight (mg)	% Inhibition of growth	Mean+ Colony Dry Weight (mg)	% Inhibition of growth
0	14.9±1.4	-	11.3±1.3	-
10	14.1±1.4	5.0	7.7±1.4	23
32	12.5±1.2	16.5	6.9±1.4	39
100	11.5±1.1	23	4.2±0.4	63
320	10.1±1.3	32	1.4±0.3	89
500	8.8±0.7	42	-	-
1000	7.2±0.9	52	0.6±0.06	95

+Mean dry weight of 10 replicate colonies

2.3.2 The effects of Steptomycin on asexual reproduction in Saprolegnia

2.3.2.1 Sporangium production

The results of one of three similar replicate experiments demonstrating the effects of Str on zoosporangium formation in S.ferax colonies grown from nylon-disc inocula, are summarised in Figs. 2.6-2.9. As with the growth studies a wide variation in the measured toxicity of Str between replicate experiments was observed. This was particularly marked between experiments such as summarised in Figs. 2.6-2.9, and earlier replicates carried out using agar plug inocula, in glass rather than plastic Petri dishes. A representative series of results from one of the latter are presented in Fig. 2.10 for comparison.

Sporangium inhibition shows an approximately linear regression when plotted on probability scale against the log of the dose (Fig. 2.8). The measured ED50 values ranged from 8 mg/l as in Fig. 2.8, to nearly a 100 mg/l as shown in the experiment summarised in Fig. 2.10.

Fig. 2.6 The effect of streptomycin on the progress of sporangium formation on induced S. ferax colonies (18h), incubated at 25°C for 20h.

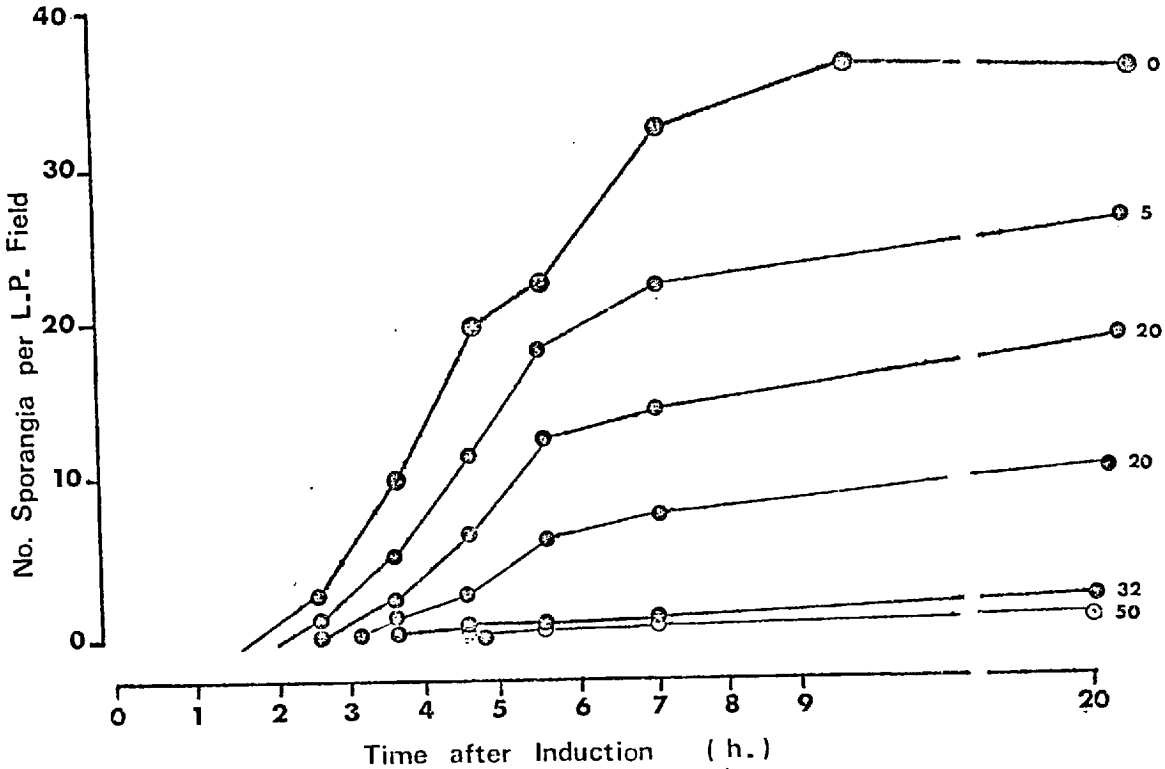


Fig. 2.7 The effect of streptomycin on sporangium formation in S. ferax, 7h and 20h after induction.

Fig. 2.8 Probit (% inhibition of sporangium formation) against log antibiotic concentration, 20h after induction.

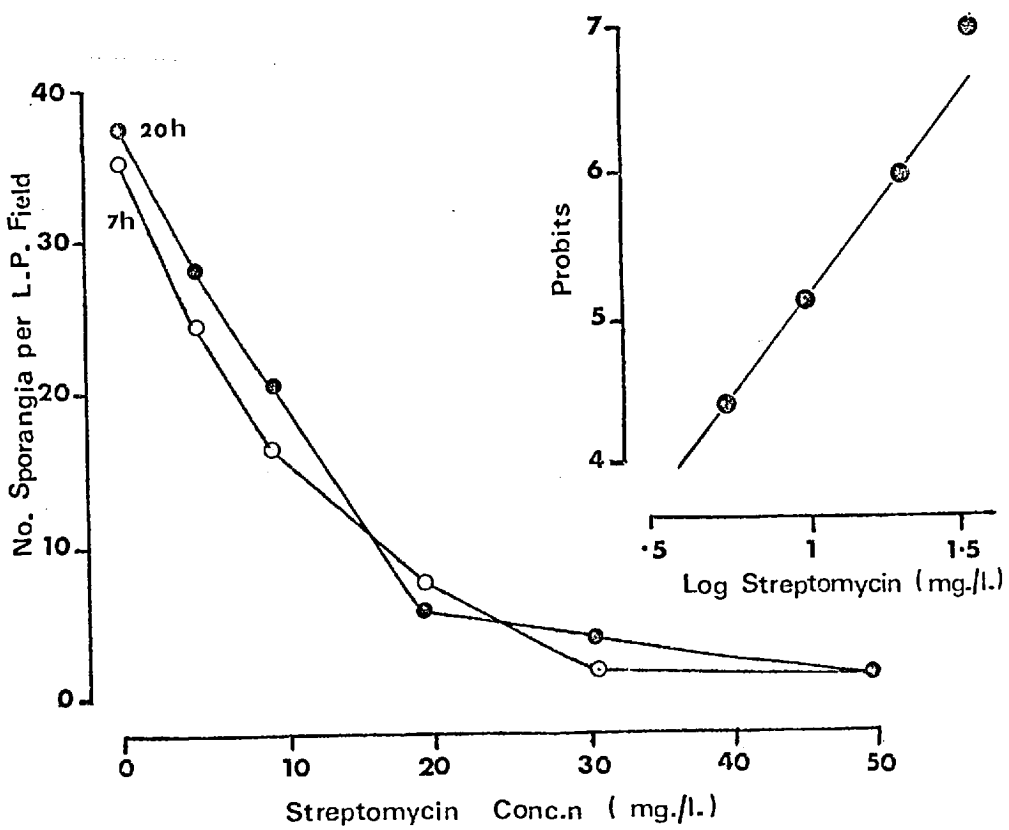


Fig. 2.9 Histograms showing the effects of streptomycin on sporangium cleavage and zoospore dehiscence in 18h-colonies of S. ferax, 20h after induction.

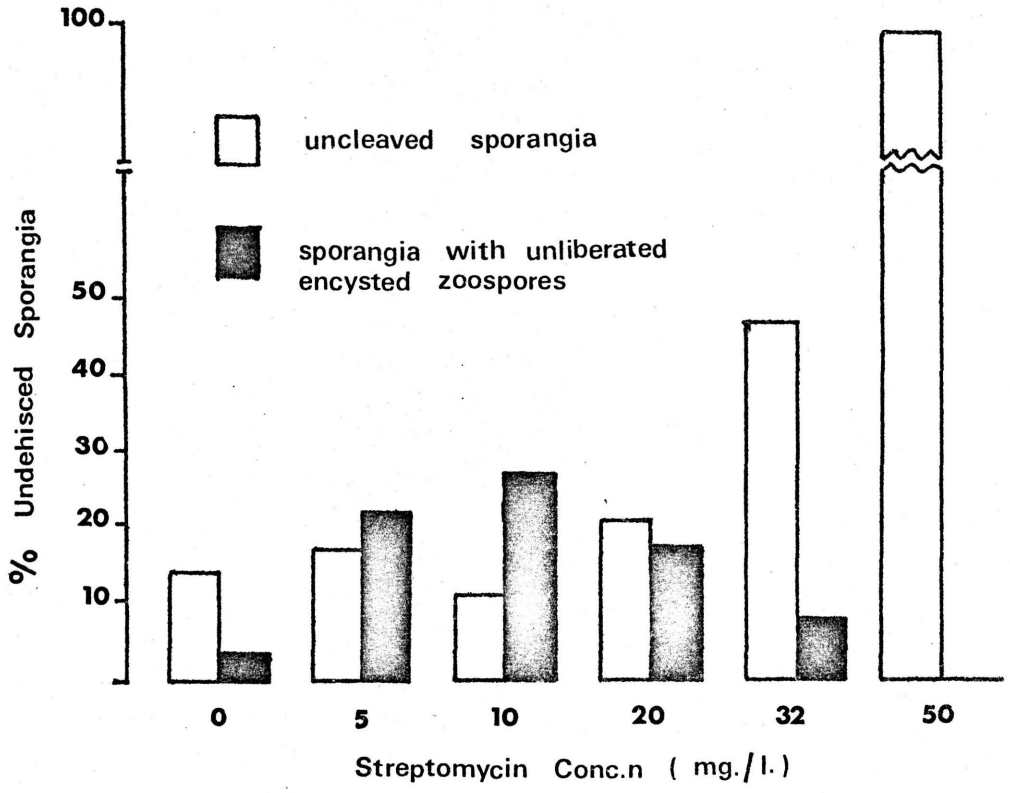
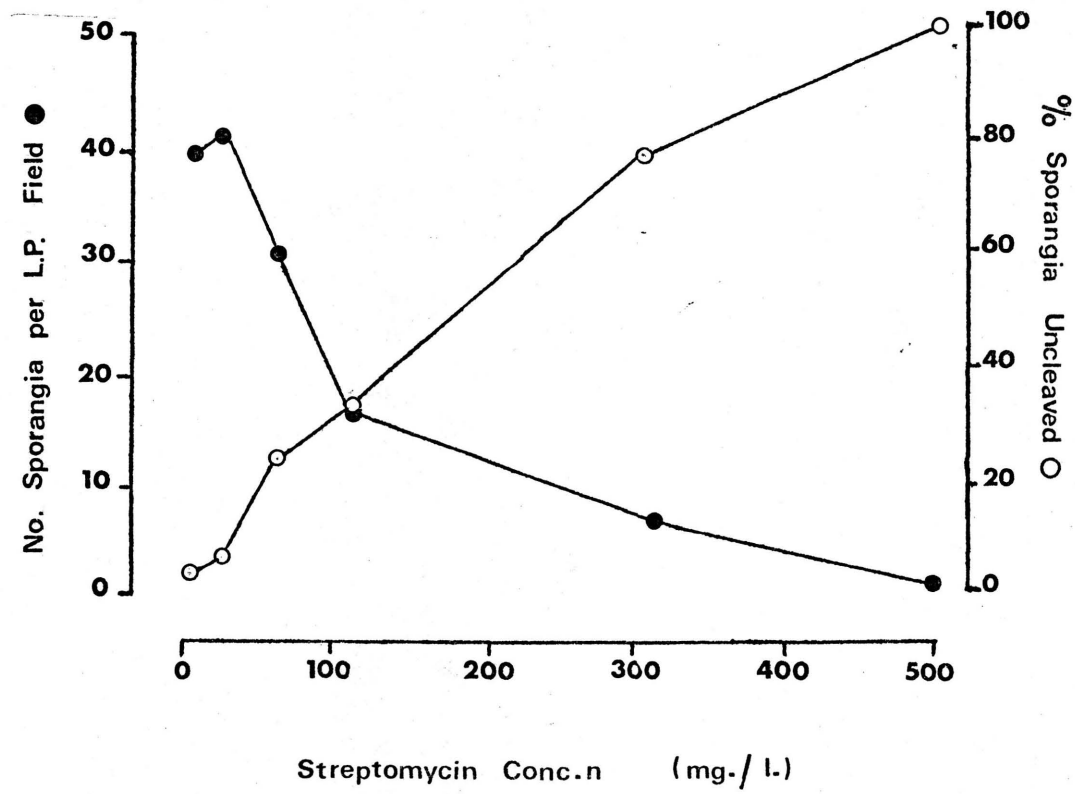


Fig. 2.10 The effect of streptomycin on sporangium production and cleavage in 18h colonies of S. ferax, assessed 20h after induction.



The antibiotic also increases the 'lag period' (Griffin & Breuker, 1969) prior to the formation of sporangium initials on induced colonies (Fig. 2.6). If the lag phase is plotted against Str concentration it shows an almost linear increase (Fig. 2.11) as demonstrated in other fungal inhibitor studies (e.g. effect of cycloheximide on conidia germination in Absidia glauca; Trinci & Gull, 1970).

The effect of Str on sporangium production in a range of Saprolegnia isolates was assessed in a single comparative experiment, the results of which are summarised in Table 2.5. Most sporangium-producing species show a similar pattern of Str-inhibition to that described for S.ferax. Only S.litoralis proved significantly less sensitive to Str, still producing gemmae in abundance in the 500 mg/l treatment (Table 2.5). In contrast the low level of sporangium production in S.furcata was completely suppressed by even 10 mg/l Str.

Table 2.5 The effect of streptomycin on sporangium production in a range of Saprolegnia spp., assessed 20 h after induction

Species		Streptomycin conc.n (mg/l)					
		0	10	50	100	500	1000
S.ferax	(8)	4	3	1	0	0	0
S.ferax	(2)	4	3	1	0	0	0
S.ferax	(3)	4	3	1	0	0	0
S.furcata	(4)	2	0	0	0	0	0
S.hypogyna	(6)	4	2	1	0	0	0
S.litoralis	(7)	4	3	3	3	2	1
S.megasperma	(8)	4	3	2	1	0	0
S.parasitica	(9)	4	3	2	0	0	0

No.sporangia per L.P. field: 0, none; 1, < 5; 2, 5-15; 3, 15-30; 4, 30-50

2.3.2.2 Sporangium cleavage

In addition to inhibiting sporangium production Str also effects the differentiation of the sporangial cytoplasm into zoospores, as shown in Figs. 2.9 and 2.10. For the experiments summarised in Figs. 2.6 and 2.10 the ED50 values for cleavage inhibition are respectively 32 mg/l and 200 mg/l. A similar effect on cleavage has been shown in sporangia of an Achlya sp. treated with cycloheximide (Griffin & Breuker, 1969). These inhibited sporangia were classified as gemmae.

At lower Str concentrations (< 32 mg/l) the proportions of sporangia containing unliberated zoospores which have encysted in situ is also increased (Fig. 2.9). This group includes both sporangia in which dehiscence has been completely supressed, and those in which there has been only a partial liberation of spores.

Fig. 2.11 The effect of streptomycin on the length of the lag phase prior to the appearance of the first sporangium initials in S.ferax

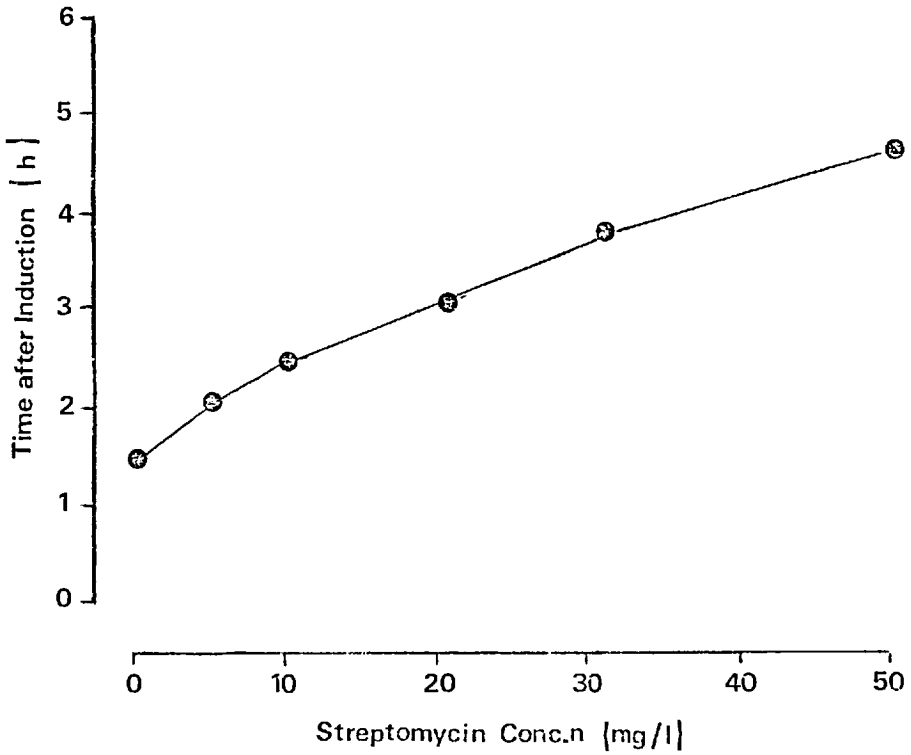
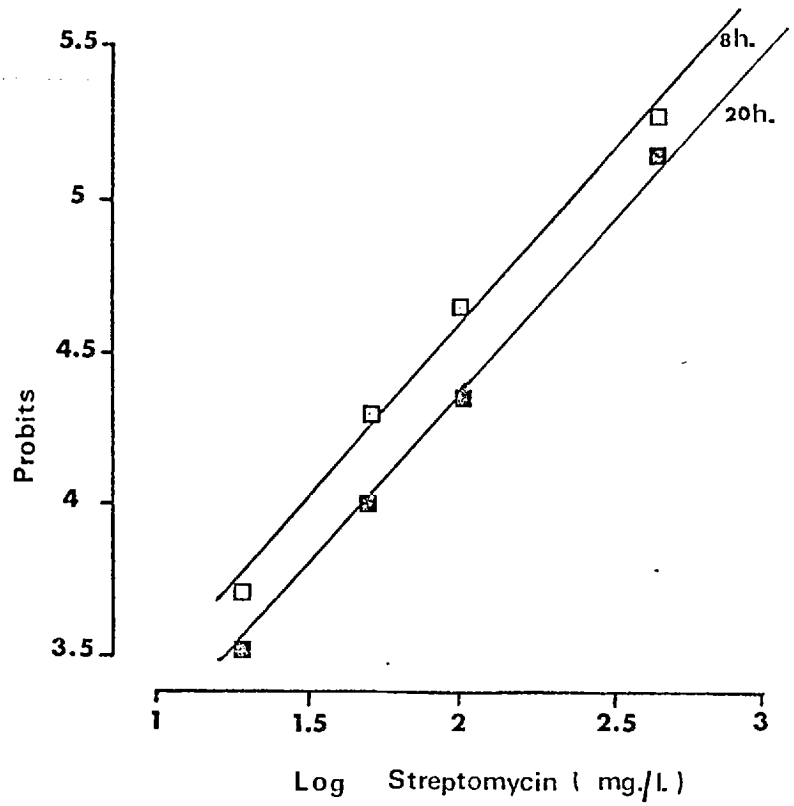


Fig.2.12 Probit (% inhibition of cyst germination) against log antibiotic concentration, assessed 8h and 20h after incubation at 25°C.



2.3.2.3 Zoospore activity

The combined effects of Str on sporangium formation, cleavage and zoospore release all contribute to the markedly reduced number of free swimming zoospores in Str-induced plates. These effects on zoospore production were not however assessed quantitatively. Particularly at concentrations of 32 mg/l and above Str reduces the period of motility from 10-15 minutes to 5 minutes or less. This probably contributes to the tendency of zoospores to encyst within the sporangium. Although small numbers of secondary zoospores are released from Str induced cysts, few can be seen 24 h after induction. This is the time when they are most abundant in control plates.

2.3.2.4 Cyst germination

A spore germination test was set up with a suspension of cysts (10^5 cysts/ml) harvested from 12 h induced colonies, andscored after 8 h and 24 h. The results are summarised by the probit-dose response curves in Fig. 2.12. Germination was determined by the formation of a germtube, which was always shorter in antibiotic treatments. The ED50 values for cyst inhibitionfrom Fig. 2.12, are 220 mg/l after 8 h, and 350 mg/l after 24 h. Clearly cyst germination is less sensitive to Str than sporangium formation. This probably reflects the relative insensitivity of the vegetative phase of S.ferax to the antibiotic.

The apparent decline in antibiotic toxicity with time (Fig. 2.12) is probably the result of the inherant variation in cyst germination times within the cyst suspension, since the two regressions have the same gradient.

2.3.3. The effects of Streptomycin on sexual reproduction in Saprolegnia

2.3.3.1 Gametangium production

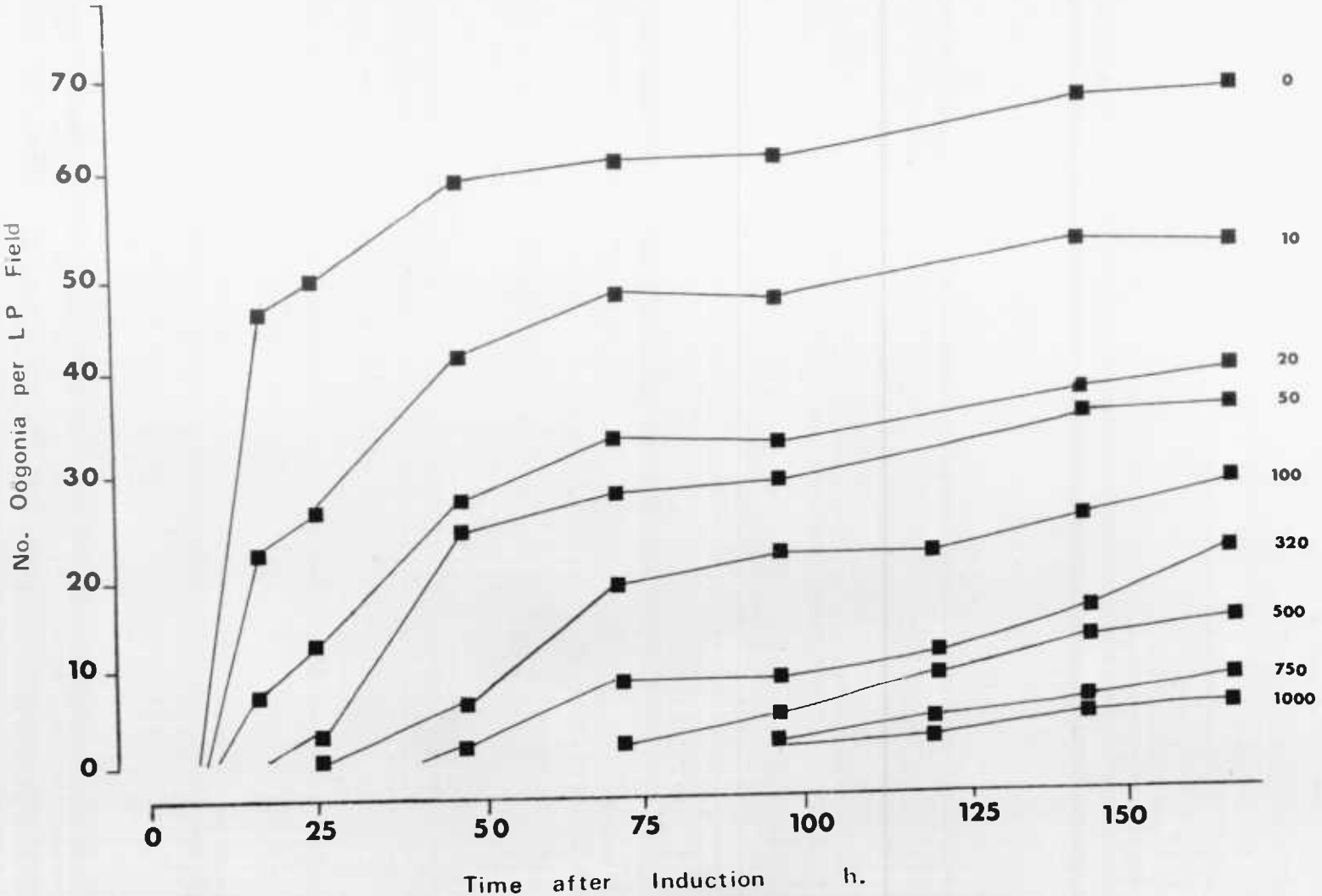
The results of a representative of one of three similar replicate experiments demonstrating the effects of Str on sexual reproduction in S.furcata are summarised in Figs. 2.13-2.17. Many of the scored reproductive structures in Str treatments are strictly classifiable as gemma types. However for the sake of these numerical studies they are classified simply as cleaved or uncleaved oogonia in the text figures and tables.

As with sporangium development Str reduces both the level of oogonium production, and increases the lag period before their appearance on induced colonies (Figs. 2.13-2.16). This increase in the lag phase follows an approximately linear increase with Str concentration, at least between 50 and 750 mg/l (Fig. 2.18). The extension of the lag phase alters the measured antibiotic toxicity assessed over a 6-8 day period. Thus after 25 h the ED50 is only 10 mg/l, whereas after 168 h it has been increased to 68 mg/l (Fig. 2.17).

The probit-dose response curves shown in Fig. 2.17 appear to be of the two phase type, showing a marked increase in gradient at high antibiotic

Fig. 2.13 The effect of streptomycin on the progress of oogonium formation on induced 18h-colonies of S. furcata at 20°C

(a) Time-course curves.



(b) Photographs of the colony margins 168h after induction.

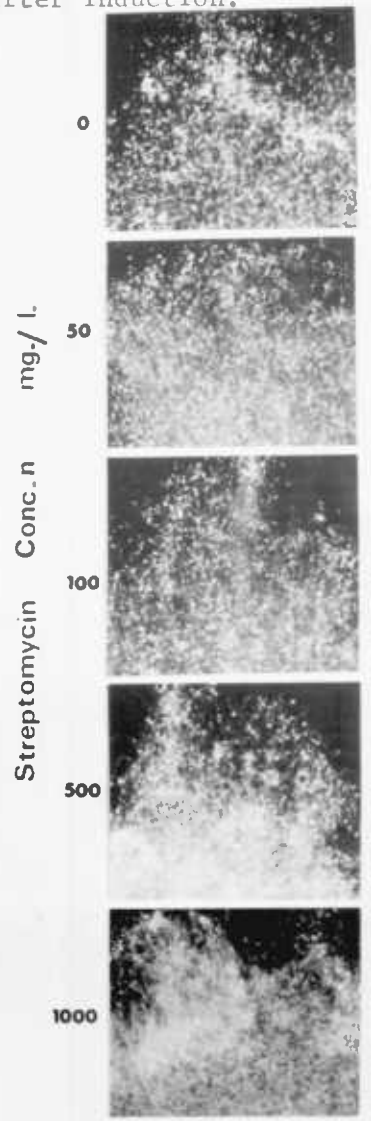


Fig. 2.14 The effect of streptomycin on oogonium formation on induced 18h-colonies of S. furcata.

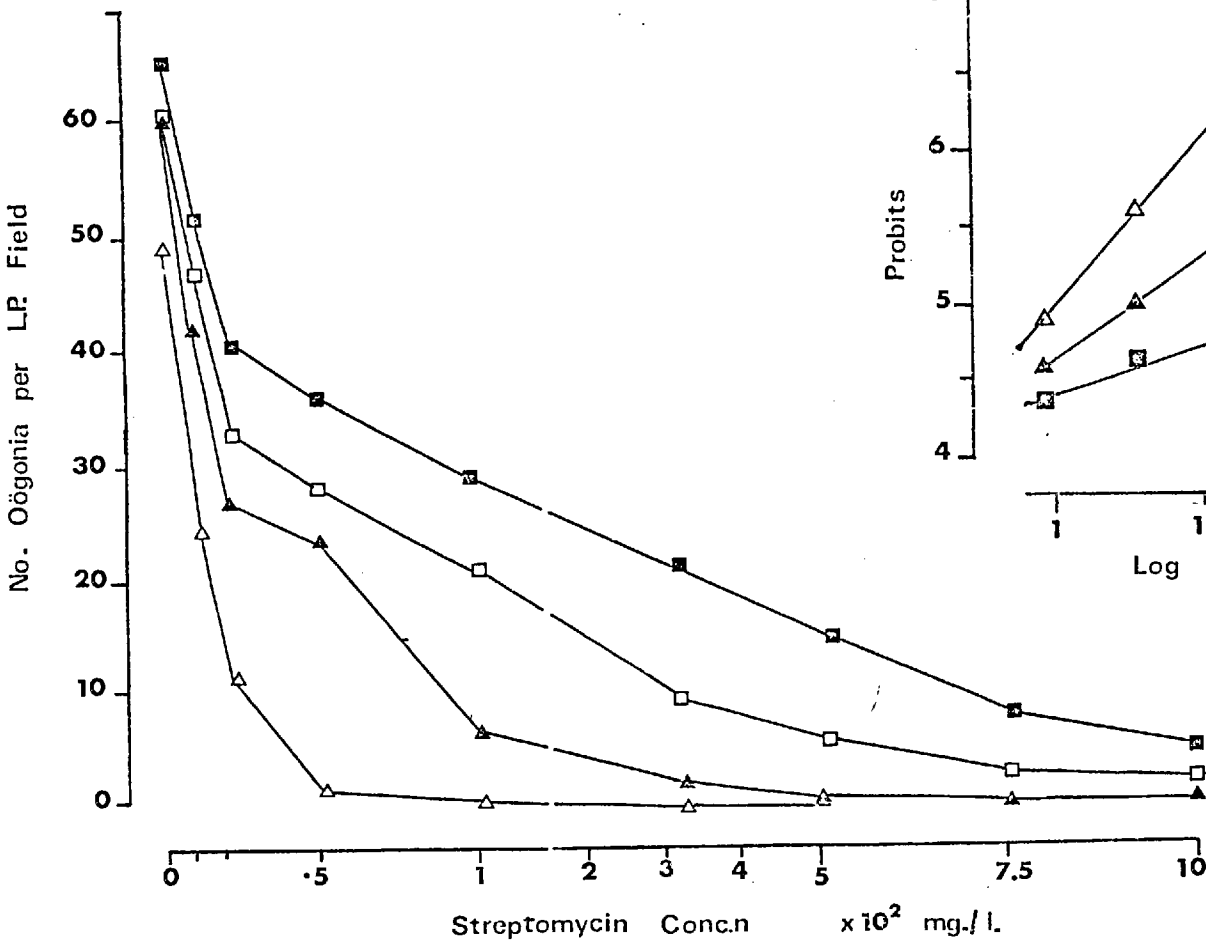


Fig. 2.15 Probit (% inhibition of oogonium formation) against log antibiotic concentration, assessed 25h, 48h and 168h after induction at 20°C.

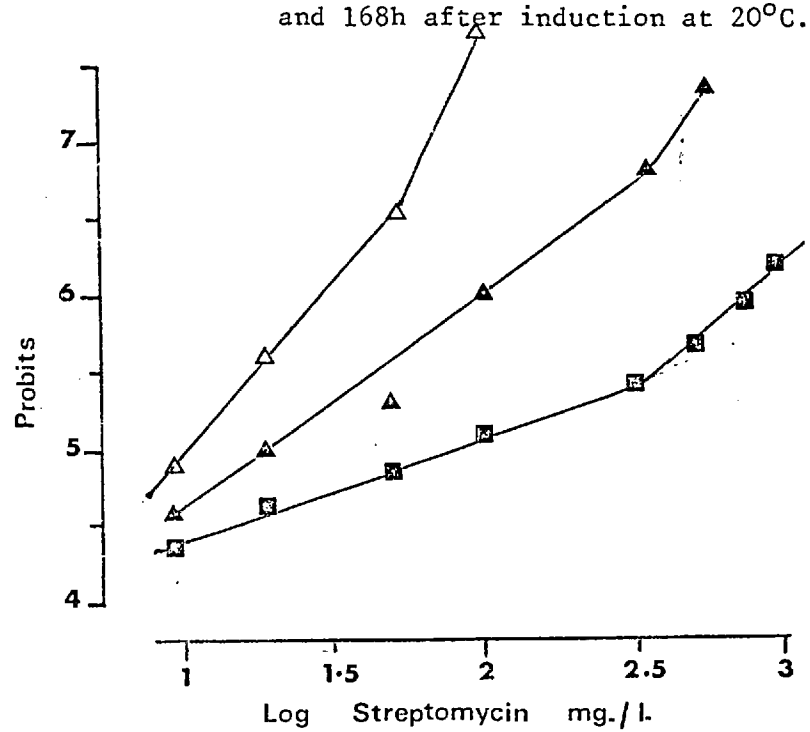


Fig. 2.16 The effect of streptomycin on oogonial cleavage in S. furcata, assessed 48h, 72h and 144h after induction.

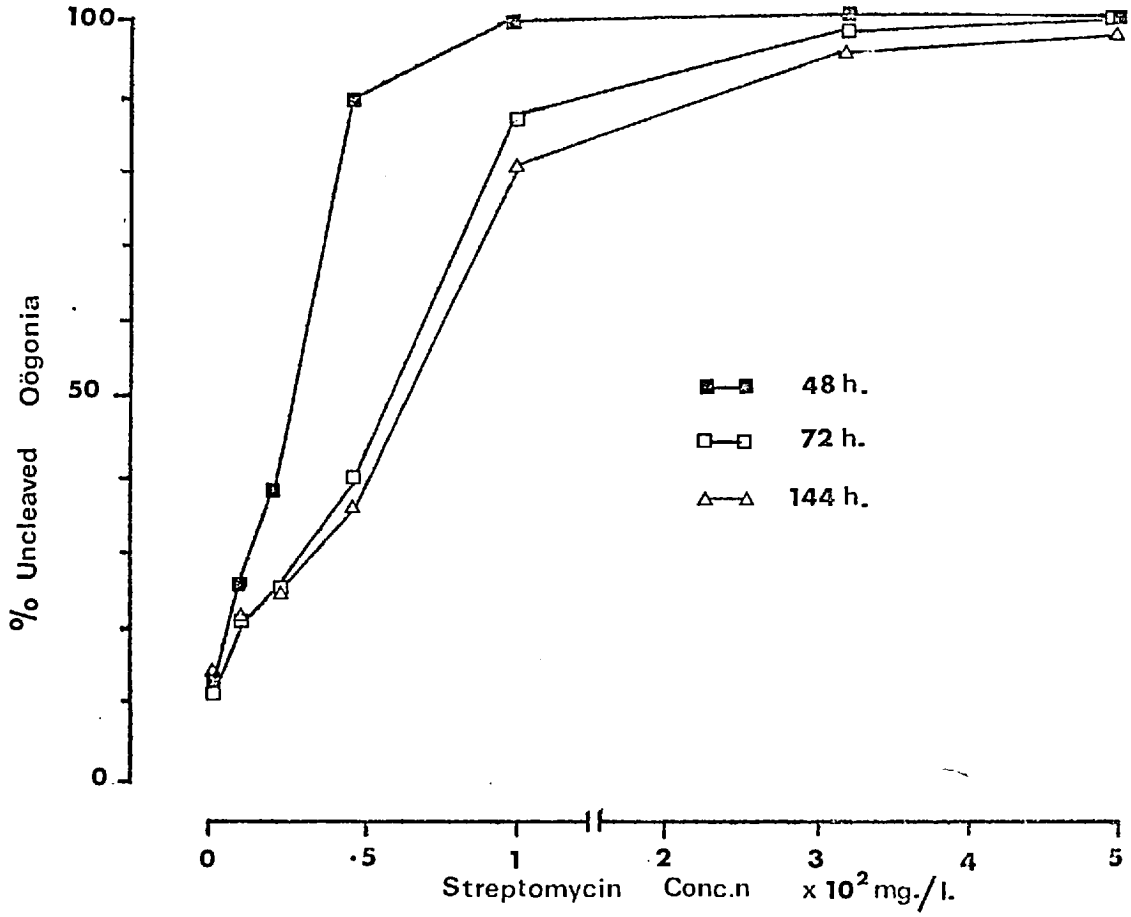


Fig. 2.17 Probit (% inhibition of oogonial cleavage) against log antibiotic concentration, assessed 168h after induction.

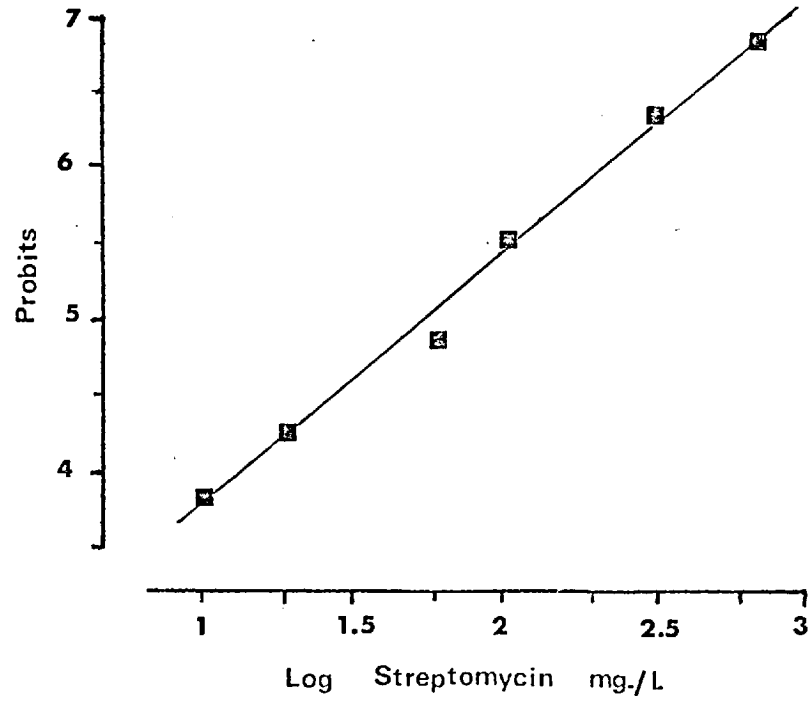


Fig. 2.18 The effect of streptomycin on the length of the lag phase prior to the appearance of the first oogonium initials in S.furcata

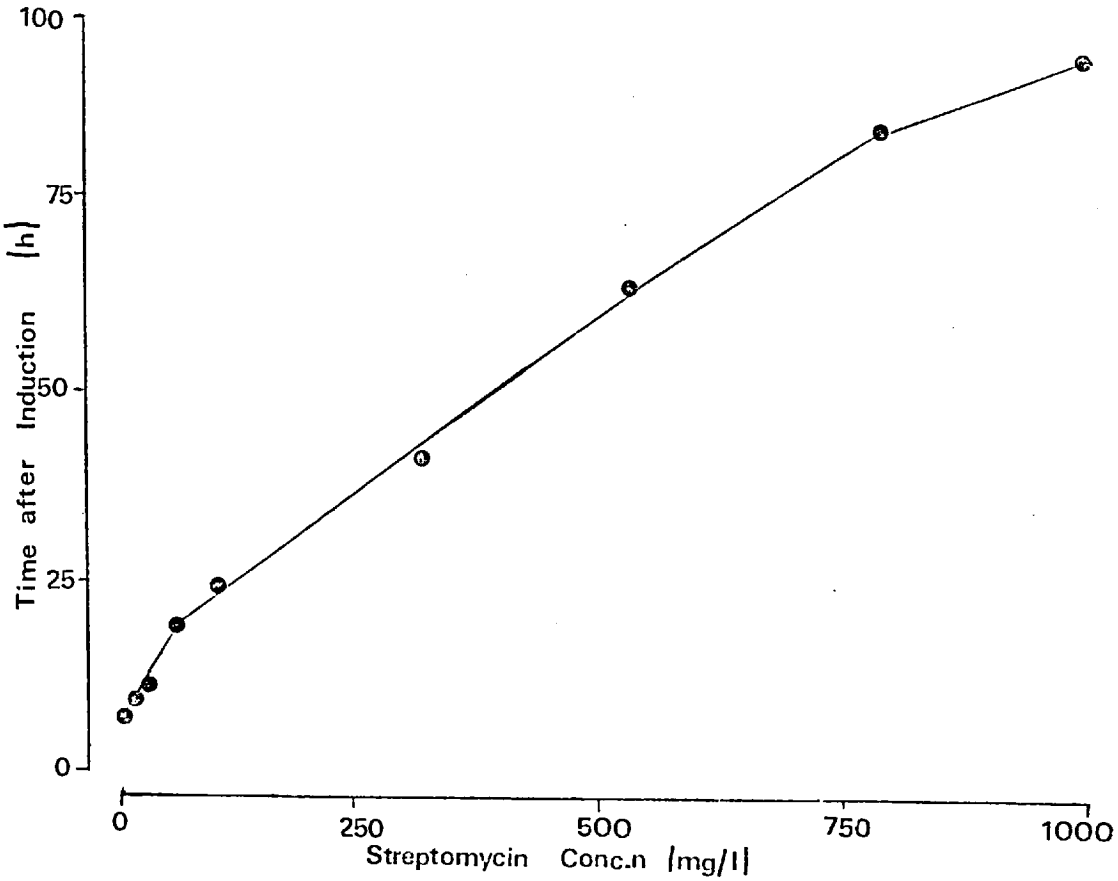
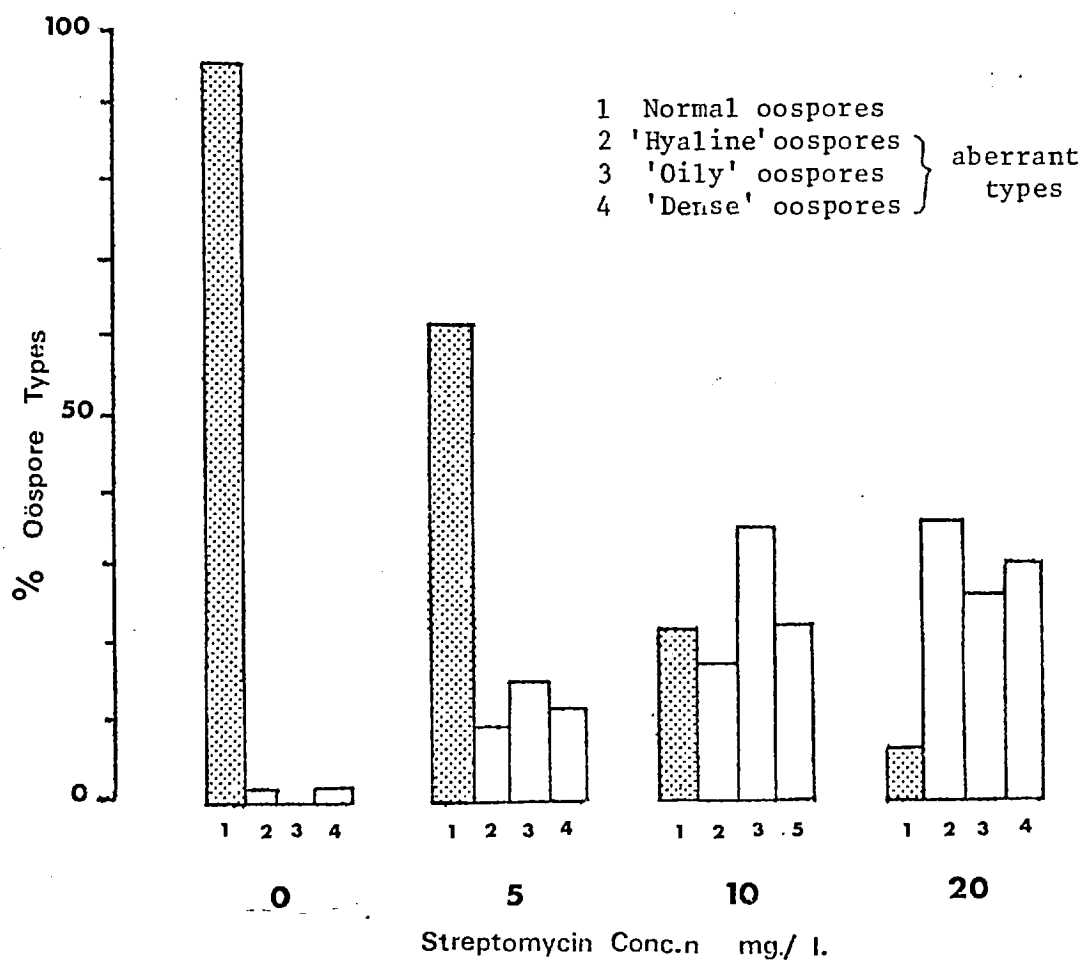


Fig. 2.19 Histograms showing the effects of streptomycin on oospore maturation, assessed 120h after induction.



concentrations. Such curves are not uncommon in fungal inhibitor studies (Cochrane, 1958) and suggests Str is affecting different physiological processes at different concentrations.

The effects of Str on sexual reproduction in other Saprolegnian species was only determined for S.megasperma, as none of the other species produced oogonia under the experimental conditions employed. As with S.furcata Str reduced the number of oogonia and the level of spore differentiation in S.megasperma. Oogonia did not form in Str concentrations above 50 mg/l, although spherical gemmae were observed up to 320 mg/l.

2.3.3.2 Oogonium cleavage

Str strongly inhibits oospore differentiation in S.furcata (Figs. 2.16, 2.17). The dose-response curves for cleavage inhibition show much less temporal change than those for oogonium production (cf. Figs. 2.14 and 2.16) In addition the probit-log dose curves follow a simple linear regression (Fig. 2.17) indicating Str behaves uniformly on this developmental process. The ED50 value taken from the cleavage data assessed 168 h after induction is 70 mg/l.

2.3.3.3 Oospore maturation

Many of the oospores which form in Str-induced oogonia abort during their maturation. This is shown by the analysis of oospore types in Str-treatments (< 20 mg/l) summarised in the histograms in Fig. 2.19. The different oospore types shown in these histograms will be described in Section 2.3.8.7.Increasing Str concentrations result in increasing numbers of abnormal oospores, so that at 20 mg/l only 5% of the spores mature normally. These results are rather more inhibitory than frequently observed. In some replicate experiments up to 30% of the differentiated oospores mature normally even in 100 mg/l Str.

2.3.4 The effects of Streptomycin on reproduction in Phytophthora cactorum

2.3.4.1 Sporangium production

The effect of Str on sporangium formation in P.cactorum is summarised in Table 2.6. Str inhibits sporangium production in this species, and the ED50 value lies approximately between 5 and 10 mg/l.

2.3.4.2 Sporangium germination

The effect of Str on zoospore differentiation and liberation from sporangia of P.cactorum was assessed in a germination test, scored 8 h after induction. The results are summarised in Table 2.7 and Fig. 2.20. The inhibition of zoospore formation in sporangia of P.cactorum follows a similar pattern to that described in Ps.humuli by Griffin and Coley-Smith (1971). The probit-dose response curves follows a linear regression, and the ED50 value for sporangium inhibition is 35 mg/l (Fig. 2.20).

Table 2.6: The effect of streptomycin on sporangium formation in P. cactorum, assessed 72h after induction at 20°C.

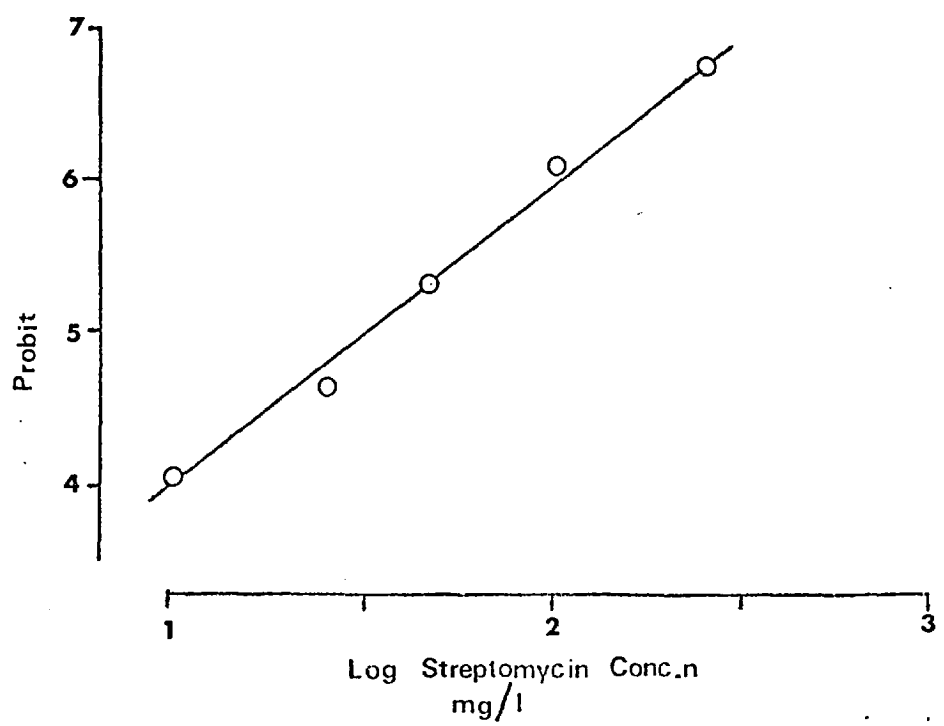
Streptomycin Concentration (mg/1)						
0	1	5	10	20	50	100
++++	++++	+++	++	+	-	-

No. Sporangia per L.P. Field: ++++, 50; +++, 20-50; ++, 5-20; +, 5; -, 0.

Table 2.7: The effect of streptomycin on sporangium germination in P. cactorum at 16°C, scored 8h after induction.

Streptomycin Conc^{n}. (mg/1)		No. Sporangia Scored	% Dehisced	% Inhibition of Germination
Before induction	0	492	5	-
After induction	0	498	81	0
	10	509	67	19
	25	569	55	34
	50	400	34	62
	100	303	15	88
	250	447	8	96

Fig. 2.20 Probit (% inhibition of sporangial germination) against log antibiotic concentrations for a suspension of P. cactorum (10^5/ml), assessed 8h after induction at 16°C.



2.3.5 The addition or removal of streptomycin at varying stages in the induction-cycle

2.3.5.1 Prior to Induction

This experiment was designed to determine if Str had any deleterious effects on the ability of antibiotic-grown vegetative colonies to sporulate after induction.

S.furcata colonies were grown on 1/2 GYPS liquid media containing 0, 50 and 500 mg/l Str. These colonies were then induced in a similar range of Str concentrations and the results, assessed 120 h after induction,are summarised in the histograms in Fig. 2.21.

Induced Str-grown colonies of S.furcata produce smaller numbers of oogonia in distilled water than the comparable control colonies (Fig. 2.21). This is expected since these colonies are smaller and have lower hyphal-densities than untreated colonies (see Section 2.3.1.2). Rather surprisingly however in the antibiotic treatments (50,500 mg/l) oogonial yields are higher in both Str-grown colonies than in the control colonies (Fig. 2.21). In addition in the 500 mg/l-treatment, the Str-grown colonies also have a significantly higher proportion of cleaved oogonia (Fig. 2.21). It appears as though colonies grown in Str are afforded some protection against its effects after induction. Although inhibiting colony-growth rate (Section 2.3.1.2) Str clearly does not impair the ability of induced-colonies to sporulate.

2.3.5.2 After Sporangial Induction

Str may be exerting its major inhibitory effects during the critical lag phase prior to reproductive-initial formation, when many of the biochemical changes associated with sporulation have been shown to be initiated (Griffin and Breuker, 1969; Timberlake et al., 1972). To determine if Str is also an effective-inhibitor of the later stages of reproductive morphogenesis, colonies of S.ferax were transferred to Str solutions (20,100 mg/l) after induction. For this purpose 5 h-induced colonies of S.ferax were selected since they possess a wide range of differentiating sporangia (Fig. 1.1). The results of this experiment, scored 8 h and 24 h after the initial colony induction, are summarised in Table 2.8.

The results in Table 2.8 demonstrate that even 20 mg/l Str added to differentiating sporangia considerably restricts further development. In particular both the proportion of uncleaved sporangia and sporangia containing encysted spores are increased. This accounts for the observed reduction in the number of liberated zoospores (Table 2.8, 24 h). The higher Str concentration (100 mg/l) effectively arrests all further differentiation on the induced colonies (Table 2.8). Clearly Str also inhibits sporangial development even when applied after the initial lag phase.

Fig. 2.21 The effect of streptomycin on oogonium production and cleavage on antibiotic-grown colonies (18h) of S. furcata, assessed 120h after induction.

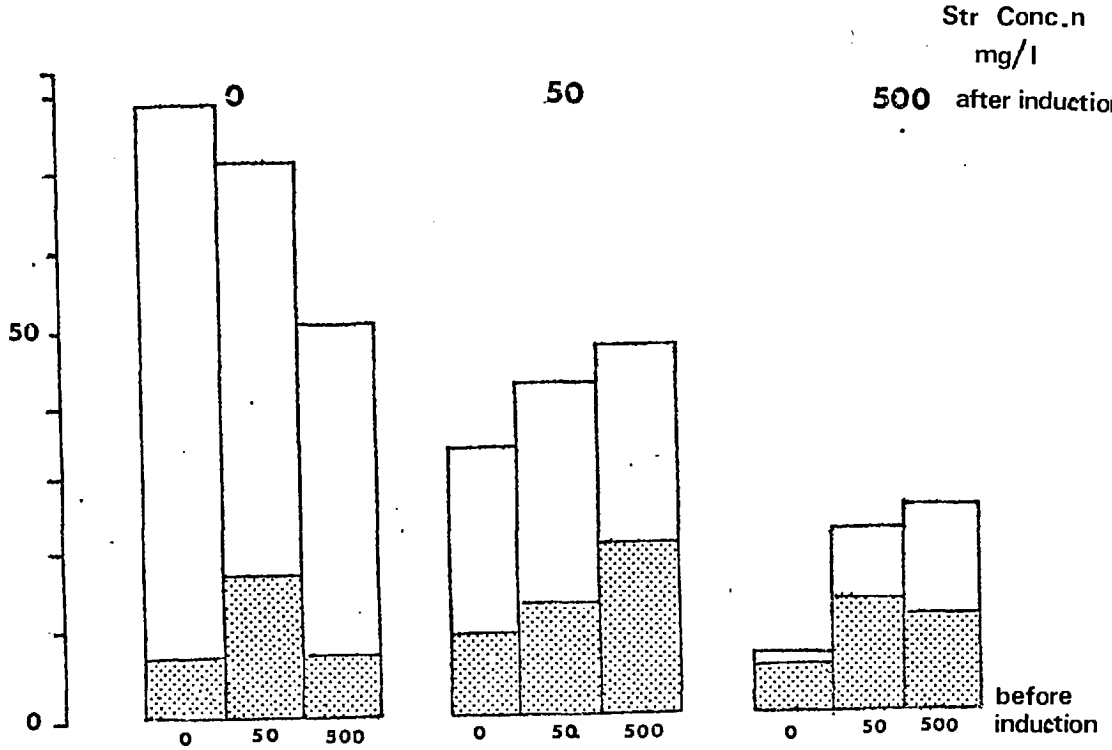


Fig. 2.22 The effect of streptomycin addition to colonies of S. furcata, 16h after induction.

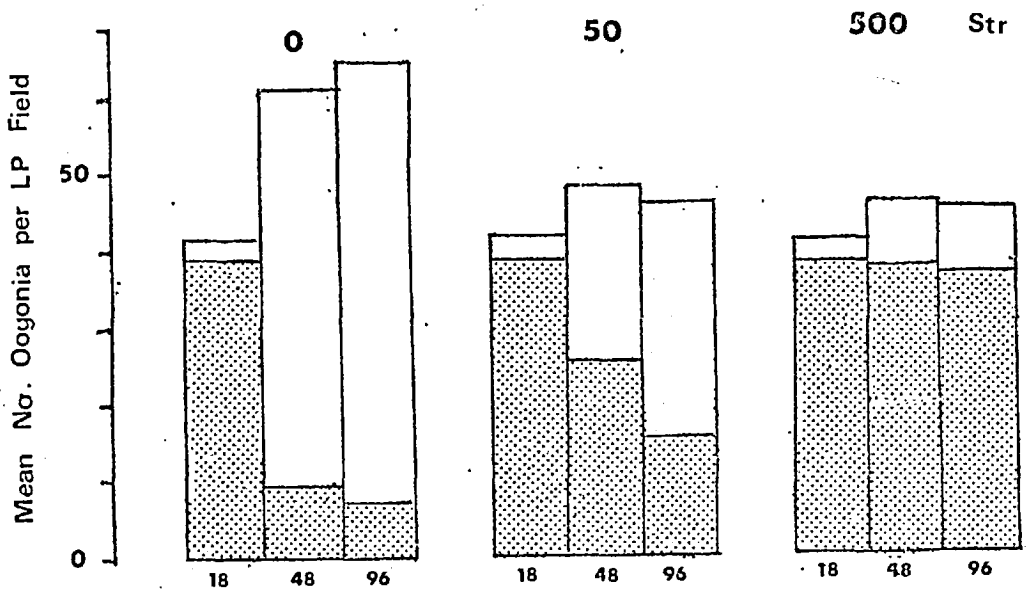


Fig. 2.23 The effect of streptomycin removal from induced colonies of S. furcata, 24h after induction, assessed after a further 48h incubation.

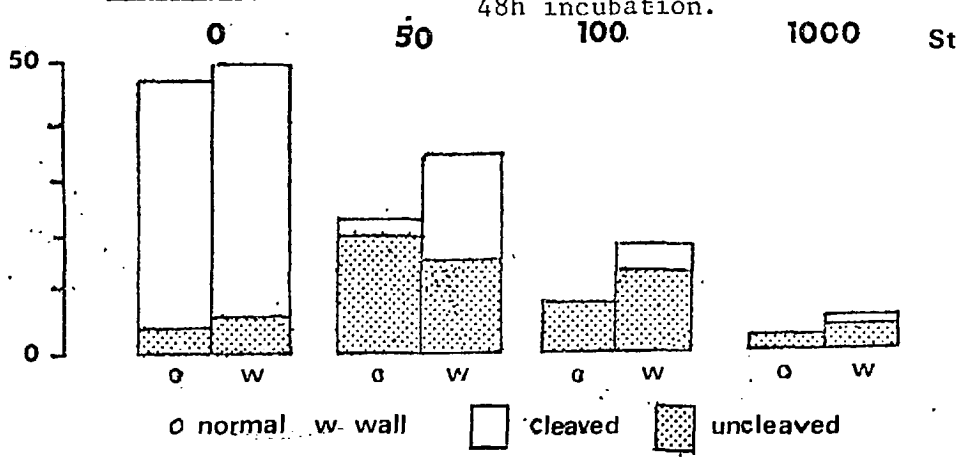


Table 2.8 The effect of Str addition to colonies of S.ferax 4 h after induction

Streptomycin conc.n (mg/l)	Time after Induction (h)						
	4		8		24		
	0	0	20	100	0	20	100
Precleavage Sporangia	+++	+++	++++	+++	+	++	+++
Post-cleavage Sporangia	+	++++	++	+	++++	+++	+
Zoospores and Cysts	+	+++	++	-	++++	++	-

Approx. No. per L.P. field: ++++, >40; +++, 40-20; ++, 20-10; +, < 10; -, 0

2.3.5.3 After Oogonium Induction

The above experiment was repeated on induced colonies of S.furcata to assess the effects of Str on partially differentiated oogonia. The colonies were transferred to Str (50,500 mg/l) 16 h after induction and the results, assessed 48,96h after the initial induction, are summarised in the histograms in Fig. 2.21 . These results are similar to those described for sporangial development in the previous section (2.3.5.2). The lower Str concentration (50 mg/l) restricts further oogonium formation after transfer and increases the proportion of uncleaved oogonia, whereas the higher concentration effectively inhibits all further differentiation (Fig. 2.22)

2.3.5.4 Removal after Induction

To assess the permanence of the Str-inhibition of oogonial differentiation the effect of antibiotic removal from induced colonies was determined. Colonies of S.furcata were induced as normal in a range of Str concentrations (0, 50, 100, 1000 mg/l) and incubated for 24 h. Half the colonies were then removed washed and placed in dishes of distilled water. All the colonies were then incubated for a further 48 h before assessing for oogonium production. The results of this experiment are summarised in the histograms in Fig. 2.23.

Although the removal of the Str results in a partial recovery of oogonial production and oospore differentiation, it is clear that at least at the higher concentrations most of the cytoplasmic damage is irreversible (Fig. 2.23). For instance in the washed colonies oogonium production is still only 64%, 35% and 10% of that of the untreated level for the three Str concentrations tested. The progressive decrease in recovery indicates that the extent of the permanent Str debilitation is directly related

to antibiotic concentration. The nature of the possible cytoplasmic effects of Str will be described in later sections

2.3.6 The Effect of other Divalent Cations on Streptomycin Toxicity

Divalent cation antagonism of Str toxicity has been widely reported in plant studies (literature review, Section 2.15). Following the results of these previous accounts the three most effective ions, viz Mn^{2+}, Ca^{2+} and Mg^{2+}, were tested in experiments with S.furcata

2.3.6.1 The effect of Ca^{2+} on the Streptomycin-Inhibition of Vegetative Growth in S.furcata

A range of Ca^{2+} concentrations (0.25 mM-25 mM) were incorporated into Str-agar containing 0.86 mM (500 mg/l) Str. These plates were inoculated with infested nylon-discs of S.furcata, and the colony-extension rate determined as described in Section 2.3.1.1. The results of this experiment are summarised in Table 2.9.

Table 2.9 The effect of Ca^{2+} ions on the colony extension rate (μm/h) of S.furcata on control and Str-agar at 25°C

Medium	Ca^{2+} Concentration (mM)				
	0	0.25	1.25	2.50	25.00
Control (1/2 GYPS)	750	725	745	763	775
Streptomycin (0.86 mM)	421	438	462	500	555

These results show that Ca^{2+} ions reduce the inhibitory effects of streptomycin on colony-extension rate. A 25-fold excess of Ca^{2+} ions increases growth rate on Str-agar by nearly 20%, although it still only reaches 75% of the untreated level (Table 2.9). The Ca^{2+} themselves have no adverse effects on colony extension rate, and may even stimulate it (Table 2.9).

2.3.6.2 Divalent Cation Antagonism of Streptomycin Toxicity to Oogonium Development

An experiment was carried out to assess the combined effects of a comparable range of Ca^{2+} and Str ion concentrations on sexual differentiation in S.furcata. The selected 72 h results from one of two similar replicate experiments are summarised in the histograms in Fig. 2.24. In this experiment all the Ca^{2+} solutions tested (0.09-1.72 mM) proved very effective at reducing the inhibitory effects of Str on sexual differentiation (Fig. 2.24). Even at the highest streptomycin concentration (0.87 mM) oogonial production is returned to a maximal level by a molar Ca^{2+} concentration 5-10 times lower than that of the antibiotic (Fig. 2.24). However at this antibiotic concentration oogonial production is still 30% lower than the control level, probably as a result of the slight toxicity of the Ca^{2+} ions themselves (Fig. 2.24).

Fig. 2.24 The effect of Ca^{2+} ions on the streptomycin-induced inhibition of oogonium development in S. furcata, assessed 72h after induction.

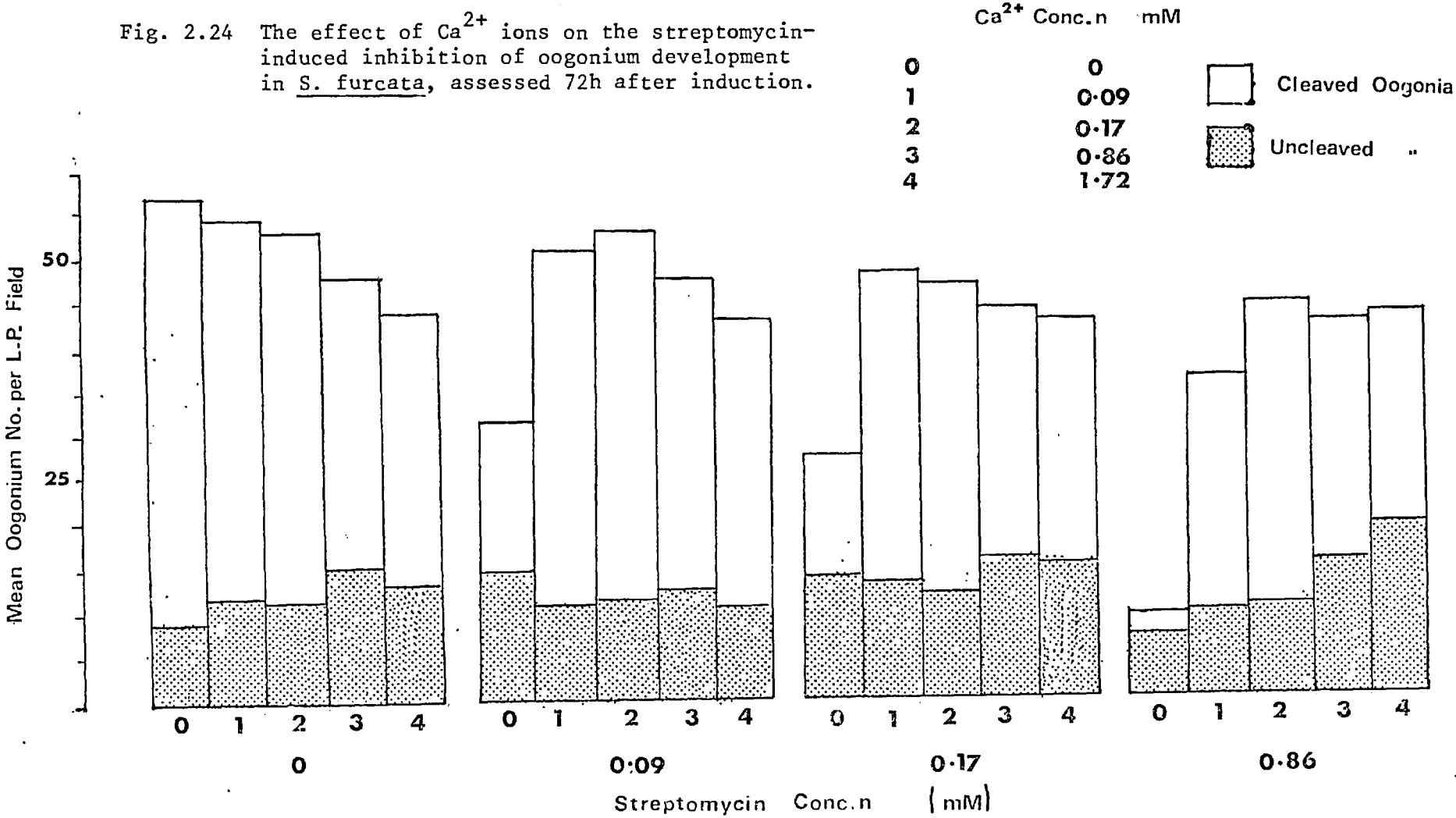


Fig. 2.25 The effect of Ca^{2+} ions on streptomycin (1.72mM) - induced inhibition of oogonium production and oospore differentiation in S. furcata, assessed 118h after induction.

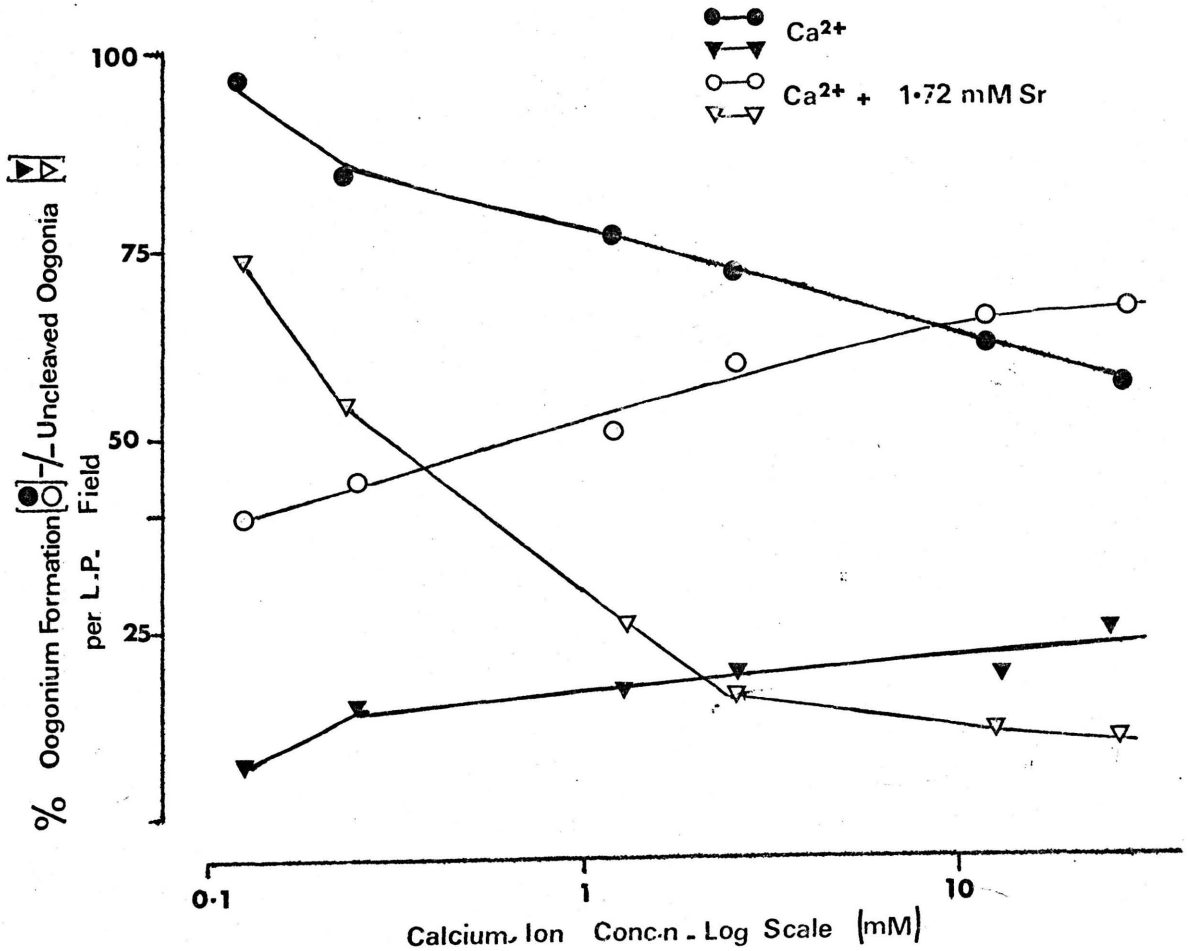
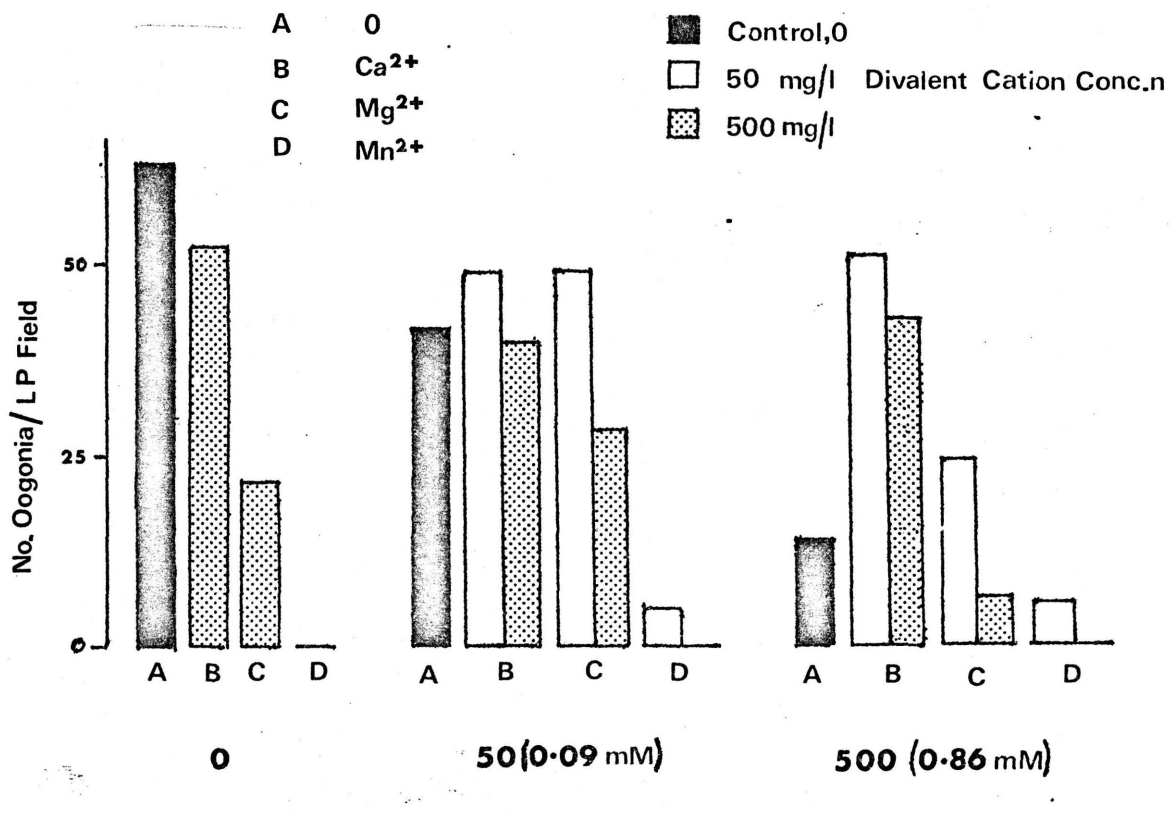


Fig. 2.26 The effect of divalent cations (Ca^{2+}, Mg^{2+}, Mn^{2+}) on the streptomycin-induced inhibition of oogonium production in S. furcata assessed 168h after induction.



This interaction between Str and Ca^{2+} ions was examined further by testing the effect of a wider range of Ca^{2+} concentrations (0.13-25 mM) against a single highly inhibitory Str concentration (1.72 mM, 1000 mg/l). The effects of these solutions on oogonium production and spore cleavage are summarised in Fig. 2.25. Clearly Ca^{2+} ions reduce both the antibiotic inhibition of oogonium formation, and cytoplasmic cleavage (Fig. 2.25). In addition Ca^{2+} ions themselves are quite inhibitory to oogonium formation, although have a less marked effect on cleavage (Fig. 2.25). What is interesting is that at high Ca^{2+} concentrations (>12.5 mM) there is a distinct synergistic effect between the two ions, resulting in higher levels of oogonium production and cleavage than when either solution is tested individually (Fig. 2.25). The maximum alleviation of Str-inhibition in this experiment occurred at Ca^{2+} concentrations of 12.5 mM and above, which is approximately 7 times the molar concentration of the antibiotic (1.72 mM). This is a similar order of magnitude to that previously reported in the Peronsporalean Oomycetes (McMeekin, 1973) and higher plants (Rosen, 1955).

The relative effectiveness of other divalent cations against Str toxicity, was assessed by testing Ca^{2+}, Mg^{2+} and Mn^{2+} in a single comparative experiment. Two concentrations of each ion (50,5000 mg/l) were selected and tested against similar levels of Str. The effects on oogonium production of these combined solutions, assessed 168 h after induction, are shown in the histograms in Fig. 2.26. The higher levels of cation used (500 mg/l: 12.5 mM Ca, 20.4 mM Mg, 9.2 mM Mn) all proved toxic to oogonium production, with Mn^{2+} being completely inhibitory (Fig. 2.26). The order of divalent cation toxicity, $Ca^{2+} < Mg^{2+} < Mn^{2+}$, was the reverse of their effectiveness as inhibitors of Str toxicity. This probably accounts for the greater effectiveness of the lower Ca^{2+} (1.25 mM) and Mg^{2+}(2.00 mM) concentrations in overcoming Str inhibition.

2.3.7 The Effects of other Protein Synthesis Inhibitors on Sexual Reproduction in Saprolegnia

2.3.7.1 Chloramphenicol (Chl)

Chloramphenicol like Str is an inhibitor of 70S ribosome function and has been shown to reduce growth-rate in Pythium (Marchant and Smith, 1968). Colonies of S.furcata were induced to sporulate in a range of Chl solutions (250-1000 mg/l) and scored for oogonium production and oospore differentiation. The results of one of two similar replicate experiments are summarized in Table 2.9.

Saprolegnia furcata proved relatively insensitive to Chl and oogonial production is only significantly reduced at concentrations of 750 mg/l (2.3 mM) and above (Table 2.9). As with the Str experiments, increasing antibiotic concentrations also increase the proportion of uncleaved oogonia

(or gemma types). For instance at a 1000 mg/l Chl only 8% of the oogonium bodies have differentiated into oospores (Table 2.9). However Chl did not produce the extended lag periods, which were such a characteristic feature of Str induction.

Table 2.9 The effect of chloramphenicol on oogonium production (mean no./L.P. field) on induced-colonies of S.furcata. The bracketed figures are the % oogonia which are uncleaved

Time after Induction (h)	Chloramphenicol Conc.n. (mg/l)				
	0	250	500	750	1000
18	31.9(100)	31.0(100)	17.8(100)	8.5(100)	3.2(100)
42	48.1(26)	49.0(25)	48.6(37)	35.6(60)	23.8(98)
120	47.5(15)	47.0(16)	48.7(28)	35.5(52)	28.1(92)

2.3.7.2 Cycloheximide (Cyc)

Unlike the previous antibiotics cycloheximide inhibits the eukaryote 80S ribosome and has been shown to block cytoplasmic protein synthesis in differentiating Achlya colonies (Cameron and LéJohn, 1971; Timberlake et al., 1972). S.furcata colonies were induced in a range of Cyc concentrations (0.5-10 mg/l) and the effects of the antibiotic on oogonium production and oospore differentiation assessed. The results of one of two similar replicate experiments are summarised in Table 2.10.

Table 2.10 The effect of cycloheximide on oogonium production (mean no./L.P. field) on induced-colonies of S.furcata. The bracketed figures are the % oogonia which are uncleaved

Time after Induction h	Cycloheximide Conc.n.(mg/l)				
	0	0.5	1.0	5.0	10.0
18	32.5(96)	25.3(100)	5.6(100)	0(-)	0(-)
42	42.1(20)	38.1(22)	10.3(82)	0(-)	0(-)
120	45.9(9)	42.8(11)	15.3(59)	0(-)	0(-)

Cyc is highly inhibitory to sexual differentiation in S.furcata, and there is a relatively narrow range of antibiotic concentrations in which oogonium development is observed (0.5-1.0 mg/l, Table 2.10). Oogonium production is completely inhibited at 5.0 mg/l Cyc (18.8 μM) and above. The proportion of uncleaved oogonia and gemma-types also increases with antibiotic concentration, although the inhibition of cleavage is not as marked as in the other inhibitors (Table 2.10). As with chloramphenicol this antibiotic does not significantly affect the length of the lag period prior to oogonium initial appearance.

2.3.8 The effect of antibiotics on gross morphology and cytology

2.3.8.1 Experimental details

Most of the morphological and cytological effects of the antibiotics on growth and reproduction were assessed during the collection of the numerical data described in the preceeding sections. In addition small portions of antibiotic-induced colonies were dissected out for more critical examination under the light microscope and photographic recording. Selected colonies were also fixed and embedded for an ultrastructural examination of antibiotic effects. The main fixations carried out in the study of Str-effects are summarised in Tables 2.11 and 2.12.

From each processed colony or suspension two samples were usually selected and blocks prepared for sectioning as described in Section 0.2.6.4. Where possible representative sections were collected throughout the whole hypha or reproductive structure selected for examination. Usually two separate specimens were examined from each of the prepared blocks. During the course of the Str studies over 20 reproductive structures from S.ferax and nearly 80 from S.furcata were examined ultrastructurally. Individual bodies were chosen on the subjective assessment that they represented fairly typical morphological types within the colony. However it is acknowledged that the relatively small specimen sample and its subjective selection impose limitations to the conclusions which can be drawn about the ultrastructural effects of the antibiotics. Unfortunately attempts to obtain a larger non-selective sample of antibiotic-induced reproductive structures proved unsuccessful.

2.3.8.2 Vegetative hyphae

Str does not alter the general hyphal morphology of Saprolegnia colonies grown either on agar media or in liquid culture (see Fig. 1.4). Increasing antibiotic concentrations reduce the overall density of hyphae within the colony although no analysis of its effect on branch frequency was undertaken.

The ultrastructural cytology of most Str-grown hyphae is similar to that described for untreated hyphae in Section 1.2.1 (Figs. 1.2-1.22). However a number of the 500 mg/l grown hyphae have a reduced ribosomal density (Fig. 2.225) and a number of other abnormal features. These will be described in the sections dealing with antibiotic effects on individual organelles (Section 2.3.9).

2.3.8. 3 Post-induction Hyphae

The first observable cytological effect in Str-induced colonies of Saprolegnia is the apparent condensation of portions of the hyphal cytoplasm into dense segments (Figs. 2.30, 2.31, 2.34). Under low power examination this gives the hyphae a distinctive 'granular' appearance. This is not a

Table 2.11 List of the fixations related to streptomycin effects on vegetative growth and asexual reproduction

Species	Stage	Incubation Time (h)	Streptomycin Conc.n.(mg/l)	Fixation	Preparation No.
S.furcata	vegetative hyphae	24	0	GaOs	3771
		24	50	GaOs	3772
		24	100	GaOs	3774
		24	500	GaOs	3775
S.ferax	zoosporangia	7	0	Os	3022
		7	40	Os	3023
		7	100	Os	3026
		96	20	Os	3323
		96	50	Os	3324
		96	100	Os	3328/9
S.ferax	encysted zoospores	8	0	Os	3885
		8	50	Os	3886
		8	100	Os	3887
		8	500	Os	3888
		8	1000	Os	3889

Table 2.12 The main colony-fixations related to streptomycin effects on sexual reproduction in S.furcata

Streptomycin conc.n. (mg/l)		Time after Induction (h)					
		9	24	48	120	168 *	240
0	A	0.6(100)	49.7(77)	79.4(19)	90.4(15)	35.2(8)	88.9(10)
	B	3444 Os	3446 Os	3449 Os	3482 GaOs	3314 Ox	3480 Km 3481
50	A	0(-)	5.1(100)	19.8(80)	40.3(44)	34.2(75)	48.2(45)
	B	-	3447 Os	3450 Os	3453 Km 3457 Os	3315 Os	3487 Os
100	A	0(-)	4.9(100)	16.9(85)	29.4(61)	26.5(79)	35.5(55)
	B	-	3448 Os	3451 Os	3454 Os 3458 GaOs	3316 Os	3483 Os
250	A	0(-)	0(-)	0(-)	6.7(100)	14.2(82)	14.2(98)
	B	-	-	-	3456 Os	3317 Os	3486 Os
500	A	0(-)	0(-)	0(-)	2.4(100)	10.9(97)	3.2(100)
	B	-	-	-	3455 Os	3319 Os	3485 Os
1000	A	0(-)	0(-)	0(-)	0(-)	9.4(100)	0.1(100)
	B	-	-	-	-	3321.Os	3484 Os

* Separate experiment

A Oogonium no.L.P. field (% uncleaved)

B Preparation no. and fixative

simple osmotic effect since it is not replicated by plasmolysis in 0.8 M sucrose, and does not usually develop until 2-3 h after induction. This condensation of hyphal cytoplasm did not normally occur at Str concentrations below 50 mg/l, and was most extensive at 320 mg/l and above (Figs. 2.30-2.37).

The condensed cytoplasm forms discrete blocks, 20-100 µm in length, which are distributed throughout the hypha including at the apex (Figs. 2.30, 2.31, 23.4, 2.37a). These segments are separated by apparently empty regions of hypha in which only a few refractile droplets and membraneous strands can be distinguished (Figs. 2.33, 2.34, 2.37a). Under ordinary optics the condensed cytoplasm appears finely particulate (Fig. 2.30) whereas it is quite refractile under anoptral phase (Figs. 2.31, 2.34, 2.37 a & b). An ultrastructural profile of one of these condensed blocks (Fig. 2.30) shows it is composed mainly of disorganised membrane fragments embedded in an osmiophilic matrix. The only recognisable components are the large droplets of coalesced lipid (Fig. 2.2?).

Not all Str-induced hyphae show such an ordered condensation of their cytoplasm. In some there appears to be a widespread dispersion of disrupted cytoplasm throughout the hypha (Fig. 2.35) whereas in others large numbers of refractile droplets develop (Fig. 2.36).

In addition, not all regions of the hyphal cytoplasm are so catastrophically affected by Str, even at concentrations of 320 mg/l and above. For instance in some of the cytoplasm continues to accumulate in the hyphal tips without them differentiating further (Fig. 2.32). The vacuole at the apex of the hypha in Fig. 2.32 contains small granules in Brownian motion. Some of the ultrastructural profiles of induced-hyphae reveal segments of cytoplasm with an abnormal organisation but still with a higher-degree of structural integrity.

The most striking example of this is the hypha treated with a 100 mg/l Str and fixed 24 h after induction shown in Figs. 2.38-2.44. The alternate segments of dense 'disrupted' cytoplasm and more normal cytoplasm(Figs. 2.38, 2.39) suggest this may be a hypha in which the condensation of cytoplasm into dense segments is still in an early stage. The 'dense phase' in this hypha shows varying degrees of organelle disruption (cf. Figs. 2.40, 2.44). It is characterised by the high ribosome density and large coalesced lipid droplets (Fig. 2.40, 2.43). The intervening cytoplasm contains the usual nuclei, mitochondria and vacuoles (Figs. 2.39, 2.41).

The interesting feature of this hypha however is that the two cytoplasmic phases are isolated from each other by fine-strands of wall material, which are between 50-80 nm thick (Figs. 2.39, 2.40, 2.41, 2.42, 2.43). These strands of proliferated wall run both parallel to the hyphal wall (Fig. 2.42),

and may either completely (Figs. 2.39, 2.40) or partially (Fig. 2.41) traverse the hyphal compartment. Similar strands of electron-transparent wall material were also observed around some of the condensed blocks of disorganised cytoplasm, although they are not present in the segment shown Fig. 1.29. Whether the presence of wall material around the dense cytoplams is the primary cause or a secondary effect of cytoplasmic damage is unclear. However it probably accounts for the well-defined outline of the condensed cytoplasmic segments.

The second abnormal hypha is illustrated in Figs. 2.45-2.49 and comes from a colony treated with 1000 mg/l Str and fixed 240 h after induction. The cytoplasm of this hypha is filled with osmiophilic droplets of neutral lipid, between 1.0-1.5 μm in diameter (Figs. 2.45-2.49). In between the lipid droplets there are elaborate whorls of membranous material and ribosome-like particles (Fig. 2.48). This hyphal segment also contains a few vacuolar vesicles (Figs. 2.45, 2.46). The vacuoles contain fine particles and a number of curious electron-dense strands organised in parallel array, which may completely traverse the vacuolar compartment (< 10 μm). Each strand is composed of osmiophilic particles, and is approximately 40 nm in diameter (Fig. 2.47).

2.3.8.4 Sporangia

Although many zoosporangia differentiate normally in Str (< 50 mg/l) their maturation is always slower than in untreated colonies (see Fig . 2.6) Frequently Str results in the formation of rather more irregularly swollen initials than in untreated colonies (cf. Figs. 2.50-2.53, 2.58,with Figs. 1.23-1.25), although their subsequent development is often normal. However, at very inhibitory antibiotic concentrations (30-50 mg/l) sporangium development may not proceed beyond a slight swelling of the hyphal tips (Fig. 2.50).

As shown in Section 2.3.2.2 Str increases the proportion of sporangia which do not from zoospores. Such streptomycin-induced gemmae may resemble the intercalary (Fig. 2.70) and terminal gemmae (Fig. 2.73) which form in small numbers on untreated colonies. Frequently Str causes the gemma cytoplasm to become disorganised and it often completely withdraws from the cell wall, forming dense blocks of cytoplasm similar to those described in the hyphae (Figs. 2.59, 2.61, 2.63-2.65, 2.71, 2.75). This phenomenon is particularly common in sporangia transferred to Str after induction (see Section 2.3.5.2). This cytoplasmic collapse does not seem to be a simple plasmolysis since it usually occurs at the time of zoospore differentiation. It is possible this is a period when the plasmalemma and tonoplast are most vulnerable to the antibiotic.

Some of the Str-induced gemmae are highly vacuolate (Figs. 2.55, 2.56, 2.70) whereas others are uniformly dense and appear to lack an axial vacuole

(Figs. 2.62, 2.68, 2.74). Ultrastructural observations confirm the rather variable pattern of vacuolation in Str-induced reproductive structures (Fig. 2.66, 2.67, 2.77, 2.78). Even in bodies in which an axial vacuole has formed the peripheral cytoplasm is less evenly distributed than in comparable untreated sporangia (cf. Fig. 2.77 and Fig. 1.47). In others, although vacuoles appear they do not show the usual axial alignment and coalescence but remain scattered throughout the cytoplasm (Figs. 2.66, 2.78). At highly inhibitory concentrations (50-100 mg/l) sporangia show considerable disruption of both the densebody vesicle and vacuolar membranes, as shown in Fig. 2.67.

Str-induced sporangia and gemmae contain similar organelles to those described in untreated bodies in Section 1.22. All Str-induced bodies examined < 7 h after induction contained both densebody granules and bars, and some contained flimmer vesicles (Fig. 1.40). However after prolonged periods of incubation (>90 h) Str-induced gemmae although still containing abundant bar bodies (Figs. 2.170-2.173) have lost their flimmer vesicles. There is some evidence to suggest bar body formation is still continuing in these bodies. They contain cup-shaped cisternae whose densely particulate contents are similar in appearance to the peripheral bar matrix. These cisternae may be bar body precursors, and in untreated sporangia have only been observed in early precleavage stages (< 5 h after induction) (Gay, personal communication). The continued presence of these cisternae and the abundant peripheral wall vesicles (Fig. 2.182) suggest streptomycin-induced sporangia are still metabolically active, eventhough cleavage has been inhibited.

2.3.8.5 Zoospores and Cysts

Although Str increases the number of zoospores which encyst within the sporangia (Section 2.3.2.2) many of these entrapped spores germinate normally. Their germtubes emerge either through the papilla or penetrate the sporangial wall (Fig. 2.76). Str does not usually affect primary zoospore morphology, although they swim more slowly and their period of motility is reduced.

In spite of careful searching very few abnormally large zoospores and cysts were produced by Str-induced colonies of S.ferax. This contrasts markedly with the effects on P.cactorum sporangia described in Section 2.3.4.2. In these abnormally large zoospores and cysts are a common result of Str-treatment (Figs. 2.234-2.237). Str-induction does however increase the proportion of encysted zoospores which lyse before germination. Lysed cysts are recognised by their uneven profile and they contain conspicuous refractile droplets. Ultrastructurally lysed cysts contain no intact organelles and are largely contentless except for abundant membrane fragments and aggregated lipid droplets (Fig. 2.89).

Cysts germinate either by releasing secondary zoospores or by producing germtubes. Str-incubated cysts frequently only partially liberate

their secondary zoospores (Fig. 1.62) and usually produce rather short convoluted germtubes. Some of these cysts, in which germination has been arrested prematurely, have an unusual ultrastructural cytology (Figs. 2.84, 2.88). They are distinguished by the almost complete loss of cytoplasmic particulate fractions, which gives these spores the appearance of $KMnO_4$-fixed material. Bundles of flimmer tubules are still abundant in these spores, and they even occur in the inflated perinuclear envelope (Figs. 2.85, 2.88). Other germinating cysts have a similar ultrastructural cytology to the untreated spores in Figs. 1.64-1.66, except wall lomasomes are more abundant and often larger (Fig. 2.83).

A number of Str-incubated cysts have a densely staining cytoplasm with degenerate cell organelles and coalesced lipid droplets (Figs. 2.79-2.82). The extent of organelle degeneration in these dense cysts is rather variable, and while some still contain recognisable nuclei and mitochondria (Figs. 2.79, 2.80) in others only membraneous whorls remain (Figs. 2.81, 2.82). These spores always however contain elaborate vacuolar complexes (Figs. 2.79-2.82) which frequently include osmiophilic material resembling expanded densebody granules (Figs. 1.66-1.67). Similar vacuolar complexes have also been described in the unicellular alga Protosiphon botryoides, treated with Str (Berkaloff & Jupin, 1974). It is possible that these dense cysts represent an early stage of antibiotic-induced lysis.

2.3.8.6. Oogonia which differentiate into oospores

Since the effects of antibiotics on sexual differentiation in S.furcata are somewhat complex the fate of gametangia which form oospores and those which do not will be described in separate sections. As with the sporangia gametangium development in Str-induced colonies is slower than in untreated colonies. In addition the gametangia form on much more elaborately coiled stalks than the untreated bodies (cf. Figs. 2.90, 2.92-2.95 with Figs. 1.68, 1.69, 1.71, 1.77). However the ultrastructural cytology of these developing Stage 1 initials is similar to that of comparable untreated bodies (cf. Figs. 2.96 and 1.70), although they probably contain a higher density of organelles.

The gametangia are delimited by septa and by Stage IV the oogonia are vacuolate and the nuclei are entering meiosis (Figs. 2.95, 2.97). Only antheridiate oogonia form oospores (Figs. 2.92-2.94, 2.95). The main effects of Str on these bodies seems to be to derange the normal pattern of expansion and to reduce the rate of differentiation.

Neither of these effects are produced by Chl and Cyc treatments. In these antibiotics the developing gametangia are similar to those described in untreated colonies. However a small number of Cyc-induced oogonia did show an unusual pattern of cleavage. Instead of forming oospores, the

oogonial cytoplasm differentiated into a much larger number of uninucleate cyst-like bodies (Figs. 2.249, 2.250). A similar pattern of differentiation has also been reported by Slifkin (1967) in colchicine-treated gametangia of S.delica.

2.3.8.7 Oospores and fertilisation tubes

The outer primary wall which forms around oospores which differentiate in the presence of Str is usually thicker (2-3 times) than in untreated spores (cf. Figs. 2.149, 2.151 and Figs 1.30, 1.31). Most of the Str-induced spores examined shortly after wall formation have the typical Stage VII organisation (Section 1.2.4.1, Figs. 1.128) and show a well redefined segregation of their neutral lipid and densebody fractions (Fig. 2.140).

Varying proportions of Str-induced oospores do not mature normally and a number of different types of aborted spore can be recognised (Fig. 2.19). There is a good deal of variation in oospore cytology even within a single oogonium (Figs. 2.143, 2.147). Ultrastructurally Str-induced mature oospores (Stage IX-X) even though poorly fixed show a well-preserved ooplast matrix and an electron transparent endospore layer (Fig. 2.156). Most mature Str-induced oospores contain the characteristic motile granules in their ooplast.

Some of the aborted oospores in Str-treatments remain uniformly dense and do not seem to acquire the inner endospore wall layer (Figs. 2.143, 2.146). These 'dense' spores contain randomly distributed neutral lipid and densebody fractions, although some of the latter are frequently beginning to coalesce (Figs. 2.141, 2.154). The densebody vesicles frequently contain elaborate myelin arrays (Figs. 2.157) and the densebody granules are sometimes aggregated in clumps (Fig. 2.158). It is usually difficult to recognise any other organelles, such as nuclei and mitochondria, in these spores.

A number of Str-induced oospores contain large oily globules and their protoplast often withdraws from the wall (Figs. 2.145, 2.146). The ultrastructural equivalents of these 'oily' spores have not been recognised with certainty. The oospore in Fig. 2.155 contains both aggregated densebody vesicles and partially coalesced lipid, both of which could account for the large refractile droplets observed in the light microscope.

Finally there are a number of oospores which have lysed and have lost most of their cytoplasmic contents. These transparent 'hyaline' spores only contain a few small refractile droplets of lipid (Figs. 2.147, 2.153). The ultrastructural profile of a hyaline spore in Fig. 1.42 shows a few large lipid droplets and numerous membrane fragments typical of lysed cytoplasm. Note the presence of an inner endospore wall layer to this spore which indicates cytoplasmic lysis occurred after Stage VIII.

In contrast Cyc results in little oospore abortion, although results in mature oospores with uniformly refractile ooplasts (Fig. 2.251). Ultrastructurally these spores always have a well preserved osmiophilic ooplast matrix (Figs. 1.142, 1.143). These differences suggest streptomycin is probably not acting solely as a protein synthesis inhibitor.

The antheridia of Str-induced oogonia produce fertilisation tubes which balloon out to form conspicuous spherical bodies up to 10 µm in diameter (Figs. 2.144, 2.152). These expanded fertilisation tubes are highly vacuolate and contain a peripheral crescent cytoplasm adjacent to the spores (Fig. 2.152). This cytoplasm contains mainly lipid droplets in addition to a few mitochondria and large multivesicular bodies.

One Str-induced (100 mg/l, 48 h) oogonium provided the only example of an ultrastructural profile through copulating gametangia (Fig. 2.148). The fertilisation tube produces a penetration peg which ruptures the oospore wall and extends nearly 4.0 µm into the oospore cytoplasm. However it does not rupture the plasmalemma. The high density of the peg cytoplasm, its buckled wall and location in a pocket in the plasmalemma all suggest it has collapsed slightly during fixation (Fig. 2.148). No recognisable organelles are discernable in the peg cytoplasm, and it is completely enclosed by a thin (50 nm diameter) wall. This suggests that plasmogamy has not yet occurred.

More elaborate peg-like inclusions were also observed in neighbouring spores (Figs. 2.149). Serial-sections revealed these pegs to be of fertilisation tube origin (Fig. 2.151). It is suggested these are older penetration pegs which have discharged their cytoplasm, collapsed and become partially sequestered by a layer of primary oospore wall (Fig. 2.149). The latter may be the result of the enhanced wall formation in Str-treated bodies and may not occur in untreated bodies. These pegs probably become further compressed by the accretion of the endospore wall layer during Stage VIII, resulting in a structure such as shown in Fig. 1.176.

2.3.8.8 Uncleaved Reproductive Structures

As shown in Sections 2.3.3.2, 2.3.7.1 and 2.3.7.2 a considerable proportion of the reproductive structures which form in the presence of all three antibiotics fail to differentiate into oospores. The morphology of these bodies and their subsequent differentiation is extremely variable, being dependent on the antibiotic, its concentration, and the period of incubation. The association of antheridia with these uncleaved bodies is also variable (see Figs. 2.101-2.139). For instance at Str concentrations < 100 mg/l antheridia may be associated with between 5-50 % of the uncleaved bodies, whereas at higher concentrations their formation is usually completely supressed.

The antheridia associated with the uncleaved oogonia in Str-treatments are usually highly vacuolate and the organelles are confined to the peripheral cytoplasm. The nuclei in these bodies were always in interphase.

Antheridia were more frequently associated (c. < 75%) with uncleaved reproductive structures in Chl (1000 mg/l) than in the other two antibiotics. There is also some evidence that the nuclei in Chl-treated antheridia may undergo meiosis independently of the oogonial nuclei. For instance the male nucleus in Fig. 2.243 is a typical post-divisional gametic nucleus, whereas the comparable female nuclei still appear to be in interphase (Fig. 2.247).

In some instances Str interferes with differentiation as early as Stage I, and results in the development of curious knots of convoluted hyphae (Figs. 2.90, 2.91). Most of these bodies do not differentiate any further, although some may develop an oogonium at their tip. The majority of antibiotic-induced bodies are delimited by septa, after which they are classifiable as oogonia or gemmae. The undifferentiated gemmae can be divided into a number of distinct morphological groups:

1. Spherical Gemma Chains

The simplest uncleaved structures resulting from antibiotic-treatment are the typical gemma-structures (see Section 12.36). These are spherical bodies 40-50 µm in diameter which occur either singly (Figs. 2.100, 2.246) or in short chains of 3-4 bodies (Fig. 2.93) which develop in acropetal succession. They usually lack antheridia (Figs. 2.98, 2.100, 2.246). When mature these bodies are highly vacuolate and have a similar cytoplasmic organisation to the Stage IV oogonia, although they always contain interphase nuclei (Figs. 2.102, 2.255). The individual gemmae in the chains are always separated by a tripartite septum, and the younger ones are frequently only partially vacuolate (Figs. 2.99, 2.101).

2. Elongate Gemmae

At the higher antibiotic concentrations (> 320 mg/l Str, 1000 mg/l Chl, 1 mg/l Cyc) many of the reproductive structures develop as elongate club-shaped bodies (Figs. 2.129, 2.131, 2.244). These bodies are often extremely large and may be upto 150 µm in length, and up to 80 µm in diameter. They are highly vacuolate, with vacuolar vesicles accounting for over 70% of the total volume fraction (Figs. 2.131, 2.244).

3. Appendate Gemmae

Vegetative development in these bodies is initiated by the formation of refractile papillae (Figs. 2.103, 2.107, 2.119) which enlarge to form small, usually spherical, appendage initials (Figs. 2.105, 2.107, 2.109, 2.112). These papillae are presumably initiated by the polarised deposition of wall vesicles since the cytoplasm of the newly formed papilla is composed

almost exclusively of wall vesicles (Fig. 2.104). The papilla develops by the formation and extension of a new inner wall layer which ruptures the overlying cell wall leaving characteristic wall scars around the base of each appendage (Figs. 2.106, 2.109, 2.113). Appendage formation is therefore similar to germtube formation in cyst germination. Usually several appendages are initiated on each gemma, although their development is not synchronous (Figs. 2.107, 2.111, 2.115, 2.116, 2.119).

Once initiated, vegetative appendages either continue to expand spherically (Figs. 2.111, 2.112, 2.121) or establish apical polarity and elongate (Figs. 2.110, 2.114-2.119). The spherical appendages may reach a diameter similar to that of the original gemma (Fig. 2.121), and may result in the formation of chains of spherical bodies (Figs. 2.111, 2.121). Although they are superficially similar to the gemma chains described above (Fig. 2.121) the individual components are never separated by septa. As these spherical appendages are frequently vacuolate and the vacuole system is continuous with that of the orginal gemma body (Figs. 2.109, 2.111). In some instances the spherical appendages may commence linear extension as shown in Fig. 2.121.

In Str the elongate appendages are extremely varied in their appearance. Most are irregularly swollen (Figs. 2.110, 2.116, 2.118, 2.121, 2.122) and have tortuous undulating profiles (Figs. 2.114, 2.119, 2.130). The appendage tip is usually refractile (Fig.2.119) and contains the usual accumulation of wall vesicles (2.108). As in the apices of cyst germtubes plasmalemmasomes are abundant at the appendage tip (Fig. 2.108). The cytoplasm from the orginal gemma body migrates into the extending appendages, until they become almost completely devoid of contents (Figs. 2.115, 2.119, 2.124-2.126, 2.128). Many of the appendages only extend for a short distance (< 100 µm) before growth ceases and the cytoplasm accumulates at the expanding apex (Figs. 2.121, 2.124). These secondary bodies are delimited by a basal septum, and the process may repeat itself. In this way chains of 3-4 bodies are formed in basipetal succession (Figs. 2.124, 2.126). Such chains are immediately distinguishable from gemma chains by the small size of the terminal body and the evacuated subtending bodies (Figs. 2.124-2.126).

Although elongate appendages from in Cyc-induced gemmae they are never as irregularly swollen as in Str (Fig. 2.252). Some are, however, terminated by simple spherical bodies, although repeated emergence was not observed (Fig. 2.252). Therefore the elaborate vegetative-appendage forms are a distinctive feature of Str action, at least in S.furcata.

4. Secondary Gemma Bodies

The secondary gemmae which develop in Str are usually spherical and between 15-30 µm in diameter (Figs. 2.125, 2.126, 2.136-2.138). Occasionally more elongate bodies are delimited such as shown in Fig. 2.133. Although

some of these secondary gemmae are vacuolate (Figs. 2.138, 2.139) most have a uniformly dense cytoplasm (Figs. 2.136, 2.137). Ultrastructural profiles of these bodies reveal considerable breakage of the vacuolar and densebody vesicle membranes (Fig. 2.134), and in some cases they have disappeared completely (Fig. 2.135). This collapse of vacuolar structure is also suggested in the light-microscope by the rather dense lumpy nature of the cytoplasm (Figs. 2.120, 2.136). Even in the vacuolate bodies the vacuolar compartment is often made up of smaller vesicles (Fig. 2.139).

Secondary-gemmae contain the usual organelles, although densebody vesicles are much scarcer (< 2% cytoplasmic volume fraction) than in primary gemmae (< 10% volume fraction). The neutral lipid droplets are still plentiful and account for upto 10% of the cytoplasmic volume fraction. In some secondary gemmae however the neutral lipid droplets are peripherally distributed (Fig. 2.139).

These secondary gemmae were scored as 'oogonia' in the quantitative studies and their formation accounts for much of the increase in production noted at higher antibiotic concentrations (>100 mg/l) with prolonged periods of incubation (>120 h) (see Fig. 2.13).

2.3.8.9 The Variation and Range of Morphological Types

The development of these various types of reproductive body in Str-induced colonies shows considerable variation both within treatments and between replicate experiments. For instance in some experiments undifferentiated gemmae with spherical appendages (Figs. 2.112) would predominate, whereas in others the repeated emergence pattern (Figs. 2.124-2.126) was more common. However in general gemma-chains and appendate gemmae were more common at Str concentrations between 50-320 mg/l, and the larger more-elongate gemmae at concentrations of 320 mg/l and above. Usually the gemmae produced vegetative appendages between 24 h-72 h after their initial delimitation. As a result the proportion of appendate bodies increased during the period of scoring, and were most abundant (< 60% total) after 120 h of antibiotic incubation. The formation of vegetative appendages and gemmae indicates the continued functional activity of these regions of the hyphal cytoplasm that are not destroyed during the early stages in induction.

The only other oogonium-forming species on which the effects of streptomycin were assessed in any detail was the unisporiate S.megasperma. In this species streptomycin also inhibits oogonium cleavage and increases the proportion of elongate clavate gemmae. Most of the oospores formed in 50 mg/l Str aborted, giving rise to typical 'oily' spores. Appendage formation on the other hand was rare. However some early preliminary experiments with an isolate believed to be S.monoica showed a morphological response to Str similar to that reported in S.furcata. Therefore the

ability to form vegetative apendages in Str-induced gemmae may be a feature of the species.

The range of morphological types which develop on antibiotic-induced colonies and the differences between Str and Cyc are illustrated in the analysis of reproductive structures summarised in Table 2.13. This data was obtained from two colonies scored 96 h after induction in 100 mg/l Str and 1 mg/l Cyc. Str results in a slightly broader spectrum of morphological types and includes a much higher proportion (50% compared with 20%) of appendate forms. This again illustrates that Str favours continued vegetative development of antibiotic-inhibited bodies, indicating that only some of the developmental pathways are blocked.

Table 2.13 The effect of Str and Cyc on the morphogenesis of reproductive structures in S.furcata. Results were assessed 96 h after induction

Morphological Type	Photographic Example in Plates (Fig.no.)	Streptomycin 100 mg/l		Cyloheximide 1 mg/l	
		No.counted	% total	No.counted	% total
Hyphal knots	2.90, 2.91	5	2	0	-
Oogonia Stage I	2.93,2.95	20	8	0	-
Oogonia Stage VII-X	2.143-2.147, 2.251	14	5.6	36	26.0
Gemmae					
Spherical	2.100	66	26.6	58	40.0
Chains	2.98	8	3.2	6	4.0
Club-shaped	2.129	3	1.2	6	4.0
Appendate Gemmae					
Appendage initials	2.103,2.107, 2.253	26	10.5	18	12.2
Spherical appendages	2.112,2.121	61	24.6	4	2.7
Elongate appendages	2.115,2.116-2.119	4	1.6	8	5.5
Delimited Secondary Bodies	2.125,2.126, 2.252	41	16.4	9	6.2

2.3.8.10 Phytophthora cactorum sporangia

The ultrastructural study into Str effects on Phytophthora sporangia was rather limited, although the results will be included for comparison with the Saprolegnian effects. In Str (50-500 mg/l) the sporangia which fail to produce zoospores have a dense, slightly contracted, cytoplasm containing large refractile droplets (Figs. 2.231, 2.232). Ultrastructural profiles of these sporangia reveal there has been a widespread lysis of the main cellular organelles (Figs. 2.238-2.240). Only the massive aggregations of coalesced lipid are clearly recognisable (Figs. 2.238, 2.239).

At Str concentations between 50-250 mg/l a large number of abnormally large zoospores are formed (Fig. 2.235). At lower concentations (< 100 mg/l) these spores are usually quadriflagellate, and approximately 5-10 µm size, whereas at higher concentrations the undifferentiated protoplast is often released (Fig. 2.234). This results in the formation of a massive zoospore 15-20 µm in diameter (Fig. 2.235) which settles to form very large cysts (Fig. 2.236). These cysts are still viable and usually germinated by producing 3-4 germtubes (Fig. 2.237). Unfortunately the ultrastructural cytology of abnormal zoospore production could not be followed.

2.3.9. The Effect of Antibiotics on Organelle Ultrastructure

2.3.9.1 Ribosomes and Endoplasmic Reticulum (ER)

Incubation in Str frequently reduces the abundance of cytoplasmic ribosomes. This phenomenon is observed in vegetative hyphae (Fig. 2.225), sporangia (Fig. 2.171), encysted zoospores (Figs. 2.84-2.88), oogonia (Fig. 2.177, 2.179) and oospores (Fig. 2.157). This reduction in cytoplasmic ribosomes is most extensive in some of the abnormal cysts (Figs. 2.84-2.88) which resemble preparations fixed in $KMnO_4$. In the uncleaved sporangia and oogonia ribosome reduction is mainly observed in Os-fixed bodies after prolonged (> 90 h) Str-incubation (Figs. 2.171, 2.177, 2.179). In some of these bodies it appears to result from the disruption of the vacuolar membranes and the dispersion of ribosome particles into the spaces previously occupied by vacuoles (Figs. 2.159, 2.161, 2.162). A similar reduction in ribosome abundance is also observed in Chl-induced gemmae (Figs. 2.242, 2.247, 2.248) whereas comparable Cyc-induced bodies always have a high ribosome density (Figs. 2.256, 2.260). Some of the hyphae and cysts in which the cytoplasm is in various stages of condensation contain a very high density of ribosome-like particles (Figs. 2. 43, 2.79).

The formation of extensive parallel arrays of rough ER in antibiotic-treated bodies only occurs in some Str-grown hyphae (Figs. 2.225, 2.226, 2.228) and in the Cyc-induced gemmae (Figs. 2.256, 2.257, 2.259). In both these cases the arrays of parallel cisternae (< 6) are aligned around the nuclei (Figs. 2.225, 2.226, 2.256) and mitochondria (Figs. 2.228, 2.257)

2.3.9.2 Mitochondria

In spite of their reported function as 70S-ribosome inhibitors, both Str and Chl resulted in suprisingly few effects on mitochondrial structure, at least in the immediate (< 90 h) post-induction phases. In most hyphae, sporangia cysts and oogonia the antibiotic-induced mitochondria are similar in size and internal structure to comparable control structures. The mitochondria contain abundant peripheral cristae and the matrix includes the usual ribosome particles (Figs. 2.175, 2.176, 2.242, 2.243). There was no evidence of any internal membrane disorganisation such as induced by Chl

in Tetrahymena pyriformis (Turner & Lloyd, 1971) and Clamydomonas reinhardi (Behn & Arnold, 1974a). The only disruption of mitochondrial membranes observed was in some of the Str-incubated cysts in which the outer membrane has ruptured, and the inner membrane inflated with the resulting loss in cristal structure (Fig. 2.88).

However after prolonged periods of Str-incubation (>90 h) many mitochondria in the sporangia and oogonia become more irregular in shape and contain less regularly arranged cristae (Figs. 2.162, 2.163, 2.177-2.179, 2.180). There is also much more variability in the density of the mitochondrial matrix (Figs. 2.178-2.181) which may indicate an effect on the ribosomes. Some of the Str-induced secondary gemmae (Fig. 2.135) contain short, nearly spherical mitochondria, most of which have a single induced droplet of lipid-like material (Fig. 2.181). In contrast the mitochondria in Chl-induced gemmae, frequently contain elongate mitochondria (Fig. 2.245). These elongate profiles often have several constrictions, perhaps indicating that they are about to split into smaller units (Fig. 2.245). Most of the mitochondria in Cyc-induced gemmae, even after prolonged antibiotic incubation (120 h), still contain abundant rather elongate cristae (Figs. 2.256, 2.257, 2.259).

2.3.9.3 Golgi Dictyosomes

There is no indication that Str reduces Golgi number or depresses their activity in antibiotic-induced sporangial and oogonial gemmae. Even after prolonged Str-incubation (>90 h) when all Golgi-activity has ceased in untreated colonies, the dictyosomes appear to be actively producing peripheral vesicles (Figs. 2.175-2.177). They also retain the ER-mitochondrian association, which is thought to be related to periods of active wall synthesis (Section 1.3.4.1). By comparison Golgi profiles are relatively scarce in comparable Chl and Cyc-induced gemmae (Figs. 2.242, 2.243), and show little sign of wall vesicle formation.

Even in some of the Str-induced gemmae (> 90 h) the dictyosomes cisternae are reduced to small clusters of electron dense vesicles, which still show a close mitochondrial association (Figs. 2.162, 2.179, 2.191). These observations indicate Golgi participation in wall synthesis is not inhibited by Str, and this is corroborated by the observations on wall development.

2.3.9.4 Wall vesicles, the cell wall, and septa

Wall vesicles are present in the peripheral cytoplasm of all antibiotic induced reproductive structures. However they are particularly abundant in Str-induced bodies and can frequently be seen in abundance in localised clusters (Figs. 2.170, 2.182, 2.183) and around the peg-like wall ingrowths (Figs. 2.195-2.199, 2.201). In some Str-affected sporangia wall vesicles are widely scattered throughout the cytoplasm (Fig. 2.66). The uneven

plasmalemma profile (Figs. 2.185, 2.186) is considered indicative of active wall vesicle deposition in these bodies. The usual apical concentrations of wall vesicles are present in both the apices of Str-grown hyphae and vegetative appendages (Fig. 2.108). The maintainence and re-establishment of polarised wall deposition is not therefore inhibited by Str.

The walls of Str-induced reproductive structures at all stages are on average between 1½-3 times thicker than either untreated or Chl or Cyc-induced bodies. This is shown in Table 2.14 which gives a summary of the measured range of wall thickness and lomosome abundance throughout development. The only stage during which Str-treatment does not increase wall thickness or lomasome frequency is the vegetative hyphae (Table 2.14). This is in contrast to two other growth-inhibitory antibiotics, griseofulvin and cycloheximide both of which are reported to increase hyphal wall thickness (Bent & Moore, 1966; Stenlight, Katz & Rosenberger, 1971).

In most reproductive structures Str does not appear to alter the texture and density of the cell walls, except that they have a more fluffy surface (Figs. 2.182, 2.184-2.187, 2.190-2.194).

Table 2.14 Summary of measured range of wall thickness and lomasome frequency in control and antibiotic-induced material

Developmental Stage	Age* (h)	Control		Str 50-1000		Chl 1000 mg/l		Cyc 1 mg/l	
		A	B	A	B	A	B	A	B
Vegetative Hyphae	20	80-90	-	80-90	-	NS		NS	
Sporangia	7-9	120-200	+	150-300	++	NS		NS	
	96	150-200	+	200-350	++	NS		NS	
Encysted zoospores	9	60-70	++	90-100	+++	NS		NS	
Oogonia Stage I	9-24	80-90	-	90-120	+	NS		NS	
Stage IV	24-48	200-300	+	350	+	200-300	+	200-250	+
Gemmae	24-168	250-300	+	350-650	+++	200-300	+	200-300	+
Oospores 1°wall	120-168	100-150	+	100-400	++	-		100-150	+

A. Wall thickness (nm): The observed range from all the material examined, of variable age and antibiotic concentration.

B. Lomasome frequency: -: absent; +: occasional lomasome profiles observed; ++: lomasome profiles frequent, but rarely more than one per section; +++: lomasomes abundant, several per section.

* Time after induction or inoculation in the antibiotic.

NS Not scored.

Some Str-induced gemma walls are more densely stained (Figs. 2.183, 2.189, 2.199) and occasionally show a lamellate sub-structure (Fig. 2.189).

Lomdsomes are believed to form when membrane addition to the plasmalemma by vesicle deposition exceeds surface expansion, as a result of the sequestration of excess membrane into the wall (Hemmes & Hohl, 1969, Heath & Greenwood, 1970a, Marchant & Moore, 1973). Their abundance in Str-induced bodies confirms the increase in wall deposition in these bodies. Str-induced lomasomes are rather varied in their size and content (Figs. 2.83, 2.183, 2.190-2.194). They range from 0.2-1.5 μm in length and between 0.2-0.8 μm across. The membranous inclusions may either form small vesicles (Figs. 2.190, 2.191, 2.193) or from more complex whorled arrays (Figs. 2.83, 2.192). Some lomasomes also contain lipid-like material (Figs. 2.183, 2.194).

In addition to the typical wall lomasomes Str also results in the formation of peg-like ingrowths of the wall (Figs. 2.46, 2.197, 2.199, 2.200) and more extensive pockets of wall-sequestered cytoplasm (Figs. 2.150, 2.198, 2.201). The pegs measure up to 2.0 μm across at their base and may project up to 4.0 μm into the cytoplasm. They are composed of alternating but often anastomosing layers (< 8) of wall and entrapped membranous material. In oblique L.S. and T.S. these pegs appear as globular whorls of wall material as shown in Figs. 2.195 and 2.196. Such pegs are present in induced hyphae (Figs. 2.46, 2.49), cysts (Fig. 2.200), gemmae (Figs. 2.197, 2.199), oospores (Fig. 2.150) and Phytophthora sporangia (Fig. 2.240). They presumably arise as the result of the localised deposition of wall material without concomitant wall softening and extension. It is perhaps significant that they occur in cysts and gemmae in which germtube or appendage formation is not observed (e.g. Fig. 2.131). These pegs are also morphologically very similar to the wall ingrowths reported in some Phytophthora hyphae (Gooday & Hunsley, 1971).

The more extensive areas of sequestered cytoplasm, as noted in the abnormal induced hypha described in Section 2.3.8.2, contain a very dense groundplasm with a high density of ribosomes and large droplets of lipid (Fig. 2.198). At a more advanced stage the cytoplasm completely condenses into dense fragments, leaving a largely empty body (Fig. 2.201).

Plasmalemmasomes were not observed in streptomycin-treated reproductive structures except at the appendage apex (Fig. 2.108). However, they are quite common in Chl-induced gemmae (Fig. 2.241). Since these bodies are believed to be intermediate in lomasome formation (Heath & Greenwood, 1970; Marchant & Moore, 1973) there presence may be a reflection of the rate at which wall components are accreted and so entrapping the excess membrane. This again points to enhanced wall synthesis in Str-induced bodies.

Further evidence for Str-enhanced wall vesicle production comes from two stages in development during which wall vesicles normally accumulate, viz

the region of fertilisation tube-oospore contact (Figs. 1.172, 2.150) and in the region of septum insertion. Although the stages at which the wall vesicle accumulations take place were not observed, there is good reason to believe enhanced vesicle deposition has occurred. Str-induced oospores always contain lomasomes in their primary wall adjacent to the fertilisation tube (Fig. 1.172) and in one oogonium massive regions of sequestered cytoplasm are present in both the oospore and fertilisation tube (Fig. 2.150). Str-induced septa are wider than comparable control bodies (cf. Figs. 1.210-1.212 and Figs 2.202-2.205), having both thicker wall layers (< 0.6 µm upper, < 0.3 µm lower) and a broader vesicular region (< 3.0 µm). This vesicular layer frequently contains poorly-fixed lipid-like material and has conspicuous empty regions as a result of the condensation of the entrapped cytoplasm (Figs. 2.204-2.206).

2.3.9.5 Vacuolar Compartments

The formation and expansion of vacuolar vesicles in Str-induced gemmae is not normally inhibited. However frequently Str results in an altered pattern of vacuolar coalescence to that described in untreated sporangia and oogonia (Sections 1.2.2.2, 1.2.3.2). The extent of vacuolar fusion is often restricted which results in the cytoplasm containing a large number of small vesicles, up to 10 µm in diameter (Figs. 2.76, 2.111, 2.139, 2.160). In some of these gemmae the vacuoles remain widely despersed (Figs. 2.66, 2.78), whereas in others they are closely juxtaposed (Figs. 2.111, 2.160). Such divided vacuolar compartments are sometimes distinguishable in the light-microscope (Fig. 2.128). Many of the simple antibiotic-induced gemmae (type 1, Section 2.3.8.9) have a single large vacuole bounded by a well defined tonoplast (Figs. 2.99, 2.101, 2.102).

Str and Chl treatments result in widespread vacuolar and densebody vesicle breakage, particularly after prolonged incubation (Figs. 2.67, 2.117, 2.135, 2.159, 2.162, 2.241, 2.244). Many of these Str-induced bodies lack well defined vacuolar compartments (Figs. 2.67, 2.135) and frequently cytoplasmic components become dispersed into the vacuolar space (Figs. 2.117, 2.159, 2.241). The disrupted vacuolar membranes are often undulating, with a suture-like profile, possibly as a result of contraction after breakage (Fig. 2.162). This breakage was only recorded in Os-fixed material and it is possible that the antibiotics act by predisposing the membranes to disruption at fixation However there is some indication that Str may disrupt vacuole integrity in living material since vacuoles are frequently difficult to observe in these bodies (Figs 2.120, 2.138, 2.137). This may also lead to the contraction of cytoplasmic contents observed in sporangia (Figs. 2.63, 2.65, 2.71-2.75).

2.3.9.6 Neutral lipid and densebody fractions

Str-induced reproductive structures have slightly increased neutral lipid

and densebody fractions compared with comparable untreated bodies. For instance the volume fraction of neutral lipid is approximately 10% in Stage I initials (Fig. 2.96) and 15-20% in Stage IV bodies (Fig. 2.97). This compares with values of 5% and 10-15% respectively for the untreated bodies. However after prolonged antibiotic incubation (>90 h) there is a marked reduction in the level of both lipid (15-2% to 4-10%) and densebody granules (10-15% to 2-5%). This decline is probably the result of the continued utilisation of these products to provide the endogenous energy for continued differentiation.

The appearance of densebody granules and their associated matrix material is rather varied in antibiotic-induced gemmae. In most Os-fixed sporangia oogonia and gemmae the densebody granules are uniformly osmiophilic (Figs. 2.208, 2.209, 2.248) although may become partially electron tansparent with prolonged antibiotic incubation (Figs. 2.207, 2.211, 2.2.2). As in untreated bodies linear arrays of myelin-like lamellae with the usual periodicity of 8-9 nm are often present in the densebody vesicles (Figs. 2.209, 2.211). Occasionally more than one granule is contained within each vesicle (Fig. 2.269).

GaOs-fixed densebody vesicles are more varied in their appearance, particularly in Str-induced gemmae (Figs. 2.210, 2.213, 2.21). In some the matrix condenses around the granule so that the two are virtually indistinguishable (Fig. 2.213). In others the matrix expands to fill the whole vesicle and forms complex reticulate patterns (Figs. 2.214-2.216). Finally a number of others have a broad banded-matrix similar to that described in the densebody vesicles of Dictyuchus sterile (Gay, Greenwood & Heath, 1971). Comparable Cyc-induced densebody vesicles also have an expanded matrix, which contains extensive myelin-like configurations (Figs. 2.258, 2.260). It seems probable that the antibiotics may be interfering with the fixation of the densebody matrix since a similar range of configurations was also induced by varying the buffer and pH conditions (J.Gay, personal communication).

2.3.9.7 Multivesicular or autophagic bodies

These are unit-membrane bound organelles which contain a particulate matrix and included vesicular configurations (Figs. 2.163-2.169). They resemble the autophogic vesicles involved in the lysosomal autolysis of cell organelles (Matile, 1974). They occur in abundance in Str-induced reproductive structures, particularly gemmae (Figs. 2.163, 2.164, 2.166-2.169), aborted oospores (Fig. 2.165) and swollen fertilisation tubes (Fig. 2.152). These organelles are extremely varied in appearance and range from small (< 0.5 μm) rather electron transparent bodies with well-defined internal membranes to larger (< 1.0 μm) densely particulate bodies, in which the membranes are barely discernible (Figs. 2.164, 2.169).

These differences in ultrastructural cytology may be related to the organelles from which they are derived. For instance the multivesicular bodies in Fig. 2.163 are closely associated with a cluster of mitochondria, with which they have similar staining properties. In contrast the cluster of larger more electron-dense structures (Figs. 2.164, 2.165) are similar in density and appearance to the advanced stages of nuclear autolysis (Fig. 2.224). Therefore these bodies are likely to represent the products of more than one organelle autolysis.

2.3.9.10 Nuclear structure

For convenience the nuclei in the antibiotic-treated material will be considered in four categories.

1. Interphase nuclei

The majority (>75%) of the nuclei observed in antibiotic-treated hyphae, sporangia, cysts and oogonia appeared to be in interphase (Figs. 2.78, 2.102, 2.131, 2.148, 2.256). Most appeared comparable in size shape and nucleoplasm organisation to the nuclei in untreated bodies, even after quite prolonged (>90 h) periods of antibiotic incubation. Each nucleus is associated with a pair of centrioles which are apparently normal in their organisation. However the centrioles associated with some of the nuclei in Chl-induced gemmae had a larger amount of fibrillar material associated with their triplet microtubules than in untreated centrioles (Fig. 1.96).

A number of Str and Chl-induced nuclei also had a curious array of amorphous granules associated with their centriolar pockets (Figs. 1.96, 2.218). When the centriole is viewed in T.S. 6-8 of these granules can be seen symetrically arranged around the centriolar pocket, approximately 60 nm from the nuclear envelope (Fig. 2.218). There is also some indication that these granules are connected to the nuclear envelope by a narrow structure which may be a short microtubule (Fig. 1.96). These bodies may therefore represent the nascent spindle apparatus. Similar arrays have also been reported in untreated interphase nuclei in sporangia of S.ferax (Gay, personal communication), and are probably not a product of antibiotic action, but are possibly stabilised in some way.

Str does not result in the development of elaborate loop-like extensions of the nuclear envelope, which have been reported to be induced by microtubule inhibitors in S.ferax (Heath, 1975a). Nevertheless a number of nuclei in Str-induced gemmae and cysts contain elaborate vesicular inclusions (Figs. 2.217, 2.219, 2.222). Serial sections suggest these included membranes may arise from invaginations of the nuclear envelope, although this has not been demonstrated unequivocably (Fig. 2.219). Some interphase nuclei in Str-grown hyphae (Fig. 2.226) and Chl-induced gemmae (Fig. 2.247) contain coiled strands of electron dense material, which may be thickened strands of DNA.

2. Dividing nuclei

Mitotic configurations were observed in most Str-grown vegetative hyphae even at the highest antibiotic concentration (500 mg/l). This suggests Str is not a primary inhibitor of nuclear division. Two of the Str-induced oogonia which were selected for examination also contained enlarged prophase I nuclei (Fig. 2.97) and showed the expected changes in centriolar structure (Figs. 1.122, 1.123). All the Str-induced oospores and fertilisation tubes contain the expected small gametic nuclei (Fig. 1.181) which suggests successful nuclear division has taken place. Therefore it appears as though Str mainly blocks the initiation of nuclear division.

3. Autolysing nuclei

Many nuclei in Str-induced gemmae undergo autolysis. This was observed most frequently in appendate gemmae and appeared to follow a similar pattern to nuclear autolysis described in Phytophthora sporangia by Hemmes and Hohl (1972a). However in these antibiotic-induced gemmae there is no evidence that nuclear autolysis is preceded by nuclear division as it is in Phytophthora. The nuclei first become surrounded by either small vesicles (Fig. 2.221) or by double-membraned cisternae (Fig. 2.220). The cisternae and vesicles coalesce and expand until the nucleus is almost completely isolated from the surrounding cytoplasm (Fig. 2.223). During this process the nucleoplasm becomes more fibrillar in appearance and the nuclear envelope begins to break down (Fig. 2.224). The final stages of autolysis probably involves the dissociation of the autophagic vesicle into a number of smaller multivesicular bodies such as shown in Figs. 2.164, 2.165. It seems likely that nuclear autolysis is enhanced by the antibiotic, as it is a common cytoplasmic response to stressed conditions (Ericsson, 1969; Heath, 1975a). However it should be remembered that phases of nuclear autolysis accompany the normal differentiation of both sporangia and gametangia.

4. Nuclei with condensed nucleoplasm

A number of Str-treated hyphae and spores contain nuclei which have osmiophilic condensed nucleoplasm (Figs. 2.84, 2.85, 2.225-2.227). In Str-grown (500 mg/l) hyphae the extensive condensed nucleoplasm occurs in a central mass but leaves small portions adhering to the nuclear envelope (Figs. 2.225, 2.226). In the cysts the electron-dense material mainly corresponds to the nucleolus (Fig. 2.85) but smaller fragments remain scattered throughout the nucleoplasm (Fig. 2.81). Apart from the electron-dense material the nucleoplasm is largely electron-transparent although often contains certain amount of particulate and fibrillar material (Fig. 2.225, 2.227, 2.84). In the hyphal nuclei fibrils of DNA like material can be discerned (Fig. 2.226) whereas some of the cyst nuclei contained small (80 nm) vesicles scattered throughout the peripheral nucleoplasm (Fig. 2.84).

Some antibiotic-induced nuclei contained condensed but fragmented nucleolar material. This is particularly well shown in some of the dense cysts (Fig 2.79) in which the nucleolar material is scattered throughout the nucleoplasm. Both condensed nucleoplasm and dispersed nucleoli have been reported in hyphal nuclei of S.ferax grown at high temperatures (30°C; Heath, 1969). Str may therefore act directly on these nuclei and result in an impairment of their normal function.

2.3.10 Physiological effects of Streptomycin

2.3.10.1 Colony respiration

Since mitochondrial ribosomes are possible sites for Str inhibition in eukaryote cells (see Section 2.1), the effect of this antibiotic on colony respiration is of interest. Respiratory activity was assessed by measuring O_2 uptake by S.furcata colonies using an oxygen electrode. The results for the effect of Str on vegetative colony respiration, measured after 24 h incubation in the antibiotic (0,50,500 mg/l) are summarised in Table 2.15.

Table 2.15 The effect of streptomycin on dry weight increase and O_2-uptake in vegetative colonies of S.furcata at 20°C, after 24 h induction

Str Conc.^{n} (mg/l)	Colony age (h)	Mean$^+$ Colony Dry Weight (mg)	% Growth Inhibition	Mean$^+$ O_2-uptake per colony µ mole O_2/h/mg	Range	% O_2-uptake Inhibition
0	24	3.1		31.8	30.0-33.6	
0	48	9.0	-	30.0	28.2-31.2	-
50	48	6.4	44	25.8	21.6-28.8	20
500	48	4.8	77	19.8	17.4-22.2	38

$^+$ 3 replicate colonies

Str reduced O_2 uptake by vegetative colonies, although there is appreciable variation between the three replicates (Table 2.15). The ratio between growth inhibition and O_2 uptake reduction is approximately the same (c.2.0) for both Str concentrations (50,500 mg/l) which suggests the two may be directly correlated. Hine (1962) also reported that Str reduced O2-uptake by colonies of Pythium ar henomanes, but noted that inhibition only occurred in the presence of an exogenous energy source. The effects of Str on respiration in induced colonies of S.furcata was therefore examined.

The respiration of individual colonies was followed throughout the course of the experiment (48 h) and the O_2 uptake measurements were always expressed as a percentage of the uptake measured immediately prior to induction. The results of such an experiment, together with the observed oogonium production are summarised in Fig. 2.266. Even in untreated colonies O_2 consumption declines rapidly following induction. By 48 h, when most of the

Table 2.16 The effect of streptomycin on oogonium production and the leakage of K^+ ions and UV-absorbing substances. Assessed on 2 18 h colonies of S.furcata, 120 h after induction

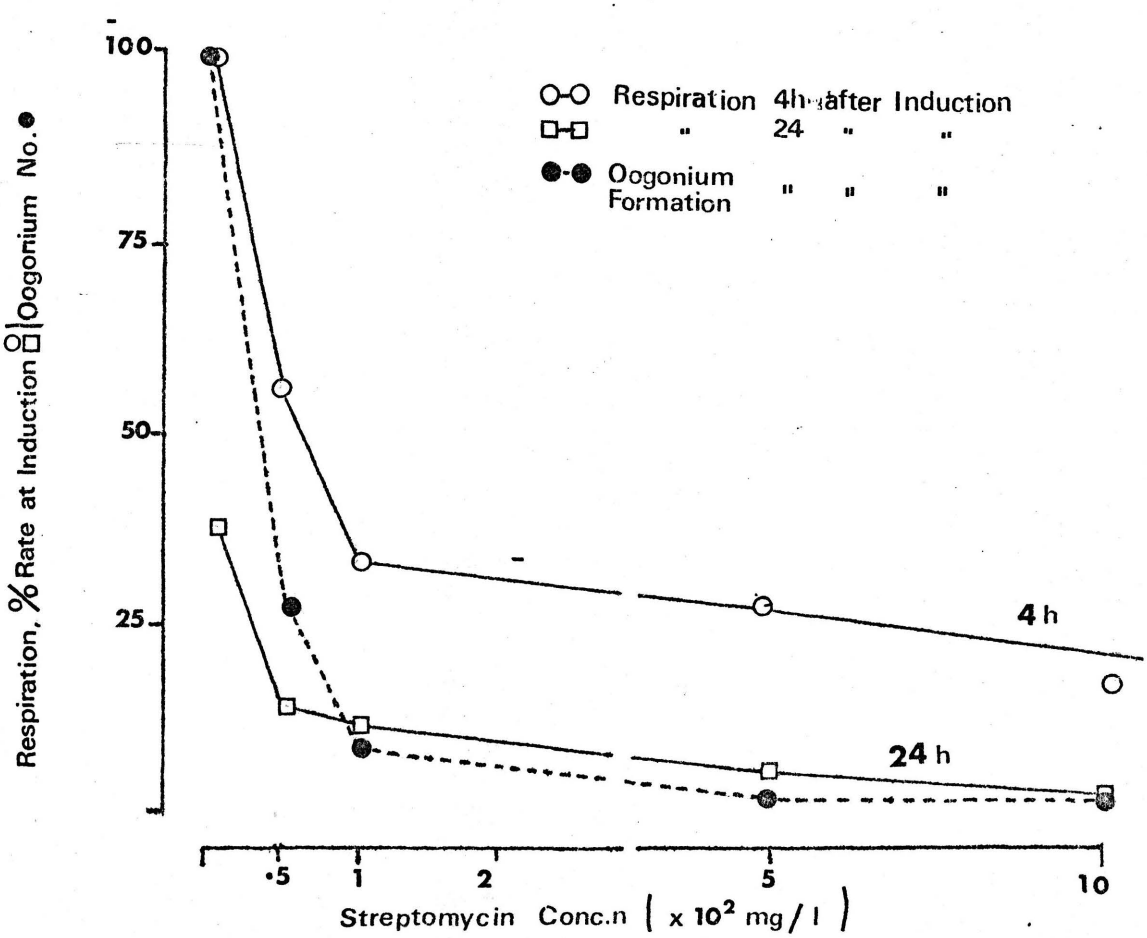
Streptomycin conc^n (mg/l)	Mean$^+$ no. oogonia per L.P. field	% Uncleaved	K^+ Conc^n (mg/l)	UV (260 nm) absorbance (x 10^{-2})
0	72.0	9	3	2
10	55.0	30	4	2
50	30.0	35	8	2
100	9.0	93	40	9
500	0.7	100	30	10

$^+$ all figures are the mean of 3 replicate plates

Table 2.17 The Ca^{2+} ion content of inducing solutions assessed 48 h after induction

Streptomycin conc^n(mg/l)	Ca^{2+} ion Concentration(µg/mg dry wt) S.furcata	S.ferax	Streptomycin conc^n(mg/l)	Ca^{2+} ion Concentration(µg/mg dry wt) S.furcata	S.ferax
heat killed	6.9	6.8	100	2.7	1.9
0	0.1	0.1	320	3.2	4.1
50	0.4	0.4	1000	5.4	5.0

Fig.2.266 The effect of streptomycin on colony respiration (% inhibition of O_2-uptake at induction) and oogonium production on induced 18h colonies of S. furcata.



gametangia have differentiated into spores, O_2 uptake is only 16% that of the pre-induction level. Str increases the rate of O_2 uptake decline (Fig. 2.266) and is accompanied by a marked fall off in gametangium development.

Unfortunately O_2-uptake proved difficult to assess in Str-induced colonies because they were more susceptible to disintegration in the electrode chamber. This mechanical damage is reported to reduce oxygen uptake (Darby and Goddard, 1950) and probably accounts for the very low recorded oogonium production (Fig. 2.266).

2.3.10.2 Membrane permeability

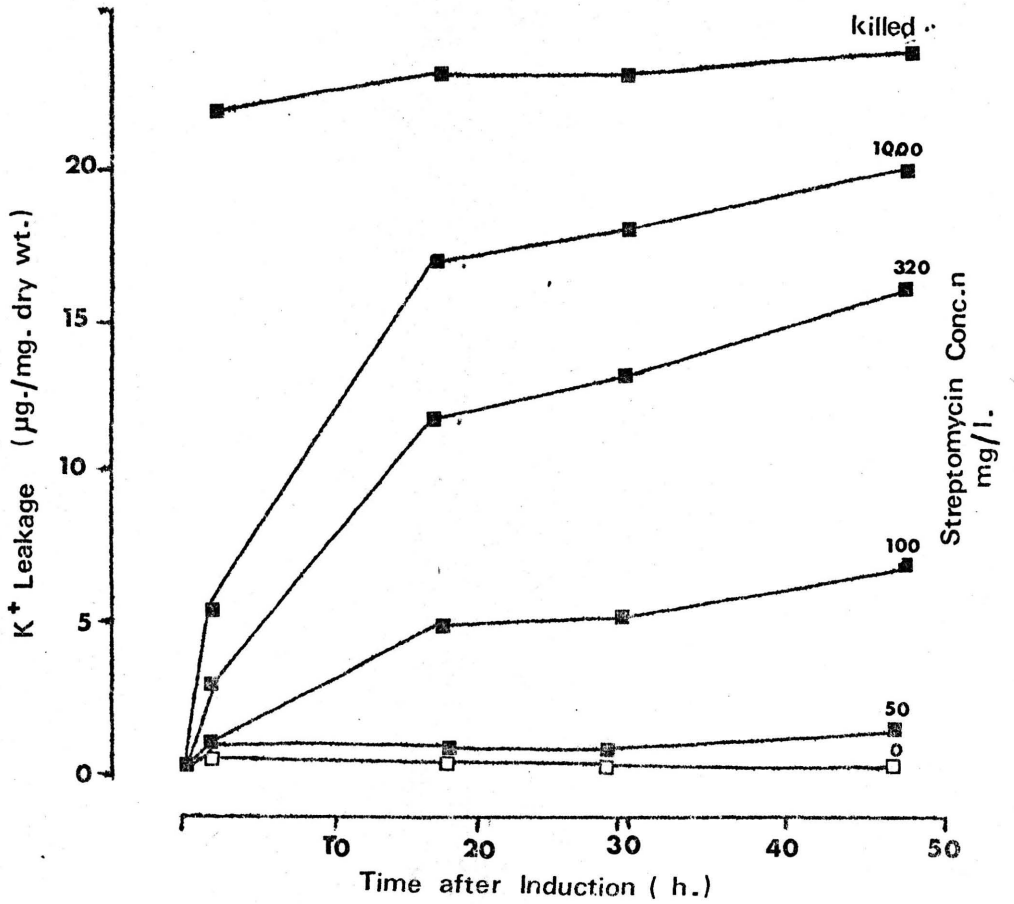
Streptomycin increases the permeability of bacterial cell membranes and results in both the leakage of ions and low molecular weight metabolites (Anand & Davis, 1960; Hancock, Dubin & Davis, 1962). Its effects on the permeability of eukaryote membranes have not been previously reported. The leakage of potassium ions (K^+) and UV-absorbing substances (absorbance at 260 nm) from 2 induced 18 h colonies (combined dry weight c. 5 mg) into the inducing solution was assessed 120 h after induction. The results are summarised in Table 2.16. Although both the amounts of detected K^+ and UV absorbance were rather small, Str clearly induces increased leakage at concentrations of 100 mg/l and above.

Following this experiment the leakage of K^+ was investigated in greater detail, using larger colonies (48 h, c. 18 mg dry weight) to obtain more easily measurable amounts of ion. To assess the extent of Str-induced membrane disruption the leakage from antibiotic treatments was compared with ion loss induced by disrupting the hyphal cytoplasm by heat treatment at 60°C for 5 minutes. The results for K^+ leakage from Str-induced colonies of S.ferax are summarised in Fig. 2.267 and for S.furcata in Fig. 2.268.

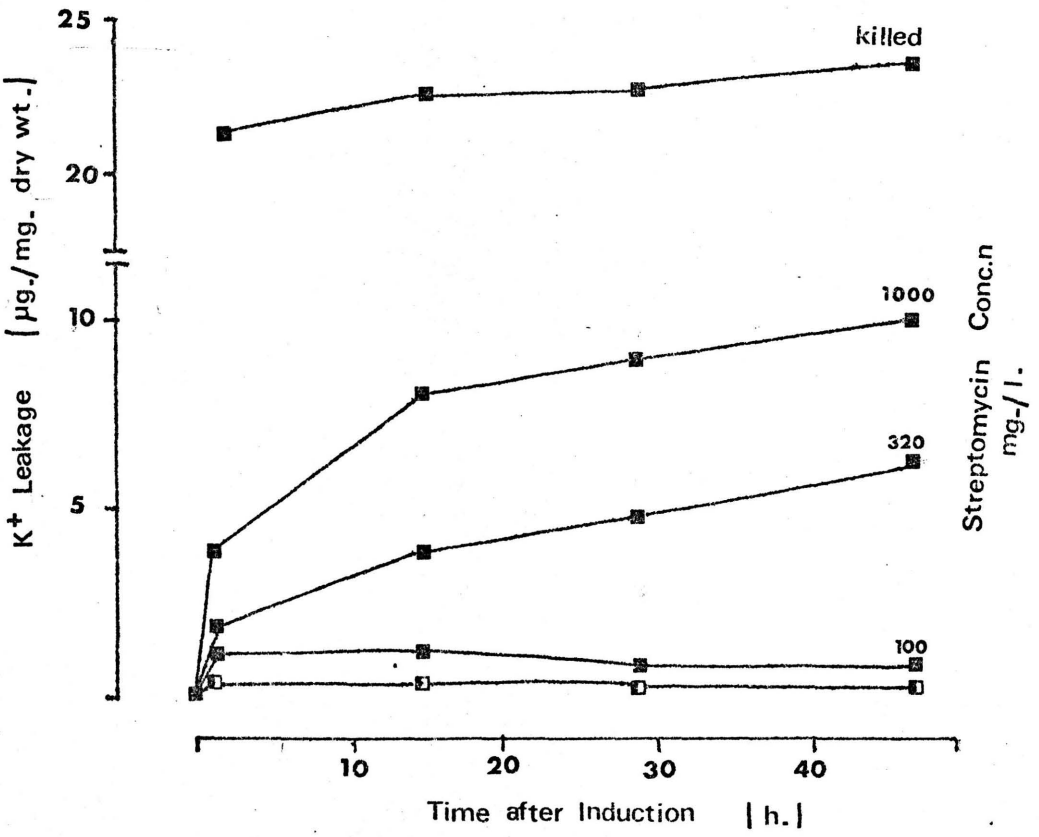
Str results in a considerable leakage of K^+ from induced colonies. In this respect S.ferax proved slightly more sensitive to Str than S.furcata (Figs. 2.267, 2.268). Significant ion loss does not occur at Str concentrations below 100 mg/l for S.ferax, and below 320 mg/l for S.furcata. However, once this critical threshold concentration has been passed ion leakage increases with antibiotic concentration. At the highest Str concentration (1000 mg/l) K^+ loss reaches 80% that measured in heat-killed colonies for S.ferax and 50% for S.furcata. Such high levels of ion leakage have also been reported in fungi treated with saponin inhibitors (Olsen, 1971 a, b). However there was no sign of any massive leakage and reabsorbance of ions from untreated colonies as noted in Pythium colonies on transfer to a citrate buffer solution (Olsen, 1971b).

In addition to analysis of K^+ the 48 h samples were also assayed for Ca^{2+}, and the results are summarised in Table 2.17. Ca^{2+} show a similar

Fig. 2.267 The effect of streptomycin on K^+ leakage from induced 48h colonies of S. ferax at 20°C.



The effect of streptomycin on K^+ leakage from induced 48h colonies of S. furcata at 20°C.



leakage pattern to that described above for K^+, with appreciable leakage only occurring at or above the critical threshold concentration of 100 mg/l. In the highest Str-treatment ion loss again reaches 70-75% that noted in heat killed colonies.

2.3.10.3 Elemental composition of differentiated oogonia

It is shown in the preceding section that Str (>100 mg/l) results in a gross increase in membrane permeability. However in S.furcata limited reproductive development still occurs at these concentrations (Fig. 2.13). Therefore it is important to determine whether Str increases the permeability of the reproductive bodies which differentiate at concentrations which induce ion leakage, or whether this loss is confined to vegetative hyphae only. Ultrastructural observations indicate that during prolonged periods of incubation in high concentrations of Str (> 100 mg/l) considerable disruption of the internal vacuolar membranes takes place, and organelle lysis occurs. It would also be useful to know whether, since it is a divalent cation, Str preferentially displaced certain elements such as Ca^{2+} and Mg^{2+} from the cells.

These possibilities were investigated by elemental analysis of oogonia from control and Str-induced colonies as described in Section C.2.6.9. Representative scans for reproductive structures mounted on aluminium supports are shown in Fig. 2.268, and for material mounted on carbon supports in Fig. 2.269. The vertical axis of these scans is an uncalibrated measure of X-ray intensity, which in Fig. 2.268 is on a linear scale and in Fig. 2.269 on a logarithmic scale. The scan in Fig. 2.268 is a typical background count (white radiation) taken from the aluminium support. Apart from the massive Al peak no other element is detectable, indicating there were no extraneous contaminating elements on the supports.

A typical cluster of air dried oogonia from an untreated colony are shown in Fig. 2.268c. Two representative elemental scans for such untreated oogonia on aluminium and carbon supports are shown in Fig. 2.268c and Fig. 2.269a respectively. All the untreated oogonia contain the following elements: Na, Mg, Al, P, S, Cl, K and Ca. Even on carbon supports the Al peak is probably derived from the backscatter of electrons from the aluminium mounting for the carbon disc. The high P peak is of interest since recent biochemical studies on Phytophthora oospore walls have also shown they contain an exceptionally high level of this element (Lippman, Erwin & Bartnicki-Garcia, 1974).

The elemental composition of reproductive structures induced in 50 mg/l Str proved similar to the untreated bodies, except that in 2 out of the 3 replicates Ca was absent (Fig. 2.268d). This is probably the result of Str competition for divalent cation sites on the cell wall such as has been demonstrated in Pseudoperonospora sporangia (Griffin & Coley-Smith, 1975).

The elemental analysis of bodies induced in 500 mg/l Str show there is a striking loss of elements at this concentration (Figs. 2.269a, c). Only Al, P and S were detected in all the 4 replicate scans which were carried out, although small amounts of Na and Mg were detected in some specimens (Fig. 2.269b, c). The absence of K correlates well with the observed leakage of K^+ at this high antibiotic concentration. Therefore it is clear that streptomycin, certainly after prolonged periods of incubation (120 h), results in an appreciable loss of ions from delimited reproductive structures as well as from the vegetative hyphae.

2.4 DISCUSSION

2.4.1 The Toxic Effects of Streptomycin on Oomycetes

This account shows that both members of the Saprolegniales and Peronosporales are sensitive to streptomycin. All stages in Saprolegnian morphogenesis are inhibited by the antibiotic, although there is considerable variation in sensitivity between species, strains and developmental stages. This is shown in the summary of ED50 estimates given in Table 2.18 and in the growth-inhibition data in Table 2.3. Previous studies report similar variations in streptomycin sensitivity in both Pythium and Phytophthora spp., with growth-inhibitory concentrations ranging from 10 mg/l to in excess of 500 mg/l (Eckert & Toa, 1962; Hine, 1962; Vörös, 1965; Shaw and Elliott, 1968; Shattock & Shaw, 1975).

In Saprolegnia the reproductive stages are clearly more sensitive to streptomycin than hyphal development (Table 2.1). The two phase inhibition curves which result when oogonium inhibition is plotted on a probability scale are not uncommon in fungal inhibitor studies (reviewed by Cochrane, 1958). Similar curves are for instance produced by another divalent cation, copper (McCallan cited by Cochrane, 1958). Such curves indicate different modes of streptomycin action at different concentrations. Speculation as to the nature of these inhibitory effects will be given in later sections.

2.4.2 The Inhibition of Cytoplasmic Cleavage

Although streptomycin is highly inhibitory to spore differentation in both sporangia and oogonia, the abnormal cleavage patterns observed in the Peronosporales (Griffin & Coley-Smith, 1971) and also described here for P.cactorum are not produced in the Saprolegniales. This supports the ultrastructural accounts of different cleavage processes in these two groups (see Section 1.1.2.4 for details). Streptomycin-inhibited sporangia of P.cactorum appear to deposit an additional inner wall layer before cytoplasmic lysis occurs. In Phytophthora it is believed that both the wall (Christen & Hohl, 1972) and at least some of the cleavage vesicles (King, Colhoun & Butler, 1968; Elsner et al., 1970) are Golgi derived. Streptomycin may therefore favour wall vesicle formation at the expense of cleavage vesicle production. This would lead to the partial or complete inhibition of cleavage plane delineation and result in the formation of the abnormally large spores observed in antibiotic treatments. Further ultrastructural evidence is required to confirm this hypothesis.

The basis of cleavage inhibition in Saprolegnia is also obscure, in spite of the more comprehensive ultrastructural evidence. The linear probit-dose response curve for the inhibition of oospore differentiation indicates that a single physiological process is involved in the cleavage

Table 2.18 A summary of toxicological data (ED50) for streptomycin at different development stages

Development Stage	ED50 values (mg/l *)		
	S.ferax	S.furcata	P.cactorum
1. Colony extension rate	>>1000+	50-750+	-
2. Dry weight increase	1000	45	-
3. Sporangium production	8-100	-	5-10+
4. Zoospore differentiation	32-200	-	35
5. Cyst germination	350	-	-
6. Oogonium production	-	68-200	-
7. Oospore differentiation	-	70-250	-

* All data assessed on standard 18 h colonies (4-5 mg dry weight) except 1, 2, 4 (P.cactorum only) and 5. One and 2 were assessed on growing colonies over a period of < 72 h, and 4 and 5 on standard suspension of sporangia and cysts

\+ These estimates were not made from a probit-log dose plot.

effect. Cleavage inhibition may be related to the various effects observed on vacuole cytology. However these effects are so varied it is impossible to cite a single response, such as a failure to get proper vacuole expansion or fusion, as the main inhibitory lesion.

It has also been demonstrated that cleavage furrow development is closely related to changes in nuclear behaviour. In the sporangia, these include alterations in nuclear shape and centriole structure (Heath & Greenwood, 1971) and in the oogonia, nuclear division (Howard & Moore, 1970). Such changes are not observed in streptomycin-inhibited bodies. This may mean streptomycin is inhibiting cleavage primarily through its effects on nuclear behaviour. However the effects of cycloheximide reported in this study and of colchicine described by Slifkin (1967), show that oogonial cleavage can occur independently of nuclear division. This results in the formation of uninucleate cyst-like bodies. Since this does not occur in streptomycin treatments it suggests that it is the cleavage apparatus itself which is affected.

Most of the bodies which do not differentiate into oospores in S.furcata lack antheridia. Mechanical inhibition of antheridium attachment in Thraustotheca clavata has also been shown to prevent oospore formation (Weston, 1918), perhaps because it interferes with the pattern of hormonal regulation described in Section 1.1.3.1. However streptomycin also inhibits cleavage in sporangia and in some antheridiate oogonia. This suggests that the inhibition of antheridium formation is not the primary lesion affecting spore differentiation.

Although Golgi vesicles have not been directly implicated in cleavage vacuole formation in Saprolegnia (Gay, Greenwood & Heath, 1971) the stimulation of wall synthesis by streptomycin may still be important. Streptomycin may alter the balance of cellular metabolism in favour of wall synthesis so that it effectively blocks the biochemical and structural changes necessary for spore differentiation. As a result continued vegetative development takes place resulting in the formation of outgrowths and appendages. Such an hypothesis is supported by observations made on gametangial differentiation in S.furcata colonies induced at 30°C. At this temperature many of the reproductive structures failed to form oospores, and produced vegetative outgrowths not unlike those induced in streptomycin. Vegetative hyphae of S.ferax grown at this temperature show both increased growth and wall vesicle production (Heath, 1969). It seems likely therefore that the metabolic balance at this temperature is also altered in favour of wall vesicle synthesis, as proposed in streptomycin.

The inhibition of sporangial cleavage has also been induced in the Saprolegniales by concentrations of cations in excess of 40 mM (Klebs, 1899; Griffin, 1966). However since streptomycin effectively inhibits zoospore

differentiation in S.ferax at concentrations between 0.6-0.8 mM, it is unlikely to be the result of such a non-specific cation inhibition

2.4.3 The Extension of the Post-induction Lag Phase

It has been shown in Achlya spp. that many of the biochemical changes associated with sporulation are initiated in the period immediately following induction, prior to the appearance of the reproductive structures (Griffin & Breuker, 1969; Horgen & Day, 1974; Day and Horgen, 1975). Presumably streptomycin increases this lag period because it impairs normal metabolism, perhaps by affecting protein synthesis or respiration. Similar increases have been reported in fungi treated with other metabolic inhibitors prior to sporulation or spore germination (e.g. Trinci & Gull, 1970; Griffin & Breuker, 1969), suggesting this is a general phenomenon.

At high streptomycin concentrations (> 100 mg/l) the extended lag phase may also allow the partial recovery of antibiotic damaged cytoplasm. The reproductive structures which develop at these concentrations form outside the region of lysed cytoplasm and frequently on hyphal branches which develop after induction. Ultrastructural studies reveal that strands of wall material rapidly form between regions of disorganised and apparently healthy cytoplasm. This phenomenon has also been reported in Saprolegnia hyphae treated with microtubule inhibitors (Heath, 1975a). This wall insertion may therefore be a non-specific response to cytoplasmic damage. Such a mechanism is particularly important in a coenocyte such as Saprolegnia in which there is direct cytoplasmic continuity throughout the hyphae. Presumably the isolation of damaged cytoplasm would allow unaffected cytoplasm to continue normal metabolic functions, including reproductive differentiation

2.4.4 The Antagonism of Streptomycin Toxicity by Divalent Cations

The antagonism of Ca^{2+} ions to the inhibitory effects of streptomycin on Saprolegnia furcata is similar to that reported previously in a wide range of eukaryote organisms (see Section 2.1.5). Neither Mn^{2+} or Mg^{2+} ions were as effective as Ca^{2+}, as they themselves were toxic to sexual differentiation. This was particularly so of Mn^{2+} ions, which in other eukaryote studies, including members of the Peronosporales (McMeekin, 1973; Griffin & Coley-Smith, 1975) were as, or more effective than Ca^{2+} ions. Zahn (1961) also concluded that the effectiveness of divalent cations at reducing the phytotoxic effects of streptomycin on higher plants was inversely related to their own toxic effects.

As in studies on Ps.humuli the maximal alleviation of streptomycin inhibition was obtained with Ca^{2+} concentrations slightly in excess of the antibiotic (Griffin & Coley-Smith, 1975). However much lower concentrations (< 10 times lower) still significantly reduced the effects of the antibiotic.

Griffin and Coley-Smith (1975) suggest that this indicates that Ca^{2+} ions have a much stronger binding affinity to suitable cellular ligands, and were able to show that Ca^{2+} actively displaced streptomycin from the sporangial walls. The observed reduction in the level of calcium in streptomycin-induced oogonia, is probably the result of the simple competitive inhibition of calcium adsorption, when streptomycin ions are present in massive excess.

2.4.5 Cell Wall Enhancement

One of the most conspicuous cytological effects of streptomycin on induced colonies of Saprolegnia is to increase both cell wall thickness and lomasome abundance. A similar enhancement of cell wall formation has also been described in Allomyces arbuscula induced to sporulate in sublethal concentrations of cycloheximide (Turian & Viswanathan, 1966). It was suggested that this inhibitor resulted in an inbalance of cellular metabolism in favour of wall synthesis, which also seems to occur in streptomycin.

The absence of enhanced wall formation in the vegetative hyphae is puzzling. Other fungal growth inhibitors have been widely demonstrated to result in increased hyphal wall thickness (e.g. griseofulvin: Bent & Moore, 1966; cydoheximide: Sternlight, Katz & Rosenberger, 1971; penta chloronitrobenzene: Threlfall, 1972; L-sorbose: Trinci & Collinge, 1973). It also suggests that streptomycin may be acting in fundamentally different ways during vegetative development and reproduction.

The development of peg-like ingrowths and 'appendage' outgrowths demonstrates that streptomycin does not inhibit the initiation of new foci of polarised wall deposition. This contrasts with the effect of cycloheximide on Aspergillus hyphae, in which the normal apical polarity of wall vesicle deposition is suppressed (Sternlight,Katz & Rosenberger, 1971). However localised wall ingrowths such as described here are not an infrequent phenomenon and in particular are often induced by microtubule disrupting agents (e.g. colchicine in Chlorella sp.: Wanda, 1968; colchicine in S.ferax: Heath, 1975a;colcemid in S.ferax: Heath, 1975a; lindane in pea roots: Charnetski, Lichtenstein & Evert, 1974).It may be significant that both increased wall deposition and the abundance of autophagic vesicles are usually correlated with 'stressed' cytoplasm (Heath, 1975a).

2.4.6 The Mechanism of Streptomycin Action in Saprolegnia

Two fundamental questions arise from the prece ding discussion of streptomycin effects on Saprolegnia. These concern the identification of the main intracellular site or sites of action and the basis of the variations in antibiotic toxicity. As Gale and his associates (1972) point out, the determination of the primary metabolic lesion caused by an antibiotic is usually extremely difficult due to the interdependent nature of cellular processes.

Nevertheless previous studies into the pleiotrop ic effects of streptomycin on eukaryote cells indicate the following sites or processes may be affected by the antibiotic (details are given in the literature review, Section 2.1).

1. Mitochondria and chloroplasts, due to the inhibition of 70S ribosome function.
2. Cytoplasmic protein synthesis.
3. Membrane permeability and integrity.
4. Cellular cationic sites, other than ribosomes and membranes.
5. Specific cellular processes such as nuclear division and carotenoid synthesis.

Each of these possible sites of streptomycin action will be discussed in relation to the observed effects on Oomycetes.

2.4.6.1 Mitochondrial function

Although few immediate effects of streptomycin on mitochondrial ultrastructure are observed the gross uptake of oxygen by vegetative colonies is reduced. It should be noted that the absence of specific ultrastructural changes in mitochondrial structure in streptomycin and chloramphenicol does not mean these organelles are not affected. For instance extracted mitochondria from chloramphenicol-grown hyphae of Pythium ultimum, although appearing normal in thin section, were deficient in cytochromes a, a3 and b (Marchant & Smith, 1968). The fibrous inclusions in the mitochondrial matrix of some streptomycin grown hyphae resemble proteinaceous inclusions recently described in yeast mitochondria (May, 1974). Their appearance in Saprolegnian mitochondria may be the result of the derangement of normal mitochondrial protein synthesis, resulting in the accumulation of abnormal or cytoplasmically synthesised proteins.

Further indirect cytological evidence for the impairment of respiratory metabolism in some streptomycin grown hyphae comes from the extensive ER arrays in these bodies. Similar ER arrays in higher plants are frequently induced by conditions of energy deficiency caused by inhibitors or anaerobic conditions (Podbielkowska et al., 1975).

The effects of streptomycin on colony respiration after induction are more difficult to interpret. The widespread lysis of hyphal cytoplasm may itself account for the observed reduction in the level of oxygen uptake. In addition there is little sign of any impairment of respiratory metabolism in the streptomycin-induced reproductive structures. Even though spore differentiation may be inhibited, the continued vegetative development of these bodies is frequent. This contrasts with chloramphenicol induced gemmae in which appendage formation is rare.

Most of the changes in mitochondrial structure observed after prolonged

antibiotic incubation probably arise as a result of the depletion of endogenous energy reserves, as similar changes are observed in control gemmae. It is suggested therefore that mitochondrial function is mainly impaired by streptomycin during vegetative growth. Even then, probably only a limited proportion of the mitochondria are affected.

2.4.6.2 Cytoplasmic Protein Synthesis

Although streptomycin is reported to inhibit protein synthesis in excised pea tissue (Venis, 1968) it is unlikely that the mechanism of inhibition is the same as in prokaryote cells (McMeekin, 1973). For instance ribosomes isolated from fungal cytoplasm are relatively insensitive to streptomycin (reviewed by Lloyd, 1974). However streptomycin may interfere with protein synthesis by competing for Ca^{2+} and Mg^{2+} sites, both of which are essential co-factors for protein synthesis in Achlya (Cameron & Lé-John, 1972). In order to assess the effects of streptomycin on cytoplasmic protein synthesis, the observations will be evaluated against those obtained with cydoheximide. This is a known inhibitor of cytoplasmic protein synthesis in the Saprolegniales (Cameron and LéJohn, 1972; Timberlake et al., 1972). The following differences on sexual reproduction in S.furcata were noted.

1. S.furcata shows a much more restricted tolerance to cycloheximide compared with streptomycin. Sexual differentiation is completely inhibited by 0.02 mM cycloheximide, compared with concentrations in excess of 1.72 mM for streptomycin.
2. Cycloheximide-induced gemmae are less varied morphologically. Appendage development is limited and does not result in the irregular swollen forms commonly found in streptomycin.
3. Cycloheximide does not induce the widespread abortion of oospores. In addition the ooplast matrix is apparently stabilised and remains in gel form.
4. Cycloheximide-induced gemma often contain parallel arrays of ER, whereas comparable streptomycin-induced bodies do not. This is significant because such arrays have been induced in plant cells by protein synthesis inhibitors (Dexheimer, cited by Podbielkowska et al., 1975).

Such differences indicate that it is unlikely that streptomycin is acting primarily as an inhibitor of cytoplasmic protein synthesis.

2.4.6.3 Membrane Permeability and Stability

Although streptomycin induced membrane leakiness has been reported in bacterial studies (Section 2.12) it has not previously been described in eukaryotic cells. Nevertheless similar effluxes of K^+ to those induced in Saprolegnia by streptomycin have been described in fungi treated with EDTA (Elferink, 1974), triterpeneglycoside saponins (Olsen, 1971a, b) and polyene

antibiotics (Kinsky, 1962; Molzahn & Woods, 1972). These inhibitors affect the membrane by either sequestering essential membrane components (e.g. Ca^{2+} by EDTA) or by binding to specific membrane components (e.g. polyenes and saponins to sterols). It seems probable therefore that streptomycin acts in one or perhaps both these ways.

The leakage of ions and UV-absorbing material is correlated quite well with the observation of condensed blocks of lysed cytoplasm in the induced hyphae. This indicates that the leakage of ions is associated with cell death as shown in EDTA treated beet tissue (Van Steveninck, 1965), and not simply an enhanced leakiness of the plasmalemma such as described by Elferink (1974) in yeast cells. In addition the critical antibiotic concentration required to induce ion leakage in colonies of S.furcata corresponds well with the observed increase in gradient of the probit-dose response curve (Fig. 2.15). This indicates that the destruction of membrane permeability is one of the major metabolic lesions induced by streptomycin.

The 'all or nothing' nature of streptomycin-induced leakiness is similar to that shown in beet tissue treated with EDTA (Van Steveninck, 1965). This is known to be related to the number of calcium ions which must be removed from the membrane before integrity is lost. It is therefore proposed that streptomycin must affect (probably by binding to) a critical number of membrane sites to induce membrane leakiness. The nature of these membrane sites is open to speculation. The elemental analysis of streptomycin induced oogonia shows that streptomycin reduces the level of cellular calcium. This element is responsible for governing membrane stability and permeability (Burström, 1968; Lucy, 1974), and is known tobind to membrane phospholipid and sterol components (Seimiya, & Ohki, 1973; Olsen, 1973 ; Elferink 1974). It is suggested that these components are likely to be involved in the building of the divalent streptomycin molecule as well. Once the antibiotic has occupied a critical number of suitable sites, membrane integrity is lost, and the rapid death of the cytoplasm ensues.

Furthermore calcium has also been shown to be essential for normal spore differentiation in Saprolegnia (Cameron & LéJohn, 1972; McCann & Stuart, 1973). Although the role of this ion in cleavage has not yet been determined, it seems probable that it is related to its regulation of membrane stability and fusion (Lucy, 1973). This would be particularly crucial during a phase of rapid membrane expension and coalescence such as occurs during cleavage vacuole formation. The binding of streptomycin to the internal vacuolar membranes in place of calcium may well interfer with the normal cleavage process. It may account for the frequent observations of partial vacuole coalescence and the enhanced breakage of membranes during fixation. Further supporting evidence for this proposal is discussed in Section 3.4 after the effects of excess Ca^{2+} ions have been described.

2.4.6.4 Other Cellular Cation Functions

In addition to effects caused by the binding of streptomycin to 70S ribosomes and membranes, a number of other cellular functions are controlled by divalent cations and likely to be affected by streptomycin interference. For instance divalent cations such as Mn^{2+}, Ca^{2+} and Mg^{2+} are known to be important enzyme co-factors (Cochrane, 1958; Ross, 1975). Therefore streptomycin may derange cellular processes governed by such enzymes. In addition in the Saprolegniales, calcium has been shown to be necessary for amino acid uptake and is a structural component of both the cell wall and possibly ribosomes, in addition to membranes (Cameron & LéJohn, 1972). The impairment of normal amino acid uptake by streptomycin may be one of the major effects contributing to the reduction in growth rate of vegetative colonies. In higher plants calcium regulates cell wall rigidity and extension (Burström, 1968) and its presence in Oomycete walls suggest it may serve this function in this group also. The observed displacement of calcium by streptomycin may alter wall extensibility, and account for the abnormally large and irregularly swollen morphological forms of Str-induced gemmae. It may also explain the enhanced twisting of oogonial initial stalks, since similar effects on root hairs have been induced by the removal of calcium (Burström, 1968).

Calcium ions are also known to be important in governing the deposition and stability of crystalline phospholipid complexes (Kavanau, 1965). This may account for the elaborate densebody matrix configurations observed in GaOs-fixed material.

2.4.6.5 Nuclear Cytology

There is no evidence that streptomycin specifically inhibits a stage in nuclear division such as reported in griseofulvin treated hyphae (Gull & Trinci, 1973). It appears as though in streptomycin-induced oogonia nuclear division either is completed normally or is not initiated. This may be the result of the derangement of the normal hormonal control of differentiation, outlined in Section 1.1.3.1. Antheridiol is a sterol derivative (Barksdale, 1969), and as indicated in Section 2.4.6.3 as such may bind the antibiotic. The presence of the membranous inclusions and 'centriolar arrays' in some of the gemma nuclei appear to be correlated to antibiotic treatment. The former are probably derived from elaborate invaginations of the nuclear envelope, although this could not be proven unequivocally. Elaborations of the nuclear envelope have recently been described in nuclei treated with microtubule inhibitors, and may be a non-specific response to metabolic poisons (Heath, 1975a). The centriolar arrays on the other hand have been previously seen in untreated sporangial nuclei (J.Gay, unpublished photograph) and therefore are probably not a direct result of antibiotic action.

However their increased incidence in antibiotic treatments suggest they are either stabilised in some way, or their fixation is enhanced.

The autolysis of nuclei is widely observed in streptomycin induced gemmae. Whether this is a specific effect of the antibiotic is uncertain since nuclear autolysis is part of the normal differentiation pattern in both sporangia and oogonia. However, nuclei with condensed osmophilic nucleoplasm are invariably associated with stress conditions: and have been previously described in hyphae grown at 30°C (Heath, 1969). Therefore although nuclear division is not specifically inhibited it is likely that streptomycin does result in some impairment of nuclear function. Whether this is a primary lesion or a secondary effect of the impaired metabolism is uncertain.

2.4.7 Variations in Streptomycin Toxicity

Oomycete fungi show many levels of variation to streptomycin inhibition. As well as variation between different strains and species, considerable differences in the sensitivity of different developmental stages are observed (see Table 2.18). This is strikingly shown by S.ferax. While vegetative development is relatively tolerant to streptomycin, asexual reproduction is extremely sensitive. The possible reasons for these observed variations will now be discussed. For convenience they will be divided into variations which arise independently of the organism, and those which are governed by the organism and its biochemistry.

2.4.7.1 Environmental Effects

Most of the observed variation in measured streptomycin toxicity between replicate experiments is the result of minor differences in experimental conditions, even though these were standardised as much as possible. For instance there is likely to be variation in the potency of the antibiotic stock solutions prepared from antibiotic which has been stored for varying lengths of time. There will also be variation in the size and hyphal density of 18 h colonies, which will influence the efficiency of washing. Such variations do not however affect the fundamental response of the fungus to the antibiotic.

The incorporation of the antibiotic into the growth medium is also likely to reduce its potency. For instance, media have been shown to complex heavy metals and render them unavailable to the fungus (Ross, 1975). The apparently lower toxicity of streptomycin on vegetative growth assessed on agar culture compared with liquid culture, has also been shown in Peronosporalean studies (Hine, 1962; Vörös, 1965; Shattock & Shaw, 1975). This may reflect the greater availability of the antibiotic to the fungus in submerged culture. In addition agar has also been shown to contain calcium (< 20 mg/l; Elliott, 1972) which would reduce streptomycin toxicity.

2.4.7.2 The Cellular Determination of Antibiotic Sensitivity

It is proposed that streptomycin exerts its pleiotropic effects on cellular metabolism by binding to cellular divalent cation ligands, in the place of calcium and other essential ions. The availability of suitable binding sites will be critical in determining streptomycin sensitivity.

The binding of streptomycin to Oomycete cell walls has been recently shown by Griffin and Coley-Smith (1975). Vörös (1962) found that Oomycete hyphae adsorbed 3 to 10 times more antibiotic than chitinous fungi. He proposed that this was due to the cellulosic nature of the Oomycete cell walls. This study suggests that streptomycin binds to the cell walls of Saprolegnia at the expense of calcium. It seems possible therefore that the binding of streptomycin to Oomycete cell walls is related to the exceptionally high calcium content of these walls compared with other fungi (Cameron & LéJohn, 1973). It is likely that, as in higher plants (Burström, 1968) the presence of cellulose and calcium are directly correlated.

The availability of suitable absorption sites on the cell wall is probably essential for the uptake of streptomycin into cells. The transport of another divalent cation, zinc, into fungal cells requires the binding of this ion to the wall before it is moved into the cell (Paton & Budd, 1967). Streptomycin may first have to bind to the wall, before it is able to attach itself to suitable membrane sites. This may explain why the naked zoospore and oosphere stages of development are surprisingly tolerant to this antibiotic.

Although the cell wall may be critical in determining the insensitivity of chitinous fungi to streptomycin, it is difficult to see how this regulates sensitivity within the Oomycetes. For instance, Vörös (1962) was unable to detect significant differences in antibiotic absorption to hyphae of resistant and tolerant Oomycetes. In addition Oomycete cell walls do not vary significantly in their composition between vegetative and reproductive stages, except in the mature oospores (Lipmann, Erwin & Bartnicki-Garcia, 1974). Yet vegetative and reproductive stages show marked variations in their sensitivity to streptomycin, so some other factor must be involved.

Variations within the Oomycetes may be related to the availability of suitable plasmalemma-located and internal binding sites. Variations in the abundance of specific membrane-located carrier molecules, shown to be involved in streptomycin uptake in Nitella (Litwack & Pramer, 1967), may be critical in this respect. It is suggested that streptomycin affects membranes by binding either to phospholipids or sterols, or both. Recently the sensitivity of different fungal isolates to membrane-binding inhibitors such as polyenes and saponins has been shown to be correlated to the sterol contents of their membranes (Olsen, 1973; Woods, Bard & Jackson, 1973). Similarly

the susceptibility of yeast strains to EDTA-induced ion leakage was shown to be inversely related to their phospholipid content (Elferink, 1974). Such variations in membrane composition may account for the intra-and inter-specific variation reported here for the effects of streptomycin on Saprolegnia.

Such a hypothesis may also explain the greater susceptibility of reproductive differentiation to this antibiotic. Sporulation in Saprolegnia has been shown to be accompanied by a marked increase in phospholipid reserves (Gay, Greenwood & Heath, 1971; Hagedorn & Weinert, 1974). Similarly reproduction in the Peronosporales has been shown to require sterols, which are not synthesised by this group (Elliott, Hendrie & Knight, 1966). It is likely that sterol synthesis also occurs during Saprolegnian reproduction as well. Since both phospholipids and sterols have been suggested as binding agents for streptomycin, the number of cellular targets is clearly going to increase during reproduction. It is interesting to note that Pythium hyphae grown on basal medium are insensitive to saponin inhibitors, whereas those grown on a sterol rich medium (which also induces sporulation) are sensitive (Défago, cited by Olsen, 1973). Clearly the incorporation of extra phospholipid and sterol components into Saprolegnian membranes following induction could increase their susceptibility to streptomycin.

Transient changes in membrane permeability following the induction of sporulation have been demonstrated in Allomyces (Turian,1975). Such changes in Saprolegnia may enhance streptomycin uptake following induction, and increase the sensitivity of the reproductive stages. In Saprolegnia, colonies grown in the presence of streptomycin were less affected by the antibiotic during induction. Perhaps the membranes become adapted in some way to the antibiotic and less susceptible during the critical induction phase.

Finally there is some evidence from studies with other inhibitors that the vegetative development of Saprolegnia spp. is generally more tolerant than reproductive differentiation. A good example of this is that hyphal nuclear divisions are apparently unaffected by microtubule inhibitors, whereas gametangial divisions are seriously deranged (Slifkin, 1967; Stuart & O'Gorman, 1971). Recently Heath (1975a, b) has demonstrated this difference cannot be explained on the basis of differences in membrane permeability to these inhibitors. Possibly the biochemical process and cytoplasmic components of vegetative hyphae are less seriously affected by metabolic inhibitors, including streptomycin, than comparable reproductive processes.

It is acknowledged that the above discussion is largely speculative. Nevertheless the morphological and ultrastructural observations presented in this study provide a sound basis on which confirmatory biochemical investigations might be initiated.

PART 3. THE EFFECTS OF TAPWATER AND DIVALENT CATIONS ON THE REPRODUCTIVE DIFFERENTIATION OF SAPROLEGNIA SPP.

This section briefly describes the effects of different inducing solutions (viz tap, distilled and deionised water) of varying ionic composition on the reproductive morphogenesis of Saprolegnia spp. The results of Part 2 indicate that streptomycin may primarily act as a competitor for cellular divalent cation sites. To evaluate this further the inhibitory effects of other divalent cations (Mn^{2+}, Ca^{2+}, Mg^{2+}) were investigated. Finally the effects of divalent cation sequestration by ethylene diamine tetracetic acid (EDTA) are included for comparison. A literature review of the sporulation induction process is also included in this section.

3.1 LITERATURE REVIEW

3.1.1 The Induction of Sporulation in Saprolegnia

At the turn of the century Klebs (1899) published the results of a classic series of experiments into the nutrient requirements necessary for growth and reproduction in the Saprolegniales. This work laid the foundations on which all subsequent studies have been based and has been summarised at some length by both Coker (1923) and Sparrow (1960). Some of the main conclusions of Klebs studies are as follows:

1. In the presence of adequate nutrients colonies of Saprolegnia will continue to grow vegetatively indefinitely.
2. Nutrient depletion will induce vegetative colonies to sporulate. The rapid removal of nutrients favours asexual zoosporangium development, whereas a more gradual depletion favours gametangium formation.
3. Oogonium formation can be preferentially induced by either 0.1% haemoglobin or leucine, although the addition of phosphate and nitrate salts are often necessary for maximal antheridium development (also Kauffman, 1908).
4. The presence of high levels (0.5-1.0%) of inorganic salts inhibits spore formation and results in the development of the so-called gemmae.

Pieters (1915) concluded that the addition of phosphate always increases the overall reproductive capa city of induced colonies. This observation can probably be correlated to the findings of result ultrastructural studies which show the accumulation of phospholipid in differentiating sporangia and oogonia (Gay & Greenwood, 1966; Gay, Greenwood & Heath, 1971; Gay, 1972).

Although satisfactory sporulation in many Saprolegnia spp. can be induced by transfer to distilled water, it has frequently been found necessary to add a variety of supplements (usually inorganic e.g. phosphates and nitrates) to obtain maximum reproductive productivity (Pieters, 1915; Reischer, 1951; Barksdale, 1962& 1970; Yang & Mitchell, 1965; Unestam, 1969). The range and quantity of these supplements varies from species to species, although some, such as Aphanomyces euteiches (Yang & Mitchell, 1965), are more demanding in their requirements than others.

Pieters (1915) was the first to notice that distilled water was frequently unsatisfactory as a sporulation-inducing agent, resulting in low yields and abnormal sporangium development. He found that this inhibition was overcome by filtration through charcoal black and concluded that his distilled water contained certain inhibitory components. The unreliability of distilled water as a sporulation-inducing agent resulted in the widespread recommendation of the use of sterilised pond water instead (e.g. Coker, 1923).

However more recently Reischer (1951) investigating the effect of charcoal filtration concluded that it probably supplemented a deficiency in the

distilled water rather than removing an inhibitor. This proposal was further explored by Griffin (1966) working with an Achlya sp. He was able to demonstrate that calcium was the necessary element lacking in most distilled waters, and supplemented by filtration or by the use of pond water. In Achlya, a 0.1 mM $CaCl_2$ solution is able to supplement the calcium requirements for sporulation. Following on from Griffin's (1966) studies, Cameron and LéJohn (1972) investigated the role of calcium in the cellular biochemistry of Achlya. Spore cleavage was found to be one of the critical calcium requiring stages, as has been noted during sexual reproduction in Saprolegnia diclina (McCann & Stuart, 1973). It was suggested this may be related to the function of calcium as regulator of membrane permeability (Cameron & LeJohn, 1972).

There have been conflicting reports as to the need to add supplements to sexually differentiating colonies of Achlya ambisexualis. Barksdale (1962) claims that C, N, P, Mg and Ca are all necessary additions for maximal oogonium production in Achlya. In addition, she claims (Barksdale, 1970) that antheridium initiation is enhanced by the presence of an exogenous energy supply. In contrast Mullins and Warren (1975) have shown that optimum oogonium production occurs in colonies induced in distilled water, and that the addition of various inorganic supplementsboth delays initiation and reduces the level of oogonium production. They suggest this descrepancy may be due to the use of hempseed-grown colonies by Barksdale.

In general tap water has not been favoured as an inducing medium for Saprolegnia colonies, although its effects have not been widely documented. Unestam (1965) does however comment that tap water is slightly less effective at inducing sporulation in Aphanomyces astaci than either distilled water or dilute pond water. In addition Unestam (1969) has succeeded in obtaining both growth and sporulation in A.astaci by growing in a dilute nutrient medium and reducing the concentrations of dissolved oxygen and carbon dioxide. He proposed that actively growing vegetative hyphae produce a sporulation-inhibiting factor, which is overcome by the removal of exogenous nutrients or by the lowering of oxygen and carbondioxide concentration.

3.1.2 Changes in cellular biochemistry which accompany induction

The biochemical changes which accompany the initiation and progress of sporulation in Saprolegnia colonies are still poorly understood. Most of the studies on the biochemistry of sporulationin the Saprolegniales have been carried out on Achlya spp. During sporulation there appears to be little net change in either the dry weight or protein content of induced colonies which means all denovo protein synthesis is achieved by the turnover of pre-existing components (Griffin & Breuker, 1969; Cameron & LéJohn, 1972; Timberlake et al., 1973; Mullins & Warren, 1975). However in spite of this,

following induction there is a rapid increase in both the rate of RNA and protein synthesis. Inhibitors show that sporangium differentiation require both the synthesis of messenger RNA and proteins throughout differentiation Thus sporangium development is arrested if either inhibitors of transcription (e.g. actinomycin D) or translation (e.g. cycloheximide) are added to the induced-colony, although there is often a lag of up to 30 minutes. Therefore at any one time the cytoplasm only contains sufficient messenger RNA to govern the following 30 minutes differentiation (Griffin & Breuker, 1969; Timberlake et al., 1973). This contrasts with differentiation in another aquatic Phycomycete, Allomyces arbuscula in which all the mRNA for sporangium development is transcribed prior to induction (Burke, Seale & McCartney, 1974). In addition there is no biochemical evidence in Achlya to indicate that sporulation is initiated by the de-repression of preformed mRNA or allosterically-inhibited enzymes (Griffin & Breuker, 1969).

Among the enzymes which are induced during the early stages of sporulation in Achlya are the lysosomal enzymes, acid phosphatase (O'Day & Horgen, 1974) and α-mannosidase (Horgen & O'Day, 1975). Both of these enzymes increase 2-3 fold during the early parts of sporulation up to septum insertion and then decline again. It is significant that the curve for ER-abundance in Saprolegnia sporangia also shows a similar pattern (Hagedorn & Weinert, 1974). Therefore the initiation and control of sporulation in the Saprolegniales involves the fundamental alteration of cellular biochemistry which appears to be governed at the chromosomal level (Griffin & Breuker, 1969).

3.2 MATERIALS AND METHODS

3.2.1 Water Types used in Induction Experiments

The water used in the induction experiments was always drawn from the same mains source. This same source was used to feed the Fisons still, from which the double glass distilled water was also derived. The deionised water was however taken from a different mains source in an adjoining laboratory. The tap water had a calcium content of between 8-10 mM and a magnesium content of 5-6 mM (analysed by Chemistry Department, Imperial College). The chlorine content of the tap water was not however determined.

The tap water was distilled in a Fisons quartz glass still, and re-distilled in a Scorah still. Deionised water was obtained by passing tap water through a column of Zeolit ion exchange resin in a Permutit deioniser. A list of these main water types together with their pH and electrical conductivities is given in Table 3.1a.

Table 3.1a. Summary of the main water types used in induction experiments

Water Type	Abbreviation	pH	Conductivity µmho
Membrane Filtered.	MFTW	6·7	630 - 650.
Tap	TW	6.7	650-700
Fisons distilled (single)	SDW	5.8	6-10
Double glass distilled	DGW	5.8	2-5
Deionised	DIW	5.9	3-4

3.2.2 Divalent Cation and EDTA Stocks

Stock solutions of Mn^{2+}, Ca^{2+} and Mg^{2+} ions and EDTA were prepared from the appropriate salts as summarised in Table 3.1b. These stock solutions were made up in 100 ml volumetric flasks, using double glass distilled water. Dilutions of these stock solutions were prepared as described in the streptomycin experiments.

Table 3.1b The divalent cation and EDTA salts used in preparation of stock solutions for use in induction experiments.

Ion	Salt	molecular wt.	Stock solution prepared (mg/l)
Mn^{2+}	$MnCl_2\ 4H_2O$	197.92	1000
Ca^{2+}	$CaCl_2\ 6H_2O$	223.06	10000
Mg^{2+}	$MgSO_4\ 7H_2O$	246.50	1000
EDTA	$CH_2\ N(CH_2\ COOH)\ CH\ COONa)_2\ 2H_2O$	372.24	10000

The experimental methods used in this section are similar to those employed in the antibiotic inhibition studies, (see Section 2.2).

3.3 OBSERVATIONS

3.3.1 The Effect of Mains Tap Water and its Pre-treatment on Saprolegnian Reproduction

3.3.1.1 Sporangium Formation in S.ferax

Colonies (18 h) of S.ferax were induced in TW, MFTW, SDW, DGW and DIW (see Table 3.1) and the effects on sporangium production assessed after 7 and 24 h. The results are summarised in Table 3.2 and shows the type of inducing-water used has little overall effect on sporangium production. Nevertheless differentiation proceeds more swiftly in TW and MFTW compared with the distilled waters, with initials appearing as soon as 1 h after induction (cf. Fig. 1.1).

Although TW does not reduce the level of sporangium production it does result in a reduction in the period of zoospore motility and the encysted spores produce more irregular germtubes. In DIW some abnormal escape of cytoplasm was observed, with a few sporangia even liberating undifferentiated masses of cytoplasm. This suggests SDW and DGW are able to supplement certain requirements for normal sporangium differentiation that DIW cannot, eventhough there is little difference in their electrical conductivities (Table 3.1).

3.3.1.2 Gametangium Formation in S.furcata

It was noticed during a series of preliminary experiments, that when S.furcata-infested hempseeds were induced in TW the resulting hyphal outgrowth was relatively sparse and few oogonia or gemmae developed (Fig. 3.3). In contrast hempseeds placed in SDW (Fig. 3.1) and GDW (Fig. 3.2) produced a luxuriant outgrowth of hyphae and abundant gametangia. The results of a comparable experiment to that described in Section 3.1.1.1 are summarised in Table 3.3. In addition to the different water types described in Table 3.1, samples of tapwater were also boiled (60 minutes, BTW) and autoclaved (15 min 15 p.s.i., ATW) to determine if effects were due to a volatile such as chlorine.

The results shown in Table 3.3 confirm that oogonium production and oospore differentiation are both severely inhibited in TW and MFTW. It is clear therefore that this inhibition is not the result of the bacteria and protozoa which are present in TW. Both autoclaving and boiling however significantly reduce the level of oogonium and oospore inhibition observed in TW (Table 3.3). This suggests the deleterious agent in TW is removed or denatured by heating. As well as driving off a volatile inhibitor such as chlorine, heating also precipitates some of the calcium, resulting in a slight reduction in the water conductivity (Table 3.3).

The most effective alleviation of TW inhibition is provided by either

Table 3.2 The effect of the pre-treatment of water on sporangium production in S.ferax, assessed 7 h and 24 h after induction

Water	Conductivity µmho	Sporangial Types			
		Pre-septum 7h	Cleaving 7h	Dehisced 7h	Dehisced 24h
TW	680-700	1	3	4	4
MFTW	680-700	1	3	4	4
SDW	6-8	2	4	1	4
GDW	2-3	2	4	1	4
DIW	3-5	2	4	1	4

Sporangia/L.P.Field: > 40, 4; 20-40, 3; 10-20, 2; < 10, 1.

Table 3.3 The effect of the pre-treatment of water on the induction of oogonia and oogonium cleavage in S.furcata, assessed 120 h after induction

Water	Conductivity µmho	Oogonia (120 h after induction)		
		Mean no per L.P.Field	% Uncleaved	Oogonium Production (% GDW value)
TW	680-700	9.9	93	22
MFTW	680-700	10.4	98	24
ATW	600-650	20.5	63	49
BTW	500-550	26.3	25	65
SDW	6-8	38.8	5	95
GDW	2-3	42.3	6	100
DIW	3-5	32.6	17	82

distillation or deionisation, both of which reduce the measured ionic contents of the water dramatically (Table 3.3). The mains tapwater contained between 8-10 mM calcium and 2-2.5 mM magnesium. It is shown in Section 3.3.2 that when present in excess both these ions have a deleterious effect on oogonium formation and differentiation. DIW results in a slightly increased proportion of uncleaved oogonia compared with the distilled waters (Table 3.3). However the abnormal patterns of oospore cleavage reported in S.diclina oogonia in the absence of calcium were not observed (McCann & Stewart, 1973).

3.3.1.3 TW-induced Gemmae: Morphology and Ultrastructure

Between 60-100% of the bodies which differentiate in TW and MFTW fail to differentiate into oospores. Most of these TW-induced gemmae were large spherical bodies, up to 80 μm in diameter, and most lacked antheridia. As with antibiotic-induced gemmae chains of these spherical bodies were frequent (Fig. 3.4). In some bodies the tips of the antheridial hyphae became greatly expanded and resembled oogonia initials (Fig. 3.5). As usual a number of abnormally swollen club-shaped gemmae also form, and these have fairly dense non-vacuolate contents (Fig. 3.6). Finally, a small proportion (c. 5%) of the uncleaved gemmae produced simple germ-tube like appendages which extended for < 500 um. Therefore the range of gemma types is similar to those reported in antibiotic-induced gemmae

Although the internal structure of TW-induced gemmae was variable a number of common effects could be recognised. The extent of vacuolar expansion and coalescence showed a good deal of variation within these gemmae (Figs. 3.7-3.9). In most the partially expanded vacuoles remain in close contact without fusion, resulting in the vacuolar compartments being divided by fine protoplasmic strands (Fig. 3.9). Some of the vacuoles contain 'doughnut-profiled' densebodies similar to those observed in germinating cysts (cf. Fig. 3.8 and Fig. 1.66). This is a rare example of the presence of densebody granules in an expanded vacuolar vesicle. There is little evidence of vacuolar membrane disruption such as observed in Str-induced gemmae.

There is no sign of the conspicuous parallel arrays of ER in these gemmae. The Golgi dictyosomes are either associated with mitochondria or nuclei, but do not appear to be particularly active 120 h after induction (Fig. 3.18). The peripheral cytoplasm contains the usual wall vesicles (Fig. 3.16, 3.18, 3.13) and the gemma walls are thickened, ranging in thickness from 280 to 450 nm (Figs. 3.13, 3.14, 3.18). Small lomasomes are frequently present in these walls (Fig. 3.13, 3.14) although they are not as abundant as in Str-induced gemmae.

The mitochondria have a dense particulate matrix and abundant orderly-arranged cristae (Figs. 3.14-3.21). Many of the mitochondria have cup-shaped profiles (Fig. 3.23) and in tangential section appear as

toruloid bodies (Fig. 3.21). Similar profiles are reported in S.terestris by Howard and Moore (1970) and are believed to be associated with the use of lipids as of endogen ous food reserves. However the intimate associations with neutral lipid droplets and densebody vesicles described in the latter are not so common in TW-induced gemmae.

The osmiophilic densebodies in these gemmae are small (< 200 nm) and some show signs of fragmentation (Fig. 3.18). Many of the densebody vesicles contain lamellar arrays with a periodicity of 8-9 nm (Fig. 3.15).

The multivesicular (autolytic) bodies are more numerous in TW-induced gemmae than in any other treatment. In addition, their structure (Figs. 3.16, 3.17, 3.19, 3.20) is different from that of comparable bodies in either differentiating sporangia (Figs. 1.50, 1.51) or Str-induced gemmae (Figs. 2.163-2.169). In TW-induced gemmae they are large (0.5-1.0 µm) ovoid or spherical bodies with a uniform particulate matrix containing myelin-like membran ous arrays (Fig. 3.17, 3.19). Smaller bodies containing more abundant spherical membran ous inclusions also occur as shown in Fig. 3.20. The multivesicular bodies are themselves frequently associated with smaller (< 300 nm) uniformly granular bodies, some of which appear either to be coalescing with or budding off from the larger body (Fig. 3.17). The large multivesicular bodies resemble the almost mature autolytic 'segregation vesicles', in which the lysed organelles are no longer recognisable (Ericsson, 1969). The smaller uniform bodies resemble the primary lysosomes which transport lytic enzymes from the dictyosome to the autolytic vesicle (Matile, 1974).

The nuclei in the TW-induced gemmae are in interphase and show no sign of any abnormal inclusions, such as observed in some Str treated bodies (Figs. 3.7-3.9).

3.3.1.4 Oospore Morphology and Ultrastructure

As mentioned in Section 1.2.4.3 many of the oospores which differentiate in TW-induced oogonia are abnormally swollen (Fig. 3.10). In extreme cases these spores may reach a diameter of 20 µm or more (Figs. 3.10, 3.11). Their wall is thinner (between 0.8-1.2 µm) and appears less rigid, with spore shape largely determined by contact with the oogonium and neighbouring spores (Fig. 3.10). The inner endospore layer has a distinctive ultrastructure (Figs. 1.151, 1.161, 3.12). It is lightly stained, without visible substructure and often with a more electron-transparent inner layer (Fig. 3.11). Small osmiophilic granules, resembling lipid, are distributed either uniformly (Fig. 3.12) or in localised bands (Fig. 1.151) within the endospore layer. The endospore wall in these spores is clearly bounded on both sides by a 'unit membrane' (Fig. 1.161). The origin of these membranes is discussed in Section 1.3.4.3.

The endospore layer in some of these spores is elaborated adjacent to

the fertilisation tube to form a conspicuous knob-like protrusion into the spore cytoplasm (Fig. 3.11). In some spores (not shown) this peg extended nearly 8 µm into the spore, and had an elaborate core of 'collapsed' wall material which was continuous with the external fertilisation tube. Such pegs are further evidence that the oospores are regularly penetrated by the fertilisation tube in this species.

The excellent fixation of the spore cytoplasm is a not able feature, and various aspects of their internal cytology has already been described in Section 1.2.4.4 . However these spores are a striking example of the importance of the endospore layer in governing spore permeability, and in relation to this probably dormancy also.

The swollen profiles of the spores suggest they may be compared with the early stages of spore germination described in living material by Zeigler (1953). The thinning endospore layer and the enhanced permeability are both consistent with germination. However until further information is available on the structural aspects which accompany oospore germination the status of these spores will remain equivocal.

3.3.2 The Effect of Divalent Metal Cations and EDTA on Saprolegnian Reproduction

3.3.2.1 The Effect of Ca^{2+} on sporangium formation in S.ferax

Colonies (18 h) of S.ferax were induced in a range of Ca^{2+} concentrations (2.5-250 mM) and the effect on sporangium development assessed after 5 h and 24 h. The results are summarised in Table 3.4, and show that Ca^{2+} concentrations up to 25 mM have no overall effect on sporangium formation, although higher concentrations are progressively inhibitory. Nevertheless at Ca^{2+} levels between 2.5-25 mM the rate of sporangium differentiation is clearly enhanced (Table 3.4). At concentrations of 125 mM and above there is severe disruption of the hyphal cytoplasm, and it degenerates into a series of 'oily' droplets such as shown in Fig. 3.63.

Table 3.3 The effect of Ca^{2+} on sporangium formation in S.ferax, assessed 5 h and 24 h after induction

		Calcium Ion Conc. n. (mM)						
		0	2.5	12.5	25	62.5	125	250
Stage	Time (h)	5.24	5.24	5.24	5.24	5.24	5.24	5.24
Precleavage		2.1	3.1	3.1	3.1	2.3	1.2	0.0
Dehisced		3.4	3.4	4.4	4.4	1.1	0.0	0.0
Zoospores		1.3	2.2	3.2	3.1	1.0	0.0	0.0
Cysts		0.4	1.4	1.4	1.4	0.1	0.0	0.0

No. Sporangia/L.P.Field 0. Absent 0; 1, < 10; 2,10-20; 3, 20-30; 4, > 40

3.3.2 The Effect of Divalent Metal Cations and EDTA on Sexual Reproduction in S.furcata

The results of a series of four separate experiments each determining the effect of Ca^{2+}, Mg^{2+}, Mn^{2+} and EDTA on oogonium production and cleavage are summarised in Figs. 3.24 and 3.25. All three metal cations and EDTA produce sigmoid log dose-response curves, which are of similar gradient (Fig. 3.24). However the toxicity of the three cations and EDTA clearly differs. In order of decreasing toxicity they can be placed as follows Mn^{2+} (ED50 c. 0.1 mM) >> Mg^{2+}, EDTA (ED50 c. 5 mM) > Ca^{2+} (ED50 c 25 mM).

The effect of the cations (with the exception of Mg^{2+}) and EDTA on oospore differentiation follow similar inhibitory patterns (Fig. 3.25) Again Mn^{2+} is more toxic than either EDTA or Ca^{2+}. In all cases spore cleavage is less sensitive to these agents than oogonium production. This is particularly apparent with Mg^{2+},which over the concentration range tested shows a gradual and approximately linear increase with the log-dose (Fig. 3.25).

3.3.2.3 Ca^{2+} Antagonism of Mn^{2+} Toxicity

Since Ca^{2+} proved such effective antagonists of Str-inhibition their effectiveness against Mn^{2+} toxicity was also tested. The results of an experiment in which a 1.25 mM Ca^{2+} concentration was tested aginst Mn^{2+} solutions of 0.9 and 18.2 mM, are summarised in Table 3.5.

Table 3.5 The effect of Ca^{2+} on Mn^{2+} induced inhibition of oogonium production (mean no. per L.P. field) and oospore cleavage (% uncleaved oogonia, bracketed figures) in S.furcata, assessed 72 h after induction.

	Calcium Conc.n. (mM)	
Manganese Conc.n. (mM)	0	1.25
0	60.4 (9)	54.0 (9)
0.9	1.8 (100)	46.1 (11)
18.2	0 (-)	17.8 (13)

Calcium ions proved highly effective antagonists of manganese toxicity. When present in slight excess (1.25 mM Ca^{2+} vs. 0.9 mM Mn^{2+}), Ca^{2+} restored oogonium production and spore formation virtually to the control level (Table 3.5). Even when Mn^{2+} ions greatly outnumber Ca^{2+} (c.15 times), the total inhibition of oogonium production was still overcome. This suggests that Ca^{2+} ions have a greater affinity for suitable cellular sites than Mn^{2+} ions eventhough the latter have a greater chelate stability (Cochrane, 1958).

Fig. 3.24 The effect of divalent cations and EDTA on oogonium production in S. furcata, assessed 120h after induction.

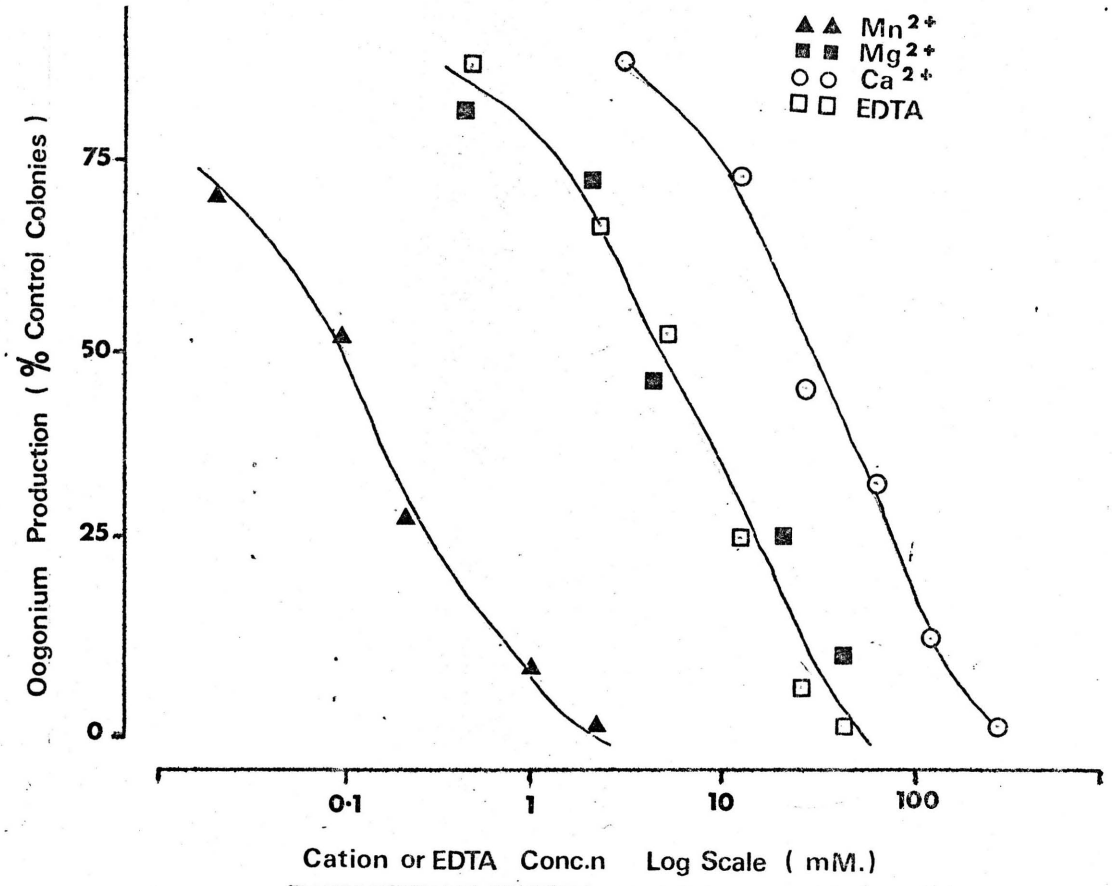
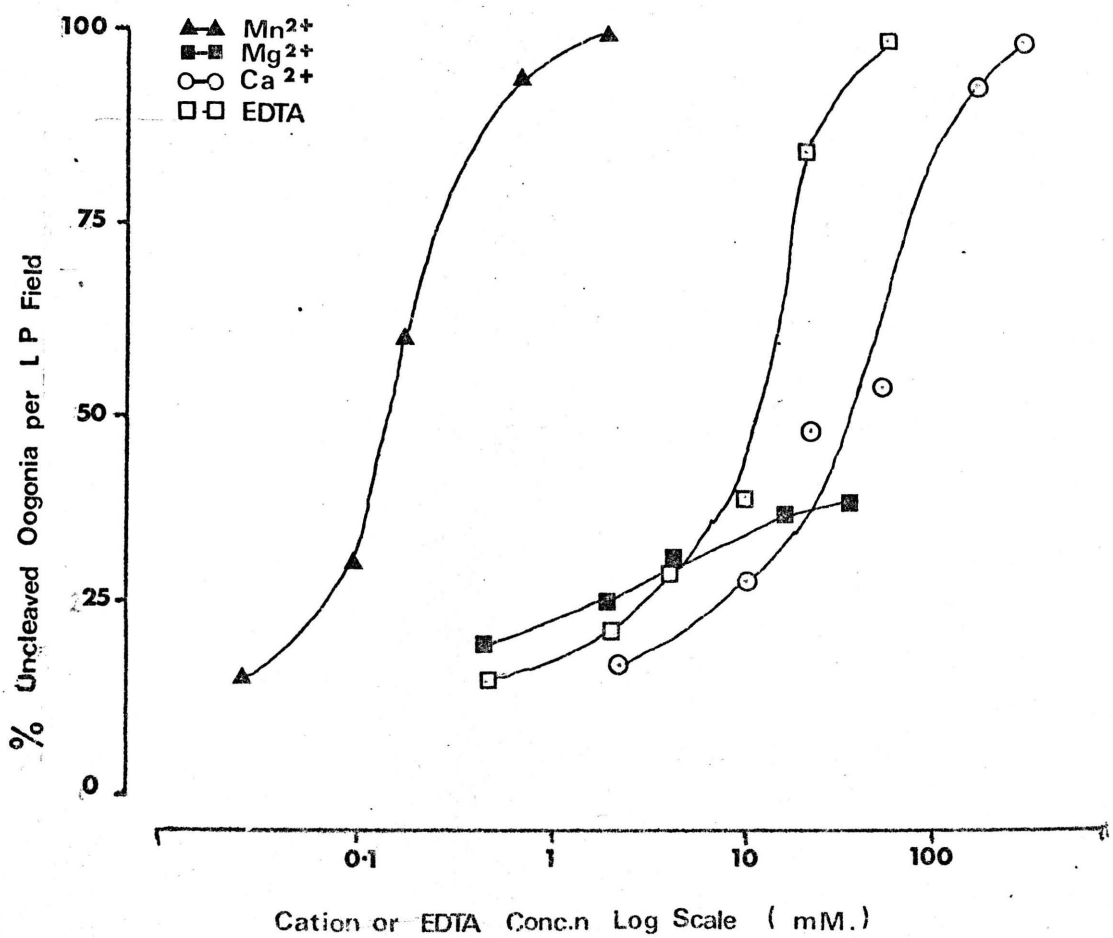


Fig. 3.25 The effect of divalent cations and EDTA on oogonial cleavage in S. furcata, assessed 120h after induction.



3.3.2.4 The Morphology and Ultrastructure of Cation and EDTA Induced Gemmae

Gemmae induced by Mn^{2+}, Ca^{2+}, Mg^{2+} and EDTA exhibit a similar range of morphological types to those described in previous sections (e.g. 2.3.8.8) Although simple spherical and clavate types predominated (Figs. 3.41, 3.45, 3.46) appendages were produced by between 10 and 30% of all the Ca^{2+} induced gemmae. In addition the latter were often very large (< 100 nm) and had a dense, apparently non-vacuolate, cytoplasm (Figs. 3.41, 3.44). The cytoplasm of many Mn^{2+}-induced gemmae lysed and most of their contents were lost. Many of the hyphae in these Mn^{2+}-induced colonies are packed with refractile oil droplets (Fig. 3.63). Although this phenomenon is also observed at high concentrations of Mg^{2+} and Ca^{2+} it never occurs to the same extent.

Ultrastructural observations have been made on EDTA, Ca^{2+} and Mn^{2+}-induced gemmae. Each treatment results in gemmae with a distinctive ultrastructural cytology, and therefore each will be described separately.

1. EDTA-induced gemmae

Most EDTA-induced gemmae are distinguished by their lack of expanded vacuolar vesicles and overall 'dense' appearance of the cytoplasm (Fig. 3.26). Some gemmae are vacuolate (Fig. 3.27), but the vacuolar areas remain partitioned by cytoplasmic strands, and the peripheral cytoplasm is densely packed with organelles and reserves.

In spite of the high density of cytoplasmic ribosomes, they lack definition (Figs. 3.29, 3.31). Mitochondria are abundant and their ultrastructural appearance (Fig. 3.29) is similar to that observed in untreated oogonia and gemmae. Golgi dictyosomes are still closely associated with both nuclei and mitochondria (Fig. 3.29), although the absence of peripheral vesicles suggest they are quiescent at this stage (120 h after induction). One of the most distinctive features of EDTA-induced gemmae is the high concentration of wall vesicles in the peripheral cytoplasm (Figs. 3.26, 3.27, 3.30). However the cell wall is not noticeably thicker than in control bodies (c. 200-300 nm, Fig. 3.30) and only contains occasional plasmalemmasomes (Fig. 3.30) and lomasomes. This suggests vesicle accumulation is the result of a partial inhibition of their secretion.

The densebodies in EDTA-induced gemmae are small and rarely exceed 300 nm in diameter (Figs. 3.29, 3.31). They are often irregular in profile, and there is no sign of any lamellar material within the densebody vesicles (Fig. 3.31). The nuclei are in interphase and are apparently unaffected by this agent (Fig. 2.29).

2. Calcium-induced gemmae

The ultrastructural effects of high Ca^{2+} concentrations (> 50 mM) on

gemmae were quite distinctive and appeared similar in both S.ferax and S.furcata. Although Ca^{2+}-induced gemmae have quite high vacuolar fractions (< 50%) the vacuolar vesicles remain small, rarely exceeding 3.0 µm in diameter (Figs. 3.42, 3.47). In addition there was frequently considerable breakage of the vacuolar and densebody vesicle membranes in these bodies, as shown in Figs. 3.50, 3.55, 3.58 and 3.60.

Mitochondria appear unaffected by high levels of calcium, and contain abundant well-ordered cristae even at Ca^{2+} concentrations as high as 100 mM. Mitochondrial profiles of up to 4.0 µm are not uncommon in Ca^{2+}-induced gemmae and toruloid or cup-shaped profiles were associated with droplets of lipid (Fig. 3.56) and densebody vesicles (Figs. 3.50, 3.55). Dictyosomes are still associated either with mitochondria (Fig. 3.57) or nuclei (Fig. 3.48) but do not appear to be particularly active at this stage (120 h after induction).

The cell walls of these gemmae are greatly thickened and may reach a diameter of 850 nm (Figs. 3.47, 3.54, 3.57, 3.58). These walls remain electron transparent, and there is little sign of the lamellar substructure observed in some of Str-induced walls (Figs. 3.54, 3.57, 3.58). However, as in Str-induced gemmae wall thickening is accompanied by an increase in lomdsome abundance (Figs. 3.57, 3.58), the formation of peg-like wall ingrowths (Fig. 3.54) and a thickening of the basal septa (Fig. 3.60). The latter is particularly conspicuous and these septa are clearly visible under the light microscope (Figs. 3.44, 3.46, 3.59).

The densebodies are also much enlarged in Ca^{2+}-induced gemmae, and may reach a diameter of 750 nm or so, (Fig. 3.50, 3.55) compared with the usual 350-450 nm size in untreated bodies. There was never any sign of lamellar material in the densebody vesicles, although they did contain small osmiophilic particles (Fig. 3.55). At concentrations up to 25 mM nuclear structure is unaffected by excess Ca^{2+} ions. However at higher levels of calcium (> 25 mM) the nuclei appear shrunken and have a indistinct, rather fuzzy outline (Fig. 3.47). High-power examination reveals that these nuclei have a coarsely particulate nucleoplasm, and a highly folded nuclear envelope (Fig. 3.48). The latter is closely associated with stacks (< 7) of proliferated membranes, forming elaborate myelin-like arrays, with a periodicity of approximately 9-10 nm (Figs. 3.52, 3.53). In extreme cases the nucleoplasm contents are lost, leaving an elaborately folded membrane complex such as shown in Fig. 3.49. The conclusion that this membrane is derived from modified nuclear envelope is supported by the presence of the typical annulate nuclear pores (Fig. 3.52). In addition to the abnormal nuclei,pairs of centrioles were observed in the cytoplasm that were not associated with nuclear profiles (Fig. 3.51). This suggests that either

the structures or forces which usually maintain their nuclear association are lost, or that their companionate nuclei have completely disintegrated.

3. Manganese-induced gemmae

The highly toxic Mn^{2+} ions result in the almost complete disruption and disintegration of gemma cytoplasm (Figs. 3.61-3.66). The recognisable components in these bodies are the mass of membrane fragments and the coalesced lipid droplets (Fig. 3.66, 3.69). In some bodies structures resembling partially lysed mitochondria (Fig. 3.69) and nuclei (Fig. 3.67) are however still discernible. The cell walls of these bodies are slightly thickened (< 500 nm, Fig. 3.68) and contain small lomasomes.

3.3.2.5 The Morphology and Ultrastructure of Cation and EDTA Induced Oospores

Both Mg^{2+}, Ca^{2+} and Mn^{2+} cations and EDTA result in the widespread abortion of oospores which differentiate in their presence (Figs. 3.32, 3.34, 3.43). In general the oospore contents degenerate into oily droplets, as described in Str-induced spores in Section 2.3.8.7. The remaining oospores mature normally and all possess an ooplast containing the usual motile granules (Fig. 3.36).

In addition to causing oospore abortion EDTA also appears to affect the normal pattern of cleavage as shown in Figs. 3.33, 3.25, 3.36. Oogonia in EDTA (< 5.0 mM) frequently contain oospores of varied size ranging from 8 µm to in excess of 20 µm (Figs. 3.33, 3.35, 3.36). Presumably these arise as a result of abnormal cleavage patterns, since similar variations in spore size have also been reported in S.diclina in a calcium-free medium (McCann & Stuart, 1973). The precise way these abnormal cleavage patterns arise could not be ascertained.

Ultrastructurally some of the aborted EDTA-induced oospores have a distinctive endospore layer. It is thinner (0.5 µm) and more electron-dense than normal and in parts has separated from the primary wall layer (Fig. 3.39, 3.40). It has an electron dense outer boundary, but there is no evidence of an inner membrane (Fig. 3.40). The internal contents of these spores show only the large coalesced droplets of lipid and the old membrane fragments. The primary wall of all EDTA-induced spores is slightly thicker than usual (350 nm cf. 250 nm, Figs. 3.38, 3.40). This may mean that the accumulated wall vesicles observed in the undifferentiated gemmae (Figs. 3.26, 3.27) may be discharged after cleavage.

3.4 DISCUSSION

3.4.1 The Effects of Tap Water

There is obviously considerable variation in the suitability of tap water as a sporulation inducing agent. While it increases the rate of sporangium formation in S.ferax, it inhibits oogonium formation in S.furcata Both of these effects could also be induced by the addition of calcium (2.5 to 25 mM) to distilled water. Since tap water contains approximately 10 mM Ca^{2+} and 5 mM Mg^{2+} ions, it suggests these effects are related to the divalent cation content of the water. While this satisfactorily explains the effects on sporangium differentiation, it does not entirely account for all the effects on S.furcata, particularly the marked inhibition of oospore formation.

The ultrastructural observations while showing similarities between tap water and Ca^{2+}-induced gemmae (e.g. thickened walls and large cup-shaped mitochondria, see Table 316) also reveal a number of differences between these treatments. Tap water–induced gemmae for instance contain unusually large multivesicular bodies, whereas Ca^{2+}-induced gemmae have much larger densebodies (Table 3.6). It therefore seems likely that there is some other component in tap water which contributes to its inhibitory effects. Recently chlorine (0.5 mg/l) has been shown to reduce the level of sporangium formation and zoospore differentiation in Peronospora trifolium on alfalfa plants (Fréid & Stuteville, 1975). This was first noticed when fresh tap water was used in the humidity chambers instead of distilled water. Since some of the inhibitory effects of tap water on Saprolegnia are alleviated by heat treatment it is possible a volatile inhibitor, such as chlorine, is also involved here. However the situation is confused by the fact that heat treatment also precipitates some of the divalent cations in the tap water. In addition, tap water is still highly inhibitory to oogonium production after it has been allowed to stand for 3-4 days to allow the chlorine to evaporate away.

3.4.2 The Effects of EDTA

In Achlya spp., EDTA (0.01 mM) has been shown to extract 40% of the cellular calcium and inhibit both growth and sporulation (Griffin, 1966; Cameron & LéJohn, 1972). Much higher concentrations (c. 5 mM) are required to produce similar effects in S.furcata. However wide variations in the sensitivity of different strains of Saccharomyces cerevisae to EDTA have been reported by Elferink (1974), and shown to be related to the phospholipid content of their membranes. EDTA does not appear to be toxic itself but exerts its effects through the sequestration of calcium and possibly other vital divalent cations (Cameron & LéJohn, 1972). It seems probable that EDTA inhibits S.furcata in the same way.

One of the most striking ultrastructural observations on EDTA-induced

gemmae is the abundance of wall vesicles in the peripheral cytoplasm. The concentration of wall vesicles in these gemmae exceeds those observed in any other treatment. However rather surprisingly this abundance of wall vesicles is not correlated with an increase in gemma wall thickness. The accumulation of these vesicles therefore may be related to the slowing down or inhibition of their discharge at the cell surface. This is supported by studies on animal cells which have shown that calcium regulates cellular secretion processes. Thus the addition of EDTA to mammalian mast cells inhibits the discharge of the peripheral secretory vesicles and results in their accumulation in the cytoplasm (Kagayama & Douglas, 1974). EDTA may affect the discharge of peripheral wall vesicles in Saprolegnia in a similar way. However EDTA-induced oospores have thicker cell walls than their untreated counterparts (c. 300 nm cf. 150 nm), which suggests the impairment of vesicle deposition is not effective after cleavage.

Calcium ions are known to stabilise amorphous polar lipid and prevent its hydration and dispersion (Kavanau, 1965). This presumably explains the presence of enlarged phospholipid densebodies in Ca^{2+}-induced gemmae, and the small densebodies in comparable EDTA-induced bodies (Table 3.6). Calcium ions are an important structural component of cell membranes where they govern permeability and fusion (Burström, 1968; Lucy, 1973). The removal of membrane bound calcium may explain the abnormal vacuolation and cleavage patterns observed in EDTA-induced gemmae and oogonia. Finally calcium has been shown to be necessary for the normal maturation of Peronosporalean oospores (e.g. Elliott, 1972). The increased incidence of oospore lysis in EDTA and excess calcium treatments, suggest this ion also plays an important role in the development of Saprolegnian oospores.

These EDTA effects indicate the importance of calcium for the normal reproductive morphogenesis of Saprolegnia. The fact that double glass distilled water is usually a perfectly satisfactory inducing agent may be explained on two counts:

a) Distilled water contains sufficient calcium ions to supplement the calcium requirement.

b) The vegetative mycelium is normally able to accrue sufficient calcium during vegetative development to supplement requirements during reproductive differentiation.

Some evidence for the former comes from the fact that distilled water (single and double) proved a better oogonium-inducing agent than deionised water. It is possible deionisation removes more calcium and magnesium than distillation. Nevertheless even in deionised water the level of sporulation is still quite high, suggesting that some calcium requirements are supplied from internal 'reserves'. However the presence of calcium in the inducing

medium may enhance the rate of sporulation as shown in S.ferax. There is also evidence that sexual reproduction in different Saprolegnian species is affected by calcium deficiency in different ways (J.Fletcher, personal communication). This may reflect variations in the ability to extract calcium from the environment or internal reserves. Such variations may explain why glass distilled water is a perfectly satisfactory inducing agent for some species and not others (see Section 3.1).

3.4.3 Divalent Cation Toxicity

Of the three divalent cations examined, manganese was the most toxic. Its ED50 value for oogonium production in S.furcata was 0.05 mM compared with 5.0 mM for Mg^{2+} and 62.5 mM for Ca^{2+}. Similar results to these have also been reported in an Achlya sp. (Cameron & LéJohn, 1972). In this species vegetative growth was completely inhibited by 0.1 mM Mn^{2+} and 2.0 mM Mg^{2+}, whereas Ca^{2+} had little effect at concentrations of upto 50 nM. However the Peronosporales are less sensitive to Mn^{2+} ions, and manganese is the most effective streptomycin antagonist in this group (McMeekin, 1973; Griffin & Coley-Smith, 1975).

The effects of heavy metals, including manganese, on fungi have recently been reviewed by Ross (1975). In general the basis of heavy metal toxicity in fungal cells is poorly understood. Since Mn^{2+} ions have a stronger chelate binding stability than Ca^{2+} and Mg^{2+} (Cochrane, 1958) they might be expected to replace these ions from their cellular sites when present in excess. Nevertheless Ca^{2+} ions effectively antagonise Mn^{2+} toxicity to S.furcata. Indeed a similar interaction to that described in the streptomycin studies is suggested. It seems likely therefore that Ca^{2+} ions are preferentially absorbed into Saprolegnian cells, and competitively reduce both the uptake of Mn^{2+} and streptomycin. This is the reverse of what has been reported in yeast cells in which Mn^{2+} ions are preferentially adsorbed at the expense of Ca^{2+} ions (Jennings, cited by Ross, 1975). However Oomycetes in general, and the Saprolegniales in particular (Griffin, 1966; Cameron & LéJohn, 1972), have been shown to have a much higher calcium requirement than most other fungi.

3.4.4 Morphological and Ultrastructural Effects of Excess Ca^{2+} ions

The most striking feature of Ca^{2+}-induced gemmae are their thickened cell walls. A similar Ca^{2+}-induced cell wall thickening has also been described in higher plants (reviewed by Burström, 1968). In these it is believed that calcium acts by binding to the cell wall and increases its rigidity. This reduces the rate of cell expansion and allows the wall to become thickened. The predominance of club-shaped and more irregular elongate structures (e.g. Figs. 3.45, 3.46, 3.59) at calcium concentrations of 50 mM and above, indicates that normal cell expansion is also being

affected in Saprolegnia.

The effect of calcium on stabilising polar lipid has been mentioned in Section 3.4.3. The binding of excess Ca^{2+} ions to vacuolar membranes may be the main factor involved in limiting their coalescence, and considering their breakage during Os-fixation. For instance, Lucy (1973) reports that conditions which prevent the localised removal of membrane-bound calcium inhibits normal membrane fusion.

However the effect of excess Ca^{2+} ions on nuclear structure in gemmae is quite unlike that observed or reported in any other treatment. The effect seems to be primarily on the nuclear envelope, which may mean this membrane is particularly 'sensitive' to calcium. Certainly the mitochondria at comparable concentrations appear structurally unaffected. Therefore it is likely that most of the morphological and structural effects produced by high levels of calcium can be explained by their binding to suitable intracellular cationic sites and deranging the normal processes of differentiation.

3.4.5 Comparison of Divalent Cation, EDTA and Antibiotic Effects

Selected morphological and cytological effects of streptomycin, calcium, EDTA and tap water on the differentiation of oogonia and gemmae in S.furcata are summarised in Table 3.6. The similarities between the tap water and calcium effects are discussed in Section 3.4.1. It was proposed in Section 2.4 that streptomycin acts by binding to suitable cellular cationic sites, where it then interferes with the cellular processes normally regulated by divalent cations, such as Ca^{2+} and Mg^{2+}. It is possible that streptomycin simply binds to the specific divalent carrier sites on the plasmalemma and prevents further cation uptake. In the event of this, one might expect to observe symptoms of intracellular cation deficiency such as produced by EDTA. However comparison of the streptomycin and EDTA effects on S.furcata reveal relatively few similarities between these two inhibitors (Table 3.6).

In fact the symptoms produced by streptomycin correlate most closely with those produced by excess calcium ions (Table 3.6). This provides additional evidence to support the hypothesis that both excess Ca^{2+} and streptomycin ions are acting by binding in a non specific way to cellular cationic sites. The cell wall and membranes appear particularly important sites for such cations. Clearly the effect of these divalent cations on cellular biochemistry is extremely variable. While spore differentiation is invariably inhibited wall synthesis is enhanced by both excess Ca^{2+} and streptomycin. These ions may be acting directly on the biochemical pathways which govern wall synthesis. On the other hand they may act indirectly by allowing cellular components which would normally be involved in other cellular processes, to be diverted into wall synthesis.

Table 3.6 Summary of the morphological and structural effects of inhibitors in induced colonies of S.furcata

Developmental Stage or structure	Inhibitor				
	Control	Str	Ca.	TW	EDTA
1. Gemma morphology					
simple	+	++	+	+++	++++
club-shaped	-	+	++	++	+
appendate	-	++++	+	+	-
2. Abnormal oospore types					
'oily' spores	+	+++	++	+	+++
swollen oospores (>20 µm dia)	-	-	-	+++	++
3. Ultrastructural cytology of gemmae					
large cup-shaped mitochondria	-	-	+++	++	-
vacuolar membrane breakage	+	+++	+++	+	+
densebody diameter (nm)	350-450	350-550	600-750	350-500	250-300
MVB abundance	+	++	+	+++	+
Wall thickness (nm)	250-300	350-650	500-800	350-600	200-300
lomasomes abundance	+	++++	+++	++	+
peg-like wall ingrowths	-	++	+	-	-

-, rare or absent; + < ++++, arbitrary scale of increasing abundance, based on comparison of effects of all inhibitors.

This hypothesis assumes that streptomycin, an alien molecule to the cell, is able to mimic in a fairly non-specific way the activities governed by ions that are normal cell constituents. Indirect biochemical evidence that streptomycin is able to substitute for divalent metal cations comes from studies with cell-free protein synthesising systems from bacterial cells. It was discovered that in a system in which Mg^{2+} ions were omitted, low levels of streptomycin actually stimulated protein synthesis by substituting for the requisite Mg^{2+} ions (Nissim & Zamir, 1974). Clearly the effect that streptomycin molecules have on cellular biochemistry will very much depend on the pathway involved. This explains the complexity of the observed morphological and structural effects.

The results of this final section show how the apparently unconnected inhibition of oogonium development in S.furcata by streptomycin and tap water are both related to some extent to the effects produced by excess Ca^{2+} ions. The critical role played by calcium in the reproductive morphogenesis of an Oomycete fungus is again demonstrated.

5. SUMMARY

This account continues the ultrastructural studies of growth and reproduction in Saprolegnia initiated by Gay and Greenwood (1966) and continued by Heath (1969). Although most of their observations are supported by this study, a number are re-evaluated in the light of these and other recent findings. For example the parallel arrays of ER seen in S. ferax (Heath & Greenwood, 1971) are correlated with periods of light turnover or depletion of proteins and the Golgi-ER-mitochondrion association (Heath & Greenwood, 1971) with wall formation. The presence of small vesicles in the regions of wall deposition noted by Heath, Gay and Greenwood (1970) is also demonstrated in a) naked oospheres, b) fertilisation tube apex, c) in the region of fertilisation tube and oospore contact, and d) in the apices of antibiotic-induced gemma appendages. Further evidence for the derivation of these wall vesicles from Golgi dictyosomes is presented. Although both streptomycin and high concentrations of calcium ions increase both gemma wall thickness and the abundance of peripheral wall vesicles, observations after treatment with EDTA indicate that effects are not necessarily correlated.

The development of the characteristic tripartite septum in Saprolegnia has still not been satisfactorily resolved. The involvement of small Golgi derived vesicles suggested by Heath (1969) is confirmed and a possible model for septum formation is proposed. Although it is not known whether the two septal wall layers are normally inserted simultaneously, single wall strands traversed the hyphal compartment in some streptomycin treatments. It is possible that experimental study of the abnormal septa developed in calcium and streptomycin treatments may prove profitable in elucidating the ultrastructural development of these curious cross walls.

Gametangial nuclear divisions in S.furcata follow a similar course to those previously described in S.terrestris by Howard and Moore (1970). They support recent light-microscopic (Flanagan, 1970; Win-Tin & Dick, 1975) and genetic studies (Mullins & Machlis, 1965; Lasure & Griffin, 1974) which indicate these divisions are meiotic. The absence of the synaptinemal complex in the Saprolegniales is again confirmed, and this may have important genetic implications. Unfortunately none of the inhibitors used in this study appeared to interfere specifically with nuclear divisions and did not contribute any further information on the nature of hyphal and gametangial divisions.

Streptomycin studies failed to contribute any further information on the mechanism of cleavage furrow delimitation in the Saprolegniales, even though this antibiotic results in abnormal cleavage patterns in the

Peronosporales. In Saprolegnia although cleavage furrow development fails to occur, abnormal cleavage rarely follows. However both EDTA and to a lesser extent deionised water, both induce abnormal oospore cleavage in S.furcata, although the ultrastructural mechanism of this could not be determined. It confirms the crucial role of calcium in this process, as previously reported in S.dioica by McCann and Stuart (1973).

The use of inhibitors and tap water as sporulation inducing agents contributed significantly to the understanding of the ultrastructural changes accompanying oospore maturation. This account of oospore maturation in S.furcata is the most comprehensive for any species of Saprolegnia to date and complements recent accounts of oospore development in the Peronosporales (Hemmes & Bartnicki-Garcia, 1975; McKeen, 1975). The examination of cycloheximide-induced oospores, fixed in glutaraldehyde-osmic shows the ooplast vacuoles contain an osmiophilic matrix in which the densebodies are embedded. Furthermore this is correlated with the transparency of these vacuoles in the light microscope. The presence of this matrix material was not detected in permanganate fixed oospores of S.terrestris (Howard & Moore, 1970). It also confirms the structural homology of the ooplast vacuole in the Saprolegniales and Peronosporales.

The formation of the inner oospore wall (endospore) is described in detail. As in the Peronosporales this wall layer is exceptional in that its accretion occurs independently of the usual wall vesicles. Furthermore there is evidence to suggest that in Saprolegnia this endospore layer may be deposited inside the original spore plasmalemma. The mature endospore layer of S.furcata is differentiated as two distinct layers, the inner of which is accreted during the late stages of oospore maturation. This has not been previously illustrated in ultrastructural accounts of oospores, although is not unexpected from the results of light microscopic observations of Saprolegnian oospores (Dick, 1969). The chemical composition of this inner layer has not been determined, although it is not due to an increased concentration of polysaccharide. Indeed its increased osmiophilia suggests it may contain lipid or lipoprotein, possibly derived from the breakdown of cell organelles during oospore maturation.

The abnormal structure of the endospore layer in tap water-induced oospores is accompanied by excellent preservation of the oospore contents with osmic fixation. The structure of the endospore layer thus appears to be critical in governing spore permeability to fixatives. In this respect it is also likely to be important in determining spore dormancy, which is poorly understood in the Oomycetes (Hemmes & Bartnicki-Garcia, 1975).

The streptomycin studies also provided the only example in the present study of a fertilisation tube penetrating an immature oospore. This

observation was probably facilitated by the larger penetration pegs formed in the antibiotic. The collapsed fertilisation tubes sequestered between the endospore and the outer wall in mature oospores indicates that the fertilisation tubes are undoubtably functional in this species, even though this has recently been questioned (Flanagan, 1970). This conclusion was corroborated by observations of oospore nuclei, which indicate karyogamy takes place during the late stages of oospore maturation. Fusion nuclei were only observed in abnormal oospores induced in tap water and were shown to be structurally different from typical vegetative diploid nuclei.

This study shows that the Saprolegniales share the sensitivity to streptomycin reported in the Peronosporales (Griffin & Coley-Smith, 1971). As in higher plants (Zahn, 1961; McMeekin, 1973) and green algae (Litwack & Pramer, 1967; Kirk, 1962) the inhibitory effects of streptomycin on the Peronosporales are again shown to be greatly reduced by divalent metal cations, and in particular by calcium. On the other hand chitinous fungi are reported to be relatively insensitive to streptomycin (Vörös, 1963). This provides further evidence to support the view that Oomycete fungi are more closely related to green algae than most other fungal groups (Manton, 1965; Heath & Greenwood, 1971).

A model for streptomycin action in Saprolegnia is summarised in Fig. 4.1 and the accompanying legend. Streptomycin has markedly different effects on vegetative and reproductive stages. In vegetative hyphae it is suggested that its action may be due mainly to its effect on mitochondrial activity. Since in green algae streptomycin has been shown to act on the 70S plastid and mitochondrial ribosomes (e.g. Behn & Arnold, 1974a), these ribosomes may also be the main target in vegetative hyphae of Saprolegnia. Furthermore changes in the structure of thes mitochondrial ribosomes, such as described in Clamydomonas (Behn & Arnold, 1974b) may account for the streptomycin resistant and dependent strains of Phytophthora infestans recently isolated by Shattock & Shaw (1975).

However, the effects of streptomycin observed on colonies of Saprolegnia which have been induced to sporulate are consistent with the antibiotic acting primarily as a competitor for a wide range of cellular divalent cation binding sites. It is proposed that this causes the morphological and cytological similarities observed between streptomycin and excess calcium ions on S.furcata. Furthermore the effects of streptomycin on membrane permeability are reminiscent of those produced by membrane acting agents such as saponins (Olsen, 1971a, b, 1973) and EDTA (Elferink, 1974). It is proposed that following induction, the number of available streptomycin binding sites, both on the plasmalemma and intracellular sites, increase and account for the greater antibiotic susceptibility of these

stages. It is important that these observed variations in streptomycin sensitivity between vegetative and reproductive stages be taken into account when selecting streptomycin resistant strains for use in genetic studies.

Obviously a study such as this, confined almost exclusively to morphological and cytological observations, is only able to reveal limited information on the derangement of cellular biochemistry by streptomycin Nevertheless it has added considerably to the understanding of the possible effects of streptomycin on Oomycete fungi, and clearly indicates a number of desirable biochemical investigations. In particular the detection and isolation of a suitable streptomycin-binding agent from the plasmalemma would be required to validate many of these proposals.

Although not all the questions posed at the onset of this investigation have been satisfactorily answered, it has shown that the use of metabolic inhibitors provides useful insights into the mechanisms operating during normal differentiation in a family such as Saprolegnia.

Fig. 4.1 Model for streptomycin action against Saprolegnia

1. Pre-requisites

a) The antibiotic binds to suitable sites (▽) on the cell (Griffin & Coley-Smith, 1975). This is perhaps related to cellulose (Vörös, 1965) or some other constituent peculiar to Oomycete walls.

b) The antibiotic is taken into the cell via a number of specific membrane-located carriers (Litwack & Pramer, 1957) (◆).

c) The cell contains a finite but variable number of suitable cellular cationic binding sites (▽ △). These may be located in membranes and cellular components such as 70S ribosomes.

2. The model

A. High streptomycin concentration (500 mg/l) against growing vegetative hyphae.

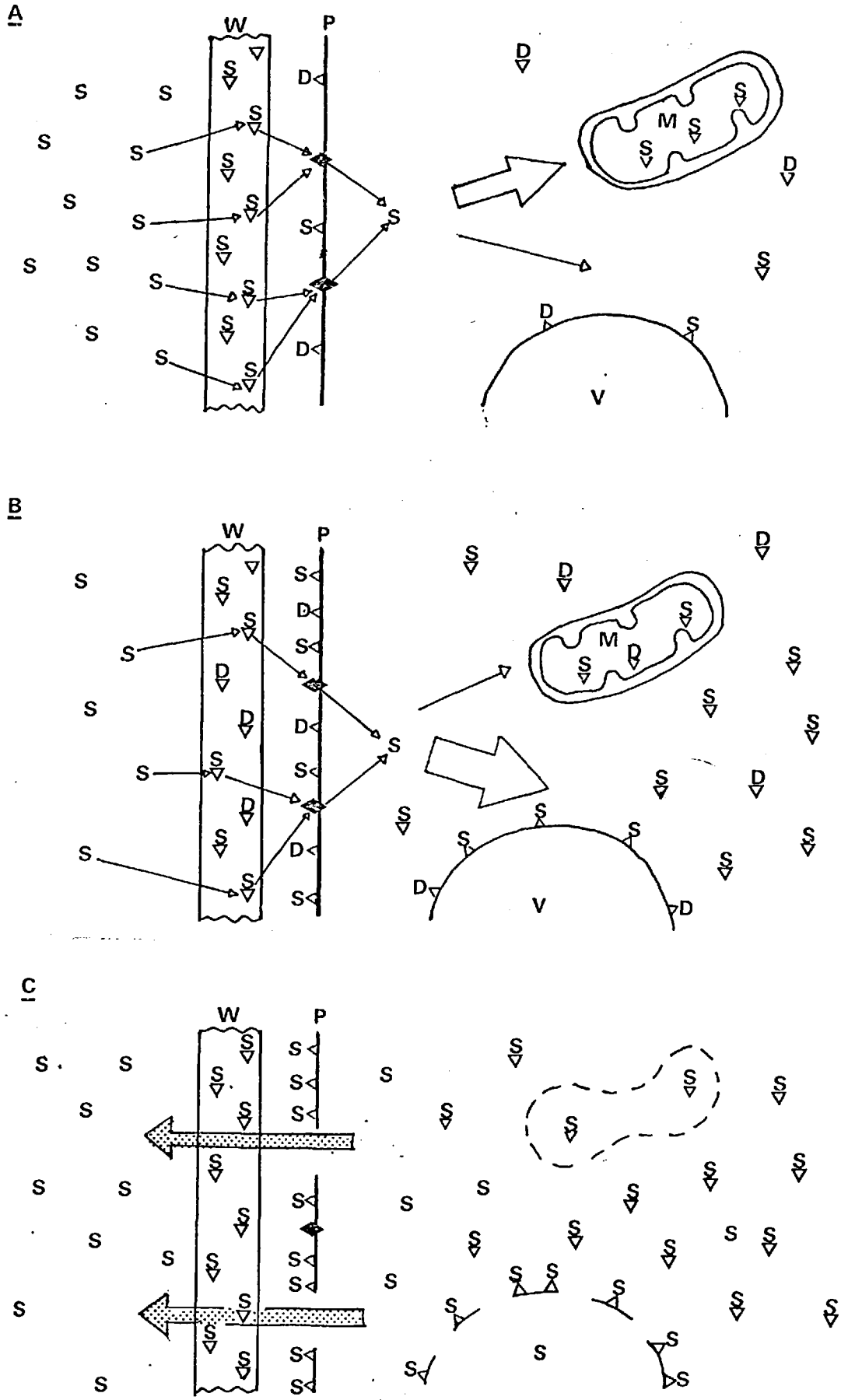
In normal vegetative hyphae it is proposed there are only a small number of specific cationic binding sites (▽) located on the plasmalemma and intracellularly. Binding still occurs to the hyphal walls (Vörös, 1965). Intracellular streptomycin mainly affects the 70S mitochondrial ribosomes and results in a partial disruption of respiratory metabolism.

B. Moderate streptomycin concentrations (< 100 mg/l) against induced colonies.

Following induction it is proposed that the number of specific antibiotic binding cationic sites increases (▽). In addition antibiotic uptake may be temporarily increased. Streptomycin competes for the cellular cationic sites and deranges cellular functions governed by calcium and other essential divalent metal cations.

C. High streptomycin concentrations (> 100 mg/l) against induced colonies.

If the antibiotic is present in sufficient quantities to saturate the plasmalemma sites, membrane permeability is destroyed. This is accompanied by a massive leakage of cellular constituents and organelle lysis and cell death follows.



D divalent cations (eg Ca^{2+})
M mitochondrion
P plasmalemma
S free streptomycin
S bound streptomycin
V vacuole
W cell wall

divalent cation binding sites
membrane located streptomycin uptake sites
path of antibiotic into and within cell
efflux of ions and low molecular wt. metabolites out of cell

5. REFERENCES

Alcorn, S.M. & Ark, P.A. (1956). Movement of certain antibiotics in cuttings of Pyracantha and carnation. Appl.Microbiol. 4, 126-130.

Aldrich, H.C. & Mims, C.W. (1970). Synaptonemal complexes and meiosis in Myxomycetes. Am.J.Bot., 57, 935-941.

Altman, J. & Bachelder, S. (1956). Susceptibility of some ornamental and vegetable plants to streptomycin injury. Pl.Dis.Reptr.,40, 1081-1083.

Altman, J. & Davis, B.H. (1958). Experiments on the control of downy midlew of broccoli and bacterial spot of lima bean with streptomycin. Pl.Dis.Reptr., 42, 416-419.

Anand, N. & Davis, B.D. (1960). Effect of streptomycin on Escherichia coli. Damage by streptomycin to the cell membrane of E.coli. Nature, Lond., 185, 22-23.

Anaud, N., Davis, B.D. & Armitage (1960). Uptake of streptomycin by Escherichia coli. Nature, Lond., 185, 23-24.

Anderson, P.J. (1956). Streptomycin for control of blue mold and bed rot of tobacco. Phytopathology 46, 240.

Anderson, H.W. & Nienow, I. (1947). The effect of streptomycin on higher plants. Phytopathology, 37, 1.

Anonymous (1972). Modern X-ray Analysis II., EDAX (Nuclear Diodes) Inc., Illinois.

Ark, P.A. & Thompson, J.B. (1957). Control of downy mildew of cucumber with antibiotics. Pl.Dis.Reptr., 41, 452-454.

Aronson, J., Meyer, W.L. & Brock, T.D. (1964). A molecular model for chemical and biological differences between streptomycin and dihydrostreptomycin. Nature, Lond., 202, 555.

Atkinson, A.W., John, P.C.L. & Gunning, B.E.S. (1974). The growth and division of the single mitochondrion and other organelles during the cell cycle of Chlorella studied by quantitative sterology and 3-dimensional reconstruction. Protoplasma, 81, 77-109.

Bakerspigel, A. (1960). Nuclear structure and division in the vegetative mycelium of the Saprolegniaceae. Am.J.Bot., 47, 94-100.

Barksdale, A.W. (1962). Effect of nutritional deficiency on growth and sexual reproduction of Achlya ambisexualis. Am.J.Bot., 49, 633-638.

Barksdale, A.W. (1963). The role of hormone A during sexual conjugation in Achlya ambisexualis. Mycologia, 55, 627-632.

Barksdale, A.W. (1966). Segregation of sex in progency of a selfed heterozygote of Achlya bisexualis. Mycologia, 58, 802.

Barksdale, A.W. (1968). Meiosis in the antheridium of Achlya ambisexualis E 87. J.Elisha Mitchell scient.Soc., 84, 181-194.

Barksdale, A.W. (1969). Sexual hormones of Achlya and other fungi. Science, 166, 831-837.

Barksdale, A.W. (1970). Nutrition and antheridial-induced branching in Achlya ambisexualis. Mycologia, 62, 411-420.

Bartnicki-Garcia, S. (1966). Chemistry of hyphal walls of Phytophthora. J.gen.Microbiol.,42, 57-69.

Bartnicki-Garcia, S. (1973a). Fundamental aspects of hyphal morphogenesis Symp.Soc.gen.Microbiol., 23, 245-266.

Bartnicki-Garcia, S. (1973b). Cell wall genesis in a natural protoplast: The zoospore of Phytophthora palmivora. In Yeast, Mould and Plant Protoplasts, 77-91. Eds. J.R.Villanueva, I.Garcia-Acha, S.Gascon and F.Umbur . Academic Press, London

Bartnicki-Garcia, S. & Lippman, E. (1969). Fungal morphogenesis: cell wall construction in Mucor ro Science N.Y., 165, 302-304.

Beckett, A., Heath, I.B. & McLaughlin, D.J. (1974). An Atlas of Fungal Ultrastructure. Longman, London.

Behn, W. & Arnold, C.G. (1974a). The effect of streptomycin and neamine on the structure of chloroplast and mitochondria in Chlamydomonas reinhardi. Protoplasma, 82, 77-89.

Behn, W. & Arnold, C.G. (1974b). On the different genetic constitution of the chloroplast and mitochondria in antibiotic dependent mutants of Chlamydomonas reinhardi. Protoplasma, 82, 91-101.

Ben Shaul, Y. & Ilana, O. (1970). Effects of streptomycin on plastids in dividing Euglena cells. Planta, 91, 195-203.

Bent, R.J. & Moore, R.H. (1966). The mode of action of griseofulvin. Symp.Soc.gen.Microbiol., 16, 82-110.

Berkaloff, C. & Jupin, H. (1974). Modifications du spectre d'emmission de fluorescence et de l'ultrastructure du plaste de l'algue verte, Protosiphon botryoides sommised l'action de la streptomycine. Protoplasma, 80, 41-55.

Berliner, M.D. (1954). A study of meiosis and the effects of certain antibiotics upon meiosis in Gymnosporangium clavipes. Am.J.Bot., 41, 93-104.

Bimpong, C.E. & Hickman, C.J. (1975). Ultrastructural and cytochemical studies of zoospores cysts and germinating cysts of Phytophthora palmivora. Can.J.Bot., 53, 1310-1327.

Blackwell, E. (1943). The life history of Phytophthora cactorum. Trans. Br.mycol.Soc., 26, 71-89.

Bliss, C.I. (1935). The calculation of the dosage-mortality curve. Ann.appl.Biol., 22, 134-163.

Bovarnick, J.G., Chang, S-W., Schiff, J.A., Schwatzbach, S.D. (1974). Events surrounding the early development of Euglena chloroplasts. J.gen. Microbiol., 83, 51-62.

Bracker, C.E. (1967). Ultrastructure of Fungi. A. Rev.Phytopath., 5, 343-374.

Bracker, C.E. (1971). Cytoplasmic vesicles in germinating spores of Gilbertella persicaria. Protoplasma, 72, 381-397.

Braselton, J.P. & Miller, C.E. (1973). Centrioles in Sorosphaera. Mycologia, 62, 220-225.

Brasier, C.M. & Sansome, E. (1975). Diploidy and gametangial meiosis in Phytophthora cinnamorni, P.infestans and P.drechsleri. Trans. Br.mycol.Soc., 65, 49-65.

Branscomb, E.W. & Galas, D.J. (1975). Progressive decrease in protein synthesis accuracy induced by streptomycin in Escherichia coli. Nature, Lond., 254, 161-163.

Brian, P.W. (1957). Effects of antibiotics on plants. A.Rev.Pl.Physiol.,, 8, 413-426.

Brinkley, B.R. & Stubblefield, E. (1970). Ultrastructure and interaction of the kinetochore and centriole at mitosis and meiosis. Adv.Cell Biol., 1., 119-185

Brock, T.D. (1966). Streptomycin. Symp.Soc.gen.Microbiol., 16, 131-168.

Bryant, T.R. & Howard, K.L. (1969). Meiosis in the Oomycetes: I. A microspectrophotometric analysis of nuclear deoxyribonucleic acid in Saprolegnia terrestris. Am.J.Bot., 56, 1075-1083.

Bullivant, S. (1973). Freeze-etching and freeze-fracturing. In: Advanced Techniques in Biological Electron Microscopy. 67-111. Ed. J.K.Koehler. Springler-Verlag, Berlin.

Bullivant, S. & Ames, A. (1966). A simple freeze-fracture replication method for electron microscopy. J.Cell Biol., 29, 435-447.

Burgeff, H. (1915). Untersuchungen über variabilität sexualitat und erbhchkeit be Phycomycomyces niteus Kuntze. Flora N.F., 108, 353-388.

Burke, D.G., Seale, T.W. & McCarthy,B.J. (1972). Protein and ribonucleic acid synthesis during the diploid life cycle of Allomyces arbuscula. J.Bact., 110, 1065-1072.

Burström, H.G. (1968). Calcium and plant growth. Biol.Rev., 43, 281-316.

Cameron, L.E. & LéJohn, H.B. (1972). On the involvement of calcium in amino acid transport and growth in the fungus.Achlya. J.biol.Chem., 15, 4729-4739.

Carbonell, L.M., Gil, F. & Yegres, F. (1973). Cell wall regeneration of; protoplasts of Histoplasma capsulatum. In: Yeasts, Mould and Plant Protoplasts. 93-103. Eds. J.R.Villanueva, I. Garcia-Acha, S.Cascon & F.Umburu, Academic Press, London & New York.

Cavalier-Smith, J. (1974). Basal body and flagellar development during the vegetative cell cycle and the sexual cycle of Chlamydomonas reinhardi J.Cell.Biol., 16, 529-556.

Chapman, J.A. & Vujičić, R. (1965). The fine-structure of sporangia of Phytophthora erythoseptica. J.gen.Microbiol., 41, 275-282.

Charnetski, W.A., Lichtenstein, E.P. & Evert, R.F. (1974). Effects of lindane on cell structure of pea roots. Can.J.Bot., 51, 2111-2117.

Christen, J. & Hohl, H.R. (1972). Growth and ultrastructural differentiation of sporangia in Phytophthora palmivora. Can.J.Microbiol., 18, 1959-1964.

Claussen, P. (1908). Uber eintwicklung und befruchtung bei Saprolegnia monoica. Ber.dt.bot.Ges., 26, 144-161.

Cochrane, V.W. (1958). Physiology of Fungi. Wiley, New York..

Coe, D.M. (1955). Streptomycin as a control for downy mildew of cucurbits. Pl.Dis.Reptr., 39, 729-730.

Cohen, Y. & Sackston, W.E. (1973). Some effects of streptomycin on Plasmopara halstedii, the downy mildew of sunflower. Phytopathology, 63, 200a.

Coker, W.C. (1923). The Saprolegniaceae with notes on other water moulds. University of North Carolina Press. Chapel Hill.

Coley-Smith, S.R. (1966). Early season control of hop downy mildew Pseudoperonospora humuli with streptomycin and protectant fungicides in severely infected plantings. Ann.appl.Biol., 51, 183-191.

Colt, W.M. & Endo, R.M. (1972). Ultrastructural changes in Pythium aphanidermatum zoospores and cysts during encystment,germination and penetration of primary lettuce roots. Phytopathology, 62, 751a.

Cotner, F.B. (1930). The development of zoospores in Oomycetes at optimum temperatures and the cytology of their active stages. Am.J.Bot., 17, 511-546.

Crosse, R., McWilliam, R., Rhodes, A. & Dunn, A.T. (1960). Antifungal action of streptomycin copper chelate against Phytophthora infestans on tomato. Ann.app.Biol., 48, 270-278.

Crump, E. & Branton, D. (1966). Behaviour of primary and secondary zoospores of Saprolegnia sp. Can.J.Bot., 44, 1393-1400.

Darby, R.T. & Goddard, D.R. (1950). Studies of the respiration of the mycelium of the fungus Myothecium verrucaria. Am.J.Bot., 37, 379-387

Davies, J. & Nomura, M. (1972). The genetics of bacterial ribosomes A.Rev.Genetics, 6, 203-234.

de Bary, A. (1887). Comparative vegetative morphology and biology of the fungi, mycetozoa and bacteria. Clarendon Press, Oxford.

Dhir, S.P. & Boatman, E.S. (1972). Location of polysaccharide on Chlamydia psiltacii by silver methionamine staining and electron microscopy. J.Bact., 111, 267-271.

Dick, M.W. (1969). Morphology and taxonomy of the Oomycetes with special reference to the Saprolegniaceae, Leptomitaceae and Pythiaceae. I. Sexual reproduction. New Phytol., 68., 751-775.

Dick, M.W. (1971). Oospore structure in Aphanomyces. Mycologia, 63, 686-688.

Dick, M.W. (1972). Morphology and taxonomy of the Oomycetes with special reference to the Saprolegniaceae, Leptomitaceae and Pythiaceae. II. Cytogenetic systems. New Phytol., 71, 1151-1159.

Dick, M.W. & Win-Tin (1973). The development of cytological theory in the Oomycetes. Biol.Rev., 48, 133-158.

Dowler, W.M. & Goodman, R.N. (1958). Downward translocation of streptomycin in Coleus sp. Phytopathology, 48, 392

Dubin, D.T., Hancock, R. & Davis, B.D. (1963). The sequence of some effects of streptomycin in Escherichia coli. Biochim.biophys.Acta, 74, 476-489.

Eagle, H. & Saz, A.K. (1955). Antibiotics. A.Rev.Microbiol., 9, 173-226.

Eckert, J.W. & Tsoa, P.H. (1962). A selective antibiotic medium for isolation of Phytophthora and Pythium from plant roots. Phytopathology, 52, 771-777.

Eisenstadt, J.M. & Brawerman, G. (1964). The protein-synthesising systems from the cytoplasm and chloroplasts of Euglena gracilis. J.molec.Biol., 10, 392-398.

Elferink, J.G.R. (1974). The effect of ethylene diaminetetra acetic acid on yeast cell membranes. Protoplasma, 80, 261-268.

Elliott, C.G. (1972). Calcium chloride and growth and reproduction in Phytophthora cactorum. Trans.Br.mycol.Soc., 58, 169-172.

Elliott, C.G. & MacIntyre, D. (1973). Genetical evidence on the life-history of Phytophthora. Trans.Br.mycol.Soc., 60, 311-316.

Elliott, C.G., Hendrie, M.R. & Knights, B.A. (1966). A sterol requirement of Phytophthora cactorum. J.gen.Microbiol., 42, 425-435.

Ellzey, J.T. (1974). Ultrastructural observations within the antheridia of Achlya ambisexualis. Mycologia, 66, 32-47.

Elsner, P.R., Vander-Molen, G.E., Horton, J.C. & Bowen, C.C. (1970). Fine structure of Phytophthora infestans during sporangial differentiation and germination. Phytopathology, 60, 1765-1772.

Ericsson, J.L.E. (1969). Mechanism of cellular autophagy. In: Lyosomes in biology and pathology. Vol. 2. 345-394. Eds. J.T.Dingle, & H.B.Fell. North-Holland Press, Amsterdam and London.

Fahnrich, P. (1974). Studies in development of the Phycomycete Allomyces arbuscula. 1. Effect of protein and nucleic acid synthesis inhibitors on differentiation of gametangia. Arch.Mikrobiol., 98, 85-92.

Finean, J.B., Coleman, R. & Michell, R.H. (1974). Membranes and their cellular functions. Blackwell Scientific Publications, Oxford.

Finney, D.J. (1971). Probit Analysis. 3rd ed. Cambridge University Press.

Flaks, J.G., Cox, E.C. & White, J.R. (1962). Inhibition of polypeptide synthesis by streptomycin. Biochem.biophys.Res.Commun., 7, 385-389.

Flanagan, P.W. (1970). Meiosis and mitosis in Saprolegniaceae. Can.J.Bot., 48, 2069-2076.

Fox, C.F. (1972). Membrane assembly. In: Membrane Molecular Biology. Ed. C.F.Fox & A.O.Keith. Sinauer Associates Inc. Stamford, Conn.

Freere, R.H. & Weibel, E.R. (1967). Sterologic techniques in microscopy Jl.R.microsc.Soc., 87. 25-34.

Freid, J. & Wintersteiner, O. (1947). Streptomycin II. Reduction and oxidation products of streptomycin and streptobiosamine. J.Am. chem.Soc., 69, 79-86.

Freid, P.M. & Stuteville, D.L. (1975). Effect of chlorine on Peronospora trifolium sporangial production and germination. Phytopathology, 65, 929-930.

Gale, E.F., Cundiliffe, E., Reynolds, P.E., Richmond, M.H.& Waring, M.J. (1972). The molecular basis of antibiotic action. 278-379. Wiley & Sons, London.

Gay, J.L. (1972). X-ray microanalysis in the development of oospores of the fungus Saprolegnia. Micron, 3, 139-143.

Gay, J.L. & Greenwood, A.D. (1966). Structural aspects of zoospore production in Saprolegnia ferax with particular reference to cell and vesicular membranes. Colston Papers, 18, 95-110.

Gay, J.L., Greenwood, A.D. & Heath, I.B. (1971). The formation and behaviour of vacuoles (vesicles) during oosphere development and zoospore germination in Saprolegnia. J.gen.Microbiol., 65, 233-241.

Gray, R.A. (1955). Inhibition of root growth by streptomycin and reversal of the inhibition by manganese. Am.J.Bot., 42, 327-331.

Greenwood, A.D. (1959). Observation on the zoospores of Vaucheria 11. J.exp.Bot., 10, 55-68.

Griffin, D.H. (1966). Effect of electrolytes on differentiation in Achlya sp. Pl.Physiol., Lancaster, 41, 1254-1256.

Griffin, D.H. & Breuker, C. (1969). Ribonucleic and synthesis during the differentiation of sporangia in the water mould Achlya. J.Bact., 98, 689-696.

Griffin, M.J. & Coley-Smith, J.R. (1971). Some effects of streptomycin on Pseudoperonospora humuli in downy mildew of hop. J.gen.Microbiol., 69, 117-134.

Griffin, M.J. & Coley-Smith, J.R. (1975). Uptake of streptomycin by sporangia of Pseudoperonospora humuli and the inhibition of uptake by divalent metal cations. Trans.Br.mycol.Soc., 65, 265-278.

Grosso, J. (1954). Control of tobacco blue mould by antibiotics. Pl.Dis. Reptr., 38, 333-337.

Grove, S.N. (1970). Zoospore encystment and germination in Pythium aphanidematum. Am.J.Bot., 57, 245-266.

Grove, S.N. & Bracker, C.E. (1970). Protoplasmic organisation of hyphal tips among fungi. Vesicles and Spitzenkörper. J.Bact., 104, 989-1009.

Grove, S.N., Bracker, C.E. & Morré, D.J. (1970). An ultrastructural basis for hyphal tip growth in Pythium ultimum. Am.J.Bot., 57, 245-266.

Gull, K. & Trinci, A.P.J. (1973). Griseofulvin inhibitis fungal mitosis Nature, Lond., 244, 292-294.

Gull, K. & Newsam, R.J. (1975). Meiosis in Basidiomycetous fungi. II Fine structure of the synaptinemal complex. Protoplasma, 83, 259-268.

Hagedorn, H. & Weinert, H. (1971). Untersuchungen uber die Ultrastruktur von Saprolegnia monoica. I. Dei vegetative hyphae. Z.Naturof., 26b, 843-849.

Hagedorn, H. & Weinert, H. (1972). The endoplasmic reticulum during the sporogenesis of S.monoica. Arch.Mikrobiol., 81, 13-24.

Hagedorn, H. & Weinert, H. (1974). Die veranderungun der ultrastruktur vährend der zoosporogenese bei Saprolegnia monoica. Protoplasma, 81, 145-162.

Hancock, R. (1964). Early effects of streptomycin on Bacillus megaterium. J.Bact., 88, 633-639.

Hartog, M. (1887). On the formation and liberation of zoospores in the Saprolegniaceae. Q.Jl.Microsc.Sci., 27, 427-438.

Hartog, M. (1891). Some problems of reproduction: a comparative study of gametogeny and protoplasmic senescence and rejuvenescence. Q.Jl. Microsc., 33, 1-79.

Hawker, L.E. (1963). Fine structure of Pythium debaryanum and its probable significance. Nature, Lond., 197, 618-619.

Hawker, L.E. & AbbottP. McV. (1963). Fine structure of young vegetative hyphae of P.debaryanum. J.gen.Microbiol., 31, 491-494.

Heath, I.B. (1969). Structural aspects of the growth and reproduction of Saprolegnia spp. Ph.D. Thesis. University of London.

Heath, I.B. (1974a). Mitosis in the fungus Thraustotheca clavata. J.Cell Biol., 60, 204-220.

Heath, I.B. (1974b). Centrioles and mitosis in some Oomycetes. Mycologia, 66, 354-359.

Heath, I.B. (1975a). The effect of antimicrotubule agents on the growth and ultrastructure of the fungus Saprolegnia ferax and their ineffectiveness in disrupting hyphal microtubules. Protoplasma, 85, 147-176.

Heath, I.B. (1975b). Colchicine and chemical binding components in the fungus Saprolegnia ferax. Protoplasma, 85, 177-192.

Heath, I.B. & Greenwood, A.O. (1968). Electron microscopic observations of dividing somatic nuclei in Saprolegnia. J.gen.Microbiol., 53, 287-289.

Heath, I.B. & Greenwood, A.D. (1970a). The structure and formation of lomosomes. J.gen.Microbiol., 62, 129-137.

Heath, I.B. & Greenwood, A.D. (1970b). Centriole eplication and nuclear division in Saprolegnia.

Heath, I.B. & Greenwood, A.D. (1971). Ultrastructural observations on the kinetosomes and golgi bodies during asexual life cycle of Saprolegnia. Z.Zellforsch, 112, 371-389.

Heath, I.B., G ay, J.L. & Greenwood, A.D. (1971). Cell wall formation in the Saprolegniales: Cytoplasmic vesicles underlying developing walls. J.gen.Microbiol., 65, 225-232.

Heath, I.B., Greenwood, A.D. & Griffiths, H.B. (1970). The origin of flimmer in Saprolegnia, Dictyuchus and Cryptomonas. J.Cell Sci., 7, 445-461.

Hegnauer, H. & Hohl, H.R. (1973). A structural comparison of cyst and germ tube wall in Phytophthora palmivora. Protoplasma, 77, 151-163.

Heintz, C.E. (1971). An ultrastructural analysis of zoosporogenesis in Pythium middletonii. In: Abstracts of First International Mycological Congress, Exeter.p.43. Eds. G.C. Ainsworth & J.Webster.

Hemmes, D.E. & Bartnicki-Garcia. (1975). Electron microscopy of gametangial interaction and oospore development in Phytophthora capsici. Arch. Microbiol., 103, 91-112.

Hemmes, D.E. & Hohl, H.R. (1969). Ultrastructural changes in directly germinating sporangia of P.parasitica. Am.J.Bot., 56, 300-313.

Hemmes, D.E. & Hohl, H.R. (1971). Ultrastructural aspects of cyst germination in Phytophthora parasitica. J.Cell Sci., 9, 175-191.

Hemmes, D.E. & Hohl, H.R. (1972). Flagellum degeneration in the fungus Phytophthora palmivora (formerly Phytophthora parasitica). J.gen. Microbiol., 73, 345-351.

Hemmes, D.E. & Hohl, H.R. (1973). Mitosis and nuclear degeneration: Simulatneous events during secondary sporangia formation in Phytophthora palmivora. Can.J.Bot., 51, 1673-1675.

Hendy, R.J. (1966). Resemblance of lomosomes of Pythium debaryanum to structures recently described in Chara and Nitella. Nature, Lond., 209, 1258-1259.

Hine, R.B. (1962). Effect of streptomycin and pimarcin on growth and respiration of Pythium species. Mycologia, 54, 640-646.

Ho, H.H., Hickman, C.J. & Telford, R.W. (1968). The morphology of zoospores of Phytophthora megasperma. Can.J.Bot., 46, 88-89.

Ho, H.H., Zacchariah, K. & Hickman, C.J. (1968). The ultrastructure of zoospores of Phytophthora megasperma. Can.J.Bot., 46, 37-42.

Hoch, H.C. & Mitchell, J.E. (1972a). The ultrastructure of Aphanomyces euteiches during asexual spore formation. Phytopathology, 62, 149-160.

Hoch, H.C. & Mitchell, J.E. (1972b). The ultrastructure of zoospores in Aphanomyces euteiches and their encystment and subsequent germination. Protoplasma, 75, 113-138.

Hohl, H.R. & Hamamoto , S.T. (1967). Ultrastructural changes during zoospore formation in Phytophthora parasitica. Am.J.Bot., 34, 1131-1139.

Hooker, J.K., Siekevitz, P. & Palade , G.E. (1969). Formation of chloroplast membranes in Clamydomonas reinhardi y-1. Effects of inhibitors of protein synthesis. J.biol.Chem.,44, 2621-2631.

Horgen, P.A. & O'Day, D.H. (1975). The developmental patterns of lysosomal enzyme activities during Ca^{2+} induced sporangium formation in Achlya bisexualis 11.α Mannosidase. Arch.Microbiol.,102, 9-12.

Horner,C.E. (1963). Chemotherapeutic effects of streptomycin on establishment of progression of systemic downy mildew infection of hops. Phytopathology,53, 472-474.

Horner,C.E. & Maier, C.R. (1957). Antibiotics eliminate systemic downy mildew from hops. Phytopathology, 47, 525.

Howard, K.L. (1971). Oospore types in the Saprolegniaceae. Mycologia, 63, 679-686.

Howard, K.L. & Bryant, T.R. (1971). Meiosis in the Oomycetes: 11 A microspectrophotometric analysis of DNA in Apodachlya brachymena.

Howard, K.L. & Moore, R.T. (1970). Ulstrastructure of oogenesis in Saprolegnia terrestris. Bot.Gaz., 131, 311-336.

Hunsley, D. & Burnett, J.H. (1970). The ultrastructural architecture of the walls of some hyphal fungi. J.gen.Microbiol., 62, 203-218.

Jacoby, J.A. & Gorini, L. (1967). Effect of streptomycin and other aminoglycoside antibiotics on protein synthesis. In: Antibiotics. Vol. I. Mechanisms of Action. pp. 726-747.

Jamieson, J.D. & Palade, G.E. (1968). Intracellular transport of secretory proteins in the pancreatic exocrine cell. IV. Metabolic requirements. J.Cell Biol., 39, 589-603.

Kagayama, M. & Douglas, W.W. (1974). Electron microscope evidence of calcium-induced exocytosis in most cells treated with 48/80 or the ionosphores A-23187 or X-537A. J.Cell Biol., 62, 519-526.

Katz, D. & Rosenberger, R.F. (1971). Hyphal wall synthesis in Aspergillus nidulans: effect of protein synthesis inhibition and osmotic shock on chitin insertion and morphogenesis. J.Bact., 108, 184-190.

Kauffman, C.H. (1908). A contribution to the physiology of the Saprolegniaceae, with special reference to variations of the sexual organs. Ann.Bot., 22, 361-387.

Kavanau, J.L. (1965). Structure and function of lipids in biological membranes. Vol. I. Holden-Day Inc.,San Francisco.

Kazama, F.Y. (1975). Cytoplasmic cleavage during zoosporogenesis in Thraustochytrium sp. Ultrastructure and effects of colchicine and D_2O. J.Cell.Sci., 17, 155-170.

Khorychev, M.P. (1973). Absorption of copper ions by cells of Candida ulilis. Mikrobiologiya, 42, 745-749.

King, J.E. & Butler, R.D. (1968). Structure and development of flagella of Phytophthora infestans. Trans.Br.mycol.Soc., 51, 689-697.

King, J.E., Colhoun, J. & Butler, R.D. (1968). Changes in the ultrastructure of sporangia of Phytophthora infestans associated with indirect germination and aging. Trans.Br.mycol.Soc., 51, 269-281.

Kinsky, S.C. (1962). Nystatin binding to protoplasts and particulate fraction of Neurospora crassa and a basis for selective toxicity of polythese antifungal inhibitors. Proc.Nat.Acad.Sci. U.S.A., 48, 1049-1056.

Kirk, J.T.O. (1962). Effect of streptomycin on greening and biosynthesis in Euglena gracilis. Biochim.biophys.Acta., 56, 139-151.

Korzybski, T., Kowszyk-Grindifer, L. & Kurylowicz, W. (1967). Antibiotics: Origin, Nature and Properties. Pergammon Press, New York.

Klebs, G. (1899). Zur physiologie fortpflazung einiger pilze: II. Saprolegnia mixta de Bary. Jb.wiss.Bot., 33, 513-593.

Lasure, L.L. & Griffin, D.H. (1974). Evidence for diploidy in Achlya bisexualis based on inheritance of cyloheximide resistance. Mycologia, 66, 391-396.

Leary, J.V., Roheim, J.R. & Zentmeyer, G.A. (1974). Ribosome content of various spore forms of Phytophthora spp. Phytopathology, 64, 404-408.

Lippman, E., Erwin, D.C. & Bartnicki-Garcia, S. (1974). Isolation and chemical composition of oospore-oogonium walls of Phytophthora megasperma var. sojae. J.gen.Microbiol., 80, 131-145.

Litwack, G. & Pramer, D. (1957). Absorption of antibiotics by plant cells. III. Kinetics of streptomycin uptake. Archs.Biochem.Biophys., 68, 394-402.

Lloyd, D. (1974). The mitochondria of micro-organisms. Academic Press, London.

Lu, B.C. (1970). Genetic recombination in Coprinus.II. Its relations to the synaptenemal complexes. J.Cell Sci., 6, 669-678.

Lucy, J.A. (1973). The chemically-induced fusion of cells. In: Membrane mediated information. Vol. 2. Structures. pp. 117-128. Ed. P.W.Kent, American Elsevier Pub. Co., New York.

Luft, J.H. (1961). Improvements in epoxy resin embedding methods. J.biophys. biochem.Cytol., 9,409, 414-417.

Luzatto, L., Apirion, D. & Schlessinger, D. (1969). Polyribosome depletion and blockage of ribosome cycle by streptomycin in Escheridia coli. J.molec.Biol., 42, 315-335.

Machlis, L. (1966). Sex hormones in fungi. In: The fungi. An advanced treatise Vol. 2. pp.415-431, Eds. G.C.Ainsworth & A.S. Sussman, Academic Press, New York & London.

Machlis, L. (1972). The coming of age of sex hormones in plants. Mycologia, 64, 235-247.

Maier, C.R. (1959). Effects of streptomycin sulphate on the hop downy mildew fungus in vivo. Phytopathology, 49, 545.

Maliga, P., Sz-Breznovits, A, Marton, L. (1973). Streptomycin-resistant plants from callus culture of haploid tobacco. Nature, Lond.,244, 29-30

Manton, I. (1965). Some phyletic implications of flagellar structure in plants. Adv.Bot.Res., 2, 1-34. (Ed. R.D.Preston).

Manton, I, Clark B. & Greenwood, A.D. (1951). Observations with the electron microscope on a species of Saprolegnia. J.exp.Bot., 2, 321-331.

Marchant, R. (1968). An ultrastructural study of sexual reproduction in Pythium ultimum. New Phytol., 67, 167-171.

Marchant, R. & Moore, R.T. (1973). Lomosomes and plasmalemmasomes in fungi. Protoplasma, 76, 235-247.

Marchant, R. & Robards, A.W. (1968). Membrane systems associated with the plasmalemma of plant cells. Ann.Bot., 32, 457-471.

Marchant, R. & Smith, D.G. (1968). The effect of chloramphenicol on growth and mitochondrial structure of Pythium ultimum. J.gen.Microbiol., 50, 391-397.

Marchant, R., Peat, A. & Banbury, G.H. (1967). The ultrastructural basis of hyphal growth. New Phytol., 66, 623-629.

Margulis, M.M. & Brubaker, C. (1970). Effect of chloramphenicol on amino acid incorporation by chloroplasts and comparison with the effect of chloramphenicol with chloroplast development in vivo. Plant Physiol. Lancaster. 45, 632-638.

Marks, G.E. (1965). The cytology of Phytophthora infestans. Chromosoma 16, 681-692.

Matile, Ph. (1974). Lysosomes. In: Dynamic aspects of plant ultrastructure. pp.178-218. Ed. A.W.Robards. McGraw Hill, London.

Marlatt, R.B. (1956). Susceptibility of some vegetables to streptomycin injury. Pl.Dis.Reptr., 40, 200-201.

May, R. (1974). Microfilaments in yeast mitochondria. Protoplasma, 82, 395-399.

McCann, M. & Stuart, M. (1973). The effect of calcium on sexual reproduction in Saprolegnia diclina. Paper given to Irish Branch of Soc. of gen.Microbiol. Trinity College, Dublin.

McClure, W.K. Park, D. & Robinson, P.M. (19-8). Apical organisation of the osmatic hyphae of fungi. J.gen.Microbiol., 50, 177-182.

McKeen, W.E. (1973). Streptomycin inhibition of Peronospora parasitica and its host reversed by manganase and calcium. Phytopathology, 63, 34-36.

Mims, C.W. (1972). Spore wall formation in the myxomycete Arcyia cinerea. Trans.Br.mycol.Soc., 59, 447-481.

Miskin, R. & Zamir, A. (1974). Inhibition of interconversion of ribosomes between forms active and inactive in 30S subunit functions by aminoglycoside antibiotics. J.molec.Biol., 87, 135-139.

Modelell, J. & Davis, B.D. (1969). Mechanism of inhibition of ribosomes by streptomycin. Nature. Lond., 224, 345-348.

Moens, P.B. (1970). The fine structure of meiotic chromosome pairing in natural and artificial Lilium polyploids. J.Cell Sci., 7, 55-63.

Moens, P.B. & Rapport, E. (1971). Spindles, spindle plaques, and meiosis in the yeast Saccharomyces cerevisiae Hansen. J.Cell Biol., 50, 344-361.

Molzahn, S.W. & Woods, R.A. (1972). Polyene resistance and the isolation of sterol mutants in Saccharomyces cerevisiae. J.gen.Microbiol., 72, 339-348.

Moore, H. & Muhlethaler, K. (1963). Fine structure in frozen-etched yeast cells. J.Cell Biol., 17, 609-628.

Moore, R.T. & McAlear, J.H. (1961). Fine structure of mycota 5. Lomosomes previously uncharacterised structures. Mycologia, 53, 194-200.

Moses, M.J. (1968). Synaptinemal complex. A.Rev.Genet., 2, 363-412.

Moskevitz, M. & Kelker, N.E. (1965). Amino acid control of streptomycin action on mammalian cells. Nature, Lond., 205, 476.

Muller, K.O., Mackay, J.H.E. & Friend, J.N. (1954). Effect of streptomycin in the host-pathogen relationship of a fungus phytopathogen. Nature, Lond., 174, 878-879.

Mullins, J.T. & Raper, J.R. (1965). Heterothallism in biflagellate aquatic fungus. Preliminary genetic analysis Science N.Y., 150, 1174-1175.

Mullins, J.T. & Warren, C.O. (1975). The entire asexual reproductive progression in Achlya ambisexualis in absence of exogenous nutrients. Am.J.Bot., 62, 770-774.

Natti, J. (1957). Control of downy mildew of brocolli with antibiotics and fungicides. Pl.Dis.Reptr.,41, 780-788.

Novaes-Liden, M. & Jimenez-Martinez, A. (1968). The structure of cell walls of phycomycetes. J.gen.Microbiol., 54. 407-415.

Novikoff, A.B. & Holtzman, E. (1976). Cells and Organelles, Holt, Rinehart and Winston Inc. London.

O'Day, D.H. & Horgen, P.A. (1974). Developmental patterns of lysosomal enzyme activities during Ca^{2+} induced sporangium formation in Achlya bisexualis. Dev.Biol., 39, 116-124.

Ogawa, J.M. McCain, A.H. & Holt, D.H. (1960). Streptomycin absorption in diseased and healthy hop tissues and its effect on the hop downy mildew organism and mildew development. Phytopathology, 50, 278-280.

Olsen, R.A. (1971a). Triterpeneglycosides as inhibitors of fungal growth and metabolism. I. Effect on growth, exogenous respiration and leakage of UV-absorbing material from various fungi. Physiologia. Pl., 24, 534-543.

Podbielkowska M., Zarska-Maciejewska B., & Kapeska-Palacz A. (1975)
Morphology of protoplasts affected by inhibition of respiration
Protoplasma 83. 201-208

Olsen, R.A. (1971b). Triterpeneglycosides as inhibitors of fungal growth and metabolism. 2. Effect on leakage of inorganic ions. Physiologia Pl., 25, 204-212.

Olsen, R.A. (1973). Triterpeneglycosides as inhibitors of fungal growth and metabolism. 5. Role of sterol contents of some fungi. Physiologia Pl., 28, 507-515.

Ott, D.W. & Brown, R.M. (1974a). Developmental cytology of the genus Vaucheria. 1. Organisation of the vegetative plant. Br.phycol.J., 9, 111-126.

Ott, D.W. & Brown, R.M. (1974b). Developmental cytology of the genus Vaucheria. 11. Sporogenesis in Vaucheria fontinalis (L) Christensen. Br.phycol.J., 9, 333-337.

Ozaki, M., Mizushima, S. & Nomura, M. (1969). Identification and functional characterisation of the protein controlled by the streptomycin-resistant locus in E.coli. Nature, Lond., 222, 333-339.

Parker, B.C., Preston, R.D. & Fogg, G.E. (1963). Studies of the structure and chemical composition of the cell walls of Vaucheriaceae and Saprolegniaceae. Proc.R.Soc.B., 158, 435-445.

Parthier, B. (1965). Effects of antibiotics on the uptake of ^{35}S-methionine and $^{32}PO_4$ and on their incorporation into protein and ribonucleic acid of green tobacco leaves. Nature, Lond., 206, 783-784.

Paton, W.H.N. & Budd, K. (1972). Zinc uptake in Neocomospora vasinfecta. J.gen.Microbiol., 72, 172-184.

Peachey, L.D. (1958). Thin sections. 1. A study of section thickness and physical distortion during microtomy. J.biophys.biochem.Cytol., 4, 233.

Pestka, S. (1971). Inhibitors of ribosome function. A.Rev.Microbiol., 25, 487-562.

Phillipi, M.L., Pansh, R.W. & Hohl, H.R. (1975). Histochemical and biochemical evidence for the presence of microbodies in Phytophthora palmivora. Arch.Microbiol.,103, 127-132.

Pieters, A.J. (1915). The relation between vegetative vigor and reproduction in some of the Saprolgniaceae. Am.J.Bot., 2, 529-626.

Regna, D.B. (1959). Chemistry of antibiotics. In: Antibiotics: their chemistry and non-medical uses. pp. 58-173. Ed. H.S.Colberg Van Nostrand, Princeton, N.Jersey.

Reischer, H.S. (1951). Growth of Saprolegniaceae in synthetic media. 11. Nutrient requirements and the role of Kreb's cycle acids. Mycologia 43, 319-328.

Reynolds, S. (1963). The use of lead citrate at high pH as an electron opaque stain in electron microscopy. J.Cell Biol., 17, 208-211.

Robards, A.W., Jackson, M.S., Clarkson, D.T. & Sanderson, T. (1972). The structure of barley roots on relation to the transport of ions into the stele. Protoplasma, 77, 291-311.

Robbins, E., Jentzsch, G. & Micali, A. (1968). The centriole cycle in synchronised Hela-cells. J.Cell Biol., 36, 329-339.

Robertson, N.F. (1965). The mechanism of cellular extension and branching. In: The fungi. Vol. I. pp.613-623. Ed. G.C.Ainsworth, & A.S.Sussman. Academic Press, New York and London.

Rogers, H.J. (1970). Bacterial growth and the cell envelope. Biol. Rev., 34, 194-214.

Rosen, W.G. (1954a). Effects of streptomycin on certain green plants. Ohio J.Science, 54, 75-78.

Rosen, W.G. (1954b). Plant growth inhibition by streptomycin and its prevention by manganese. Proc.Soc.exp.Biol.Med., 34, 194-214.

Ross, I.S. (1975). Some effects of heavy metals on fungal cells. Trans.Br. mycol.Soc., 64, 175-193.

Sager, R. (1954). Mendelian and non mendelian inheritance of streptomycin resistance in Clamydomonas reinhardi. Proc.nat.Acad.Sci. U.S.A., 40, 356-363.

Sager, R. & Tsubo, Y. (1962). Mutogenic effects of streptomycin in Clamydomonas. Achiv.Mikrobiol. 42, 159-175.

Sansome, E.R. (1961). Meiosis in the oogonium of Pythium debaryanum Hesse. Nature, Lond., 911, 827-828.

Sansome, E.R. (1963). Meiosis in Pythium debaryanum Hess and its significance in the life-history of the biflagellatae. Trans.Br.mycol.Soc., 66, 63-72.

Seimiya, T. & Ohki, S. (1973). Ionic structure of phospholipid membranes and binding of calcium ions. Biochim.biophys.Acta., 298, 546-561.

Shatla, M.N., Yang, C.Y. & Mitchell, J.E. (1966). Cytological and fine-structure studies of Aphanomyces euteiches. Phytopathology, 56, 923-928.

Skattock, R.C. & Shaw, D.S. (1975). Mutants of Phytophthora infestans resistant to and dependent upon antibiotics. Trans.Br.mycol.Soc., 64, 29-41.

Shaw, D.S. & Elliott, C.G. (1968). Streptomycin resistance and morphological variation in Phytophthora cactorum. J.gen.Microbiol., 51, 75-84.

Shaw, D.S. & Khaki, I.A. (1971). Genetical evidence for diploidy in Phytophthora. Genet.Res., 17, 165-167.

Shatz, A., Bugie, E., & Waksman, S.A. (1944). Streptomycin, a substance exhibiting antibiotic activity against gram positive and gram negative organisms. Proc.Soc.exp.Biol.Med., 55, 66-69

Sietsma, J.H., Eveleigh, D.E. & Haskins, R.H. (1975). Cell wall composition and protoplast formation in some oomycete species. Biochim. biophys.Acta.,184, 306-3.17.

Sing, V.O. & Bartnicki-Garcia, S. (1975). Adhesion of Phytophthora palmivora zoospores: electron microscopy of cell attachment and cyst wall fibril formation. J.Cell Sci., 79, 11-20.

Slifkin, M.K. (1967). Nuclear division in Saprolegnia as revealed by colchicine. Mycologia, 59, 431-445.

Smith, F.E.V. (1923a). On direct nuclear divisions in the vegetative mycelium of Saprolegnia. Ann.Bot., 37, 63-73.

Smith, J.H. (1923b). On apical growth of fungal hyphae. Ann.Bot., 37, 341-343.

Sparrow, F.K. (1960). Aquatic Phycomycetes. Second revised edition. University of Michigan Press, Ann Arbor.

Stephenson, L.W., Erwin, D.C. & Leary, J.V. (1974). Meiotic configurations in the oospore of Phytophthora capsici. Can.J.Bot., 52, 2141-2143.

Sternlicht, E., Katz, D. & Rosenberger, R.F. (1973). Subapical wall synthesis and wall thickening induced gy cycloheximide in hyphae of Aspergillus nidulans. J.Bact., 114, 819-823.

Stiers, D.L. (1974). Fine structure of ascospore formation in Poronia punctata. Can.J.Bot., 52, 999-1003.

Stuart, M.R. & O'Gorman,A.M. (1971). The effect of griseofulvin on growth and reproduction in Saprolegnia. In: Abstracts of First International Mycological Congress. pp. 91-92. Eds. G.C.Ainsworth & J.Webster.

Szallosi, D., Callarco, P. & Donahue, R.P. (1972). Absence of centrioles in the first and second meiotic spindles of mouse oocytes. J.Cell Sci., 11, 521-541.

Thiery, J-P. & Rombourg, A. (1974). Cytochemie des polysaccharides. J.Microcopie, 21, 225-232.

Threlfall, R.J. (1972). Effect of pentochloronitrobenzene (PCNB) and other chemicals on sensitive and PCNB-resistant strains of Aspergillus nidulans. J.gen.Microbiol., 71, 173-180.

Timberlake, W.E., McDowell, L., Cheney, J. & Griffin, D.H. (1973). Protein synthesis during the differentiation of sporangia in the water mould Achlya. J.Bact., 116, 67-73.

Timmer, L.W., Castro, J., Erwin, D.C., Belser, W.L. & Zentmeyer, G.A. (1970). Genetic evidence for zygotic meiosis in Phytophthora capsici Am.J.Bot., 57, 1211-1218.

Tokunaga, J. & Bartnicki-Garcia. S. (1971). Structure and differentiation of cell walls of Phytophthora palmivora sycts, hyphae and sporangia. Achiv.Mikrobiol., 79, 293-310.

Trinci, A.P.J. (1971). Influence of the width of peripheral growth zone on radial growth rate of fungal colonies on solid media. J.gen.Microbiol., 67, 325-344.

Trinci, A.P.J. & Collinge, A. (1973). Influence of L.sorbose on growth and morphology of Neurospora crassa. J.gen.Microbiol., 78, 179-192.

Trinci, A.P.J. & Gull, K. (1970). Effect of actidione, griseofulvin, and tripehytin acetate on the kinetics of fungal growth. J.gen.Microbiol., 60, 287-292.

Trow, A.H. (1895). The karyogamy of Saprolegnia. Ann.Bot., 9, 609-652.

Trow, A.H. (1899). Observations on biology and cytology of a new variety of Achlya americana. Ann.Bot., 13, 131-177.

Trow, A.H. (1901). Observations on the biology andccytology of Pythium ultimum n.sp. Ann.Bot., 15, 269-312.

Trow, A.H. (1904). On fertilisation in the Saprolegnieae. Ann.Bot., 18, 541-569.

Turian, G. (1975). Differentiation in Allomyces and Neurospora. Trans. Br. mycol.Soc., 64, 367-380.

Turian, G., & Viswanathan, M.A. (1966). Facteurs nucle o-cytoplasmiques et differenciation sexuelle des allomyces. Inhibitions selectives par les accridines et l'actinomycine D.

Turner, G. & Lloyd, O. (1971). Effect of chloramphenicol on growth and mitochondrial function of ciliate protozoan Tetrahymena pyriformis. J.gen.Microbiol., 67, 175-188.

Unestam, T. (1965). Studies on the crayfish plague fungus, Aphanomyces astaci. Physiologia Pl., 18, 483-505.

Unestam, T. (1969). On the physiology of zoospore production in Aphanomyces astaci. Physiologia Pl., 22, 236-245.

Van Steveninck, R.F.M. (1965). The significance of calcium on the apparent permeability of cell membranes and the effects of substitution with other divalent cations. Physiologia Pl., 18, 54-69.

Vasquez, D. (1974). Inhibitors of protein synthesis. F.E.B.S. letters. 40. (supplement) 5.63-84.

Venis, M.A. (1968). Streptomycin inhibition of protein synthesis in pea reversed by divalent cations. Nature Lond., 221.

Von Euler, H. (1947). Nukelein Sauren als vauch staffe in gagenwart von colchicin an und von streptomycin. Arkiv fur Kemi-Mineral och.Geol., 24, 1-9, cited by Goodman, 1959.

Vörös, J. (1963). Mode of action of selective fungistatic effect of streptomycin. Nature, Lond., 199, 1110-1111.

Vörös, J. (1965). Streptomycin sensitivity of Oomycetes due to the increased absorption of streptomycin by their mycelia. Phytopath. Z., 54, 249-255.

Vörös, J., Kiraly, Z. & Farkas, G.L. (1957). Role of polyphenolase in streptomycin-induced resistance in Phytophthora in potato. Science, N.Y., 126, 1178.

Vujičić, R. (1971). An ultrastructural study of sexual reproduction in Phytophthora palmivora. Trans.Br.mycol.Soc., 57, 525-530.

Wanda, F. (1968). Ultrastructural changes during normal and colchicine initiated cell division of Chlorella. Protoplasma, 66, 105-130.

Wang, M.C. & Bartnicki-Garcia, S. (1966). Biosynthesis of β-1_s-3- and β-1,6- linked glucose by Phytophthora cinnamoni hyphal walls. Biochem.biophys.Res.Commun., 24, 832-837.

Wang, M.C. & Bartnicki-Garcia. S. (1973). Novel phosphoglucans from the cytoplasm of Phytophthora palmivora and their selective occurrence in certain life cycle stages. J.biol.Chem., 248, 4112-

Westergaard, M. & von Wettstein, D. (1970). Studies on the mechanism of crossing over. IV. The molecular organisation of the synaptinemal complex in Neotiella (Cooke) Saccardo (Asomycetes). C.R.Trav.Labs. Carlsberg, 37, 239-268.

Westergaard, M. & von Wettstein, D. (1972). The synaptinemal complex. An.Rev. Genet., 6, 71-109.

Weston, W.H. (1918). The development of Thraustotheca a peculiar water mould. Ann.Bot., 32, 115-173.

Win-Tin & Dick, M.W. (1975). Cytology of oomycetes. Evidence for meiosis and multiple chromosome associations in Saprolegniaceae and Pythiaceae, with an introduction to the cytotaxonomy of Achlya and Pythium. Arch. Microbiol., 105, 283-293.

Williams, W.T. & Webster, R.K. (1970). Electron microscopy of the sporangium of Phytophthora capsici. Can.J.Bot., 48, 221-227.

Woods, R.A., Bard, M. & Jackson, I.E. (1973). Resistance to polyene antibiotics and correlated sterol changes in clinical isolates of Candida tropicalis. Soc.gen.Microbiol.Abstracts,Imperial College, London.

Yang, C.Y.D. & Mitchell, J.E. (1965). Cation effect in reproduction of Pythium spp. Phytopathology, 55, 1127-1131.

Zahn, G. (1962). Streptomycin und metallionen. Phytopath., 245, 345-365.

Zalokar, M. (1959). Growth and differentiation of Neurospora hyphae. Am.J.Bot., 46, 602-610.

Zaumeyer, W.J. & Doolittle, S.P. (1956). Control of later blight of tomato with streptomycin. Phytopathology, 46, 32.

Zeigler, A.W. (1953) Meiosis in the Saprolegniaceae. Am.J.Bot., 40, 60-66.

Zevenhuizen, L.P.T.M. & Bartnicki-Garcia, S. (1969). Chemical structure of insoluble hyphal wall glucan of Phytophthora cinnamoni. Biochemistry, N.Y., 8, 1496-1502.

Zickler, D. (1970). Division spindle and centrosomal plaques during mitosis and meiosis in some Ascomycetes. Chromosoma, 30, 287-304.

THE EFFECTS OF STREPTOMYCIN AND DIVALENT CATIONS ON THE DEVELOPMENT AND FINE-STRUCTURE OF SAPROLEGNIA SPP.

VOLUME II

by

Gordon William Beakes, B.Sc., A.R.C.S.

A thesis submitted for the degree of Doctor of Philosophy of the University of London and for the Diploma of Imperial College

June 1976

Department of Botany and Plant Technology,
Imperial College of Science and Technology,
London SW 7

6. PHOTOGRAPHIC PLATES

The legends for each plate of photographs are headed by a title and a Section number relating to the relevant part of the the accompanying text. The negative number of each individual micrograph is given at the bottom left corner of each legend. In addition electron micrographs are also given their fixation schedule and preparation numbers, and the light micrographs the optical system under which examined. Both the negative and preparation numbers are those of the Analytical Cytology Section of the Department of Botany, Imperial College, London. All the material in the electron micrographs, except the freeze-fracture oospore and the PASM stained endospore wall has been stained using the standard uranyl acetate-lead citrate procedure.

The time after inoculation or induction and the appropriate inducing medium are included at the bottom right of each legend. Where the latter has been omitted from the legend the standard inducing procedure using single or double distilled water has been employed.

The photograph magnification is indicated by the bar scales, which unless otherwise labelled, represent a length of 1 µm. The magnifications of some of the light-micrographs have been included with the legends.

6.1 ABBREVIATIONS

6.1.1 Fixatives

GaOs	glutaraldehyde - osmic acid
$KMnO_4$	potassium permanganate
Os	osmic acid

6.1.2 Optical Systems

AP	Anoptral phase contrast
NP	Nomarski (differential interference phase)
OI	Ordinary optics

6.1.3 Inducing Solutions

ATW	autoclaved tap water
Chl	chloramphenicol
Cyc	cycloheximide
MFTW	membrane-filtered tap water
Str	streptomycin
TW	tap water

6.1.4 Plates and Legends

A	antheridium
am	aster microtubules
Ap	apical papilla
B	bar body
C	centriole
Ca	microtubular array in nucleoplasm radiating from centriole pocket
Cp	centriole pocket in nuclear envelope
cf	cleavage furrow
cm	cytoplasmic microtubules
cz	encysted zoospore
DB(V)	densebody granule (or vesicle)
DN	degenerating nucleus
ER	rough endoplasmic reticulum
E(W)	endospore wall layer of the oospore
FB	fibrous body
FT(t)	fertilisation tube
FTp	penetration peg produced by fertilisation tube
FV	flimmer vesicle
G	Golgi dictyosome
GV	Golgi vesicle
L	lomasome
Li	neutral lipid droplet
M	mitochondrion
Mf	fibrous material within mitochondrial matrix
MVB	multivesicular autophagic vesicle
N	nucleus
Nu	nucleolus
Ne	nuclear envelope
Np	nuclear pore
Op(v)	ooplast vacuole in oospore
OW	oogonium wall
P	peg-like ingrowth of wall
PL	plasmalemmasome
PS	pellucid spot (oospore nucleus)
Se	tripartite septum
Sm	spindle microtubules
UE	uniaxial element in prophase I nuclei
W	cell wall
WV	wall vesicles
V	vacuoles
Vg	granular vacuolar contents

PART 1

1.2.1 Vegetative hyphae of Saprolegnia furcata

The observations on vegetative hyphae were made on 20 h colonies, grown in 1/2 GYPS liquid medium.

Fig. 1.4 Light micrograph of vegetative hyphae at the margin of a 20 h colony. Note the tapered hyphal apices and their refractile contents.
151/26 O.I. x c.250 20 h

Fig. 1.5 Light micrograph of a single hyphal tip examined by Nomarski phase optics showing the absence of visible organelles at the extreme apex. Filamentous mitochondria, spherical lipid droplets and nuclei can be seen in the immediate subapical region. There are no large vacuoles in hyphae in this region.
110/5 N.P x c.1300 20 h

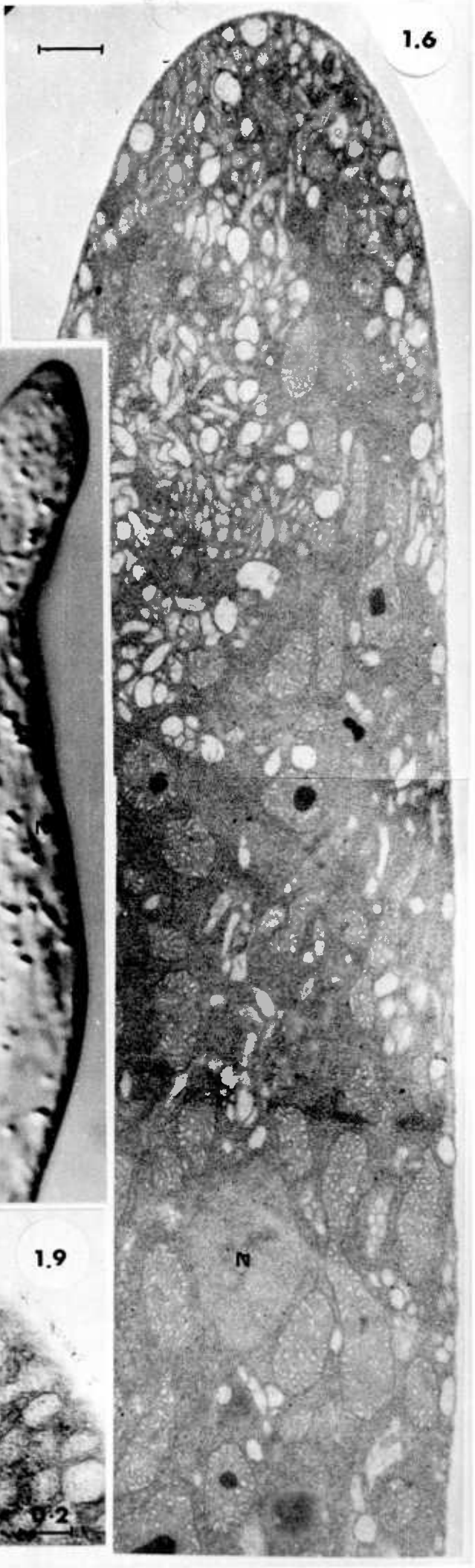
Fig. 1.6 Montage of a typical LS through a main hyphal apex showing the characteristic organisation of organelles. The tapered apical region (< 10 μm) mostly contains elongate and spherical wall vesicles, behind which is the mitochondrial zone (10–25 μm). The nuclei and vacuolar vesicles only appear at a distance more than 25 μm from the apex.
29684/5 GaOs 3773 20 h

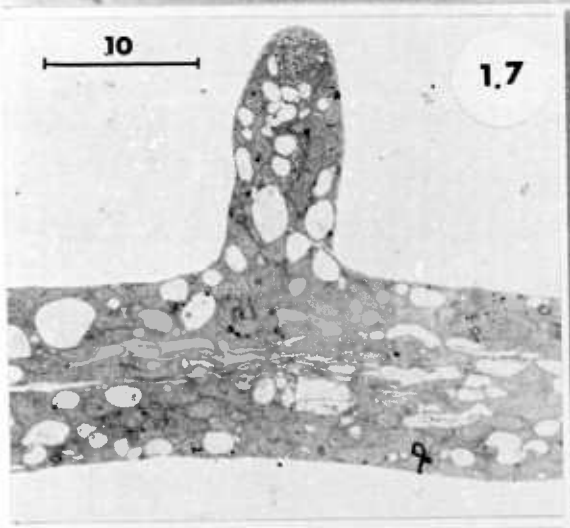
Fig. 1.7 A subapical portion of the hypha in Fig. 1.6, showing the first lateral branch (c.250 μm behind tip). Elongate vesicles contribute to the developing axial vesicle in the main hypha. 20 h
29691 GaOs 3773

Fig. 1.8 Detail of the lateral branch in Fig. 1.7 showing the foreshortened organelle zones. The wall vesicles are spherical and large vacuolar vesicles occur within 5 μm of the tip.
29701 GaOs 3773 20 h

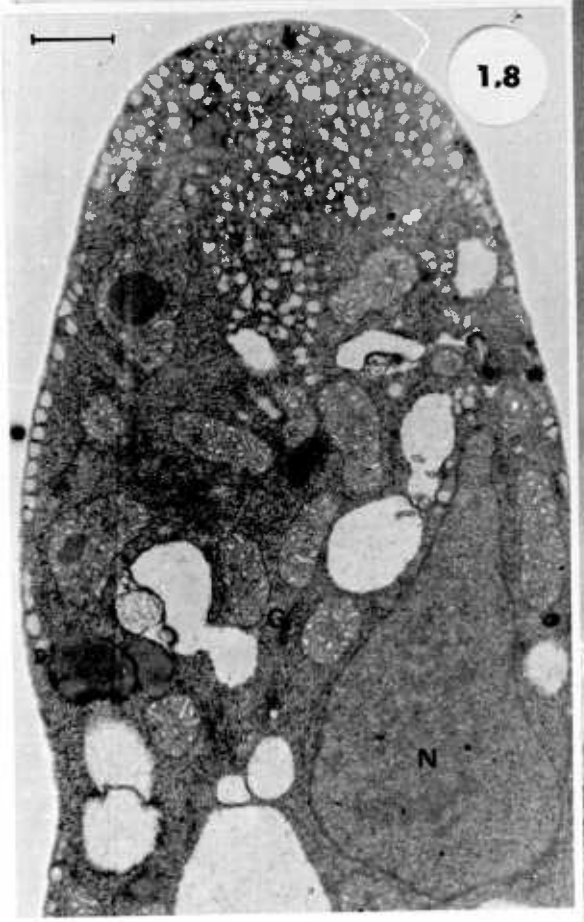
Fig. 1.9 Detail of the apical vesicle zone in Fig. 1.8 showing the spherical apical wall vesicles, some of which have coalesced. The fine fibrillar contents of these vesicles is characteristic of GaOs fixation. The hyphal wall is very thin and completely electron transparent except at its surface.
29695 GaOs 3773 20 h

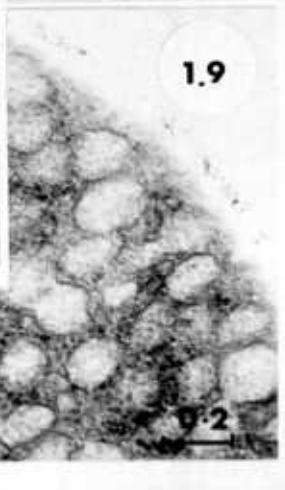

1.4


1.6
N


10
1.7


1.5
N
20


1.8
N


1.9

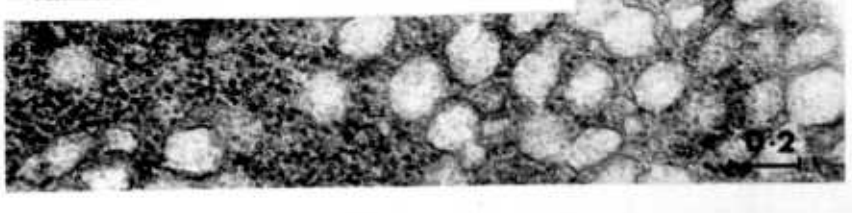

0·2

Fig. 1.10 TS hyphal profile from the subapical region, (approximately 50 to 200 µm behind the tip) showing the small discrete vacuolar vesicles and abundant nuclei and mitochondria.
29705 GaOs 3773 20 h

Fig. 1.11 Detail of the peripheral ctyoplasm of a hypha similar to that shown in Fig. 1.10. Note the absence of wall vesicles and the presence of whorls of electron dense membranous material. Similar structures occur throughout the hyphal cytoplasm.
29712 GaOs 3773 20 h

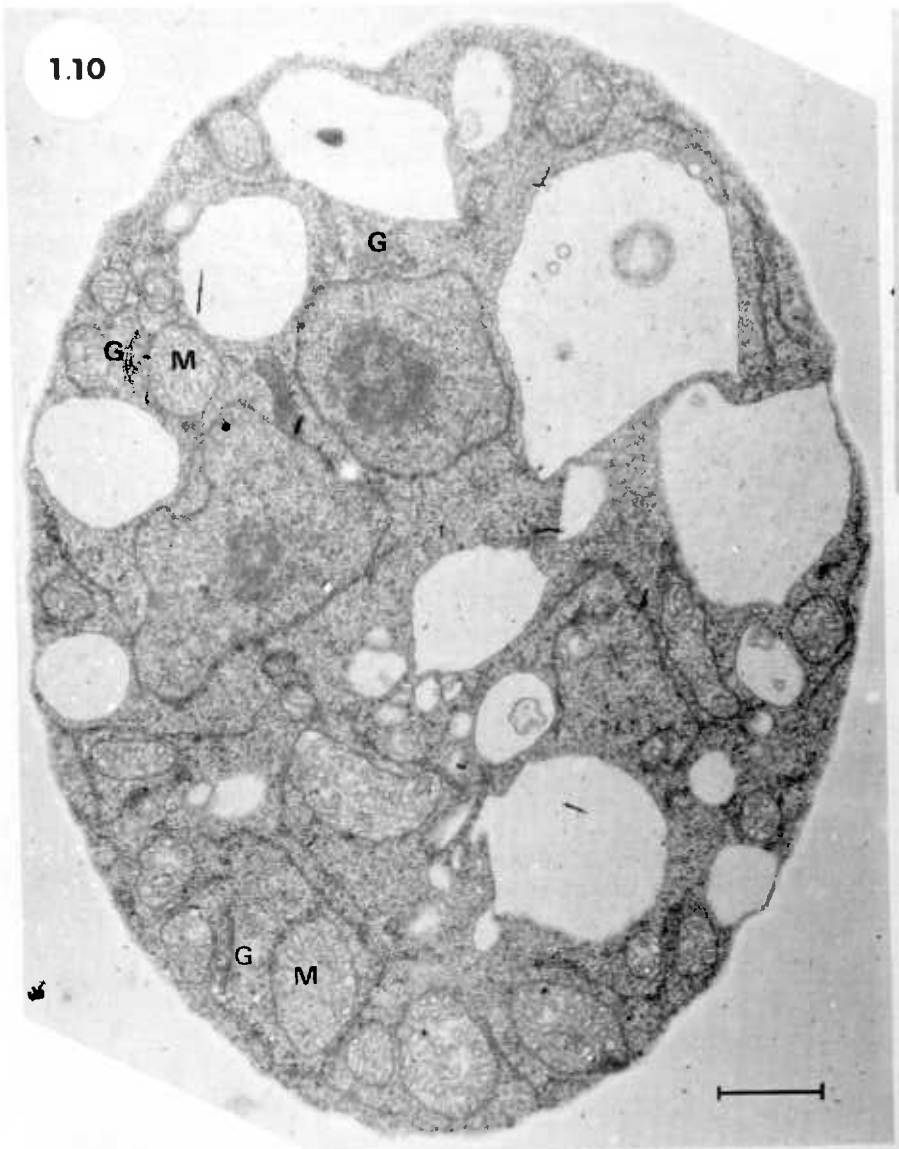
Fig. 1.12 Profile of a typical hyphal Golgi dictyosome showing association with a cisterna of ER and intermediate vesicles Both the membranes and contents of the dictyosome cisternae stain more densely than ER cisternae. Although the cisternal margins are not especially inflated, small electron dense vesicles seem to be separating from them.
29712 GaOs 3773 20 h

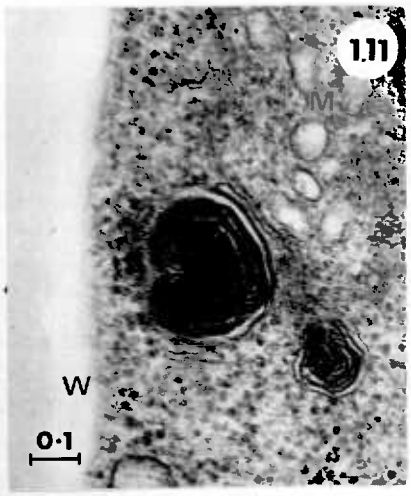
Fig. 1.13 Golgi dictyosome showing the characteristic ER-mitochondron association.
29669 GaOs 3773 20 h

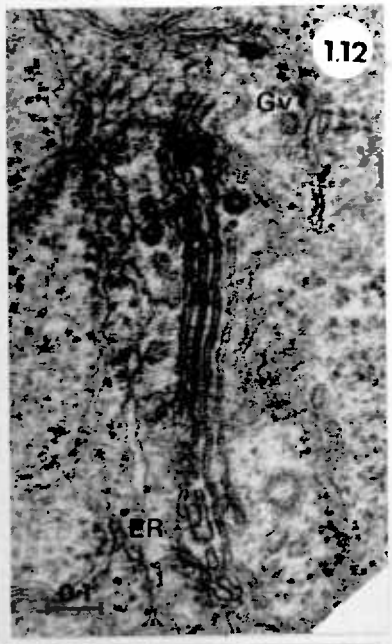
Fig. 1.14 Light micrograph of a hyphal branch arising from the mature hypha region, > 500 µm behind the apex. Note the large vacuole and peripherally distributed cytoplasm containing mitochondria and nuclei.
110/7 NP x c.1,200 20 h

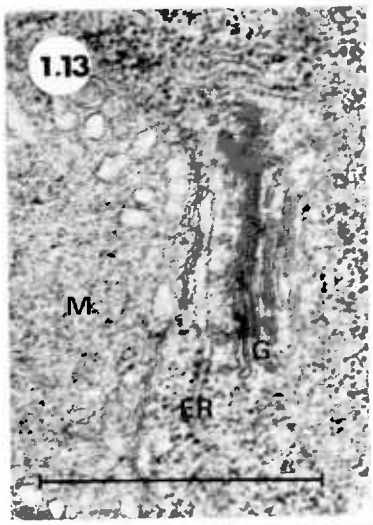
Fig. 1.15 Electron-micrograph of a comparable region to that in Fig. 1.14, showing that the vacuolar region is composed of contiguous but separate vacuoles.
29693 GaOs 3773 20 h

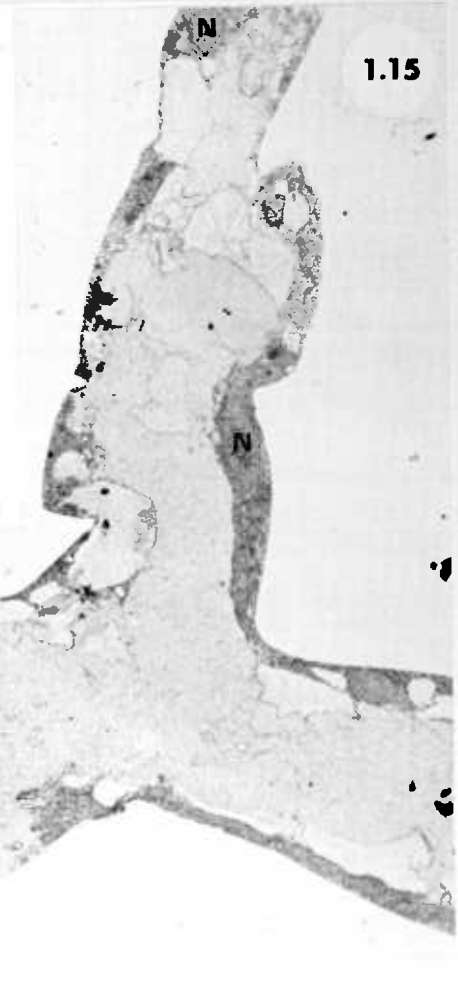
Fig. 1.16 Detail of peripheral cytoplasm in a mature hyphal region showing the extent of vacuolation. Wall vesicles are the only organelle present in this narrow cytoplasmic band.
29723 GaOs 3773 20 h


1.10
G
G
M
G
M


1.11
M
W
0·1


1.12
GV
ER
0·1


1.13
M
G
ER


1.15
N
N
10

0·1
1.16
V
W
W


1.14
L
N
M
10

Fig. 1.17 A typical interphase nucleus in the subapical hyphal region. The nucleoplasm is uniformly particulate and contains a more electron dense but diffuse nucleolar region. This nucleus is closely associated with both ER cisternae and mitochondria.
29670 GaOs 3772 20 h

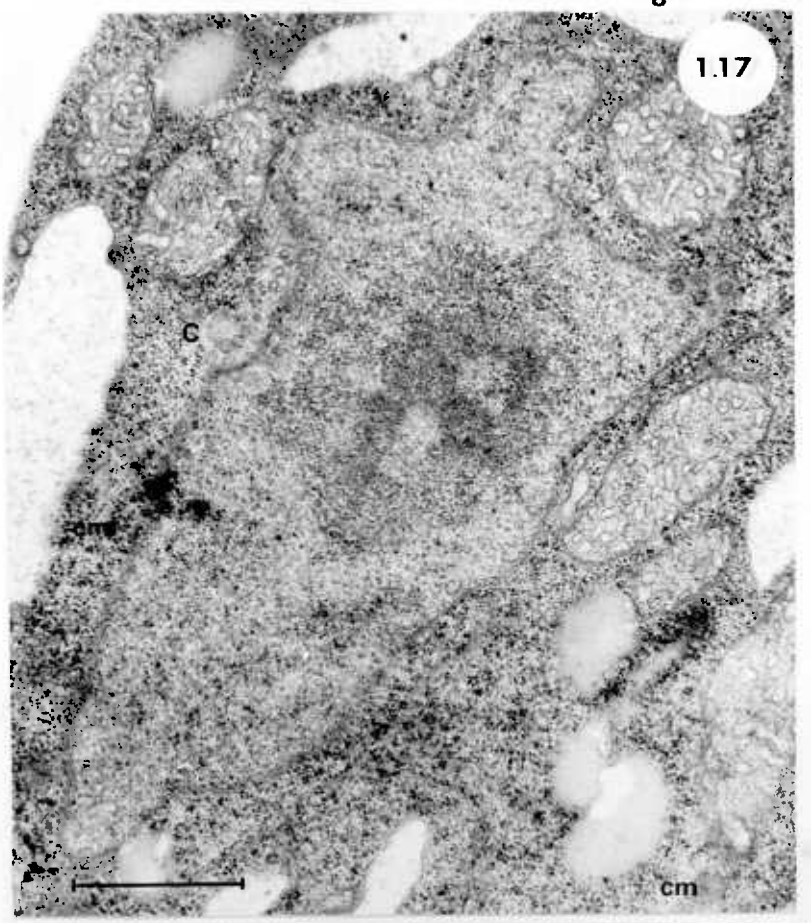
Fig. 1.18 Detail of the surface of the nucleus in Fig. 1.17 showing the centriolar pocket, and 80 nm diameter nuclear pores. Microtubules radiate from the centriolar region over the nuclear surface.
29670 GaOs 3772 20 h

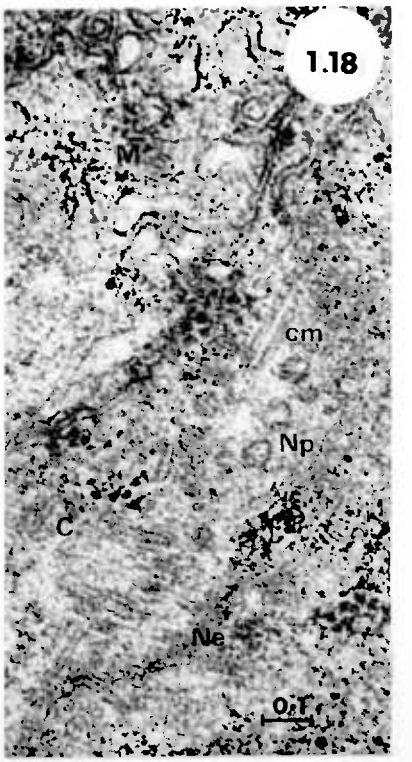
Fig. 1.19 An elongate dumbell-shaped telophase nucleus. The nucleolar material has separated into two discrete bodies. Serial sections reveal there are two pairs of centrioles associated with this nucleus and their location is indicated (Cp).
29 GaOs 3772 20 h

Fig. 1.20 An oblique nuclear section showing the intranuclear spindle microtubules, terminating at the centriolar pocket. This is probably a late prophase or metaphase stage.
29666 GaOs 3772 20 h

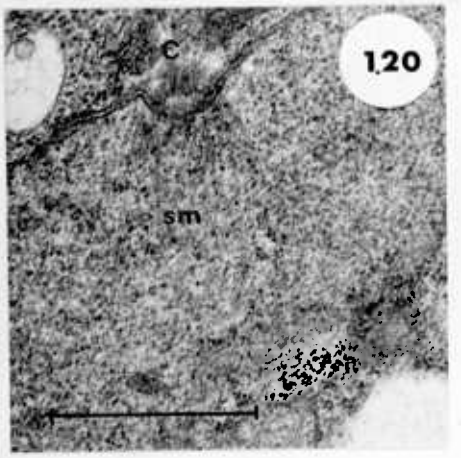
Fig. 1.21 An elongate interphase nucleus from a mature region of a hypha showing an unusually extensive nucleolar region. The horn-like projections extending from the upper part of the nucleus are closely associated with cytoplasmic microtubules. Note the close proximity of the Golgi dictyosome with the centriolar pocket, which is also shown in Fig. 1.22.
29667 GaOs 3772 20 h

Fig. 1.22 LS profile of one of the pair of polar centrioles associated with the telophase nucleus in Fig. 1.19. The end to end orientation of these centrioles is typical of oomycete fungi. Remnants of spindle apparatus terminate against the nuclear envelope adjacent to the centrioles.
29713 GaOs 3772 20 h

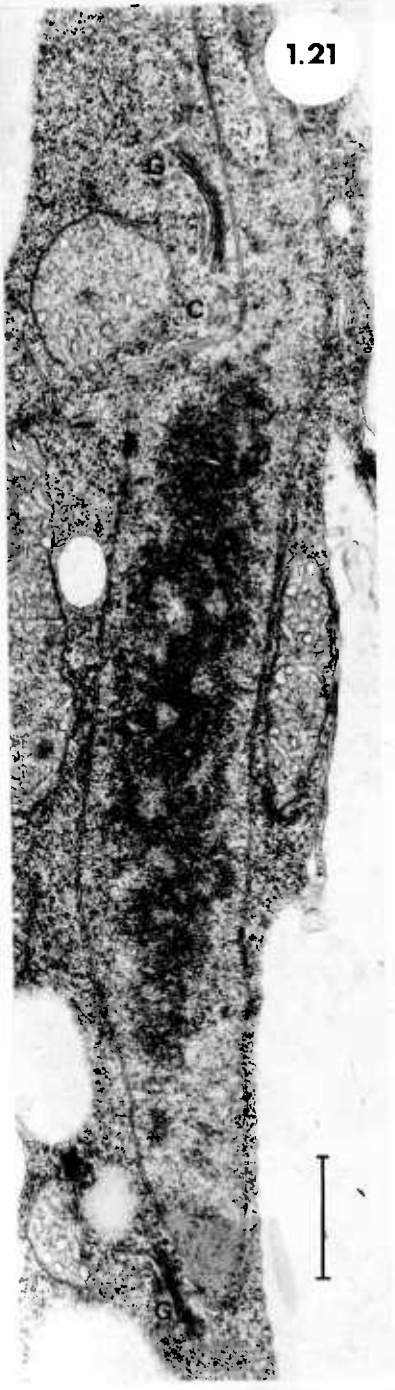

1.17
C
cm
cm


1.18
M
cm
Np
C
Ne
0,1


1.19
Cp
Nu
Nu
Cp


C
1.20
sm


1.22
C
C
sm
0,1


1.21
G
C
G

1.2.2.1 Asexual Reproduction: Sporangium development in Saprolegnia ferax

Fig. 1.23 A newly initiated sporangium developing on a peripheral hyphal tip, showing that expansion commences at the apex.
55/5 O.I. x c.500 3 h

Figs. 1.24-1.26 Clavate sporangium initials showing the accumulating cytoplasm. Papilla formation occurs shortly before or shortly after septum insertion.
55/5, 57/12, 56/25 O.I. x 500 4 h

Figs. 1.27, 1.28, 1.30 Vacuolate sporangia showing progressive stages in the delineation of the uninucleate spore initials. The papilla appears highly refractile throughout this period.
57/12, 56/25, 57/8 O.I. x 650 5-6 h

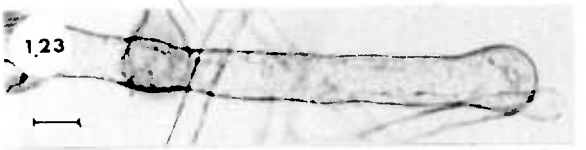
Fig. 1.29 Post cleavage sporangium containing swollen spores, which are no longer clearly discernible (homogeneous phase)
57/16 x 600 6 h

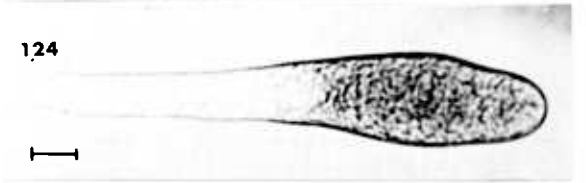
Fig. 1.30 Sporangium with clearly defined zoospores. This has acquired both flagella and contractile vacuoles, and are in gently jostling motion.
57/8 O.I. x 600 6 h

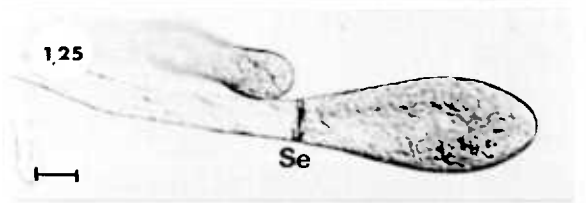
Fig. 1.31. Photographic sequence showing sporangium dehiscence. The frames were taken at approximately 3 second intervals, and show the rapidity of spore escape. Dehiscence is initiated by a single spore making contact with the papilla end wall (2). The papilla is ruptured and the first spore squeezes out. This is followed in rapid succession by the others (3-5). The last few spores escape with the aid of flagella (6). Once liberated the spores swim away from the sporangium (4-5). They swim for 10-15 minutes before settling and encysting.
57/1-6 O.I. X 500 6 h

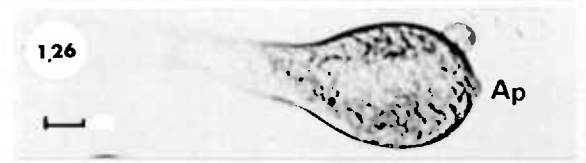
Fig. 1.32 Newly dehisced sporangium showing the formation of a new sporangium initial by outgrowth of the basal septum (proliferation)
57/20 O.I. x 650 7 h

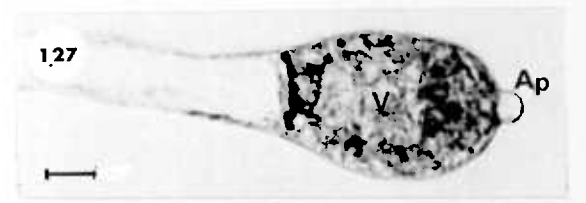
Fig. 1.33 Reniform secondary zoospores, showing laterally inserted flagella.
58/16 O.I. x 1000

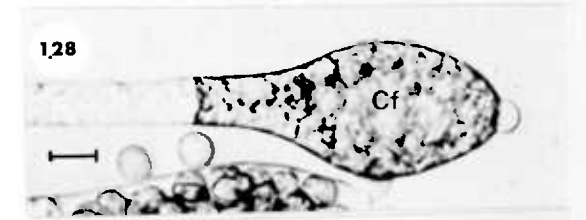


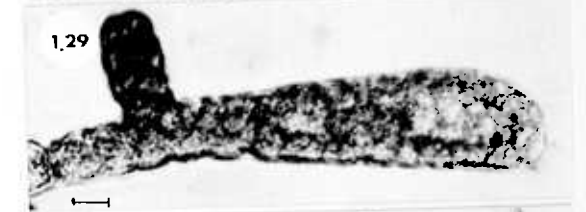


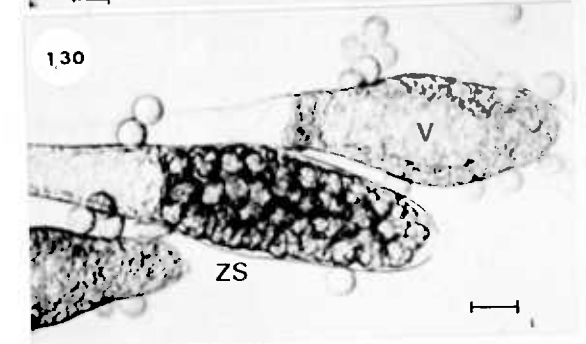




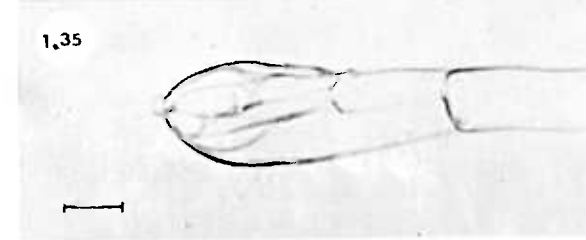


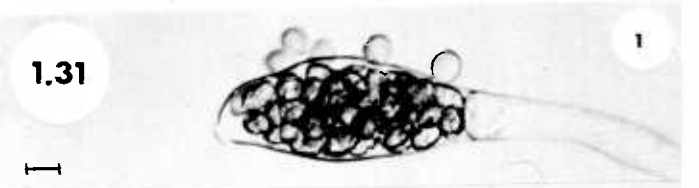


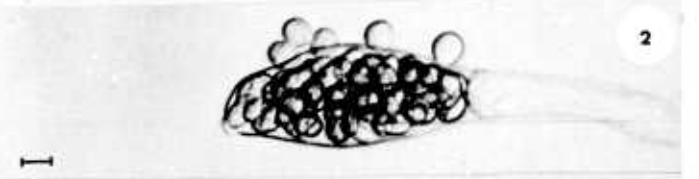


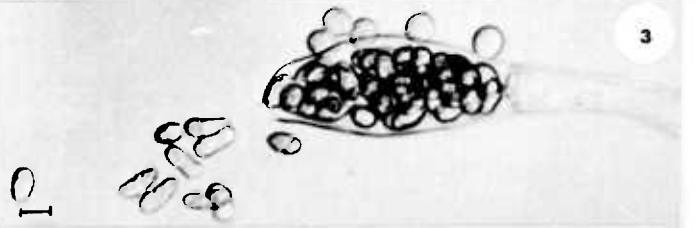




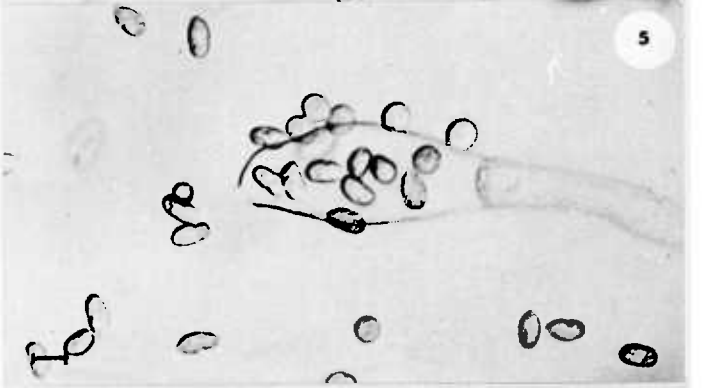


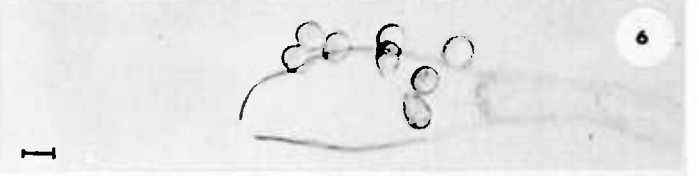




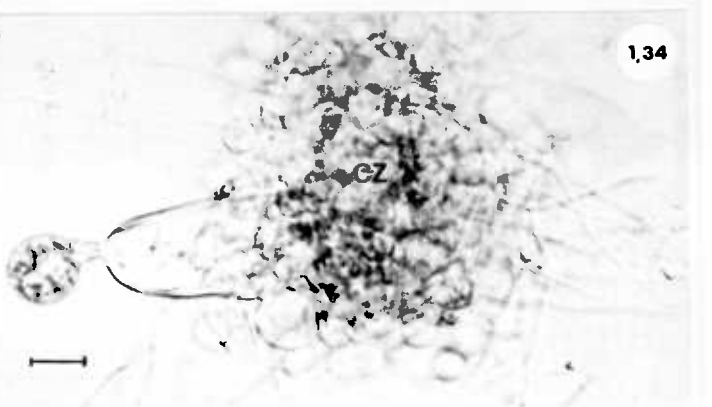












all bar scales = 0.10 µm

Fig. 1.34 A proliferated sporangium emmerging through the apical pore of a dehisced sporangium, which is surrounded by a clump of encysted secondary zoospores.
58/20 O.I. x 600 24 h

Fig. 1.35 Remains of three dehisced sporangia formed by successive proliferation. The absence of cytoplasmic contents in the subtending hypha shows how efficiently cytoplasm is collected and dispatched during sporulation.
58/18 O.I. x 600

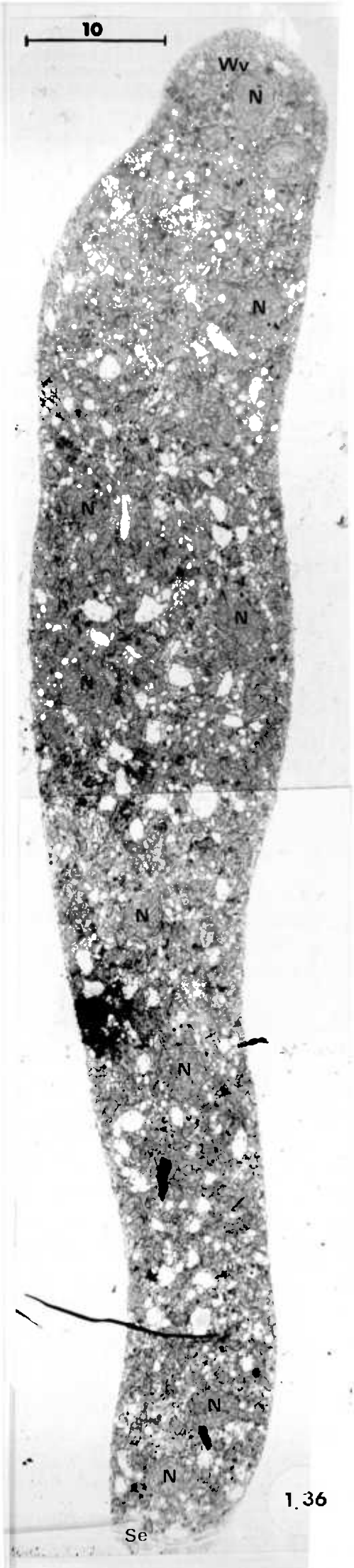
1.2.2.2 Sporangium ultrastructure of S.ferax (3024, 3727) and S.furcata (3444)

Fig. 1.36 Montage of an LS pre-cleavage sporangium. The cytoplasm is densely filled with organelles, but lacks large vacuolar vesicles at this stage.
27471-72 $KMnO_4$ (1% 5 min) 3727 4 h

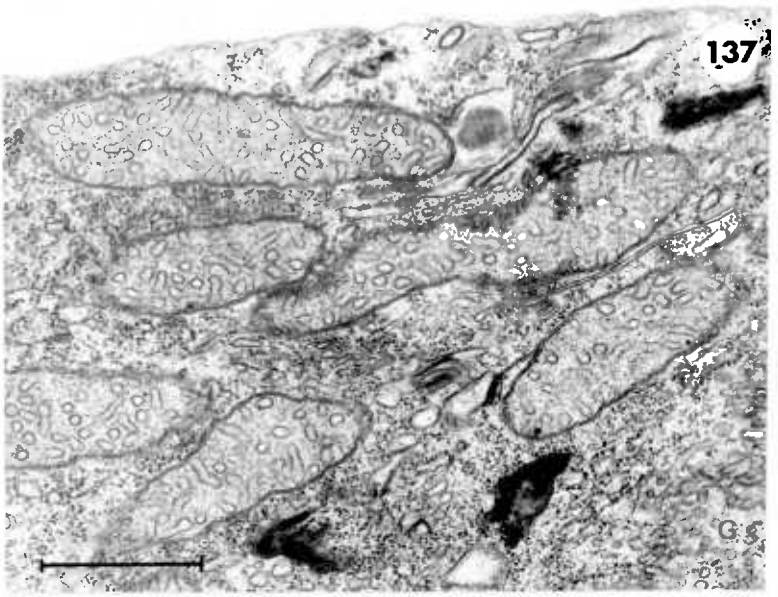
Fig. 1.37, 1.38 Details of the cytoplasm of a young pre-septal sporangium showing the parallel orientation of organelles, indicating the flow of cytoplasm into the sporangium. The mitochondria are elongate and contain abundant tubular cristae.
21476
21474 OS 3444 9 h

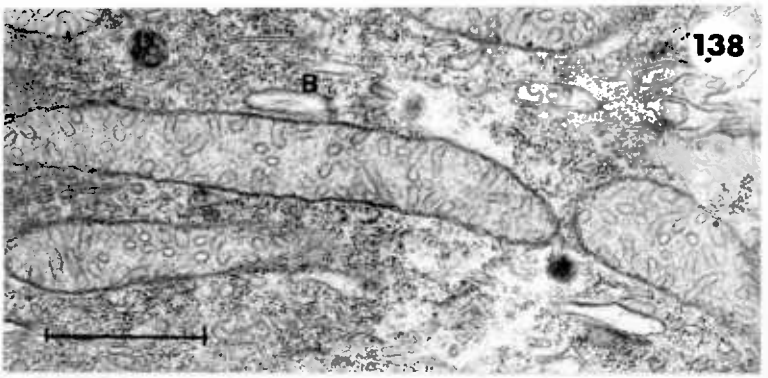
Fig. 1.39 Newly formed densebody vesicles in a pre-septum sporangium. As well as the osmiophilic granule each vesicle also contains small particles. Note how in Os the vesicle membranes have broken slightly. The face view of dictyosome shows many small peripheral vesicles with electron dense contents.
21498 OS 3444 9 h

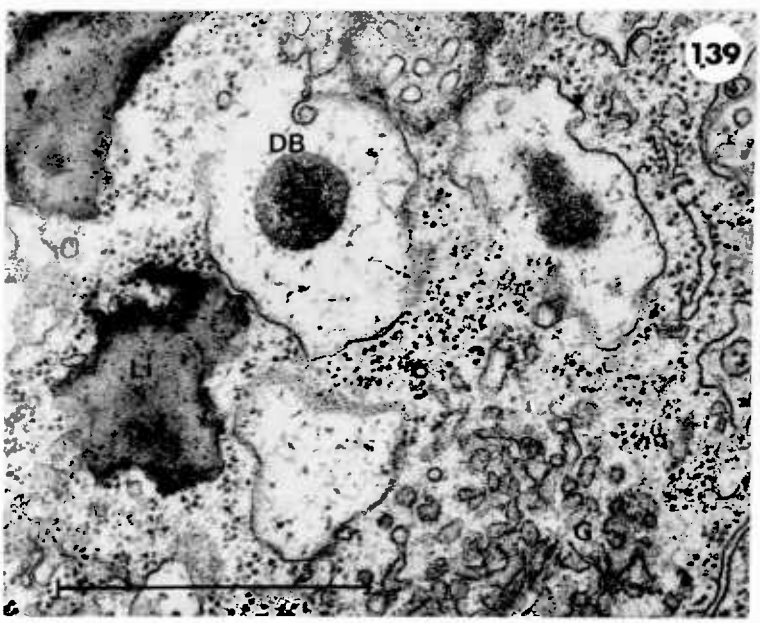
Fig. 1.40 Cytoplasm of a delimited pre-cleavage sporangium showing the abundant dictyosome vesicles, cisternae of rough ER, osmiophilic bar bodies, and newly formed flimmer vesicles with ribosomes attached.
13204 OS 3023 4 h



1.36







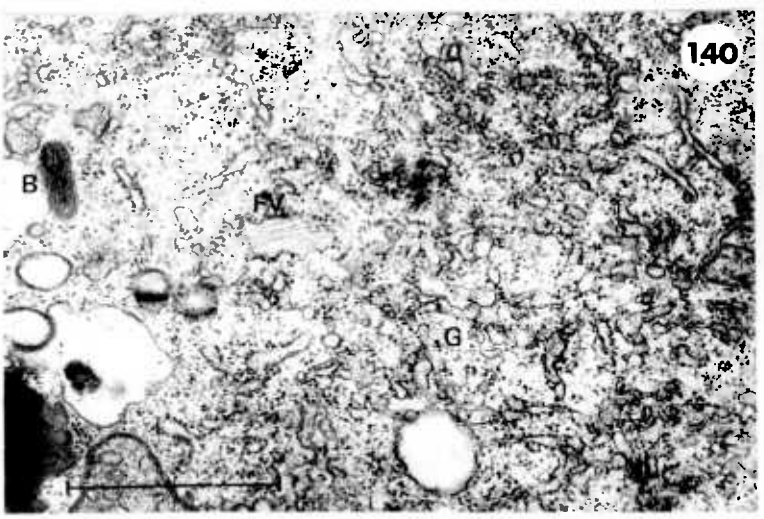
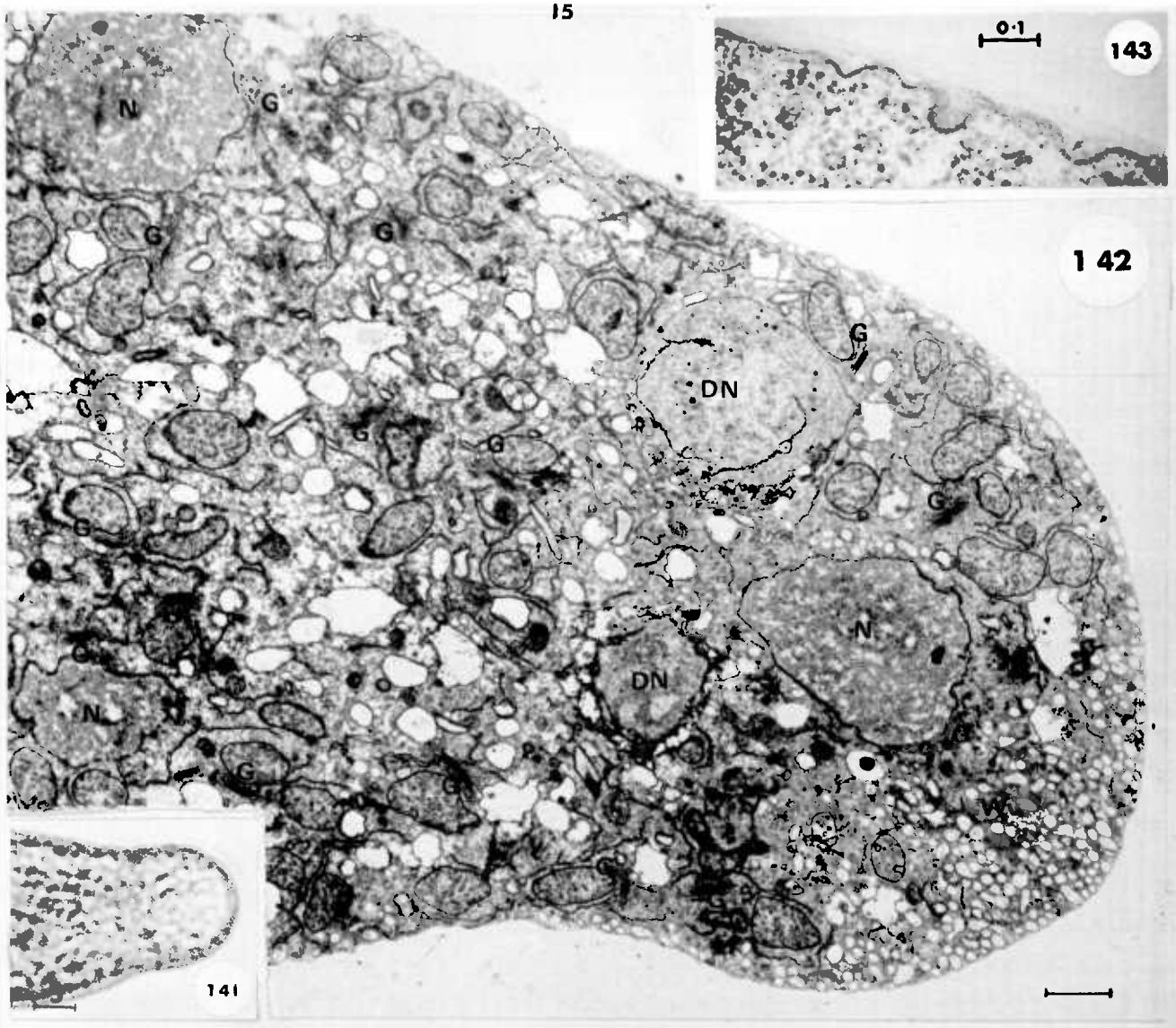


Fig. 1.41 Light micrograph of the refractile apex of a newly delimited sporangium
68/6 O.I. x 1200

Fig. 1.42 Electron micrograph of a sporangium apex such as shown in Fig. 1.41. The apex contains a large number of wall vesicles preceeding papilla initiation. Golgi dictyosomes are abundant, and show either ER-mitochondrion, or nuclear associations. Some of the nuclei are undergoing autolysis.
27470 $KMnO_4$ (1% 5 min) 3727 4 h

Fig. 1.43 Detail of the wall and peripheral cytoplasm of an undelimited sporangium. The wall is very thin and almost electron transparent. The plasmalemma is uneven and contains numerous invaginations containing lightly stained material.
27463 OS 3444 9 h

Fig. 1.44 TS of a delimited sporangium showing the development of the axial vacuolar vesicle complex.
13346 OS 3024 4 h


0·1
143
142
N
G
DN
141

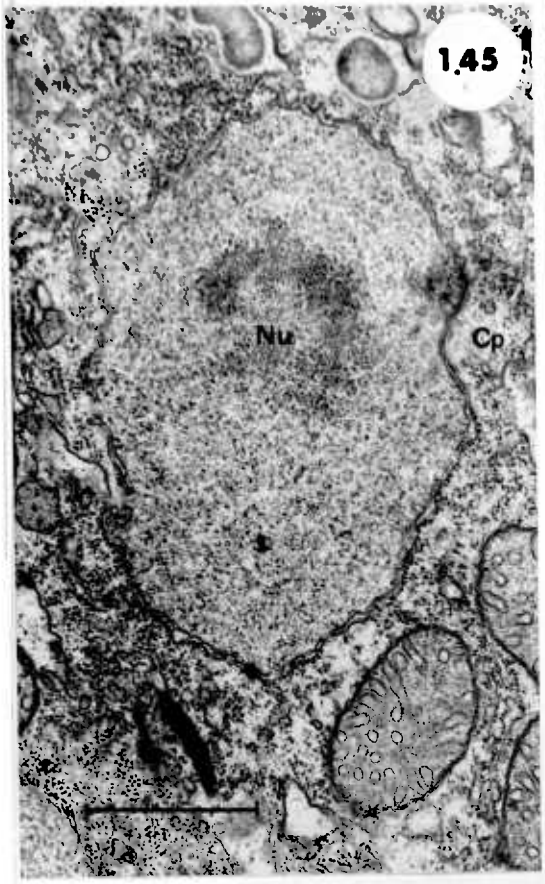

144
ER
Vv
Vg

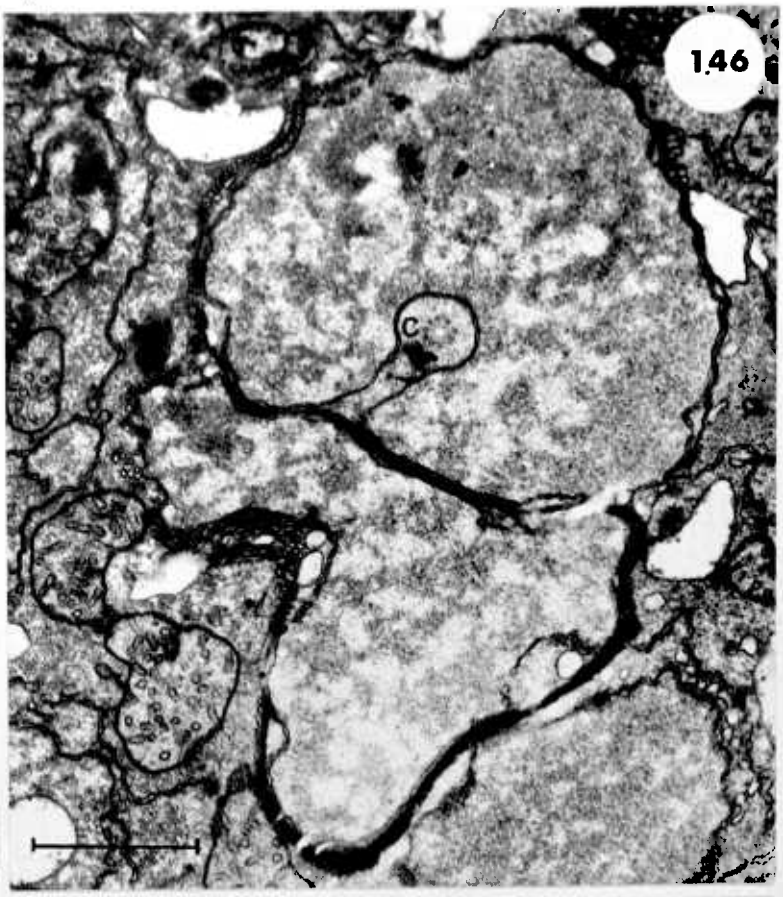
Fig. 1.45 Typical interphase nucleus in a pre-cleavage sporangium. The centriole is not in the plane of section, but the lateral centriolar pocket can be seen.
21472 O_s 3444 9 h

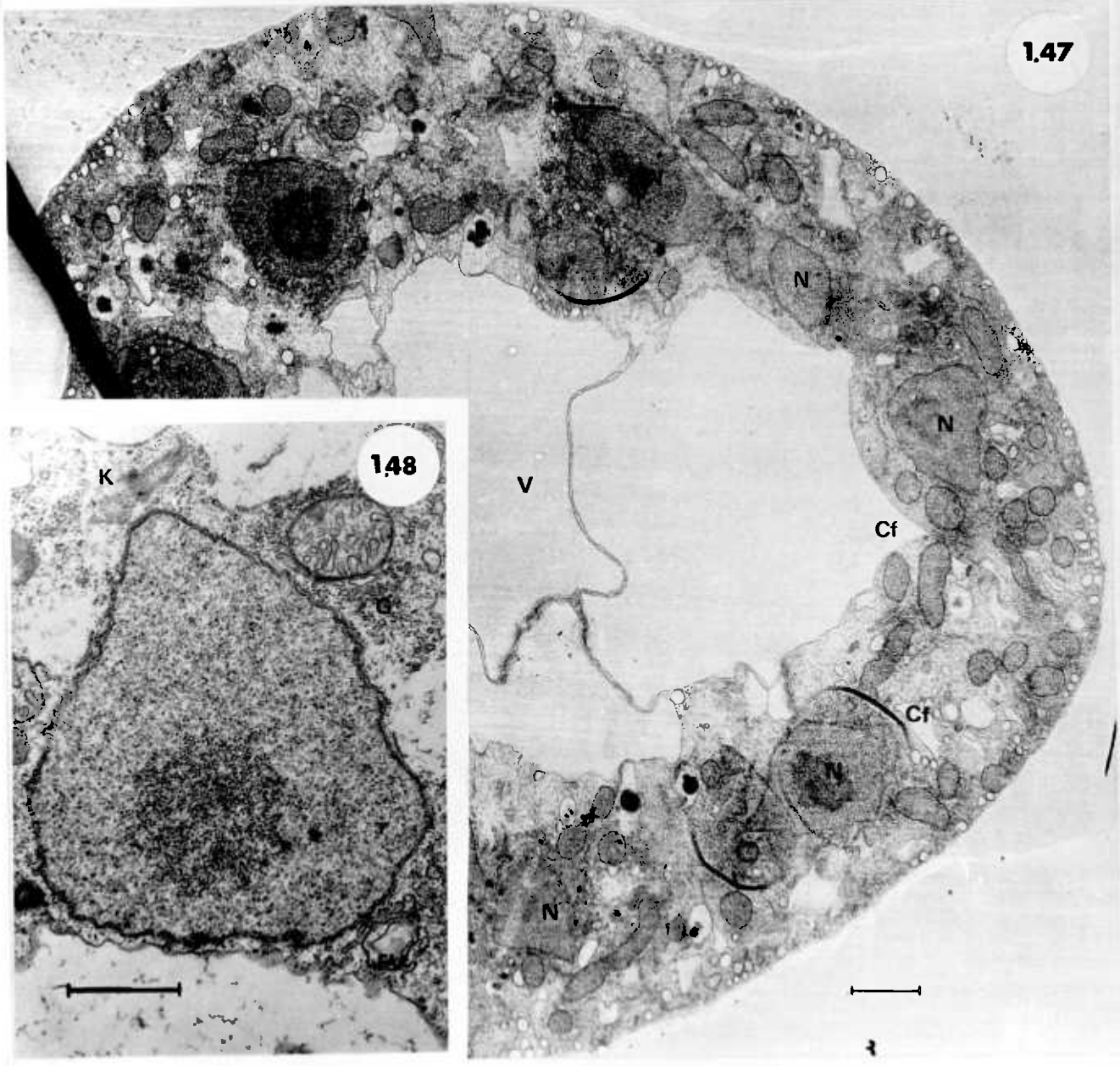
Fig. 1.46 A pair of atypical nuclei showing early stages of autolysis in a pre-cleavage sporangium. The two nuclei are surrounded by electron dense membranes and small vesicles, which makes the nuclear envelope difficult to discern. The poorly-fixed centriole lies in a deep invagination of the nuclear envelope.
27478 $KMnO_4$ (1% 5 min) 3727 4 h

Fig. 1.47 TS profile of a late cleavage sporangium showing the large axial vacuolar area. The uninucleate spore initials are becoming delimited by the formation of cleavage furrows (arrowed). The vacuoles are separated by fine strands of cytoplasm.
13319 O_s 3024 6 h

Fig. 1.48 Pyriform nucleus from a late cleavage sporangium. The centrioles have developed into a pair of apical kinetosomes. Note the close association of an ER-mitochondrion-Golgi complex with this nucleus.
29843 O_s 3024 6 h


1.45
Nu
Cp


1.46
C


1.47
N
N
V
Cf
Cf
N
N

1.48
K
G

Fig. 1.49. Detail of cytoplasm in the pre-cleavage sporangium in Fig. 1.36. The abundant parallel arrays of ER are aligned around both nuclei and mitochondria. Nuclear envelope - ER connections are also clearly shown.
27481 $KMnO_4$ (1% 5 min). 3727 4 h 4 h

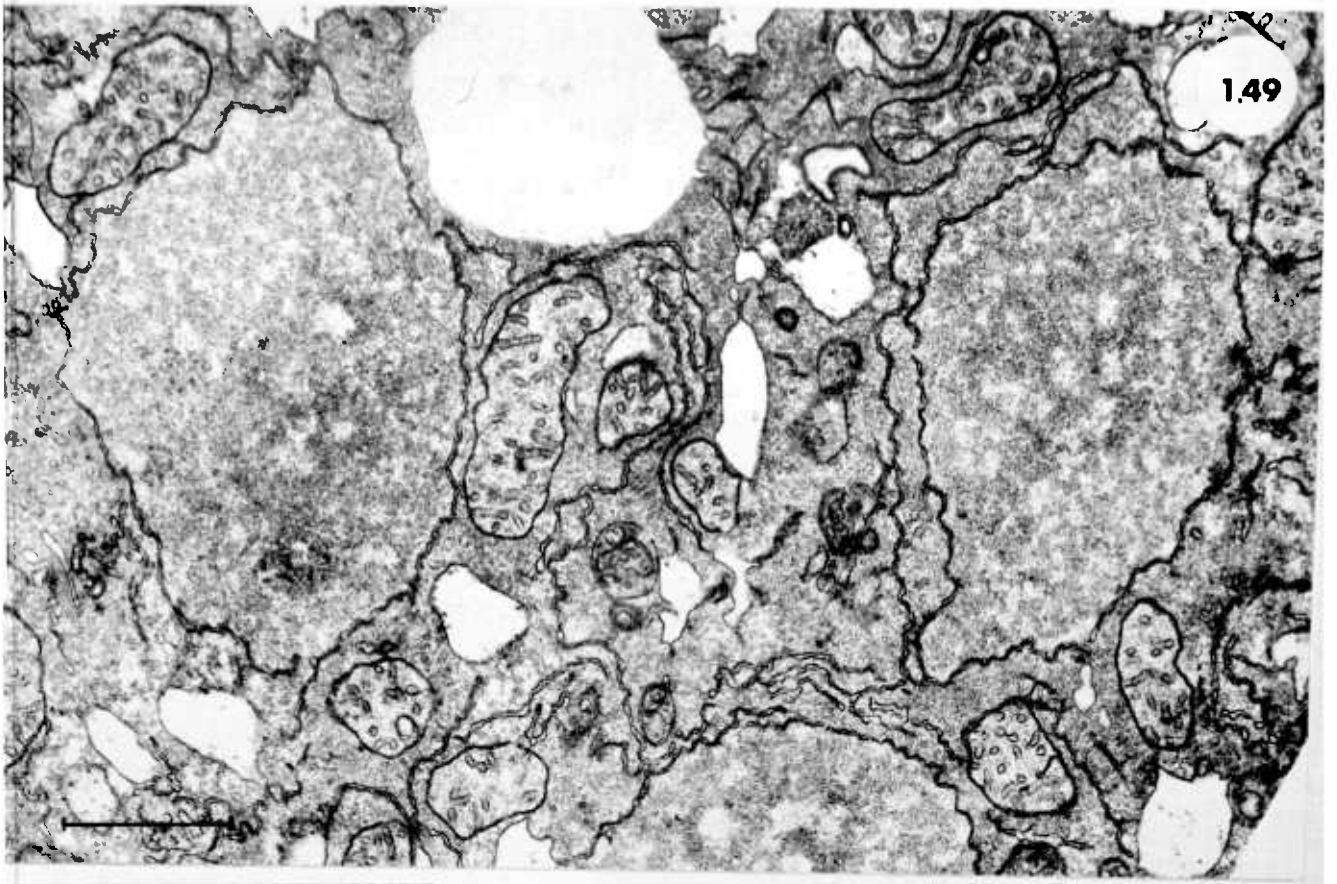
Fig. 1.50 A typical form of multivesicular body from a pre-cleavage sporangium after Os fixation.
21501 Os 3444 9 h

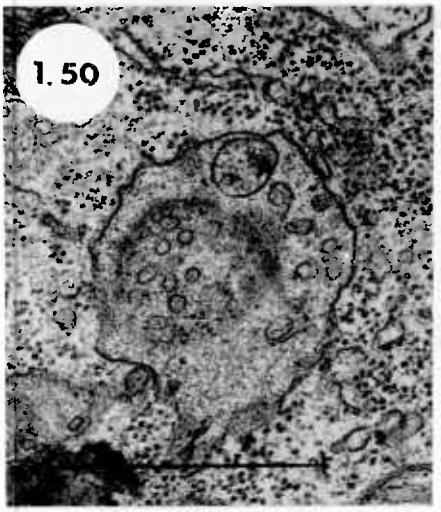
Fig. 1.51 Cluster of multivesicular bodies from a pre-cleavage sporangium. Note the bar body with peripherally distributed tubules.
27247 $KMnO_4$ (1% 5 min) 3727 4 h

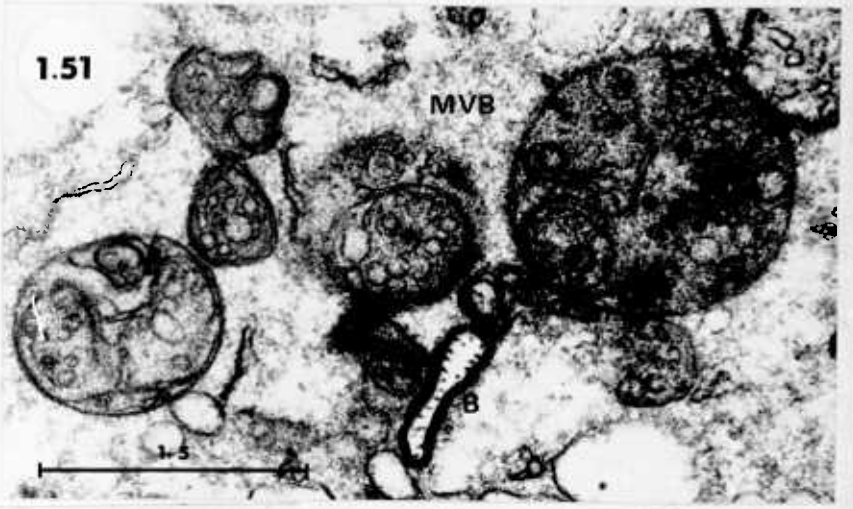
Fig. 1.52 Dictyosome in the peripheral cytoplasm of a pre-cleavage sporangium showing the typical association with a cisterna of ER, and a mitochondrion. The peripheral dictyosome cisternae are much more inflated in sporangia than in hyphae (Fig. 1.12). The large electron-transparent body to the right of the mitochondrion is an extracted droplet of neutral lipid.
27470 $KMnO_4$ (1% 5 min). 3727 4 h

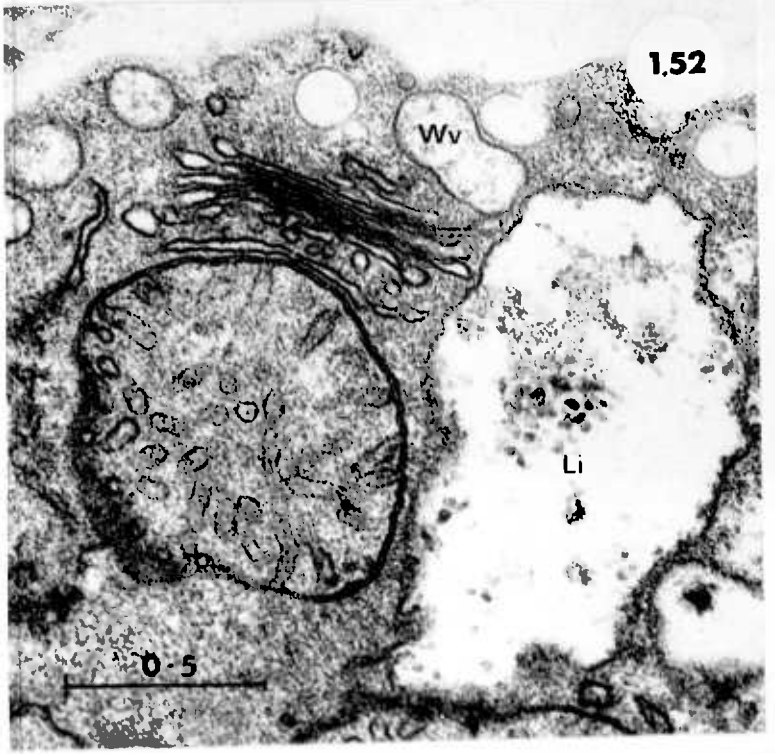
Figs. 1.53, 1.54 Typical bar bodies in a pre-cleavage sporangium showing the peripheral tubules, which may be helically coiled.
27282 $KMnO_4$ (1% 5 min) 3727 4 h
27284

Fig. 1.55 Bar in an undelimited body showing the widely dispersed tubules, and a well-defined limiting membrane.
21499 Os 3444 9 h


1.49

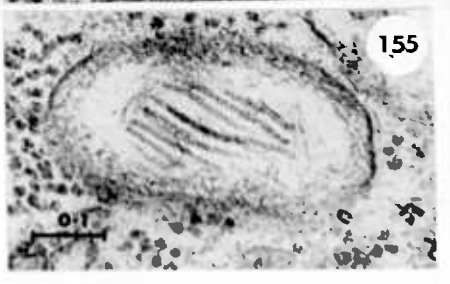

1.50


1.51
MVB
B
1·5


1.52
Wv
Li
0·5


0·1
1.53


0·1
1.54


1.55
0·1

1.2.2.6 Encysted spores of S.ferax

Figs. 1.56, 1.57. Part sections of a newly encysted primary zoospores showing the single nucleus and peripheral mitochondria. Note that the mitochondria are shorter and have more elongate cristae than in sporangia. Golgi vesicles are common and are mainly clustered near to the nucleus. The cyst wall is thin, and has an electron dense outer layer, in which the short spines are attached.

13310 0_s 3022 unknown
13312

Fig. 1.58 The peripheral cytoplasm of a mature cyst showing wall vesicles, and a small concentrically layered body.

29852 0_s 3885 8 h;

Fig. 1.59 Nucleus with centriole in a pre-germination cyst, showing the reversion to interphase structure.

29863 0_s 3885 8 h

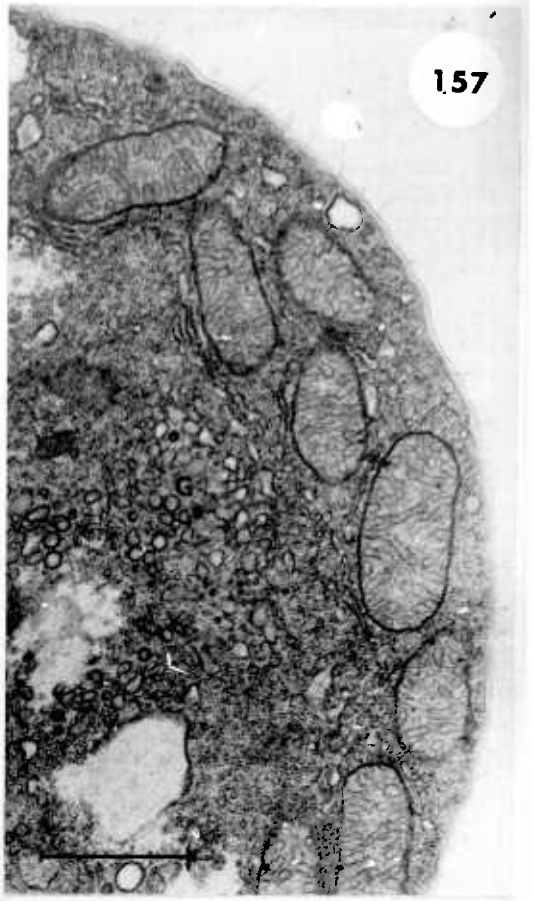
Fig. 1.60 Pre-germination cyst still containing a pyriform nucleus and apical kinetosomes (cf. Fig. 1.59). Note the condensed osmiophilic nucleolus. The mitochondria are still peripherally concentrated, but there is little evidence of Golgi activity at this stage.

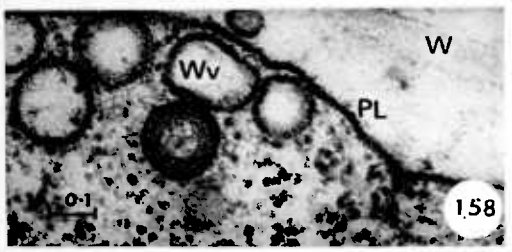
29898 0_s 3885

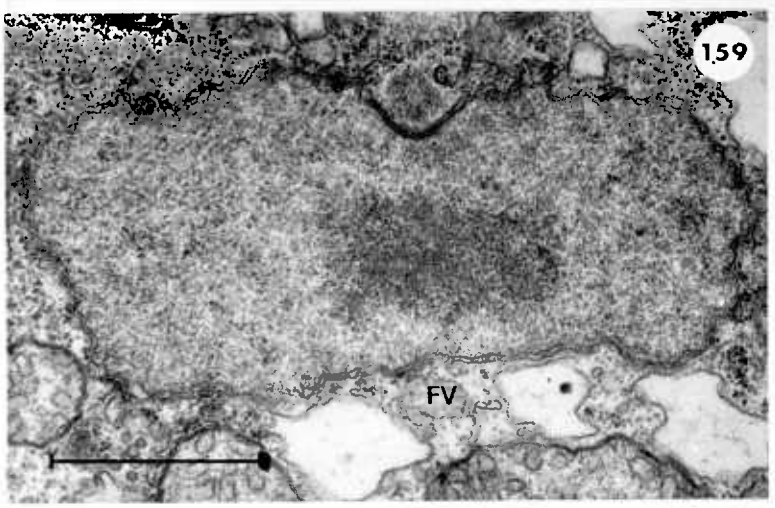
Fig. 1.61 Cyst with an expanded vacuolar compartment. The cytoplasm has plasmolysed slightly during the fixation procedure.

29641 0_s 3885

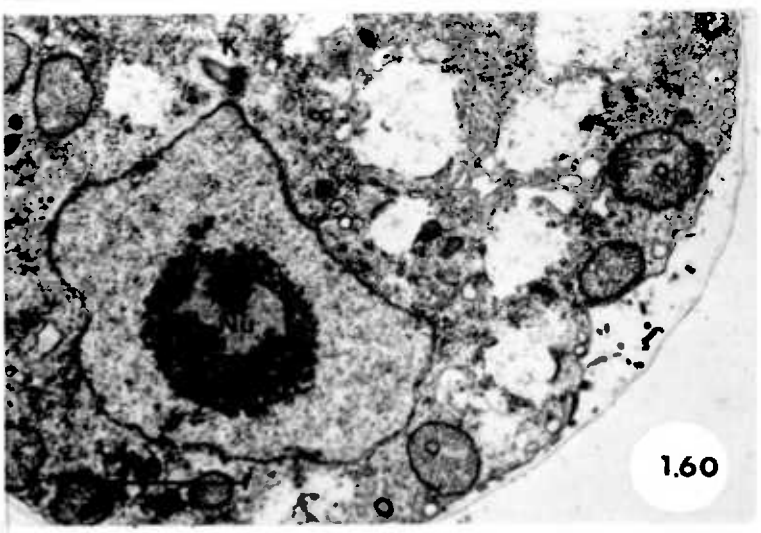

1.56
N


1.57
G
L


W
Wv
PL
0·1
1.58


1.59
FV


1.61
FV
V


Nu
1.60

1.2.2.6 Cyst germination in S.ferax

Fig. 1.62 Primary cyst incubated in Str (50 mg/l) showing a secondary zoospore being liberated through a narrow pore in the cyst wall.

29889 O_s 3886 50 mg/l Str 8 h

Fig. 1.63 Profile of a germinating cyst showing two nuclei and many expanded vacuolar vesicles. The mitochondria have elongated and become widely dispersed.

29896 O_s 3886 50 mg/l Str 8 h

Fig. 1.64 Directly germinating cyst with a short germtube. The cytoplasm is highly vacuolate with fine protoplasmic strands traversing the vacuolar region.

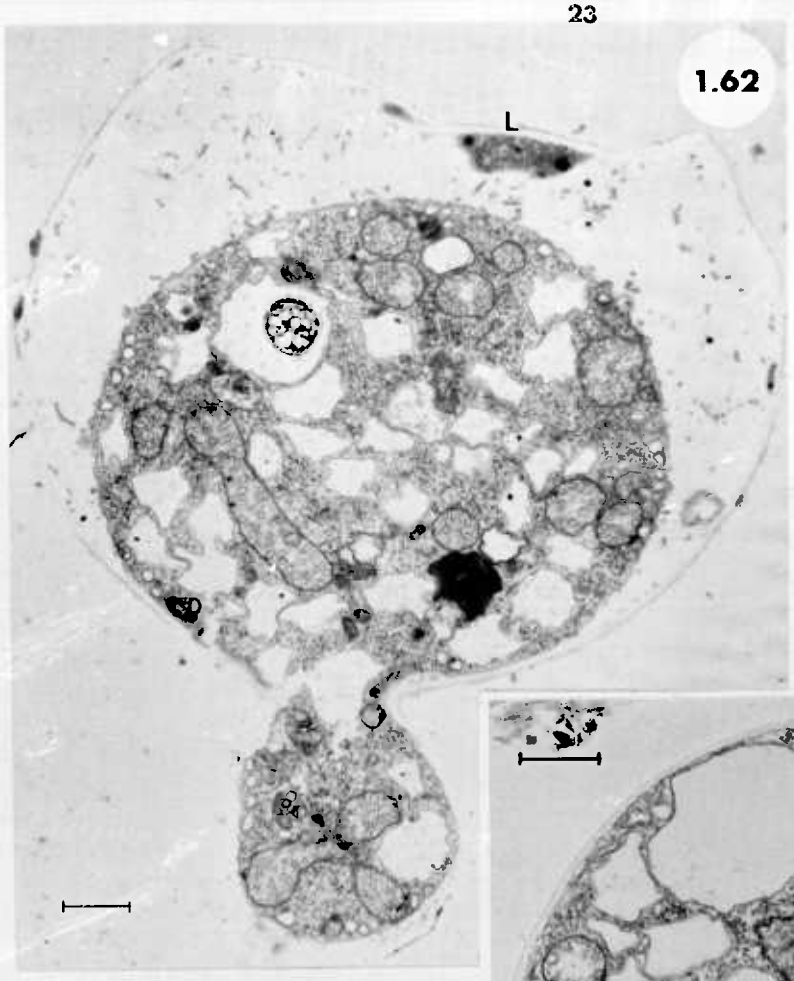
29915 O_s 3885 8 h

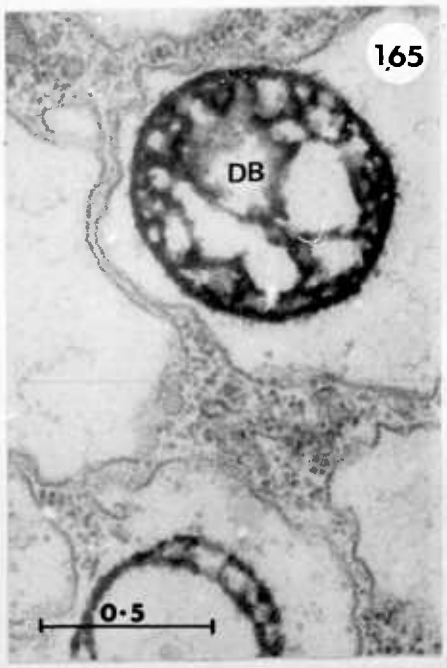
Fig. 1.65, 1.66, 1.67 A series of densebody vesicles in germinating cysts showing the progressive expansion and erosion of the osmiophilic granules. Note the characteristic 'ring' profiles which are assumed prior to the disappearance of these bodies.

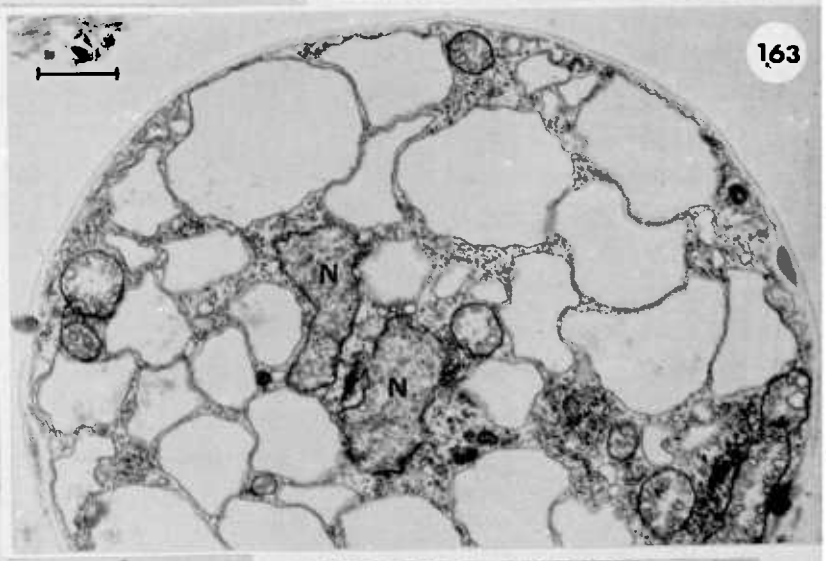
29863

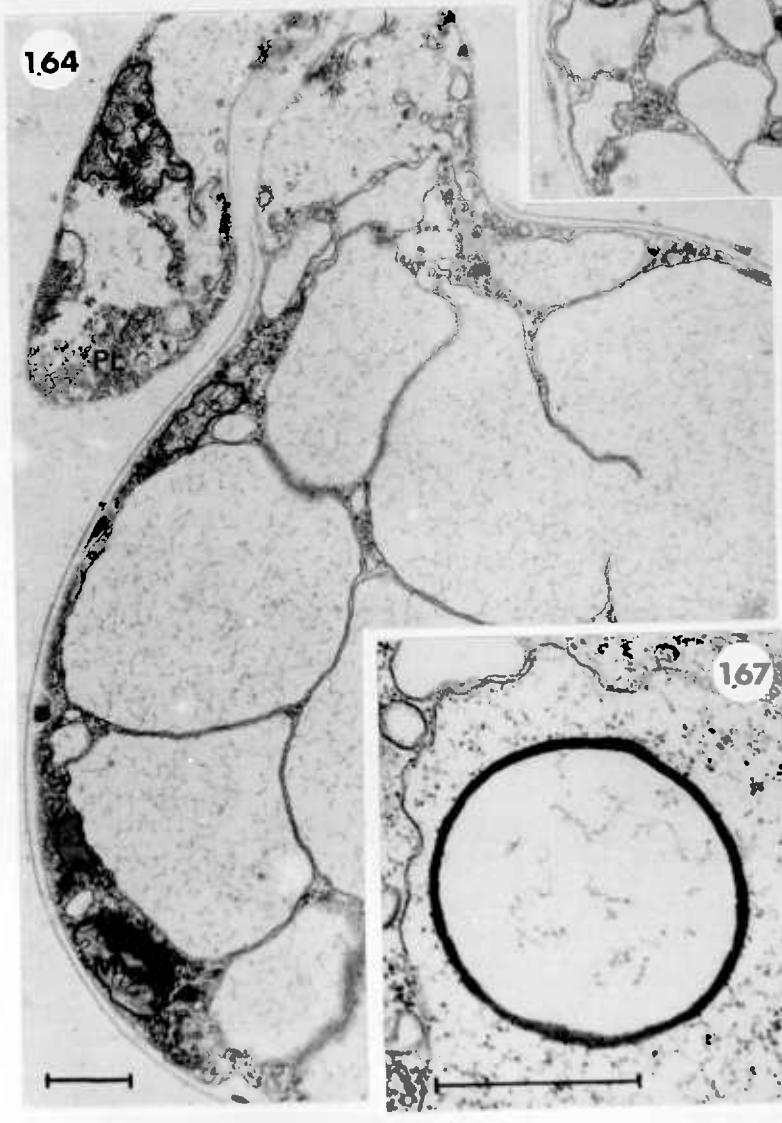
29894 3886 O_s 50 mg/l Str 8 h

29910

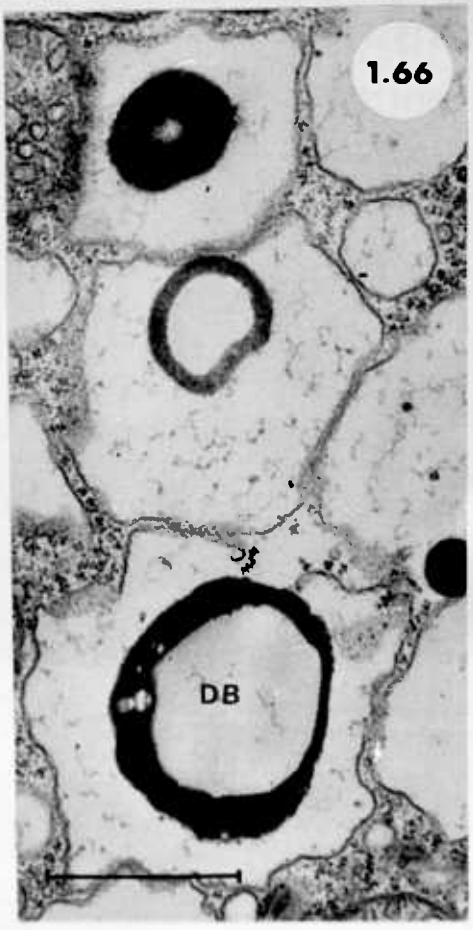

1.62
L


1.65
DB
0·5


1.63
N
N


1.64
PL

1.67


1.66
DB

1.2.3 Sexual differentiation in S.furcata: Gametangium development

Fig. 1.68 Characteristic hooked hyphal tips which later develop into oogonial initials.
107/1 0 I x 350 12 h

Fig. 1.69 A typical Stage I oogonium initial
107/2 0 I x 350 12 h

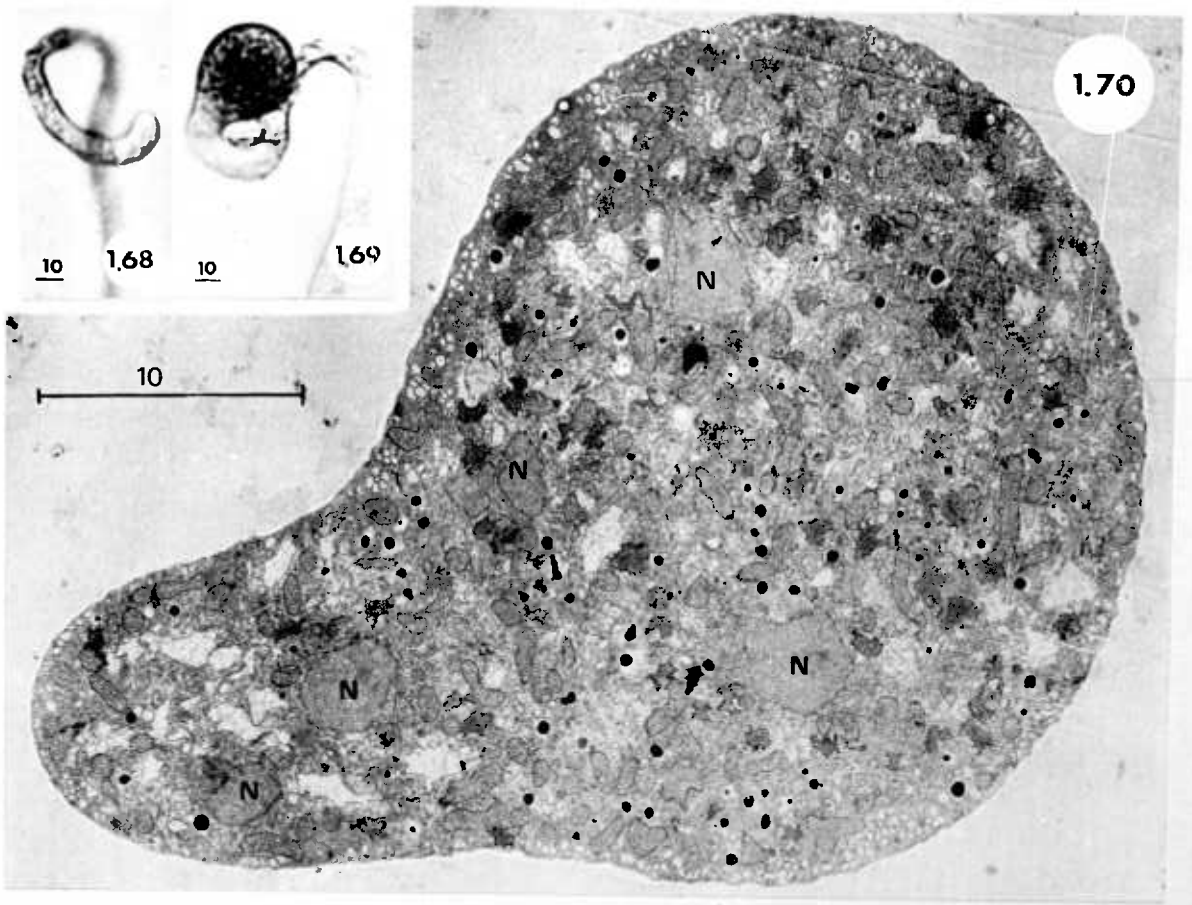
Fig. 1.70 LS of an expanding Stage I oogonium showing the high concentration of organelles, the absence of large vacuolar vesicles, and the peripheral wall vesicles.
21203 0_s 3444 9 h

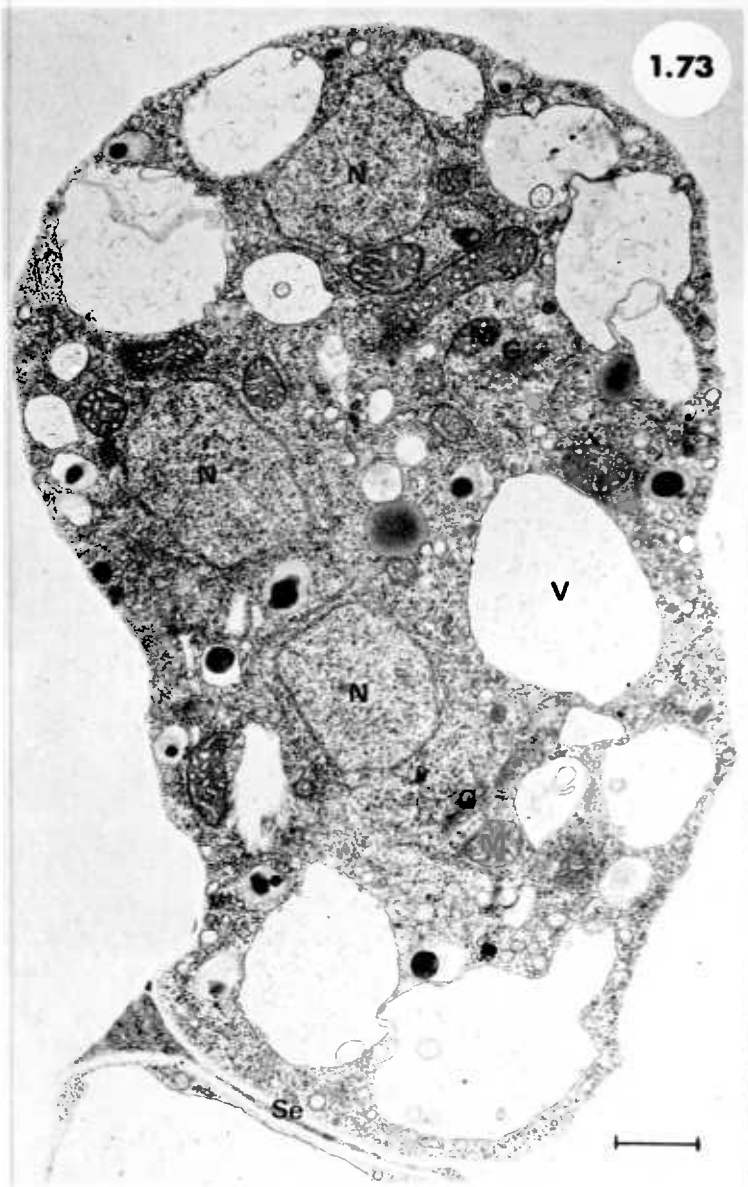
Fig. 1.71 A Stage II oogonium showing the androgynous development of antheridial hyphae from the oogonium stalk.
103/21 0 I 18 h

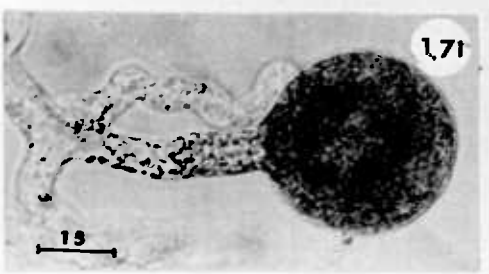
Fig. 1.73 LS of a Stage III antheridium following its delimitation The nuclei are in interphase and the vacuolar vesicles are peripherally distributed.
29178 GaOs 3883 24 h

Fig. 1.74 A pre-septum Stage III oogonium showing the elaborate complex of vacuolar vesicles at this stage.
29314 GaOs 3878 24 h

10
1.68
10
1.69


1.70
10
N
N
N
N
N


1.73
N
N
V
N
Se


1.71
15

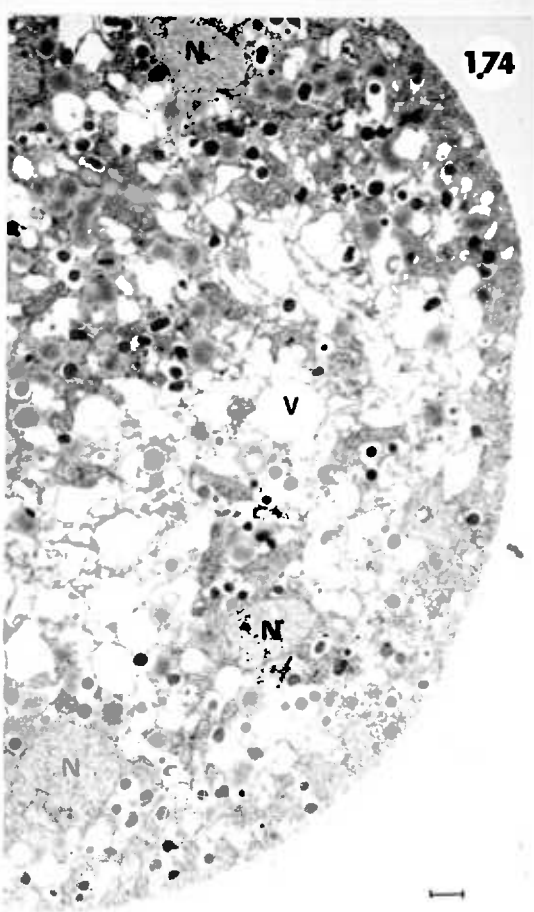

1.74
N
V
N
N

Fig. 1.75 Stage IV gametangia showing the well developed oogonium vacuole and large prophase I nuclei in both the oogonium and antheridium. Both bodies are delimited by a basal septum.
29105 GaOs 3878 24 h

Fig. 1.76 Another Stage IV oogonium in which the vacuolar compartment is still divided by fine strands of cytoplasm
21315 Os 3446 24 h

Fig. 1.77 Light micrograph of Stage IV gametangia showing the conspicuous prophase I nuclei in the oogonial cytoplasm (arrowed).
103/50 O I 24 h

Fig. 1.78a Detail of adjacent oogonium (upper) and antheridium (lower) showing the large number of wall vesicles where the gametangia contact.
50834 GaOs 3665 24 h

Fig. 1.78b LS of antheridium (stage IV) showing the synchronously dividing prophase I nuclei containing conspicuous linear elements, many of which are aligned in pairs.
31914 GaOs 2895 24 h

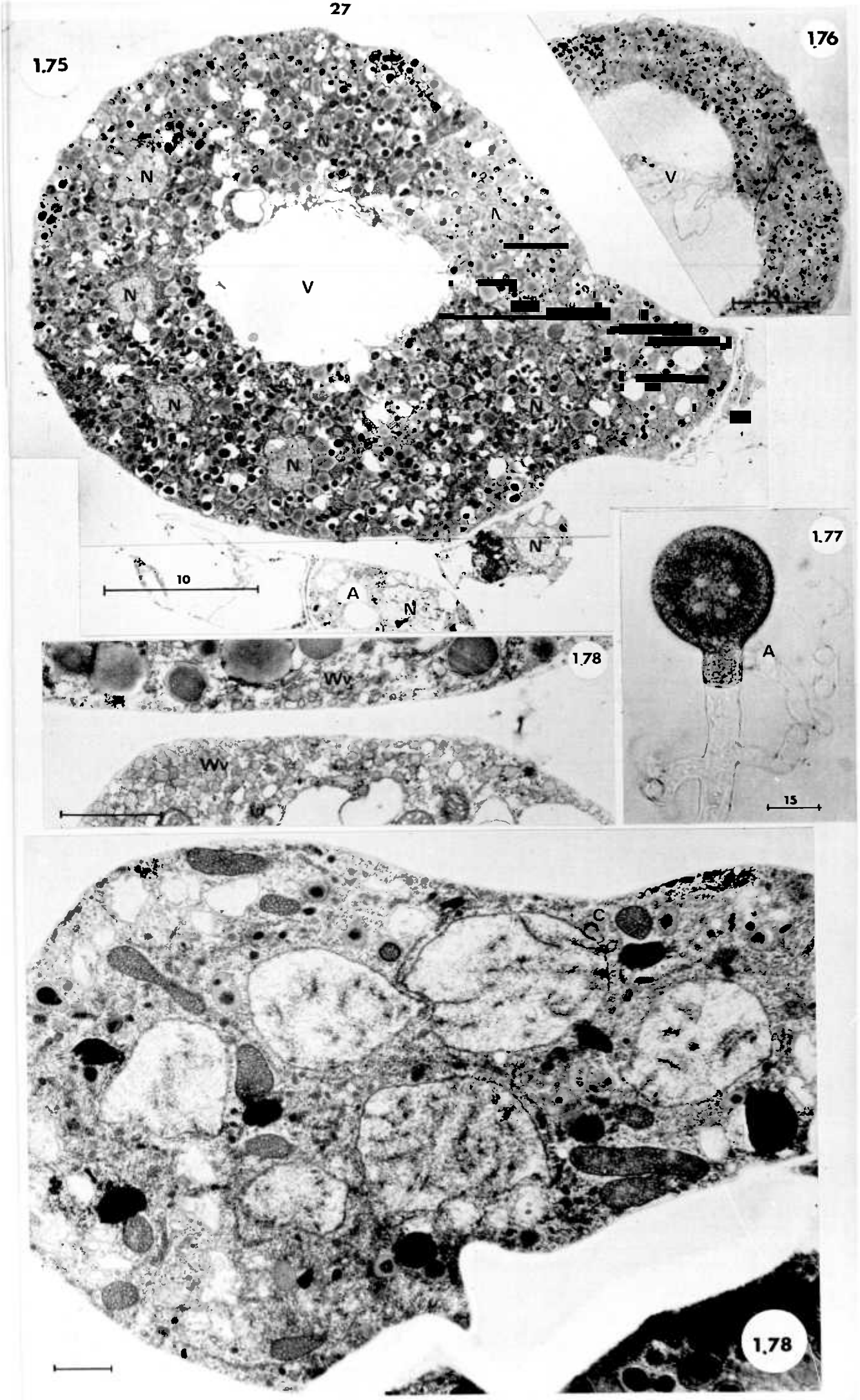
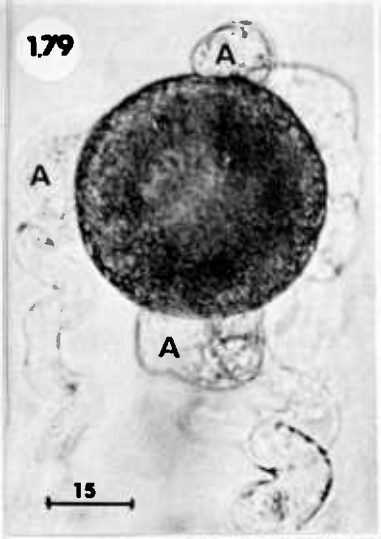

1.75
N
N
N
V
N
N
N
1.76
V
10
A
N
N
1.77
A
15
1.78
Wv
Wv
C
1.78

Fig. 1.79 Light micrograph of a late Stage IV oogonium which lacks conspicuous nuclei.
103/54 O I 24 h

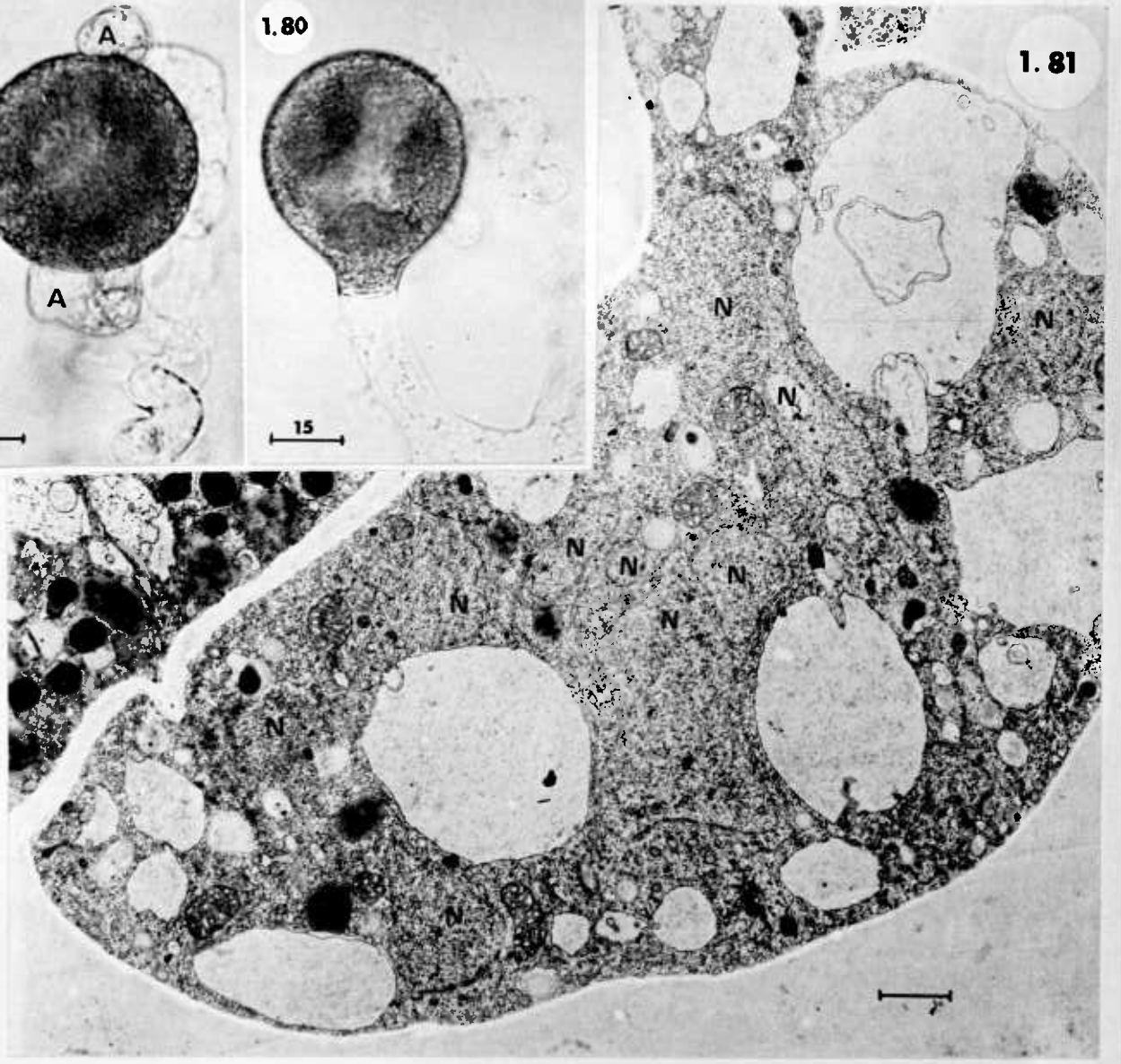
Fig. 1.80 Stage V oogonium in which the peripheral cytoplasm is aggregating into mounds as the cleavage furrows develop.
103/55 O I 24 h

Fig. 1.81 LS of an antheridium (late Stage IV) containing numerous nuclear profiles. The close association of 4 such nuclei suggest these may be late second divisional stages. Accumulations of wall vesicles in the region of gametangium contact are no longer present.
29274 GaOs 3883 48 h

Fig. 1.82 Mature antheridium (Stage V) showing the enlarged vacuolar compartment and small post meiosis gametic nuclei.
29612 GaOs 3883 48 h


1.79
A
A
A
15

1.80
15


1.81
N
N
N
N
N
N
N
N
N
N
N

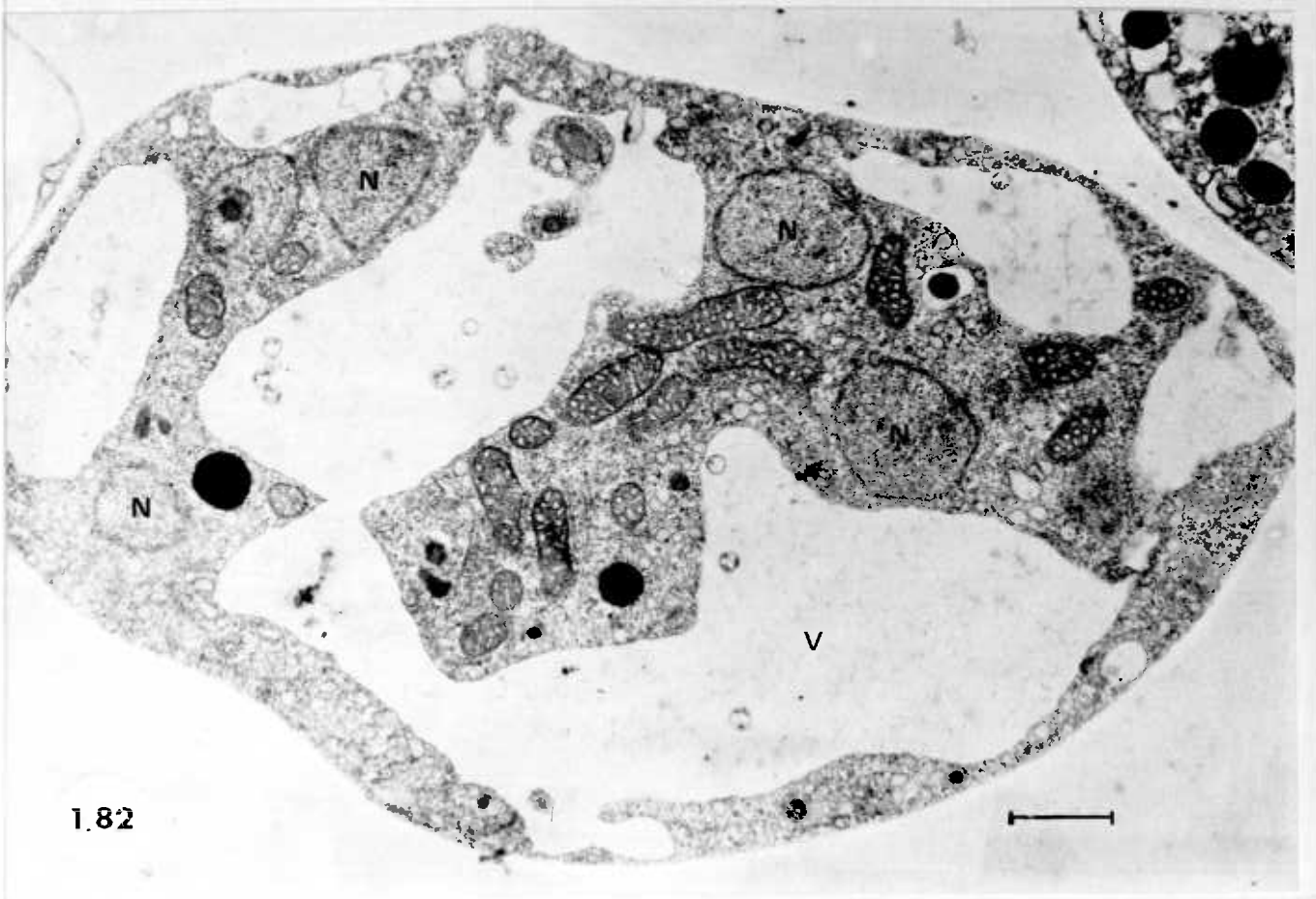

N
N
N
N
V
1.82

Fig. 1.83 Cytoplasm in a Stage I oogonium showing the typical golgi-ER-mitochondrion association. Note the similarity between the contents of the inflated ER cisterna in the upper part of the figure, and the contents of the densebody vesicle in the lower.
21346 Os 3444 9 h

Fig. 1.84 Dictyosome with many associated vesicles in a Stage IV oogonium. This dictyosome lies close to the tonoplast and does not appear to show the usual mitochondrial or nuclear association.
21318 Os 3446 24 h

Fig. 1.85 The peripheral cytoplasm of a Stage IV oogonium showing the structural similarity between Golgi-derived and peripheral wall vesicles. Note how the densebody granules are poorly preserved in this body.
21575 Os 3446 24 h

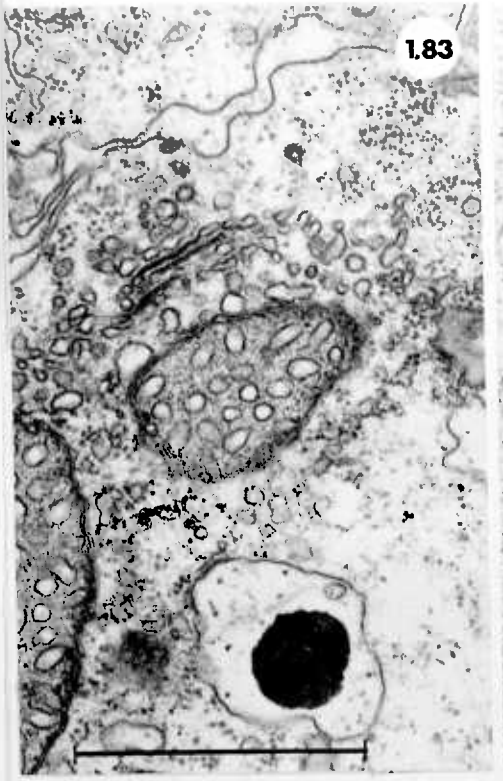
Fig. 1.86 Densebody vesicles in a Stage III oogonium. Apart from their densebodies these vesicles are indistinguishable from the expanding vacuolar vesicles.
29512 GaOs 3878 24 h

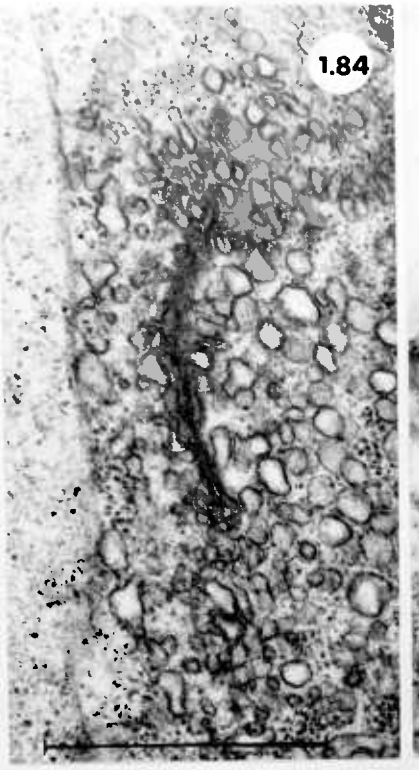
Fig. 1.87 GaOs-fixed densebody vesicle in a Stage IV oogonium. The densebody is surrounded by concentric myelin-like arrays.
22024 GaOs 3452 48 h

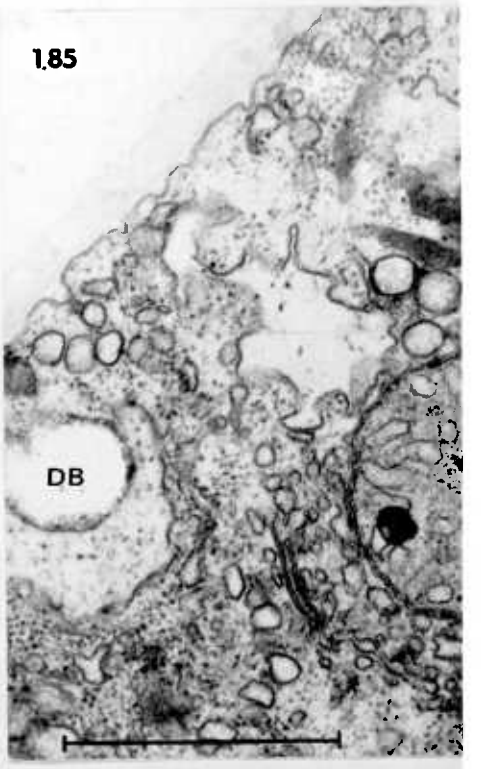
Fig. 1.88 GaOs-fixed densebody vesicle in a Stage III oogonium, showing an unusual reticulate condensation of the vesicle matrix.
29574 GaOs 3878 24 h

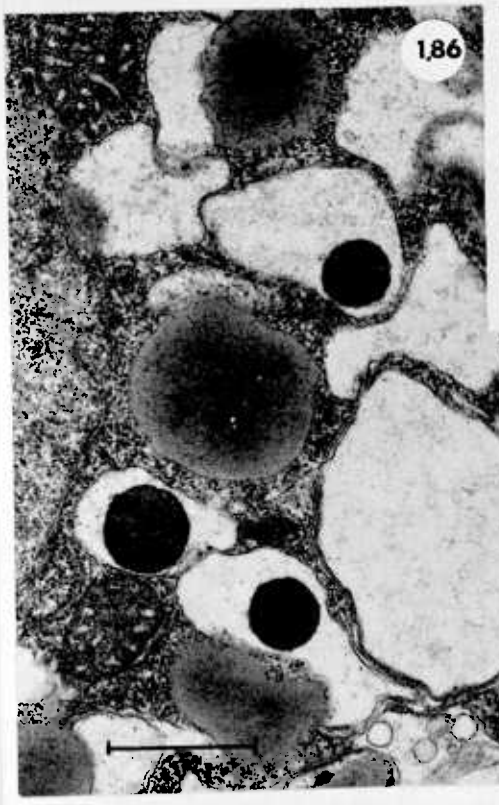
Fig. 1.89, 1.90 Densebody vesicles in Stage IV oogonia showing structure typical of Os-fixation. Note the variation in the preservation of vesicle membranes, and the extent of the myelin arrays.
21229 Os 3446 24 h
21615

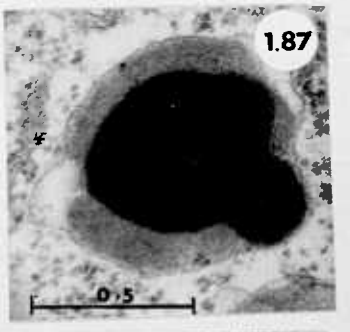
Fig. 1.91 Stage IV oogonium cytoplasm with densebody vesicle which has expanded and fused with the tonoplast membrane.
46940 GaOs 3666 24 h

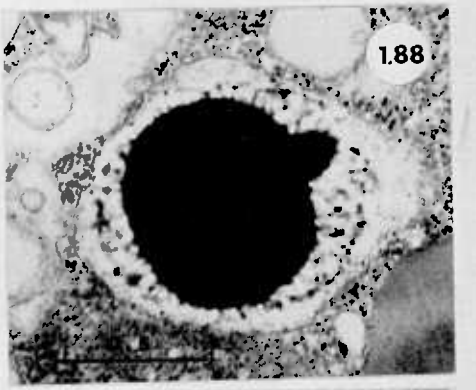

1.83

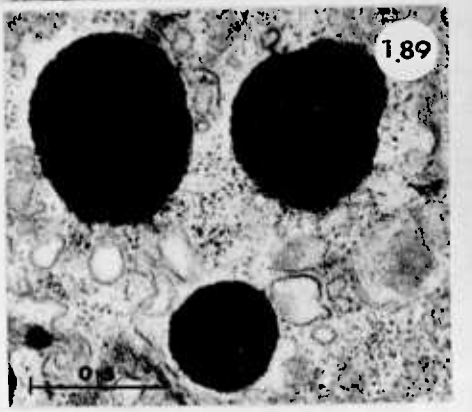

1.84

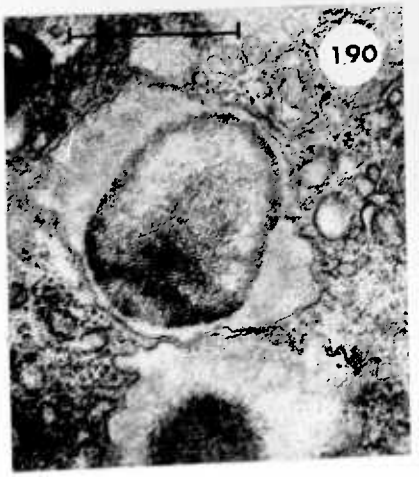

1.85
DB

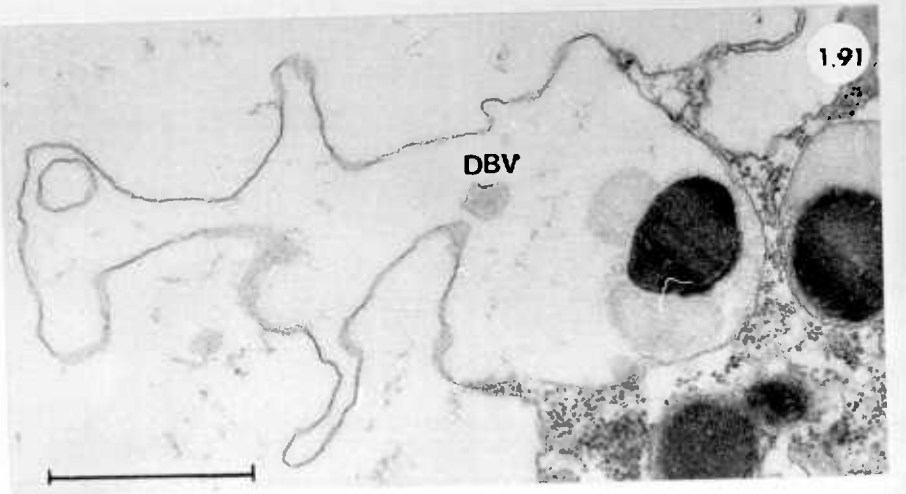

1.86


1.87
0,5


1.88


1.89


1.90


1.91
DBV

1.2.3.4 Gametangial nuclear divisions in S.furcata

Fig. 1.92 Interphase nucleus from a Stage III oogonium showing structure typical of GaOs fixation. A centriole (TS profile) lies in the nuclear envelope pocket, from which microtubules radiate. This nucleus is surrounded by cisternae of rough ER.
29309 GaOs 3878 24 h

Fig. 1.93 Interphase nucleus from a Stage I oogonium showing structure typical of Os fixation. Note the close proximity of the dictyosome to the centrioles.
21503 Os 3444 9 h

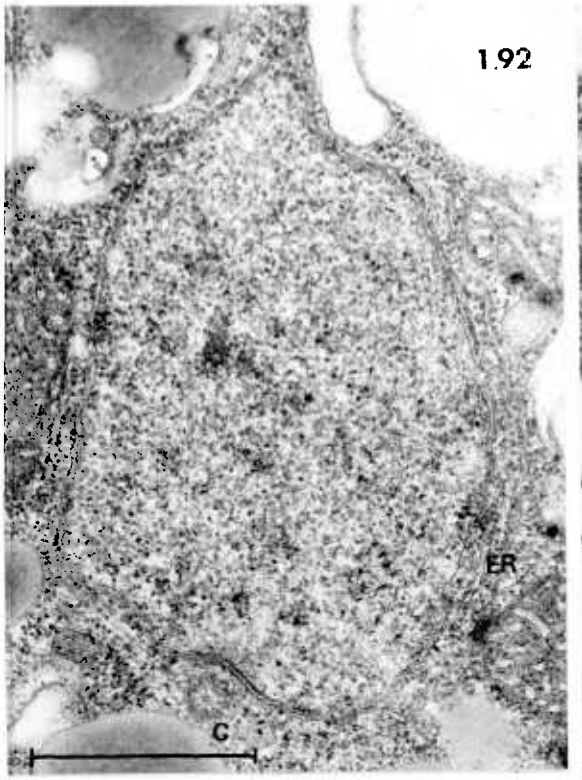
Fig. 1.94 Early prophase I nucleus from a Stage IV oogonium. Note the condensing nucleolus lying close to the nuclear envelope, and the beginning of uniaxial element development.
29076 GaOs 3878 24 h

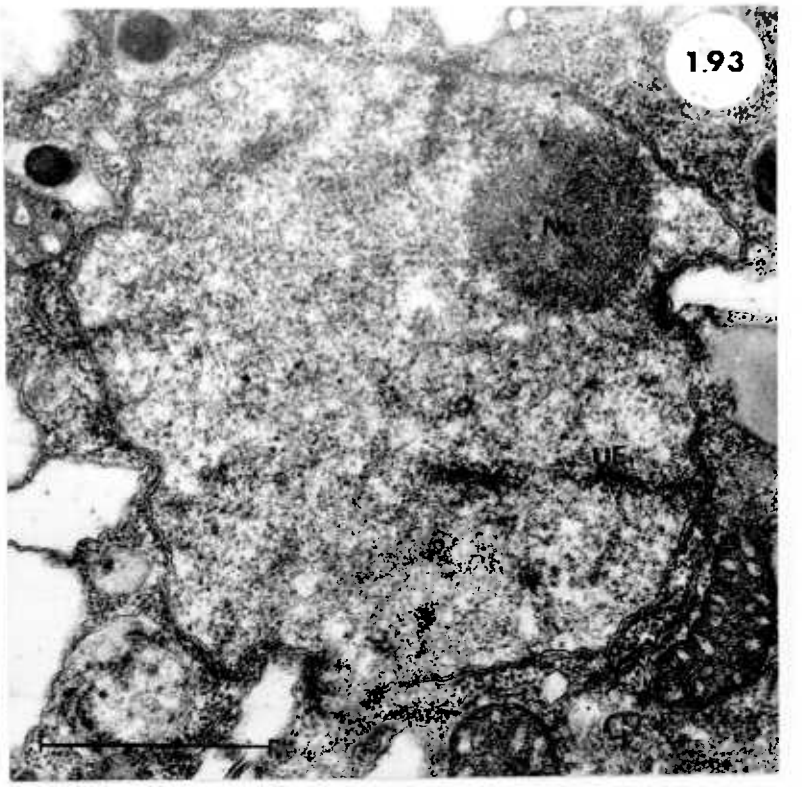
Fig. 1.95 Prophase I nucleus showing the features indicated in Fig. 1.94. Note in Os-fixed material the nucleoplasm is finely granular and the nuclear envelope is uneven and deeply invaginated.
21337 Os 3446 24 h

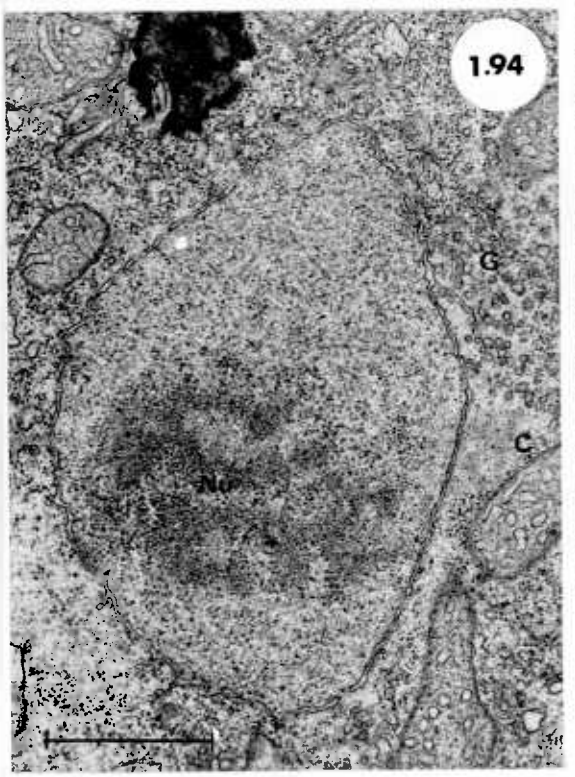
Fig. 1.96 An interphase centriole in TS from a Chl-induced gemma showing the 9 triplet microtubules linked by the central cartwheel structure. Note the loose fibrillar material surrounding the microtubules, which is more extensive than usually observed.
29954 Os 3881 Chl 1000 mg/l 96 h

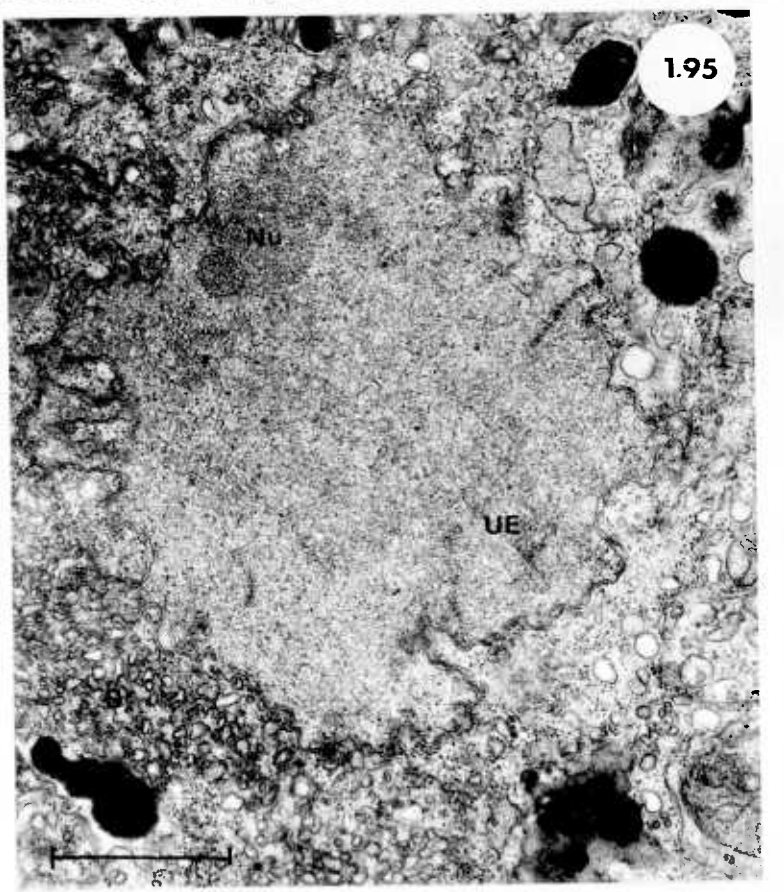
Fig. 1.97 Detail of the interphase centrioles associated with the nucleus in Fig. 1.94. Note the poor preservation of microtubule structure typical of Os-fixed material, and the characteristic end to end (180°) orientation.
21503 Os 3444 9 h

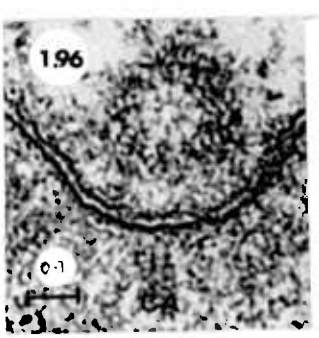
Fig. 1.98 Two pairs of centrioles shortly after separation and replication, associated with a prophase I nucleus.
21693 Os 3448 24 h

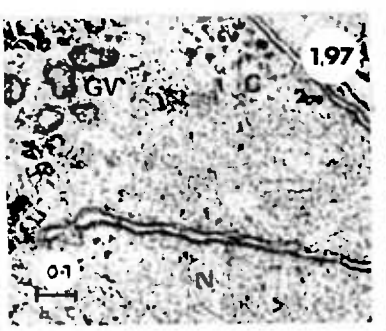

1.92
ER
C


1.93
Nu
UE


1.94
G
C
Nu


1.95
Nu
UE


1.96
0·1


1.97
GV
C
0·1
N

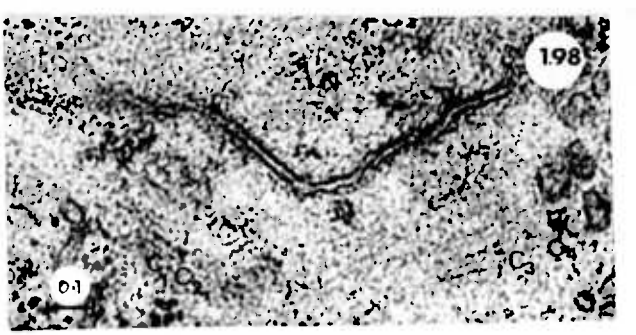

1.98
0·1

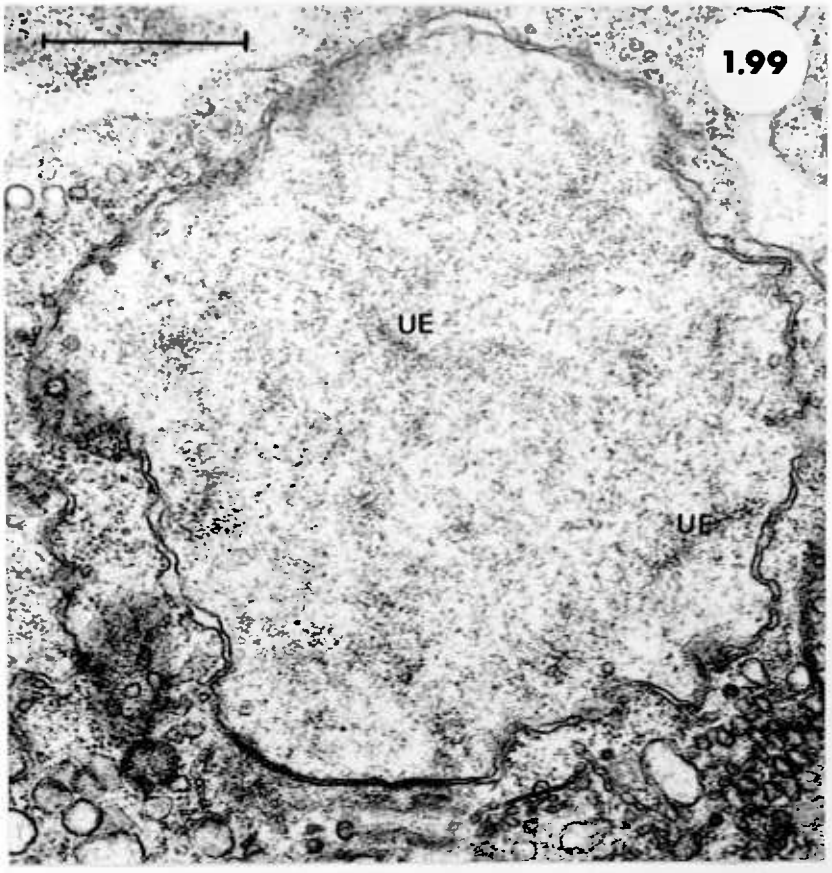
Fig. 1.99 A typical prophase I antheridial nucleus. Note the more electron transparent nucleoplasm and more regular outline than in comparable oogonial nuclei ((Fig. 1.95).
21321 Os 3446 24 h

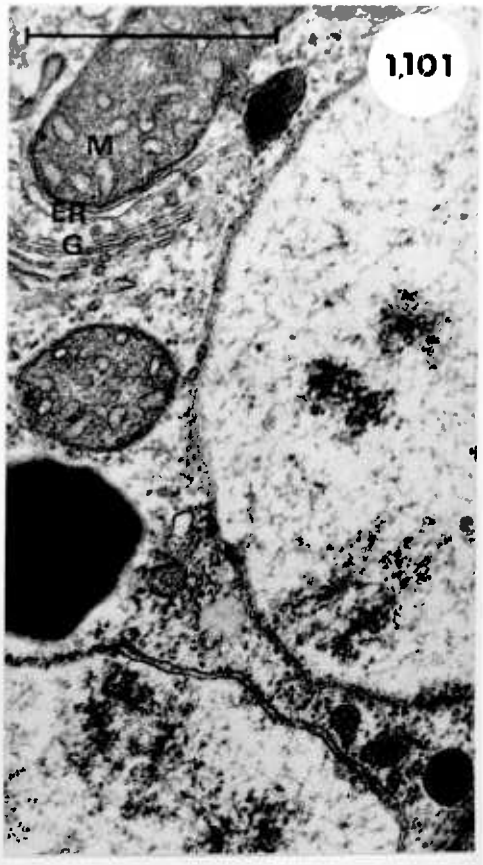
Fig. 1.100 An antheridial prophase I nucleus showing a pair of centrioles and well-defined uniaxial elements. Two of these terminate at the nuclear envelope opposite cytoplasmic microtubules.
29083 GaOs 3878 24 h

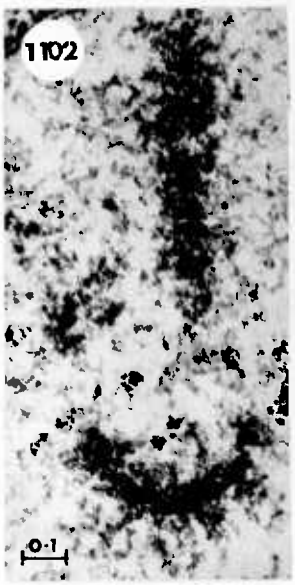
Fig. 1.101 Prophase I antheridial nuclei at a late zygotene-early pachytene stage. Note the association of lateral elements into well defined pairs. There is no evidence of SC development between these paired elements.
23150 GaOs 3452 48 h

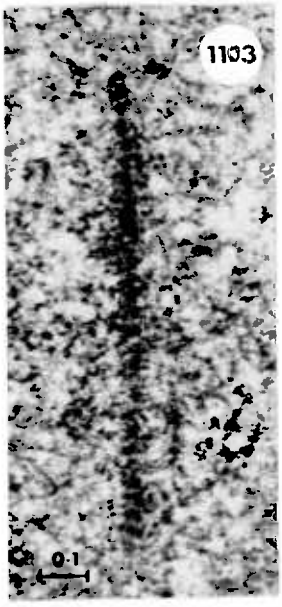
Fig. 1.102 Detail of an uniaxial element in a GaOs-fixed nucleus, showing its dense particulate substructure.
22140 GaOs 3452 48 h

Fig. 1.103 Detail of an uniaxial element in an Os-fixed nucleus, which is narrower and less conspicuous than GaOs-fixed body.
22059 Os 3451 Str 50 mg/l 48 h


1.99
UE
UE


1.101
M
ER
G


1102
0·1


1103
0·1

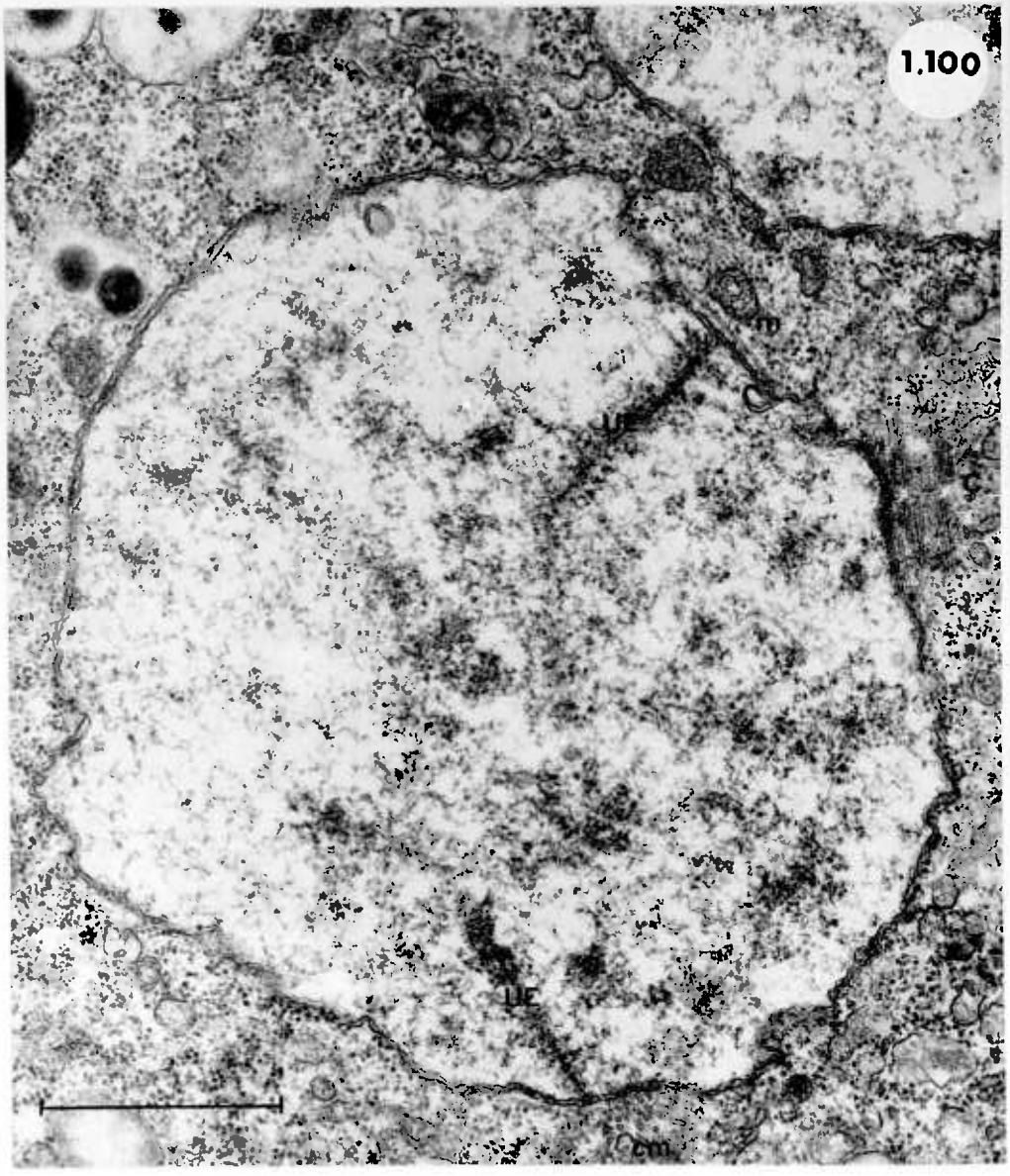
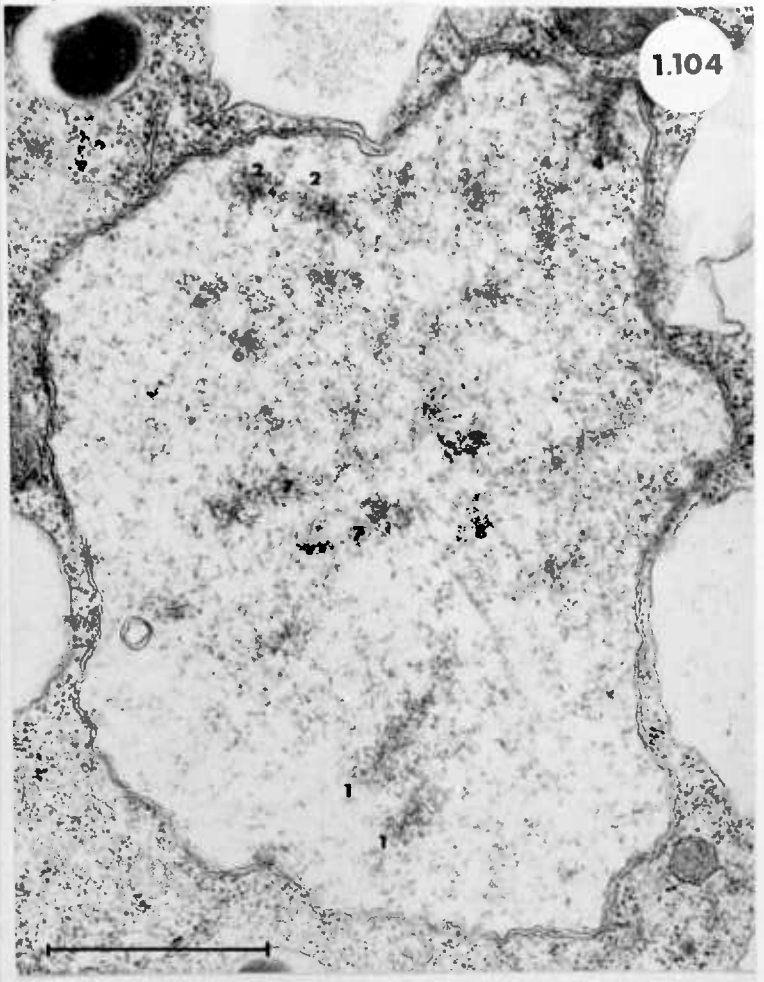

1.100
UE
cm

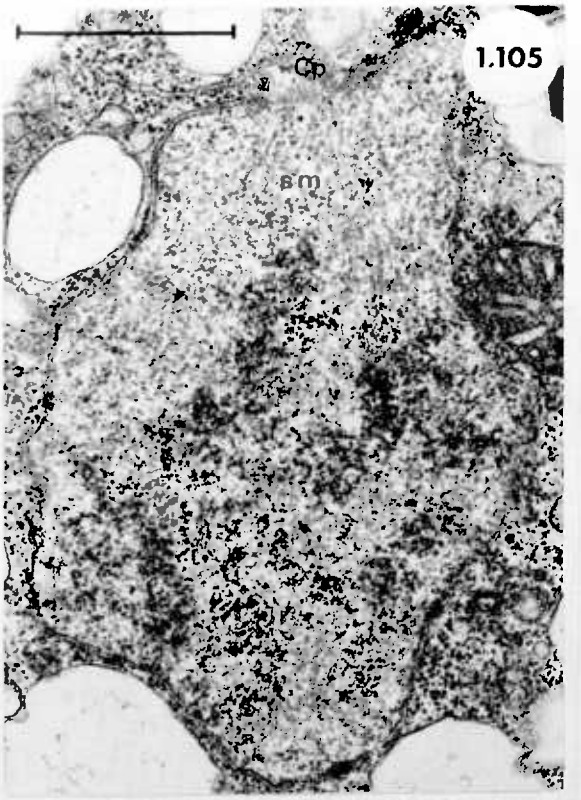
Fig. 1.104 Late prophase I nucleus in oogonium showing signs of paired unaxial elements (indicated by numbers), and the appearance of intranuclear spindle microtubules.
29198 GaOs 3878 24 h

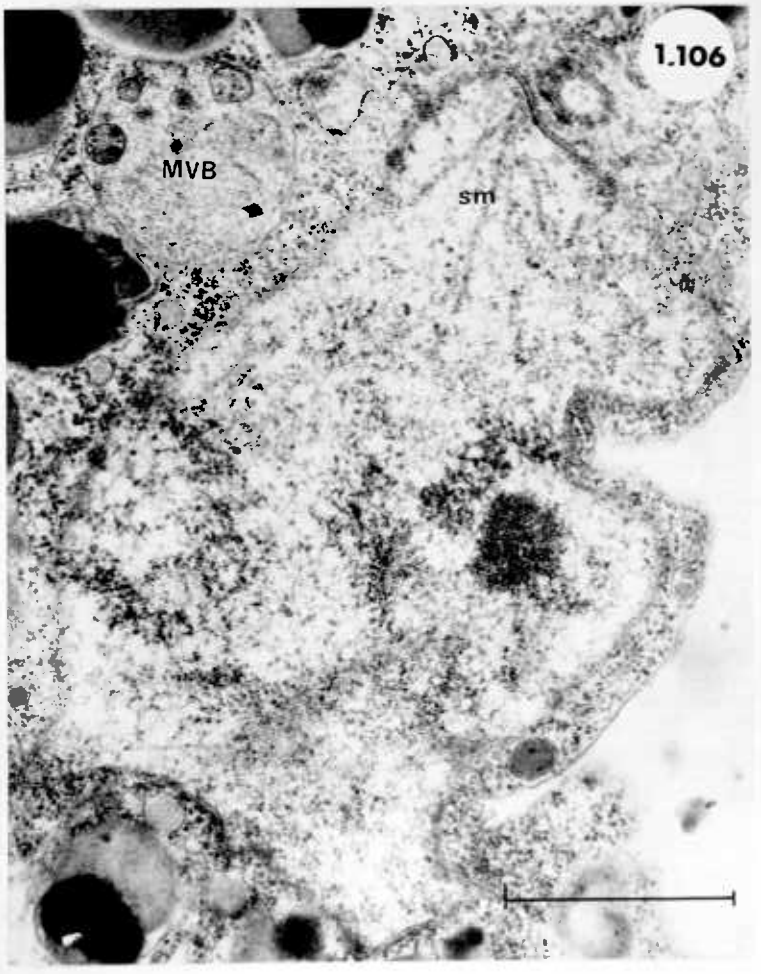
Fig. 1.105 A comparable antheridial prophase I nucleus to that shown in Fig. 1.104. The chromatin is now diffuse and is becoming aligned along the nuclear equator. Intranuclear spindle microtubules terminate adjacent to the centriolar pocket, as in mitotic divisions.
29177 GaOs 3887 24 h

Fig. 1.106 An oblique profile of a metaphase I nucleus in an oogonium showing the chromatin aligned in the equatorial region. The lateral nucleolus is still present.
22125 GaOs 3452 48 h

Fig. 1.107 An elongate anaphase I nucleus in an oogonium showing the separation of the diffuse chromatin along the intranuclear spindle which extends between the two pairs of polar centrioles.
46951 GaOs 3665 24 h


1.104
2
2
1
1


1.105
Cp
sm


1.106
MVB
sm

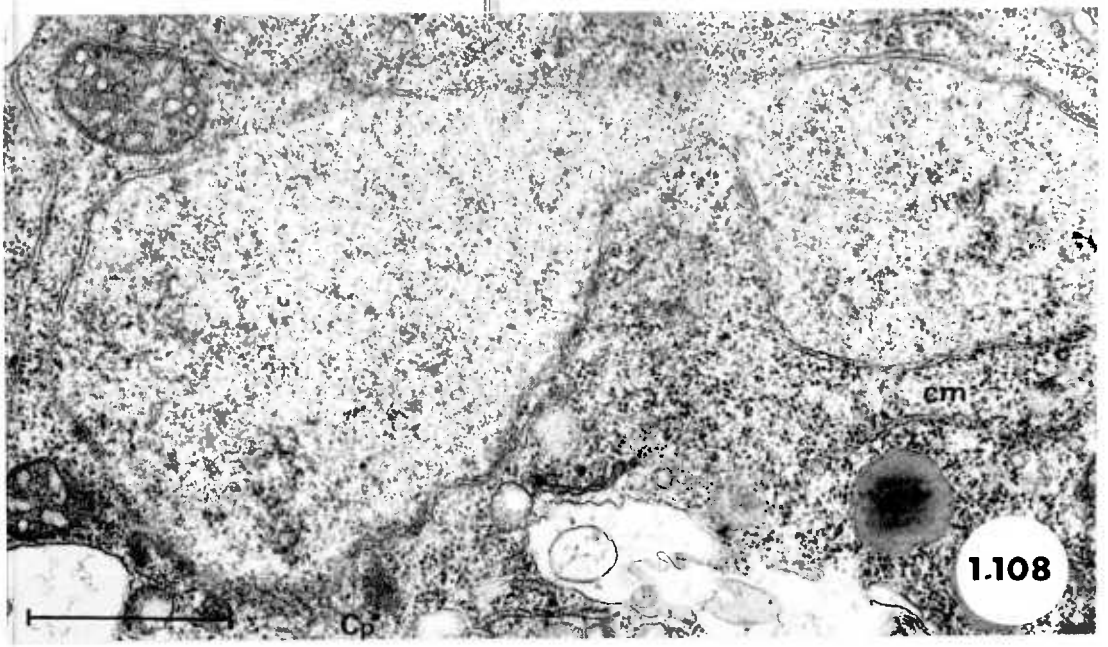

1.107
C
C

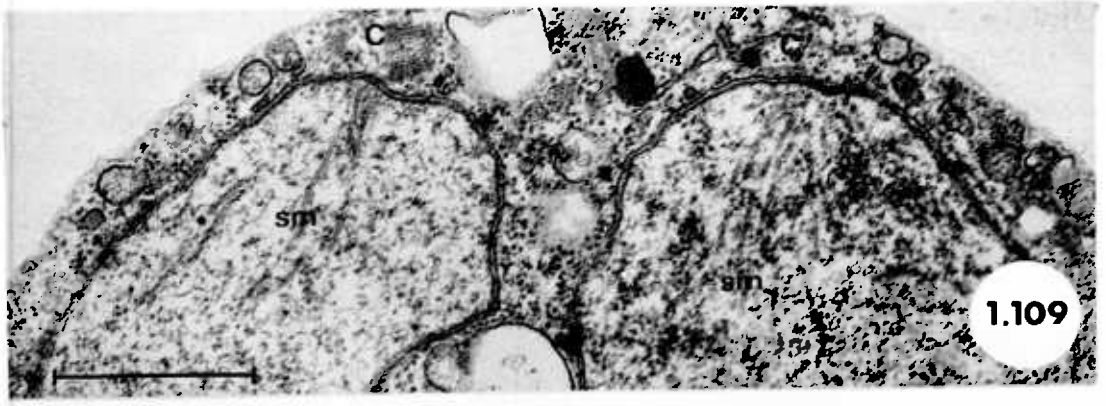
Fig. 1.108 A dumbell shaped nucleus at late telophase I in an antheridium, showing the separating products of the first nuclear division. The nucleoplasm is regaining its particulate structure. Centriolar position determined from serial section is marked Cp.
29164 GaOs 3883 24 h

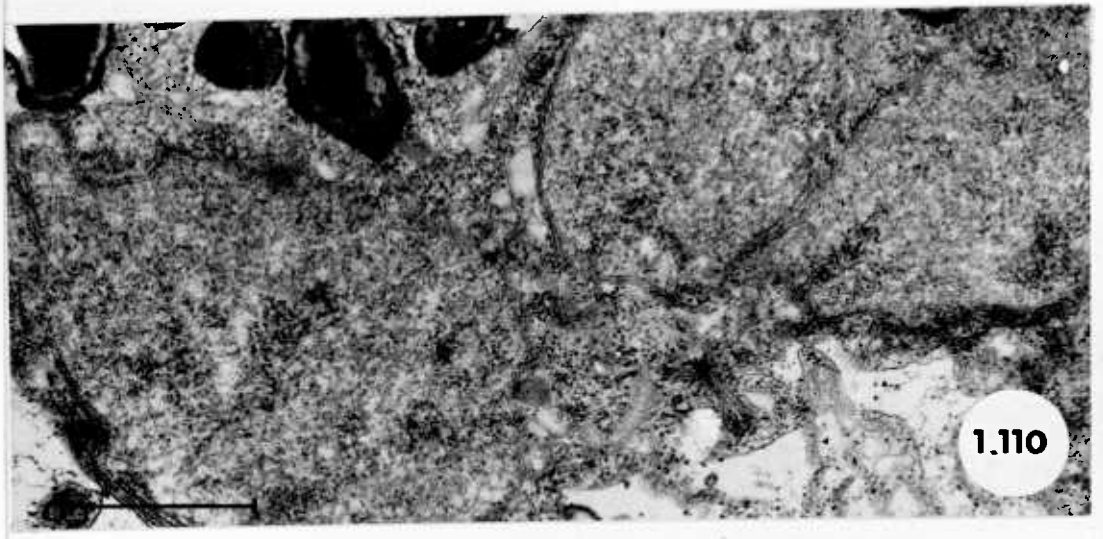
Fig. 1.109 Two adjacent nuclei in an antheridium with their spindles orientated in the same plane. Serial sections show there is only a single centriole located at each nuclear pole. This suggests these nuclei are in a second divisional stage of meiosis.
29161 GaOs 3883 24 h

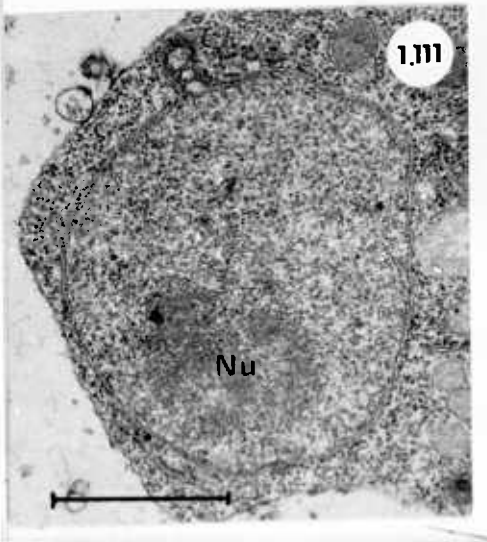
Fig. 1.110 Three adjacent nuclear profiles in a Stage IV oogonium. All three contain spindle microbutules indicating they are in division.
24429 GaOs 2395 24 h

Fig. 1.111 A post divisional gametic nucleus in a Stage V antheridium. Note the dense particulate nucleoplasm and diffuse nucleolus.
27550 GaOs 3931 24 h


cm
Cp
1.108


C
C
sm
sm
1.109


1.110


1.111
Nu

1.2.3.5 Centriolar changes during meiosis in S.furcata

Fig. 1.113 LS of a centriole pair associated with an early prophase I antheridial nucleus. They show a normal interphase structure (cf. Fig. 1.97) except they have slightly longer triplet microtubules.
29083 GaOs 3878 24 h

Fig. 1.114 An LS of a centriole pair associated with a late prophase I antheridial nucleus, showing the presence of a sheath of electron dense material enveloping the distal part of each centriole.
29117 GaOs 3878 24 h

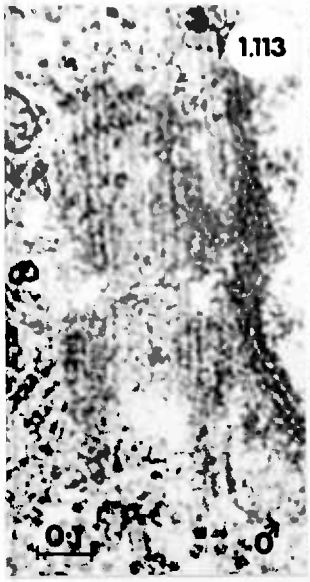
Figs. 1.115, 1.116 LS profiles of centrioles associated with anaphase I antheridial nuclei. Note how the centricles have separated and acquired a cap of endomembrane cisternae. Spindle microtubules terminate adjacent to the centriolar pockets.
25147 GaOs 3452 48 h
58016 3665 24 h

Fig. 1.117 TS of a centriole associated with an interphase oogonial nucleus, sectioned beyond the proximal cartwheel apparatus. Note the absence both of the sheath and endomembrane cap.
29173 GaOs 3883 24 h

Fig. 1.118 TS of a centriole associated with an anaphase I oogonial nucleus sectioned beyond the proximal cartwheel apparatus, showing both the amorphous sheath and the endomembrane cap. Some aster microtubules pass through pores in this cap and terminate at the sheath.
48107 GaOs 3668 24 h

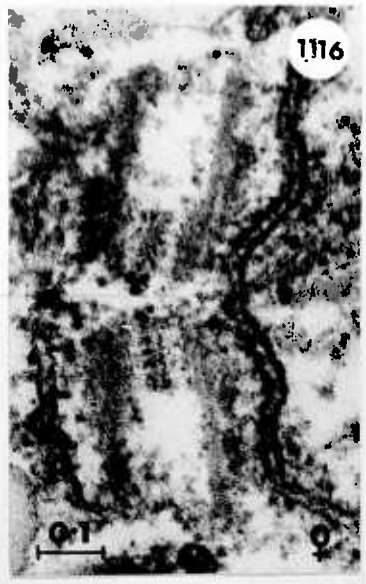
Fig. 1.119 Comparable TS of centriole associated with an anaphase I antheridial nucleus, showing fibrillar material radiating from the sheath. Microbutules are not preserved in this fixation.
22632 Os 3451 50 mg/l Str 48 h

Figs. 1.120, 1.121 Oblique serial sections through a centriole associated with a metaphase I oogonial nucleus. The nuclear envelope in face view shows the 80 nm pores. Abundant aster microtubules radiate from the region of the centriolar pocket.
22132 3452
22123

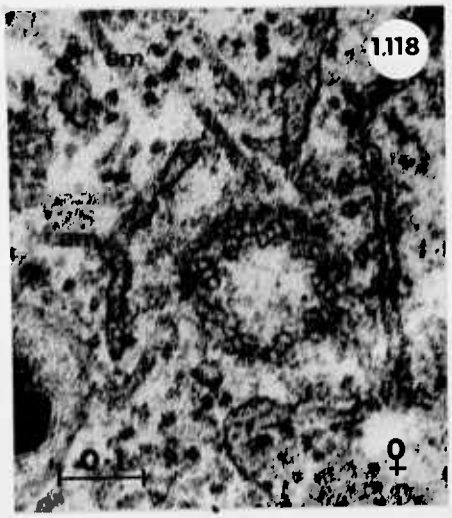

1.113
0·1

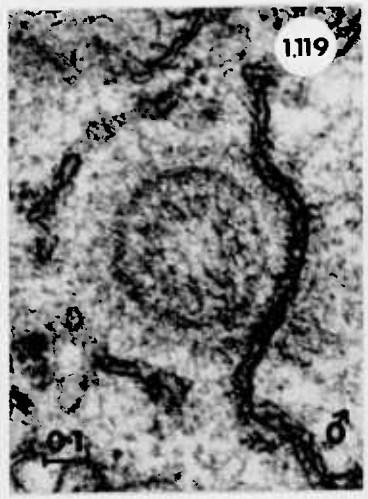

1.114
0·1

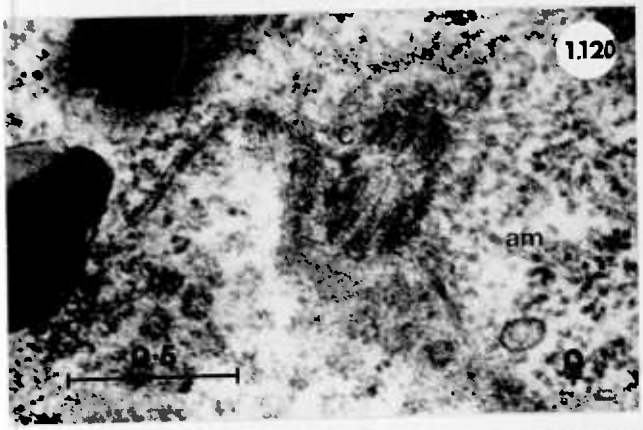

1.115
0·1

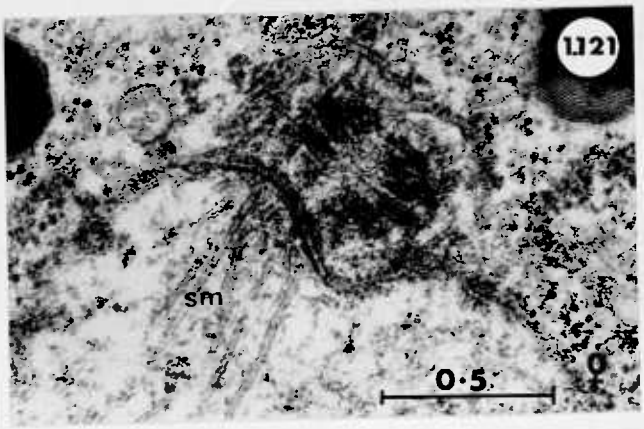

1.116
0·1

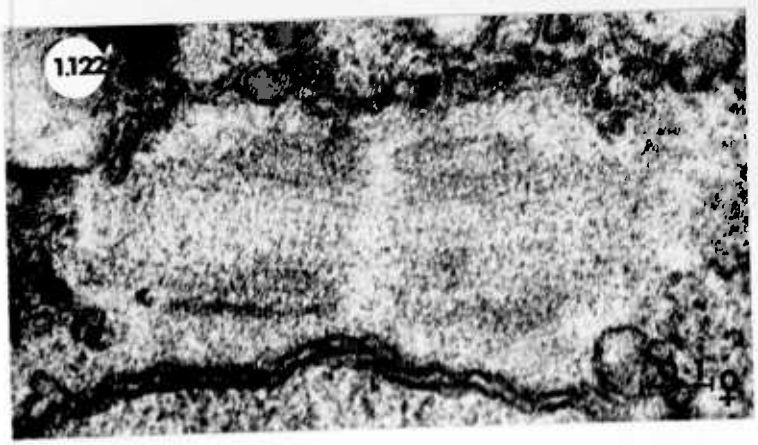

1.117
Ne
0·1


1.118
0·1


1.119
0·1


1.120
am
0·5


1.121
sm
0·5


1.122


1.123
0·1

Figs. 1.122, 1.123 LS and TS centriole profiles associated with late prophase I oogonial nuclei. The microtubules are poorly preserved in this Os fixation. Both the nucelar envelope and endomembrane cap are more irregular than in GaOs-fixed material. The divisions in the lamina spoke in LS profile can be detected.

22018 Os 3451 50 mg/l Str 48 h
22019

1.2.4 Oospore cleavage and oospore maturation in S.furcata

Fig. 1.124 Photographic sequence showing the differentiation and maturation of oospores in an oogonium. The figure in the top left corner of each frame indicates the time before and after cleavage. Times on frames 1-18 are in minutes, and in 19-36 in hours. The development of oospores can be conveniently considered in a number of stages, as shown in the following frames.
152/1-108 O.I. x 1400

Frames 1-3 Pre-cleavage phase during which the final stages in cleavage vacuole formation are completed.

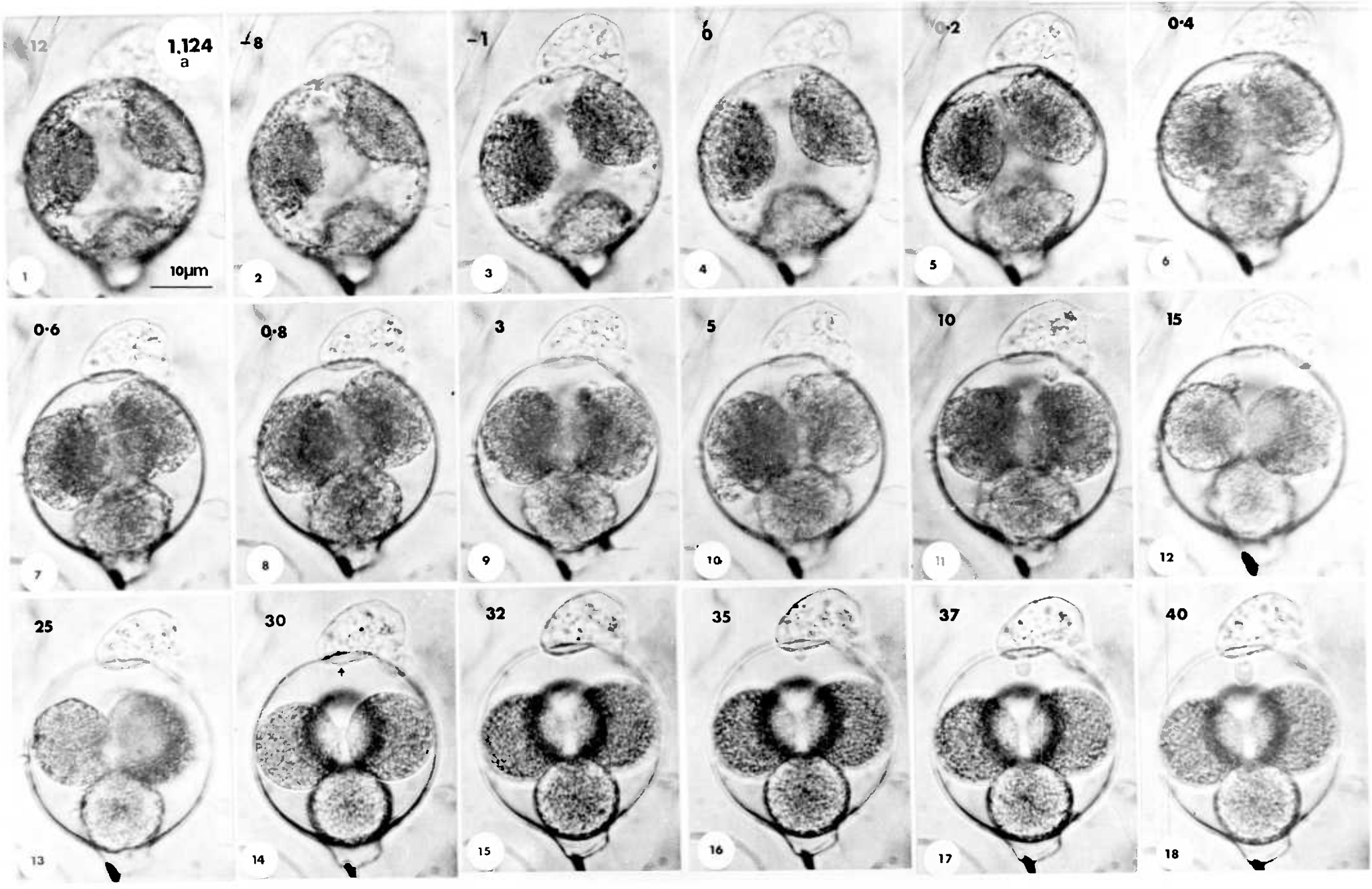
Frames 4-6 Cytoplasmic cleavage when the tonoplast fuses with the plasmalemma and the oospheres separate from the oogonium wall.

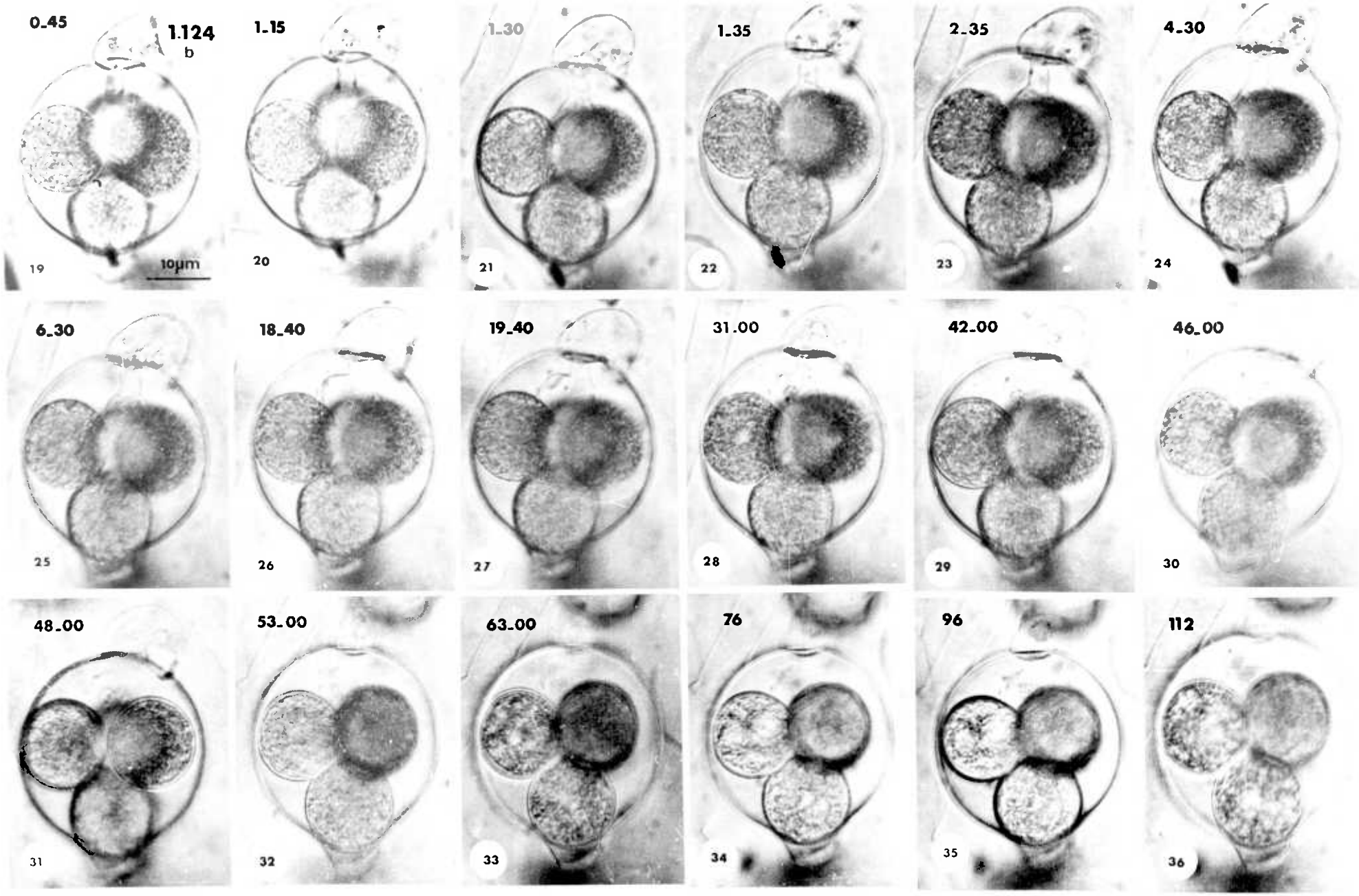
Frames 7-13 Naked cytoplasmic phase when the spores (Stage VI) have an irregular, changing outline accompanied by changes in spore volume. Cytoplasmic extrusion from these spores is shown in frames 9-12. The globule extruded from the top righthand spore (Frame 10) migrates across the intersporal space and appears to fuse with the lefthand spore (Frame 12).

Frames 14-27 The spores have a smooth spherical outline, indicating that the primary wall has formed, and uniformly dense contents (Stage VII). The development of the fertilisation tube from the antheridium is shown in Frames 14-20.

Frames 28-31 The thick refractile inner endospore wall is accreted and the spore cytoplasm becomes less uniform in appearance (Stage VIII). The conspicuous transparent bodies seen in Frame 28 are probably the pre-fusion oospore nuclei.

Frames 32-36 Internal vacuoles appear in the oospore cytoplasm, which expand by coalescence to form the single ooplast vacuole (Frame 36) (Stage IX).

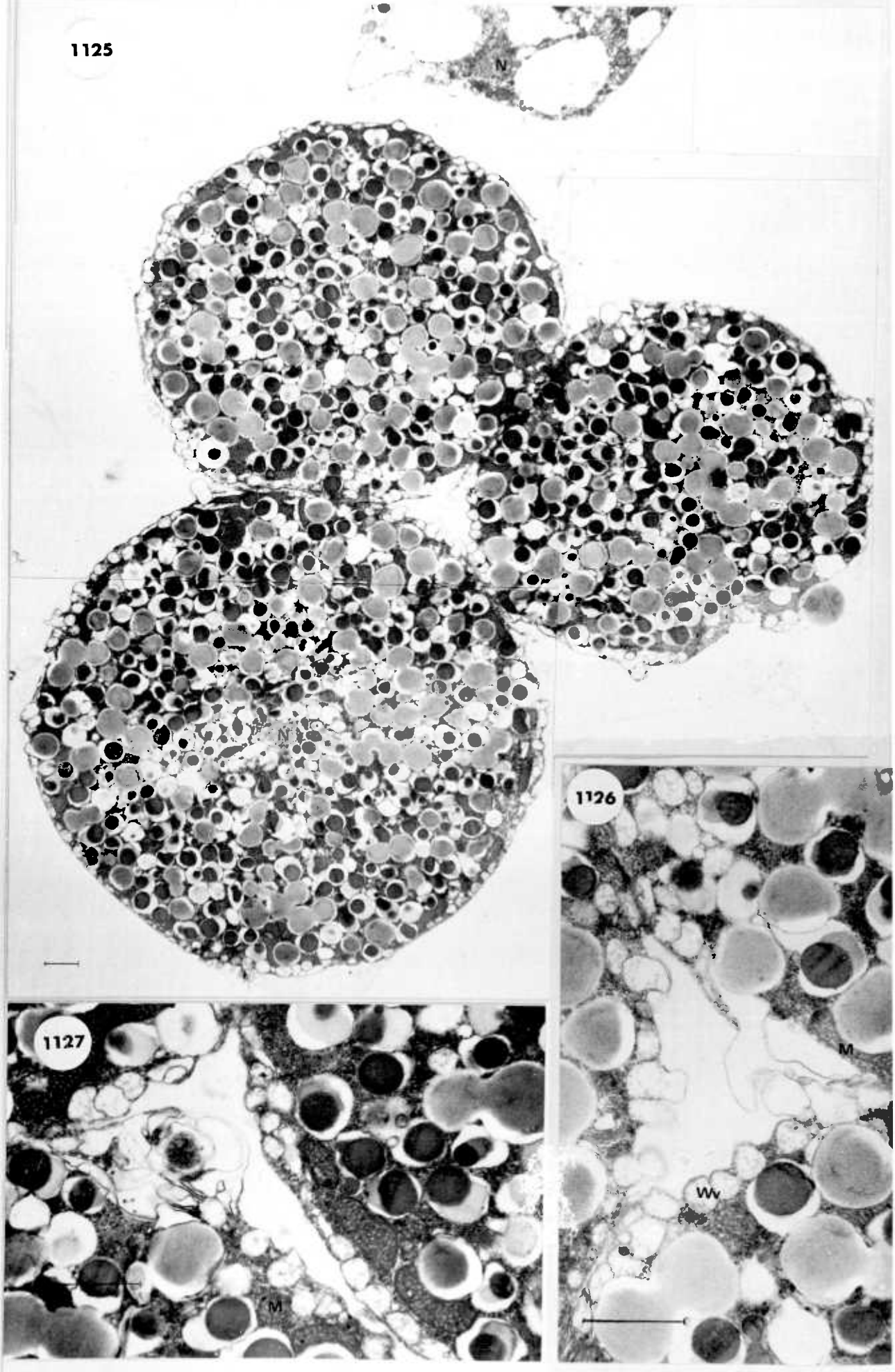

1.124
a
10µm
0·2
0·4
0·6
0·8
3
5
10
15
25
30
32
35
37
40


0_45
1.124
b
19
10µm
1_15
20
1_30
21
1_35
22
2_35
23
4_30
24
6_30
25
18_40
26
19_40
27
31.00
28
42_00
29
46_00
30
48_00
31
53_00
32
63_00
33
76
34
96
35
112
36

1.2.4.2 Stage VI oospheres of S.furcata

Fig. 1.125 Montage through three prewall oospheres and part of an antheridium. These spores show a characteristically irregular outline and clearly lack a cell wall. Droplets of neutral lipid and densebody vesicles are randomly distributed throughout these spores.
50819-21 GaOs 3665 24 h

Figs. 1.126-1.127 Serial sections through the peripheral cytoplasm of the 3 oospores shown above in Fig. 1.125, showing the peripheral wall vesicles and localised membraneous evaginations, composed of both plasmalemma and cytoplasmic membranes.
50836 GaOs 3665 24 h
50822


1125
N
N
1126
M
Wv
1127
M

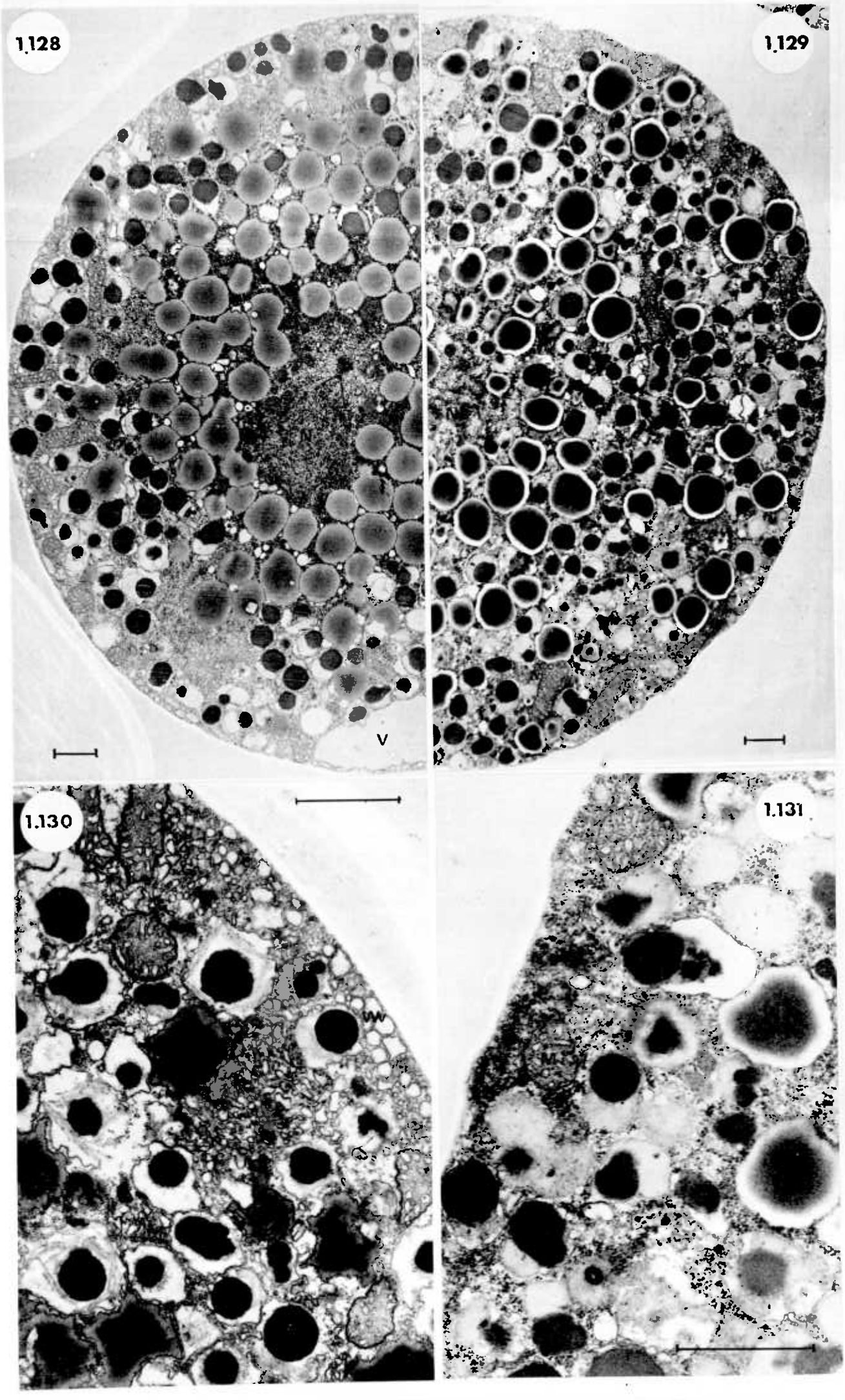
1.2.4 Stage VII oospores of S.furcata

Fig. 1.128 A typical Stage VII oospore showing the thin primary wall. The densebody vesicles are mostly peripherally distributed as are the mitochondria and the single vacuolar vesicle. The pyriform nucleus lies near the spore centre and is surrounded by droplets of neutral lipid.
29578 GaOs 3716 24 h

Fig. 1.129 Late Stage VII spore immediately prior to endospore wall formation. The lipid droplets and densebody vesicles are again becoming intermixed.
27563 GaOs 3452 48 h

Fig. 1.130 The peripheral cytoplasm of an early Stage VII spore showing that peripheral wall vesicles and active Golgi dictyosomes are still present at this stage.
29525 Os 3830 48 h

Fig. 1.131 The peripheral cytoplasm of a late Stage VII spore. Note the absence of wall vesicles and Golgi dictyosomes. The densebody vesicle matrix is considerably expanded and contains myelin configurations.
27561 GaOs 3452 48 h


1.128
V
1.129
1.130
1.131

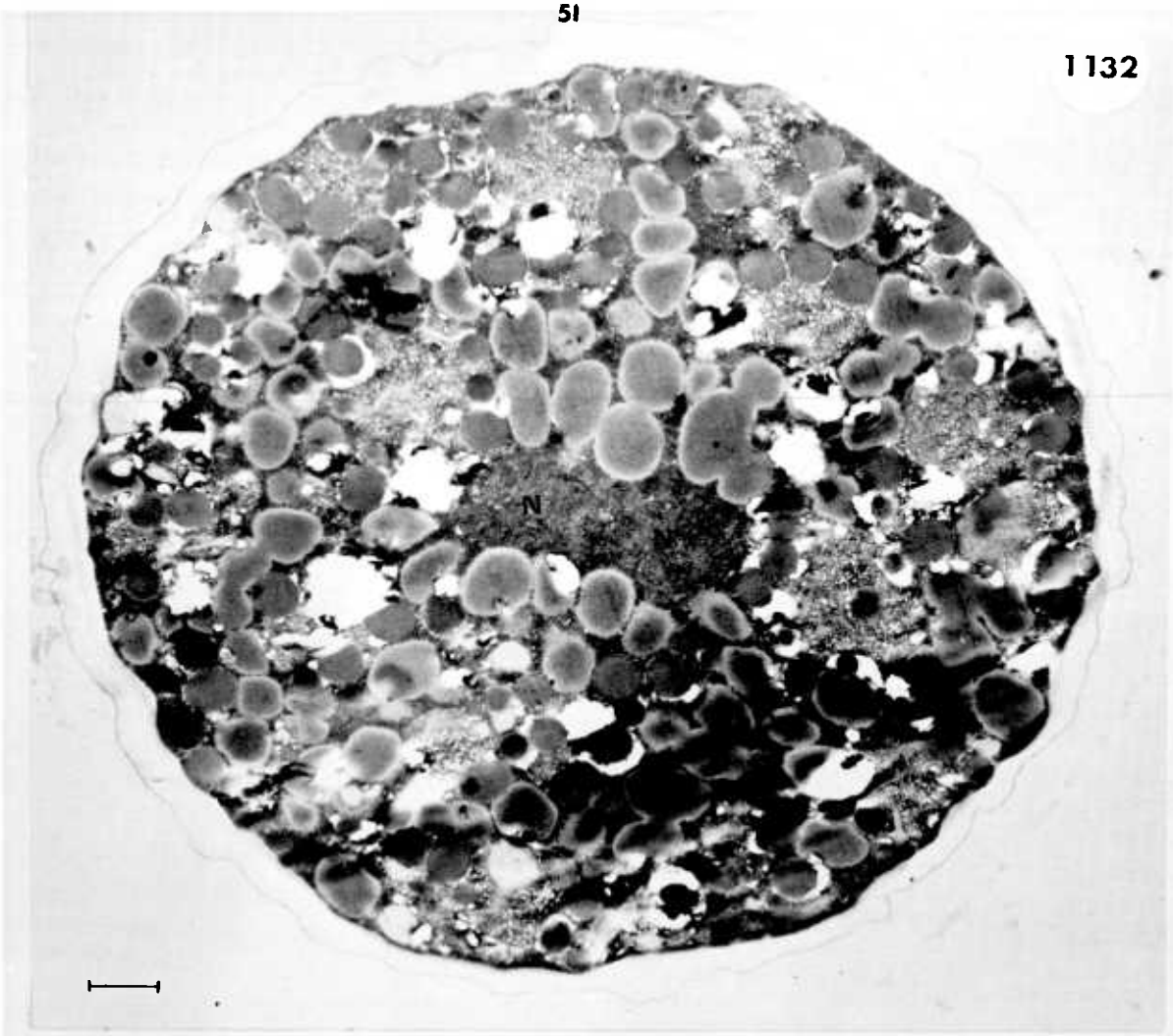
1.2.4.3 Stage VII oospores of S.furcata: Endospore wall formation

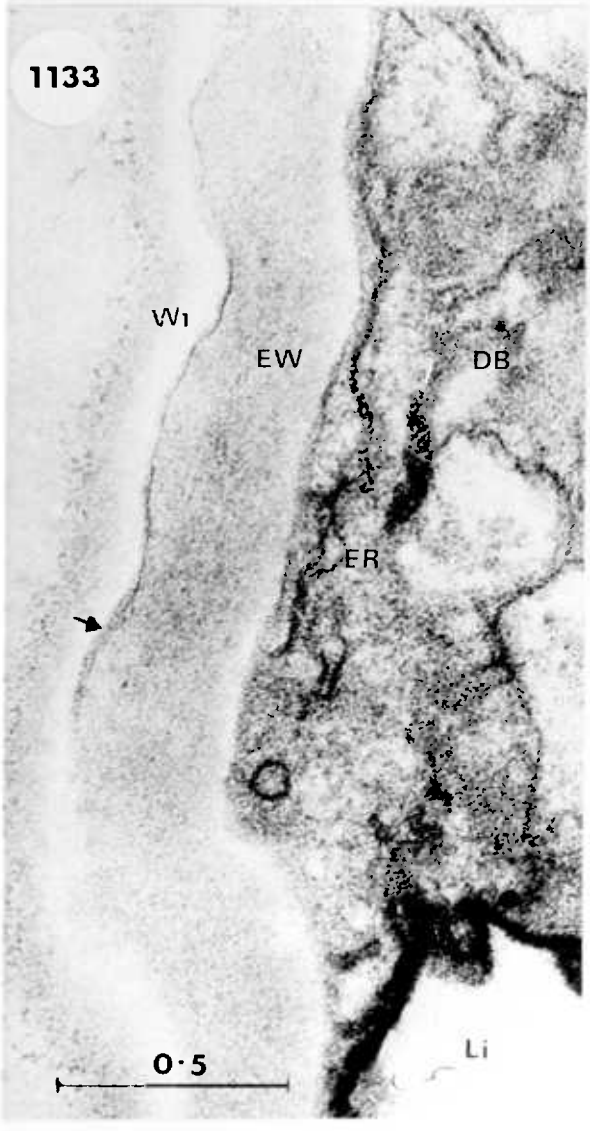
Fig. 1.132 Stage VII spore showing a well developed endospore wall layer. The quality of cytoplasmic organelle preservation is poor and typical of the fixation at this stage. However two nuclear areas can be discerned in the spore centre, and the densebody vesicles are beginning to aggregate together.
27533 GaOs 3452 48 h

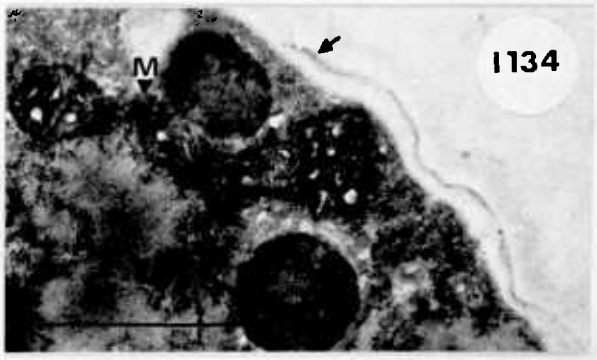
Fig. 1.133 Detail of the peripheral cytoplasm of a spore showing a developing endospore wall. Note the absence of wall vesicles in the peripheral cytoplasm. A faint tripartite membrane-like structure is present (arrowed) between the primary and the endospore walls.
31014 $KMnO_4$ (2% 5 min) 3954 48 h

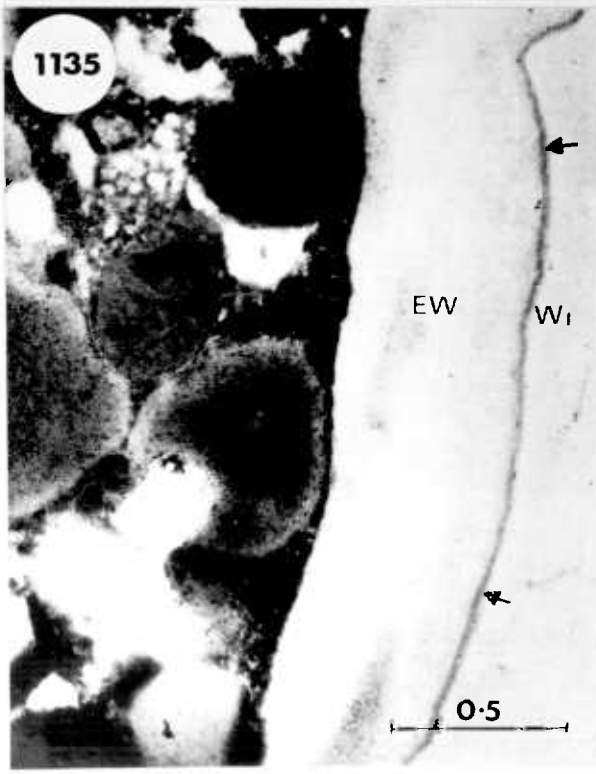
Fig. 1.134 Peripheral cytoplasm of a spore immediately following the initiation of endospore wall acretion. Even though the endospore layer is barely 100 nm thick, the preservation of cytoplasmic organelles is already poor. A collapsed mitochondrion is just recognisable. The thin membrane-like layer between the primary wall and the endospore is also shown.
27562 GaOs 3452 48 h

Fig. 1.135 Detail of an almost completely developed endospore wall showing a completely electron transparent structureless appearance characteristic of GaOs fixation. The tripartite layer between the primary and endospore wall layers is shown.
27554 GaOs 3482 120 h


1132
N


1133
W1
EW
DB
ER
Li
0·5


1134
M


1135
EW
W1
0·5

1.2.4 Stage IX oospores of S.furcata: Ooplast vacuole development

Figs. 1.136-1.140 A series of light micrographs showing the development of ooplast vacuoles within the spore cytoplasm.

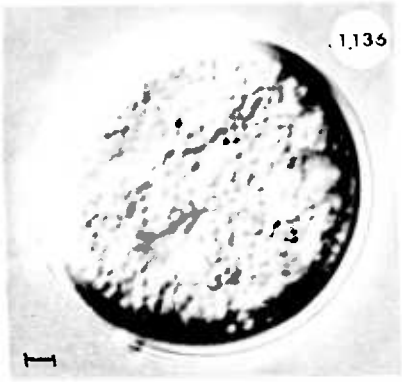
Fig. 1.136 An early Stage VIII spore showing small vacuoles between the lipid droplets.
109/18 NP x 3,500 72 h

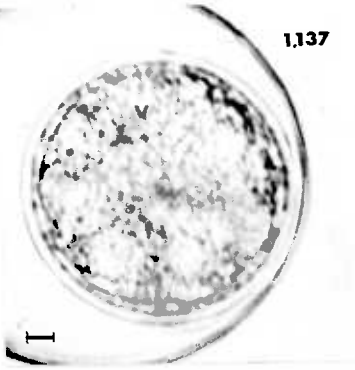
Figs. 1.137-1.140 A series of spores showing the progressive enlargement of ooplast vacuoles. Note throughout the development of the ooplast, the vacuoles are transparent and there is no sign of the granules which appear in mature spores (compare Fig. 1.140 and 1.144).
138/10 OI x 3000 72 h
109/5 OI x 3000 72 h
109/10 OI x 3500 72 h
122/5 OI x 2800 72 h

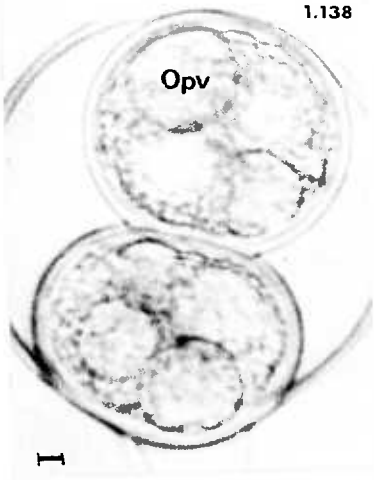
Fig. 1.141 An Os-fixed Stage VIII oospore showing 4 ooplast vacuoles in spite of the poorly-fixed cytoplasm. The contents of these vacuoles are not preserved although densebody granules are still attached to their edges.
21757 Os 3449 48 h

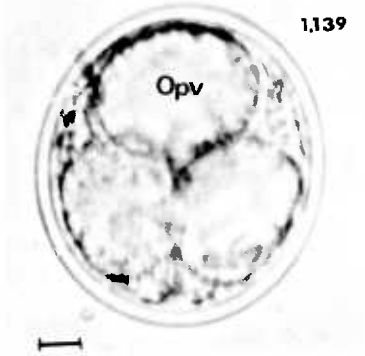
Fig. 1.142 Oospore developed in the presence of Cyc. (1 mg/l) showing 4 ooplast vacuoles with an osmiophilic matrix. Most of the densebody granules are missing.
27539 GaOs 3930 Cyc. 1 mg/l 96 h

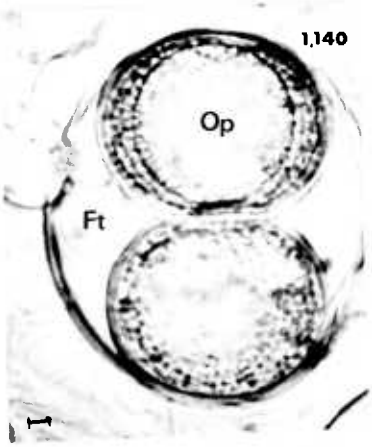
Fig. 1.143 A Cyc-induced oospore with a mature ooplast vacuole. The peripheral cytoplasm contains an orderly arrangement of lipid droplets. The osmiophilic matrix has been partially folded during preparation.
27531 GaOs 3930 Cyc. 1 mg/l 96 h

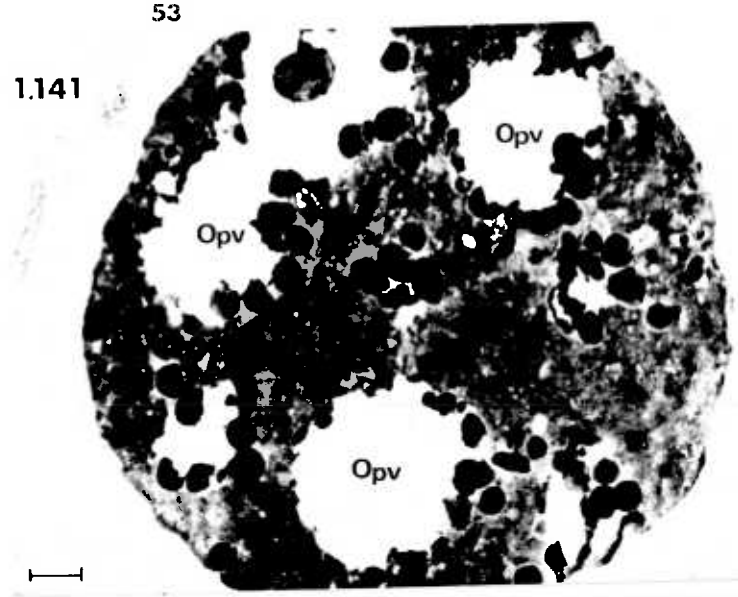

1.136

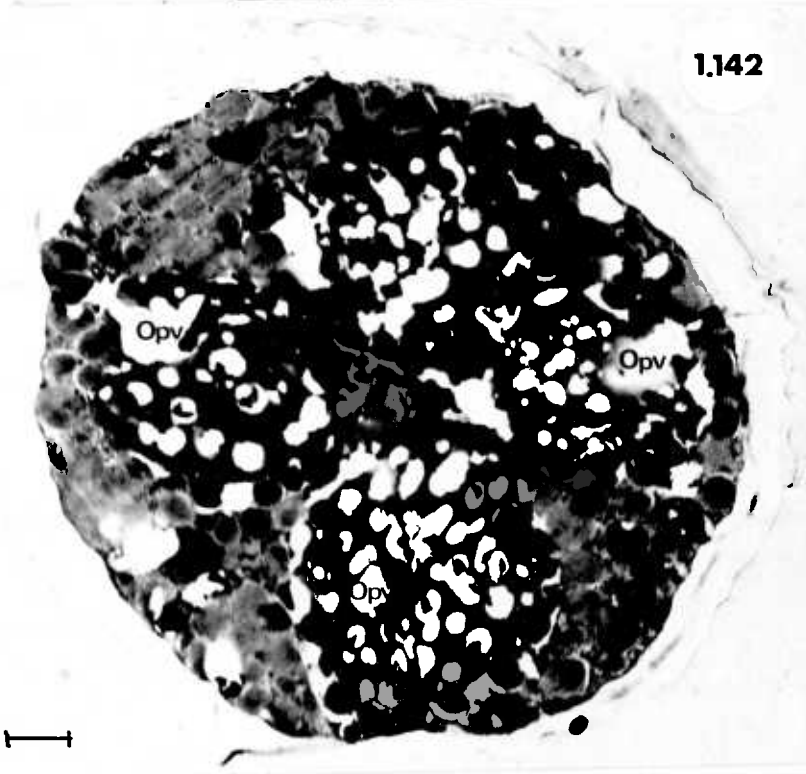

1.137

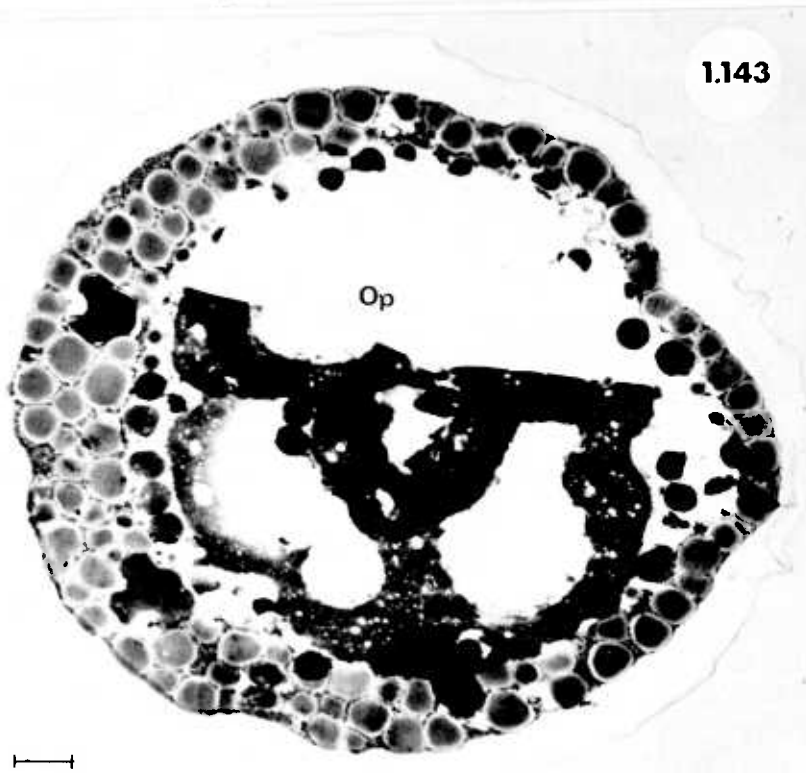

1.138
Opv


1.139
Opv


1.140
Op
Ft


1.141
Opv
Opv
Opv


1.142
Opv
Opv
Opv


1.143
Op

1.2.4 Stage X oospores of S.furcata

Figs. 1.144-1.147 Light micrographs of mature oospores.

Fig. 1.144 Oogonium with a single oospore containing a single mature spore, showing an ooplast vacuole containing particles in Brownian motion. Note the refractile pellucid spot in the peripheral cytoplasm.
102/21 OI x 3,200 96 h

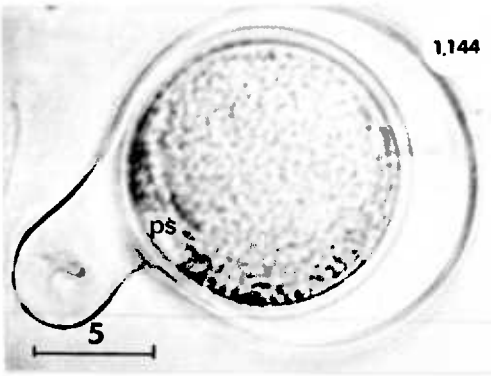
Fig. 1.145 Mature oogonium containing 3 mature oospores. Note that the ooplast vacuole in the lower spore is not completely surrounded by lipid droplets.
43/25 OI x 2,800 96 h

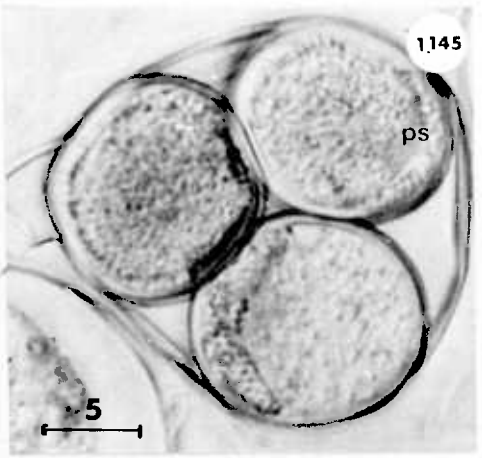
Fig. 1.146 An optical section through the peripheral lipid layer of 3 mature oospores. The pellucid spot can be seen in the upper spore.
109/17 NP x 3,200 96 h

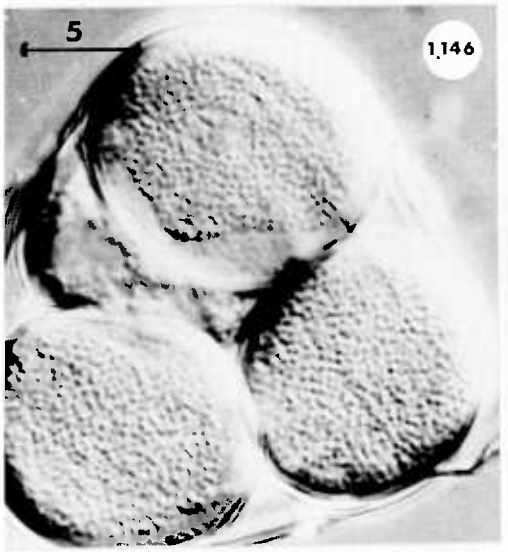
Fig. 1.147 Mature oospores under Nomarski optics, showing the boundary between the ooplast and the peripheral lipid containing cytoplasm. The ooplast granules and pellucid spots are clearly visible.
106/22 NP x 3,000 96 h

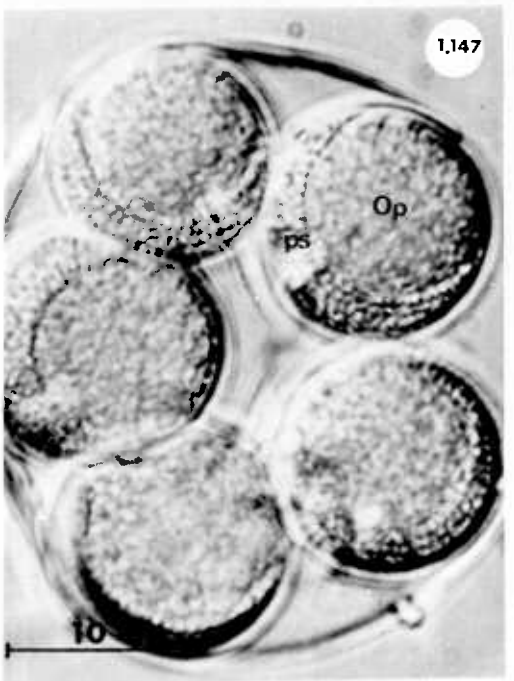
Fig. 1.148 A mature Os-fixed spore. The ooplast contents are not preserved and the peripheral cytoplasm is highly osmiophilic.
19789 Os 3314 168 h

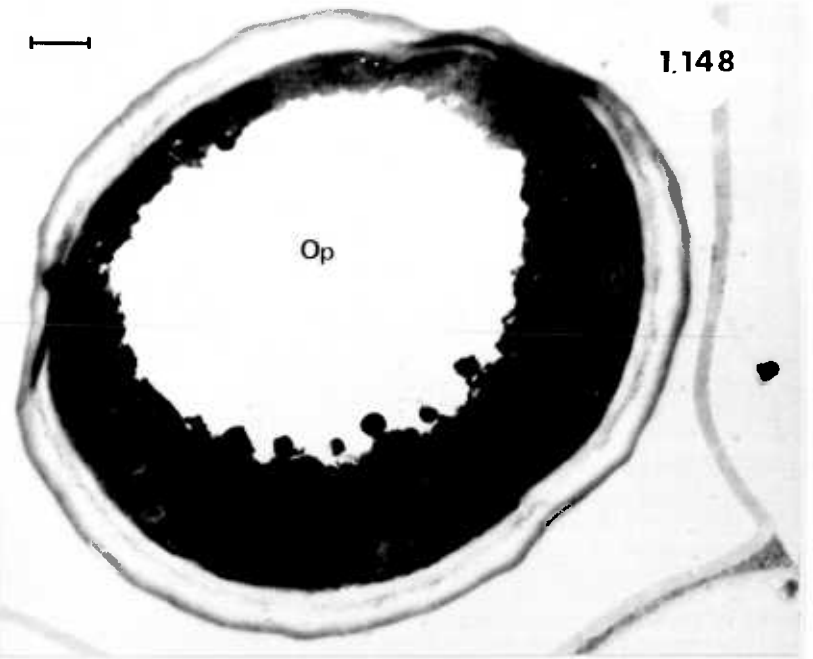
Figs. 1.149, 1.150 Two mature oospores showing the variety of spore appearances obtained with this fixative. The ooplast granules are well preserved, although the peripheral lipid droplets show signs of varying degrees of extraction. The position of the pellucid spot can be discerned, eventhough the internal membranes are not preserved.
23718 $KMnO_4$ (2% 5 min) Os 3480 240 h
31007 $KMnO_4$ (2% 25 min) Os 3954 96 h

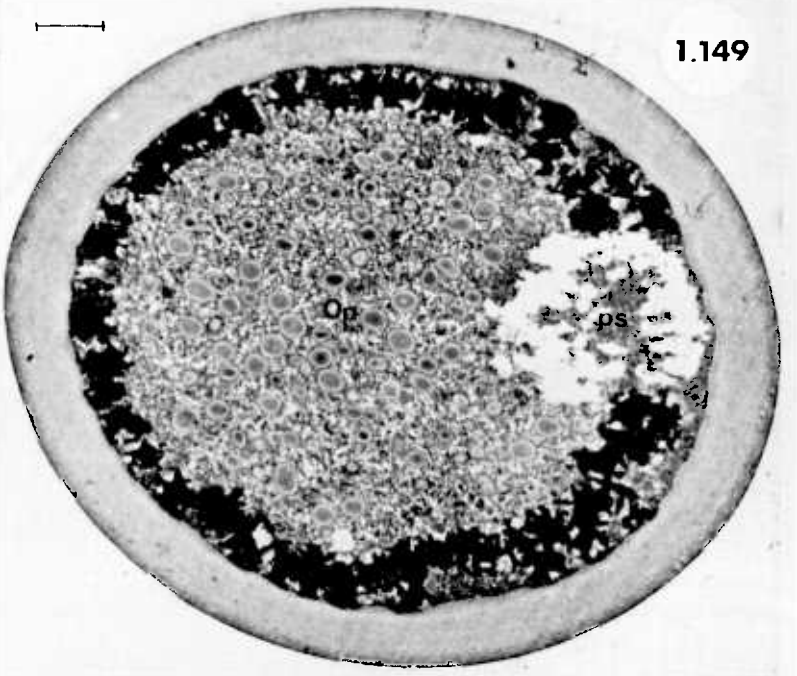

1.144
ps
5

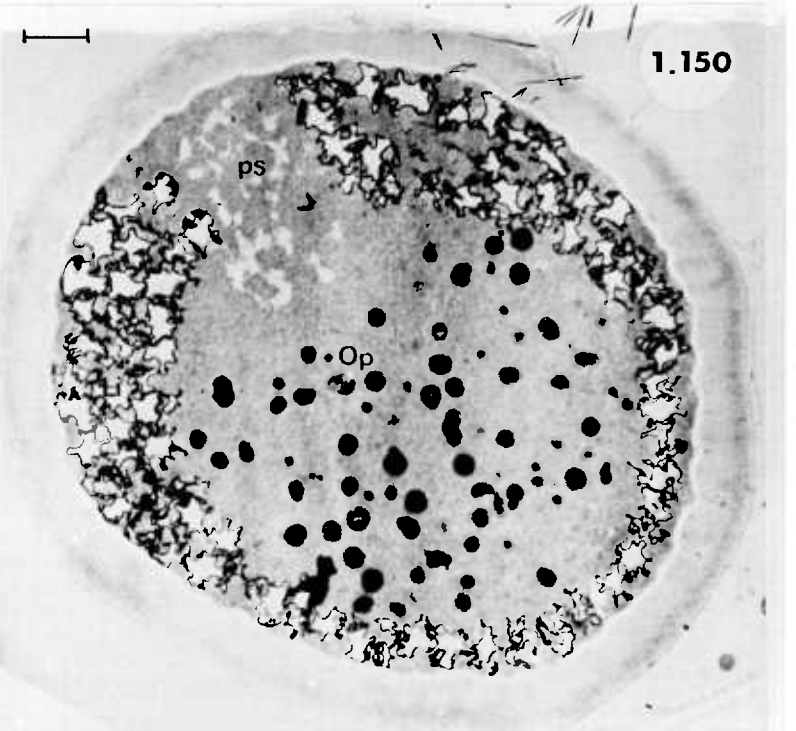

1.145
ps
5


5
1.146


1.147
Op
ps
10


1.148
Op

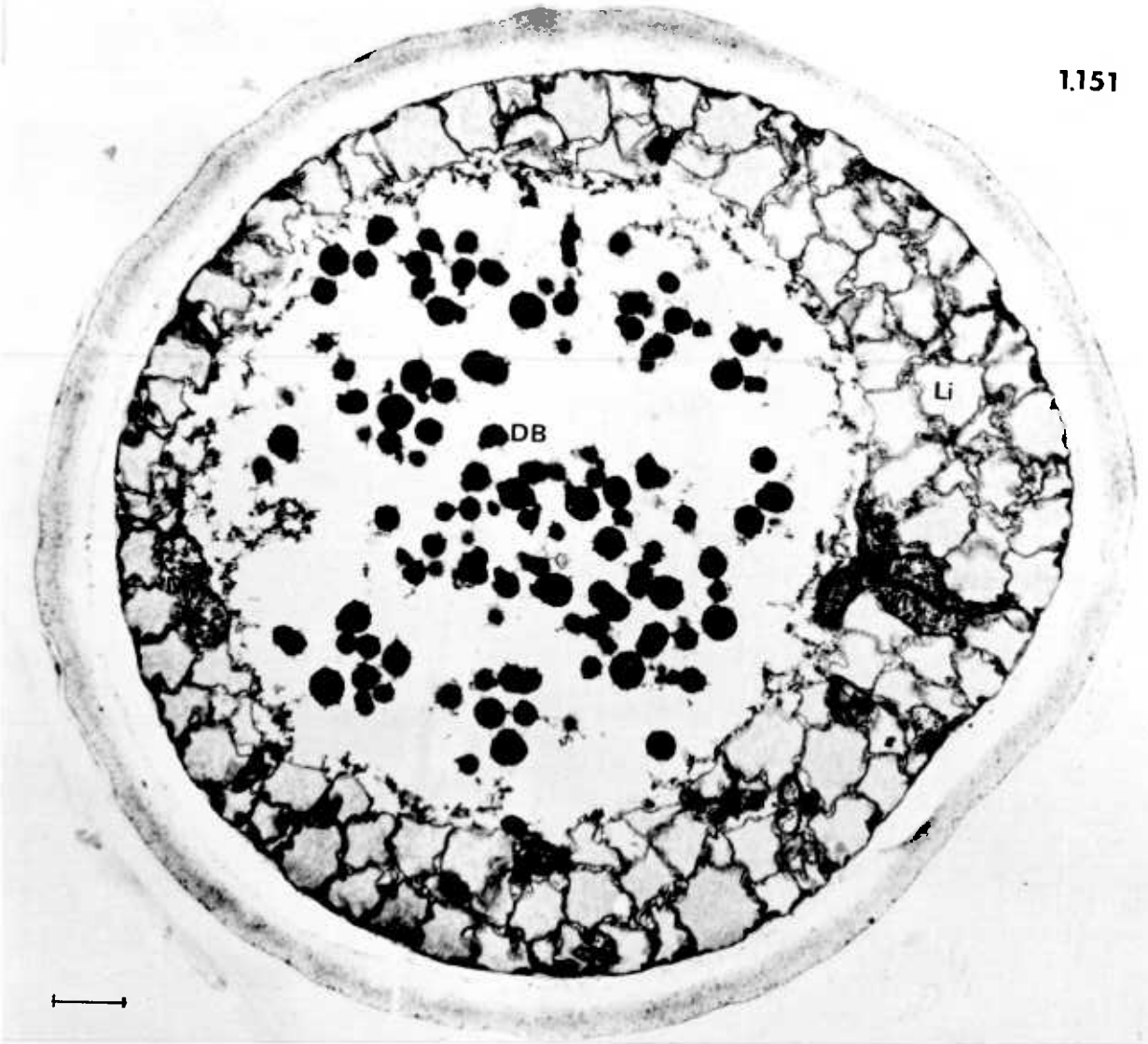

1.149
Op
ps

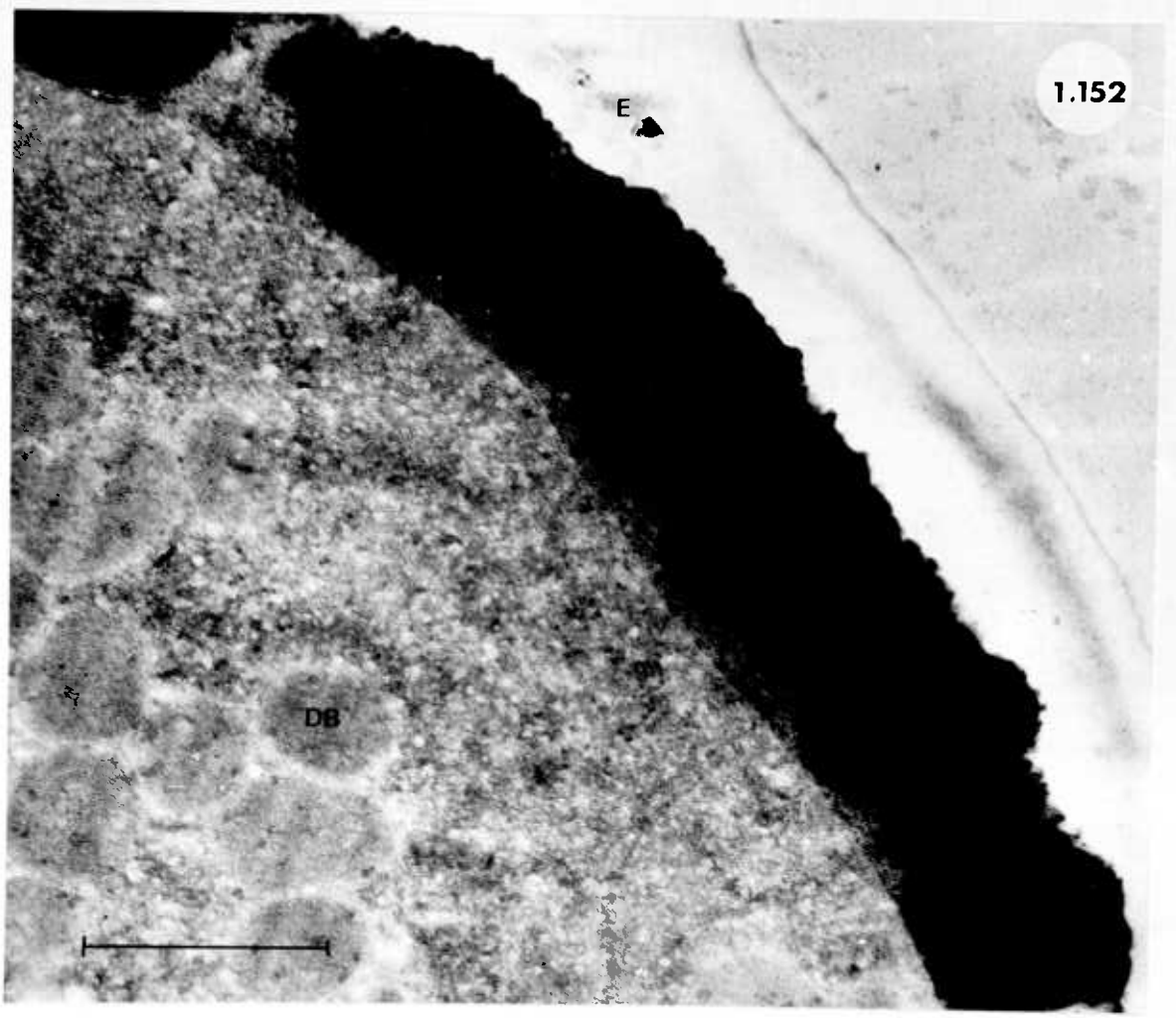

1.150
ps
Op

1.2.4 Mature Stage X oospores of S.furcata

Fig. 1.151 A comparatively well-preserved oospore after $KMnO_4$ fixation. The boundary between the ooplast and the peripheral cytoplams is well defined. The latter contains several mitochondria and other membranous inclusions. The endospore wall layer is comparatively thin and has atypical structure.
25667 $KMnO_4$ 9(2% 10 min) 3416 TW 96 h

Fig. 1.152 The peripheral cytoplasm of a mature GaOs fixed oospore induced in Str (100 mg/l). The boundary between the ooplast and peripheral cytoplasm is clearly shown, although the internal membranes are not preserved. Ooplast densebody granules are embedded in a relatively dense matrix.
23943 GaOs 3483 Str 100 mg/l 240 h


1.151
Li
DB


1.152
E
DB

1.2.4 Oospore wall morphology of S.furcata

Fig. 1.153 Wall of a Stage X spore showing the well defined inner electron dense layer. Note also the increased osmiophilia towards the primary wall.
25562 Os 3487 Str 50 mg/l 240 h

Fig. 1.154 Wall of a Stage X spore stained for polysaccharides by the PASM staining procedure. Silver granules are deposited approximately evenly throughout the endospore wall layer, but there is a much heavier deposit in the region of the primary wall-endospore boundary.
25562 Os 3487 Str 50 mg/l 240 h

Fig. 1.155 An abnormal $KMnO_4$-fixed oospore wall, showing the presence of osmiophilic islands and lamellate bands in the endospore wall.
25666 $KMnO_4$ (2% 10 min) 3416 TW 96 h

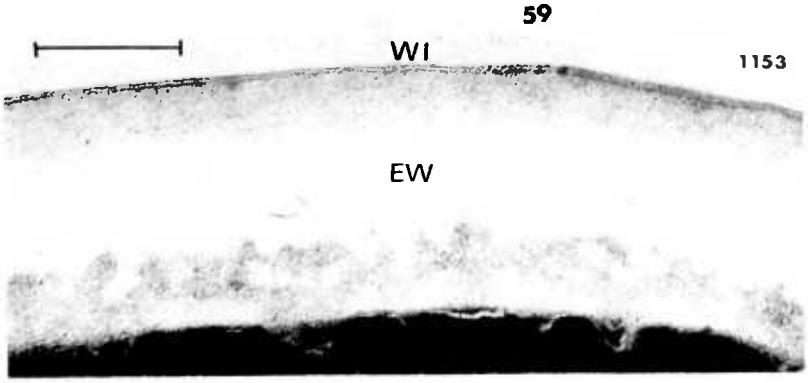
Figs. 1.156, 1.157 Two oospore walls from the same preparation showing the effect of different lengths of $KMnO_4$ fixation on endospore wall structure. The wall in Fig. 1.156 was fixed for 20 minutes and shows the osmiophilic inner layer, whereas the wall in Fig. 1.157 was only fixed for 5 minutes, and does not.
25706 3481 $KMnO_4$ (2% 20 min) Os 240 h
23488 3480 $KMnO_4$ (2% 5 min) Os 240 h

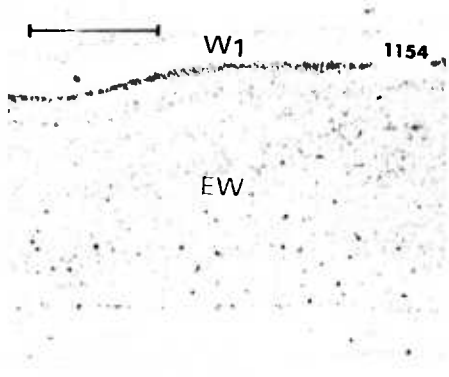
Fig. 1.158 An abnormal oospore wall induced by tap water. Osmiophilic islands are distributed throughout the endospore layer, and tripartite membrane-like layers can be seen bounding this wall on both sides. Note also the membranous whorls in the cytoplasm adjacent to the wall.
25971 Os 3669 TW 96 h

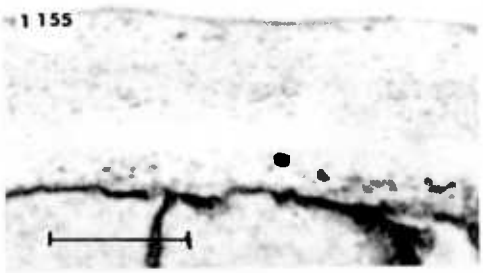
Fig. 1.159 Detail of the tripartite membrane at the outer surface of the endospore wall.
25882 $KMnO_4$ (2% 25 min) Os 3481 240 h

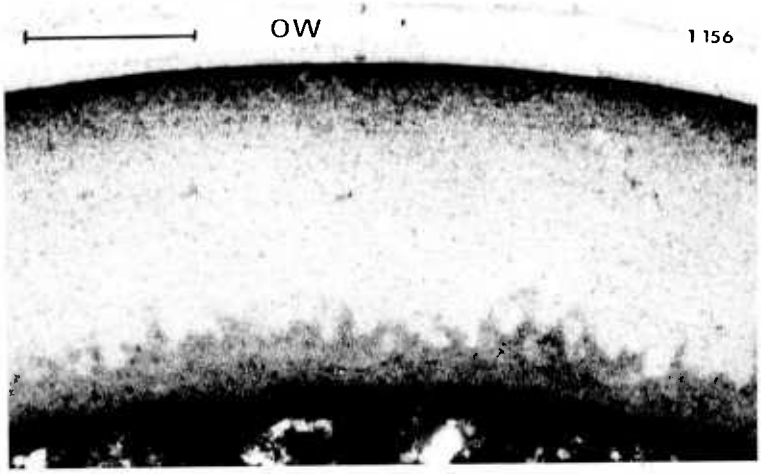
Fig. 1.160 Detail of the inner membrane between the endospore wall and the cytoplasm in a TW induced spore. Note its uneven contour.
25971 Os 3669 TW 96 h

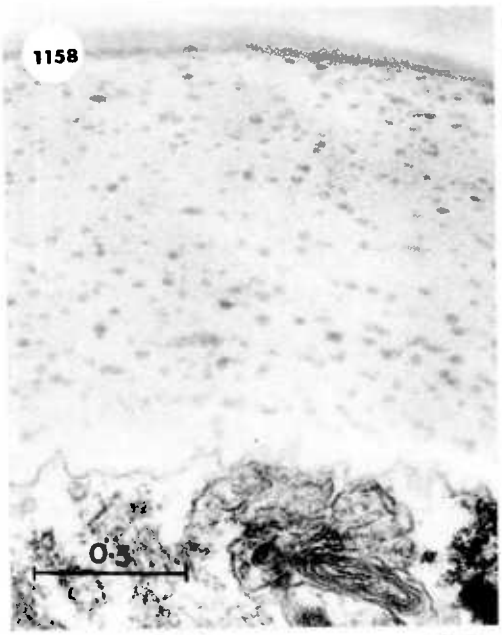
Fig. 1.161 A wall of TW-induced spore showing the two membranes associated with the endospore. The endospore layer is thinner than usual and contains small osmiophilic islands.
25930 Os 3617 TW 96 h

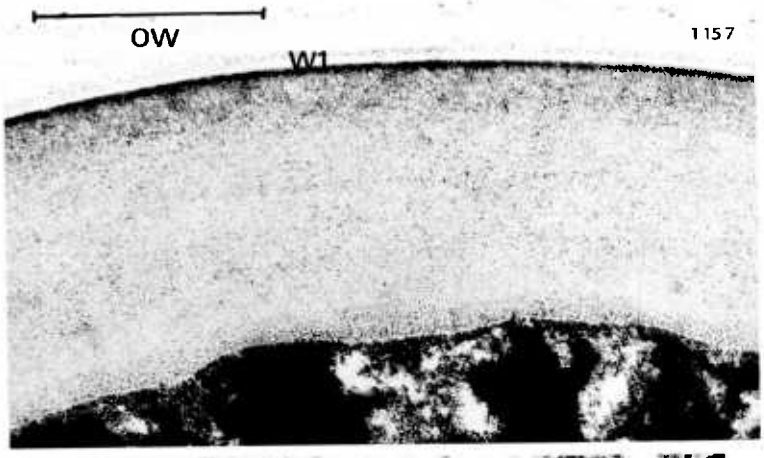

W1
1153
EW

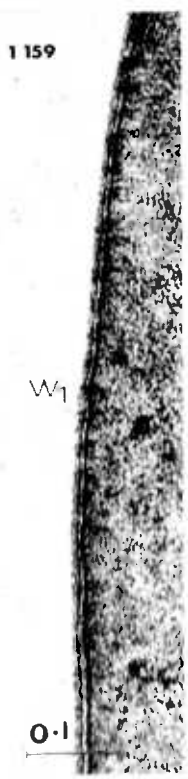

W1
1154
EW


1155

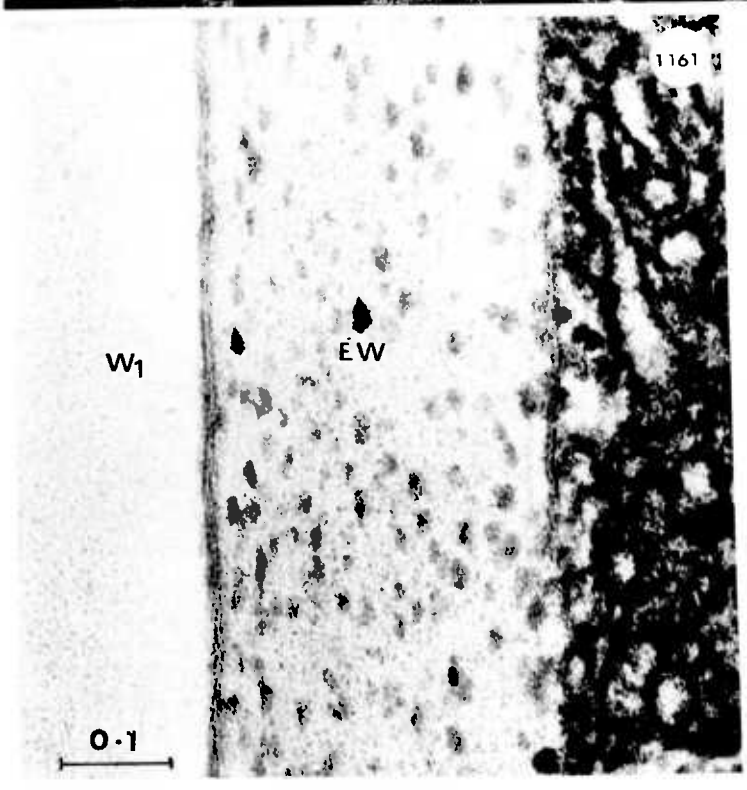

OW
1156


1158
0·3


OW
1157
W1


1159
W1
0·1


1160
0·1


1161
W1
EW
0·1

1.2.4.4 Oospore ultrastructure of S.furcata: Contents of densebody and ooplast vesicles

Figs. 1.162, 1.163 Densebody vesicles from Stage VII spore showing the extensive concentric myelin-like arrays around the densebodies in GaOs fixation.

21393
GaOs 3452 48 h
21394

Fig. 1.164 Os-fixed densebody vesicle from a Stage VII spore, showing the less extensive and more linear myelin elements.

29525 Os 3449 48 h

Fig. 1.165 Detail of the densebody vesicle matrix of an expanding ooplast vesicle from a Stage VIII GaOs-fixed spore.

27554 GaOs 3452 48 h

Fig. 1.166 Densebody granule from a freeze fractured spore showing the series of layers typical of myelin-like phosphatid configurations.

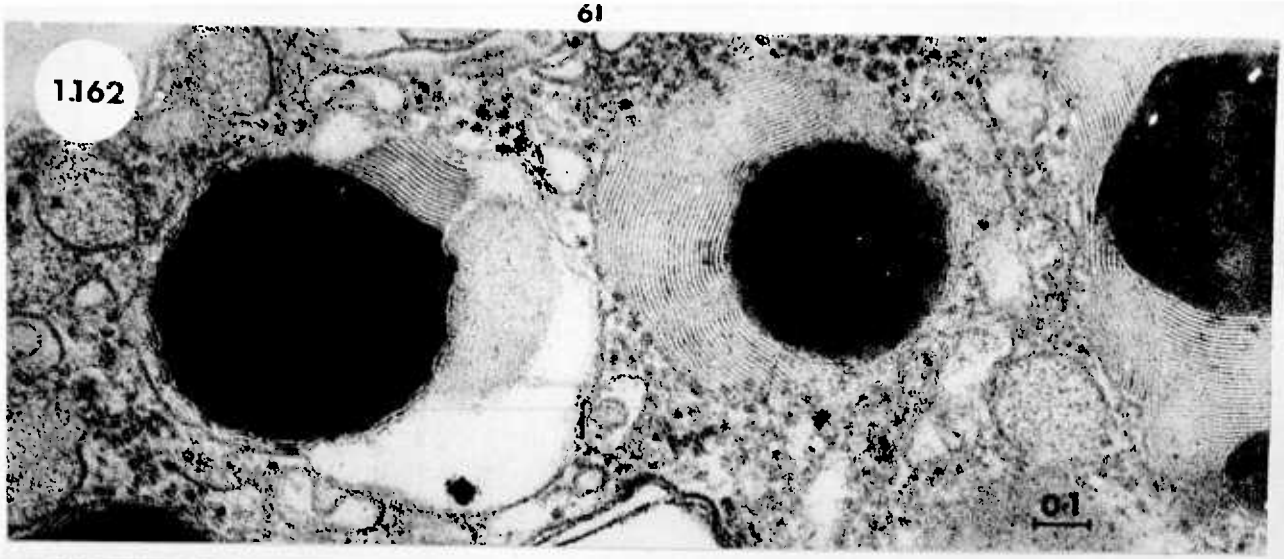
27157 Freeze-fracture

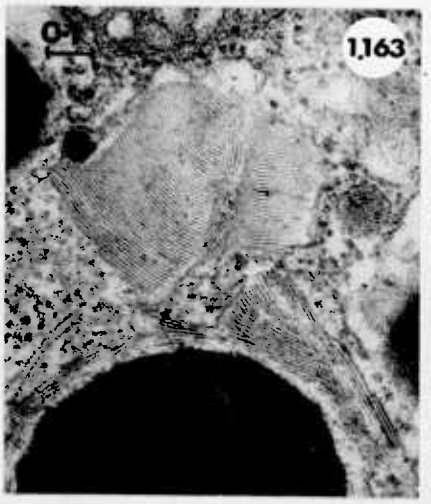
Figs. 1.167, 1.168 Densebodies from a GaOs-fixed Stage VIII spore. Although the cytoplasm is poorly preserved the myelin arrays can still be discerned.

27558
GaOs 3452 48 h
29253 3830 96 h

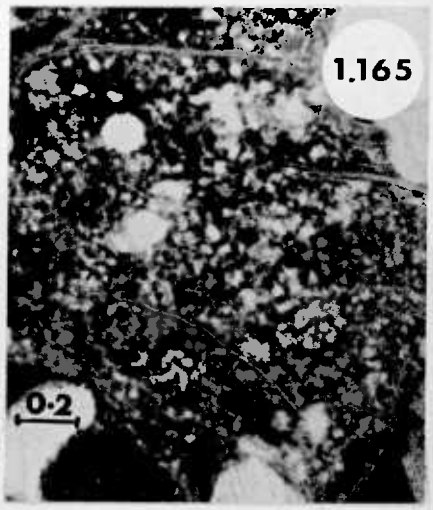
Figs. 1.169, 1.170 Large palmate arrays of matrix material from the ooplast vacuole of a mature TW-induced spore. The myelin-like structure indicates the similarity in the contents of densebody vesicles and the ooplast.

27769
Os 3891 96 h
29789

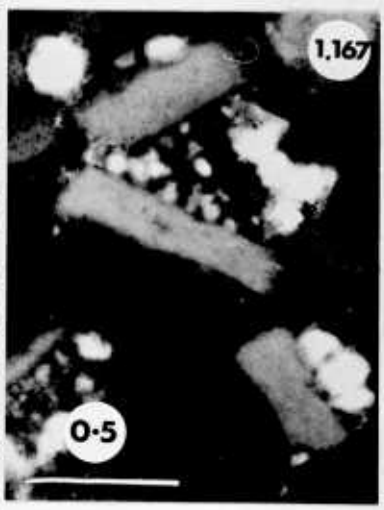

1.162
0·1


0·1
1.163

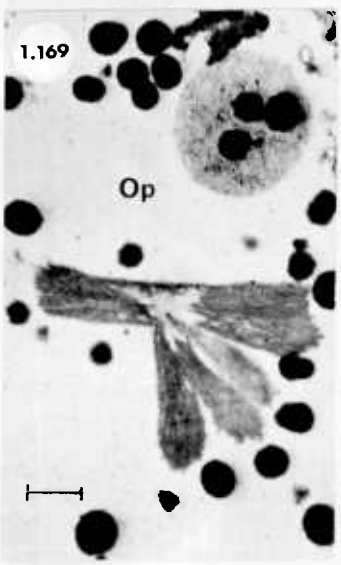

1.164
0·2

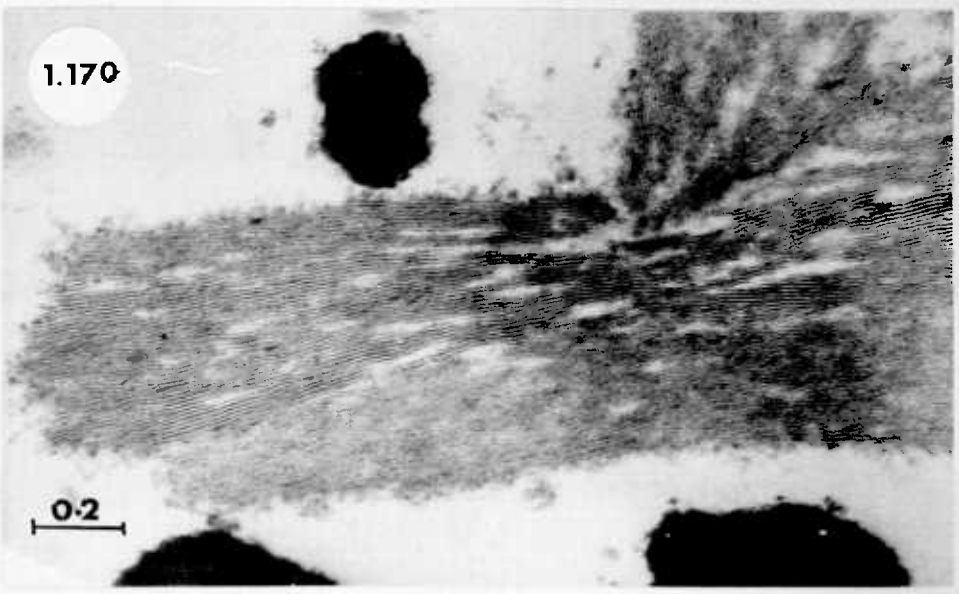

1.165
0·2


0·1
1.166


1.167
0·5


1.168


1.169
Op


1.170
0·2

1.2.4.5 Ultrastructural aspects of fertilisation in S.furcata

Fig. 1.171 Fertilisation tube in contact with a Stage VII oospore. The fertilisation tube contains wall vesicles at its apex, a gametic nucleus, several mitochondria and the usual storage reserves. Note at the point of contact the oospore wall has thickened and wall vesicles have accumulated.
29601 GaOs 3983 96 h

Fig. 1.172 Fertilisation tube and three adjacent Stage VII oospores from a Str-induced oogonium. Note the lomasome in the spore walls opposite the fertilisation tube.
22098 Os 3451 Str 100 mg/l 48 h

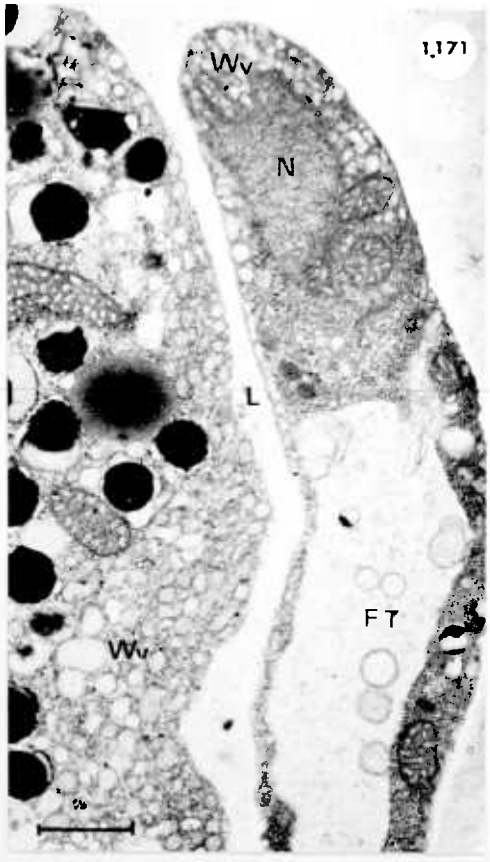
Fig. 1.173 Fertilisation tube showing a nucleus, several mitochondria and abundant peripheral plasmalemmasomes
19153 Os 3331 96 h

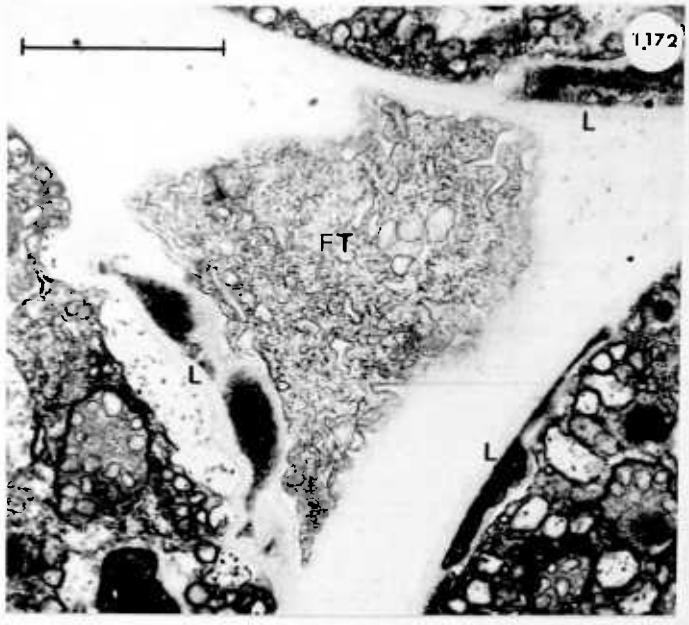
Fig. 1.174 Profile through a pair of copulating gametangia induced in Str.
22098 Os 3451 Str 100 mg/l 48 h

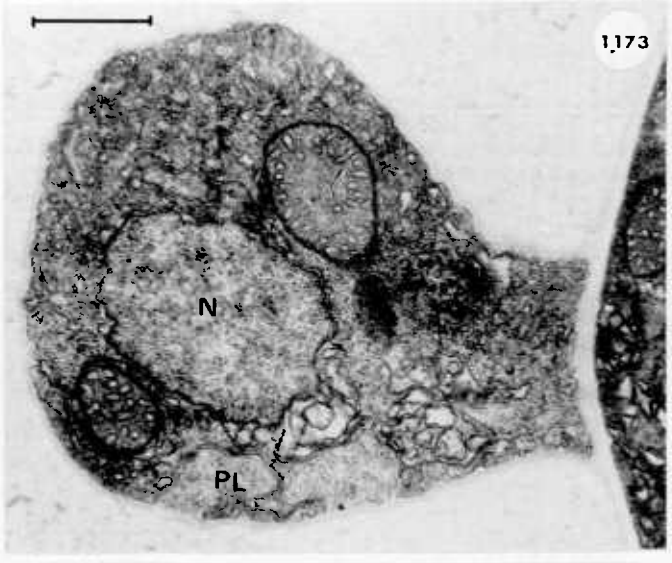
Fig. 1.175 Remnants of the fertilisation tube in a Stage VIII spore. Note the enclosure of the collapsed penetration peg by the acruing endospore material.
21382 Os 3449 48 h

Fig. 1.176 Remnants of a comparable fertilisation tube in a Str treatment.
25572 Os 3487 Str 50 mg/l 240 h

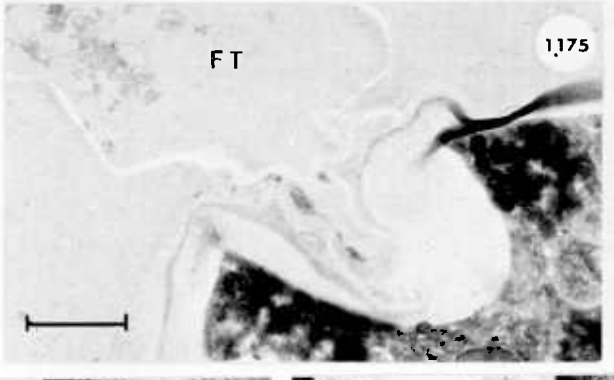
Figs. 1.177, 1.178 Remnants of collapsed fertilisation tubes and penetration pegs in Stage X oospores.
23725, 23717 3480 $KMnO_4$ (2% 5 min) 240 h


1.171
Wv
N
L
FT
Wv


1.172
L
FT
L
L

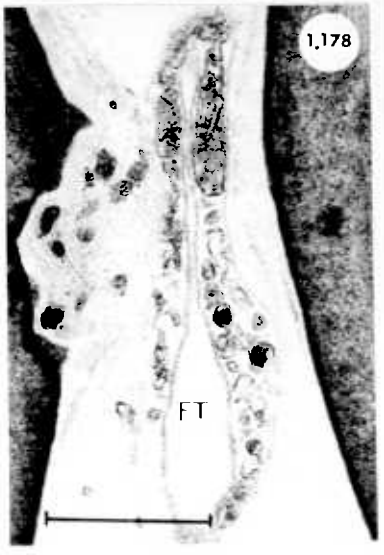

1.173
N
PL


1.174
L
FT


1.175
FT


1.176
FT


1.177


1.178
FT

1.2.4.6 Oospore nuclei in S.furcata

Fig. 1.181 Typical nucleus in a Stage VII oospore. Note the irregular profile characteristic of Os fixation, and the amorphous body located at the nuclear apex.
22075 Os 3451 Str 100 mg/l 48 h

Fig. 1.182 A comparable Ga-Os fixed nucleus. Note the smooth rounded profile and associated dictyosomes and ER cisternae.
29104 GaOs 3878 96 h

Fig. 1.184 Cytoplasmic microtubules in the nuclear region of a Stage VII spore.
27562 GaOs 3878 96 h

Fig. 1.185 Detail of a post fertilisation oospore (Stage VII) showing two nuclei.
29562 GaOs 3883 96 h

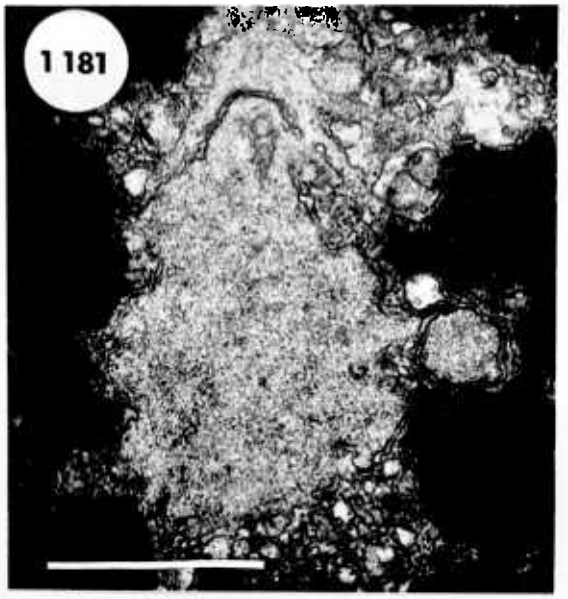
Fig. 1.187 Degenerating male nucleus in a fertilisation tube of an oogonium containing Stage VIII oospores. Note the inflated nuclear envelope and loss of nucleoplasm density.
21732 Os 3449 48 h

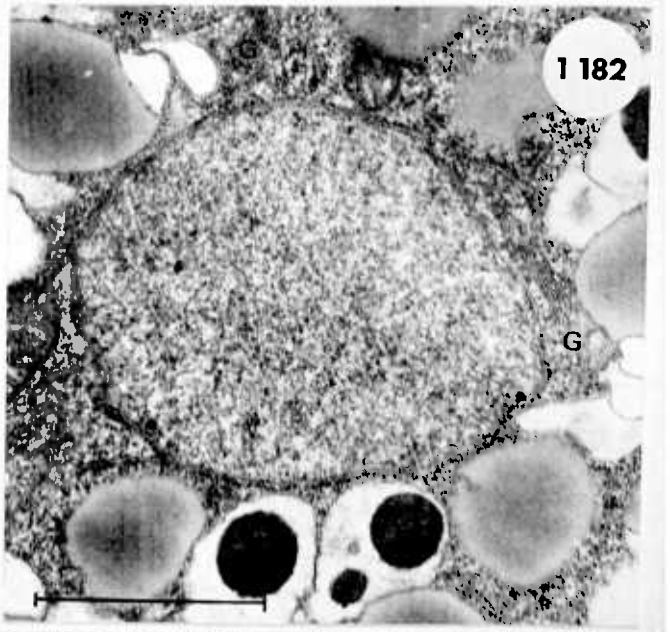
Figs. 1.188, 1.189 Nuclei in abnormal TW-induced oospores.

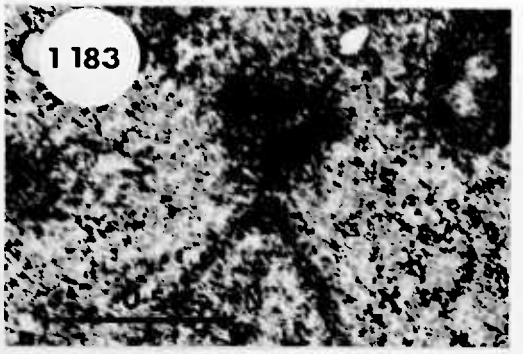
Fig. 1.188 Nucleus from the periphery of an oospore showing typical Stage X organisation. Note the large size of this nucleus and its fine fibrillar nucleoplasm.
25924 Os 3617 TW 96 h

Fig. 1.189 The irregular profile of a centrally located nucleus in an oospore with Stage VIII organisation.
25914 Os 3617 TW 96 h

Fig. 1.183. Detail of amorphous centriolar body associated with Stage VII oospore nucleus
29578 GaOs 3716 24 h

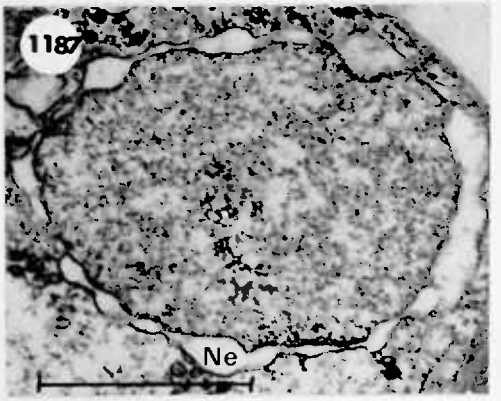

1 181

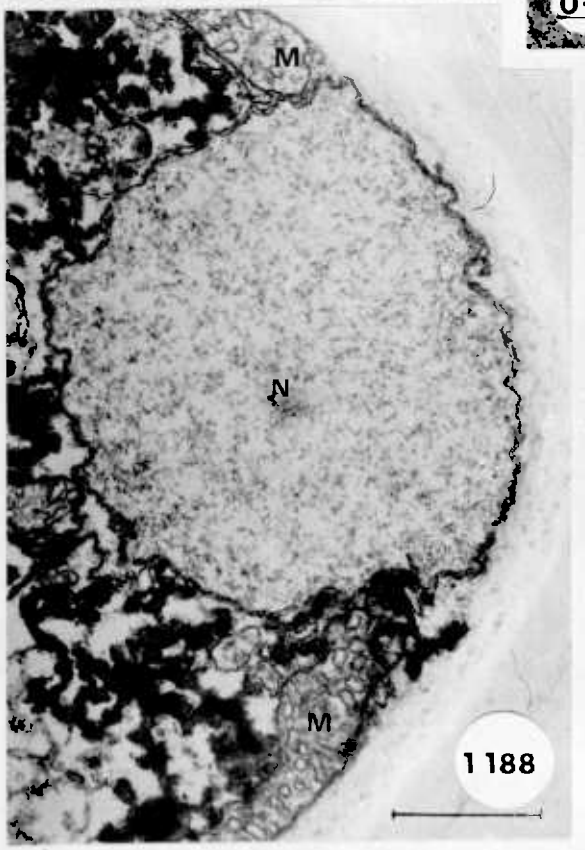

1 182
G

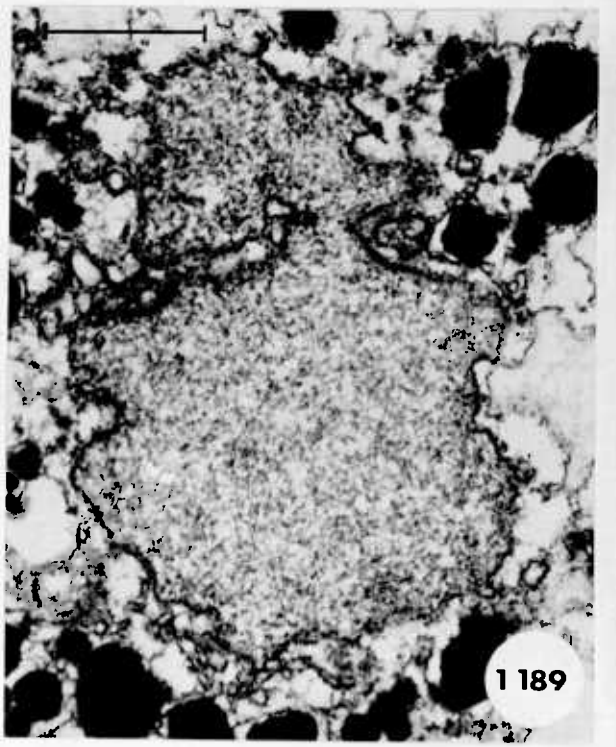

1 183


1 184
0·1


1 185
N1


1187
Ne


M
N
M
1 188


1 189

1.2.3.6 Gemmae in colonies of S.furcata

Fig. 1.190 Gemma showing large central vacuole. Note the irregular distribution of the peripheral cytoplasm. The gemma wall remains relatively thin (150 nm) and lomasomes are scarce.

29413 $KMnO_4$ (2% 25 min) Os 3481 240 h

Figs. 1.191-1.195 Light micrographs showing a range of gemma form. Note most gemmae are part of acropetally developing chains, which are separated by septa.

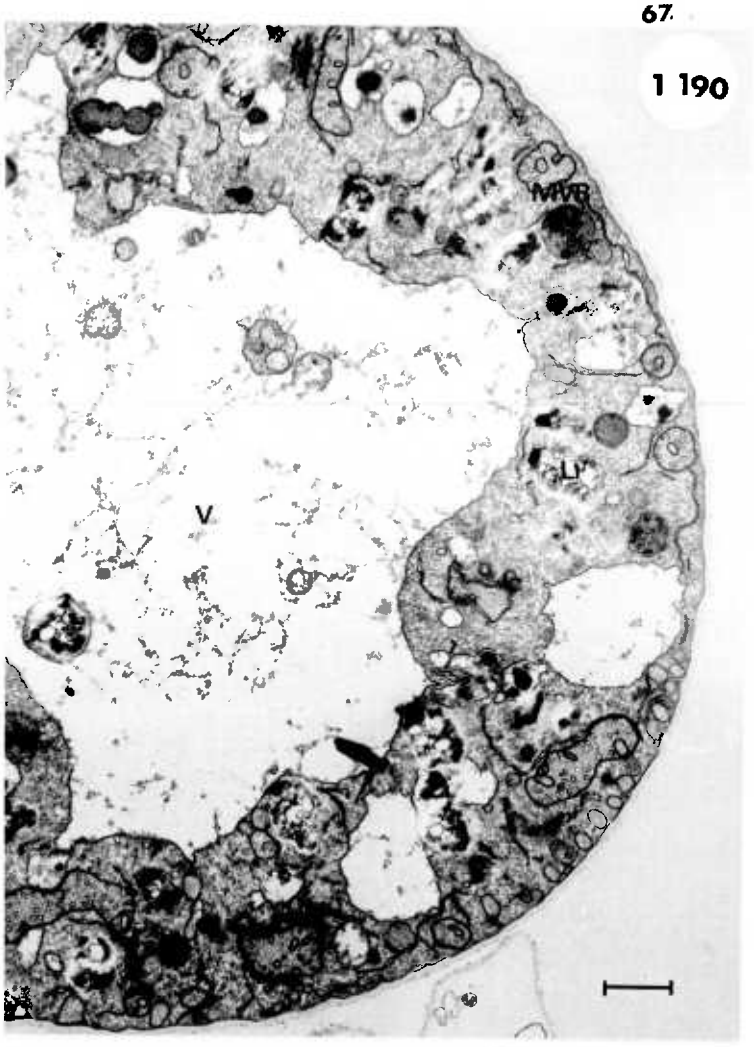
154/29 OI x 700	168/4 x 650		
154/13 OI x 600	154/27 x 700	96-240 h	
154/14 OI x 600	68/10 x 650		

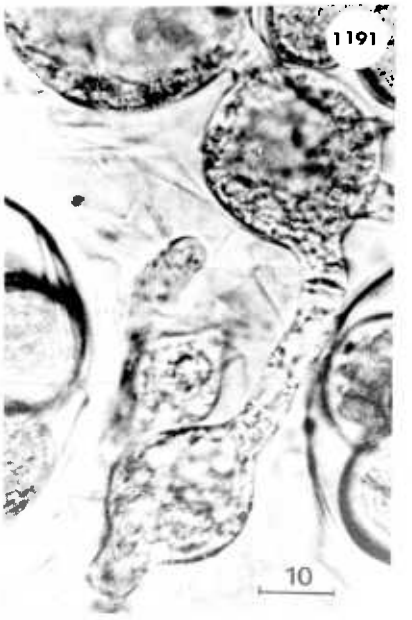
Fig. 1.194 Simple spherical gemma which has pproduced a short germ-tube after colony transfer to fresh distilled water. Note the uniform width and linear growth of this germtube.

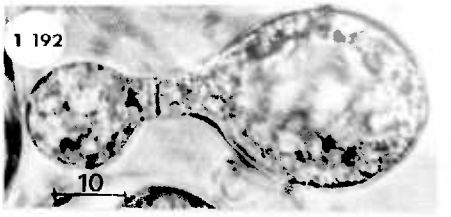
154/27 OI x 700 96 h

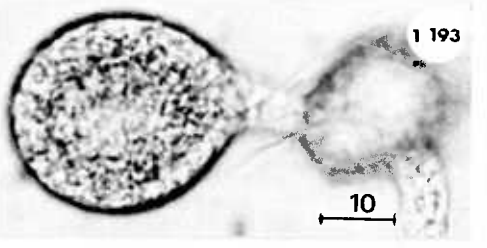
Figs. 1.196, 1.197 Serial sections of the peripheral cytoplasm of the gemma shown in Fig. 1.190, showing the nucleus and other cell components. The nucleus has a typical $KMnO_4$-fixed morphology, and the lipid droplets are largely extracted. Note the absence of vesicles associated with the dictyosome, and the paucity of wall vesicles (1.197).

1.196 23904
1.197 23901 $KMnO_4$ (2% 25 min) Os 3481 240 h


1 190
MVB
Li
V

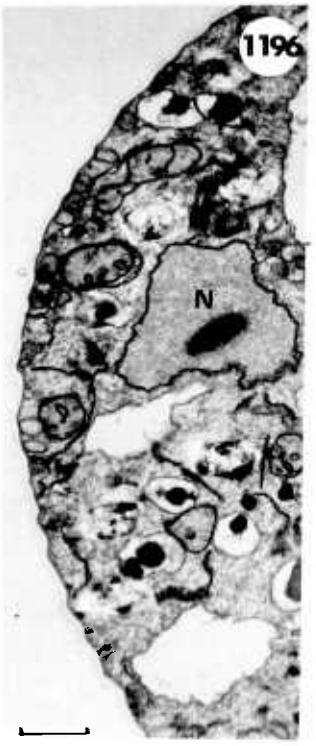

1 191
10

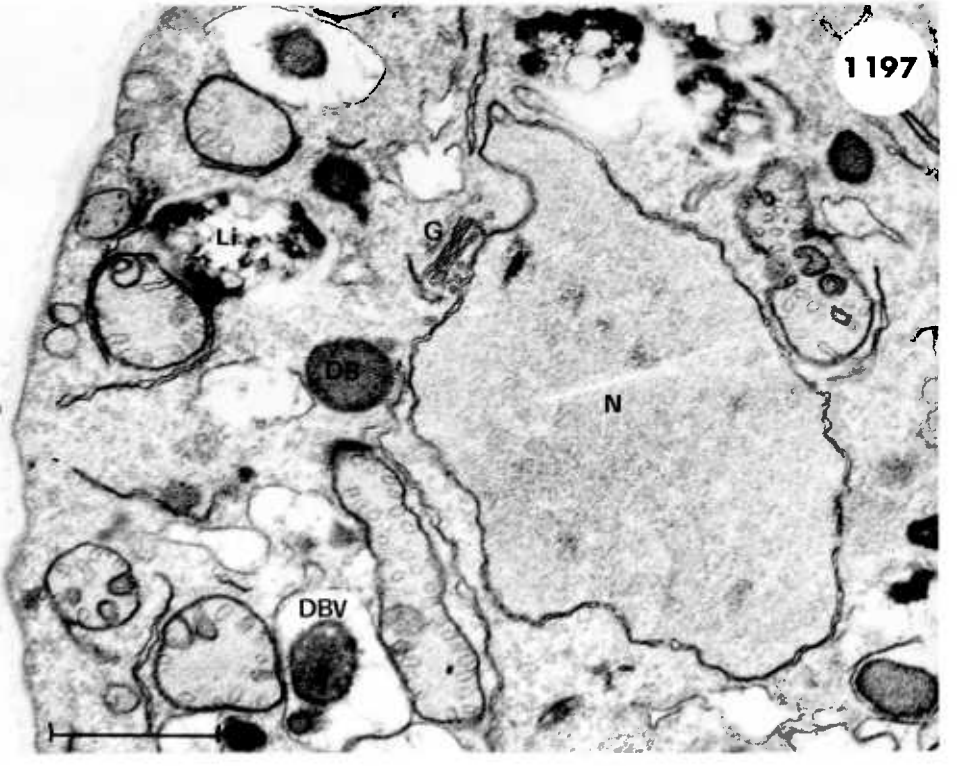

1 192
10


1 193
10


1 194
10


1 195
10


1196
N


1 197
Li
G
DB
N
DBV

1.2.5.1 Septum formation in sporangia of S.ferax and S.furcata

Figs 1.198-1.205 Selected light micrographs showing the probable sequence of septum formation in sporangia of S.furcata.

Fig. 1.198 The basal region of a sporangium prior to septum formation.
82/8 OI x 1200 7 h

Figs. 1.199, 1.200 Basal region of a sporangium showing the refractile zone which appears prior to septum insertion.
82/3
82/23 OI x 1200 4 h

Fig. 1.201 The immediate pre-septum stage in which a dense cytoplasmic band differentiates beyond the refractile zone. This disappears during septum insertion.
82/24 OI x 1200 4 h

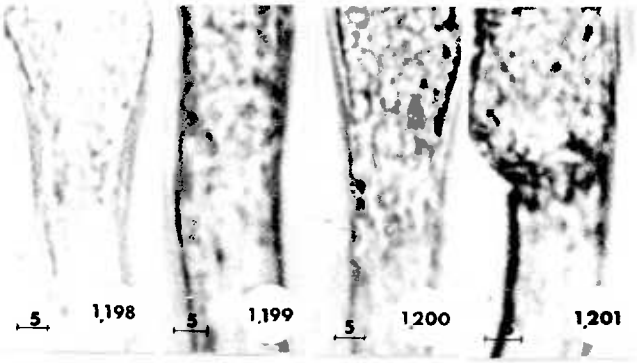
Figs. 1.202, 1.203 Newly inserted crosswalls, which are difficult to discern at this stage. Note absence of refractile zone.
82/10
82/4 OI x 1200 4 h

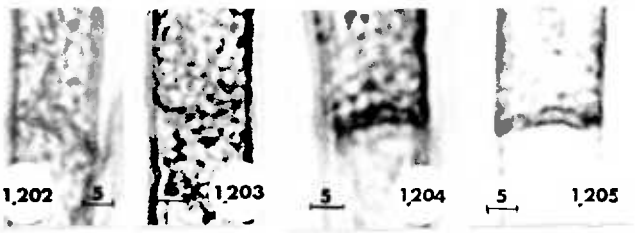
Figs. 1.204-1.205 Mature septa showing their double convexo-concave profile.
82/12
82/14 OI 9 h

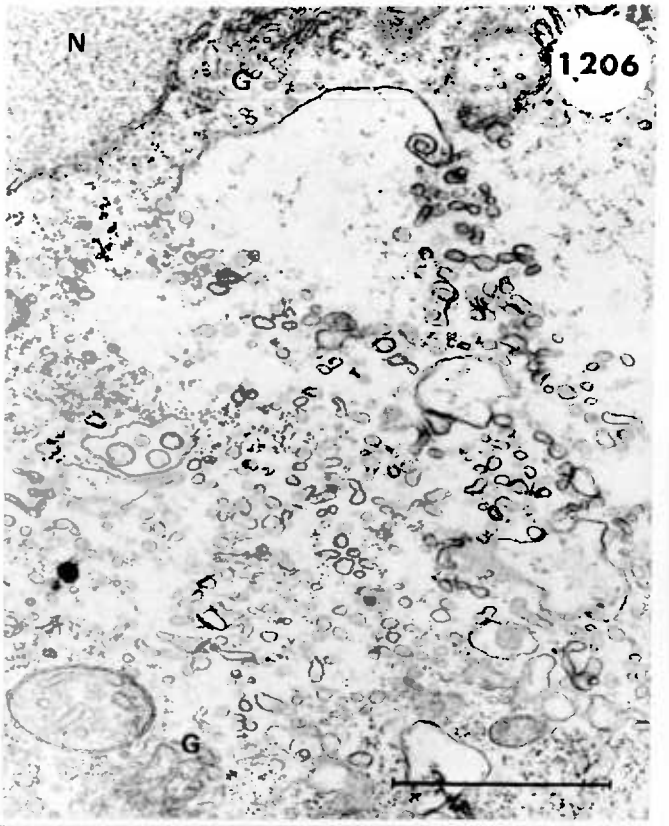
Fig. 1.206 Ultrastructure of pre-septal cytoplasm in the region of septum development. A large number of small electron dense vesicles, similar to those produced by the dictyosomes, predominate in this region.
21479 OS 3022 4 h

Fig. 1.207 LS montage of the basal region of a preseptum sporangium. Note the dense blocks of cytoplasm in the region of septum development.
27237 -38 $KMnO_4$ (2% 5 min) 3728 4 h

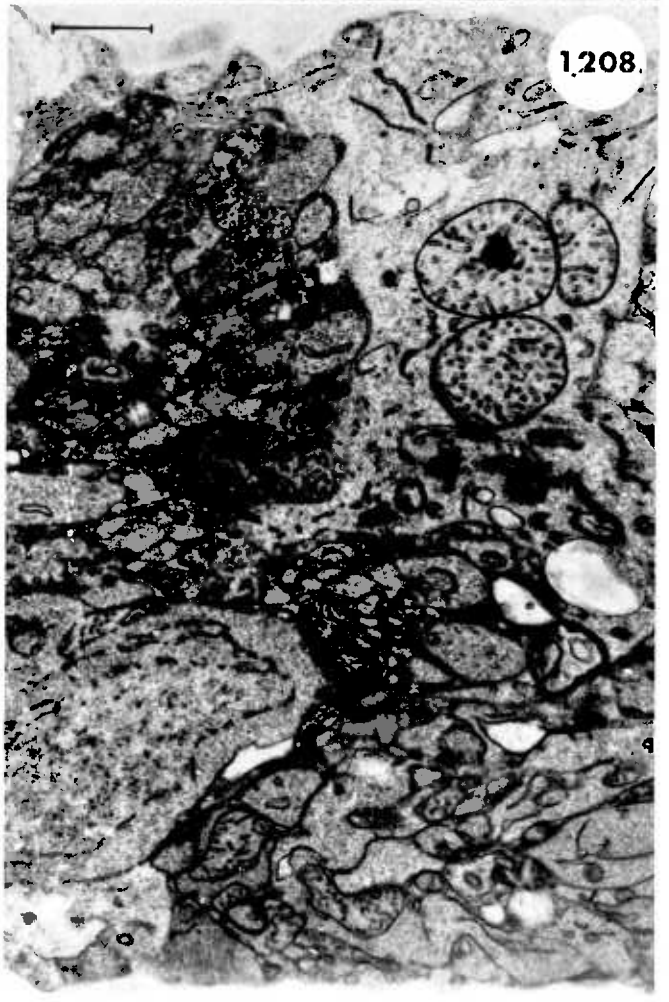
Fig. 1.208 Detail through basal region shown in Fig. 1.207. It is composed of tightly packed mitochondria and vesicles. There is a well-defined boundary formed by flattened cisternae between the 'dense' vesicular blocks and the less dense cytoplasm.
27239 $KMnO_4$ (2% 5 min) 3728 4 h


5
1,198
5
1,199
5
1,200
1,201


1,202
5
1,203
5
1,204
5
1,205


N
G
1,206
G


1,207
N


1,208.

1.2.5 Mature septum structure in S.ferax and S.furcata

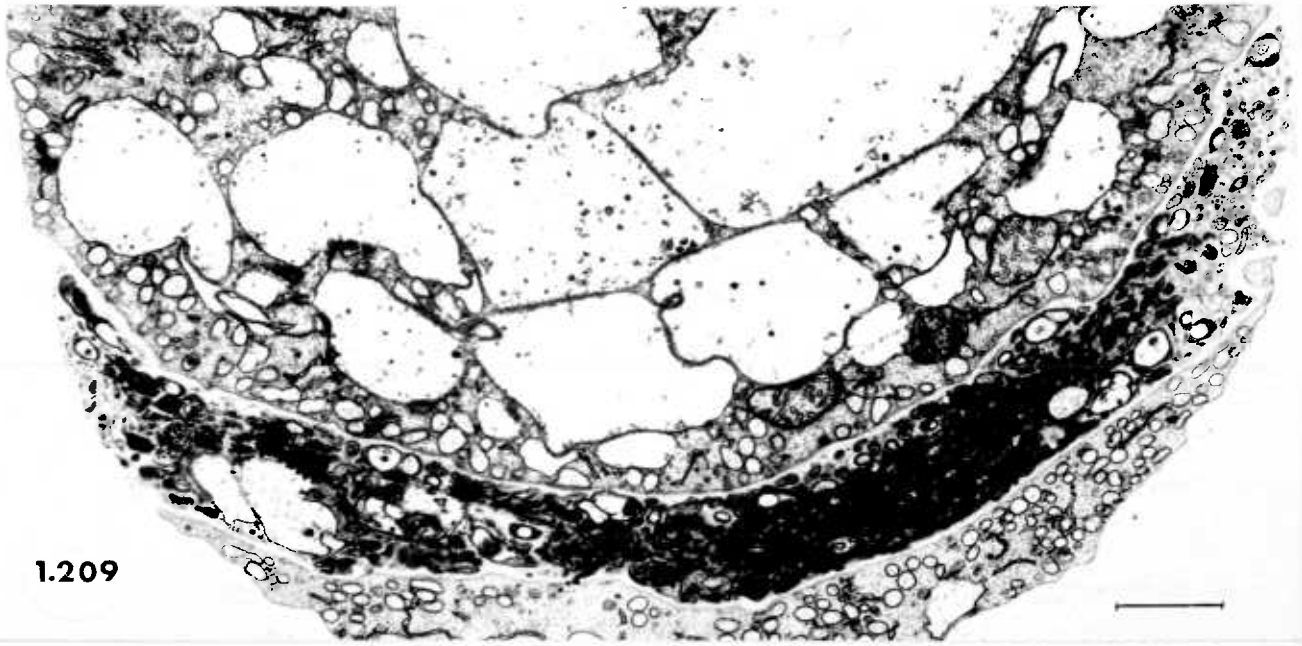
Fig. 1.209 Oblique LS of a basal septum sporangium. The thin upper and lower wall layers and the thick densely packed intermediate layer suggests this is an immediate post insertion stage.
27288 $KMnO_4$ (2% 5 min) 3727 4 h

Fig. 1.210 Median LS of mature sporangial septum, showing the characteristic convexo-concave structure. The upper and lower wall layers are appreciably thicker than the septum in Fig. 1.209, and the vesicular layer is much more compacted and discontinuous.
27459 $KMnO_4$ (2% 5 min) 3728 4 h

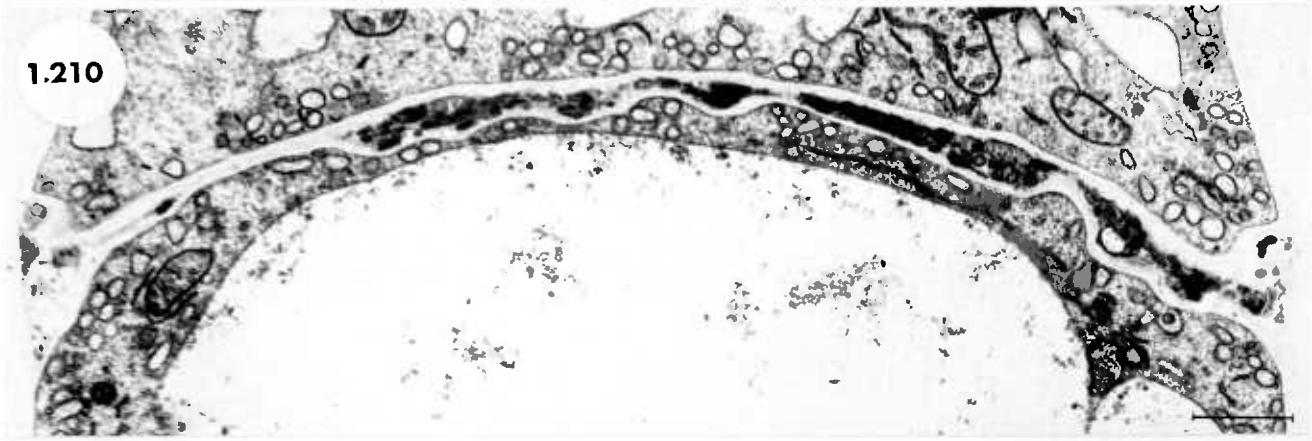
Fig. 1.211 A mature oogonial septum, showing the typical tripartite structure, but with a concavo-convex profile (cf Fig. 1.210). Note how fine strands of wall material traverse the vesicular zone.
29115 GaOs 3878 24 h

Fig. 1.212 A mature antheridial septum showing the characteristic 'trumpet' shaped profile, formed as a result of thickening of septum at the side adjacent to the oogonium.
29127 GaOs 3878 24 h

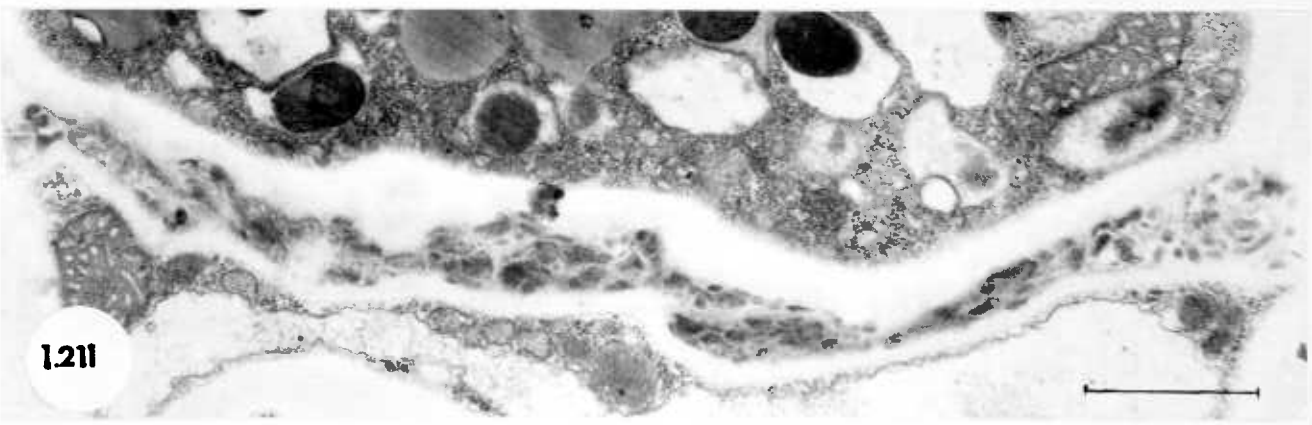
Fig. 1.213 Oblique TS through the central vesicular layer of a mature septum in a Str-induced gemma S.ferax.
27107 Os 3325 Str 70 mg/l 120 h



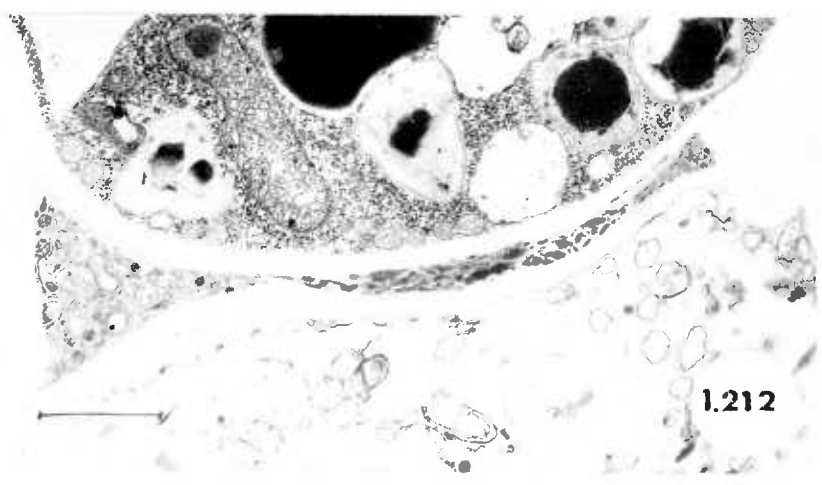
1.209



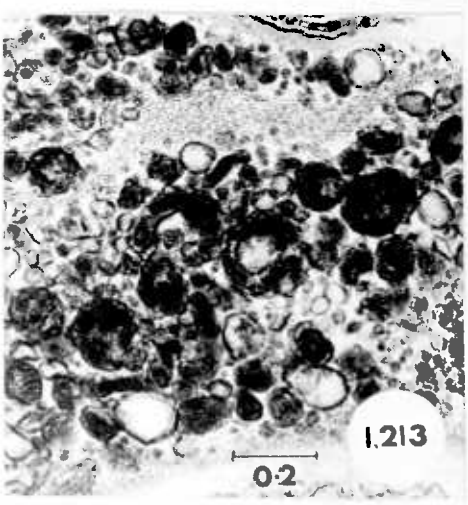
1.210



1.211



1.212



1.213

0·2

1.2.6 Sporangia of Phytophthora cactorum

Fig. 1.215 Light micrograph of a typical deciduous sporangium showing its ovoid profile and prominent apical papilla.
109/29 OI x 1,200

Fig. 1.216 LS of a sporangium showing electron transparent papilla and dense non-vacuolate cytoplasm rich in neutral lipid and densebody vesicles.
27992 GaOs 3837 48 h

Fig. 1.217 TS of a sporangium 3 h after germination induced by chilling. Note the formation of a central vacuole, the spindle shaped nuclei, and the peripheral axonemal vesicles.
25945 Os 3706 48 h

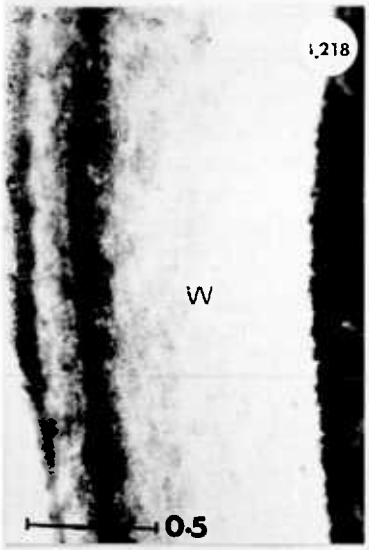
Fig. 1.218 Sporangium wall showing the thin outer-layer which is continuous with the wall of the stalk, and the thick inner layer with its electron dense outer and transparent inner regions.
27985 GaOs 3837 48 h

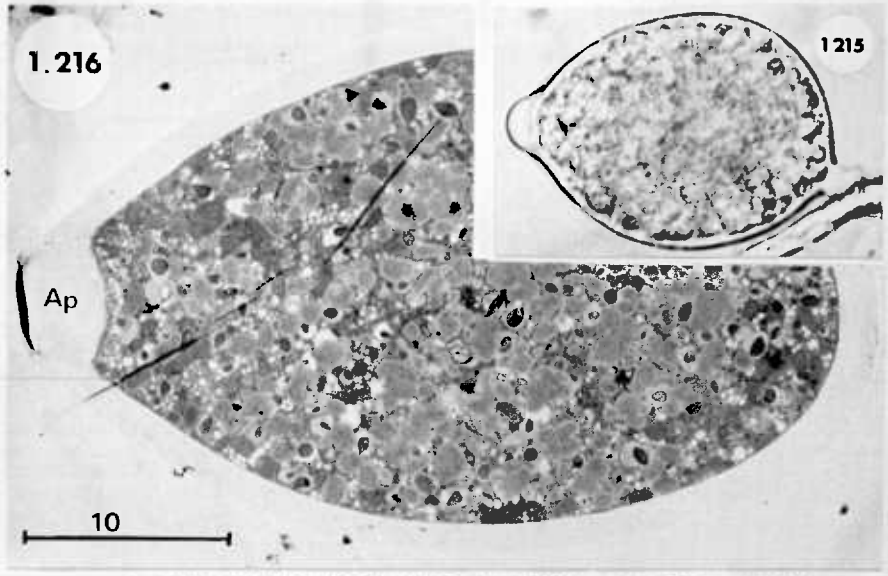
Figs. 1.219, 1.220, 1.221 Densebody vesicles in sporangia showing the variation in appearance with fixative procedure. The Os-fixed bodies have an electron transparent core and a uniformly dense periphery. In contrast the GaOs fixed bodies are osmiophilic and show the usual myelin-like striations.
25846 Os 3706 48 h
27796 GaOs 3837 48 h
27785 GaOs 3837 48 h

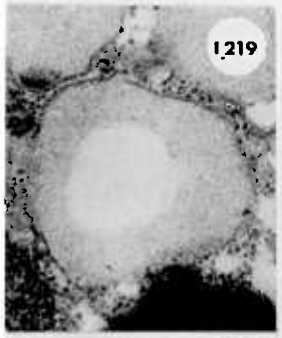
Fig. 1.222 A peripheral axoneme vesicle containing a flagellar axoneme sectioned near its base. The closely associated electron transparent vesicles are Golgi-derived and seem to be contributing to the developing vesicle. The swollen vesicles with fibrillar contents are wall vesicles.
27997 GaOs 3837 48 h

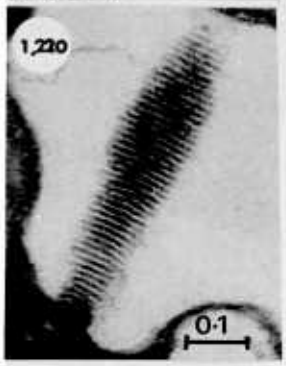
Fig. 1.223 Detail of nucleus from an uninduced sporangium. Note the spherical profile and dense nucleolar region. The small vesicles with dense particulate contents (FB) are the functional equivalents of bar bodies.
27996 GaOs 3837 48 h

Fig. 1.224 Two dictyosomes in the peripheral cytoplasm of an induced sporangium. Note these dictyosomes appear to be producing electron transparent 'axonemal' vesicles at this stage
27997 GaOs 3837 48 h

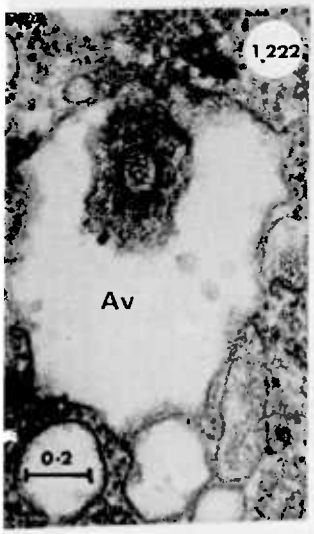

1.218
W
0·5

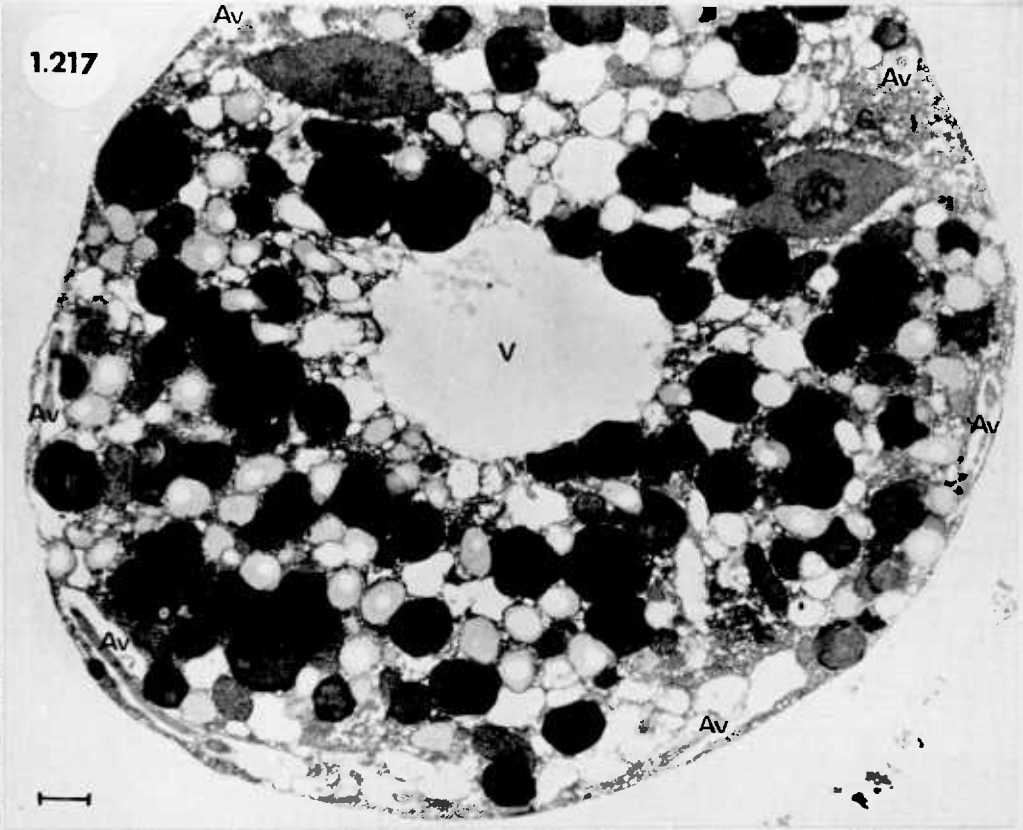

1.216
Ap
10
1.215

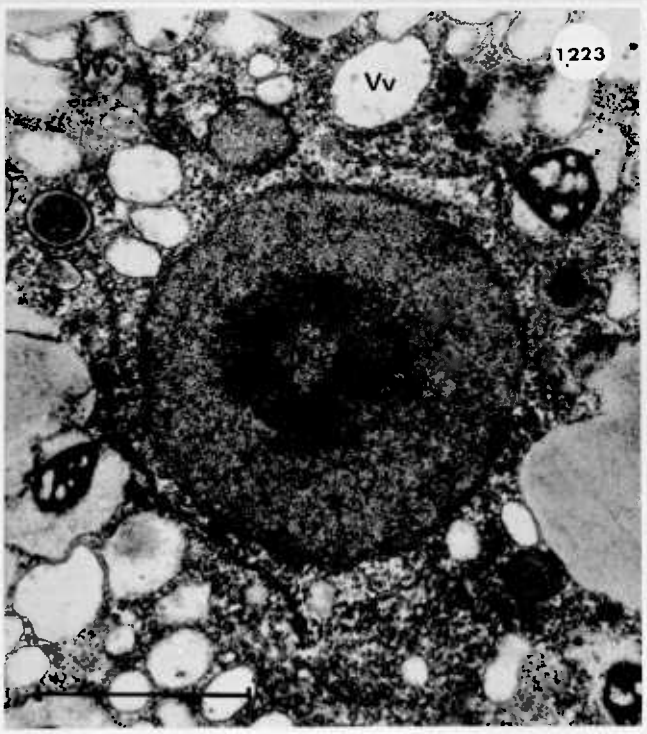

1.219


1.220
0·1


1.221
0·1


1.222
Av
0·2


1.217
Av
Av
V
Av
Av
Av
Av


Vv
Vv
1.223

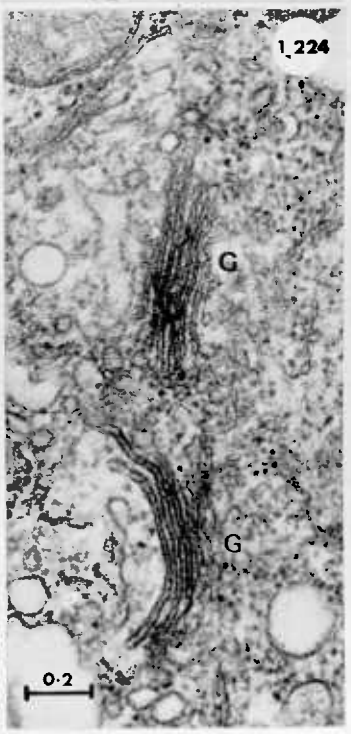
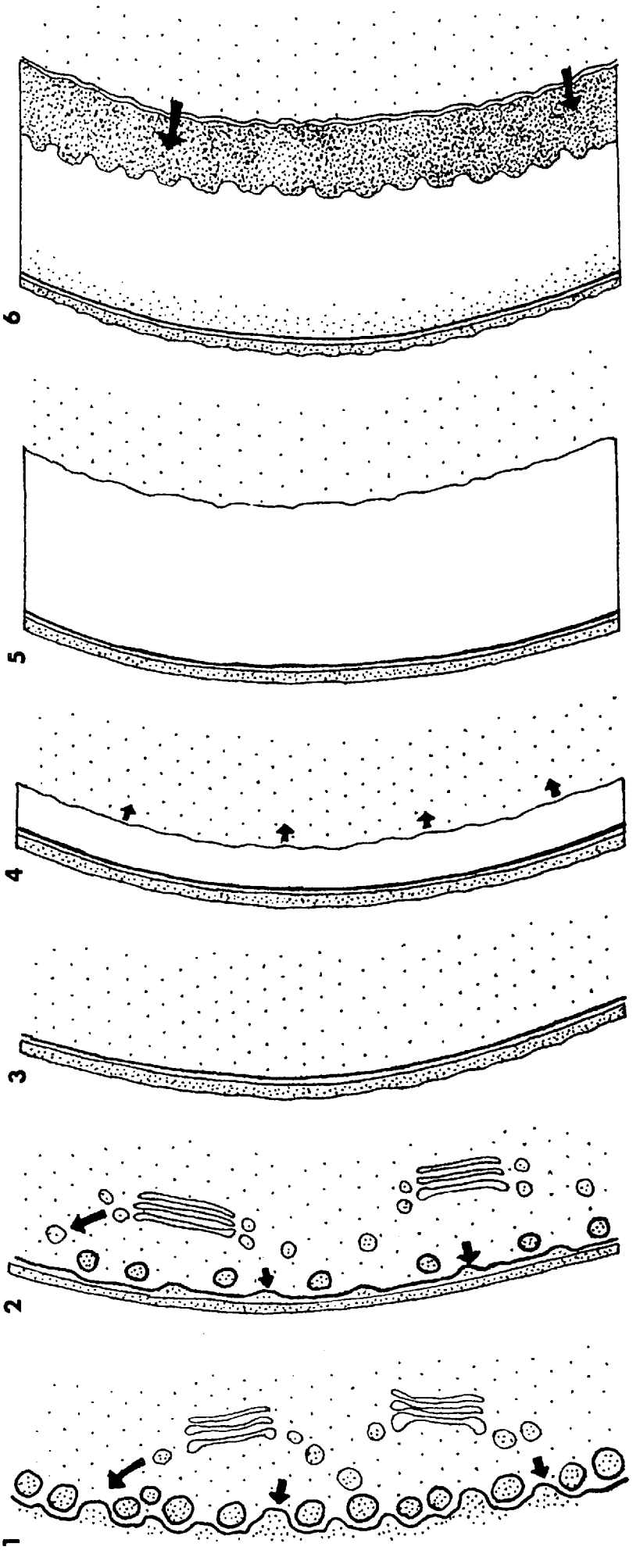

1.224
G
G
0·2

Fig. 1.225 Diagram summarising the main stages in oospore wall formation

1	Stage VI	Golgi-derived wall vesicles deposit the outer primary wall
2	Stage VII (early)	Golgi-derived wall vesicles continue to thicken the primary wall until about the time of fertilisation
3	Stage VII (late)	Primary wall formation is completed prior to endospore wall accretion. Both wall vesicles and Golgi dictyosomes are absent at this stage
4-5	Stage VIII-IX	The inner endospore wall layer is accreted centripetally without the involvment of the usual wall vesicles. An electron dense tripartite layer separates the primary wall from the developing endospore layer.
6	Stage X	An electron dense inner layer to the endospore wall differentiates during the final stage of oospore maturation. A membrane-like layer can be traced on both sides of the inner wall layer in some spores.


6
5
4
3
2
1

PART 2

THE EFFECT OF STREPTOMYCIN ON GROWTH AND REPRODUCTION IN SAPROLEGNIA

2.3.8.3 The effect of streptomycin on hyphal structure in induced colonies of S.ferax and S.furcata

Fig. 2.29 Montage of LS through a typical antibiotic-induced hypha of S.ferax showing a region of condensed cytoplasm. The main cell organelles are completely disorganised and the lipid droplets have coalesced into large aggregates.
27089/90/91 Os 3329 1000 mg/l Str 150 h

Figs. 2.30-2.37b Light micrographs illustrating the range of Str-induced hyphal effects on S.furcata.

Fig. 2.30 Hyphal segment showing a condensed block of cytoplasm which has separated completely from the cell wall.
47/3 OI 500 mg/l Str 150 h

Fig. 2.31 Hyphal tip containing condensed cytoplasm. Note its refractile appearance with anoptoral phase optics.
152/48 AP 500 mg/l Str 150 h

Fig. 2.32 Hyphal tip containing accumulated cytoplasm. The extreme apex is vacuolate.
47/1 OI 500 mg/l Str 124 h

Fig. 2.33 Hyphal tip from which cytoplasm has retracted.
152/44 AP 500 mg/l Str 150 h

Fig. 2.34 Sub-apical hyphal region showing condensation of cytoplasm into bead-like refractile segments.
152/34 AP 500 mg/l Str 150 h

Fig. 2.35 Hyphal segment containing totally disorganised cytoplasm dispersed throughout.
47/16 OI 500 mg/l Str 124 h

Fig. 2.36 Hyphae containing disorganised cytoplasm with large refractile droplets of lipid.
46/21 OI 500 mg/l Str 124 h

Figs. 2.37 a, b Apical (a) and sub-apical (b) segments of the same hypha showing the extent of cytoplasmic condensation. Small droplets of lipid, and vacuole-like compartments can be seen between the cytoplasmic aggregates.
152/36 AP x 400 500 mg/l Str 150 h
152/38


2.29
230
10
231
232
15
233
234
10
235
10
236
10
237
a
237
b

2.3.8.3 Effect of streptomycin on hyphae of S.furcata

Fig. 2.38 LS of a hypha showing the differention of the cytoplasm into dense and apparently normal segments.
21658 Os 3448 100 mg/l Str 24 h

Fig. 2.39 Part of the hypha in Fig. 2.38 showing partition by thin layers of cell wall material. The nucleus and mitochondria in the central segment appear normal.
21687 Os 3448 100 mg/l Str 24 h

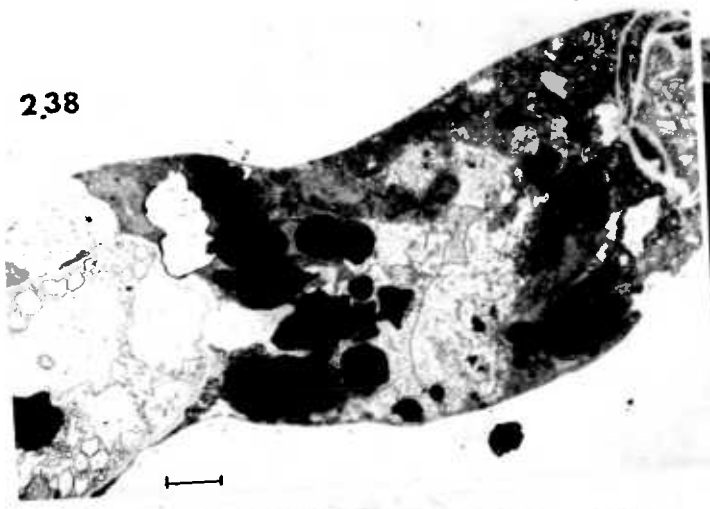
Fig. 2.40 Boundary between regions of dense and normal cytoplasm, showing the thin partition of wall material. Note the aggregation of lipid droplets in the dense phase.
21676 Os 3448 100 mg/l Str 24 h

Fig. 2.41 Detail of part of the hypha in Fig. 2.38, showing a wall ingrowth extending c. 2/3 rds across the hyphal compartment.
21662 Os 3448 100 mg/l Str 24 h

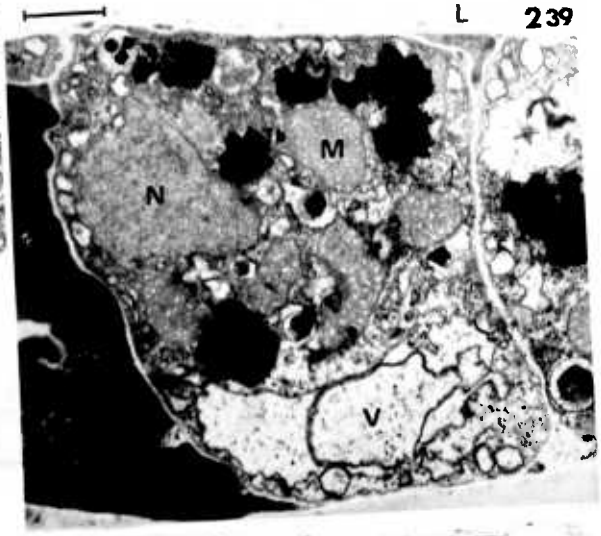
Fig. 2.42 Detail of the peripheral cytoplasm showing the complexity of wall layers (W1, W2, W3). The wall vesicles are large and have sparse contents.
21663 Os 3448 100 mg/l Str 24 h

Fig. 2.43 Detail of boundary wall between dense and normal cytoplasmic phases. Note the presence of a membrane on both sides of this wall, and the marked difference in ribosome frequency.
21677 Os 3448 100 mg/l Str 24 h

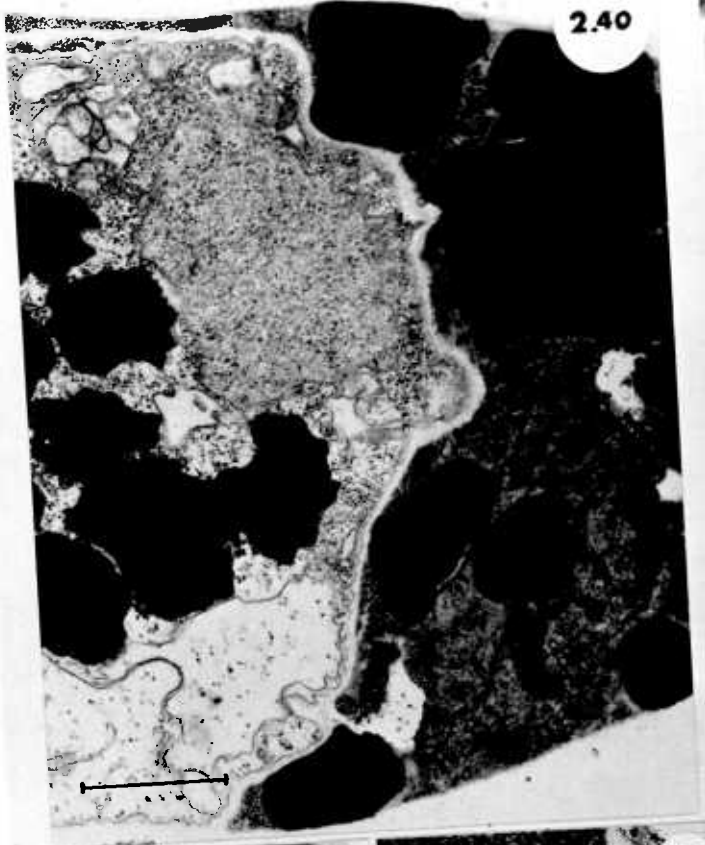
Fig. 2.44 Segment of cytoplasm in which change to the dense phase is probably still in early stages. Vacuolar compartments and mitochondria can still be seen. Note however the abundance of membrane complexes both within the cytoplasm, and between the wall layers.
21657 Os 3448 100 mg/l Str 24 h



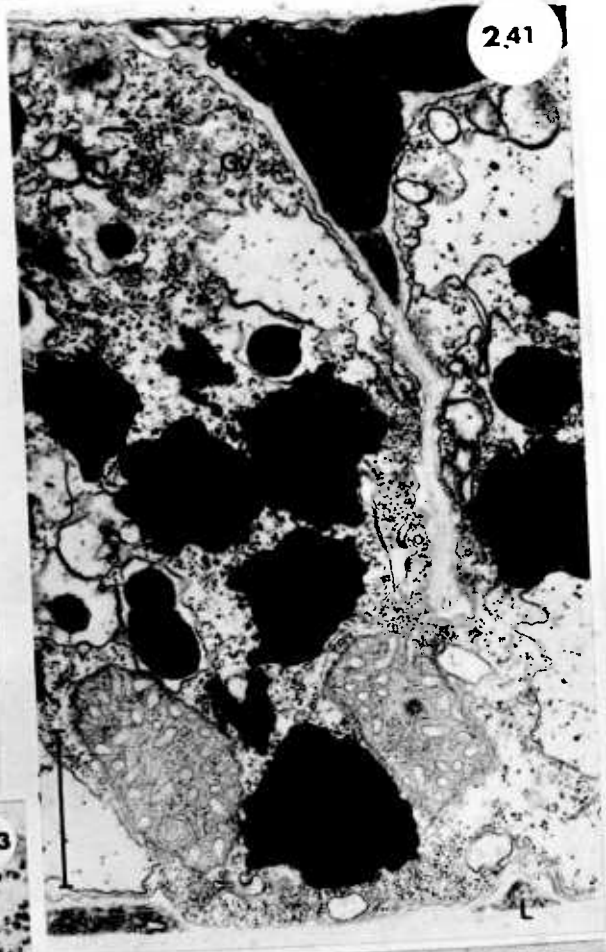
2.38



2.39



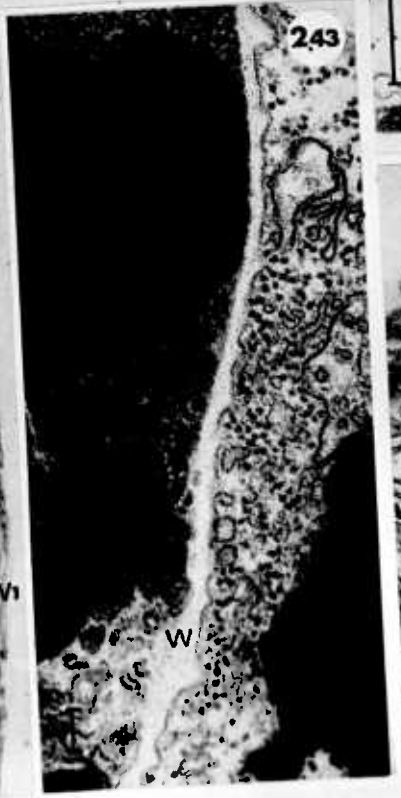
2.40



2.41



2.42



2.43



2.44

2.3.8.3 Effects of streptomycin on hyphae of S.furcata

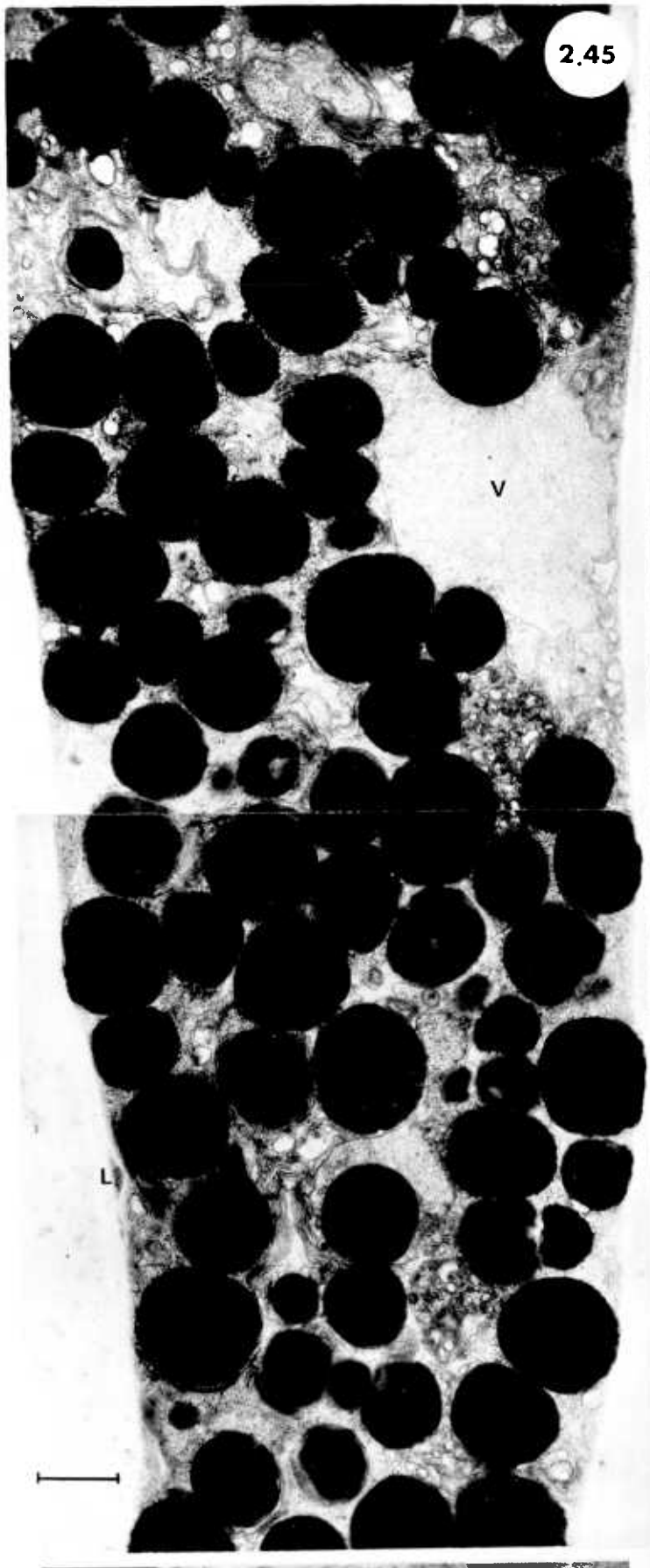
Fig. 2.45 LS montage of a segment of streptomycin-induced hypha showing the accumulation of highly osmiophilic neutral lipid droplets. The intervening cytoplasm contains membranous material and vacuolar compartments.
25167/68 Os 3484 1000 mg/l Str 240 h

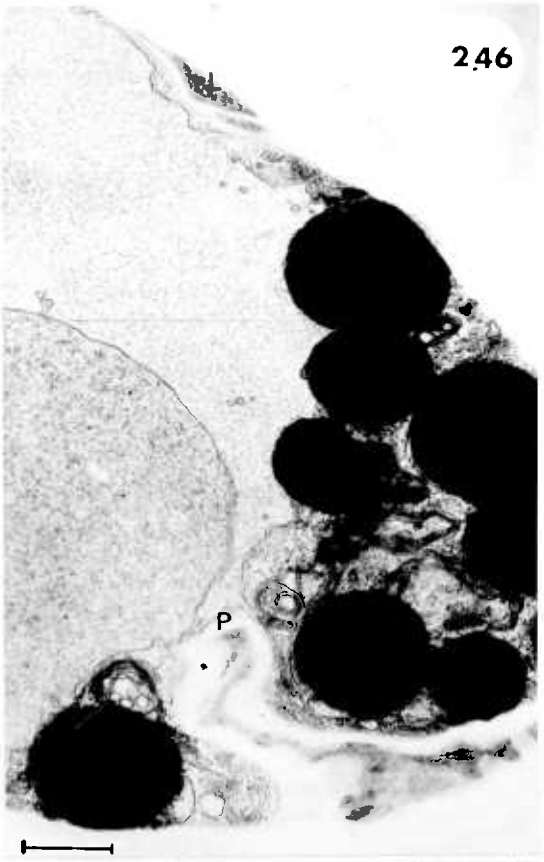
Fig. 2.46 Detail of the hypha in Fig. 2.45, showing part of a large vacuole and a peg-like wall ingrowth.
25180 Os 3484 100 mg/l Str 240 h

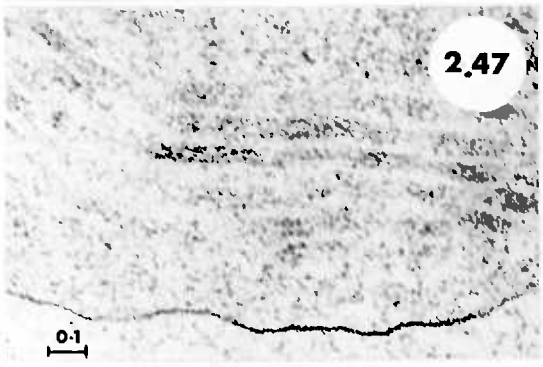
Fig. 2.47 Detail of the vacuolar contents showing curious bands of particulate electron-dense material.
25182 Os 3484 1000 mg/l Str 240 h

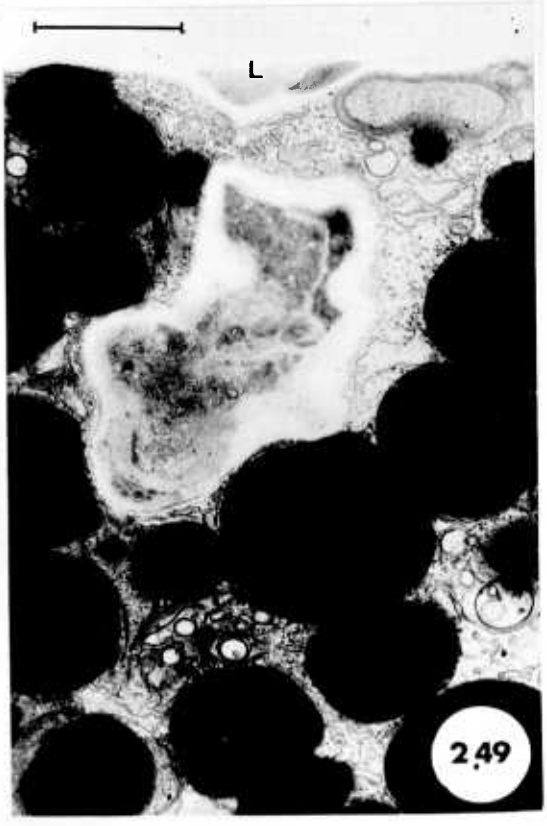
Fig. 2.48 Cytoplasm between lipid droplets. Note the elaborate membrane complexes and ribosome-like particles.
25181 Os 3484 1000 mg/l Str 240 h

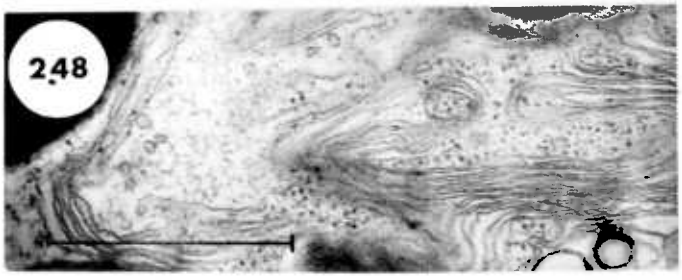
Fig. 2.49 Oblique section through peg-like wall ingrowth.
25184 Os 3484 1000 mg/l Str 240 h


2.45
V
L


2.46
P


2.47
0·1


L
2.49


2.48

2.3.8.4 The effect of streptomycin on the sporulation of induced colonies of S.ferax

Fig. 2.50 A slightly swollen hyphal tip containing condensed peripheral cytoplasm.
55/15 OI 100 mg/1 Str 4 h

Figs. 2.51-2.53 A selection of pre-septum sporangial initials, illustrating the effects of Str on their morphology.
61/11; 61/13; 61/12 OI 20 mg/1 Str 4 h

Figs. 2.54-2.56 Post septum sporangia showing axial vacuole and papilla development.
57/13; 58/10; 58/10 OI 50 mg/1 Str 7 h

Fig. 2.58 An abnormal Str-induced gemma with an elongate profile.
54/15 OI 100 mg/1 Str 30 h

Fig. 2.59 A Str-induced gemmae, in which cytoplasm has contracted slightly and become dense.
64/16 OI 100 mg/1 Str 30 h

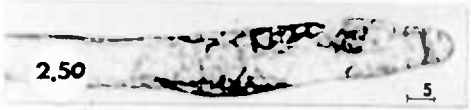
Figs. 2.60-2.61 Undelimited initials showing widespread cytoplasmic disorganisation.
69/12, 69/17 OI 100 mg/1 Str 8 h

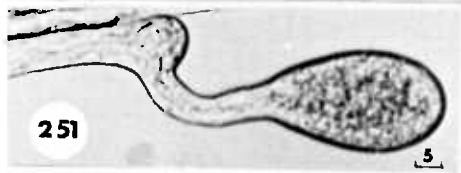
Fig. 2.62 A Str-induced gemma which shows little evidence of a vacuole. Note absence of apical papilla.
58.22 OI 50 mg/1 Str 10 h

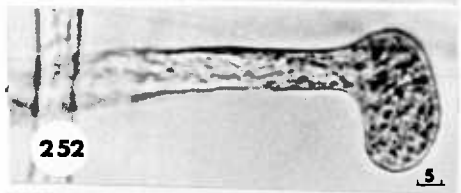
Figs. 2.63-2.65 Delimited sporangia in which the cytoplasm has condensed into dense aggregates like those observed in induced hyphae.
69/7; 68/8; 69/16 100 mg/1 Str. 28 h

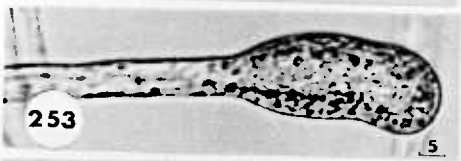
Fig. 2.66 TS of a pre-septum sporangium showing widely distributed vacuolar vesicles and wall vesicles.
13338 Os 3023 40 mg/1 Str 4 h

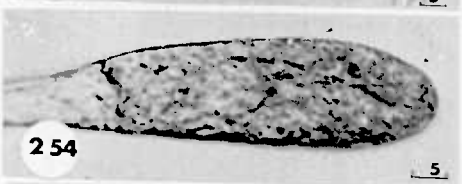
Fig. 2.67 TS of pre-septum sporangium with a thickened cell wall and poorly preserved vacuolar and densebody vesicle membranes.
13251 Os 3022 100 mg/1 Str 4h

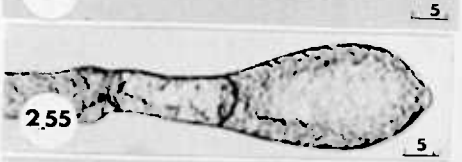

2,50
5

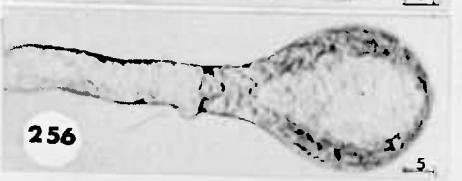

251
5

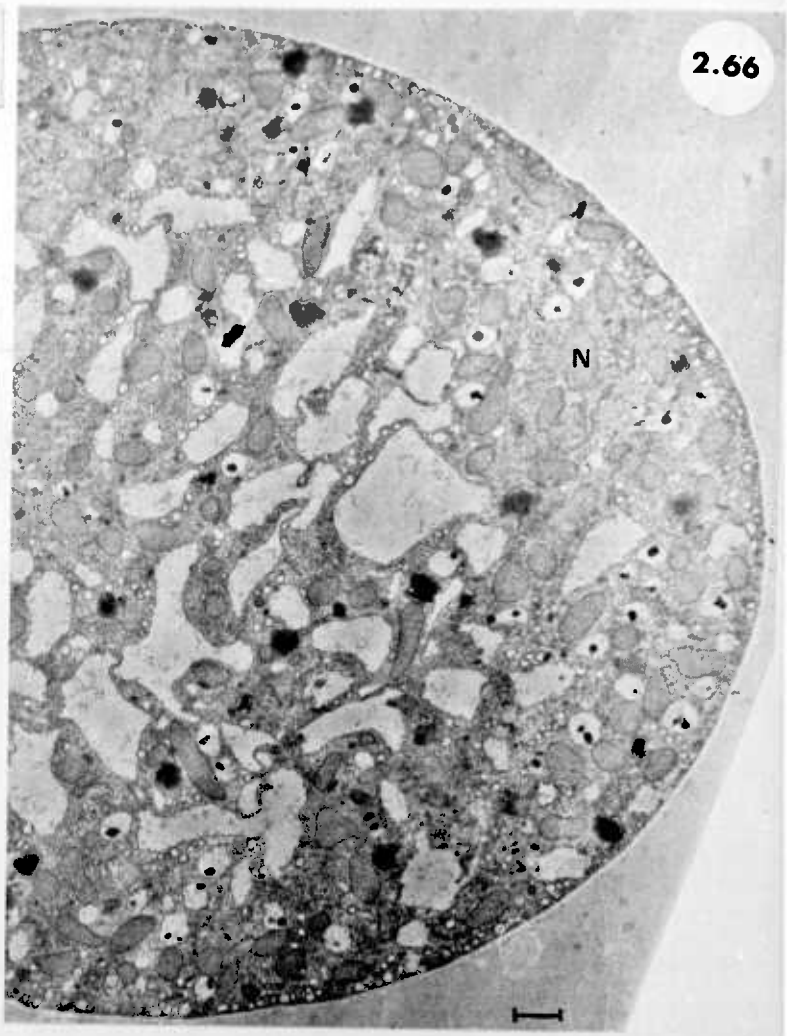

252
5

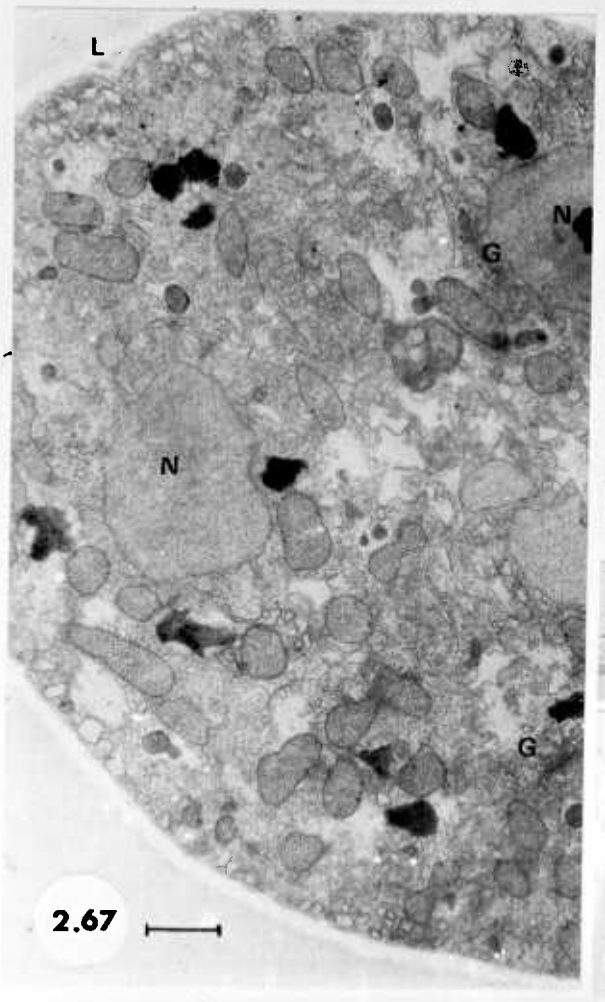

253
5

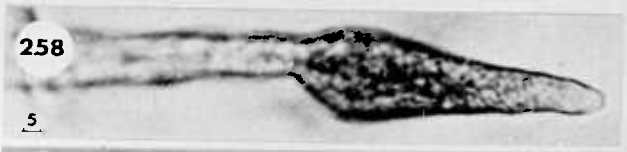

254
5


255
5


256
5


2.66
N

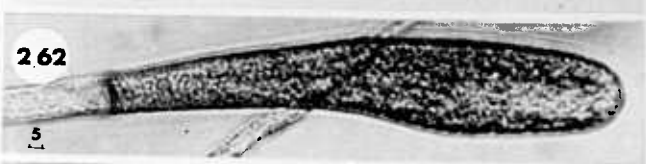

L
N
G
N
G
2.67

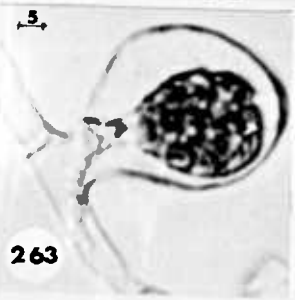

258
5


259
5


260
5


261
5
S


262
5


5
263


10
264


265

2.3.8.4 Str-induced gemmae in S.ferax

Figs. 2.68-2.76 Light micrographs illustrating the range in morphology of Str-induced gemmae.

Figs. 2.68, 2.69 Gemmae showing continued vegetative extension of their apices.

64/14 60 mg/1 Str 48 h

64/11 70 mg/1 Str

Fig. 2.70 A typical intercalery gemma.

59/24 200 mg/1 Str 30 h

Figs. 2.71, 2.72 Two gemmae with elaborate vegetative outgrowths and collapsed internal cytoplasm.

59/18 200 mg/1 48 h

59/19

Fig. 2.73 A typical chain of gemmae, which form in acropetal succession.

64/3 60 mg/1 Str 48 h

Fig. 2.74 Gemma showing vegetative extension of apex.

64/7 100 mg/1 Str 48 h

Fig. 2.75 Gemma containing condensed cytoplasm. The shape of the sporangial tip shows this occurred after papilla formation.

69/15 100 mg/1 Str 48 h

Fig. 2.76 Sporangium containing germinated cysts.

58/25 50 mg/1 Str 30 h

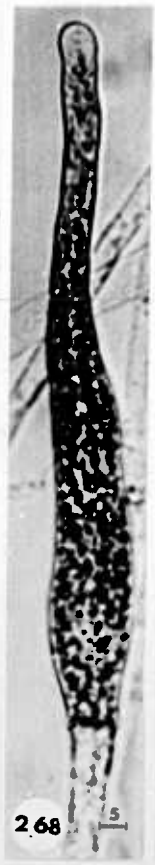
Fig. 2.77 Gemma TS showing well developed vacuolar system. Note the presence of all the typical sporangial organelles, including wall vesicles, and the abundance of lomasomes associated with the wall.

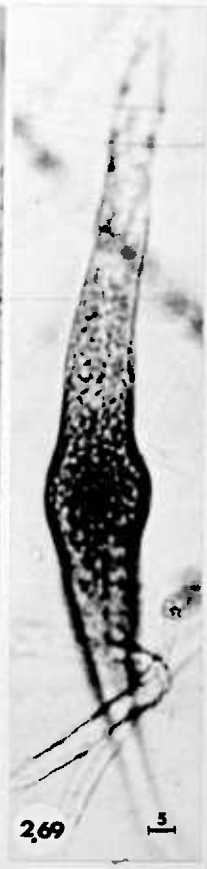
27109 Os 3324 50 mg/1 Str 96 h

Fig. 2.78 Part of TS of a gemma which contains only a few small scattered vacuolar vesicles.

27140 Os 3323 20 mg/1 Str 96 h


2.77
L
L
L
L
N
N
N


2.68
5

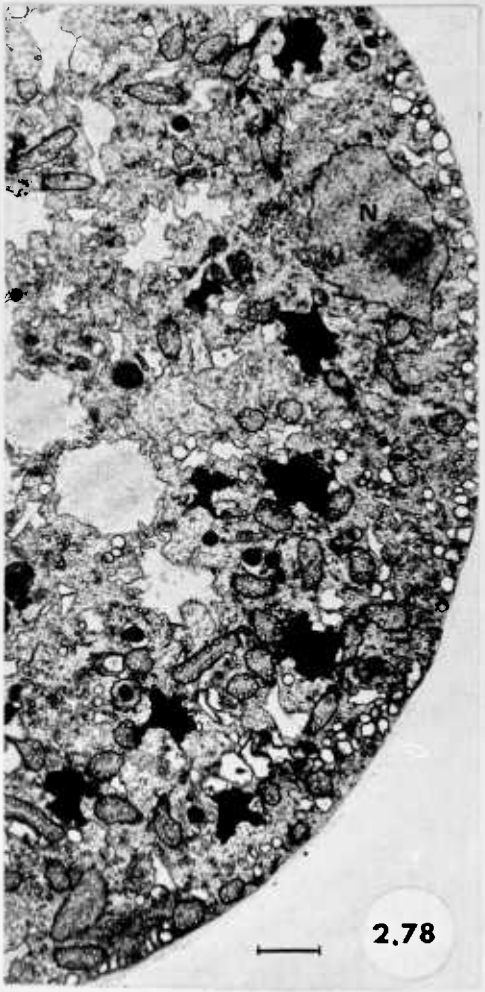

2.69
5


2.70
10


2.71
5

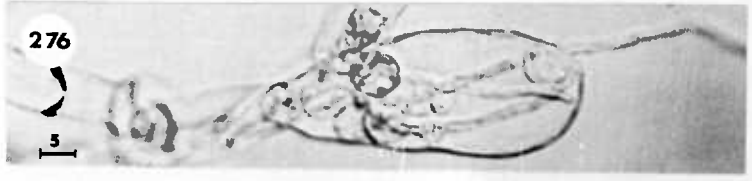

2.72
5


2.73
5


N
2.78


2.74
5


2.75
5


2.76
5

2.3.8.5 Effect of streptomycin on the cysts of S.ferax

Figs. 2.79-2.89 A selection of antibiotic incubated cysts illustrating their abnormal ultrastructure.

Fig. 2.79 Cyst still containing well-preserved organelles. The mitochondria retain their peripheral distribution and characteristic elongate cristae. The nucleolar material has become dispersed throughout the nucleoplasm. Note the elaborate vacuolar vesicles.

29931 Os 3889 500 mg/l Str 8 h

Fig. 2.80 Cyst containing slightly plasmolysed contents, and showing the beginnings of organelle degeneration.

29929 Os 3889 500 mg/l Str 8 h

Figs. 2.81-2.82 Part of two 'dense' cysts in which most of the cell organelles have become disorganised into complex membranous arrays. The complex vacuolar vesicles contain profiles of expanded osmiophilic densebody-like material.

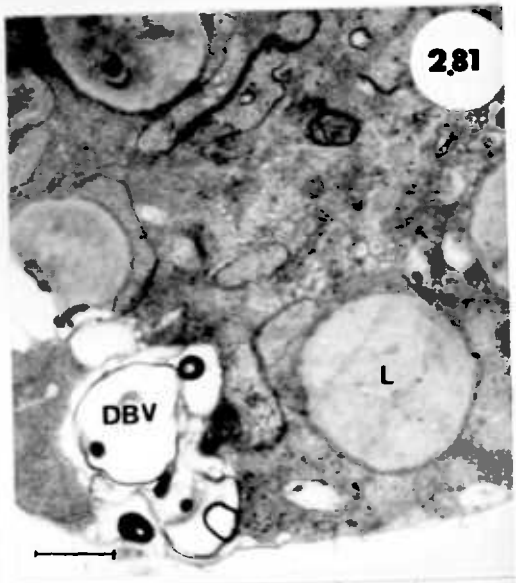
29904
29906 Os 3887 100 mg/l Str 8 h

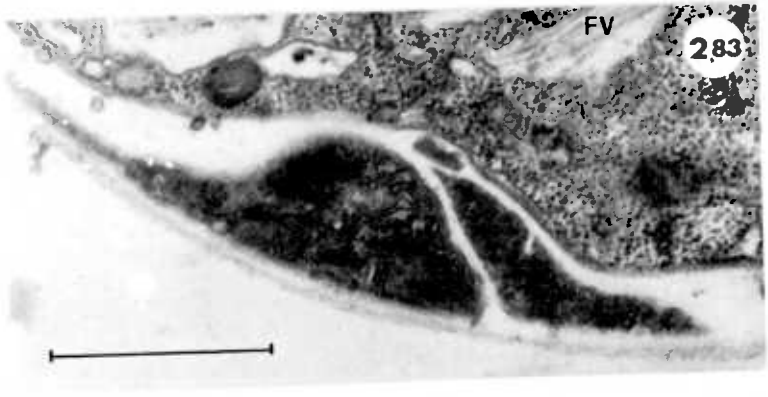
Fig. 2.38 Detail of a large lomasome associated with the inner wall of an Str-incubated cyst. Note the elaborate whorls of membranous material included in this lomasome.

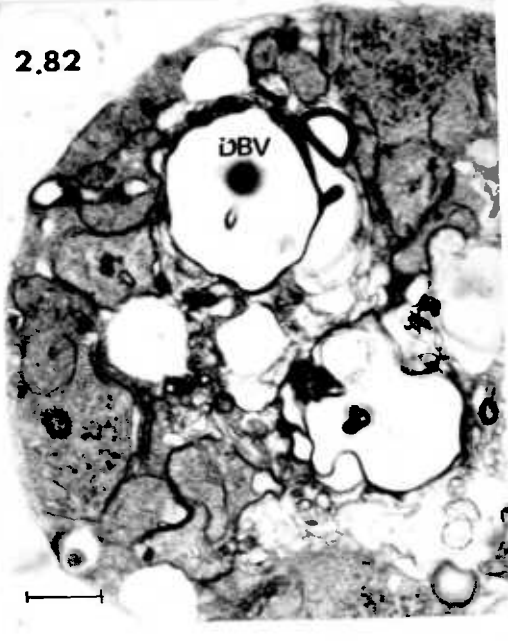
29866 Os 3886 50 mg/l Str 8 h


2.79
N
FV


2.80


2.81
L
DBV


FV
2.83


2.82
DBV

2.8.8.5 Abnormal Str-incubated cysts of S.ferax

Fig. 2.84 Abnormal cyst which has produced a short germtube. Note the paucity of staining in the groundplasm and the small number of ribosomes. This gives these cysts the superficial appearance of $KMnO_4$-fixed material. Note also the presence of small vesicles in the nucleoplasm close to the nuclear envelope.
29879 Os 3886 50 mg/l Str 8 h

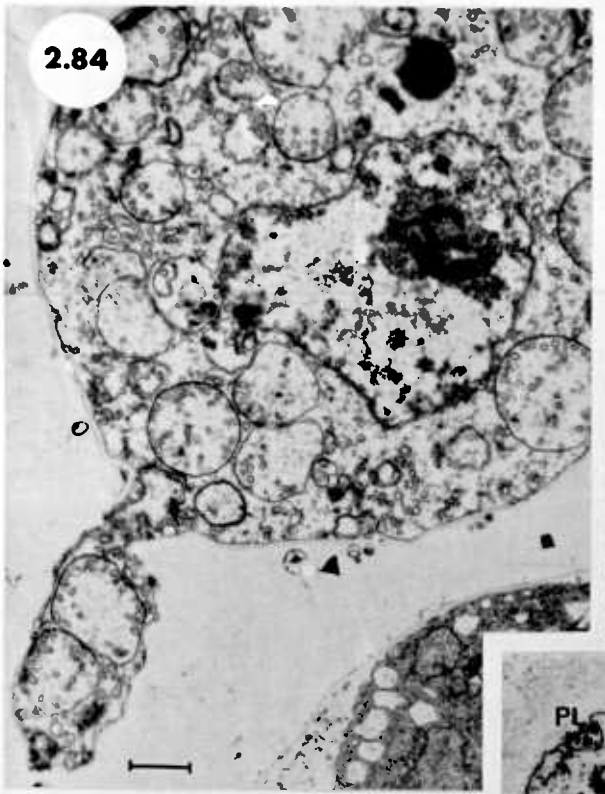
Fig. 2.85 Nucleus from an abnormal cyst such as shown in Figs. 2.84, 2.87. Note the low density of nuclear contents except for the dense condensed nucleolus. Flimmer tubules are present in the inflated nuclear envelope cisterna.
29874 Os 3886 50 mg/l Str 8 h

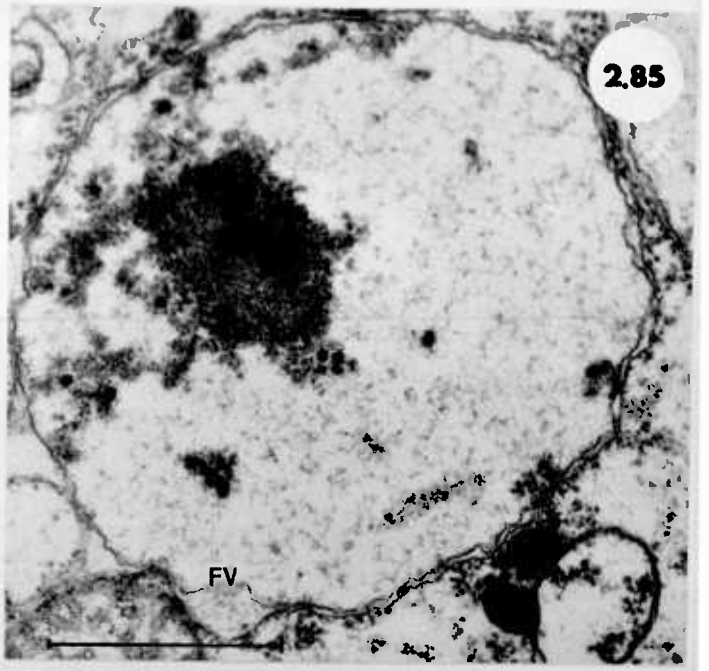
Fig. 2.86 Detail of the cytoplasm of the cyst shown in Fig. 2.87, showing the absence of ribosomes. The proteinaceous flimmer tubules are still well preserved.
29874 Os 3886 50 mg/l Str 8 h

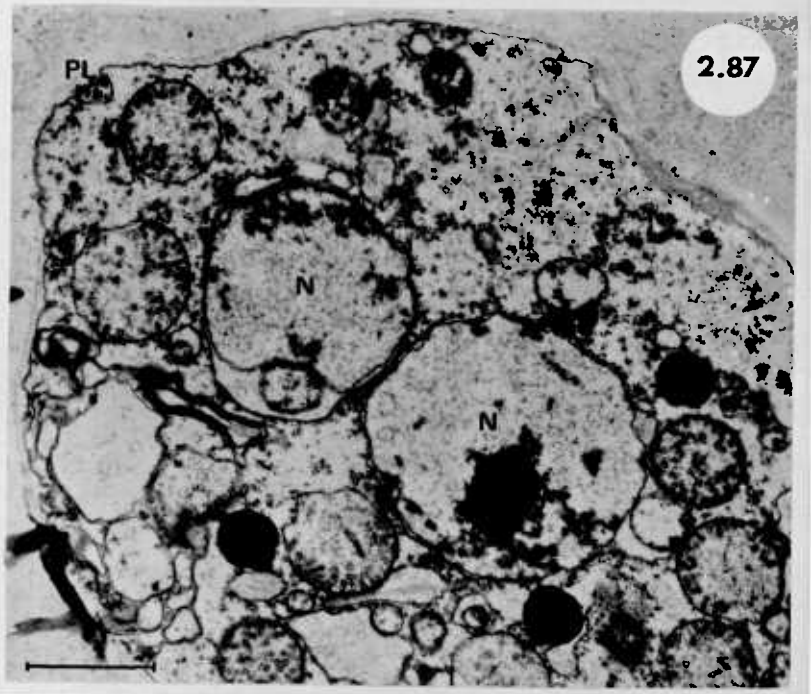
Fig. 2.87 Profile of an abnormal cyst with a lateral bulge, suggesting an early stage in germination. Note there are two nuclei in this cyst.
29874 Os 3886 50 mg/l Str 8 h

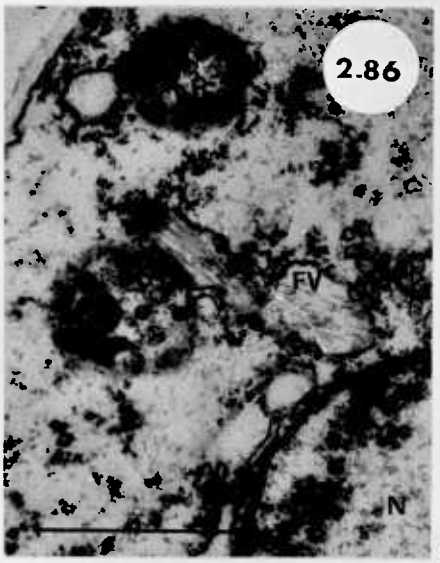
Fig. 2.88 A mitochondrion from the cyst shown in Fig. 2.87, showing the ruptured outer membrane and inflated inner membrane.
29874 Os 3886 50 mg/l Str 8 h

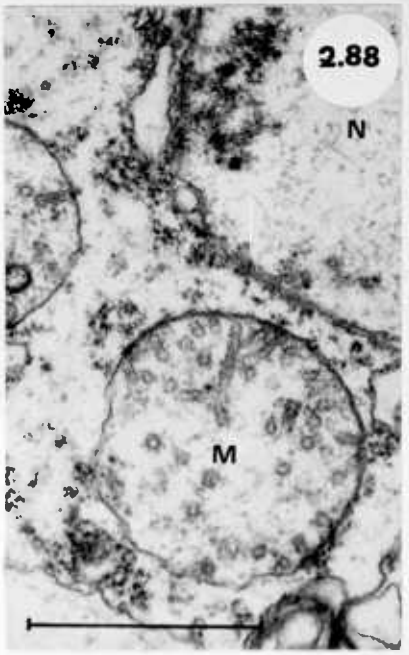
Fig. 2.89 Profile of a cyst in which the cytoplasm has become completely disorganised, leaving only membrane fragments and lipid droplets recognisable.
29845 Os 3887 100 mg/l Str 8 h

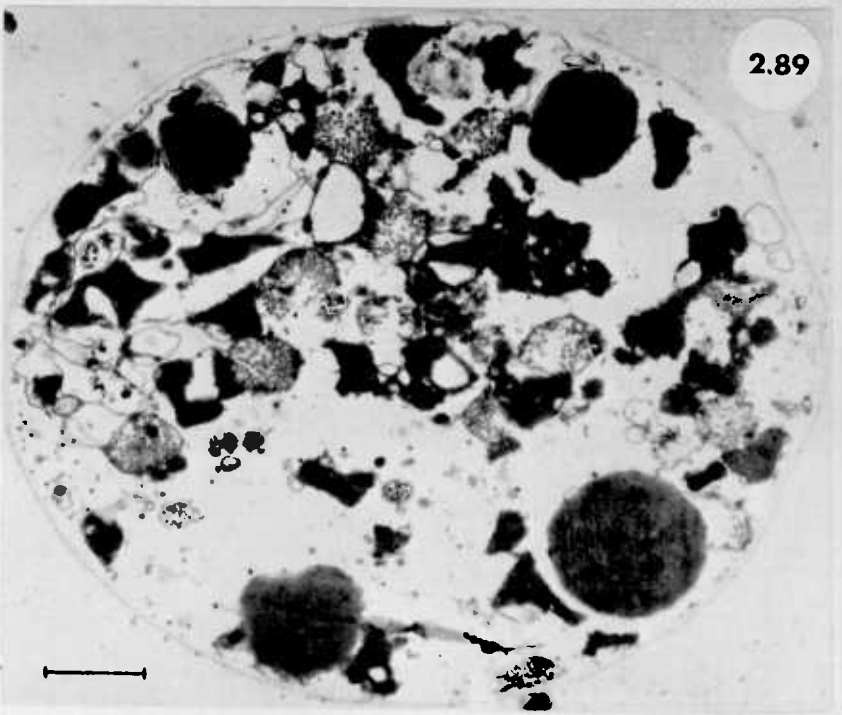

2.84


2.85
FV


PL
2.87
N
N


2.86
FV
N


2.88
N
M


2.89

2.3.8.6 The effect of streptomycin on gametangium development in S.furcata

Figs. 2.90, 2.91 Hyphal tips, showing elaborate Str-induced twisting. The elaborate knot-like structure in Fig. 2.91, probably would not differentiate further.

53/27, 62/7 OI 100 mg/l Str 48 h

Fig. 2.92 A Stage II-III oogonium initial showing elaborate stalk, and attachment of helical antheridial hyphae.

62/23 OI 150 mg/l Str 48 h

Fig. 2.93 A Stage I oogonium initial on an elaborate stalk.

62/22 OI 100 mg/l Str 48 h

Figs. 2.94, 2.95 Stage IV oogonia containing transparent prophase I nuclei. The helical coiling of the antheridial and oogonial stalks is also shown.

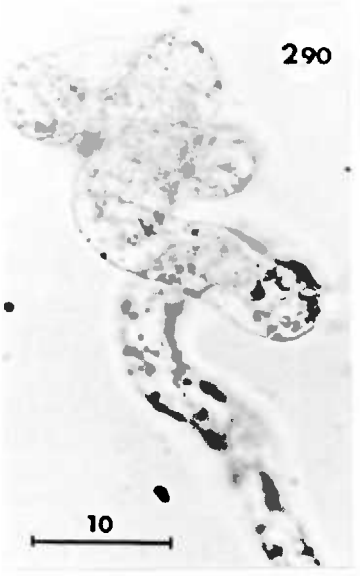
62/4, 62/12 OI 100 mg/l Str 48 h

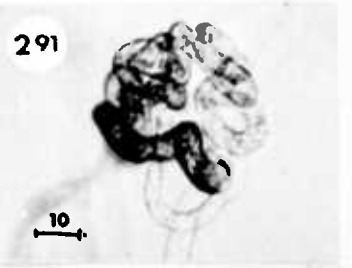
Fig. 2.96 Montage of a Stage I oogonium initial. Note the high concentration of neutral lipid and densebodies, and virtual absence of vacuolar vesicles.

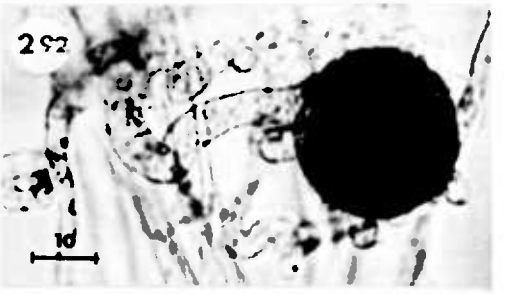
21674/75 Os 3448 100 mg/l Str 24 h

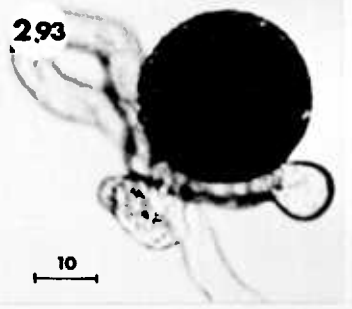
Fig. 2.97 A vacuolate Stage IV oogonium showing the peripheral prophase I nuclei (Os-fixed) and high density of lipid and densebody reserves. Note also the very thick oogonial wall.

22015 Os 3451 100 mg/l Str 48 h

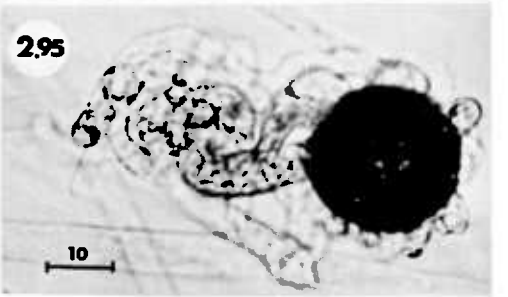

2.90
10

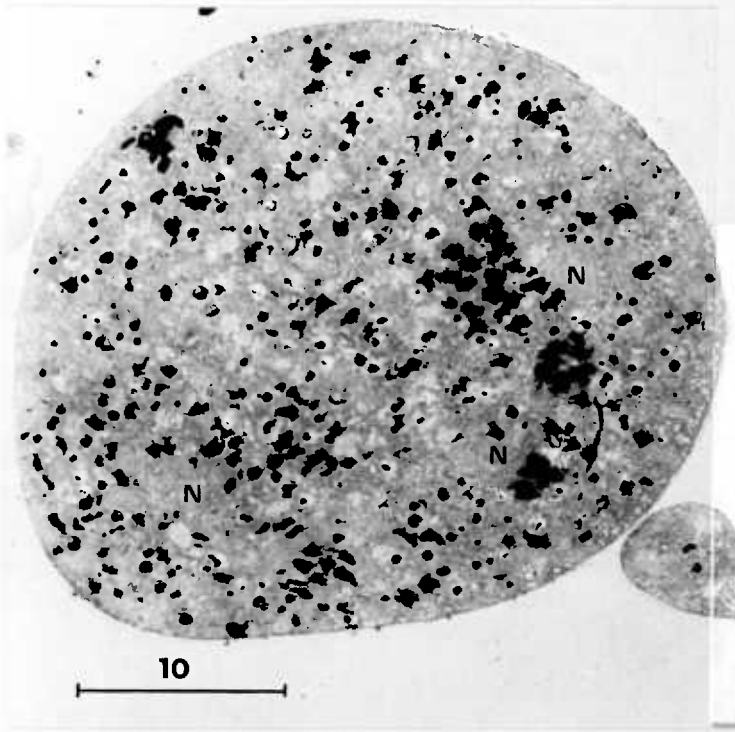

2.91
10

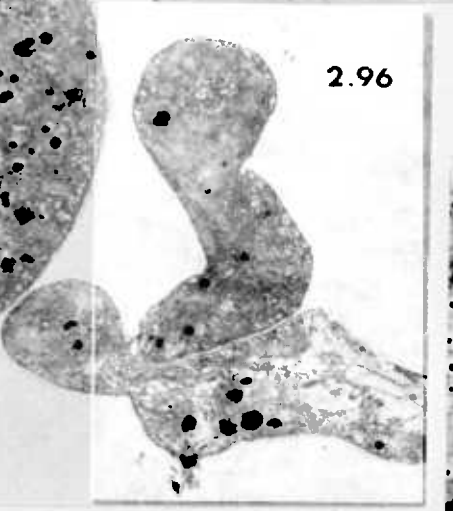

2.92
10

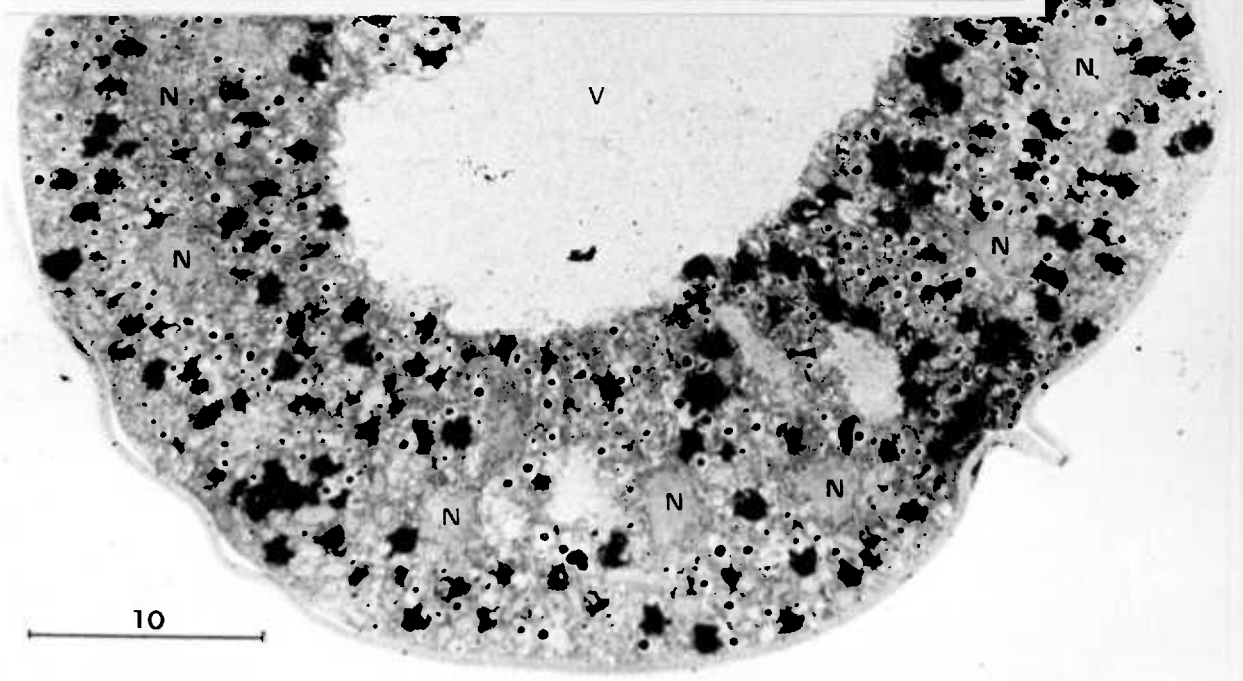

2.93
10


2.94
10


2.95
10


N
N
N
10


2.96


2.97
N
N
N
N
V
N
N
N
N
10

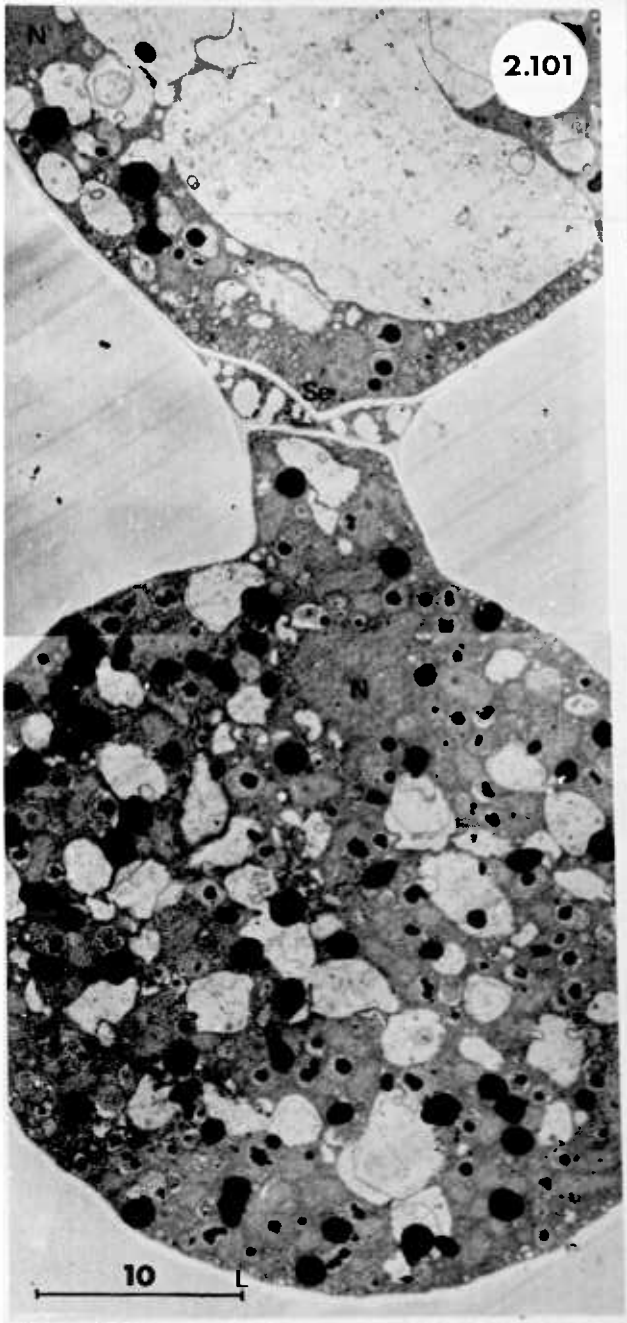
2.3.8.8 Streptomycin-induced gemmae in S.furcata: Gemma chains

Fig. 2.98 A typical chain of Str-induced gemmae, showing the order of differentiation (numbered). A newly-formed septum between the 3rd and 4th body can just be distinguished.
152/12 OI 500 mg/l Str 120 h

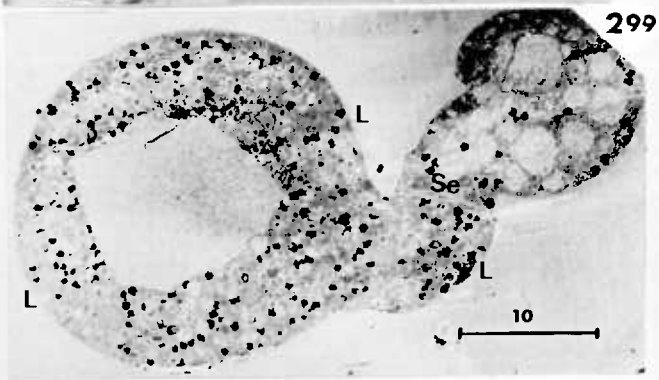
Figs. 2.99, 2.101 Sections through the terminal and second bodies of two gemma chains, showing the tripartite septa which separates them. The terminal body contains a large expanded vacuole, while the second body is only partially vacuolate.
19219 Os 3319 400 mg/l Str 120 h
21674/75 GaOs 3457 50 mg/l Str 120 h

Fig. 2.100 A single spherical gemma
67/21 OI 100 mg/l Str 96 h

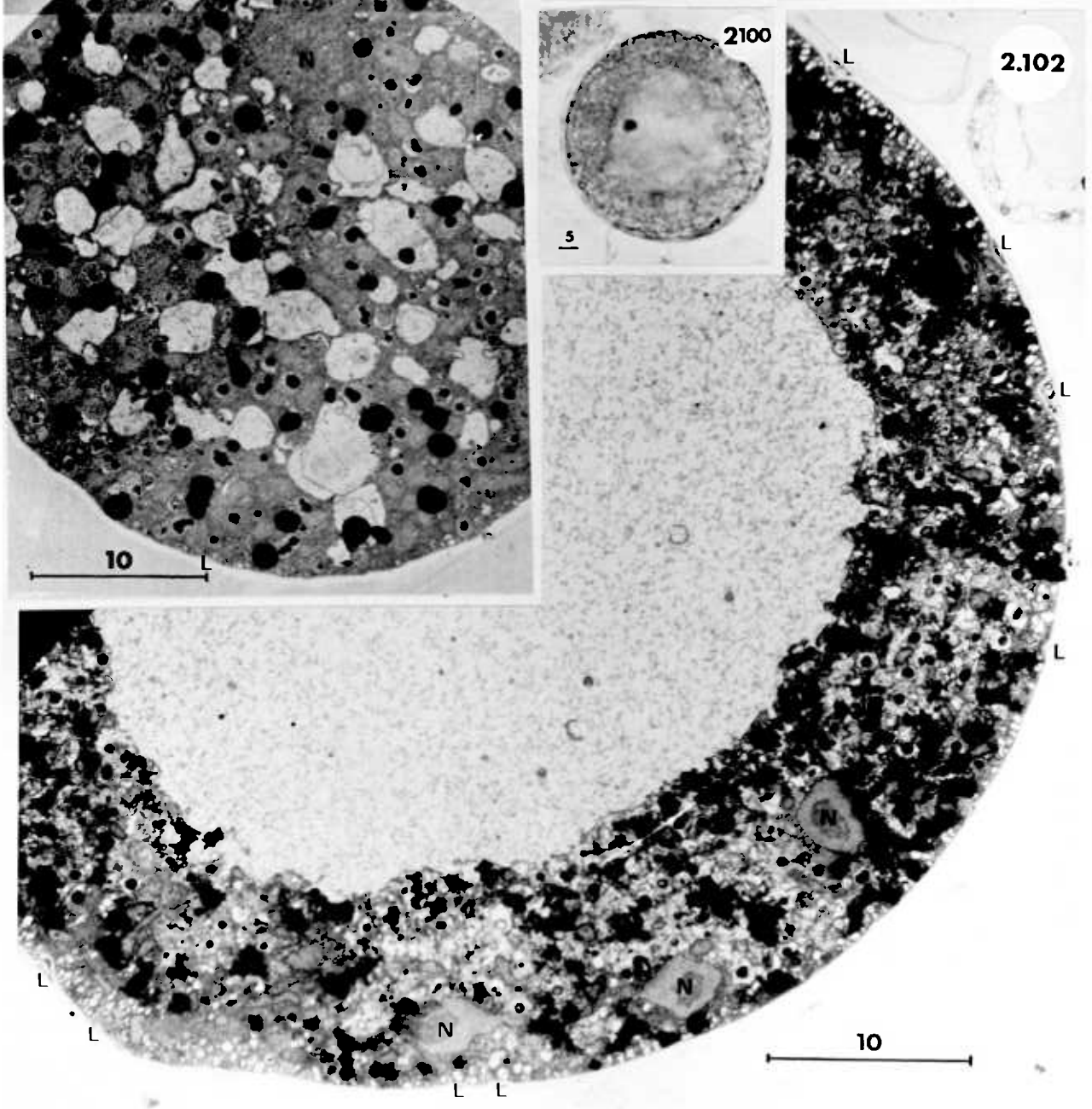
Fig. 2.102 Median section through part of a spherical gemma body, showing the large central vacuole bounded by a single tonoplast membrane. Note the large number of lomasomes associated with the cell wall.
22015 Os 3319 400 mg/l Str 120 h


2.101
N
Se
N
10
L


298
5
2
3
4
1


299
L
Se
L
L
10

2100
5


2.102
L
L
L
L
N
N
N
L
L
L
L
10

2.3.8.8 Streptomycin-induced gemmae in S.furcata: Appendage initiation

Fig. 2.103 A Str-induced gemma showing a newly initiated appendage. Note its refractile appearance at this stage.
67/23 OI 100 mg/l Str 96 h

Fig. 2.104 Section through an appendage initial. The cytoplasm is composed almost exclusively of wall vesicles.
23116 $KMnO_4$ (2% 20 min) 3453 50 mg/l 120 h

Fig. 2.105 A gemma with a more advanced appendage. Note the rather indistinct appearance of the vacuolar area within the gemma.
152/60 OI 500 mg/l 120 h

Fig. 2.106 A poorly-fixed section of a young appendage. The appendage wall is derived from a new inner wall layer. The orginal gemma wall ruptures as the appendage grows out leaving the well defined wall scars at its base.
23533 GaOs 3458 100 mg/l 120 h

Fig. 2.107 A Str-induced gemma with two developing appendages.
68/4 OI 500 mg/l 120 h

Fig. 2.108 The apex of a developing appendage showing the apical wall vesicles and abundant plasmalemmasomes.
25064 Os 3483 100 mg/l 240 h

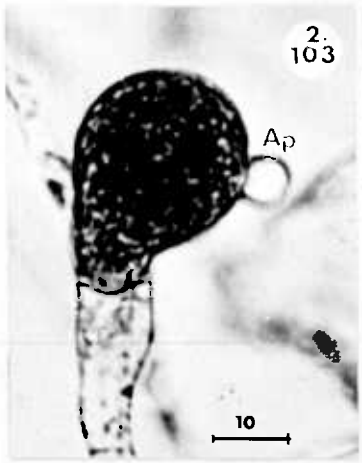
Fig. 2.109 Profile of a swollen appendage, which is already highly vacuolate. Note the apical concentration of wall vesicles and prominent basal wall scars.
19722 Os 3319 400 mg/l 120 h

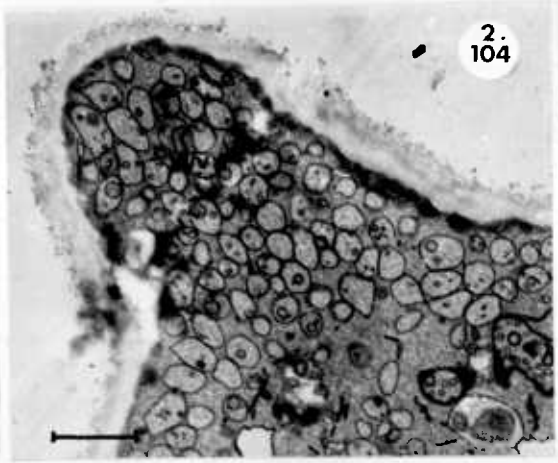
Fig. 2.110 Light-micrograph of a comparable swollen vacuolate appendage.
83/30 50 mg/l 96 h

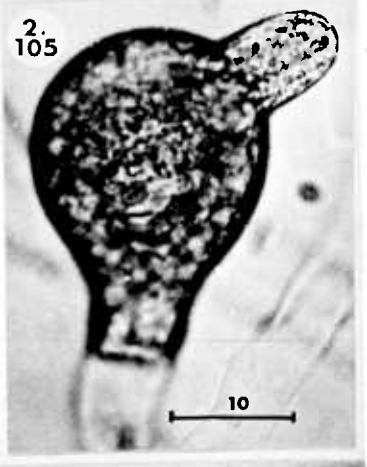
Fig. 2.111 Section of gemma with two developing appendages. Note the partially coalesced vacuolar vesicles.
19561 Os 3317 200 mg/l 120 h

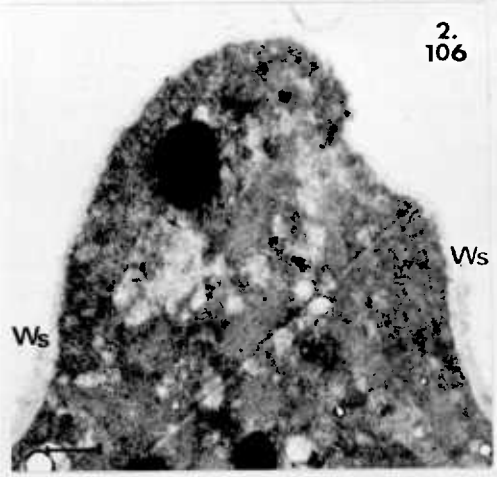
Fig. 2.112 Gemma with two spherical appendages, such as shown in Fig. 2.111.
54/23 OI 500 mg/l 96 h

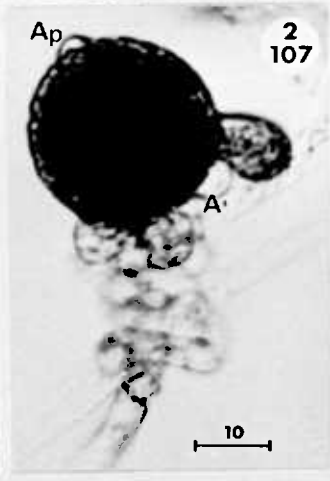
Fig. 2.113 Base of an elongate appendage showing the basal wall scars.
25474 Os 3486 250 mg/l 240 h

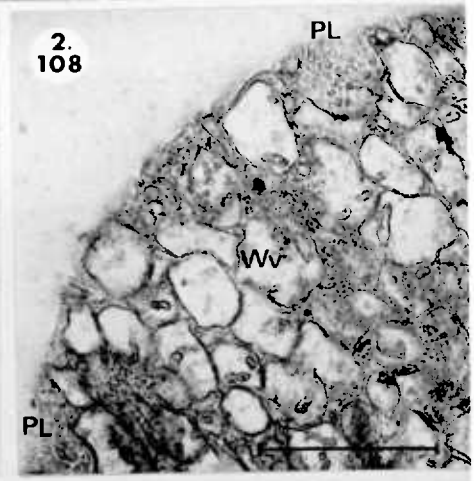

2.
103
Ap
10

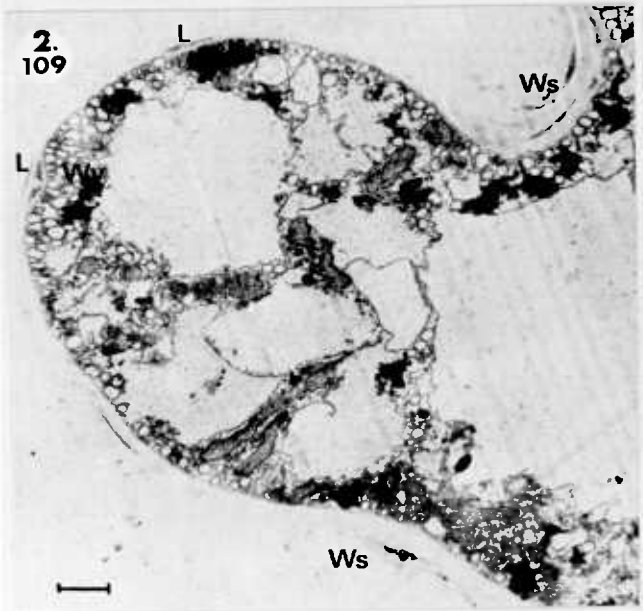

2.
104

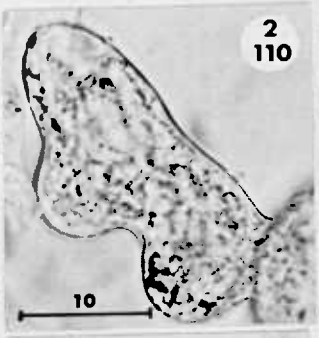

2.
105
10

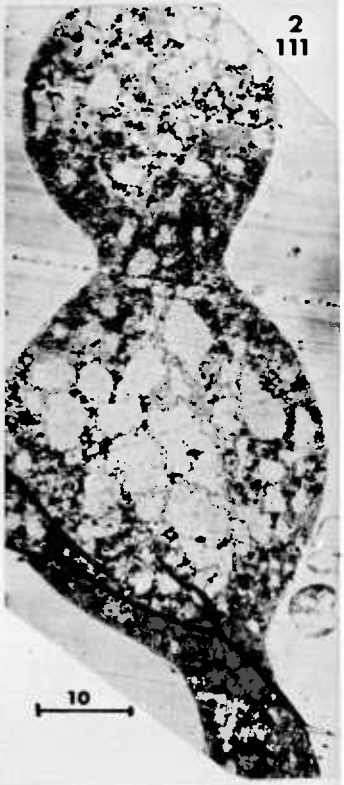

2.
106
Ws
Ws


Ap
2
107
A
10

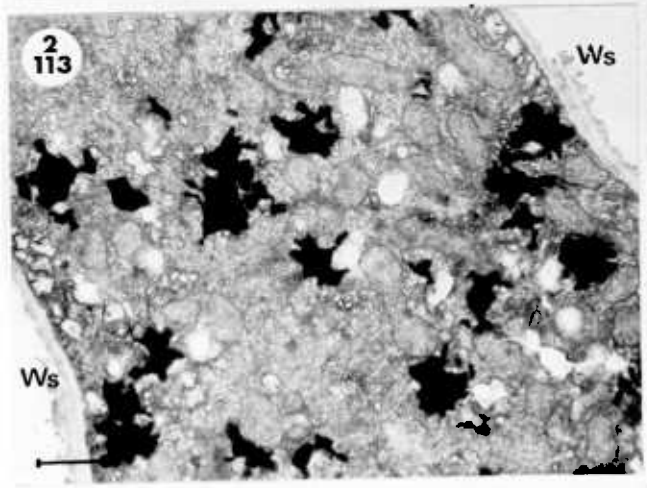

2.
108
PL
Wv
PL


2.
109
L
Ws
L
Wv
Ws


2
110
10


2
111
10


2.
112
1 0


2
113
Ws
Ws

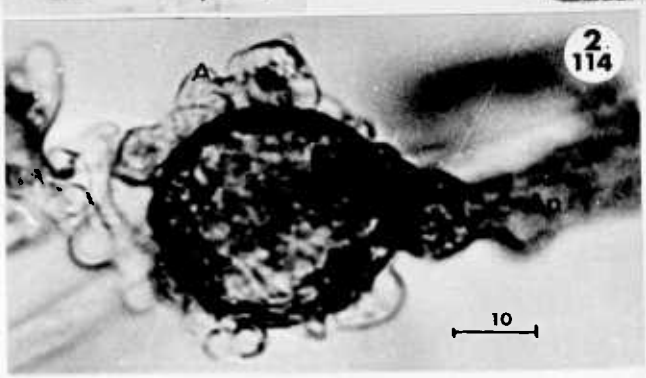

2.
114
A
10

Fig. 2.114 An appendate gemma, showing that appendage formation can also occur from antheridiate bodies.

68/8 OI 500 mg/1 120 h

2.3.8.8 Streptomycin induced gemmae in S.furcata: Appendate gemmae

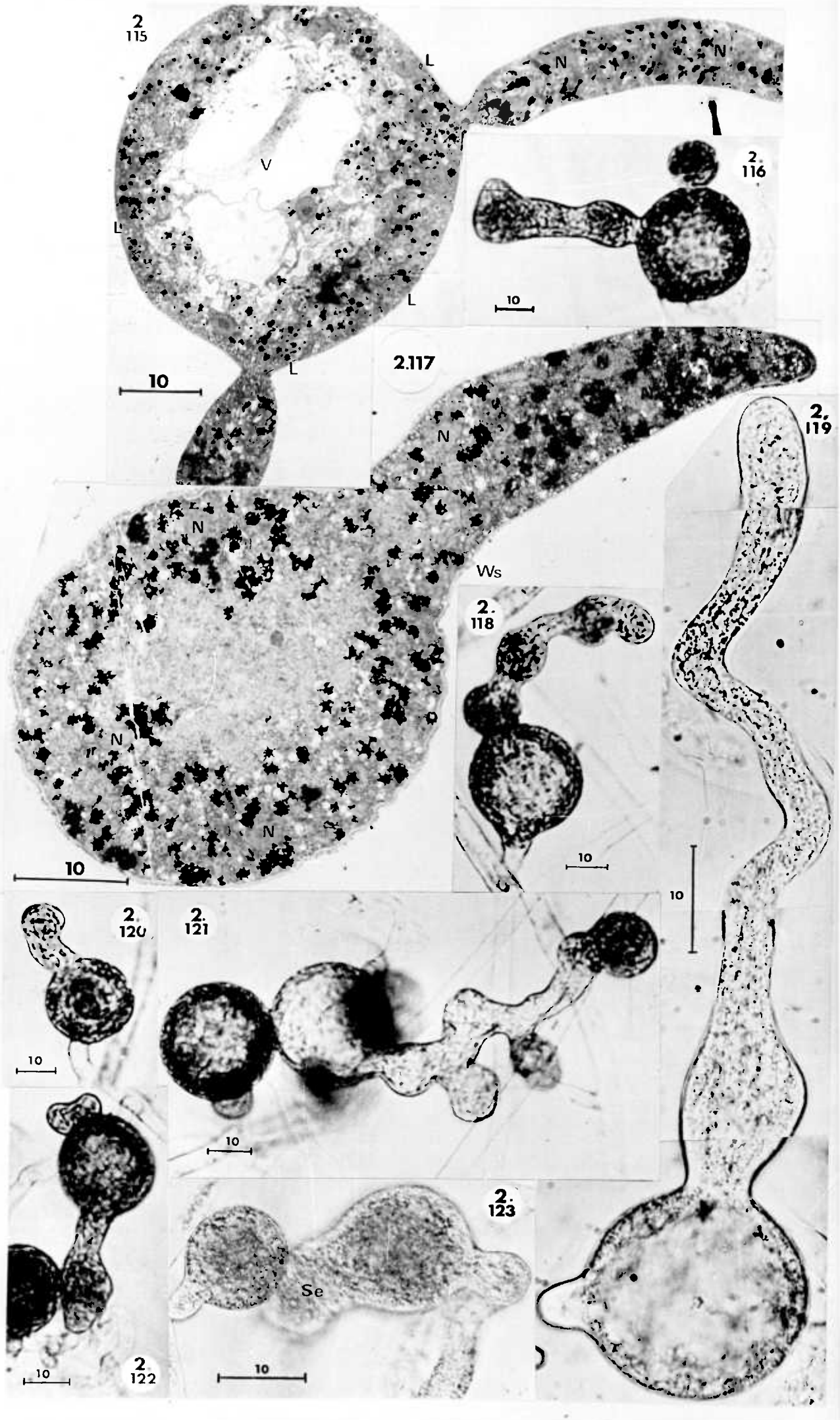
Fig. 2.115 Montage of a young appendate gemma. The gemma cytoplasm in contrast with the appendage, is highly vacuolate.
21783/84/85 Os 3450 50 mg/1 Str 48 h

Fig. 2.116 Light micrograph of an appendate gemma, showing two appendages at differing stages of development. Note the irregularly swollen profile of the larger appendage.
87/16 OI 200 mg/1 Str 120 h

Fig. 2.117 Montage of an appendate gemma after prolonged antibiotic incubation. Note the rather indistinct appearance of the vacuoles, and diameter of appendage cf. Fig. 2.115.
25475/76 Os 3486 250 mg/1 Str 240 h

Figs. 2.118-2.123 Light micrographs of selected appendate gemmae to illustrate the variability of appendage morphology.

118	67/30	OI	400 mg/1 Str 120 h
119	122/11-16	OI	50 mg/1 Str 160 h
120	67/24	OI	300 mg/1 Str 120 h
121	67/15	OI	100 mg/1 Str 120 h
122	67/24	OI	300 mg/1 Str 120 h
123	46/14	OI	500 mg/1 Str 96 h


2
115
L
N
N
V
L
L
L
10
2.
116
10
2.117
N
2.
119
N
Ws
N
N
N
10
2.
118
10
10
2.
120
2.
121
10
10
2.
122
10
2.
123
Se
10

2.3.8.8 Streptomycin-induced gemmae in S.furcata: Appendate and club-shaped forms

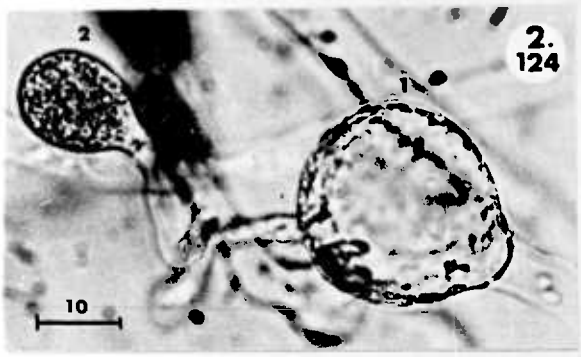
Figs. 2.124-2.126 Three light micrographs showing the successive development of secondary gemmae. They are numbered in order of their formation. Note the efficiency with which the cytoplasm migrates from one body to the next.
152/54
152/33 OI 500 mg/l Str 120 h
68/1

Fig. 2.128 Light micrograph of a gemma showing an unusual pattern of vacuolation.
45/14 OI 1000 mg/l Str 200 h

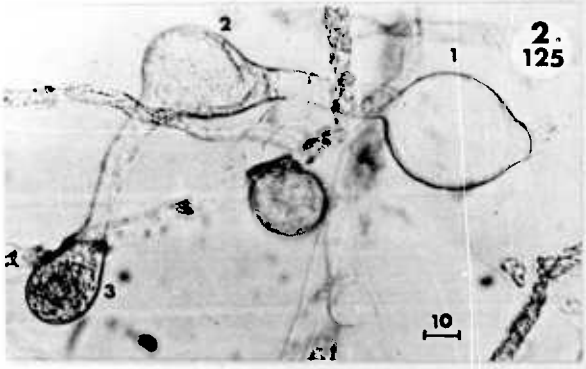
Fig. 2.129 A typical clavate gemma body.
46/19 OI 500 mg/l Str 200 h

Fig. 2.130 Mature gemma showing an extremely elongate appendage, and thinly distributed cytoplasm.
67/32 OI 500 mg/l Str 120 h

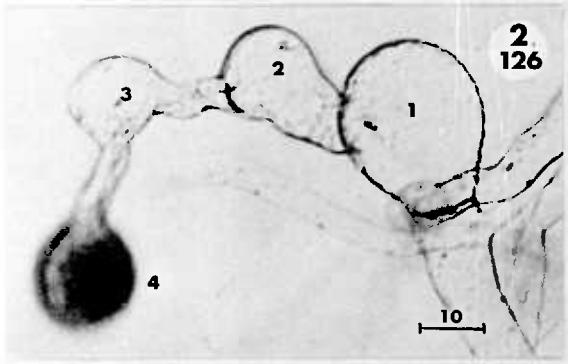
Fig. 2.131 Montage of slightly oblique LS through a clavate gemma. Note its large size, the distribution of the vacuolar compartments and the abundance of lomasomes.
25232/33 Os 3485 500 mg/l Str 240 h



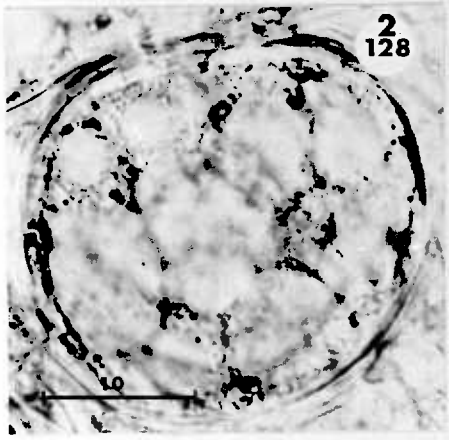
2.
124



2.
125



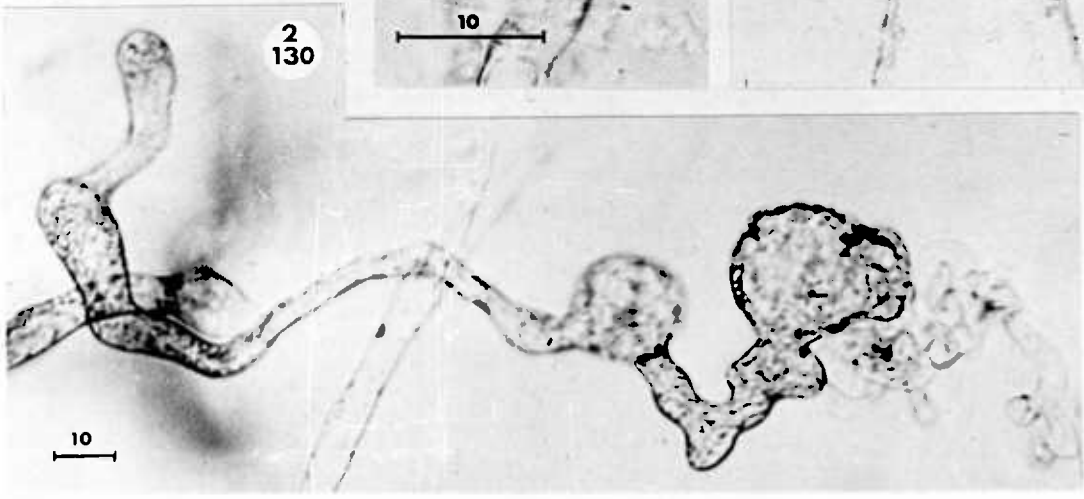
2
126



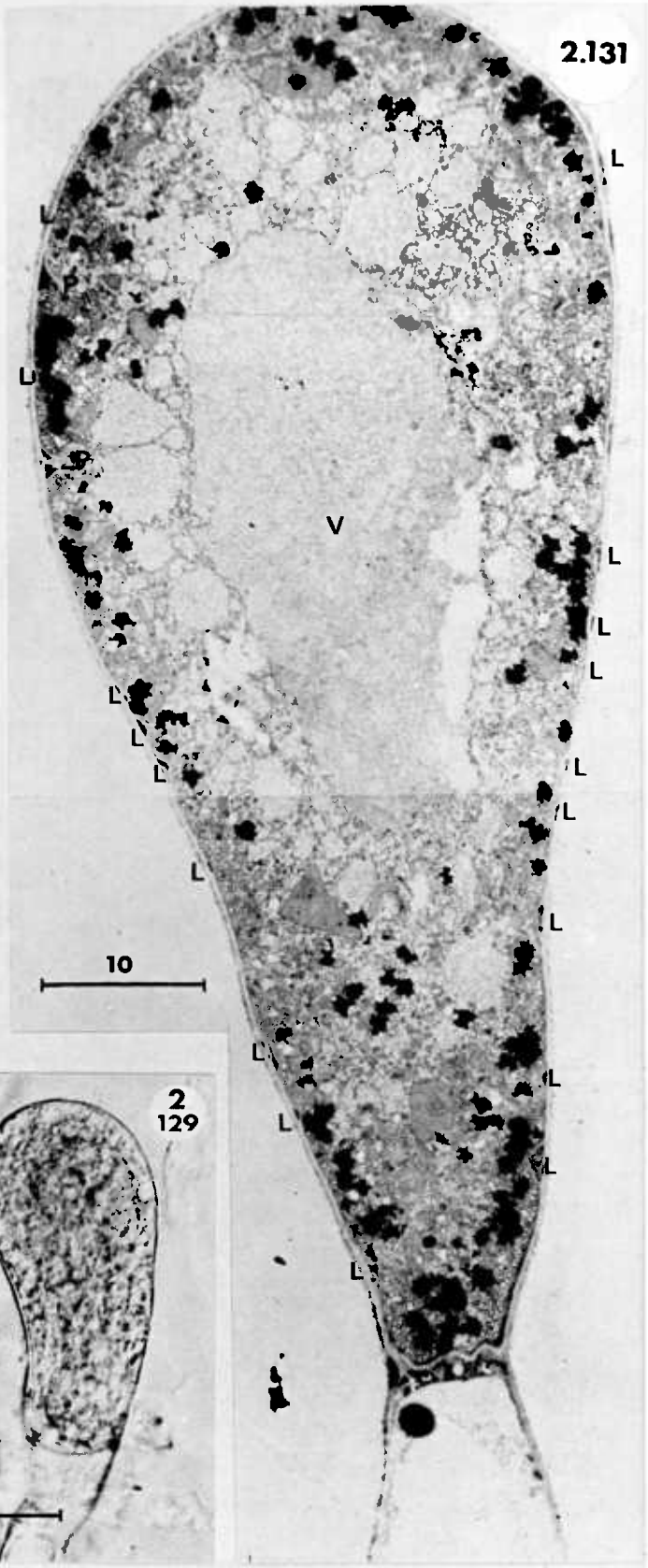
2
128



2
129



2
130



2.131

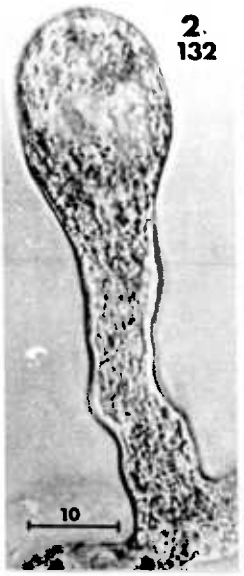
2.3.8.8 Streptomycin-induced gemmae in S.furcata: Secondary gemmae

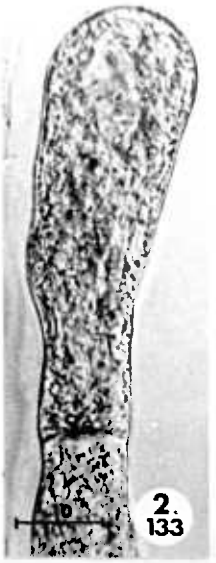
Figs. 2.132, 2.133. Swollen tips of two elongate appendages, one of which has been delimited by a septum.
53/10 53/13 OI 500 mg/1 Str 150 h

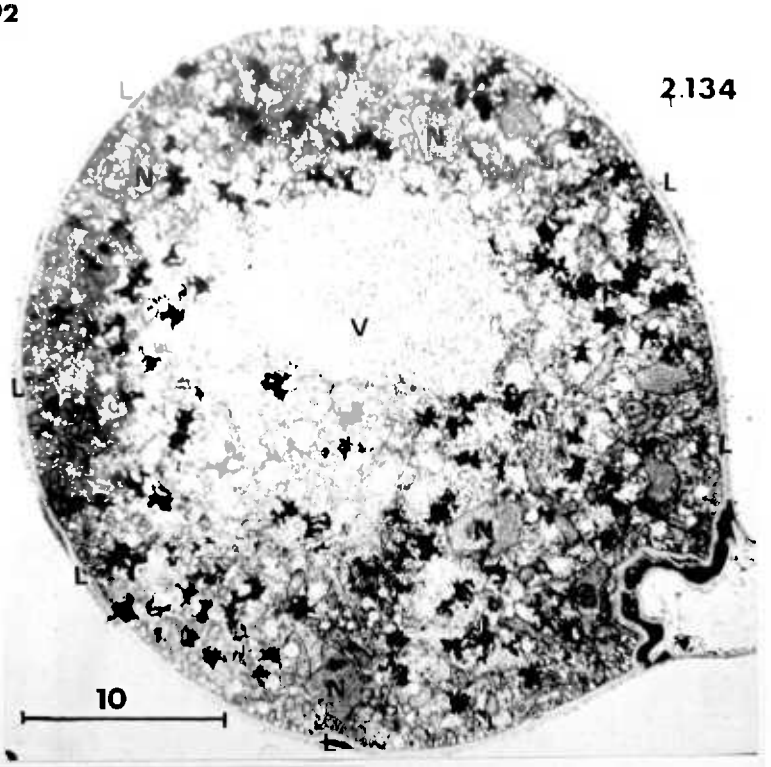
Figs. 2.134, 2.135 Sections of two secondary gemmae. Note the abundence of lomasomes and the absence of vacuolar vesicles in Fig. 2.135.
25403 Os 3485 200 mg/1 Str 240 h
25586 Os 3486 100 mg/1 Str 240 h

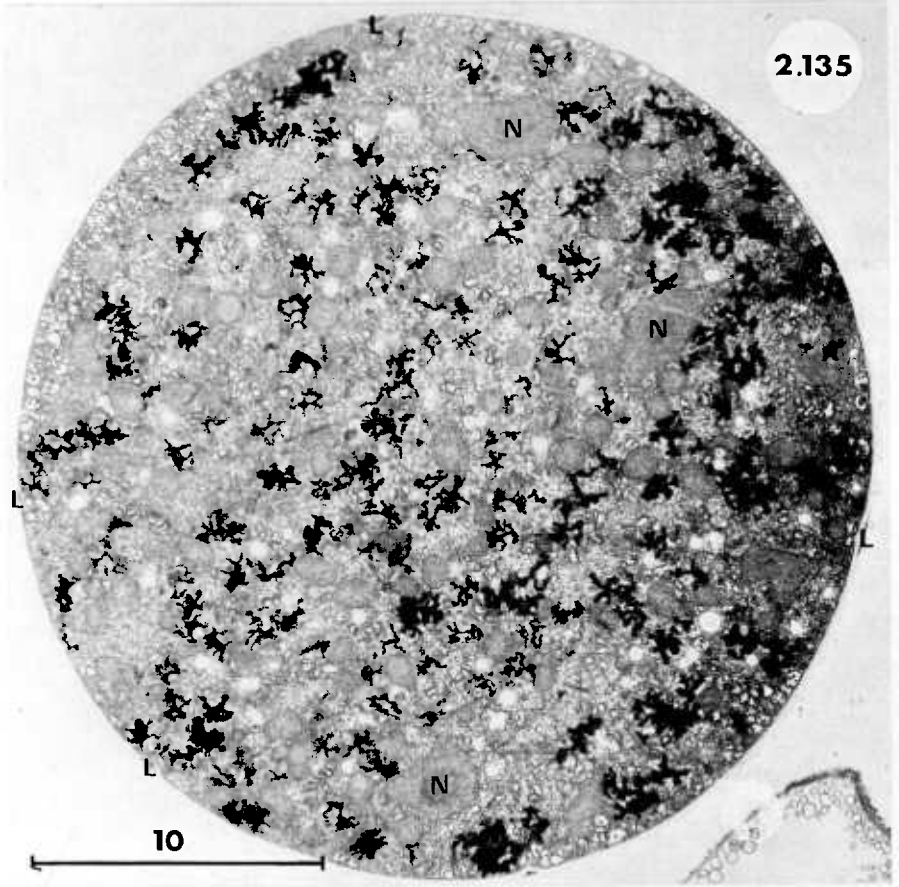
Figs. 2.136-2.138 Light micrographs of terminal secondary gemmae illustrating the variability in cytoplasmic density.
46/27, 46/17, 46/15 OI 500 mg/1 Str 150 h

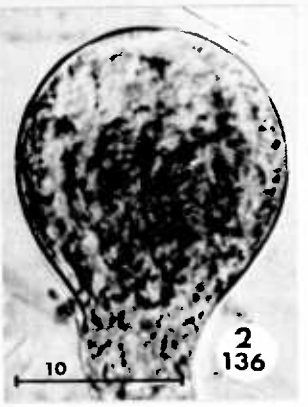
Fig. 2.139 Part of a vacuolate secondary gemma, showing the central vacuolar zone made up of small vesicles. Note how the neutral lipid droplets have become peripherally distributed.
25588 Os 3487 500 mg/1 Str 240 h

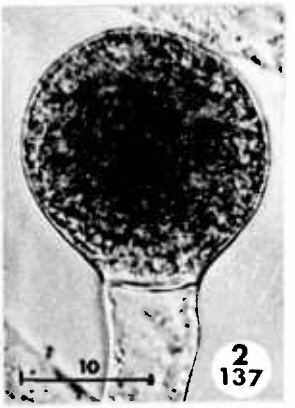

2
132
10


10
2
133

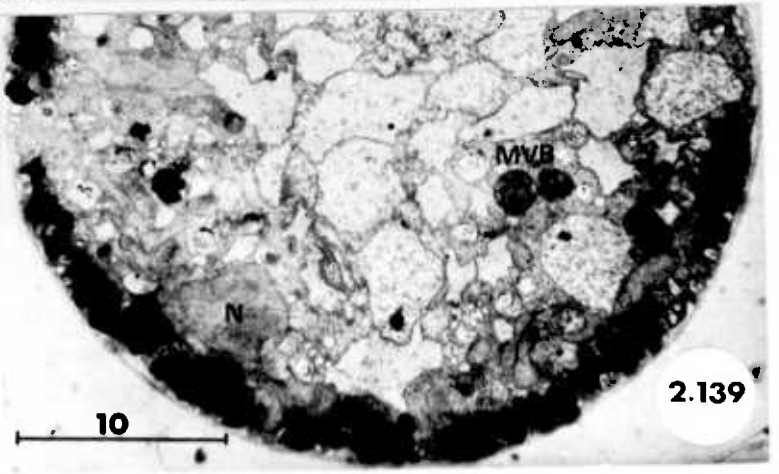

2.134
L
N
L
V
L
N
L
10


2.135
L
N
N
L
L
N
10


10
2
136


10
2
137


2
138
10


MVB
N
2.139
10

2.3.8.7 The effect of streptomycin on oospore structure in S.furcata

Fig. 2.140 Stage VII oospore showing the segregation of neutral lipid and densebody vesicle fractions.
22073 Os 3451 100 mg/l Str 48 h

Fig. 2.141 Abnormal oospore in which the neutral lipid and densebody fractions have remained randomly distributed. Most other organelles are poorly preserved.
27485 GaOs 3832 5 mg/l Str 170 h

Fig. 2.142 Oospore with lysed contents. Note the presence of a thin endospore wall layer indicating lysis occurred during the late stages of oospore maturation.
27401 Os 3932 5 mg/l Str 170 h

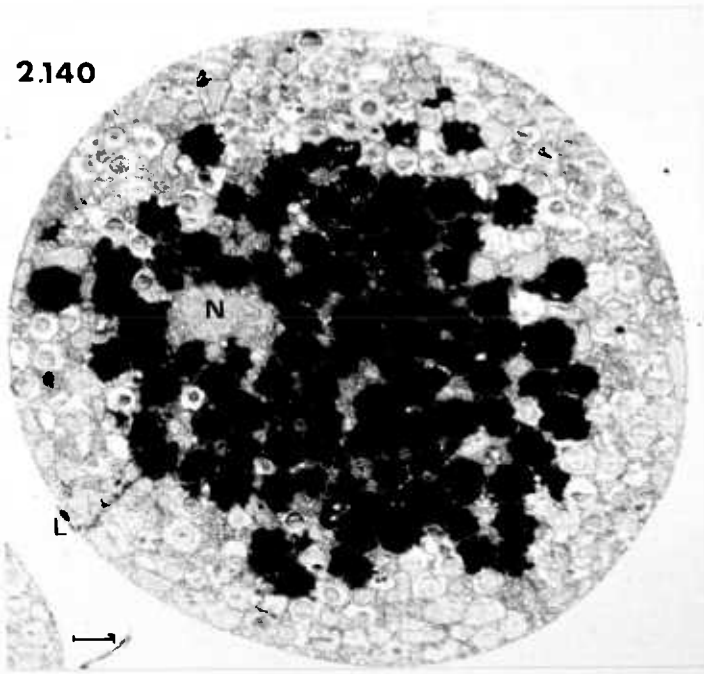
Fig. 2.143 Oogonium containing two oospores with dense cytoplasm, and others with lysed contents
154/4 5 mg/l Str 120 h

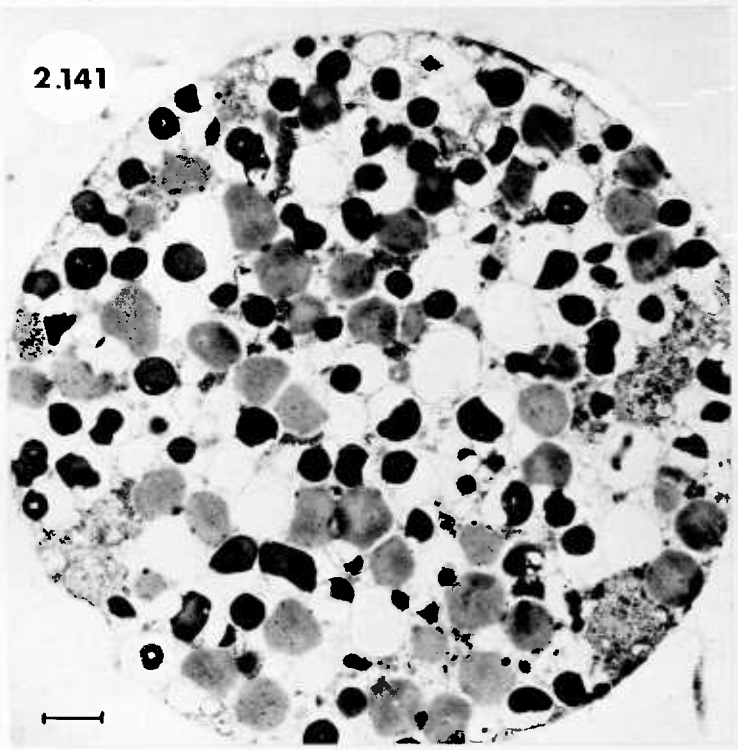
Fig. 2.144 Oogonium containing two normal Stage X oospores (upper) and several 'oily' oospores (lower). Note also the conspicuous flask shaped fertilisation tube.
154/5 5 mg/l Str 120 h

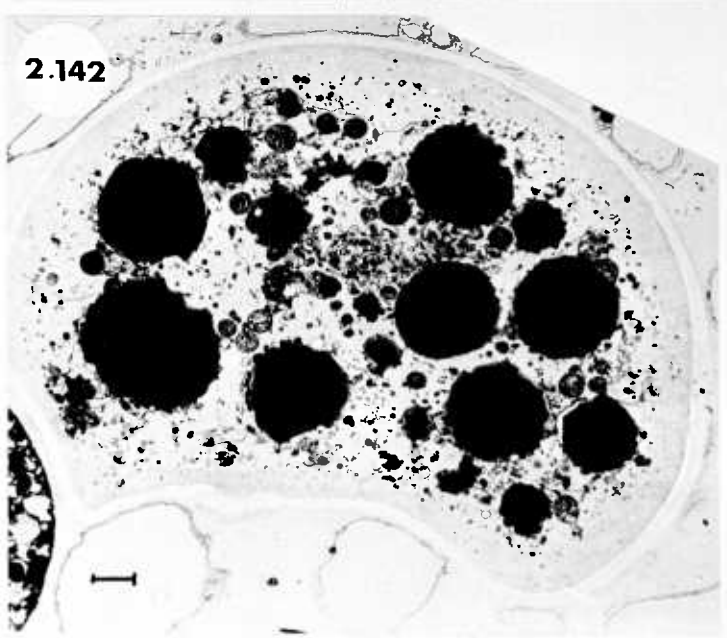
Fig. 2.145 Oogonium with a single normal and several aborted 'oily' spores.
154/6 5 mg/l Str 120 h

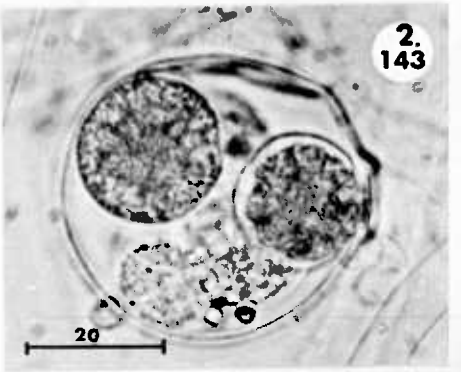
Fig. 2.146 Oogonium containing both dense and oily spores. The antheridium has almost encompassed the oogonium. This degree of development is unusual in this species.
154/18 5 mg/l Str 120 h

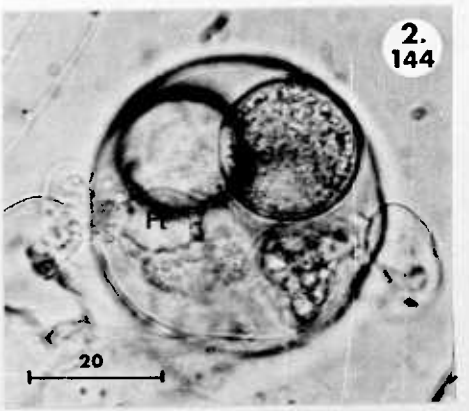
Fig. 2.147 Oogonium containing aborted 'hyaline' oospores.
154/3 5 mg/l Str 120 h


2.140
N

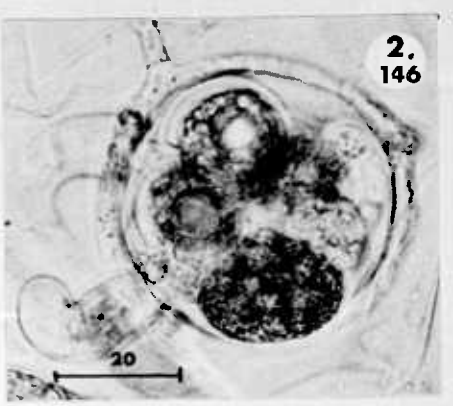

2.141

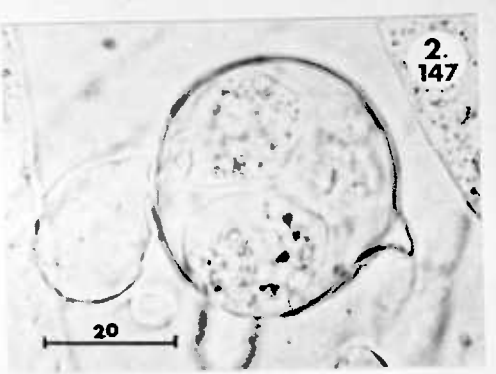

2.142


2.
143
20


2.
144
20


2.
145
20


2.
146
20


2.
147
20

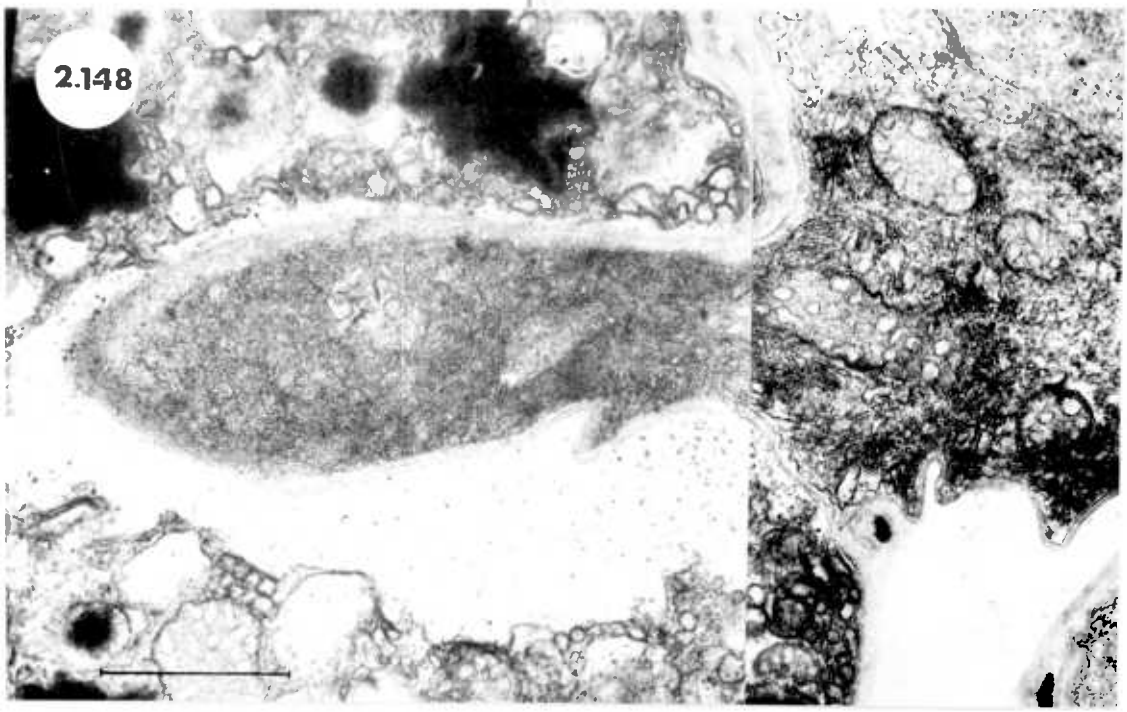
2.2.8.7 The effect of streptomycin on fertilisation tube structure in S.furcata

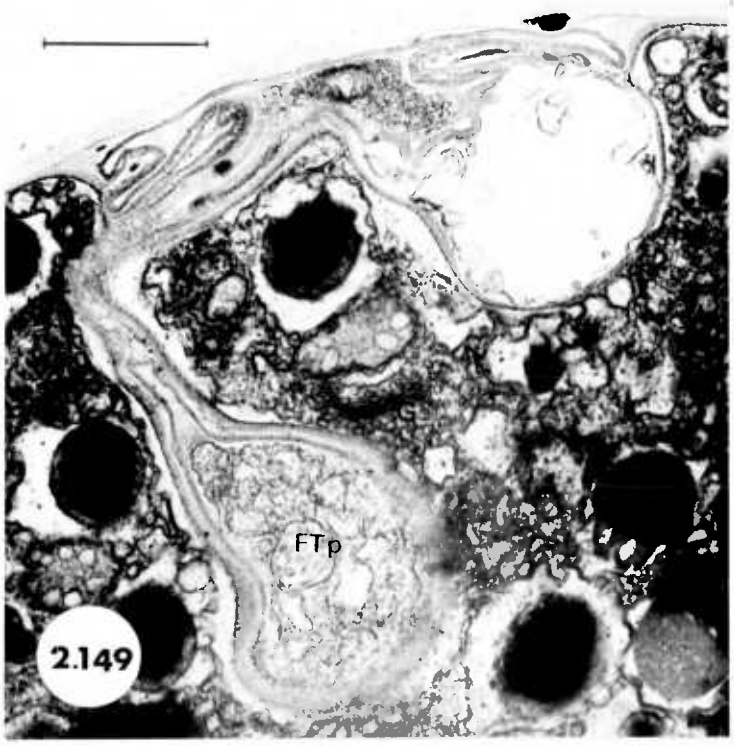
Fig. 2.148 LS montage of a fertilisation tube which has penetrated a Stage VIII oospore. The dense contents of the penetration peg and its buckled wall suggests it may have collapsed slightly during preparation. The fertilisation tube ruptures the oospore wall but does not penetrate the plasmalemma.
27139/40 Os 3450 50 mg/l Str 48 h

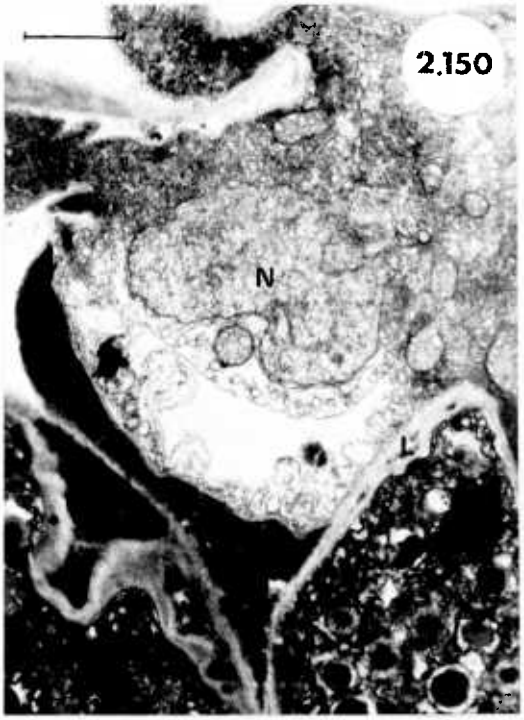
Fig. 2.149 Collapsed penetration peg of a fertilisation tube in a Stage VII oospore. Note that it is surrounded by wall material that is continuous with the oospore wall. A Golgi-mitochondrion complex is also shown adjacent to this body.
21872 Os 3450 50 mg/l Str 48 h

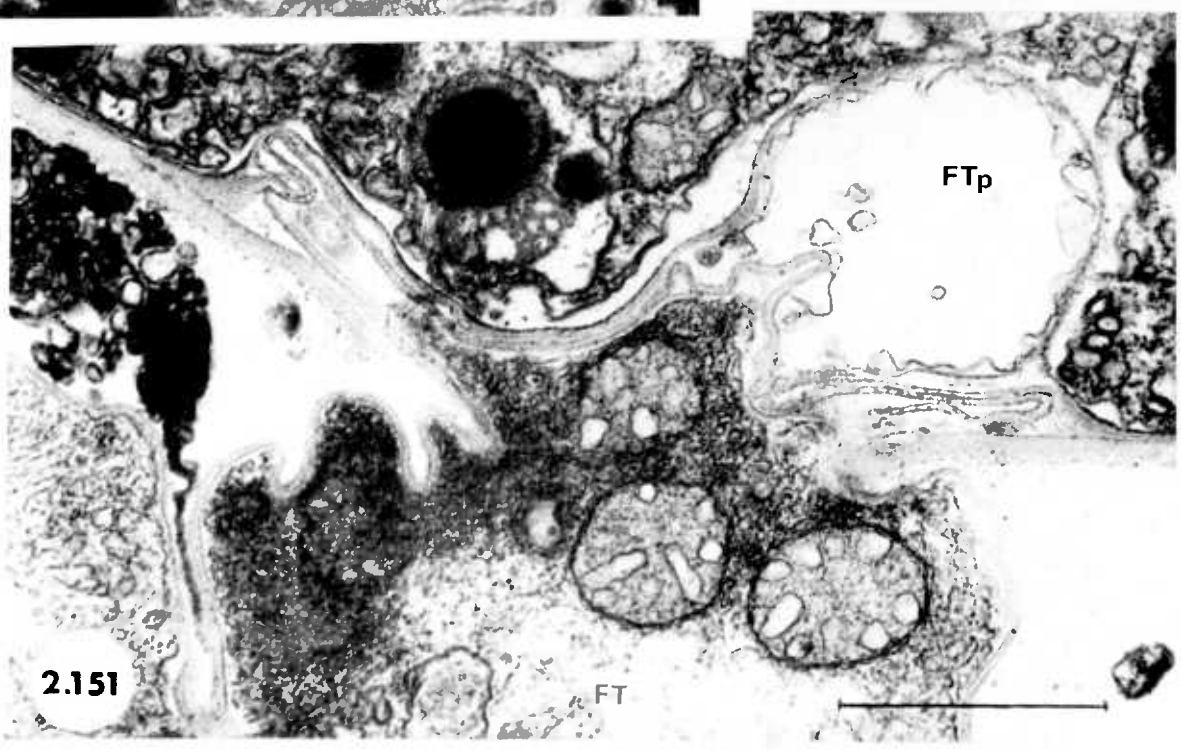
Fig. 2.151 Serial section of the penetration peg shown in Fig. 2.149 showing that it is derived from the fertilisation tube. The points of oospore wall ruptured are clearly shown.
21877 Os 3450 50 mg/l Str 48 h

Fig. 2.150 Fertilisation tube and adjacent oospores showing the massive oospore wall ingrowth and band of sequestered fertilisation tube cytoplasm (dense osmiophilic material) in the region of contact.
21874 Os 3450 50 mg/l Str 48 h


2.148


FTp
2.149


2.150
N
L


FTp
2.151
FT

2.3.8.7 The effect of streptomycin on oospore and fertilisation tube structure in S.furcata

Fig. 2.152 LS of an abnormally swollen Str-induced fertilisation tube. Note the concentration of its cytoplasm in a peripheral crescent adjacent to the aborted oospores.
29429 GaOs 3931 1 mg/l Str 170 h

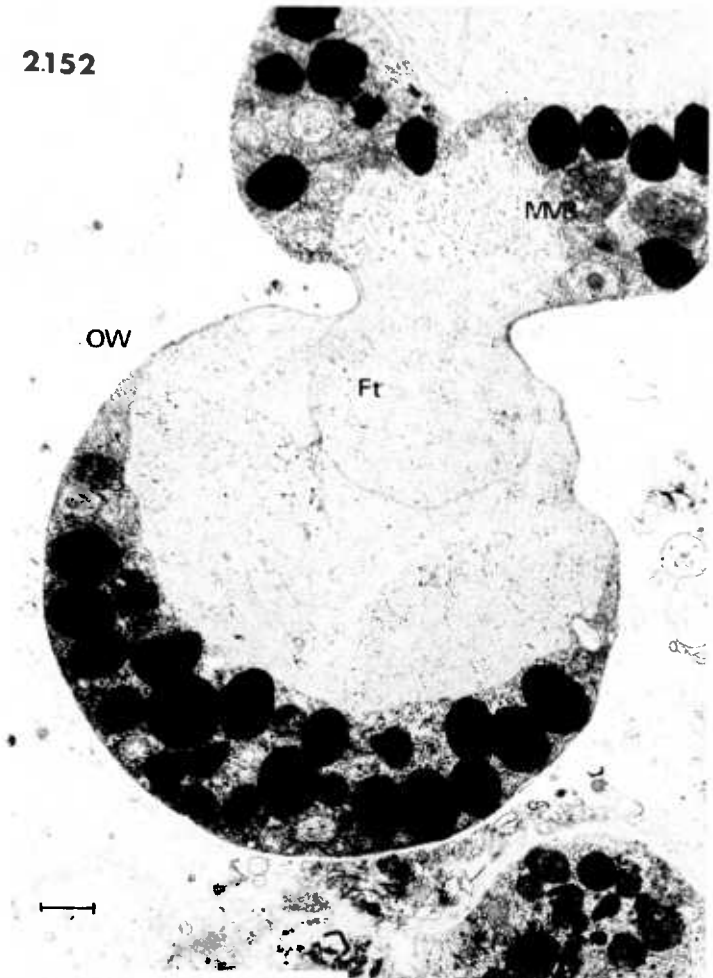
Fig. 2.153 Light micrograph of a comparable oogonium to that shown in Fig. 2.152, showing the aborted oospores and swollen fertilisation tubes.
154/8 OI 5 mg/l Str 120 h

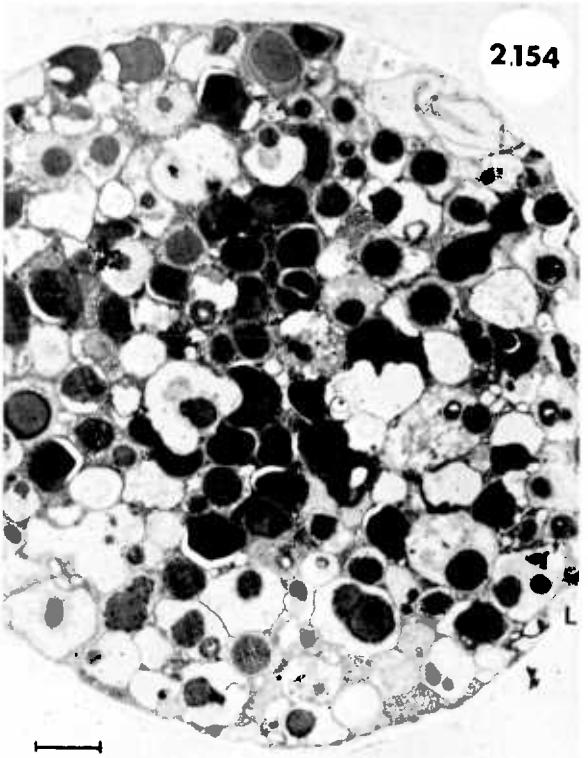
Fig. 2.154 Profile of an abnormal Str-induced oospore containing partially enlarged and coalesced densebody vesicles. Note the absence of endospore accretion.
29487 GaOs 3932 5 mg/l Str 170 h

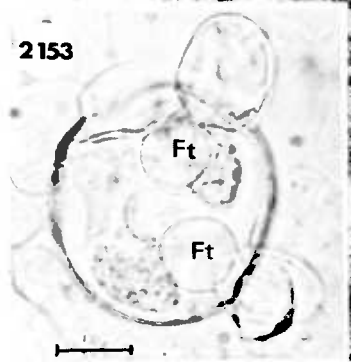
Fig. 2.155 An abnormal oospore in which the densebody vesicles have coalesced into distinct vacuoles, containing electron dense matrix material. The neutral lipid droplets which lie between these vacuoles also show signs of coalescence.
23658 GaOs 3458 50 mg/l Str 72 h

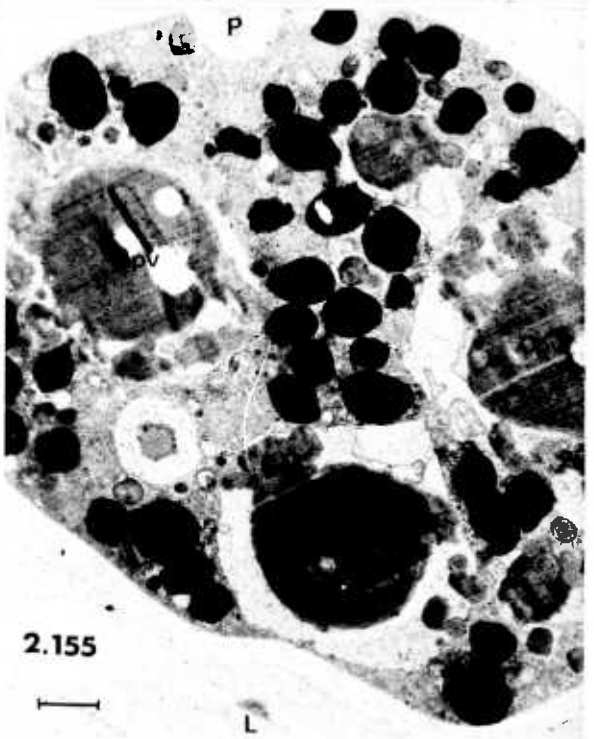
Fig. 2.156 Str-induced oospore with a mature endospore layer and fully-formed ooplast vacuole. The densebody granules have been lost from the dense matrix.
23859 GaOs 3458

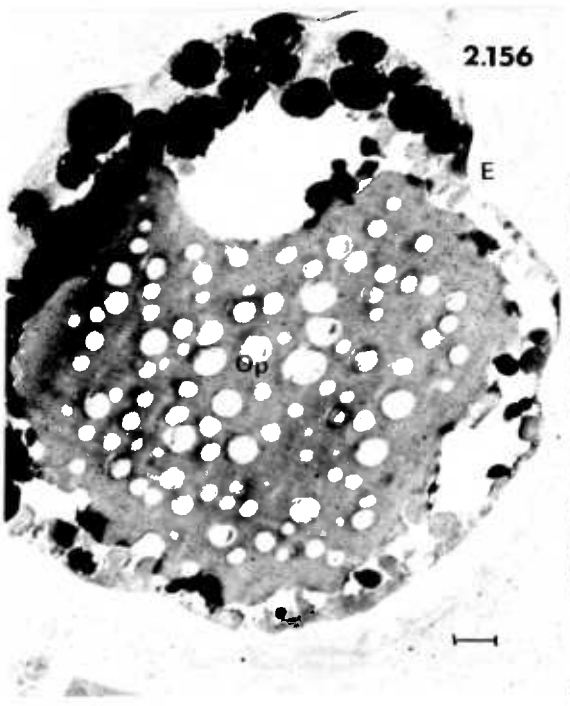
Figs. 2.157, 2.158 Detail of the densebody vesicles in the oospore in Fig. 1.154, showing the elaborate matrix and partial coalescence of the densebody granules.
27488 GaOs 3932 5 mg/l Str 170 h
27491


2.152
MVB
OW
Ft

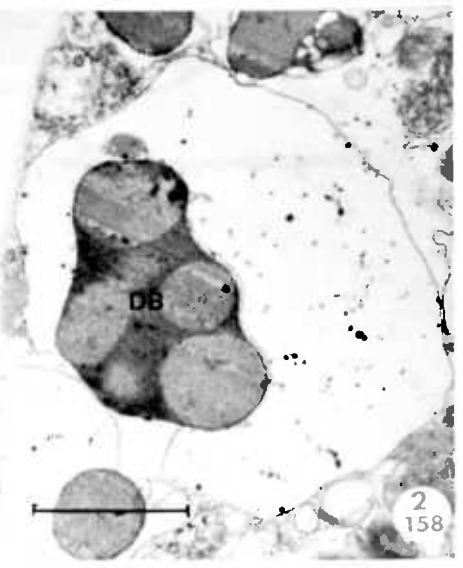

2.154
L


2153
Ft
Ft


P
OV
2.155
L


2.156
E
Op


0·5
2.157

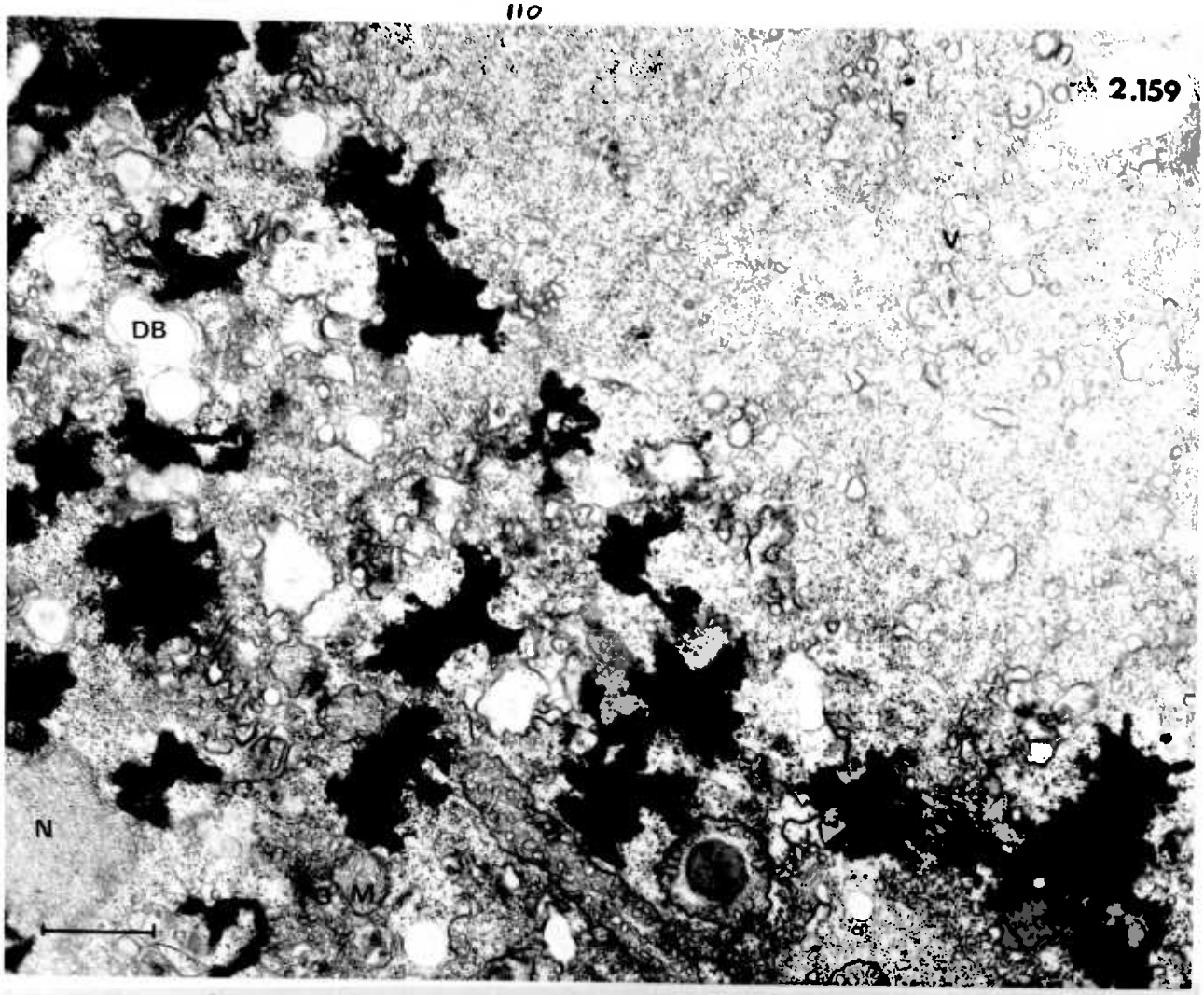

DB
2.158

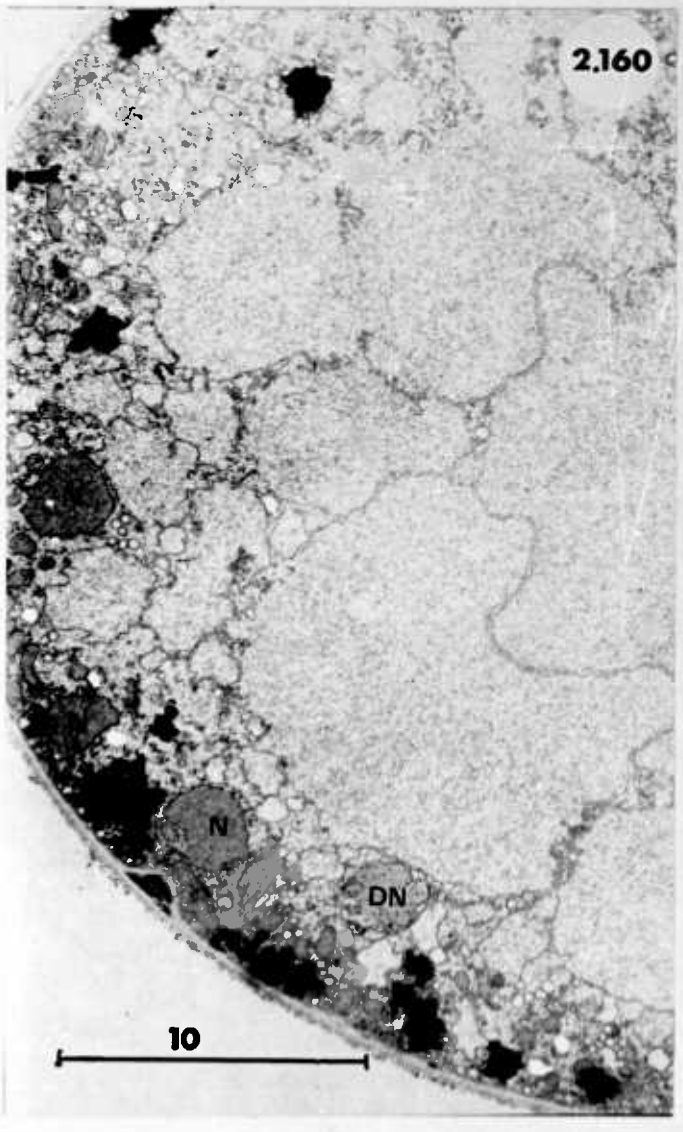
2.3.9 The effects of streptomycin on vacuole ultrastructure in gemmae of S.furcata

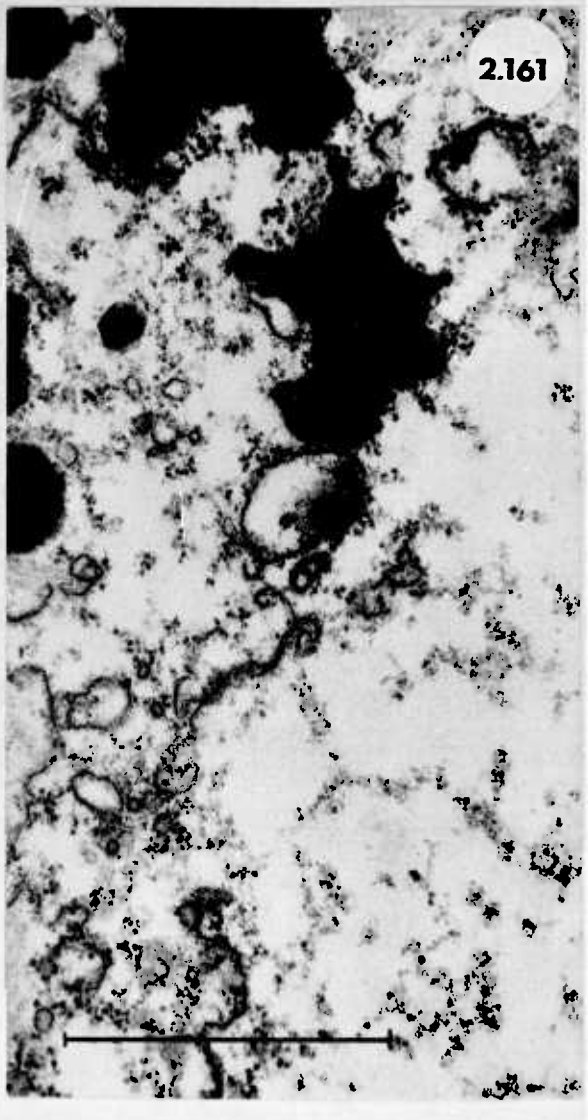
Fig. 2.159 Detail of the cytoplasm-vacuole boundary in the appendate gemma shown in Fig. 2.117, showing the disorganisation of the vacuolar membranes. Mitochondrial structure is normal and the Golgi association is still present. The densebody granules are electron transparent in this type of structure after Os-fixation.
25482 Os 3486 250 mg/l Str 240 h

Fig. 2.160 Detail of the clavate gemma shown in Fig. 2.131. Note the peripheral distribution of the main cell organelles, and the elaborate network of vacuolar vesicles.
25153 Os 3485 500 mg/l Str 240 h

Fig. 2.161 Detail of the cytoplasm-vacuole boundary in the spherical gemma shown in Fig. 2.102, showing thebreakup of the tonoplast into fragments, and the redistribution of ribosome-like particles into the vacuolar area on the right.
38266 Os 3316 100 mg/l Str 168 h


2.159
DB
V
N
M


2.160
N
DN
10


2.161

2.3.9 The effects of streptomycin on vacuolar and multivesicular body structure in gemmae of S.ferax and S.furcata

Fig. 2.162 Vacuolar membranes from a spherical gemma, showing their undulating profile. Note the clusters of Golgi derived vesicles, and ribosome-like particles distributed throughout.
19124 Os 3319 500 mg/l Str 168 h

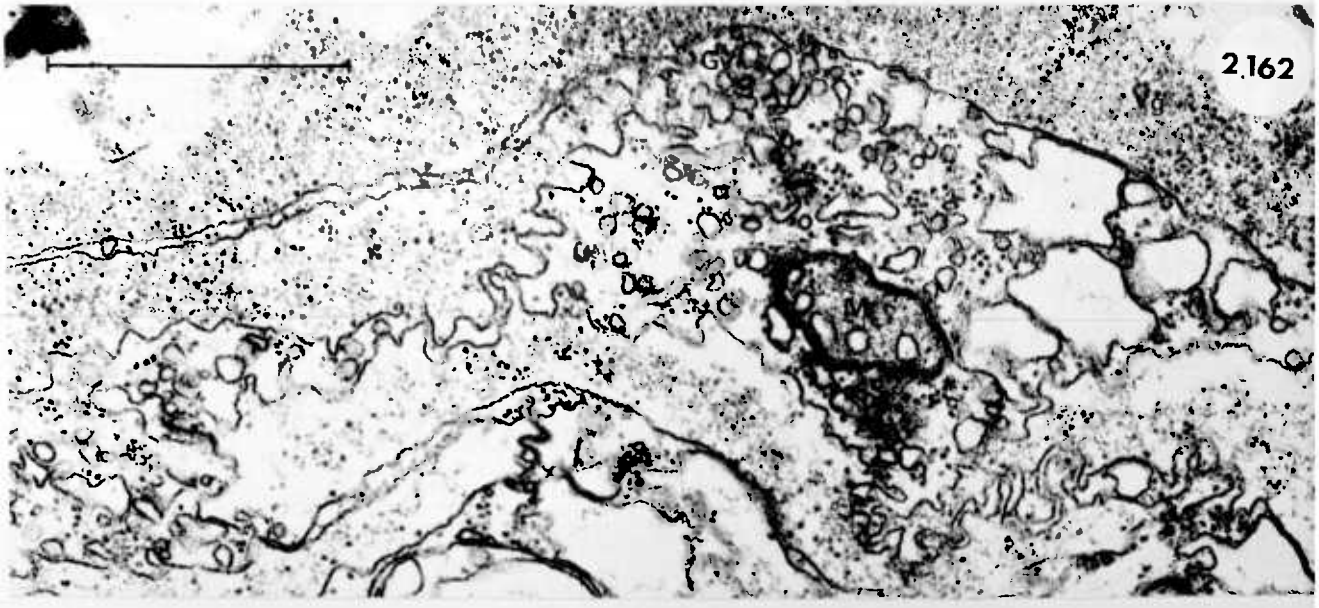
Fig. 2.163 A cluster of mitochondria and multivesicular bodies in the peripheral cytoplasm of a spherical gemma. The similarity in the appearance of the mitochondrial and multivesicular body matrix should be noted.
19138 Os 3319 500 mg/l Str 168 h

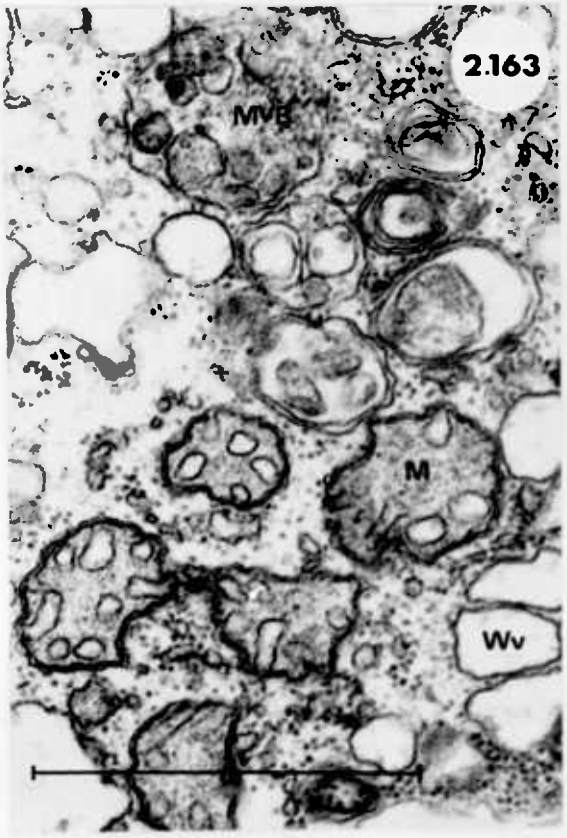
Fig. 2.164 Multivesicular body complexes in the cytoplasm of an appendate gemma. Note the dense particulate matrix and indistinct internal membranes.
25055 Os 3450 50 mg/l Str 48 h

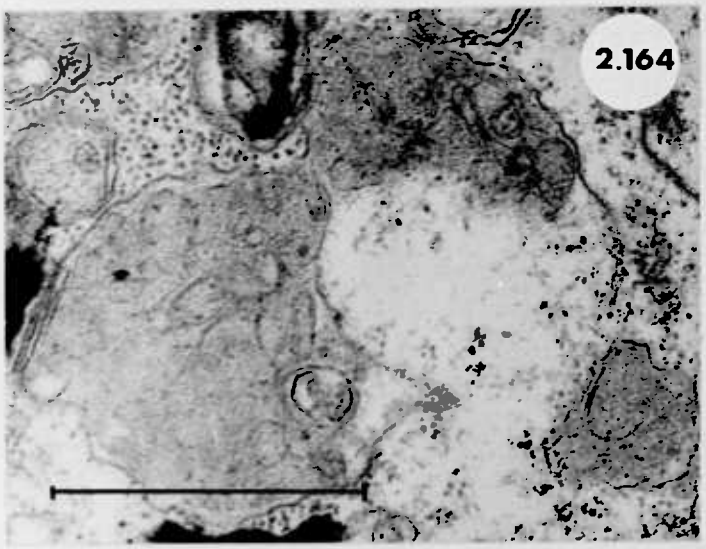
Fig. 2.165 Multivesicular body complexes in the peripheral cytoplasm of an expanded fertilisation tube, such as shown in Fig. 2.152.
29426 GaOs 3931 1 mg/l Str 168 h

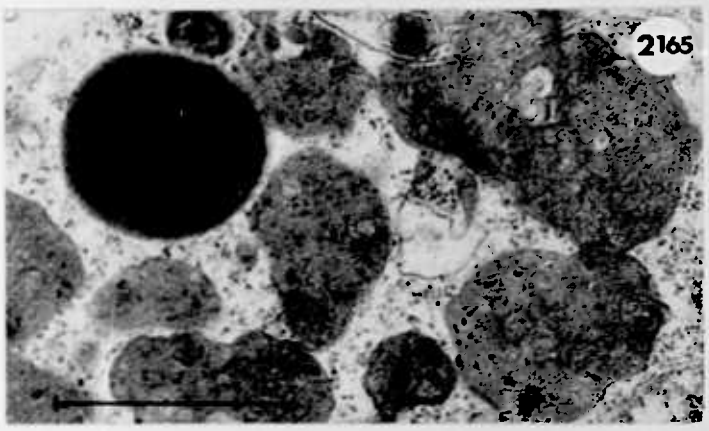
Figs. 2.166-2.168 Detail of multivesicular bodies from Str-induced gemmae in S.furcata showing the variation in their structure. Note differences in matrix density and membranous content.
38266 Os 3316 100 mg/l Str 168 h
19713 Os 3319 500 mg/l Str 168 h
19202 Os 3315 50 mg/l Str 168 h

Fig. 2.169 A multivesicular body in a Str-induced gemma of S.ferax.
27148 Os 3323 20 mg/l Str 96 h


2.162
G
M


2.163
MVB
M
Wv


2.164


2165


2166
0·5


2167
0·5


0·5
2168


0·5
2169

2.3.9.2 The effects of streptomycin on bar body and mitochondrial structure

Fig. 2.170 Detail of the peripheral cytoplasm of a Str-induced gemma of S.ferax showing a localised accumulation of wall vesicles. The mitochondria contain few cristae and the dictyosomes have become reduced to clusters of small vesicles.
27133 Os 3325 70 mg/l Str 96 h

Fig. 2.171a,b Cup-shaped cisternae in S.ferax gemmae, in profile (a) and in face view (b). Note the similarity between the fine particulate contents of these bodies and the peripheral bar body matrix (Fig. 2.173) and the close proximity of Golgi vesicles in Fig. 2.171a.
27111 Os 3324 50 mg/l Str 96 h

Fig. 2.173 Mature bar in a Str-induced gemma of S.ferax.
27133 Os 3325 70 mg/l Str 96 h

Fig. 2.175-2.181 Selected mitochondria from Str-induced gemmae and oogonia illustrating the variation in matrix density and cristae abundance.

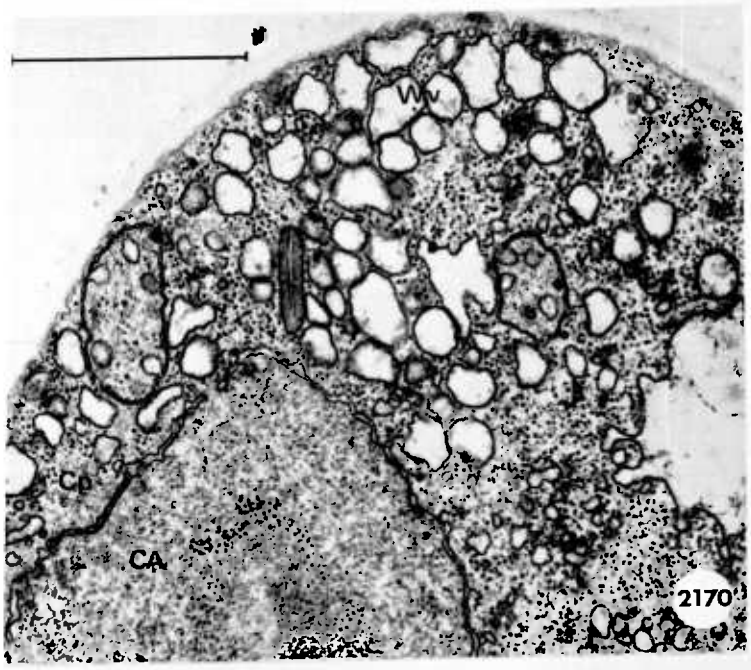
Fig. 2.175 Mitochondrion in a Stage IV oogonium showing a well ordered array of cristae and an associated dictyosome.
27144 Os 3450 50 mg/l Str 48 h

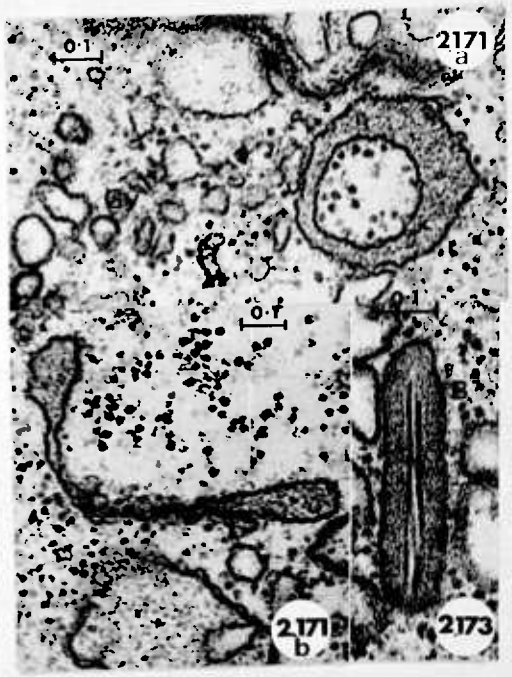
Fig. 2.176-2.178 Mitochondria in S.ferax gemmae after prolonged antibiotic incubation. Note the less regular organisation of the cristae.
27119 3324 50 mg/l Str 96 h
27139 Os 3323 20 mg/l
27130 3324 50 mg/l

Fig. 2.179 Lobed mitochondrion from an appendate gemmae of S.furcata. Note the dense matrix.
25187 Os 3485 500 mg/l Str 96 h

Fig. 2.180 Small mitochondria in S.ferax gemmae after prolonged antibiotic incubation.
27111 Os 3324 50 mg/l Str 96 h

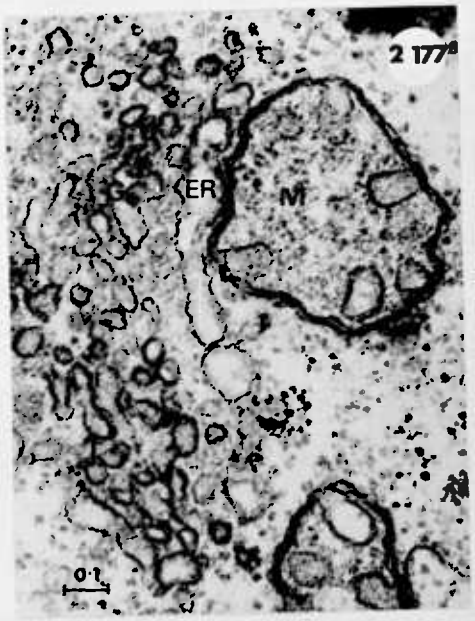
Fig. 2.181 A typical mitochondrion from the gemma shown in Fig. 2.135. Note its spherical profile and central reserve droplet.
25528 Os 3486 250 mg/l Str 240 h


W
Co
CA
2170

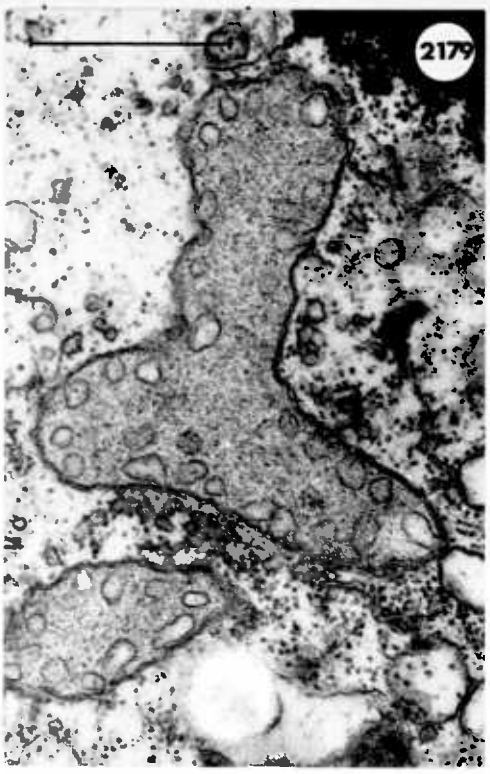

0·1
2171
a
0·1
0·1
B
2171
b
2173

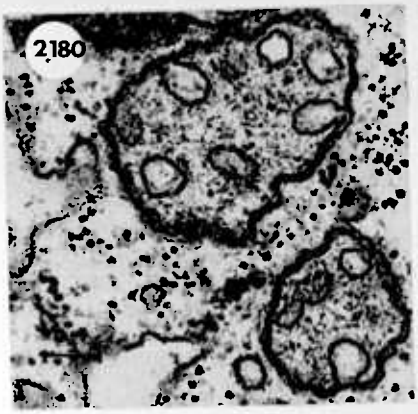

2175

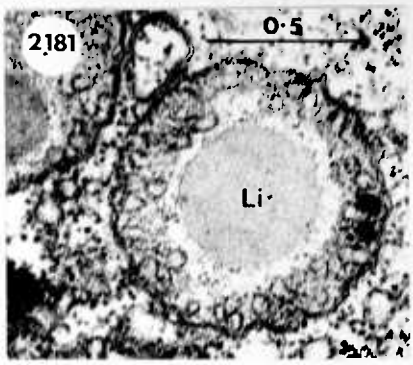

2176


2177
ER
M
0·1


2178
0·5


2179


2180


2181
0·5
Li

2.3.9.4 The effect of streptomycin on cell wall structure in S.ferax and S.furcata

Fig. 2.182 A localised cluster of wall vesicles in the peripheral cytoplasm of a S.ferax gemma.
27132 Os 3323 20 mg/l Str 96 h

Fig. 2.183 The peripheral cytoplasm of a S.furcata gemma showing a large lomasome and peripheral wall vesicles. Note the loose outer wall layer and the membranous material trapped between the wall and the plasmalemma (upper part of picture).
25437 Os 3485 500 mg/l Str 240 h

Fig. 2.184 Peripheral cytoplasm of a S.ferax gemma showing the abundant peripheral wall vesicles.
27134 Os 3323 20 mg/l Str 96 h

Fig. 2.185-2.186 Gemma walls of S.ferax (2.185) and S.furcata (2.186) showing the plasmalemma with conspicuous pocket-like invaginations.
27119 Os 3324 50 mg/l Str 96 h
21905 3450 48 h

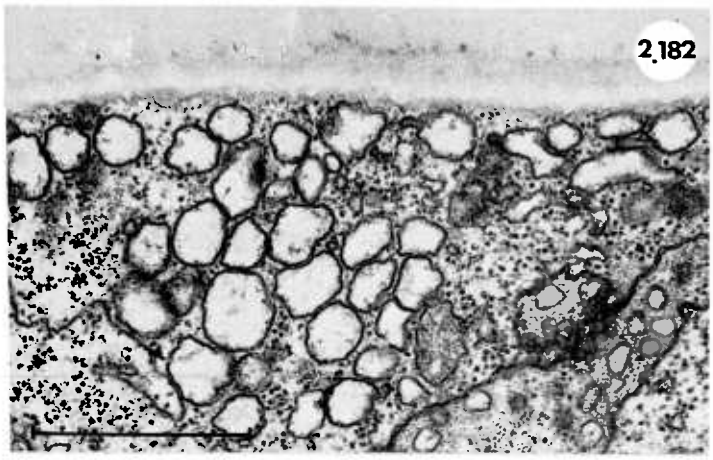
Fig. 2.187 Cell walls of mature gemmae of S.furcata. Note the variations in the staining density and substructure of these walls.
25526 Os 3486 250 mg/l Str 240 h
25587 Os 3485 500 mg/l Str 240 h

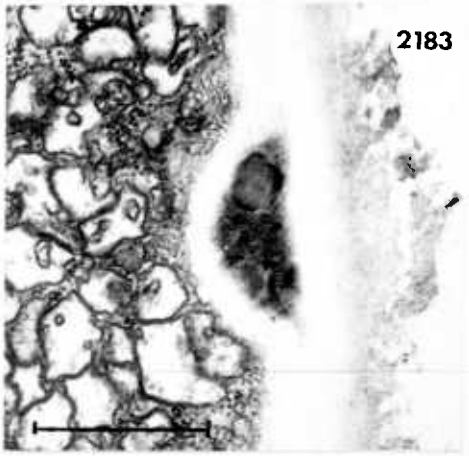
Figs. 2.190-2.193 Lomasomes in Str-induced bodies illustrating the variation in their size and structure.

Figs. 2.190, 2.191, 2.192 Lomasomes with vesicular contents in gemmae of S.ferax.
27111 Os 3323 20 mg/l Str 96 h
27113 Os 3324 50 mg/l Str 96 h
27114 Os 3323 20 mg/l Str 96 h

Fig. 2.193 Lomasome in primary wall of a Str-induced oospore.
27492 CaOs 3992 120 h

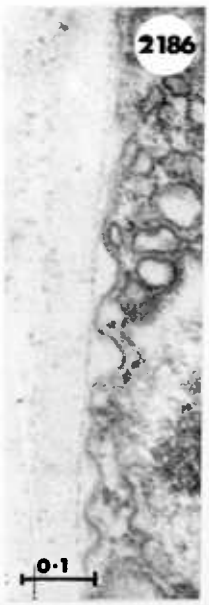
Fig. 2.194 Large lomqsome with osmiophilic lipid-like contents in a gemma of S.furcata.
19122 Os 3319 500 mg/l Str 168 h


2.182


2183


2184
0·5

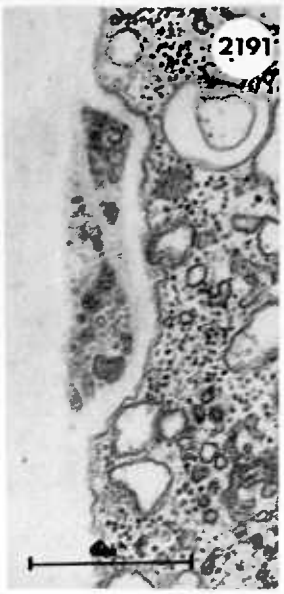

2185
0·5


2186
0·1


2187
0·5


2189
0·5


2190
0·1


2191


2192
0·5


2193
0·


2.194

2.3.9.4. The effect of streptomycin on cell wall structure in S.ferax and S.furcata

Figs. 2.195, 2.196 Oblique profiles of peg-like ingrowths from walls of S.furcata gemmae, showing concentric arrays of wall and vesicular material.

19138 Os 3319 500 mg/l Str 188 h
19853 3316 100 mg/l Str 188 h

Figs. 2.197, 2.199 Median LS profiles of wall ingrowths in gemmae of S.furcata. Note the abundance of wall vesicles surrounding each peg.

19854 Os 3316 100 mg/l Str 168 h
25243 3485 500 mg/l Str 240 h

Fig. 2.198 Section of an abnormally large wall ingrowth containing a pocket of dense degenerating cytoplasm, from a gemma of S.furcata.

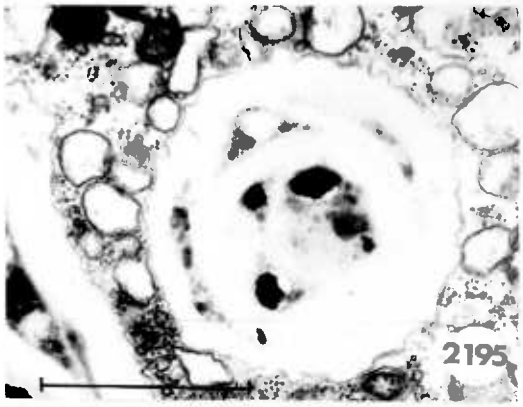
25183 Os 3485 500 mg/l Str 240 h

Fig. 2.200 Wall ingrowth from a Str-incubated cyst of S.ferax. Note the elaborate myelin figures between the wall layers, suggesting the presence of lipid.

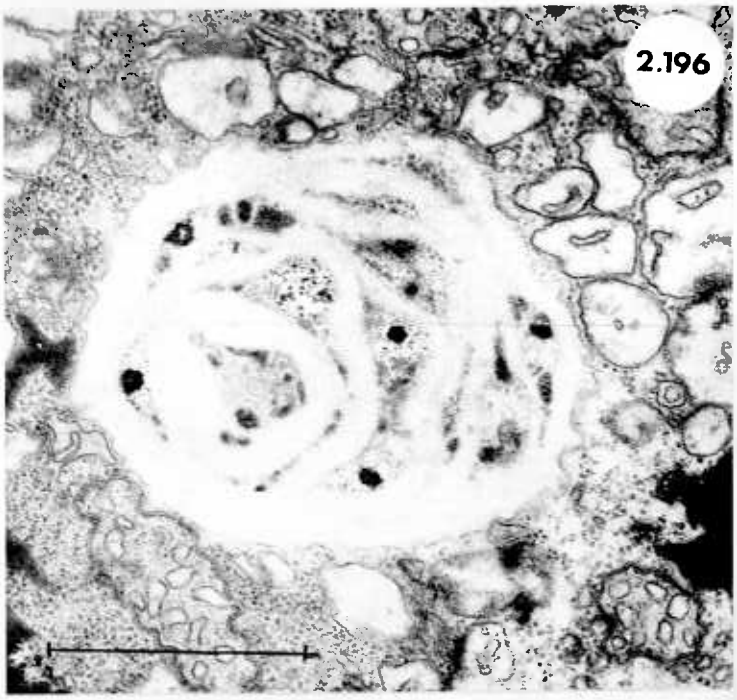
29918 Os 3887 Str 8 h

Fig. 2.201 An unusually large lomasome associated with the primary wall of a Stage VII oospore. The osmiophilic lipid like contents have condensed against the outer wall.

21792 Os 3451 100 mg/l Str 48 h



2.195



2.196



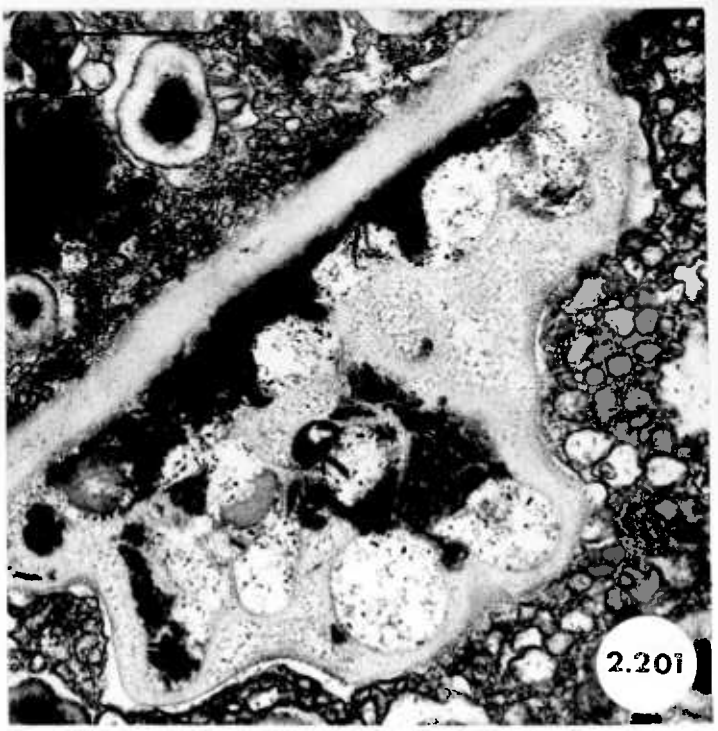
2.197



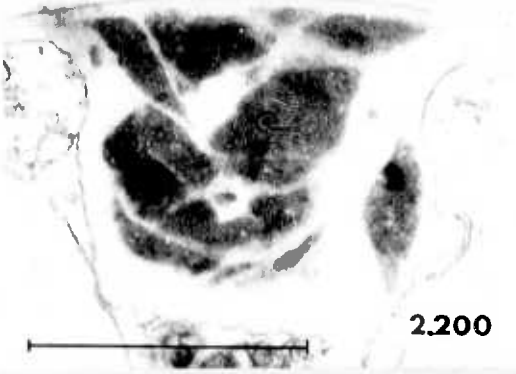
2.198



2.199



2.201



2.200

2.3.9.4 The effect of streptomycin on septum structure in S.furcata

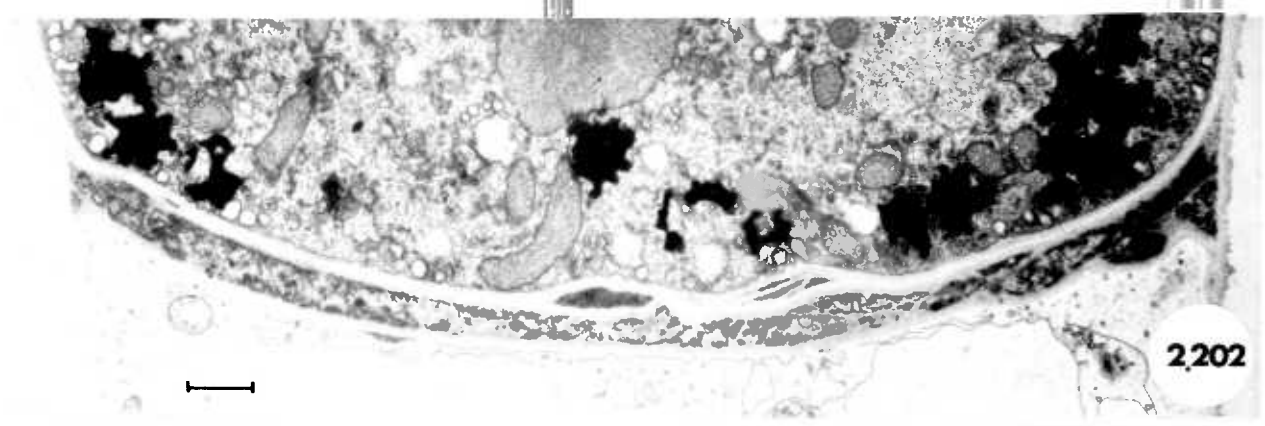
Fig. 2.202. The basal septum of the club-shaped gemma shown in Fig. 2.131. Note the thickness of both wall and vesicular layers.
25155 Os 3485 500 mg/l 240 h

Fig. 2.203 Septum of the secondary gemma shown in Fig. 2.134. Note the dense lipid-like globules included in the vesicular layer.
25408 Os 3485 500 mg/l 240 h

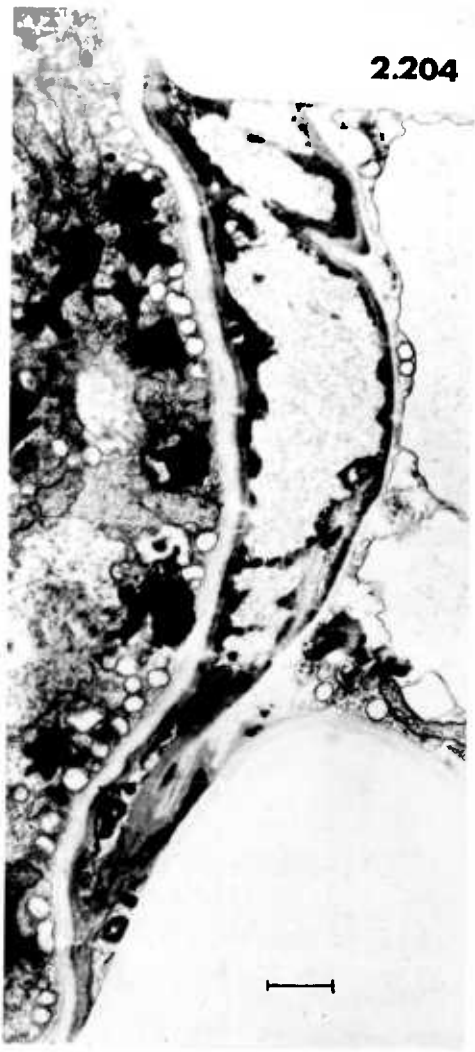
Fig. 2.204 The basal septum of an appendate gemma showing the increased thickness of both the wall and central vesicular layer. The vesicular material has condensed against the two wall layers.
19560 Os 3317 200 mg/l 168 h

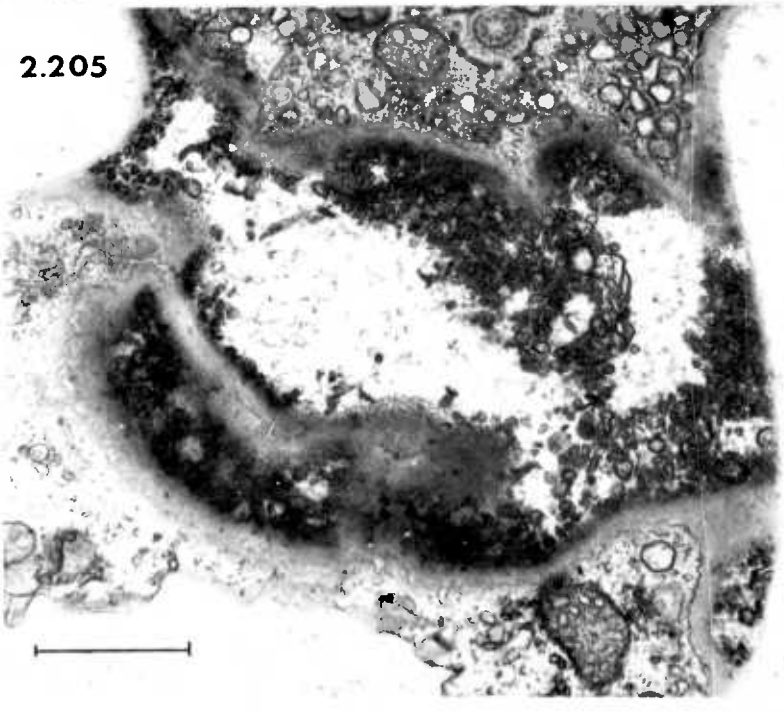
Fig. 2.205 An antherial septum showing enlarged vesicular layer (cf. Fig. 1.212).
22632 Os 3451 100 mg/l 48 h

Fig. 2.206 Detail of the included vesicular layer of the septum shown in Fig. 2.204. Note the presence of lipid-like droplets in this layer.
19601 Os 3317 200 mg/l 168 h


2.202


2.203


2.204


2.205


2.206
Li

2.3.9.6 The effect of streptomycin on the structure and contents of densebody vesicles in S.ferax and S.furcata

Figs. 2.207, 2.208 Densebody vesicles in gemmae of S.ferax. Note the small size and frequently poor preservation of the osmiophilic granule.

27111 Os 3224 50 mg/l Str 96 h
27130 3225 70 mg/l Str 96 h

Fig. 2.209 Detail of densebody vesicles in the spherical gemma shown in Fig. 2.102. These vesicles are lined with osmiophilic material and contain conspicuous myelin arrays.

33256 Os 3316 100 mg/l Str 168 h

Fig. 2.210 An unusual elongate densebody vesicle from a GaOs fixed spherical gemma of S.furcata. Note how the matrix material is organised into grouped lamella, giving the vesicle a banded appearance.

28624 GaOs 3457 50 mg/l Str 48 h

Fig. 2.211 An Os-fixed densebody granule from a Stage IV oogonium.

21905 Os 3450 50 mg/l Str 48 h

Fig. 2.212 Typical Os-fixed densebody granules from a gemma of S.furcata after prolonged antibiotic incubation. The granules themselves are electron transparent and their vesicle membranes are not preserved.

25377 Os 3485 500 mg/l Str 240 h

Figs. 2.213-2.216 Selected GaOs-fixed densebody vesicles from gemmae of S.furcata, illustrating the variability in matrix form.

Fig. 2.213 Vesicle in which the osmiophilic matrix material has condensed around the granule.

23432 GaOs 3458 100 mg/l Str 140 h

Fig. 2.214 Vesicle containing whorl-like arrays within the matrix.

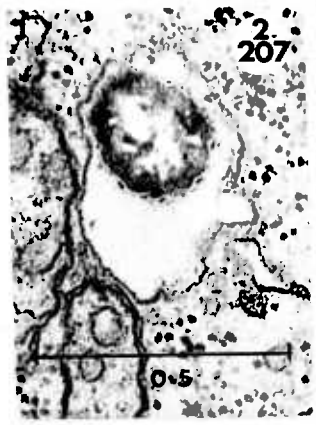
23210 GaOs 3457 50 mg/l Str 140 h

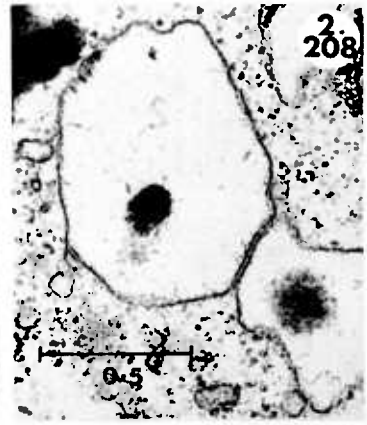
Fig. 2.215 Vesicle in which the expanded matrix forms a reticulate pattern.

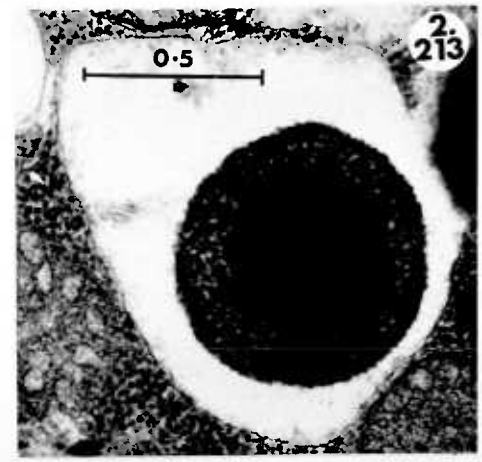
23641 GaOs 3458 100 mg/l Str 140 h

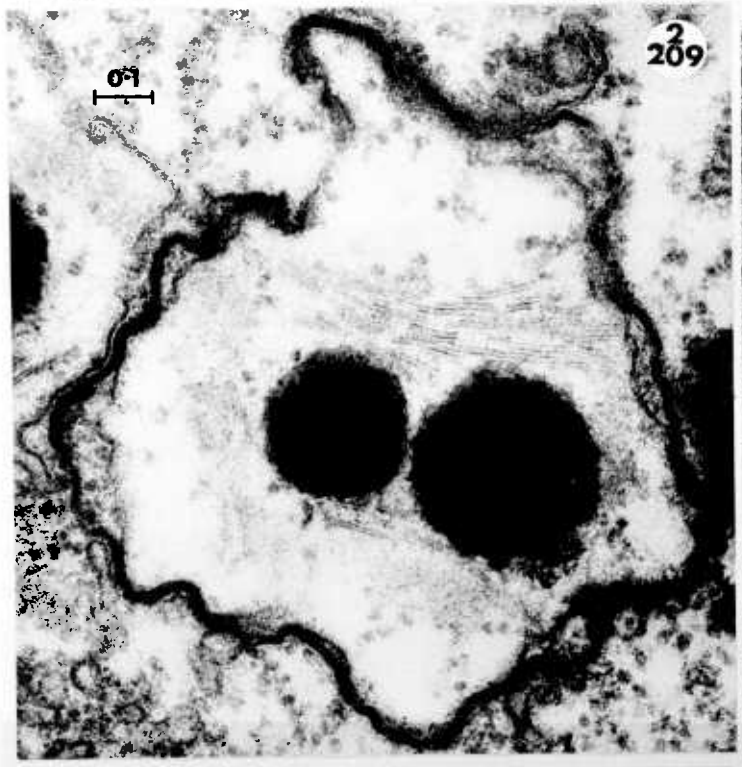
Fig. 2.216 Vesicle in which matrix forms osmiophilic bands surrounding the granule.

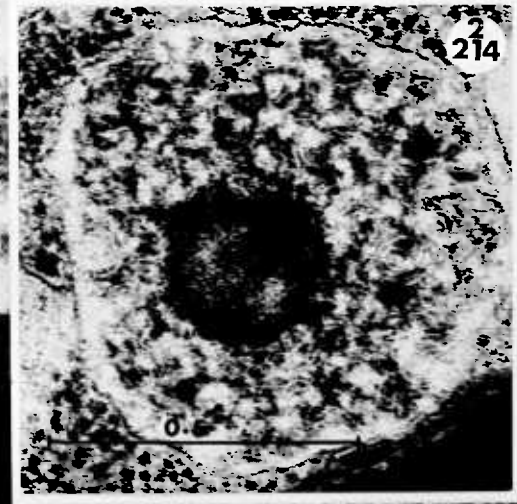
23794 GaOs 3457 50 mg/l Str 140 h

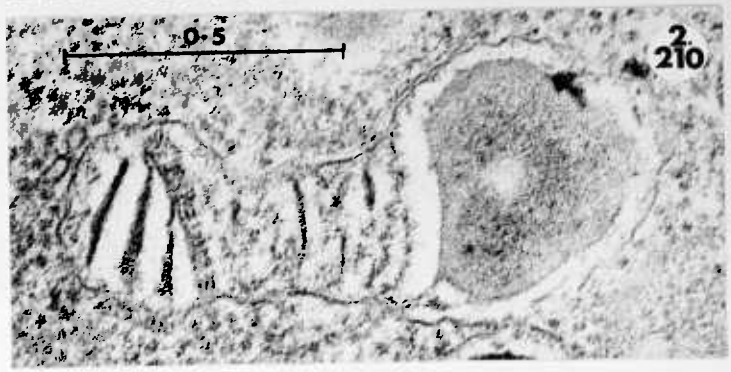

2
207
0·5

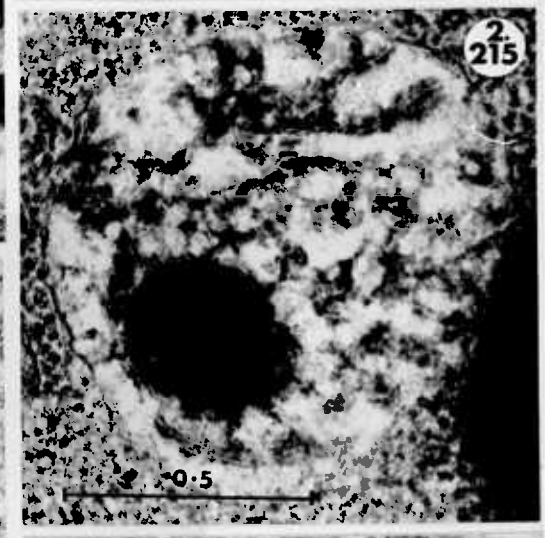

2
208
0·5

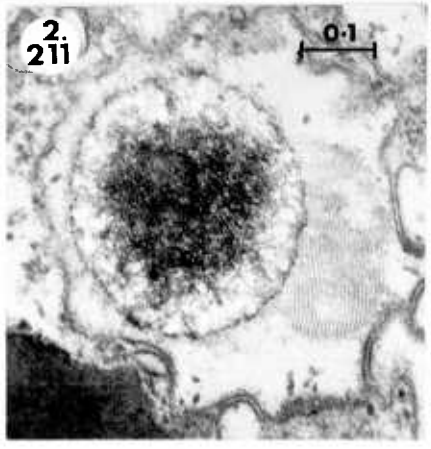

0·5
2
213

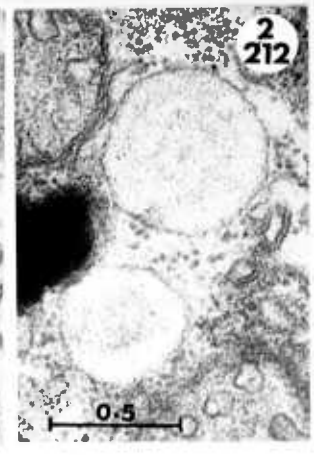

0·1
2
209

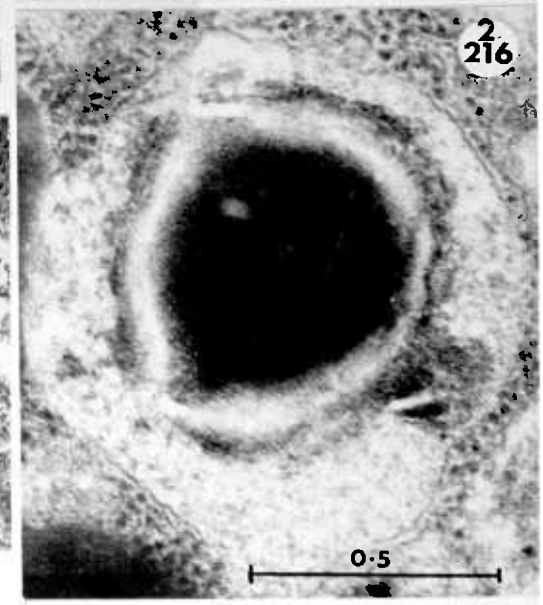

2
214


0·5
2
210


2
215
0·5


2
211
0·1


2
212
0·5


2
216
0·5

2.3.9.10 Effects of streptomycin on nuclear structure in S.ferax and S.furcata

Fig. 2.217 Interphase nucleus in a gemma of S.ferax. Note the array of short microtubules radiating from the centriolar pocket and the included membranous material.
27149 Os 3323 20 mg/l Str 120 h

Fig. 2.218 A dictyosome adjacent to the nuclear envelope, near the centriolar pocket (cp).
27149 Os 3323 20 mg/l Str 120 h

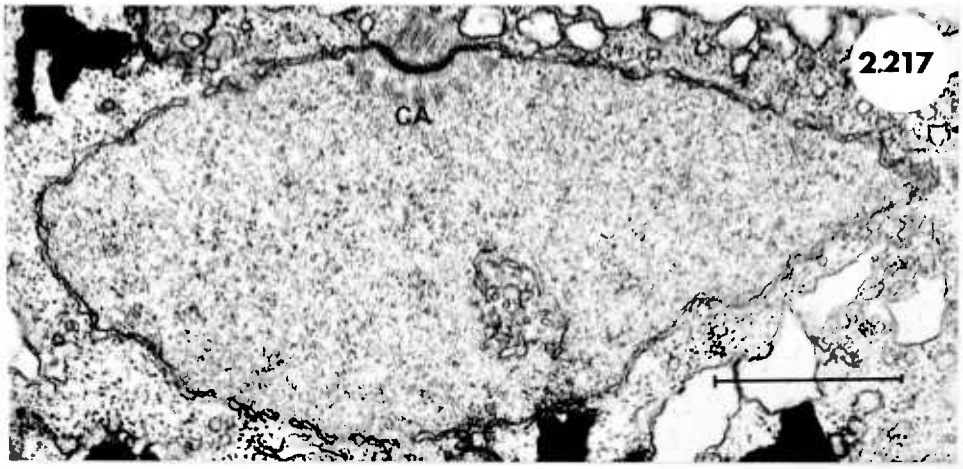
Fig. 2.219 Interphase nucleus in an uncleaved sporangium showing elaborate vesicular inclusions, which are probably derived from invagination of the nuclear envelope.

Figs.2.220-2.221 Interphase nuclei in the appendate gemma shown in Fig. 2.115. Note the disposition of small vesicles and cisterae around each nucleus preceeding autolysis.
21836 Os 3350 50 mg/l Str 48 h
21895

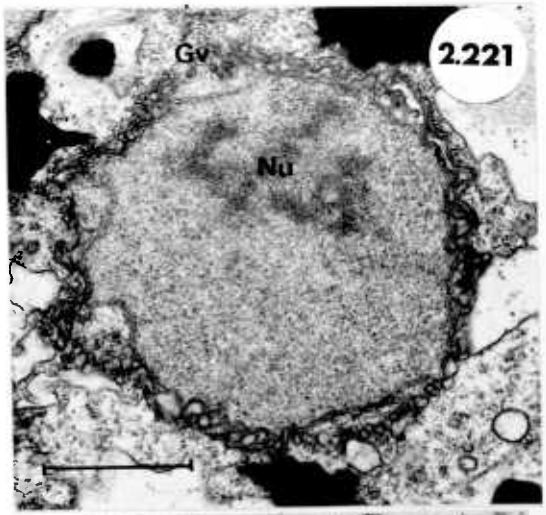
Fig. 2.222 Interphase nucleus in a gemma of S.furcata, showing typical vesicular inclusions. The nuclear envelope is very irregular and vesiculate.
191201 Os 3315 50 mg/l Str 168 h

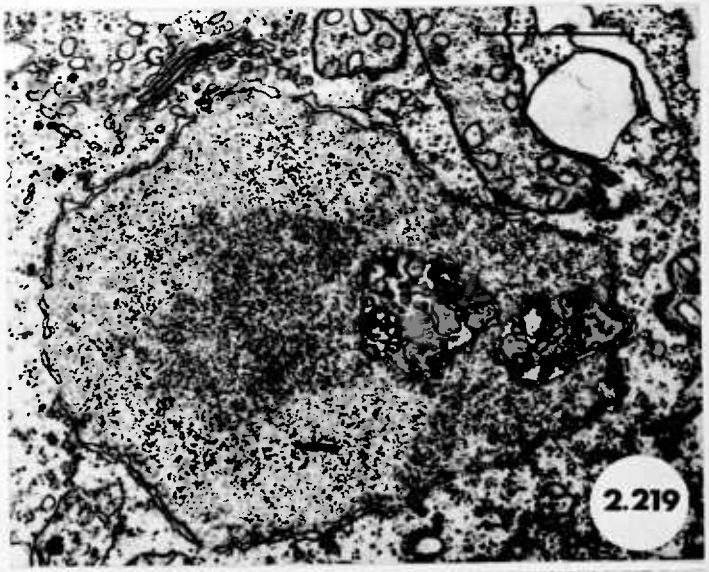
Fig. 2.223 A nucleus from a gemma of S.furcata in an advanced state of autolysis. The surrounding vesicles and membranes have coalesced and expanded to form a compartment which isolates the nucleus from the surrounding cytoplasm. Note the uniform appearance of the nucleoplasm and the beginning of nuclear envelope disintegration.
21843 Os 3450 50 mg/l Str 48 h

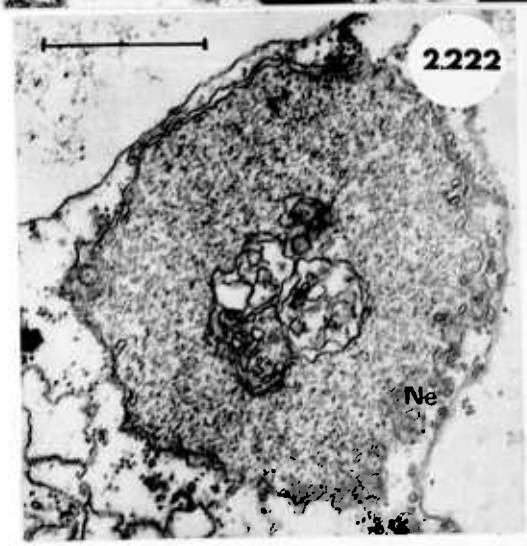
Fig. 2.224 A nucleus from a gemma of S.furcata showing final stage of autolysis. The nuclear envelope is dense and greatly fragmented, and the nucleoplasm is barely discernible from the surrounding cytoplasm.
19201 Os 3315 50 mg/l Str 140 h

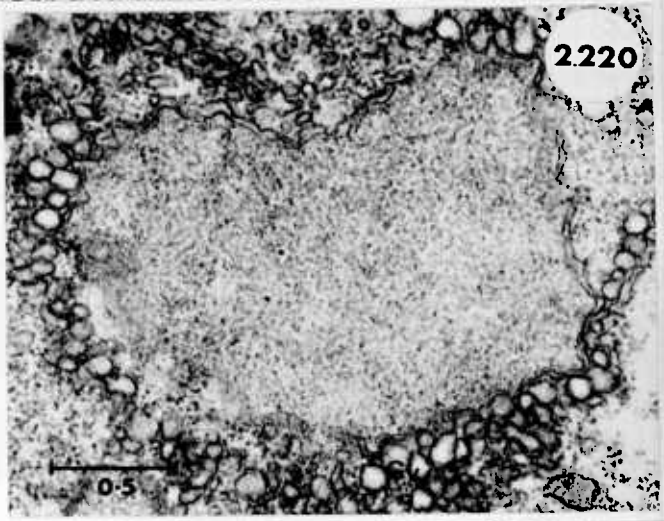

2.217
CA

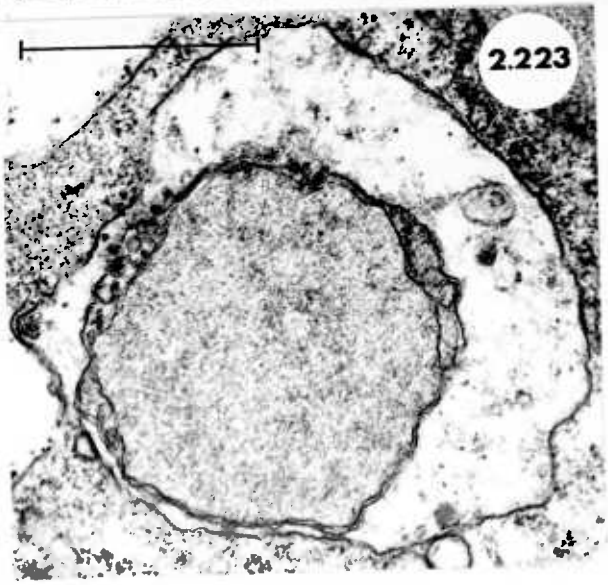

0·5
2.218

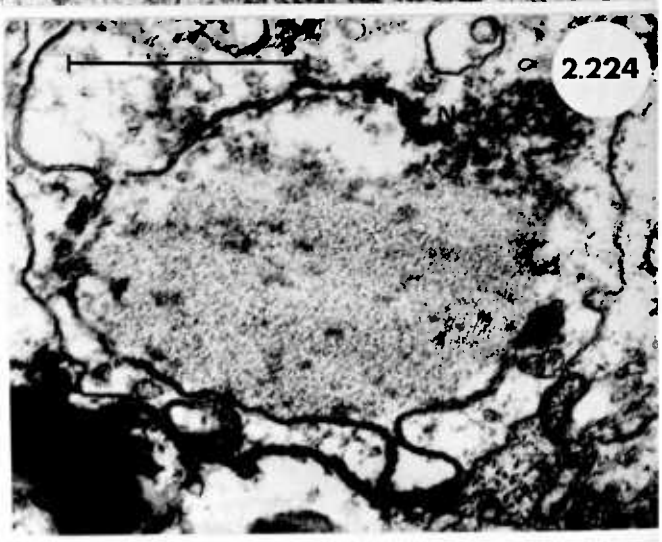

2.221
Gv
Nu


2.219


2.222
Ne


2.220
0·5


2.223


2.224

2.3.9.2 Effects of streptomycin on nuclear and mitochondrial structure in S.ferax and S.furcata

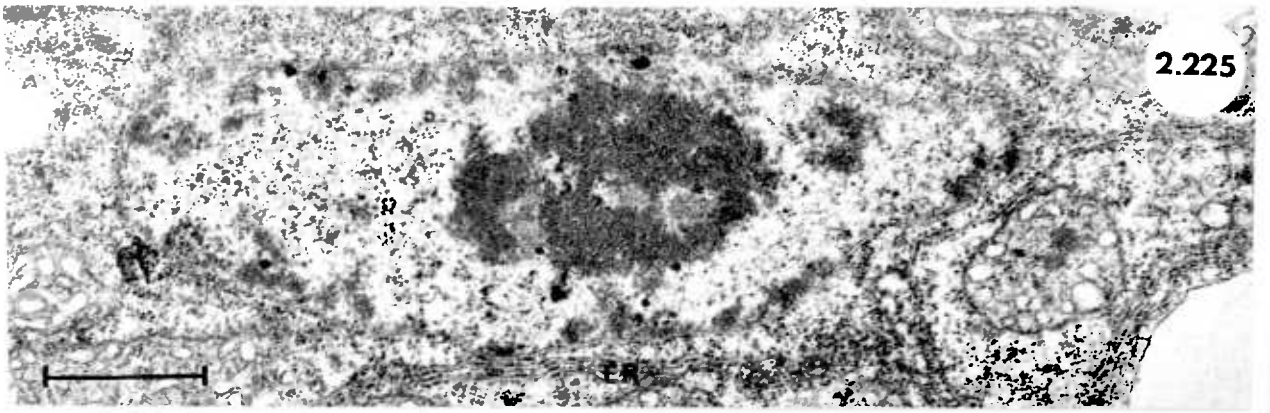
Figs. 2.225-2.226 Abnormal nuclei in streptomycin grown vegetative hyphae. Part of the nucleoplasm has condensed into osmiophilic masses, some of which are clearly associated with the nuclear envelope. Note also the presence of electron dense fibrils, resembling DNA-like material. Conspicuous arrays of rough ER surround these nuclei.
29721 GaOs 3772 500 mg/l Str 24 h
29744

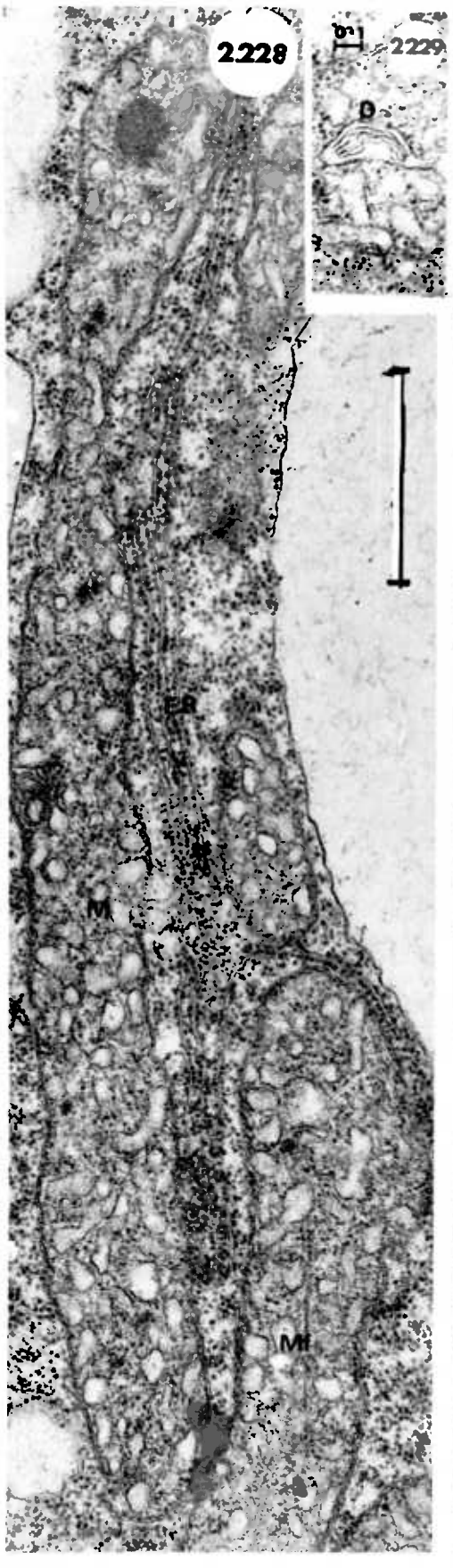
Fig. 2.227 Haploid oospore nucleus showing fragmented nucleolar material dispersed throughout the peripheral nucleoplasm.
27483 GaOs 3932 5 mg/l Str 140 h

Fig. 2.228 Elongate hyphal mitochondria containing strands of electron dense fibrillar material. Note the parallel arrays of ER cisternae surrounding the mitochondria.
29724 GaOs 3772 500 mg/l Str 24 h

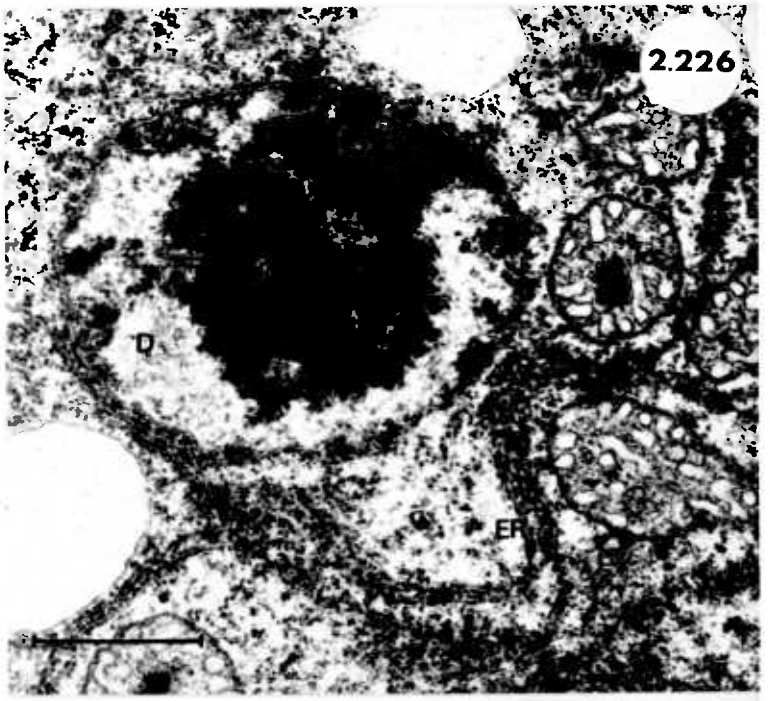
Fig. 2.229 Dense coiled DNA-like strands within the mitochondrial matrix.
29723 GaOs 3772 500 mg/l Str 24 h

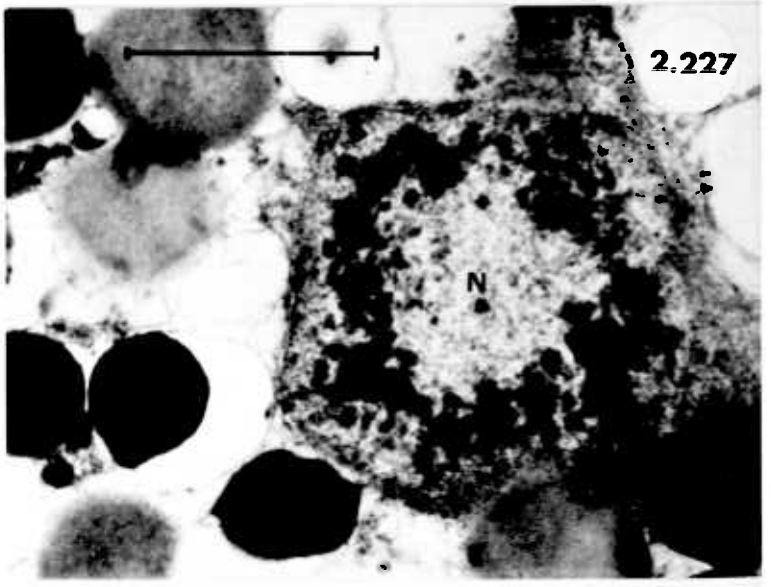
Fig. 2.230 Detail of the fibrous strands in the mitochondria matrix in Str grown hyphae. The difference in size between the mitochondrial and cytoplasmic ribosomes is clearly shown.
29725 GaOs 3772 500 mg/l Str 24 h

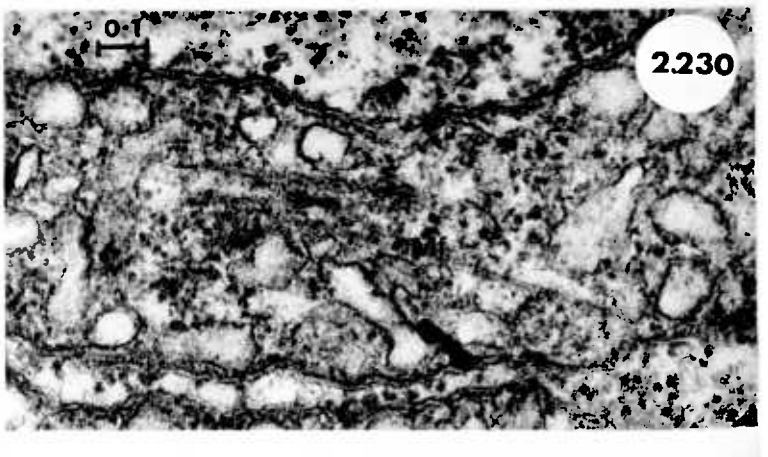

2.225
R
ER


2.228
ER
M
M

0·1
2229
D


2.226
D
ER


2.227
N


0·1
2.230

2.3.8.10 Effects of streptomycin on sporangia of P.cactorum

Figs. 2.231-2.237 Series of light-micrographs showing the effects of Str on zoospore formation in sporangia, after 12 h incubation in the antibiotic.

Figs. 2.231, 2.232 Sporangia with slightly shrunken cytoplasmic contents.

115/6 OI 50 mg/l Str 12 h
115/16 250 mg/l Str

Fig. 2.234 Sporangium liberating undifferentiated protoplast. The flagella can be distinguished on the left of the cytoplasm.

115/17 OI 250 mg/l Str 12 h

Fig. 2.235 A large motile protoplast induced in Str.

115/15 OI 250 mg/l Str 12 h

Fig. 2.236 A newly encysted giant zoospore.

112/15 NP 100 mg/l Str 12 h

Fig. 2.237 Giant cyst with two germ tubes.

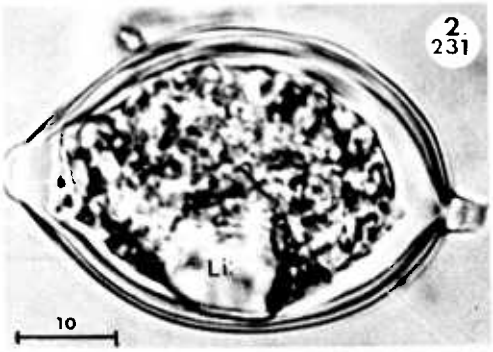
115/13 100 mg/l Str 12 h

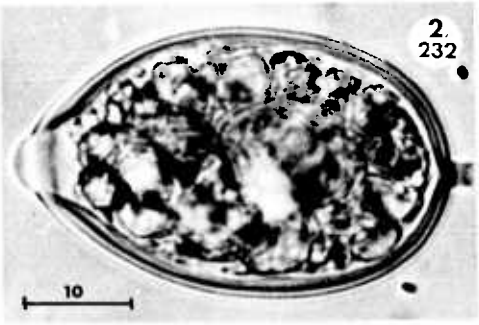
Figs. 2.237, 2.239 TS's of Str-induced sporangia showing the disorganised cytoplasm and coalesced lipid droplets.

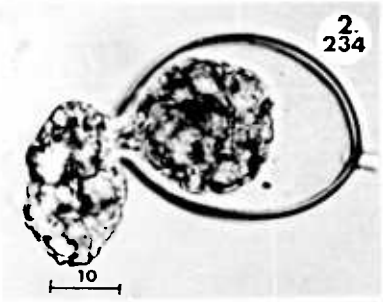
25977 Os 3708 50 mg/l Str 5 h
25975 3710 250 mg/l Str 5 h

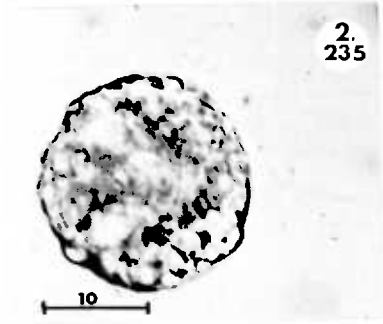
Fig. 2.240 Detail of peripheral cytoplasm of a Str-induced sporangium showing the ingrowth of the sporangial wall.

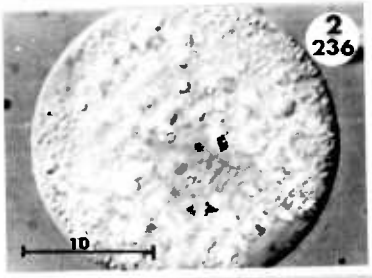
25851 Os 3708 50 mg/l Str 5 h

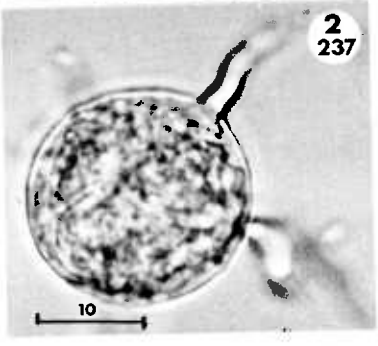

2.
231
Li
10

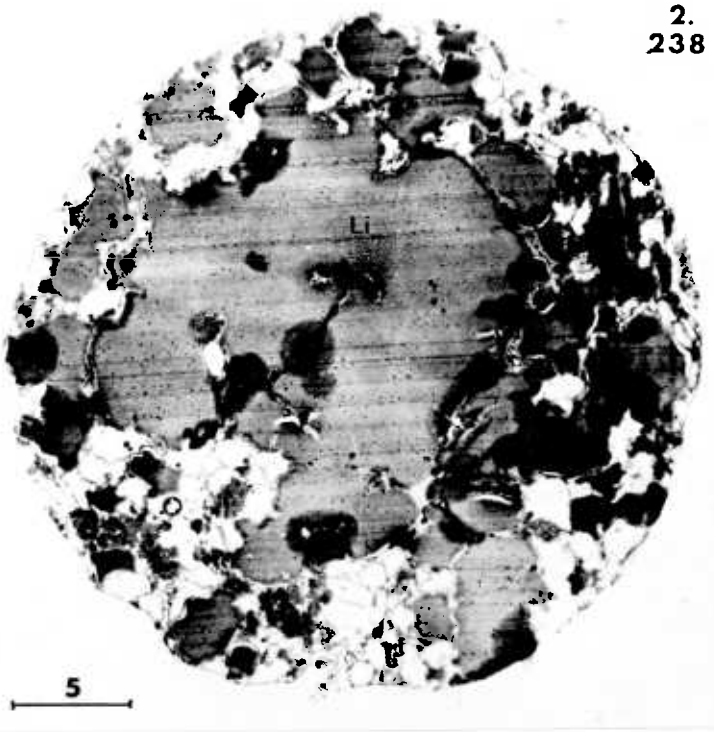

2.
232
10

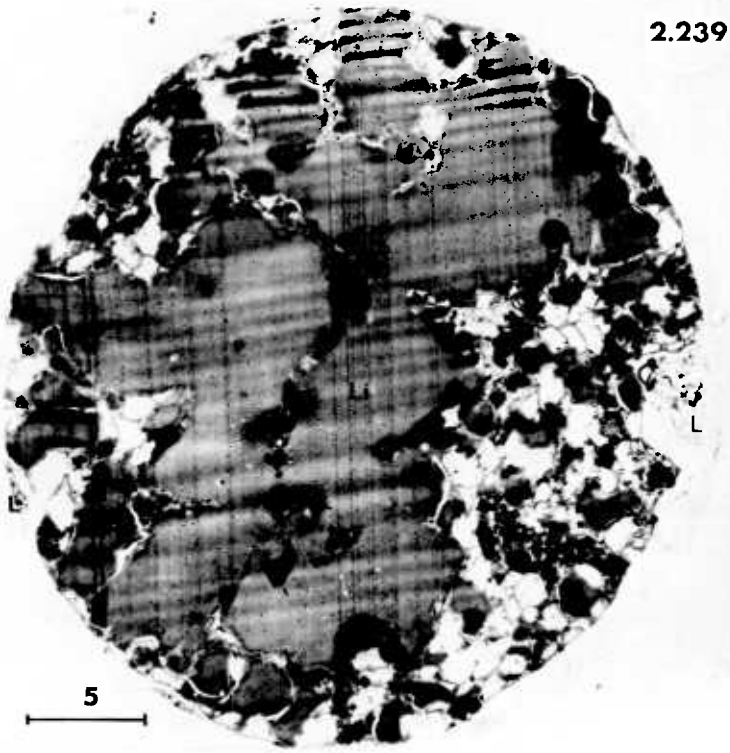

2.
234
10

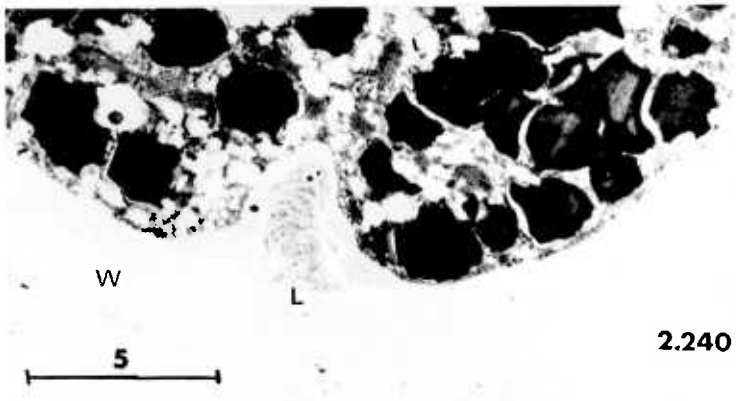

2.
235
10


2
236
10


2
237
10


2.
238
Li
5


2.239
Li
L
5

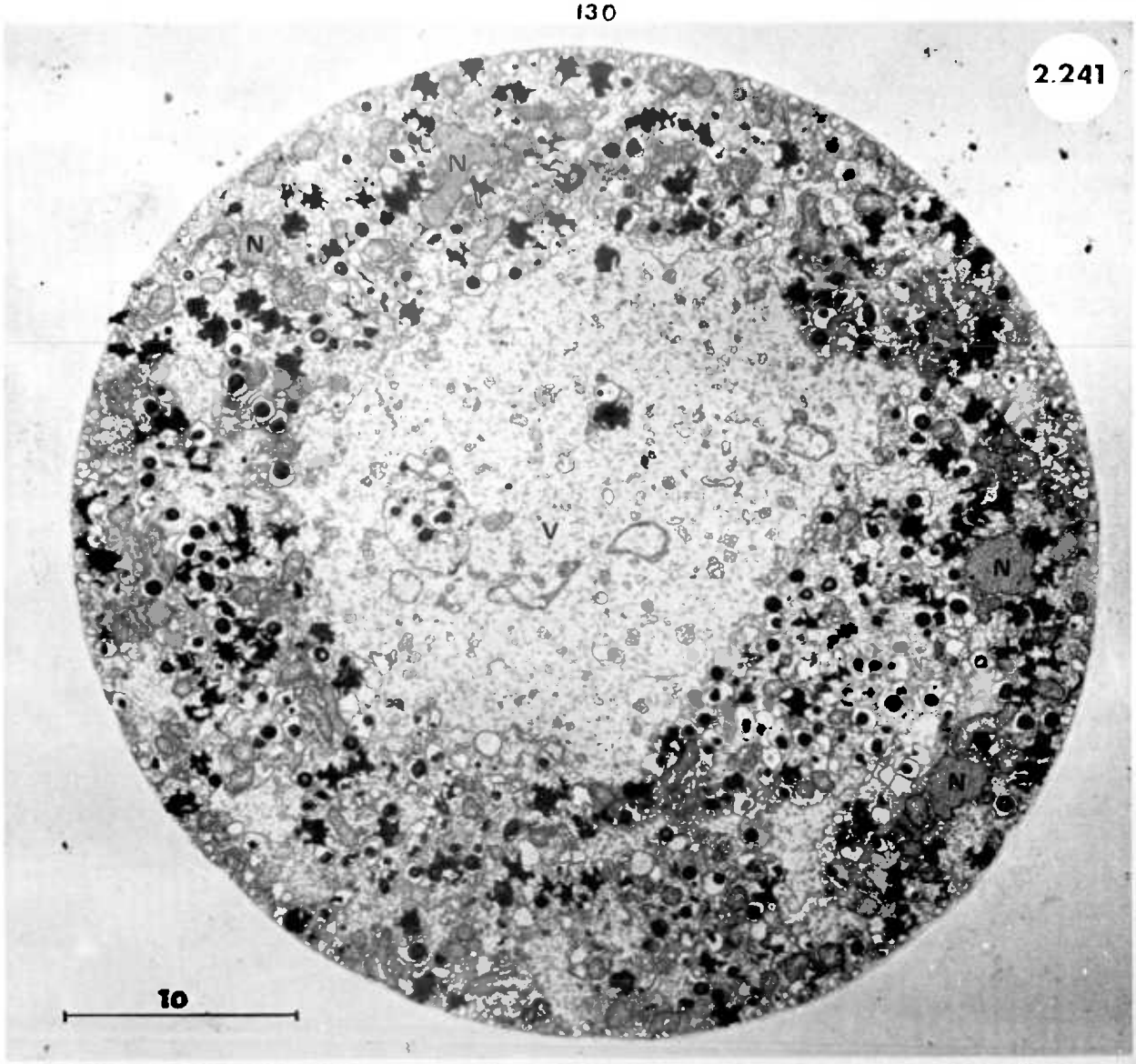

W
L
2.240
5

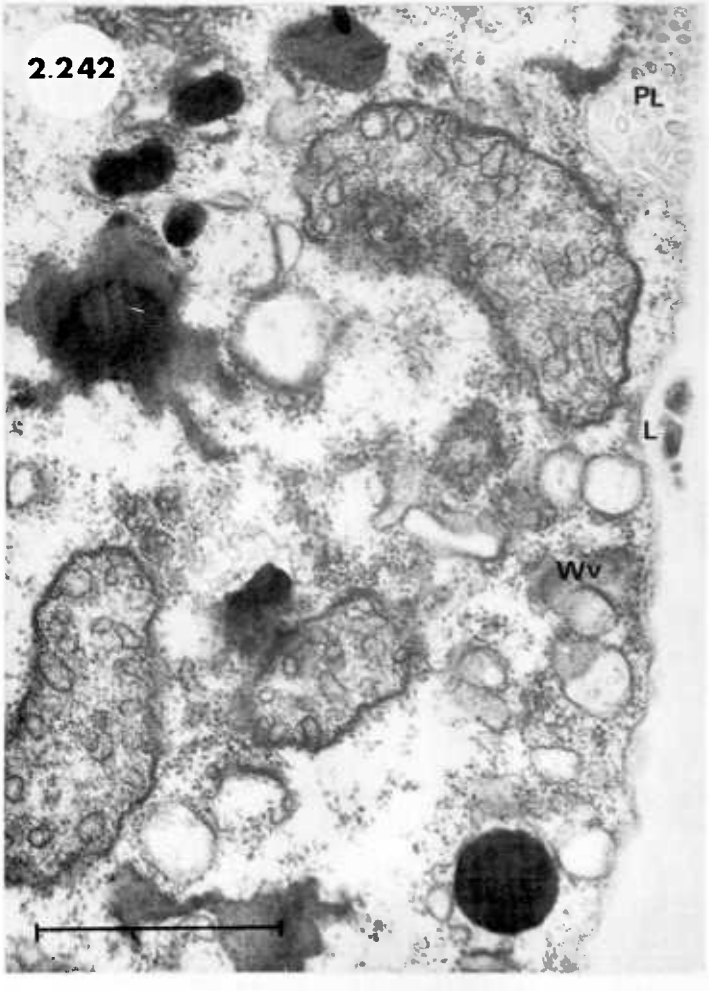
2.3.8.9 Effects of chloramphenicol on reproduction in S.furcata

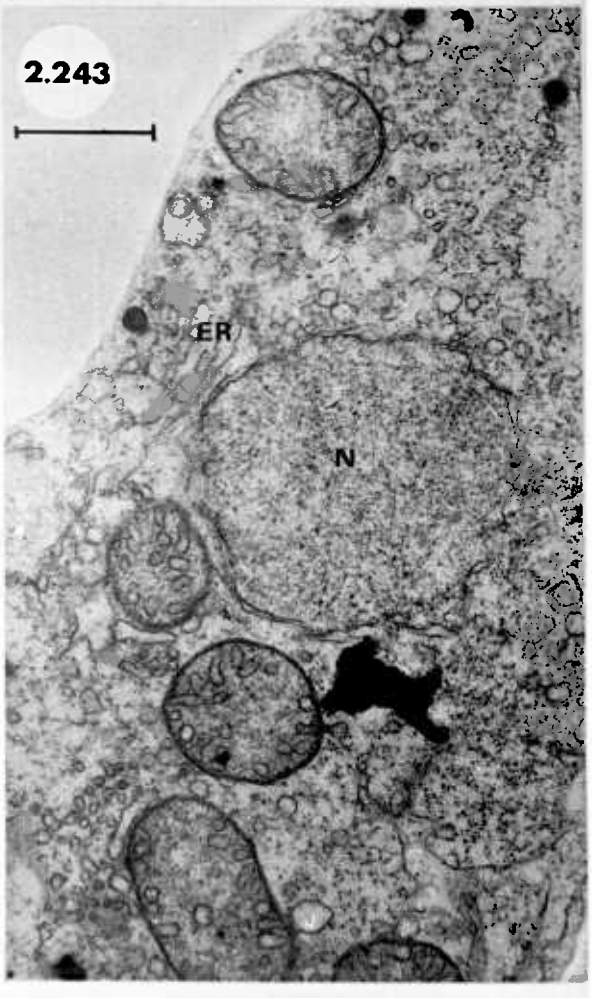
Fig. 2.241 Profile of a Chl-induced gemmae showing a certain amount of vacuolar disruption with fragments of cytoplasm dispersed throughout the vacuole.
29621 Os 3882 1000 mg/l Chl 168 h

Fig. 2.242 Peripheral cytoplasm of a Chl-induced gemma. Although the wall is not especially thickened it contains a small lomasome. The mitochondria appear normal with abundant cristae and a dense particulate matrix.
29262 Os 3881 1000 mg/l Chl 48 h

Fig. 2.243 Cytoplasm of an antheridium associated with an uncleaved 48 h oogonium. The small nuclear size suggests meiosis has already taken place.
29445 Os 3881 1000 mg/l Chl 48 h


2.241
N
N
V
N
N
1o


2.242
PL
L
Wv


2.243
ER
N

2.3.8.9 Effects of chloramphenicol on reproduction in S.furcata

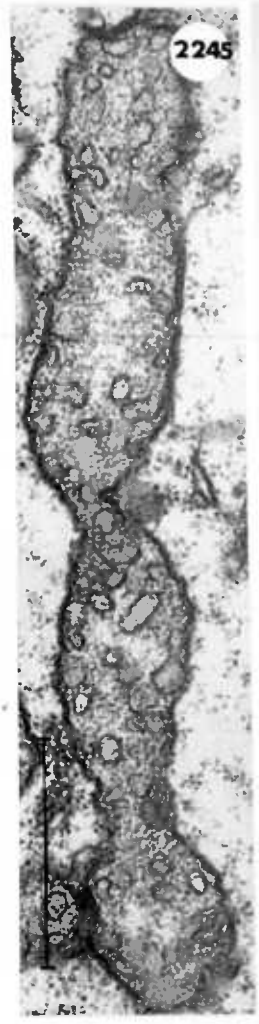
Fig. 2.244 Montage of median LS through a large uncleaved oogonium. The large central vacuolar zone is partitioned by membrane fragments. There are no lomdsomes in the cell wall.
29958/59 Os 3882 1000 mg/l Chl. 168 h

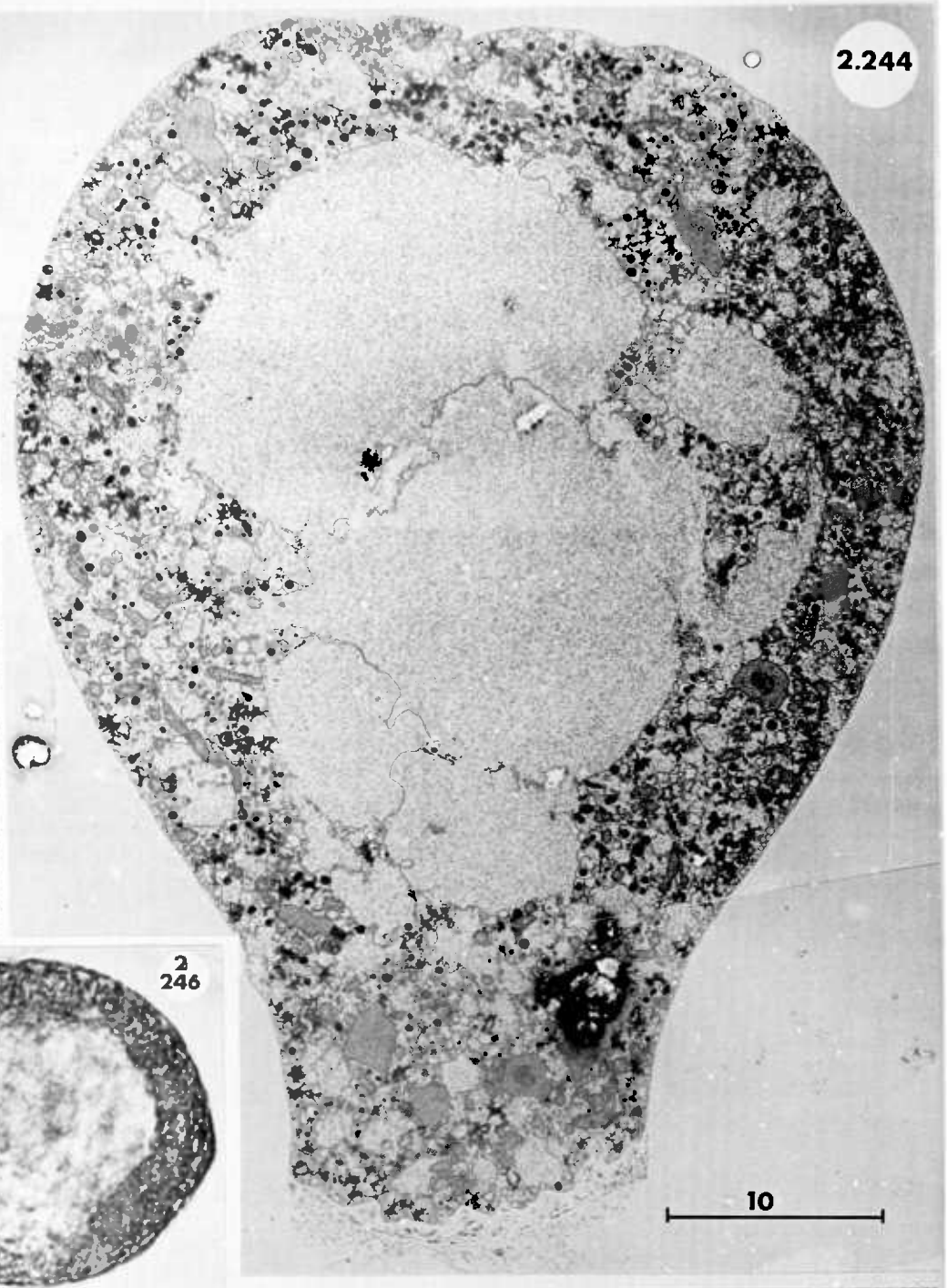
Fig. 2.245 An elongate mitochondrion in the gemma shown in Fig. 2.244.
29944 Os 3882 1000 mg/l Chl 168 h

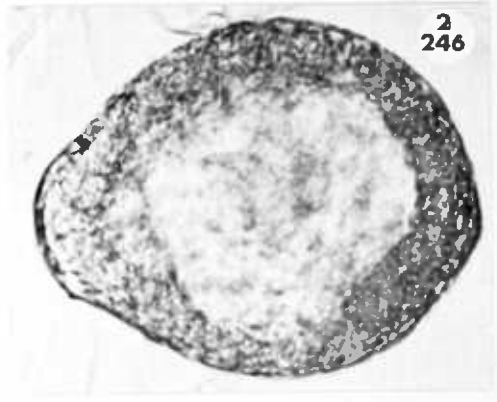
Fig. 2.246 Light-micrograph of a spherical Chl-induced gemma.
121/18 OI 1000 mg/l Chl 168 h

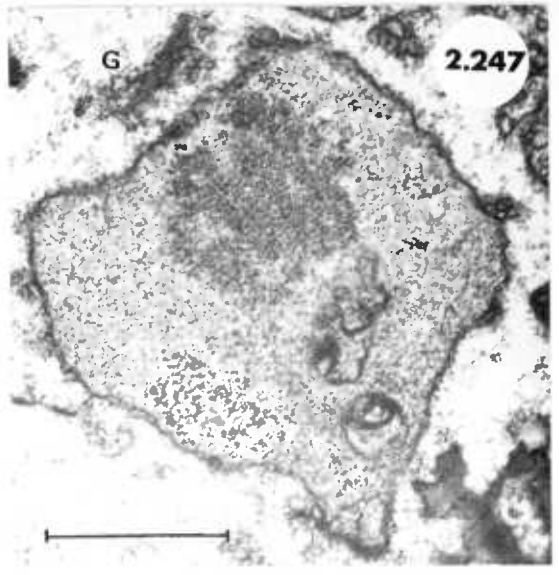
Fig. 2.247 Interphase nucleus in a gemma. Note the dense osmiophilic strands in the nucleoplasm, the low density of cytoplasmic ribosomes, and absence of peripheral golgi vesicles.
29946 Os 3882 1000 mg/l Chl 168 h

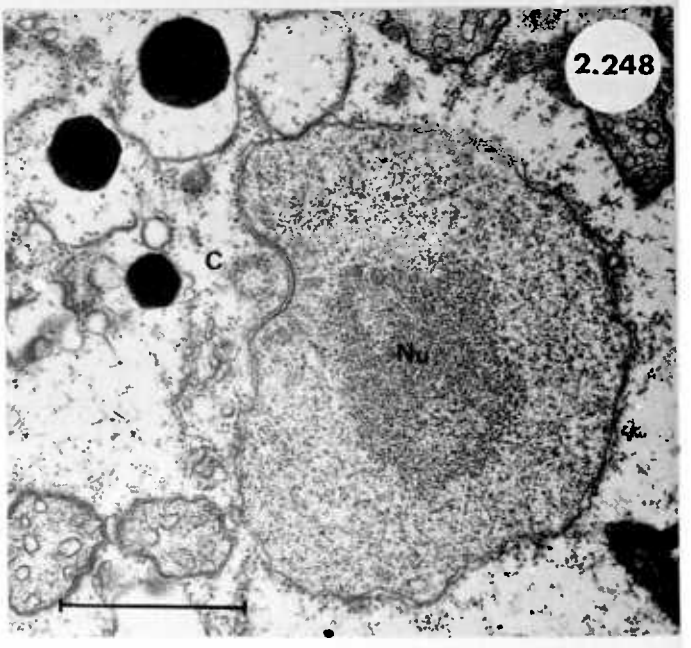
Fig. 2.248 Interphase nucleus in the gemma shown in Fig. 2.244, showing well-defined nucleolus and amorphus granules adjacent to the centriole pocket.
29954 Os 3882 1000 mg/l Chl 168 h


2245


2.244
10


2
246


G
2.247


2.248
C
Nu

2.3.8.9 The effect of cycloheximide on sexual reproduction in S.furcata

Fig.2.249 Light micrograph of Cyc-induced gemma, containing cyst-like structures.
121/7 OI 1 mg/l Cyc 120 h

Fig. 2.250 Gemma containing cyst-like structures. Each 'cyst' contains a single nucleus, vacuoles and conspicuous electron dense mitochondria.
27505 Os 3733 1 mg/l Cyc 120 h

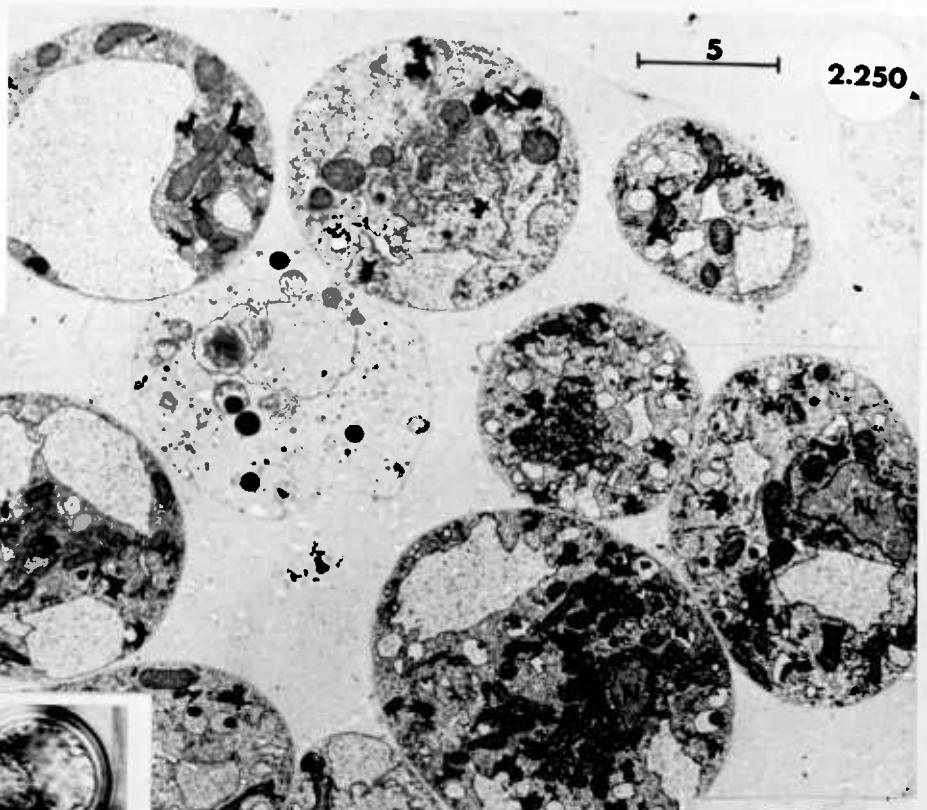
Fig. 2.251 Light micrograph of Cyc-induced oospores containing transparent ooplast vacuoles.
121/3 OI 1 mg/l Cyc 120 h

Fig. 2.252 Light micrograph of an elongate appendate gemma, with a single spherical secondary body at the appendage tip.
121/5 OI 1 mg/l Cyc 120 h

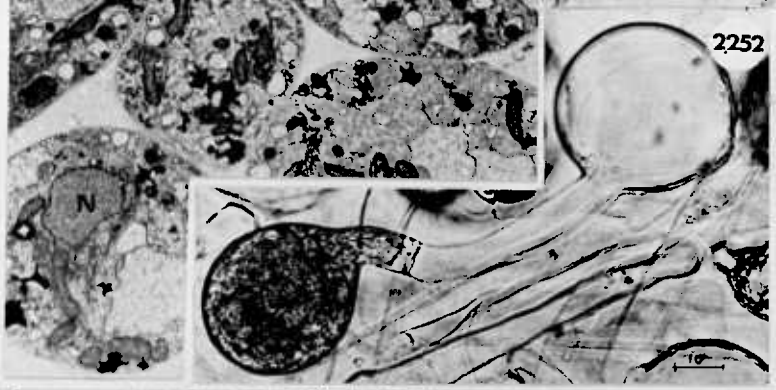
Fig. 2.253 Gemma with two developing appendages.
121/20 OI 1 mg/l Cyc 120 h

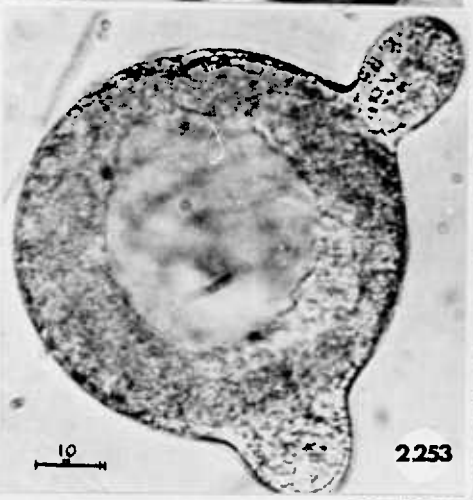
Fig. 2.254 An oblique LS through a gemma with an appendage initial developing.
27500 Os 3733 1 mg/l Cyc 120 h

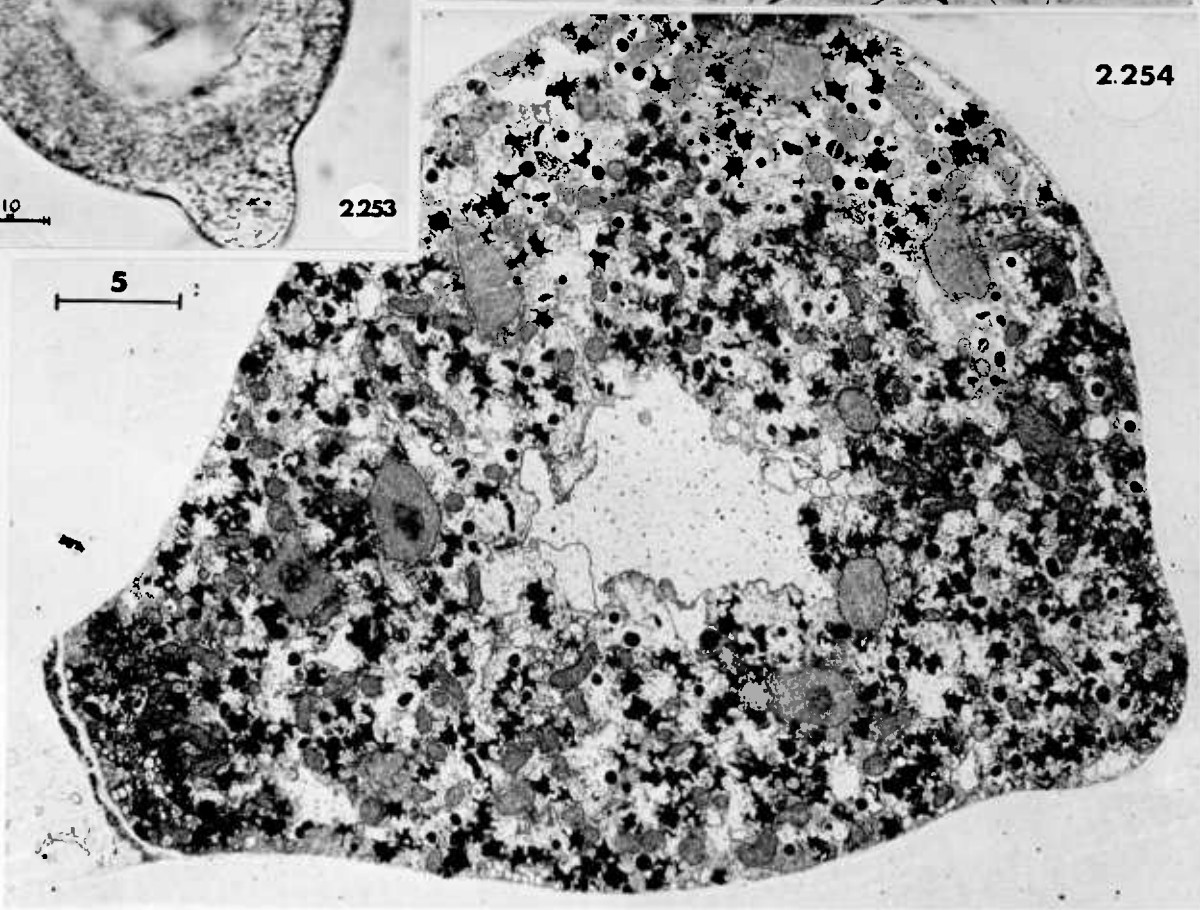

2249
10


5
2.250
N


2251


2252
N


10
2253


5
2.254

2.3.8.9 The effect of cycloheximide on sexual reproduction in S.furacta

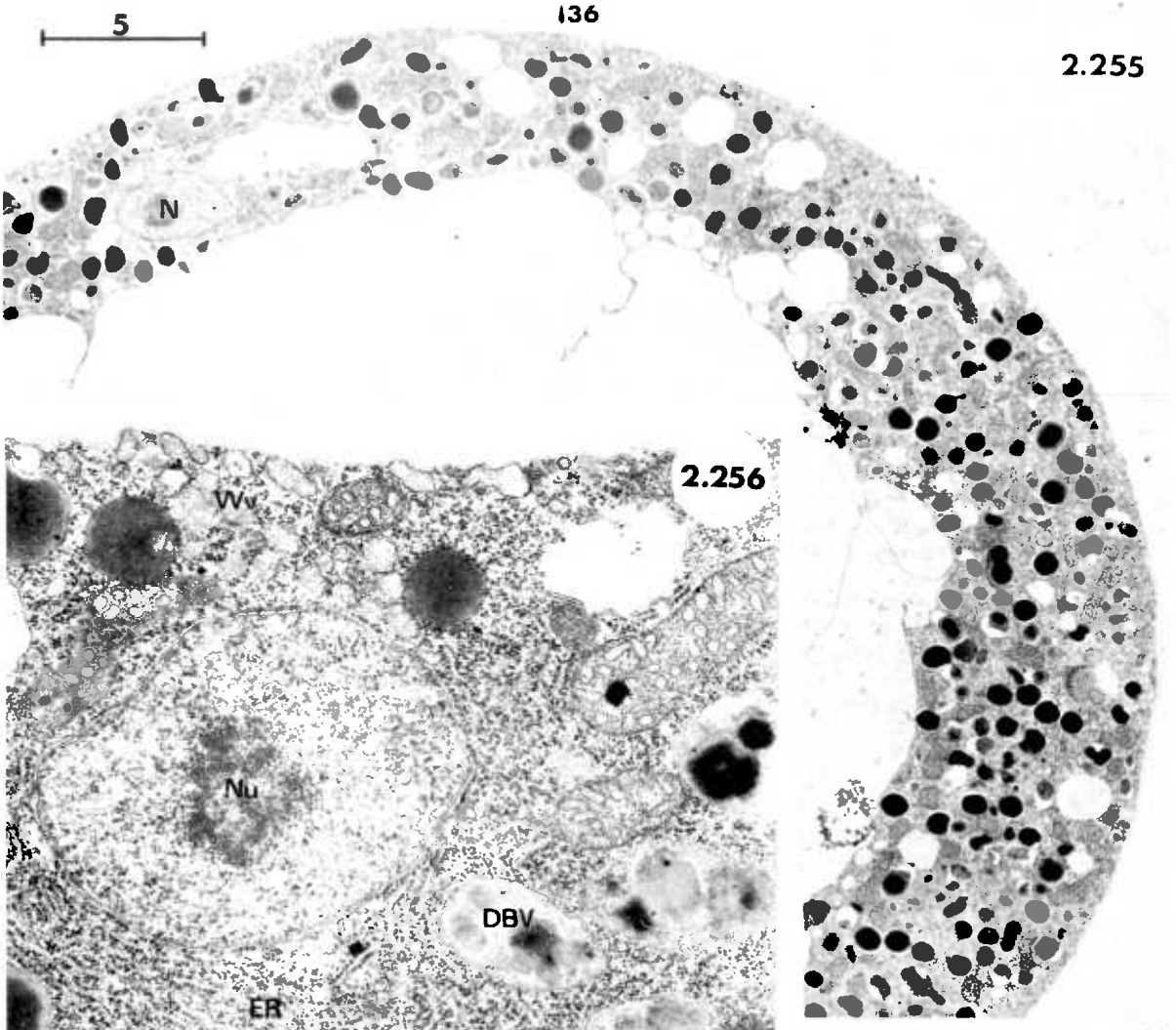
Fig. 2.255 Profile of a simple spherical gemma, showing large central vacuole.
27516 GaOs 3730 1 mg/l Cyc 120 h

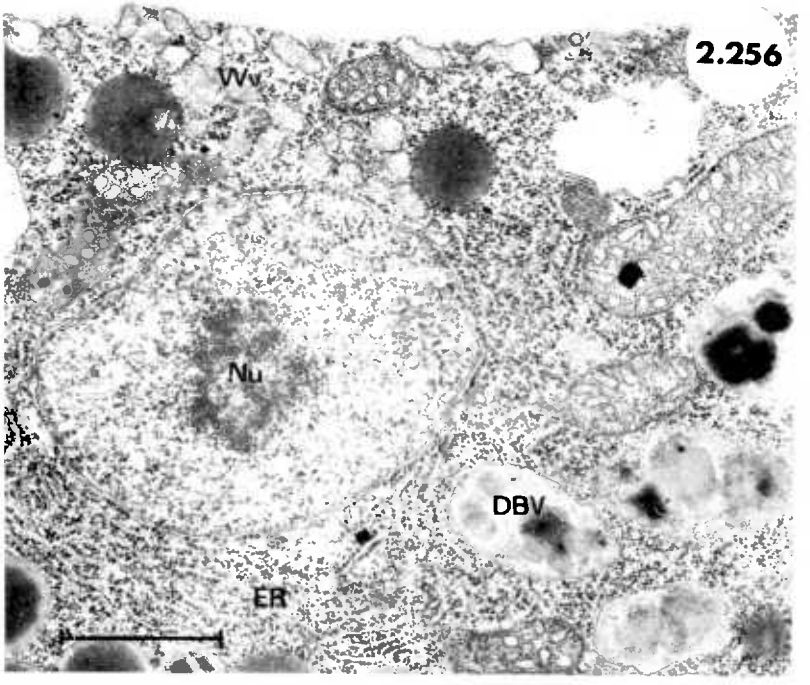
Fig. 2.256 Detail of the peripheral cytoplasm of the gemma in Fig. 2.255. Note the extensive arrays of rough ER around both the nucleus and mitochondria, and the localised accumulation of wall vesicles between the wall and nucleus.
27508 GaOs 3730 1 mg/l Cyc 120 h

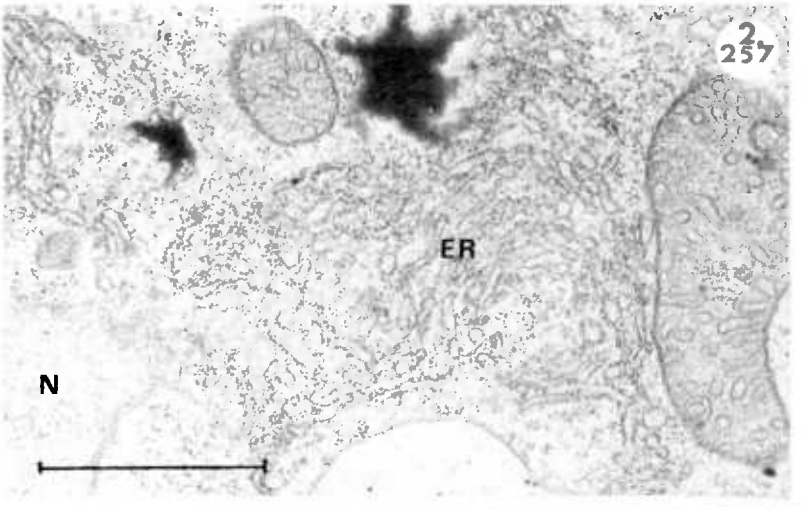
Fig. 2.257 Detail of the cytoplasm of one of cyst-like bodies shown in Fig. 2.250, showing a similar abundance of rough ER.
27563 Os 3733 1 mg/l Cyc 120 h

Figs. 2.258, 2.260 Detail of densebody vesicles in the gemma shown in Fig. 2.255, showing the expanded matrix, with characteristic myelin-like configurations.
27533 GaOs 3930 1 mg/l Cyc 120 h

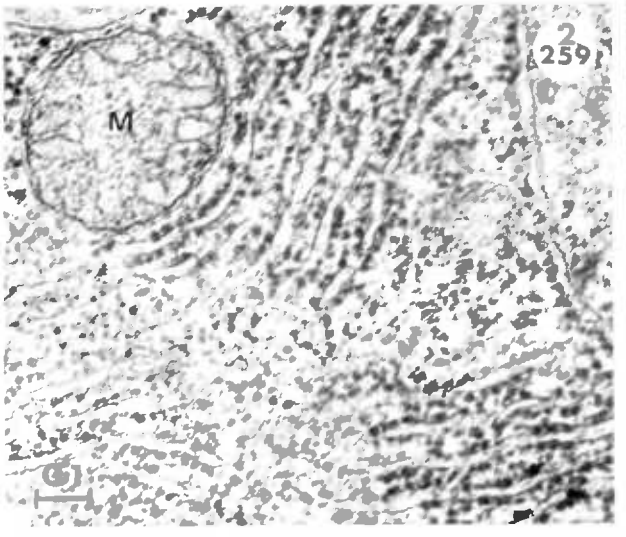
Fig. 2.259 Detail of the rough ER cisternae surrounding a mitochondrion and nucleus.
27508 GaOs 3730 1 mg/l Cyc 120 h

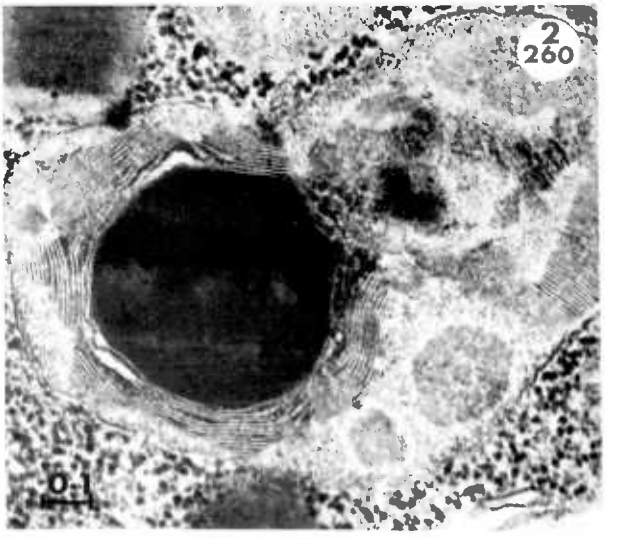

5
2.255
N


2.256
Wv
Nu
DBV
ER


2
257
ER
N


2
258
0.1


2
259
M


2
260
0.1

2.3.10.3 The elemental composition of normal and streptomycin induced oogonia

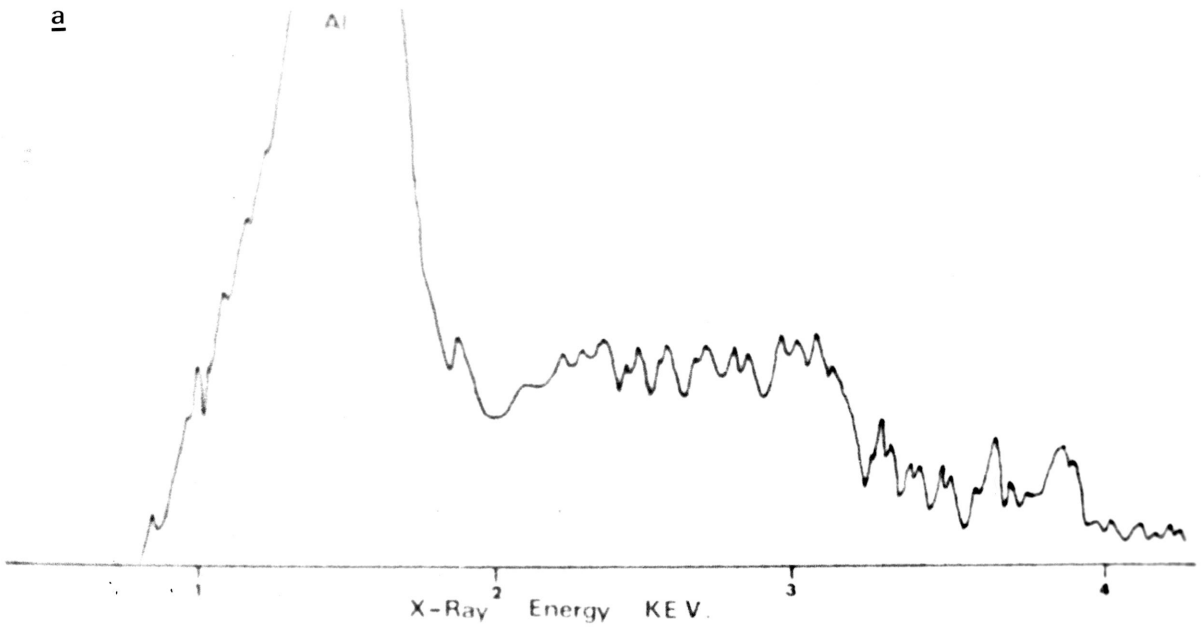
Fig. 2.268 A series of elemental microanalysis (EDAX) scans of aluminium coated specimens of S.furcata. In each case the count time is 500 seconds, and the scans are plotted in a linear scale.

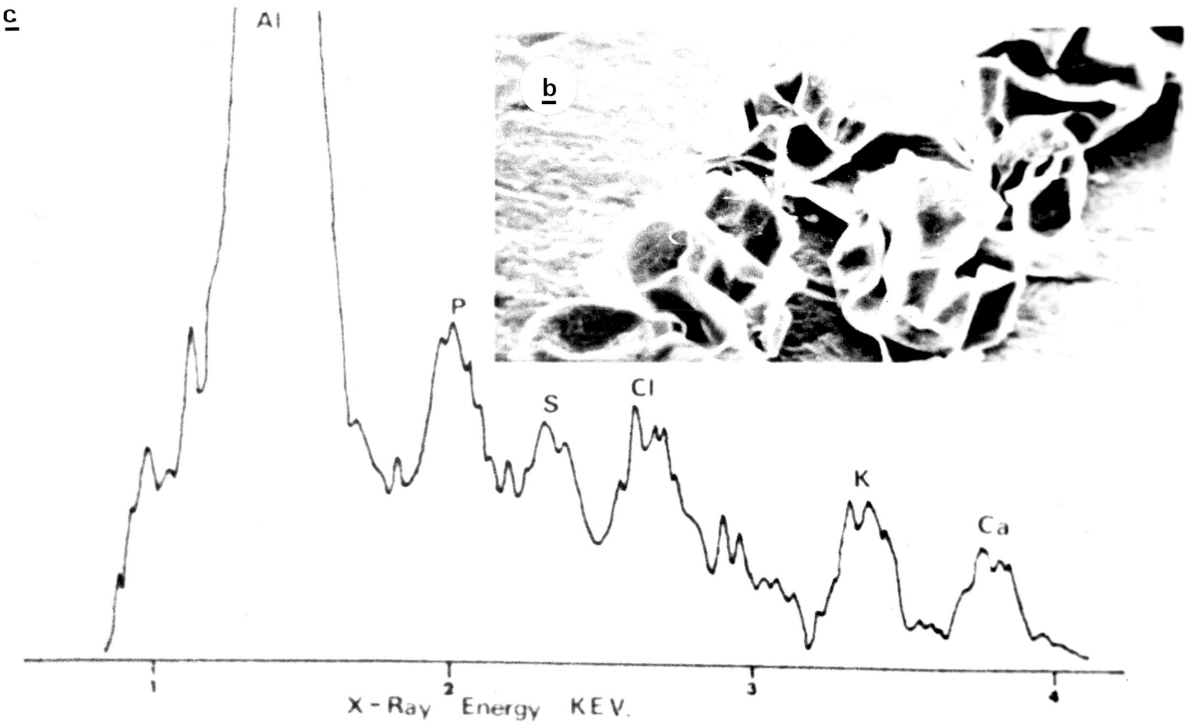
a) The background count of 'white radiation'. This was taken from the mounting stub to one side of the specimens. The aluminium peak is the only one visible.

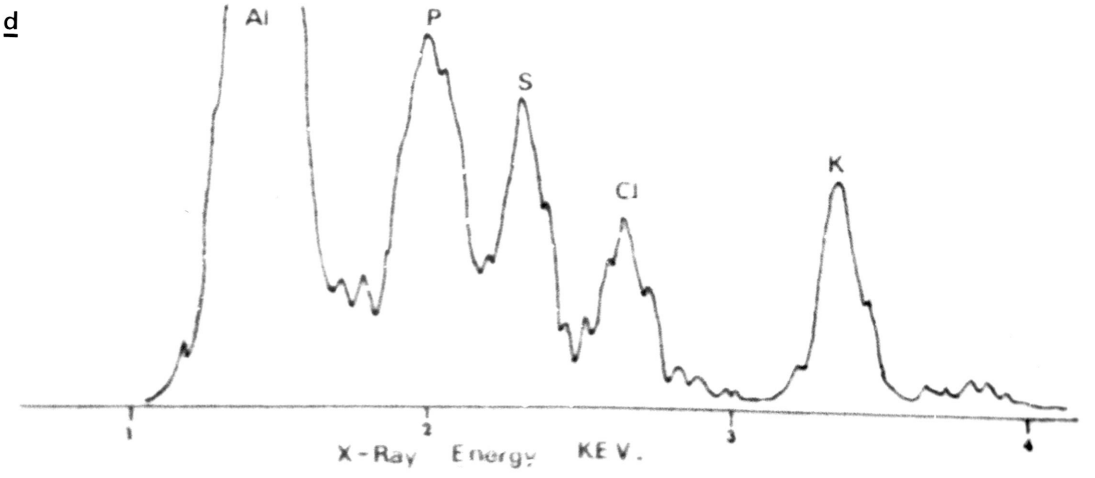
b) A scanning-electron micrograph of a number of normal oogonia dried on aluminium stubs and coated in aluminium. Parts of individual oogonia were selected for the elemental analysis scans.
838/2 x c.6000 GDW 120 h

c) Elemental analysis of an oogonium induced in glass distilled water, 120 h after induction. The main elements, excluding the Al peak, are P,S, ClK and Ca GDW 120 h

d) Elemental analysis of an oogonium induced in 50 mg/l Str, 120 h after induction. Note the absence of the Ca peak.
50 mg/l Str 120 h


a
Al
1
2
3
4
X-Ray Energy KEV.


c
Al
b
P
S
Cl
K
Ca
1
2
3
4
X-Ray Energy KEV.


d
Al
P
S
Cl
K
1
2
3
4
X-Ray Energy KEV.

2.3.10.3 The elemental composition of normal and streptomycin induced oogonia

Fig. 2.268 A series of elemental microanalysis (EDAX) scans of carbon coated specimens of S.furcata. The count time for a and b is 500 seconds, and for c, 1000 seconds. The scans are plotted on a logarithmic scale.

a) Elemental analysis of an oogonium induced in glass distilled water, 120 h after induction. The Al peak is probably from the aluminium rivot on which the carbon is mounted. The elements present are Na, Mg, Al, P, S, Cl, K and Ca

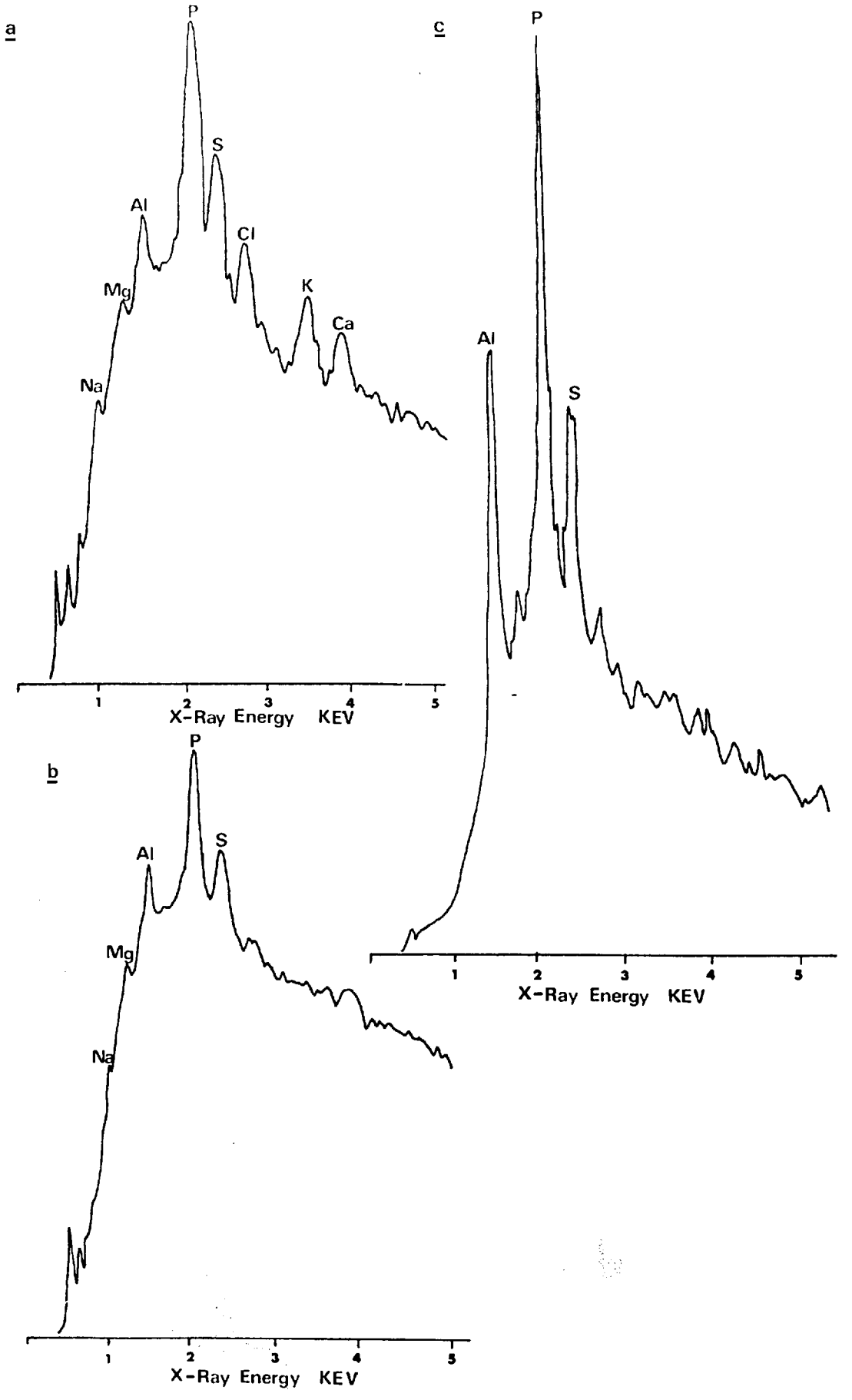
GDW 120 h

b) Elemental analysis of a gemma induced in 500 mg/l Str. 120 h after induction. Note the absence of Cl, K and Ca.

500 mg/l Str 120 h

c) Elemental analysis of a gemma induced in 500 mg/l Str, 120 h after induction, again showing the absence of all elements except Al, P and S.

500 mg/l Str 120 h


a
P
S
Al
Cl
Mg
K
Ca
Na
1
2
3
4
5
X-Ray Energy KEV
b
P
Al
S
Mg
Na
1
2
3
4
5
X-Ray Energy KEV
c
P
Al
S
1
2
3
4
5
X-Ray Energy KEV

PART 3. THE EFFECTS OF TAP WATER AND DIVALENT CATIONS ON THE REPRODUCTIVE DIFFERENTIATION OF SAPROLEGNIA SPP.

3.3.1 The effects of tap water on reproduction in S.furcata

Figs. 3.1, 3.3 Light-micrographs of hemp seed colonies induced in GDW, SDW and TW respectively. Note the effects on oogonium production and colony outgrowth.
60/2,6,8 x c.4 120 h

Fig. 3.4 A gemma chain induced in TW.
63/25 OI TW 96 h

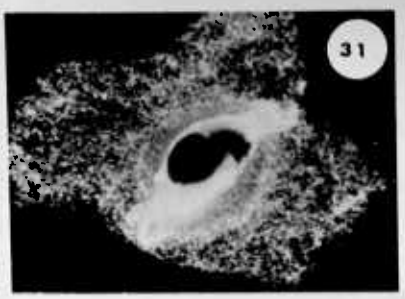
Fig. 3.5 Gemmae developing on oogonial and antheridial branches.
63/13 OI TW 96 h

Fig. 3.6 A clavate gemma with dense non-vacuolate cytoplasm.
63/14 OI MFTW 120 h

Fig. 3.7 LS of an elongate gemma induced in MFTW. The vacuolar compartments show an irregular disposition.
25903 Os 3672 MFTW 120 h

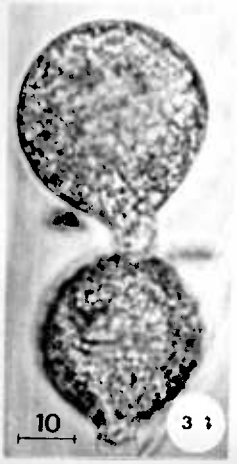
Fig. 3.8 Part of a spherical gemma showing a partially developed vacuolar zone. Note the presence of lomasomes in the wall and the expanded ring-like densebody granules in the vacuoles.
25907 Os 3672 MFTW 120 h

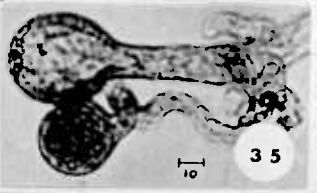
Fig. 3.9 Part of an appendate gemma showing the peripherally distributed organelle-containing cytoplasm and divided vacuolar zone.
25965 Os 3669 TW 96 h

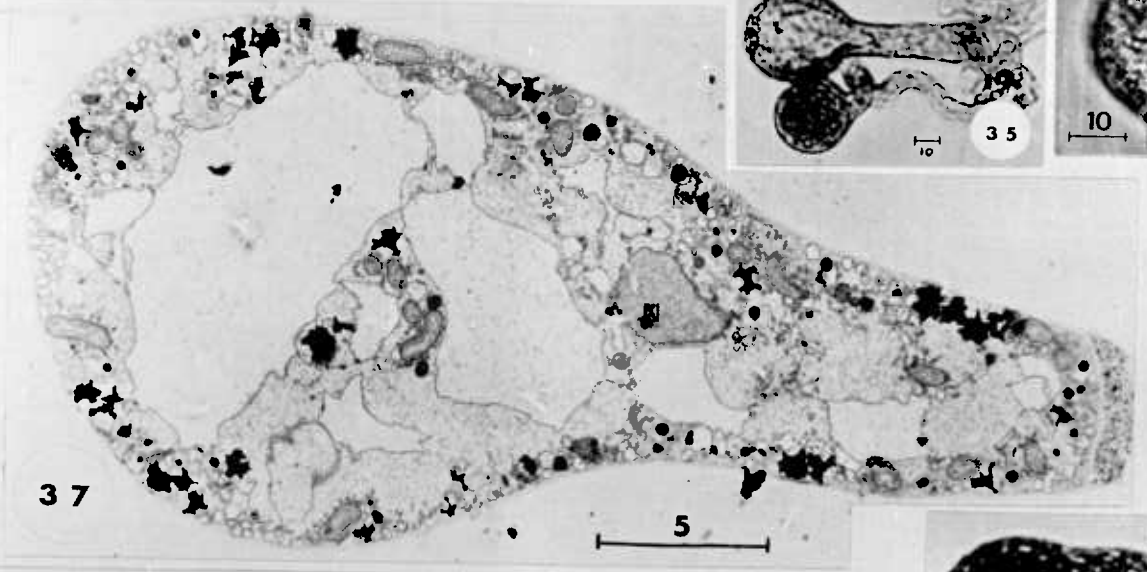

31

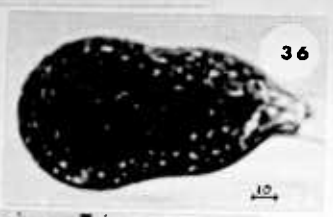

32

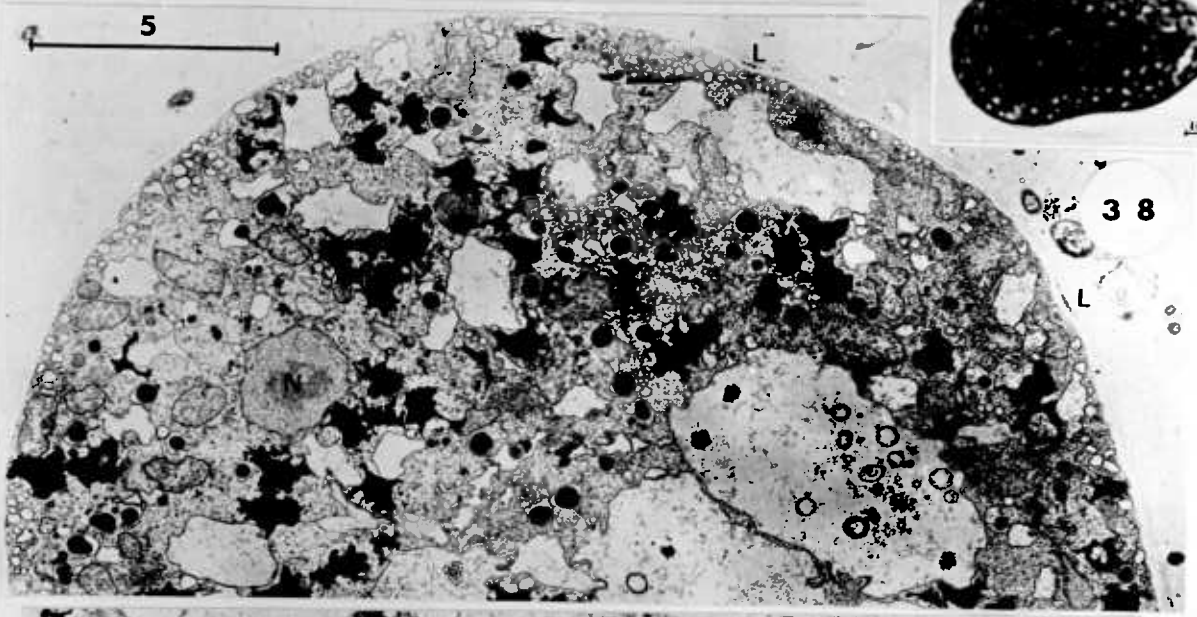

33

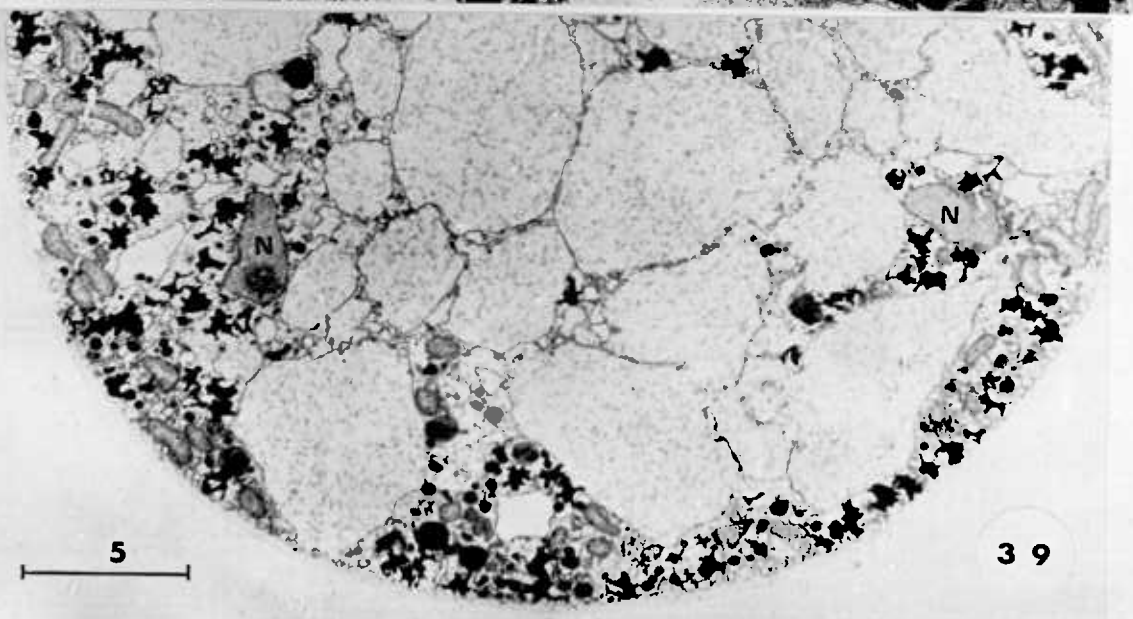

10
34


10
35


37
5


36
10


5
L
N
38
L


N
N
5
39

3.3.1 The effects of tap water on reproduction in S.furcata

Fig. 3.10 A TW-induced oogonium showing characteristically swollen oospores. Note how the peripheral lipid-containing cytoplasm is still peripherally distributed and the enlarged ooplast still contains particles in Brownian motion.
114/7 OI TW 96 h

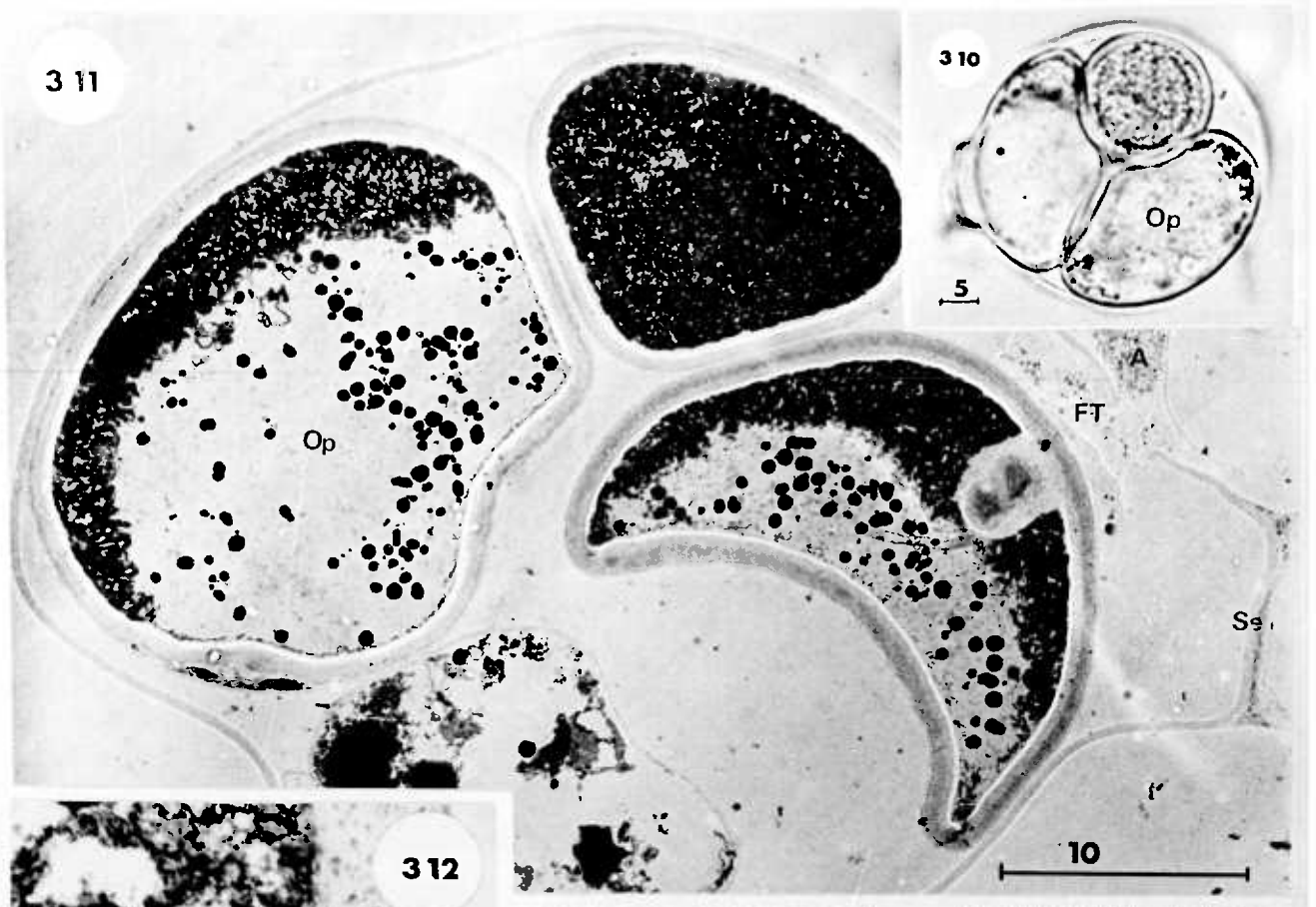
Fig. 3.11 LS of an oogonium containing oospores like those shown in Fig. 3.10. Note the peg-like ingrowth of the endospore wall where the fertilisation tube contacts the spore.
29775 Os 3991 TW 96 h

Fig. 3.12 Detail of the wall and peripheral cytoplasm of a swollen oospore. Note the thickness and structure of the endospore layer, and the good preservation of cytoplasmic organelles. The mitochondrial membranes are more electron dense and the matrix more electron transparent than usual.
25920 Os 3617 TW 96 h

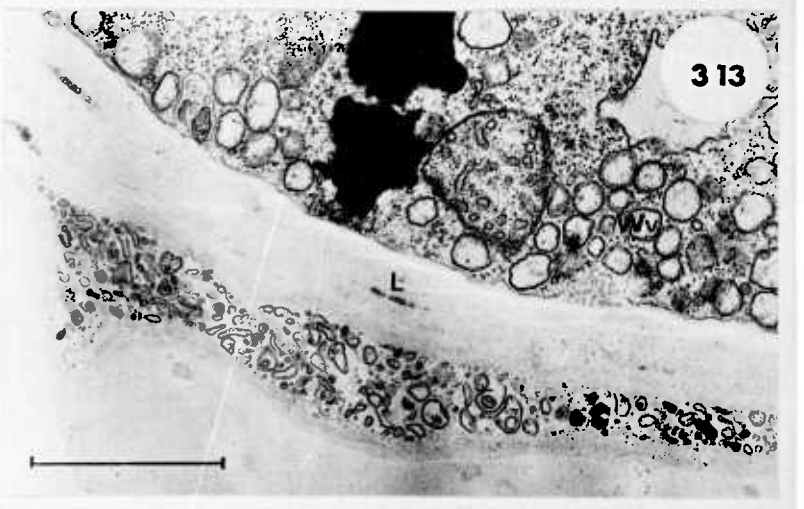
Fig. 3.13 Detail of part of a septum of the gemma shown in Fig. 3.8. Note the thickened upper layer and abundance of wall vesicles in the adjacent cytoplasm.
25968 Os 3672 MFTW 120 h

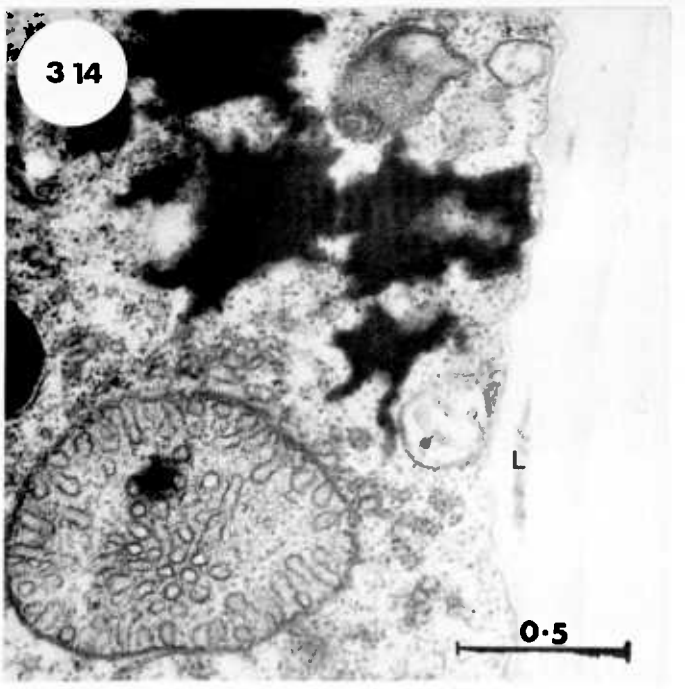
Fig. 3.14 Peripheral cytoplasm of a gemma induced in TW, showing the thick wall and large mitochondrion with abundant cristae.
25911 Os 3672 TW 96 h

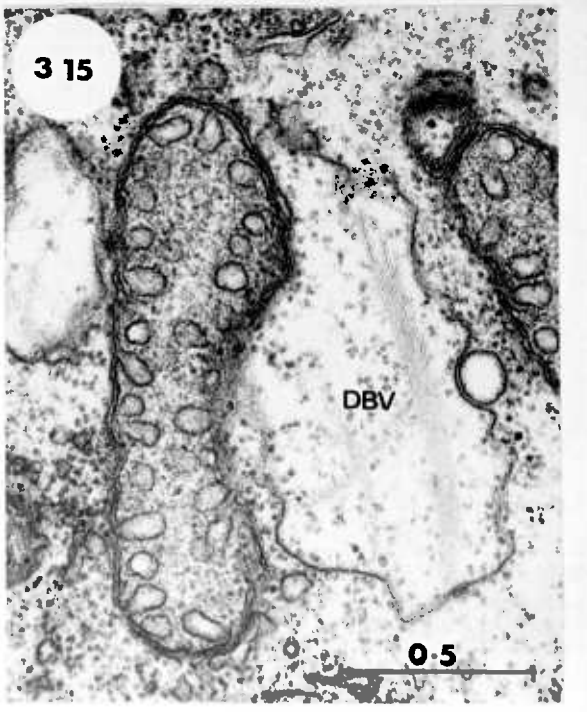
Fig. 3.15 A shallow cup shaped mitochondrion closely associated with a densebody vesicle containing myelin-like banding.
27022 Os 3333 ATW 120 h


3 11
Op
3 10
Op
5
A
FT
Se
10


3 12
M
EW
0·5


3 13
L


3 14
L
0·5


3 15
DBV
0·5

3.3.1 The effects of tap water and EDTA on reproduction in S.furcata

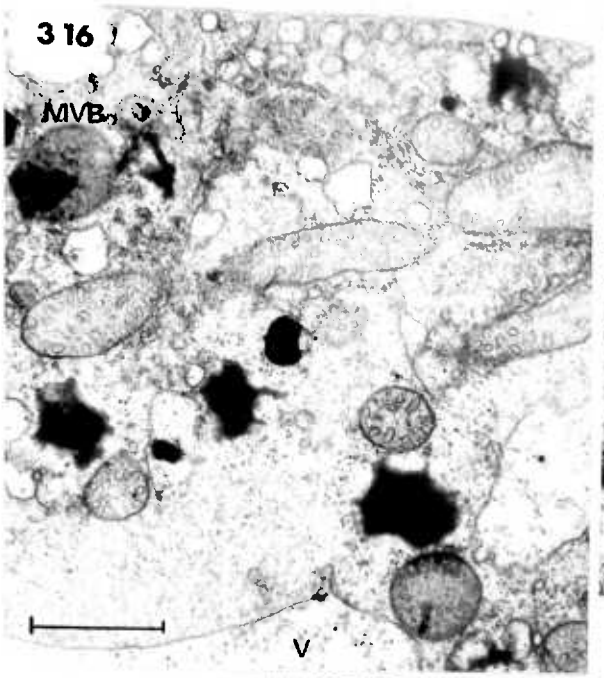
Fig. 3.16 Peripheral cytoplasm of an EDTA-induced gemma showing the small number of cytoplasmic ribosomes. Note the presence of multi vesicular bodies.
27022 Os 3704 100 mg/l EDTA 144 h

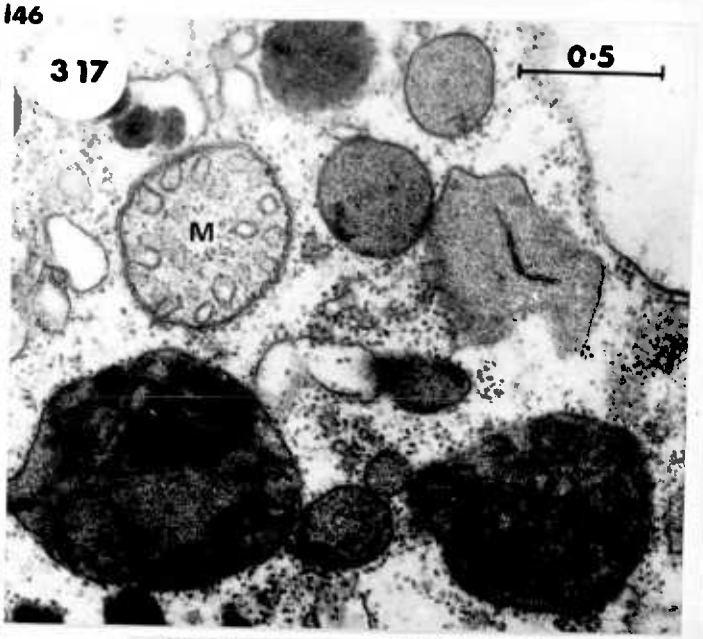
Fig. 3.17 A cluster of multivesicular bodies in a MFTW-induced gemma. Note the presence of smaller more uniformly particulate vesicles in addition to the more usual bodies with membranous inclusions.
25909 Os 3672 MFTW 144 h

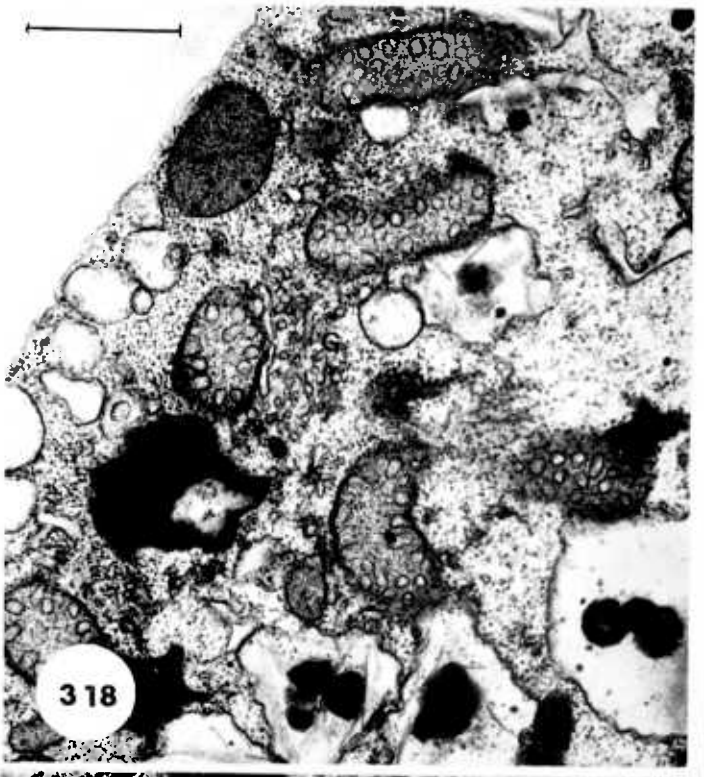
Fig. 3.18 Peripheral cytoplasm of a ATW-induced gemma, showing thickened cell wall. Note the dense particle filled vesicle adjacent to the wall and the Golgi-ER-mitochondrion complex.
27080 Os 3333 ATW 144 h

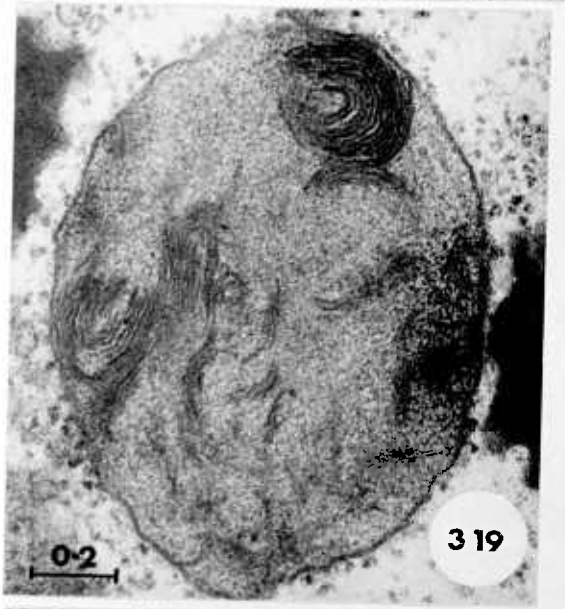
Figs. 3.19, 3.20 Multivesicular bodies in MFTW-induced gemmae. Note their uniform particulate matrix and myelin-like membranous inclusions.
25913 Os 3672 MFTW 144 h
25968 3669

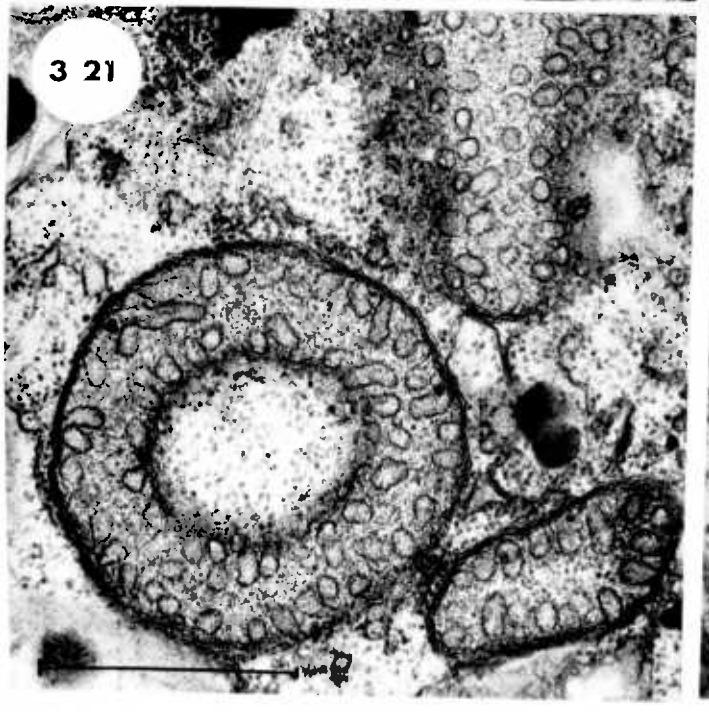
Figs. 3.21, 3.23 Two profiles of the cup-shaped mitochondria commonly found in TW-induced oogonia.
27079 Os 3333 ATW 144 h
29522 3391

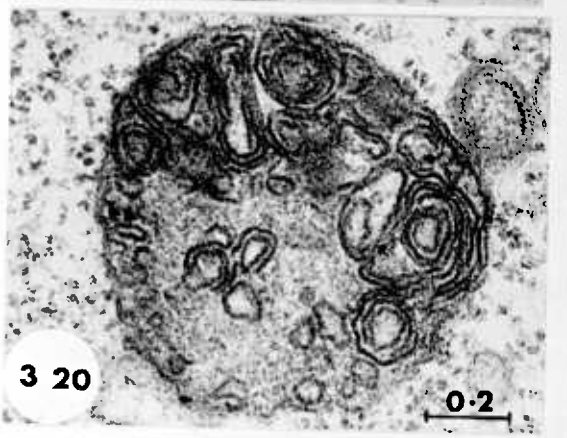

3 16
MVB
V

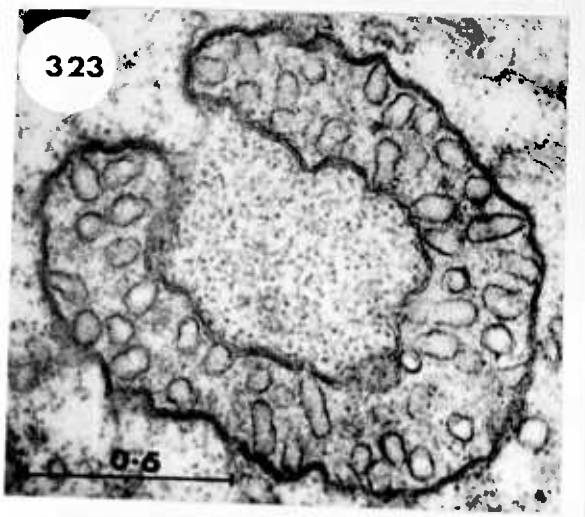

3 17
0·5
M


3 18


0·2
3 19


3 21


3 20
0·2


3 23
0·6

3.3.2.4 Effects of EDTA on reproduction in S.furcata

Figs. 3.26, 3.27 Part profiles of typical EDTA-induced gemmae. Note the high frequency of peripheral wall vesicles and absence of expanded vacuolar vesicles in Fig. 3.26.

27028 Os 3705B 500 mg/1 EDTA 144h
27021 3704B 100 mg/1

Figs. 3.28 A single spherical EDTA-induced gemma.

108.8 OI 500 mg/1 EDTA 196 h

Fig. 3.29 Detail of gemma cytoplasm. Note the interphse nucleus densebody granules and Golgi-mitochondrion associations.

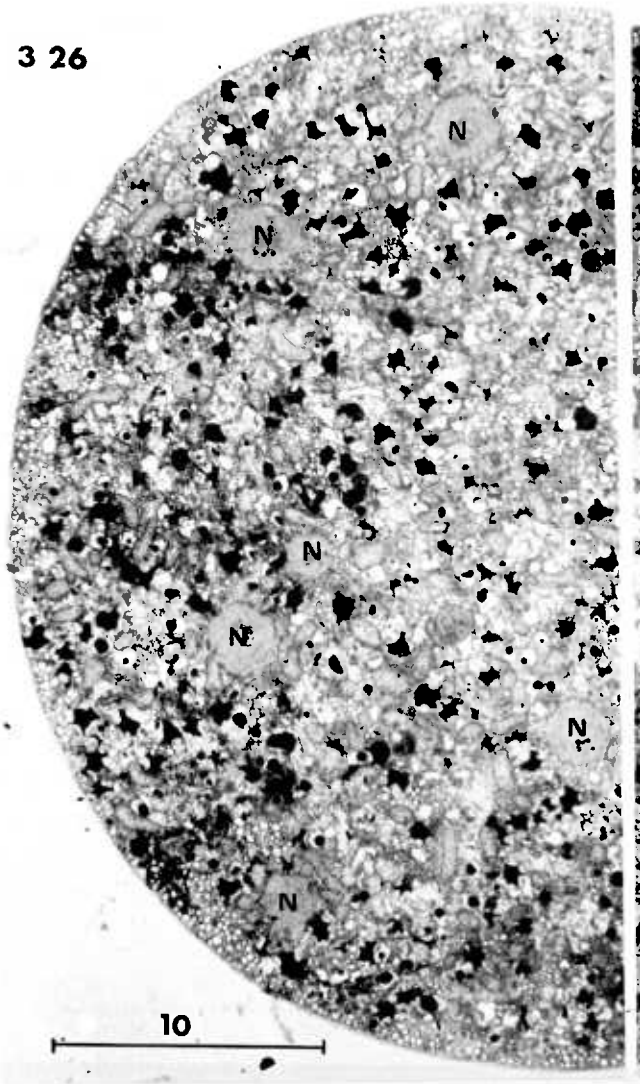
27055 Os 3705B 500 mg/1 EDTA 144 h

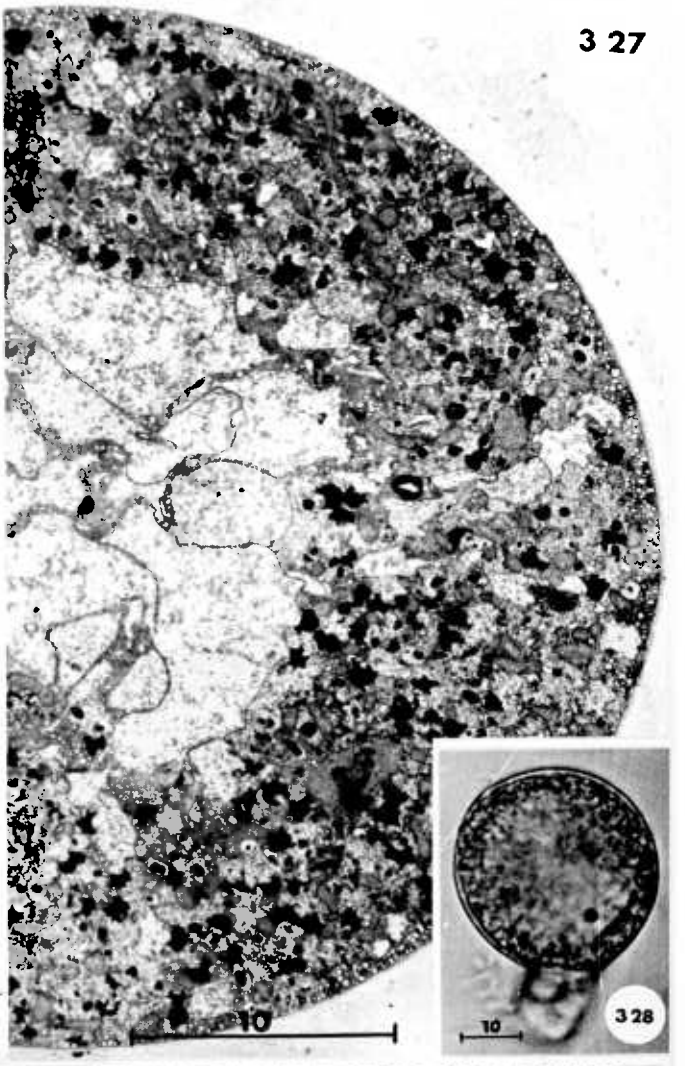
Fig. 3.30 Peripheral gemma cytoplasm showing large accumulation of wall vesicles.

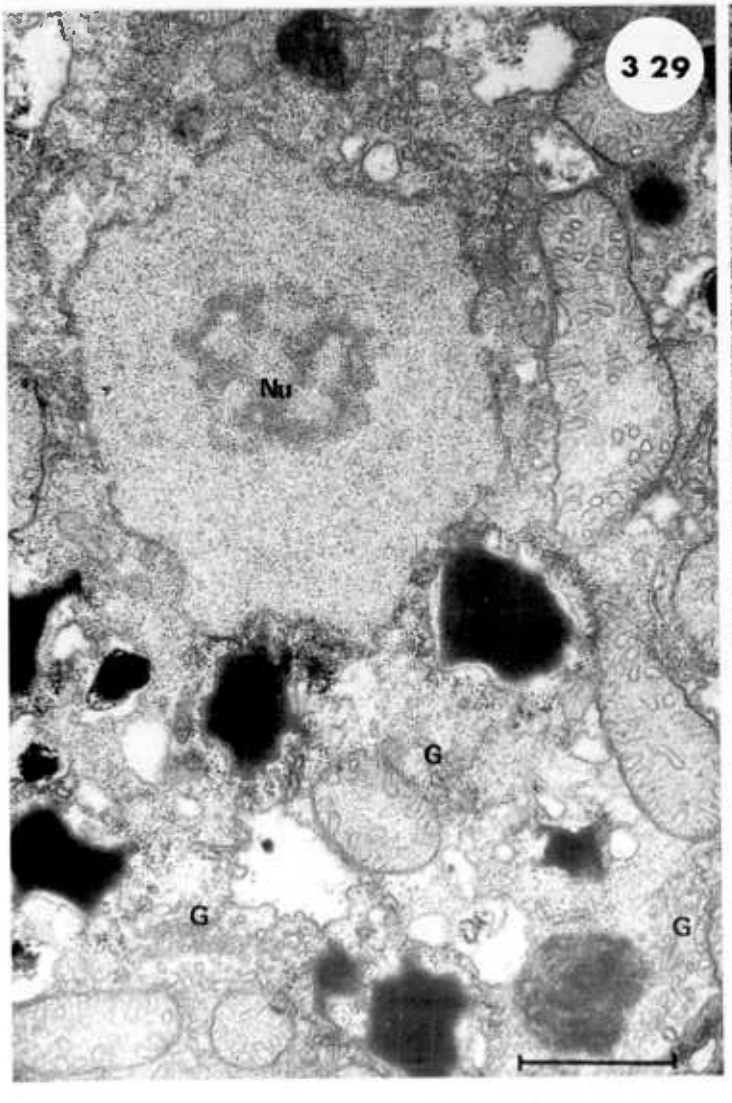
27043 Os 3705B 500 mg/1 EDTA 144 h

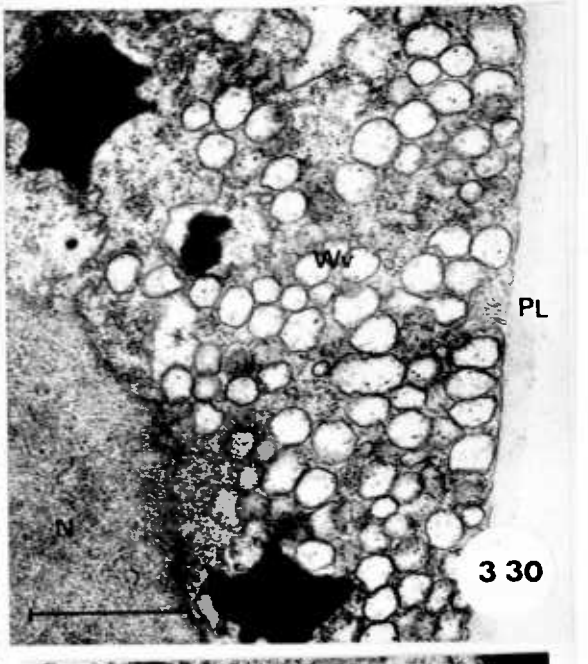
Fig. 3.31 Densebody vesicles in a gemma, showing the small granules and particulate matrix material.

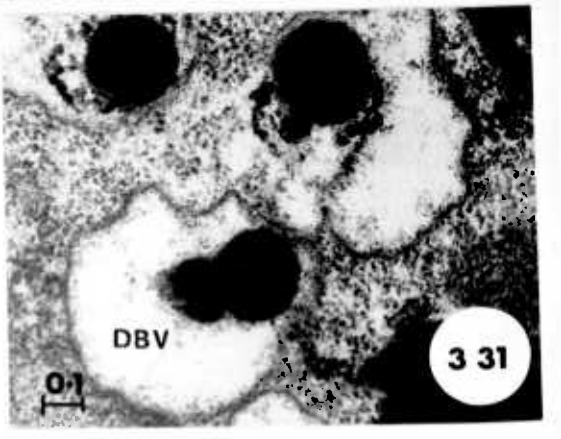
27057 Os 3706B 1000 mg/1 EDTA 144 h


3 26
N
N
N
N
N
N
10


3 27
10
3 28
10


3 29
Nu
G
G
G


Wv
PL
N
3 30


DBV
0·1
3 31

3.3.2.5 Effects of EDTA on reproduction in S.furcata

Figs. 3.32-3.37 Light-micrographs showing the effect of EDTA differentiated oospores. Note the large proportion of aborted spores and the variability in spore size.

108.22 OI	1000 mg/l EDTA 198 h
108.14 OI	500 mg/l EDTA 198 h
108.21 OI	1000 mg/l EDTA 198 h
108.12 OI	1000 mg/l EDTA 198 h
108.19 OI	500 mg/l EDTA 198 h
108.20 OI	1000 mg/l EDTA 198 h

Fig. 3.38 Detail of fertilisation tube and a mature oospore. Note the degenerate nuclei in the fertilisation tube, and thick primary wall of the oospore.

29557 Os 3704B 100 mg/l EDTA 144 h

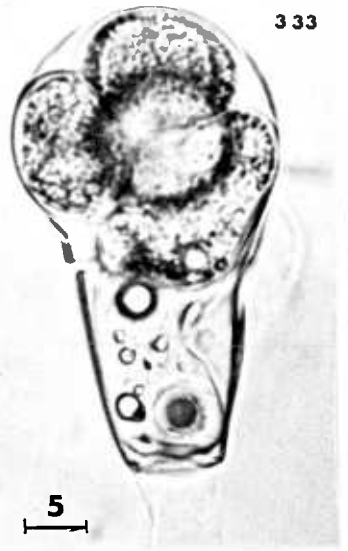
Fig. 3.39 Aborted EDTA-induced oospore showing the uniform electron dense endospore, which is partially separated from the primary oospore wall, and the large lipid droplets.

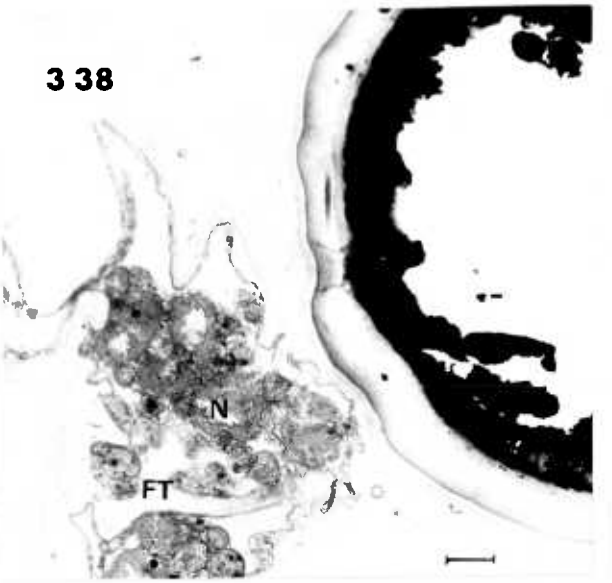
25995 Os 3704B 100 mg/l EDTA 144 h

Fig. 3.40 Detail of the wall layers of the oospore shown in Fig. 3.39. The electron dense outer layer of the endospore is conspicuous where the primary wall has separated from the outer wall. Note the absence of a membrane inside the endospore wall.

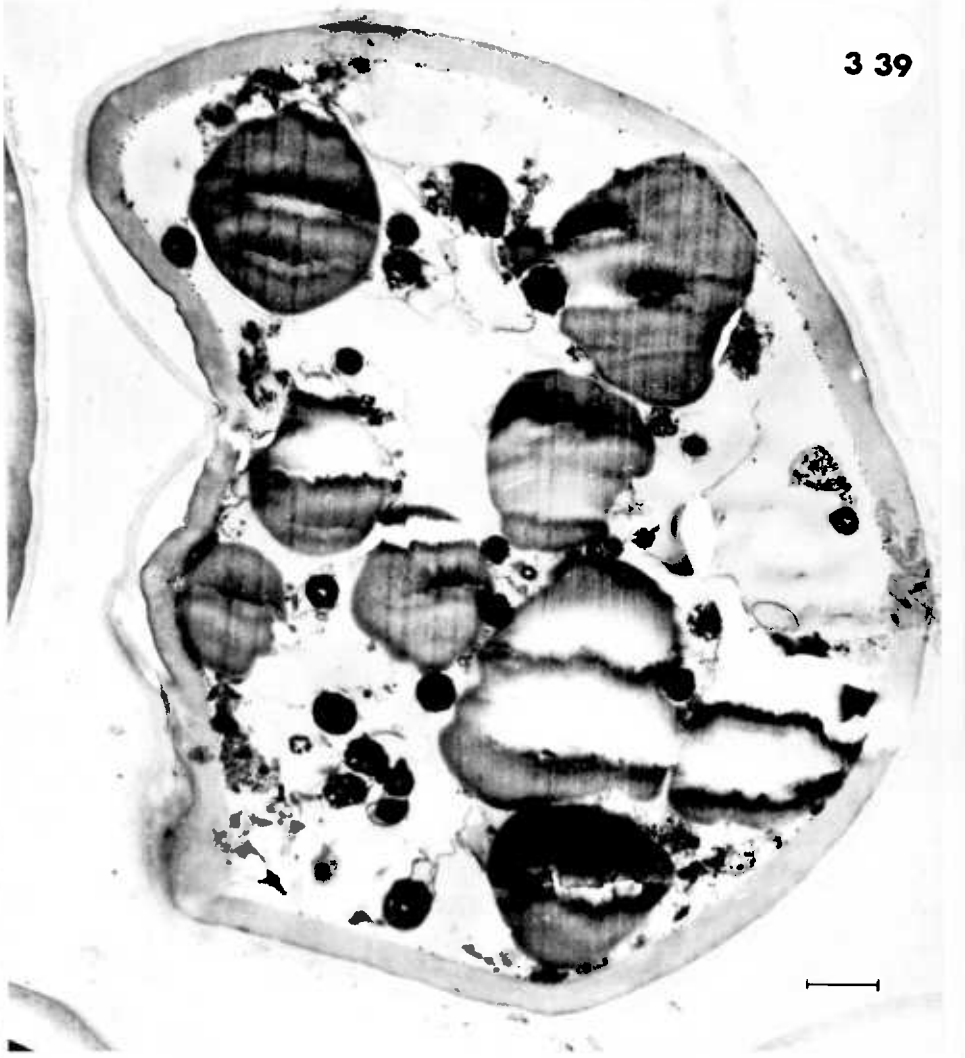
25996 Os 3704B 100 mg/l EDTA 144 h


3 32
5

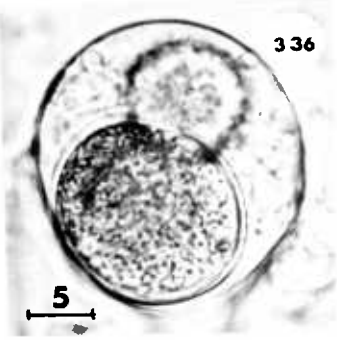

3 33
5

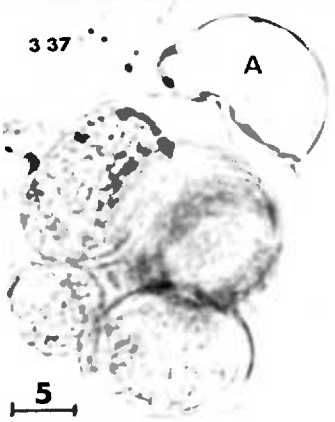

3 38
N
FT


3 34
5


3 39


5
3 35


3 36
5


3 37
A
5


340
5

3.3.2.4 The effect of high concentrations of calcium on reproduction in S.furcata

Fig. 3.41 Light-micrograph montage of a typical dense appendate Ca^{2+}-induced gemma.
152/51,52 OI 2500 mg/l Ca^{2+} 196 h

Fig. 3.42 Section of a comparable appendate gemma showing a developing appendage. Note the absence of large vacuolar vesicles and the abundance of lomasomes in the cell wall.
29455 Os 3492 1000 mg/l Ca^{2+} 196 h

Fig. 3.43 A typical Ca^{2+} induced oogonium containing aborted oospores.
152/22 OI 2500 mg/l Ca^{2+} 196 h

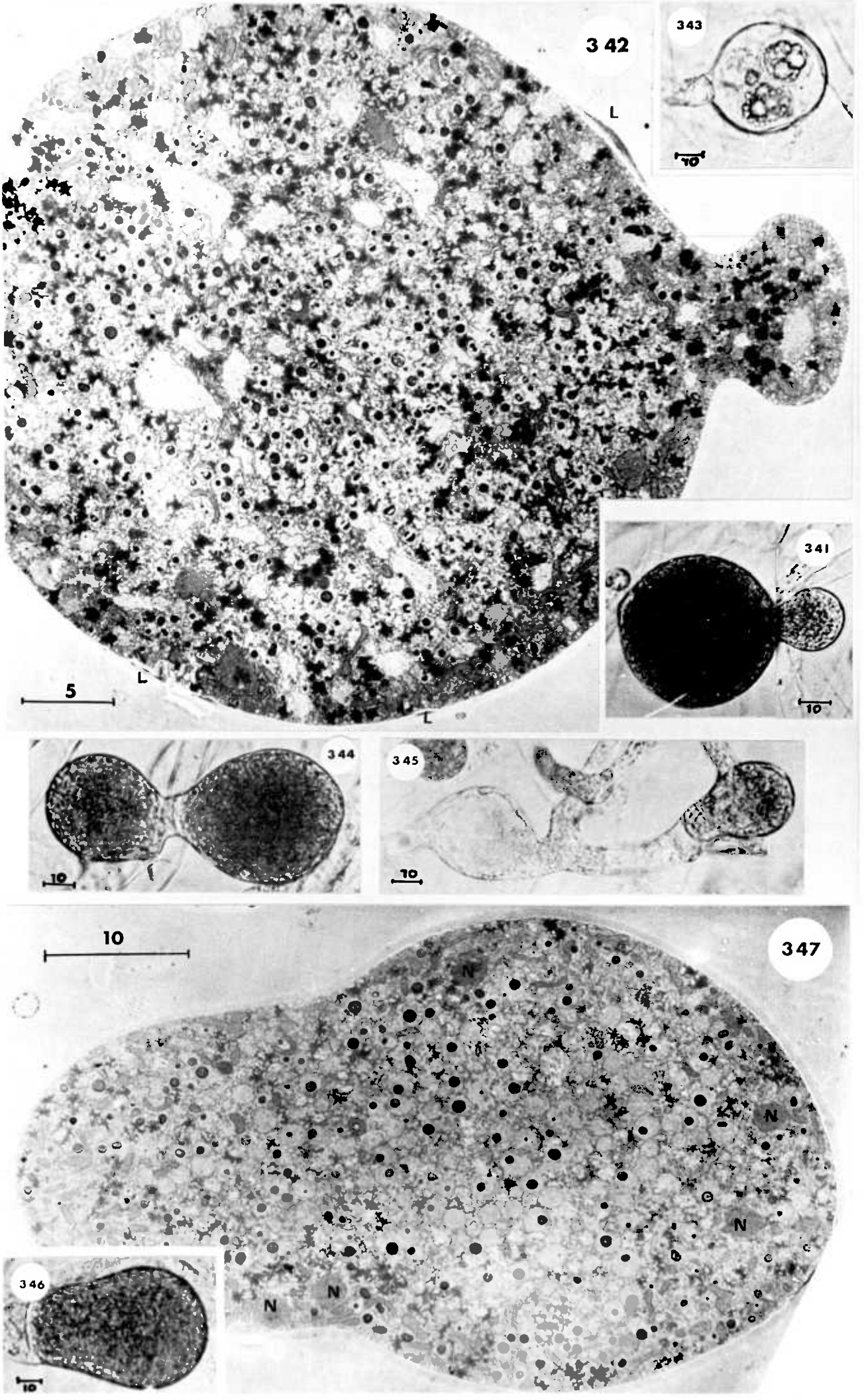
Figs. 3.44, 3.46 Light-micrographs illustrating the range of abnormal Ca^{2+} induced gemma.

Fig. 3.44 Pair of terminal gemma showing the conspicuous dividing septum and dense non-vacuolate cytoplasm.
152/49 OI 2500 mg/l Ca^{2+} 196 h

Fig. 3.45 Appendate gemma with a delimited secondary body.
152/36 2500 mg/l Ca^{2+} 196 h

Fig. 3.46 Typical club-shaped gemma.
152/12 OI 5000 mg/l Ca^{2+} 196 h

Fig. 3.47 LS of a clavate gemma showing the thickened cell wall and large osmiophilic densebodies.
29972 Os 3893 2500 mg/l Ca^{2+} 196 h


342
L
L
L
5
343
10
341
10
344
10
345
10
10
347
N
N
N
N
N
346
10

3.3.2.4 The effect of high concentrations of calcium^{+} on reproduction in S.furcata

Fig. 3.48 An abnormal nucleus typical of Ca^{2+}-induced gemmae. The nuclear envelope is indistinct and the nucleoplasm fibrillar. Note the Golgi association is still retained.
29288 Os 3893 2500 mg/l Ca^{2+} 196 h

Fig. 3.49 An elaborate membranous complex composed of nuclear envelope membranes.
29490 Os 3893 2500 mg/l Ca^{2+} 196 h

Fig. 3.50 Large osmiophilic densebody granule in a Ca^{2+}-induced gemma.
29479 Os 3893 2500 mg/l Ca^{2+} 196 h

Fig. 3.51 A pair of interphase centrioles which have become dissociated from the nucleus.
29479 Os 3893 2500 mg/l Ca^{2+} 196 h

Figs. 3.52, 3.53 Detail of the nuclear envelope proliferations shown in Fig. 3.49. Note the nuclear pores seen in tangential section.
29490 Os 3893 2500 mg/l Ca^{2+} 196 h

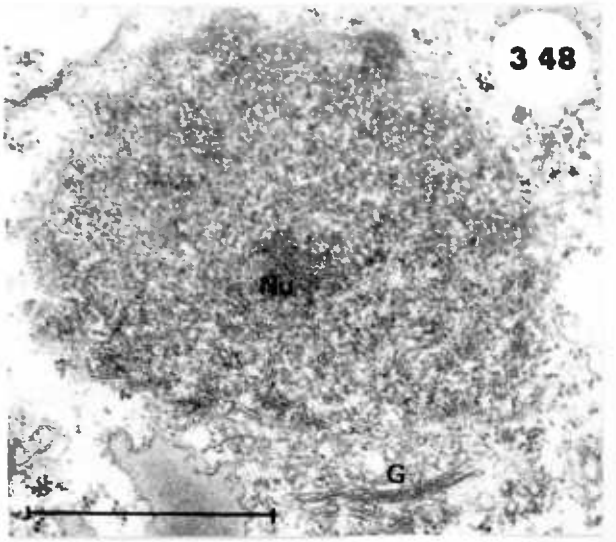
Fig. 3.54 Detail of thickened gemma wall showing peg-like ingrowth.
29465 Os 3892 1000 mg/l Ca^{2+} 196 h

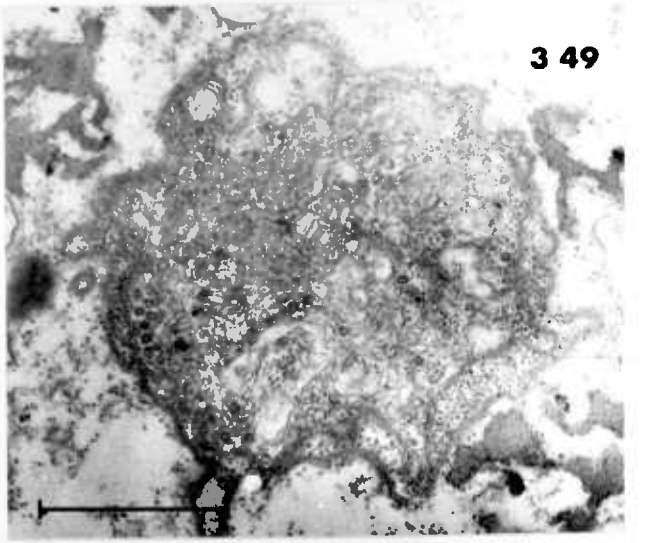
Figs. 3.55, 3.56 Mitochondrial profiles showing close associations with densebody vesicles (Fig. 3.55) and neutral lipid (Fig. 3.56).
29485, 29290 Os 3893 2500 mg/l Ca^{2+} 196 h

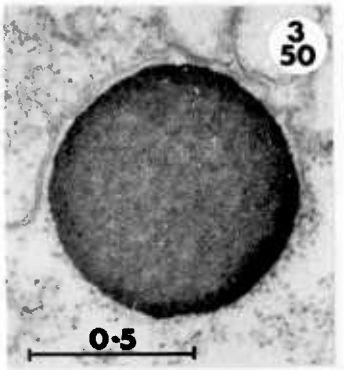
Figs. 3.57, 3.58 Detail of a thickened gemma wall showing the small sponge-like lomqsomes.
29296, 29295 Os 3893 2500 mg/l Ca^{2+} 196 h

Fig. 2.59 Light-micrograph of a thick biconcave septa in a Ca^{2+}-induced gemma.
152/15 OI 2500 mg/l Ca^{2+} 196 h

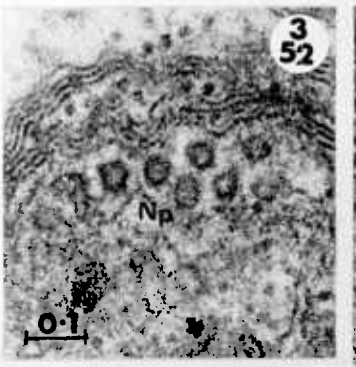
Fig. 2.60 LS through the basal septum of a gemma showing the thickened wall layers and characteristic biconcave profile.
29290 Os 3893 2500 mg/l Ca^{2+} 196 h

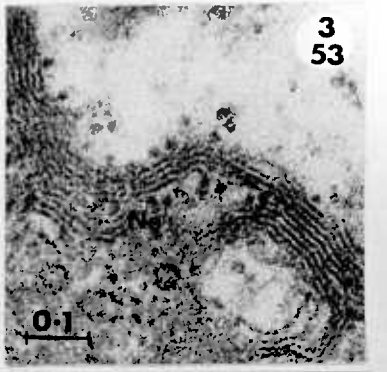

3 48
Nu
G

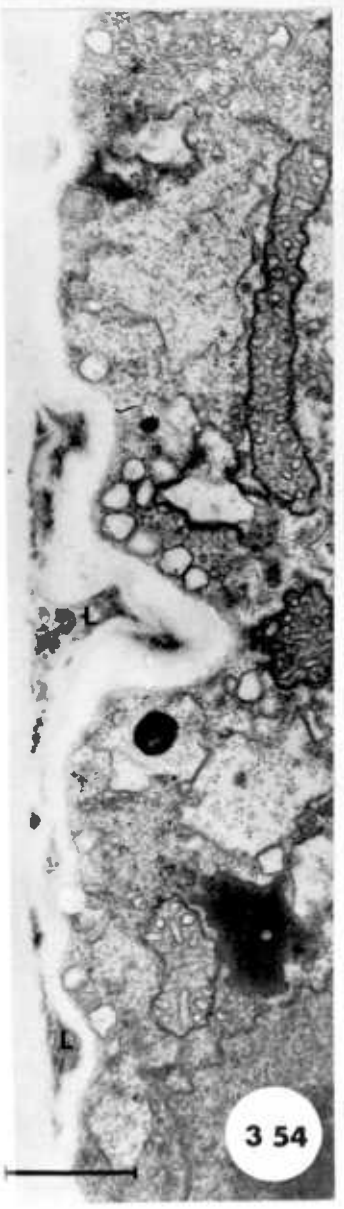

3 49

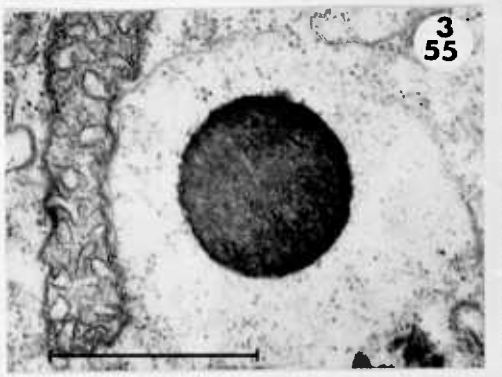

3 50
0·5

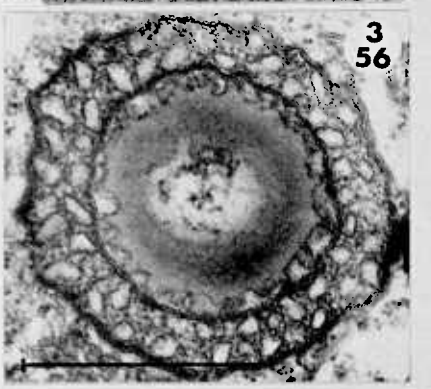

3 51
C
C
0·1

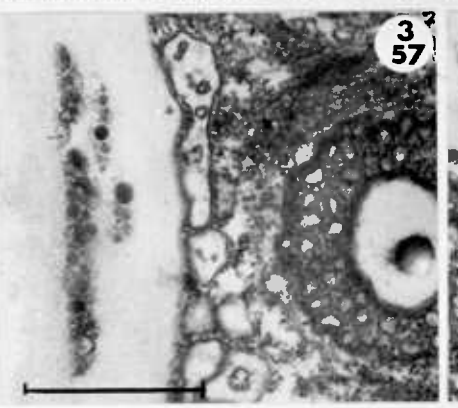

3 52
Np
0·1

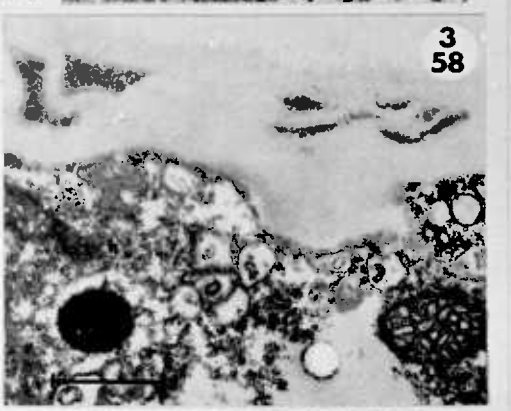

3 53
0·1

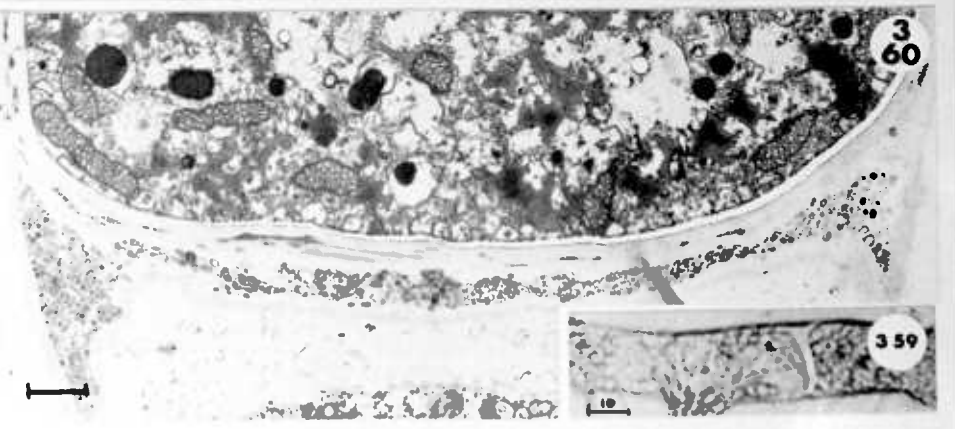

L
L
3 54


3 55


3 56


3 57


3 58


3 60

3 59

3.3.2.4 The effect of manganese on reproduction in S.furcata

Figs. 3.61-3.65 Light-micrographs showing the range of form of gemmae in Mn^{2+}-induced colonies.

Fig. 3.61 A hooked tip, suggesting a oogonial initial arrested in its early development.
149/50 OI 50 mg/l Mn^{2+} 120 h

Fig. 3.62 An elongate gemma in which the cytoplasm has degenerated.
149/70 50 mg/l Mn^{2+} 120 h

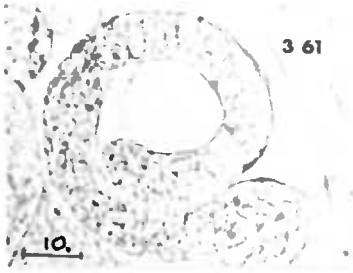
Fig. 3.63 Hyphae packed with refractile lipid droplets.
149/73 50 mg/l Mn^{2+} 120 h

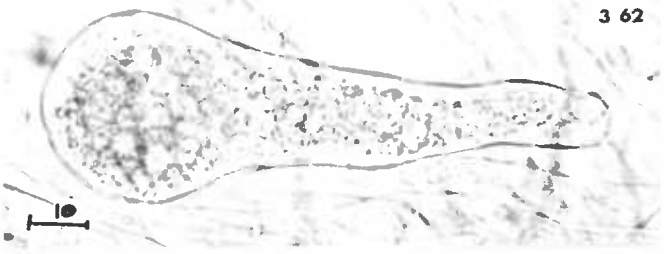
Fig. 3.64 Part of a Mn^{2+}-induced gemma showing the widespread disorganisation of cellular components.
29981 Os 3959 50 mg/l Mn^{2+} 120 h

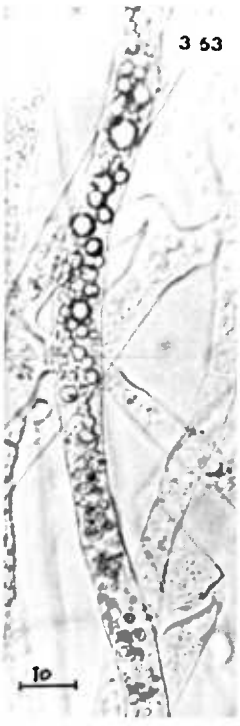
Fig. 3.67 Profile of a lysed nucleus in gemma shown in Fig. 3.64. The inflated nuclear envelope is just discernible.
29987 Os 3959 50 mg/l Mn^{2+} 120 h

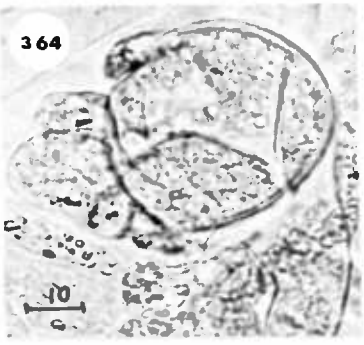
Fig. 3.68 Detail of the cell wall in the gemma in Fig. 3.64.
29978 Os 3959 50 mg/l Mn^{2+} 120 h

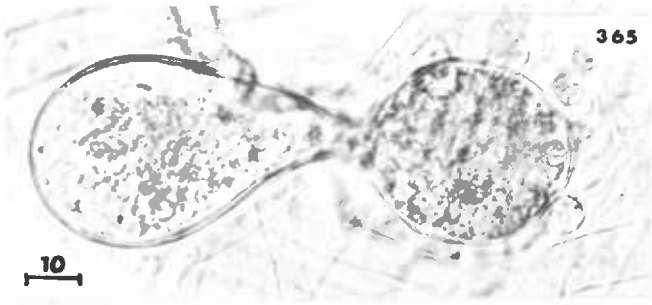
Fig. 3.69 Detail of lysed cytoplasm showing the disorganised membranes and organelles.
29982 Os 3959 50 mg/l Mn^{2+} 120 h

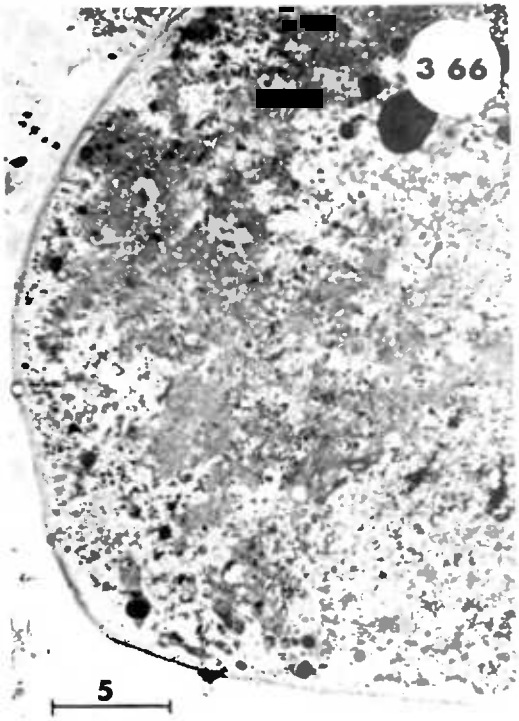

3 61
10

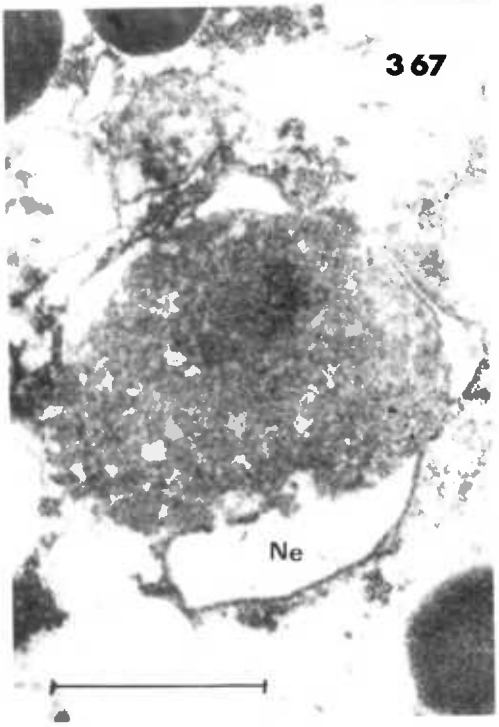

3 62
10

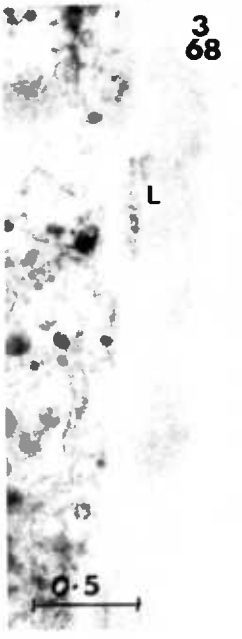

3 63
10

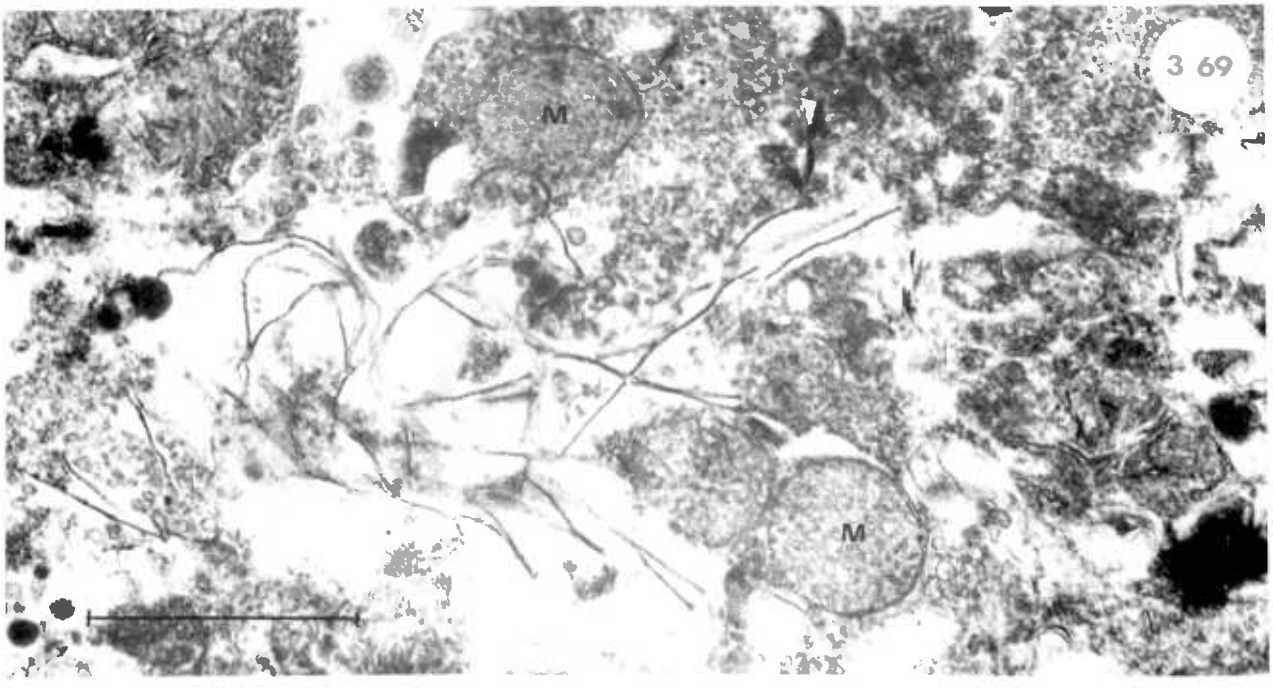

3 64
10


3 65
10


3 66
5


3 67
Ne


3
68
L
0·5


3 69
M
M